UNIVERSITY OF SOUTHAMPTON

FACULTY OF NATURAL AND ENVIRONMENTAL SCIENCES

School of Biological Sciences

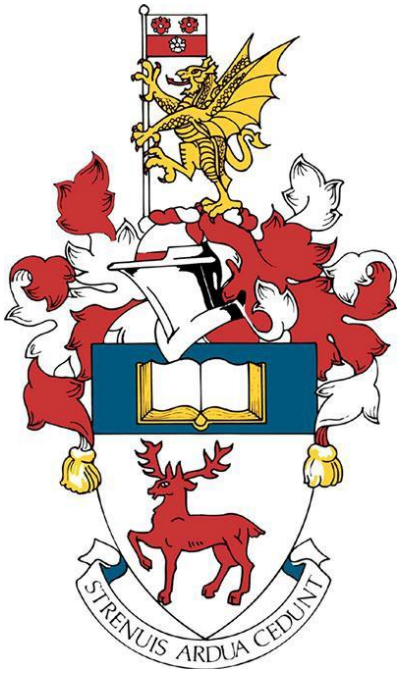

Developmental requirements and network properties of the *Drosophila* circadian clock circuit

by

Alexander Hull

Thesis for the degree of Doctor of Philosophy

June 2018

UNIVERSITY OF SOUTHAMPTON

ABSTRACT

FACULTY OF NATURAL AND ENVIRONMENTAL SCIENCES

Biological Sciences

Thesis for the degree of Doctor of Philosophy

Developmental requirements and network properties of the *Drosophila* circadian clock circuit

Alexander Hull

CLOCK/CYCLE (CLK/CYC) and PERIOD/TIMELESS (PER/TIM) are heterodimers which cyclically inhibit one another transcriptionally and post-translationally, required in adult *Drosophila* for the molecular oscillation controlling daily rhythms in activity. Prior work in the lab established that developmental reduction of PER and subsequent adult reintroduction does not affect adult rhythmic behaviour, whilst developmental PER overexpression or CYC reduction does. I sought to characterise the developmental role of CYC. Developmental CYC reduction specific to metamorphosis can impact adult behavioural rhythms, but CYC restriction throughout development does not appear to disrupt adult molecular rhythms. Developmental CYC restriction results aberrant neuroanatomy of small lateral ventral neurons (s-LN_v), which control freerunning rhythmicity, with increased complexity and defects indicative of defective axonal function, which are present in late larval and early pupal stages. Spatial mapping reveals loss of CYC in neurons other than the s-LN_vs contributes to this defect. However, the adult behavioural phenotype of a developmental CYC deficit is also associated with apparent defects in other clock neurons and expression markers for other clock-gene-expressing neurons indicate that developmental specification of these cells is altered in the absence of CYC. CYC mutants display a nocturnal profile in light-dark cycles, which cannot be rescued by adult-specific CYC. Nocturnality is a circuit property independent of s-LN_vs, or the neuropeptide that bolsters s-LN_v function, pigment-dispersing factor (PDF), which can be overriden by developmental CYC expression within s-LN_vs.

I characterised a network state, driven by continued photic stimulation via the visual pathway, histamine signalling and large lateral ventral neurons (l-LN_vs) which, in the absence of activation of a blue-light photoreceptor, CRY, encoded by the *cryptochrome* gene, which allows autonomous light sensitivity in clock-gene-expressing cells, results in a hierarchical shift in which s-LN_vs, and the neuropeptide through which they interact with other clock neurons, PDF, are dispensible for behavioural rhythms. Behaviour is not rescued in this network state following developmental CYC loss, echoing additional defects beyond the PDF cells, though developmental CYC rescue in PDF-negative clock cells can restore rhythmicity in this condition.

Contents

0 - Abstract i

- Table of Contents ii
- List of tables v
- List of figures v
- Declaration of authorship x
- Abbreviations xi

1 - Introduction

1.1 - The molecular basis of circadian rhythms in *Drosophila* 3

1.2 - The neuronal basis of circadian behavioural rhythms in *Drosophila* 7

1.3 - Interactions between clock neurons in generating behavioural rhythmicity 12

1.4 – Output pathways: Connecting the molecular clock to rhythmic phenotypes 19

1.5 - Clock output rhythms in sleep and nocturnality 23

1.6 – Involvement of circadian rhythms in developmental timing in *Drosophila* 27

1.7 - Development of circadian rhythms in *Drosophila* 28

1.8 - Developmental requirements for CLK/CYC in behavioural rhythmicity 33

1.9 - Advantages of *Drosophila* as a model organism 36

1.10 - Study Aims 37

2 - Materials and methods

2.1 - Fly culture 40

2.2 - Fly strains 40

2.3 - Locomotor assay setup 45

2.4 - Locomotor data analysis 48

2.5 - Pupariation assay 53

2.6 - Immunofluorescence 53

2.7 - Image analysis 56

3 - Results: Behavioural analysis of conditional modulation of *cycle* expression

3.1 - Validated cyc^{01} $[elav.cyc]^{ts}$ lines become arrhythmic following developmental loss of *cycle* 62

3.2 – Expression of *cycle* conditionally alters nocturnality in an adult-specific manner 69

3.3 - Developmental loss of *cycle* results in a cyc^{01}-like behavioural profile in light-dark cycles, even in cases of adult *cycle* re-introduction 73

3.4 - Spatial reintroduction of *cycle* in specific clock neuron clusters reveals 76

expression within the PDF cells promotes diurnality, whilst loss within the PDF cells promotes nocturnality

3.5 – Nocturnal behaviour of *cyc*^{01} flies is not due to aberrant PDF cell exciteability or signalling 82

3.6 – Nocturnal behaviour following loss of *cycle* is dependent on light wavelength during the day and persists following the ablation of PDF-expressing cells 88

3.7 - Conditional loss of *cycle* across developmental timepoints suggests post-larval developmental requirements for *cycle* in establishing adult behavioural rhythms 93

3.8 – Flies lacking adult expression of *cycle*, but not flies over-expressing *period* as adults, are able to entrain in light-dark cycles at adult restrictive temperature 98

3.9 - Molecular rhythms persist in *cyc*^{01} *[elav.cyc]*^{ts} sLN$_v$s following return to permissive conditions during adulthood 99

3.10- Loss of *cycle* expression in the adult is capable of damping the molecular oscillator in s-LN$_v$s 102

3.11 - Discussion – Chapter 3 105

4 - Clock cell network morphology following developmental CYC loss

4.1 - *cyc*^{01} flies, lacking functional *cycle*, possess dorsal PDF+ve projections that exhibit defasciculation and misrouting defects 116

4.2 – Developmental, but not adult loss of *cycle* expression phenocopies *cyc*^{01} projection phenotype 122

4.3 – Following loss of *cycle*, increased branching complexity is observable within PDF-expressing neurons from third-instar larvae onwards 126

4.4 - Increased complexity of PDF-expressing dorsal projections is not solely indicative of projection dysfunction and can occur in behaviourally rhythmic populations 132

4.5 – Bouton number and localization in PDF-expressing dorsal projections is altered in the absence of *cycle*. 134

4.6 –Post-synaptic targets of PDF-expressing neurons in the dorsal brain appear altered in the absence of *cycle*. 137

4.7 - The projection and behavioural phenotypes caused by 139

developmental loss of *cycle* are not due to aberrant PDF signalling

4.8 – Expression of *cycle* within PDF-expressing neurons is required, but not neccesarily sufficient, for PDF projection formation 141

4.9 - Adult-specific expression of *cycle* is required for ITP neuropeptide expression within clock neurons, and loss of cycle reduces expression of multiple clock-neuron drivers. 154

4.10 – Loss of *pdp1* or *Clock*, which regulate levels of each other, results in related phenotypes to loss of *cycle*, but ectopic expression of either fails to rescue phenotypes caused by loss of the other 162

4.11 - Discussion- Chapter 4 168

5 - Characterisation of red-light mediated clock circuit network changes and relevance to developmental requirement for *cycle*

5.1 - PDF cell firing states are dominant, yet dispensable for behavioural rhythms in constant red light 176

5.2 - s-LN_vs are dispensable for behavioural rhythmicity in constant red light, contingent upon l-LN_v presence 181

5.3 - Spatial mapping of pacemaker function confirms the importance of CRY+ve but not PDF+ve cell molecular oscillators for behavioural rhythmicity in constant red light 187

5.4 - Spatial reintroduction of PER onto per^{01} maps oscillator requirement in constant red light to the Evening Cells. 200

5.5 - Behavioural rhythms in constant red light are dependent upon compound eye signalling in the absence of PDF signalling 205

5.6 - Interrogation of red light clock cell hierarchy reveals new insights into circuit layout and plasticity 211

5.7 - Interrogating known output signalling pathways required for behavioural rhythms during constant darkness reveals certain output pathways are required under constant red light conditions, whlist others are marginalised. 221

5.8 - Network requirements for behavioural rhythms in constant red light appear separable, and more stringent than requirements for evening anticipation in 12:12hr light-dark cycles 227

5.9 – The behavioural arrhythmia induced by developmental loss of *cycle* is not rescued by exposure to constant red light, nor does developmental expression of *cycle* within putative red-light pacemaker cells allow behavioural rhythms in 231

constant red light
5.10 - Discussion – Chapter 5 240
6 - Conclusions 252
7 - Appendix 260
8 - References 354

List of tables

3.1 – Freerunning behavioural rhythms following conditional manipulation of CYC levels across varied developmental and adult temperatures 65

List of Figures

1.1 - Basic Terminology accompanying research in biological timekeeping 3
1.2 - Outline of the core molecular clock circuit and associated regulatory loops 4
1.3 - Neuroanatomy of the Drosophila circadian clock network 9
1.4 - Borbely-Achermann model of sleep 24
1.5 - Proposed mechanism of nocturnality following loss of *Clock* or *cycle* 25
1.6 - Diagram of the larval neural clock circuit 30
1.7 - Developmental overexpression of period results in adult behavioural arrhythmia 34
1.8 - Schematic of the Gal4-UAS system 37
2.1 - Absorption spectra for different experimental light conditions. 47
2.2 - Example actograms across a spectrum of Relative Rhythmic Power 49
2.3 - Presentation of activity profile data 50
2.4 - Diurnality/Nocturnality ratio calculation 51
2.5 - Schematic of Evening Anticipation Index. 52
2.6 - Demonstration of E-peak phase calculation 53
2.7 - Demonstration of quantification of axonal phenotypes 58
2.8 - Demonstration of quantification of clock protein levels and localization within the soma. 59
3.1 - A genetic scheme for conditional regulation of *cycle* levels 63
3.2 - Both developmental and adult *cycle* expression are required for behavioural rhythms in constant darkness 64

3.3 - Development-specific loss of *cycle* expression results in persistant behavioural arrhythmia 66
3.4 - Expression of transgenic *cycle* results in shortened period length 68
3.5 - Developmental and adult-loss of *cycle* expression result in distinct changes in day and night behavioural activity. 71
3.6 - Relative day and night activity differs dependent on temperature, and presence of *cycle*. 72
3.7 - Day and night behavioural activity levels are altered dependent on development- and adult expression of *cycle* 75
3.8 - Activity profiles in light-dark cycles following modulation of adult levels of *cycle* 76
3.9 - Expression of *cycle* specifically within PDF cells is sufficient for anticipatory behaviours at night 77
3.10 - Loss of *cycle* within the PDF cells impacts the distribution of day and night behavioural activity 79
3.11 - *cycle* expression in either PDF-expressing or non-PDF cells can generate anticipatory behaviour, but result in altered distribution of day and night activity 81
3.12 - Nocturnal behaviour in *cycle* mutants is independent from PDF signalling but dependent on dopaminergic neurons 84
3.13 - Tetanus toxin expression within peptidergic neurons reduces nocturnal behaviour stemming from loss of *cycle* 86
3.14 - PDF cell hyperexcitation reduces both day and night activity levels 88
3.15 - Increased nocturnal behaviour following loss of *cycle* is primed by white-light exposure during the day 89
3.16 - Ablation of PDF cells does not disrupt nocturnal behaviour caused by loss of *cycle* 91
3.17 - Loss of *cycle* expression through later developmental stages progressively weakens adult behavioural rhythms 95
3.18 - Loss of *cycle* expression during pupation significantly lowers adult behavioural rhythmicity 97
3.19 - Conditional overexpression of *period* during adulthood, unlike adult-specific loss of *cycle*, results in loss of behavioural rhythms, which can be rescued by exposure to light 99
3.20 - Developmental loss of *cycle* expression does not prevent molecular rhythms 102

re-emerging in adulthood
3.21 - Persistant lack of *cycle* expression in the adult results in loss of molecular rhythms in PER 104
3.22 - Model for developmental and adult roles for *cycle* in behaviour during light-dark cycles 114
4.1 - Loss of *cycle* expression results in increased axonal complexity of PDF cells 118
4.2 - Temperature has a negligible effect of PDF cell axonal complexity following loss of *cycle* 120
4.3 - PDF-expressing cell number is not reduced following loss of *cycle* 121
4.4 - Axons from both small and large lateral ventral neurons are misrouted dorsally following loss of *cycle* expression 122
4.5 - Developmental loss of *cycle* expression, but not adult loss, results in increased axonal complexity of PDF cells. 124
4.6 - Developmental overexpression of period increases the axonal complexity of PDF cells 126
4.7 - Loss of *cycle* expression results in increased axonal complexity of PDF cells in larval brains 128
4.8 - Loss of *cycle* expression results in increased axonal complexity in mid-pupal brains 131
4.9 - Mild increases in axonal complexity are observable in both behaviourally rhythmic and arrhythmic flies 133
4.10 - PDF cell synapses are more numerous and mis-localised following loss of *cycle* expression 135
4.11 - Loss of *cycle* expression alters the morphology of dorsal synapse-forming termini of pacemaker neuron axons 136
4.12 - Loss of *cycle* expression results in a decrease in identifiable dorsal clock neurons 138
4.13 - PDF receptor is required for correct PDF axon termini morphology, but loss of PDF receptor is distinct from loss of *cycle* expression. 140
4.14 - Inhibition of ectopic *cycle* rescue within PDF cells results in a decrease in molecular period rhythms 144
4.15 - Loss of *cycle* within PDF cells increases their axonal complexity, and expression of *cycle* only within PDF cells decreases their axonal complexity 146

4.16 - Rescue of *cycle* expression within PDF cells is sufficient for molecular period rhythms 147
4.17 - Rescue of *cycle* expression within PDF cells fails to fully rescue synapse number and morphology within PDF axonal projections 150
4.18 - Robust behavioural rhythms are only achievable when *cycle* is expressed across multiple clock cell groups 153
4.19 - Loss of *cycle* expression results in fewer ITP neuropeptide-expressing clock cells 155
4.20 - An evening cell driver line, R78G02-gal4, expresses in fewer cells following loss of *cycle* expression 157
4.21 - Fewer cells induce transcription from the *cry*-promotor region following loss of *cycle* 159
4.22 - Fewer CRY-expressing cells are identifiable following loss of *cycle* 161
4.23 - Fewer PDF cell soma are identifiable in following loss of *Clock* than loss of *cycle* 164
4.24 - Loss of either *Pdp1* or *Clock* results in fewer PDF cell soma 166
4.25 - PDP1 expression fails to rescue the PDF projection stunting identified in CLK mutants 168
4.26 - Model for effect of developmental loss of *cycle* on the adult clock circuit 174
5.1 - PDF signalling is required for freerunning behavioural rhythms in constant darkness, but not in constant red light 178
5.2 - PDF-cell silencing through ectopic expression of Kir2.1 potassium channel decreases behavioural rhythmicity in constant red light and constant darkness 179
5.3 - Hyperexcitation of PDF-cells fails to impact freerunning rhythmicity in constant red light 180
5.4 - Ablation of PDF cells reduces behavioural rhythmicity in constant darkness and constant red light 182
5.5 - Conditional ablation of small lateral ventral neurons does not remove behavioural rhythms in constant red light, so long as large lateral ventral neurons are intact 183
5.6 - Conditional ablation of small lateral ventral neurons does not affect evening anticipation, suggesting PDF control of evening anticipation timing is derived from large lateral ventral neurons 186
5.7 - Inhibition of molecular oscillations in CRY-expressing, but not PDF- 189

expressing clock neurons, results in a loss of behavioural rhythmicity in constant red light
5.8 - Loss of PDF cell molecular oscillations results in split behavioural rhythms in constant red light, with a short-period component which is independent of PDF signalling splitting 192
5.9 - Molecular oscillator function within CRY-ve clock cells in the dorsal brain can influence rhythms in constant red light 194
5.10 - Molecular oscillations are not required in CRY-expressing evening cells for behavioural rhythms in constant red light 196
5.11 - ITP neuropeptide is not required for behavioural rhythms in the presence or absence of PDF signalling in constant darkness or constant red light 199
5.12 - *period* expression solely within evening cells is sufficient for behavioural rhythmicity in constant red light 203
5.13 - *disco*^{1} mutants, lacking small lateral ventral neurons and visual connectivity, are broadly behaviourally arrhythmic in constant darkness and constant red light 206
5.14 - Loss of both visual system function and PDF signalling completely removes behavioural rhythmicity in constant red light 208
5.15 - Histamine receptor *HisCl1* is not required within clock cells for behavioural rhythms in constant red light in the absence of PDF signalling 210
5.16 - Hyperexcitation of CRY-negative clock neurons represses rhythmic behaviour in constant darkness, but not in constant red light 213
5.17 - Hyperexcitation of CRY-expressing evening cells results in decreased behavioural rhythmicity in constant red light relative to constant darkness 215
5.18 - Reduction of signalling from CRY-expressing evening cells results in decreased behavioural rhythmicity in constant red light 218
5.19 - Hyperexcitation of downstream clock neurons, $DN1_{p}s$, has limited effect on behavioural rhythms in both constant red light and constant darkness 220
5.20 - Ablation of SIFamide-expressing neurons results in decreased behavioural rhythmicity in constant red light 222
5.21 - Increased signalling from Dh44-neuropeptide-expressing neurons results in decreased behavioural rhythmicity in constant red light and constant darkness. 223

5.22 - Loss of Dh31 neuropeptide does not alter behavioural rhythmicity in constant red light or constant darkness 225
5.23 - Loss of leucokinin signalling results in decreased behavioural rhythmicity in constant darkness, but not constant red light 226
5.24 – Loss of behavioural rhythmicity in constant red light does not result in a loss in evening anticipatory activity 228
5.25 – Dopaminergic hyperexcitation does not remove anticipatory behaviours in light-dark cycles, despite loss of behavioural rhythmicity in constant red light 230
5.26 – Loss of developmental *cycle* expression results in behavioural arrhythmia in constant red light 232
5.27 – Loss of LAR within PDF cells results in lowered behavioural rhythmicity in constant darkness, but not constant red light, and evening anticipation is maintained 233
5.28 – Behavioural arrhythmia in constant darkness caused by adult loss of *cycle* within PDF cells can be partially rescued in constant red light 235
5.29 - Rescue of behavioural rhythmicity through ectopic expression of *cycle* is only achievable through pan-neuronal expression 237
5.30 - Developmental overexpression of *period* results in adult behavioural arrhythmia in both constant darkness and constant red light 239
5.31 - Summary model of differing networks of rhythmic behavioural generation in constant darkness and constant red light 252

Academic Thesis: Declaration Of Authorship

I, Alexander Hull

declare that this thesis and the work presented in it are my own and has been generated by me as the result of my own original research.

Developmental requirements and network properties of the *Drosophila* circadian clock circuit

I confirm that:

1. This work was done wholly or mainly while in candidature for a research degree at this University;

2. Where any part of this thesis has previously been submitted for a degree or any other qualification at this University or any other institution, this has been clearly stated;

3. Where I have consulted the published work of others, this is always clearly attributed;

4. Where I have quoted from the work of others, the source is always given. With the exception of such quotations, this thesis is entirely my own work;

5. I have acknowledged all main sources of help;

6. Where the thesis is based on work done by myself jointly with others, I have made clear exactly what was done by others and what I have contributed myself;

7. Either none of this work has been published before submission, or parts of this work have been published as: [please list references below]:

Signed: ……

Date: ……

Abbreviations

aMe: Accessory medulla

AR: arrhythmic

BMP: Bone morphogenetic protein

CLK: clock

CRY: cryptochrome

CT: Circadian time

CYC: cycle

DBT: Doubletime

Dcyc: UAS-cycΔ^{103}

DD: constant darkness

DH31: Diuretic hormone 31

DH44: Diuretic hormone 44

DN: dorsal neuron (1a,1p,2,3)

E: Evening

EB: Ellipsoid body

ECR: Environmentally controlled room

Elav: Embryonic lethal, abnormal vision

FMN: Fumin

GFP: Green fluorescent Protein

Hdc: Histamine decarboxylase

Hid: Head involution defective

HisCl1: histamine-gated chloride channel subunit 1

Hr: hour

Inc: Including

IP: Immunoprecipitation

ITP: Ion transport peptide

L3: Third-instar larvae

LD: 12:12 light-dark cycle

l-LN_v: Large ventral lateral neuron

LN_d: Dorsal lateral neuron

M: Morning

NPF: Neuropeptide F

Ort: Ora transientless

P6: Pupal stage 6 (24-48hr PPF)

PDP1: Par domain protein 1

PDF: Pigment dispersing factor

PDFR: Pigment dispersing factor Receptor

PER: Period

PI: Pars intercerebralis

PPF: Post-puparium formation

RNAi: RNA interference

RR: constant red light

RRP: Relative rhythmic power

SIFa: *SIFa*mide

s-LN_v: small ventral lateral neuron

sNPF: small Neuropeptide F

TAU: Period Length

TIM: Timeless

TUG: *tim-UAS-gal4*

VGlut: Vesicular Glutamate Transporter

VRI: vrille

Wt: wild-type

UAS: Upstream activating sequence

ZT: Zeitgeber time

Chapter 1 – Introduction

Circadian clocks, ~24 hr endogenous oscillators that control numerous physiological, behavioural and developmental events through the cycling of transcriptional and translational regulatory elements, are present across phyla. The simplest circadian organisms are cyanobacteria, a photosynthetic group of bacteria that photosynthesise during the day, controlled by a molecular clock entrained by light (Huang et al., 1990). Clocks exist across eukaryotic phyla and are present in protists, fungi, plants and animals. The breadth of processes under circadian regulation has necessitated further study of the system, in which an increased understanding of the workings of circadian rhythmicity and the mechanisms by which it controls multiple systems will have important applications in health and food security (Dunlap, 1999, Young and Kay, 2001). For instance, medicine effectiveness and wound healing are under circadian regulation and of clinical concern (Smolensky, 2001, Hoyle et al., 2017), circadian rhythm sleep disorders (CRSD) affect a significant proportion of the population (Schrader et al., 1993), clock defects are a cause and symptom of neurodegeneration (Musiek and Holtzman, 2016) and a broader human cost emerges from desychrony between internal clock and lifestyle, with numerous health defects in shift workers and a greater rate of accidents during unsociable hours (Harrington, 2001, Akerstedt et al., 2002). Understanding the interplay of rhythms in crop immune response (Wang et al., 2011) and in pest species, including Drosophilids, has agricultural relevance and can inform crop protection strategies (Hamby et al., 2013).

Fundamentally, clocks are capable of maintaining time and re-entraining to external environmental conditions. In constant darkness (DD) conditions, the clock freeruns, maintaining circadian rhythms in the absence of an external cue. Animal rest and activity over a 24-hour period manifests this rhythm, with distinct periods of sleep, broadly in the subjective night in the case of diurnal species and wakefulness in the subjective day. In addition to entrainability, clocks are temperature compensated, possessing uncharacterised mechanisms which allow them to maintain time irrespective of kinetic changes associated with temperature (Kidd et al., 2015).

Figure 1.1 - Basic Terminology accompanying research in biological timekeeping. *Shown is a schematic of light regimens comprising a Light-dark (LD) cycle or one day of LD and one day of Constant dark (DD) light conditions, and the accompanying terminology. Zeitgeber time (ZT), refers to an entrained timepoint, in which ZT is the initiation of an entraining stimulus, whilst Circadian time (CT), refers to the relative 24-hour timepoint of the ZT, even in the absence of the entraining stimulus.*

1.1 - The molecular basis of circadian rhythms in *Drosophila*

Across phyla, the principle of the molecular clock is the same, a negative feedback loop with translated components directly or indirectly negatively regulating their transcription, that through temporal lag in the accumulation or degradation of components of the circuit generates an oscillation with an approximately 24 hour period, that can be adjusted or reset via external stimuli.

The core clock of eukaryotes consists of a transcription/translation negative feedback loop with multiple input pathways. Additional loops regulate the individual components of this to add further specificity to the timing of the clock. The first established clock gene was discovered in *Drosophila*, which continue to possess one of the most thoroughly characterised molecular clockworks (Konopka and Benzer, 1971). *Clock* (*Clk*) and *cycle* (*cyc*) genes encode transcription factors, which gain enhanced stability when dimerised and target conserved enhancer sites, termed E-boxes, which facilitate transcription factor binding (Hao et al., 1997). The positive arm of the circadian oscillation is driven by CLK/CYC, and targets of these transcription factors can be regulated by the clock (Rutila et al., 1998). In cyc^{01} and Clk^{Jrk} loss of function mutants, behavioural rhythms are lost, as is transcription of other rhythmically expressed genes (Rutila et al., 1998, Allada et al., 1998, Mcdonald and Rosbash, 2001).

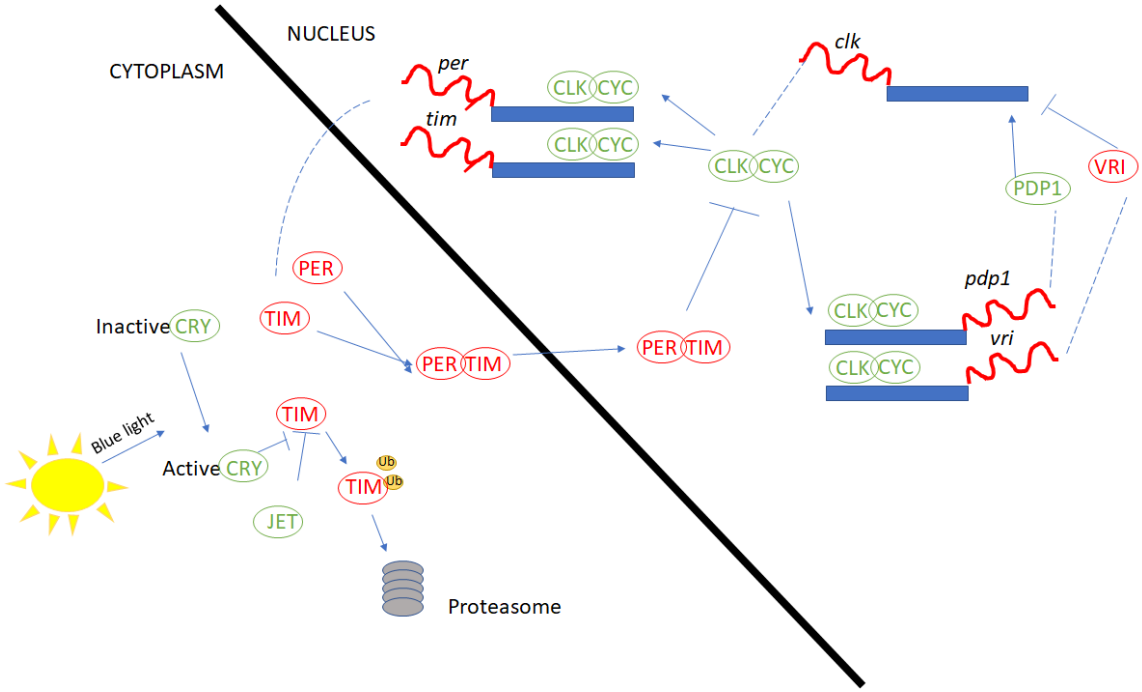

Figure 1.2 - Outline of the core molecular clock circuit and associated regulatory loops. *CLK/CYC heterodimers control transcription of numerous factors, most notably PER and TIM, which feed-back to regulate the functional levels of CLK/CYC with an approximately 24 hr cycle. CRY is capable of degrading TIM in a light-dependent fashion, allowing the dynamics of the clock to be reset, or "entrained". Proteins labelled in green are factors in the positive arm of the molecular circuit, whilst red signifies antagonistic factors comprising the negative arm of the circuit. Pointed arrows represent translocation or enhancing effects, whilst blunt arrows represent repressive effects. Dotted lines indicate processing of mRNA into mature protein. Ub stands for Ubiquitin.*

CYC is mainly cytoplasmically based and requires dimerisation to CLK in order to accumulate within the nucleus and to resist degradation (Kim and Edery, 2006, Liu et al., 2017). CLK/CYC activates multiple genes implicated in rhythmicity, notably *period* (*per*) and *timeless* (*tim*), the 1st and 2nd identified genes in *Drosophila* required for circadian rhythms. per^{01} and tim^{01} null mutants were isolated through screens assaying rest-activity behaviour in flies treated with the mutagen Ethyl methanesulfonate (EMS), which generates primarily point mutations (Konopka and Benzer, 1971, Sehgal et al., 1994). These genes were key in identifying the clock as a negative feedback loop, as PER and TIM, both transcription factors, are incapable of inducing their own transcription.

Like CLK/CYC, PER and TIM are capable of dimerising to enter the nucleus and

maintain stability, and PER is completely cytoplasmic in *tim*^{01} flies, appearing to require TIM for nuclear entry (Vosshall et al., 1994)(Figure 1.2). Both TIM and PER contain cytoplasm-localisation domains (CLDs) which are potentially blocked by the formation of a PER/TIM dimer (Vosshall et al., 1994, Saez and Young, 1996). This dimer enters the nucleus and inhibits CLK/CYC binding of E-boxes, which reside upstream of *per* and *tim* coding regions (Lee et al., 1999), hence inhibiting PER/TIM transcription, leading to derepression of CLK/CYC, and a completion of the negative feedback loop (Figure 1.2).

Neither protein nor mRNA levels of *cyc* oscillate, unlike *Clk* which has a rhythmic mRNA, but non-rhythmic protein (Rutila et al., 1998, Bae et al., 2000, Houl et al., 2006). CYC overexpression does not affect oscillations, demonstrating that CYC does not confer rhythmicity to the clock and that CLK/CYC formation is dependent on and limited by levels of CLK (Peng et al., 2003). Contrary to this, PER and TIM overexpression and knockdown leads to a partial loss of rhythmicity, indicating that the rhythmicity of these components, in addition to rhythmic *Clk*, is required for a functioning molecular clock (Blanchardon et al., 2001, Yang and Sehgal, 2001).

PER and TIM appear individually capable of preventing CLK/CYC binding to certain E-box substrates, and of inhibiting other proteins containing a BHLH motif, which imparts DNA-binding function (Lee et al., 1999). It has been subsequently demonstrated that PER alone is capable of repressing CLK/CYC transcription, in the absence of TIM (Rothenfluh et al., 2000).

One property distinguishing clocks from simple oscillations is their entrainability to external stimuli, primarily light and temperature, termed zeitgebers. As circadian timing is approximate, and no clock has evolved to perfectly mimic the period of the earths rotation, entrainability is a necessary property to maintain phase with rhythmic environmental conditions and appropriately exploit these changes. In the absence of PER, TIM is unstable and can be targeted for degradation by the photosensitive protein CRY, encoded by the gene *Cryptochrome* (Emery et al., 1998, Stanewsky et al., 1998)(Figure 1.2). CRY contains a flavin chromophore and in the presence of light undergoes photoreduction, electron transfer resulting in an active conformation of the "tail" region of CRY and allowing CRY to bind TIM in a light-dependent manner (Ceriani et al., 1999, Berndt et al., 2007). Light-activated CRY facilitates TIM degradation via ubiquitination, through recruitment of JETLAG, an E3 ligase (Emery et

al., 2000, Koh et al., 2006)(Figure 1.2). CRY degradation is light-dependent and can be stabilised by a return to dark conditions, whilst TIM degradation is irreversible once bound to CRY (Busza et al., 2004). The arrhythmia of flies in LL is a due to constitutive repressive effect on the clock via this process.

Transcriptional cycling, as mentioned above, is of importance in determining behavioural rhythms. For instance, a robust correlation exists between damping of transcript cycling and concurrent behavioural damping (Marrus et al., 1996, Peng et al., 2003).

DBT *(doubletime)* is a kinase that phosphorylates monomeric PER and facilitates its degradation via binding to SLIMB, an F-box containing E3 ligase and component of the ubiquitination pathway leading to degradation (Price et al., 1998, Ko et al., 2002, Glickman and Ciechanover, 2002). This process is similar to JETLAG-mediated light-dependent TIM degradation, occurring in freerunning conditions. Mutant variants of *dbt* exist, that produce long or short periods, or arrhythmia, without affecting DBT protein levels, indicating the pivotal role of PER degradation on maintaining a correct period length. Furthermore, loss of DBT results in an accumulation of PER in a TIM-independent fashion, indicating that the heterodimeric form of PER cannot be targeted by DBT, and indicates a role for TIM in stability of PER. In dbt^{p} tim^{01} flies, which lack appreciable TIM or DBT protein, PER is found constitutively in the nucleus, identifying not only that PER is capable of nuclear entry in the absence of TIM, but that this is mediated by DBT (Cyran et al., 2005). DBT is bound to nuclear PER, and DBT acts as a non-catalytic component in PER-mediated phosphorylation and inhibition of CLK (Yu et al., 2009). Constant clock protein levels are a result of this rhythmic post-translational modification. The peak of CLK phosphorylation, preceding degradation is in the same phase as clock mRNA cycling, indicating that this rhythmic regulation may extend to translation, but is blunted by rhythmic degradation (Kim and Edery, 2006).

SGG (*shaggy*) is another kinase that regulates the clock, where loss of SGG lengthens period and overexpression shortens period. In this case, SGG regulates TIM (Martinek et al., 2001). These pathways add another negatively regulating loop to the clock, which operates in a post-translational manner. Beyond that, these post-translational components of the clock appear to be most involved in setting the speed of the clock, through degradation of components as opposed to synthesis, which, considering the number of initially non-oscillatory transcripts of proteins involved in the clock, shows that

refinement of clock timing can occur most precisely via degradative pathways (Brown et al., 2012).

A second negative feedback loop regulating CLK expression further controls molecular cycling. VRI (*Vrille*) is rhythmically expressed in clock neurons and acts as a transcriptional repressor of CLK, damping molecular rhythms when overexpressed (Glossop et al., 2003). PDP1 (*par domain protein 1*) is a transcription factor involved in muscle development, with eight specific isoforms, of which a single isoform, PDP1ε, is expressed in clock cells, demonstrates rhythmicity, accumulation of transcript and protein levels at night (Lin et al., 1997, Reddy et al., 2000).

PDP1ε has been shown, somewhat controversially, as a positive regulator of CLK transcription, acting antagonistically to VRI through competitive binding of E-box sites on the CLK promotor. Both VRI and PDP1 promotor regions contain E-boxes, and thus both factors are activated by CLK/CYC (Blau and Young, 1999, Cyran et al., 2003). As these factors are regulated by and regulate CLK, they are proposed to form a further loop that controls rhythms in CLK transcription. Modulating VRI levels cannot fully damp molecular cycling, indicating that other factors may limit total repression of CLK (Glossop et al., 2003).

This VRI/PDP1ε loop forms another negative feedback loop that makes up part of the core molecular clock and is responsible for CLK mRNA cycling. The earlier phase of VRI compared to PDP1 leads to an early morning repression of CLK, and an evening activation when PDP1 levels supersede waning VRI levels (Cyran et al., 2003).

The core molecular clock has been studied in detail, and whilst many intricacies are unknown, the broad mechanics of an oscillator formed from a central transcription-translation loop, buffered by further transcriptional loops is well understood and conserved across phyla. So too is the role of post-translational events in regulating molecular timing, and the requirement for a molecular mechanism of entrainment.

1.2 - The neuronal basis of circadian behavioural rhythms in *Drosophila*

Molecular clocks are located in numerous tissues, but behavioural rest-activity rhythms are controlled by, and dependent upon, a circuit of clock-bearing cells within the

protocerebrum.

A core of 150 clock neurons exist within the brain, identifiable through their expression of core clock genes *tim*, *per, Clk* and *cyc*, many of which are thought to contribute to behavioural circadian function. Of these, it is possible to subdivide into neurons expressing CRY, and certain neurons within the dorsal brain which lack CRY, namely approximately forty neurons termed “DN3s”, of enigmatic function, and two neurons termed ”DN2s”. The fly brain is translucent, and all clock neurons are light accessible, so CRY+ve neurons are thus capable of autonomous light entrainment without cues from the clock network whilst CRY-ve neurons cannot autonomously entrain and must rely on entraining signals from other clock neurons. If larvae are placed into constant darkness (DD), these CRY-ve DN2s contain clock proteins cycling in anti-phase, which can be rectified by ectopic CRY expression, though the mechanism underlying this is not understood (Klarsfeld et al., 2004).

Clock neurons can be further subdivided by their expression of a neuropeptide, Pigment dispersing factor (PDF), which is present only in four-five large lateral ventral neurons (l-LN_vs) and four small lateral ventral neurons (s-LN_vs). These PDF+ve cells are all CRY+ve, with the remaining CRY+ve, PDF-ve clock neurons being a set of three out of six Lateral Dorsal Neurons (LN_ds), a 5^{th} s-LN_v that does not express PDF and a selection of ~sixteen dorsal neurons, the DN1s (Figure 1.2). The DN1 cells can be further subdivided into anterior and posterior classes, 2 $DN1_a$ and the remaining $DN1_p$s (Shafer et al., 2006).

All studies of CRY mRNA and protein expression identify the l-LN_vs, several LN_ds, the 5^{th} s-LN_v, the $DN1_a$s, and a pair of the $DN1_p$s alongside widespread expression outside the brain (Figure 1.2)(Emery et al., 2000, Zhao et al., 2003, Klarsfeld et al., 2004, Yoshii et al., 2008, Dissel et al., 2014).

.

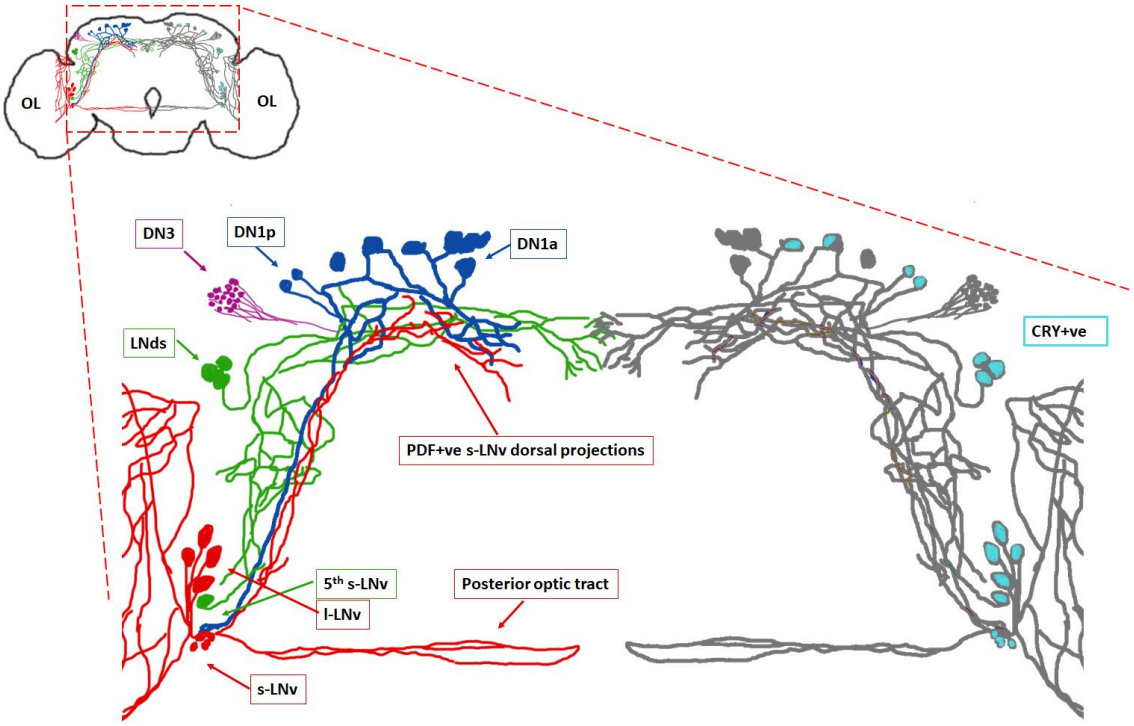

Figure 1.3 - Neuroanatomy of the Drosophila circadian clock network. *Cartoon of clock-neurons within the fly brain, traced from multiple source images. The top left shows the localisation of clock neurons within a whole fly brain, with OL referring to optic lobes. The left half of the cartoon is coloured by neuronal subset type, with PDF neurons, the s-LN$_v$s and l-LN$_v$s labelled in red, the LN$_d$s and 5th s-LN$_v$ labelled in green, DN1s in blue and DN3s in magenta. Not shown are DN2s and LPNs. Whilst all neurons labelled express core clock genes encoding CLK, CYC, PER and TIM, the right half of the diagram identifies CRY-expressing neurons in blue, the LN$_v$s, three of the LN$_d$s and a subset of dorsal neurons.*

The PDF neurons were initially determined as the pace-setting neurons for behavioural rhythms, and loss of PDF expression with the *Pdf*^{01} null mutant led to widespread, though not total, arrhythmicity in freerunning (DD) conditions. Expression of ectopic PDF in *Pdf*^{01} mutants served to rescue this arrhythmia, demonstrating the importance of PDF, and by extension, the importance of the PDF neurons (Renn et al., 1999). However, one study showed CYC expression in the s-LN$_v$s on a *cyc*^{01} background restores molecular rhythms, but does not restore behavioural rhythmicity, such that s-LN$_v$s cannot drive behavioural rhythms alone and demand an interplay between LN$_v$ rhythms and other clock neurons for WT behaviour (Peng et al., 2003). PER expression within the s-LN$_v$s alone was shown to be sufficient for rhythmic behaviour, indicating CYC may have roles

beyond that of a transcriptional activator of PER/TIM (Grima et al., 2004).

Transgenic *Kir2.1 (Potassium channel, inward-rectifying 2.1),* a potassium channel, was used as a tool to conditionally silence PDF cell activity. Potassium ion efflux in response to sodium ion influx is a precursor for action potential formation within neurons, which potentiates changes in Ca^{2+} levels resulting in release of synaptic vesicles and subsequent neuronal communication. On the basis that overexpression of constitutively open potassium channels would hyperpolarise the membrane and "silence" neurons, *Kir2.1* was expressed within PDF cells, resulting in complete behavioural arrhythmia and confirming the importance of signalling from these neurons (Nitabach et al., 2002).

Tetanus toxin, which inhibits neurotransmitter release through cleavage of synaptobrevin, a SNARE-complex component involved in mediating vesicle exocytosis at the pre-synapse, was also expressed in PDF cells. Bizarrely, tetanus expression within PDF cells fails to reduce behavioural rhythmicity, whilst tetanus expression within all clock neurons results in severe arrhythmia, suggesting PDF cell function at the circuit level, presumably including PDF release, is independent of tetanus-sensitive SNARE-mediated exocytosis, whilst this is not the other case for other clock neurons (Sweeney et al., 1995, Kaneko et al., 2000, Blanchardon et al., 2001)

It was found ectopic PDF overexpression in the PDF neurons did not diminish rhythmicity nor cycling in staining intensity at the dorsal termini, whilst aberrant expression in non-clock neurons disrupted behavioural rhythms, likely a result of the conservation of closely-interacting PDF-receptive clock neurons (Helfrich-Förster et al., 2000).

This demonstrates that s-LN_v importance in rhythmicity is not solely due to the molecular properties of the clocks they harbour, but due to the function of PDF. In the absence of PDF, clock neurons remain rhythmic, with normal molecular dynamics of periodic transcription and nuclear entry. However, whilst all molecular clocks remained rhythmic, over time there was a dispersal of phase and damping of rhythms within clock neuron subsets, and desynchrony between rhythms in individual clock cells, indicating PDF in the s-LN_vs is required for controlling synchrony across the clock circuit (Lin et al., 2004).

A sodium channel derived from halophilic bacteria, NaChBac, was transgenically introduced into *Drosophila* as a tool to modify neuronal firing (Nitabach et al., 2006). Ostensibly, NaChBac expression within neurons results in an increased sodium ion influx, depolarising the membrane more rapidly and resulting in more frequent action potentials, therefore increasing vesicle release events. The PDF cells are hypothesised to display rhythmic release of PDF, and potentially other factors, which may be dysregulated by increased electrical activity within the PDF cells (Park et al., 2000). Hyperexcitation of PDF neurons via expression of NaChBac results in an uncoupling of rhythms between clock neurons, and clock neurons cease to oscillate through the same rhythm as the s-LN_vs, demonstrating the role of PDF neuropeptide in synchrony (Nitabach et al., 2006). This phenotype is replicated by aberrant expression of PDF in clock cells, and identifies natural differences in oscillation speed of individual clock neurons, likely a result of subtly different upstream regulating components in each cell type (Helfrich-Förster et al., 2000).

Despite both s-LN_vs and l-LN_vs expressing PDF, these subsets differ in important ways, and the role of PDF in the s-LN_vs is not shared by the l-LN_vs. Whilst other clock neurons display robust rhythms in DD, rhythms in l-LN_vs are weaker, and they do not express detectable rhythmic TIM, hence their ability to synchronise neurons without a functioning clock present seems suspect, and whilst s-LN_vs control freerunning rhythms, it is thought l-LN_vs control aspects of behaviour in variable light-dark (LD) conditions (Yang and Sehgal, 2001, Schlichting et al., 2016).

PDF has been observed to cycle both in LD and DD conditions, but with a much greater amplitude in LD, indicating photic inputs of regulation alongside circadian control (Helfrich-Förster et al., 2000). Several clock cells groups express PDF receptor (PDFR), such as the s-LN_vs, the 5^{th} s-LN_v and the LN_ds (Parisky et al., 2008). It is argued that CLK/CYC-mediated transcription controls PDF expression within the s-LN_vs, as Clk^{Jrk} mutants lack detectable PDF+ve s-LN_vs, and an intermediate phenotype in cyc^{01}. l-LN_vs are PDF+ve in both Clk^{Jrk} and cyc^{01}, indicating cell-type-specific divergences in clock control of the neuropeptide, likely at the transcriptional level via control by genes downstream of CLK/CYC (Park et al, 2000, Mezan et al., 2016).

Dorsal neuron groups possess projections that innervate numerous structures of the fly brain, notably the pars intercerebralis (PI) and mushroom bodies (MB), alongside

connections to other clock cells. l-LN_vs extensively arborise the accessory medulla of the optic lobe. s-LN_vs, LN_ds, DN1s and DN2s additionally arborise the medulla to a minor extent, though the majority of connections, and the most lateral connections arise from the l-LN_vs (Helfrich-Förster et al., 2007).

s-LN_vs notably send processes dorsally, which appear to interact extensively with LN_ds and dorsal neurons and likely form a core part of the clock circuitry, facilitating interactions between s-LN_vs and the other neurons (Kaneko and Hall, 2000, Shafer et al., 2006). Dorsal and lateral neurons are connected via this pathway, which through a network of synaptic connections enables partial dissociation of behavioural rhythms from a sole molecular timekeeper, but as an emergent rhythmic property influenced by multiple molecular oscillators, facilitated by a neural circuit (Helfrich-Förster, 2003). LN_d processes additionally follow this pathway, arborizing into the dorsal protocerebrum and contralaterally to the dorsal neurons (Kaneko and Hall, 2000).

Axonal growths of s-LN_vs are not fixed, however, and exhibit neural plasticity in a circadian manner, exhibiting a higher degree of arborisation during relative daytime and a closed conformation, with fewer projections at night. s-LN_v arborisations were of normal length in per^{01} flies, but with reduced branching and no rhythmic changes in projection or fasciculation state, the amount of axonal branching or bundling of second-order processes (Fernandez et al., 2008). PDF neurons target a range of circuits throughout the day, connecting to $DN1_p$s at all timepoints, and with very limited connections with arborisations of the LN_ds at CT22, prior to subjective dawn, a point of incidentally high PDF secretion (Park et al, 2000). The existence of an LN_d/s-LN_v interaction has implications for the nature of the clock hierarchy, as both subsets are capable of influencing rhythms (Gorostiza et al., 2014).

1.3 - Interactions between clock neurons in generating behavioural rhythmicity

Drosophila are crepuscular, and so activity peaks around dawn and dusk. These peaks are not purely a startle response to light, as flies in LD cycles show an anticipatory response to lights-on and lights-off. This can be separated from normal masking and paradoxical masking, the startle response to lights-on and lights-off respectively, which can show a partially overlapping phenotype to the anticipatory response (Mrosovsky, 1999). Peaks of morning and evening anticipatory activity are under circadian control, yet operate via

different mechanisms and under the control of different clock neurons. This divergence was discovered in *Pdf*^{01} flies, which are majority behaviourally arrhythmic in DD, and the fraction that are rhythmic show a loss of morning anticipatory peak, and a robust, but significantly advanced evening peak, demonstrating this evening part of the rhythm operates with partial independence of PDF (Renn et al., 1999).

Apoptosis of CRY expressing lateral neurons and $DN1_a$s led to complete arrhythmia, indicating that the remaining dorsal neurons are incapable of generating behavioural rhythms alone. Expression of apoptotic HID in CRY+ve PDF-ve cells did not result in arrhythmicity, but a loss of evening anticipatory response, whilst PDF-specific expression of HID, like *Pdf*^{01} lines, lack morning anticipatory peaks. This identifies a PDF+ve specific morning oscillator and CRY+ve, PDF-ve E oscillator (Stoleru et al., 2004, Grima et al., 2004). PDF+ve cells can therefore be termed morning cells (M cells), and CRY+ve LN_ds and the 5th s-LN_v can be termed evening cells (E-cells). The re-emergent l-LN_v rhythm corresponds to that of the DN2s, indicating that the l-LN_vs are controlled independently to the remainder of the lateral neurons and $DN1_a$s (Stoleru et al., 2005).

In DD, s-LN_v-specific expression of PER is sufficient to restore behavioural rhythms on a *per*^{0} background in DD, whilst LN_d and 5th-s-LN_v-specific expression is not, seeming to indicate that the morning oscillator is the dominant driver of freerunning behaviour. However, the LN_v-specific clock possessed only a morning activity peak, and rhythms were required in both neural subsets to drive a subsequent evening peak (Grima et al., 2004). It was also shown through ectopic expression of period shortening kinase SGG in clock neuron subcomponents that when M + E cells had different periodicities, so as to distinguish dominant oscillations in behaviour, behavioural period length was determined by the PDF neurons in DD. In DD, M cells retain behavioural control, but whilst the periodicity is dependent on M cells, the duration of the subjective night is dependent on the E-cells, indicating an E-cell dependent-resetting signal is required for morning onset. In DD, differences in molecular phase emerge and only LN_d, DN1 and DN3 molecular rhythms corresponded to those of the s-LN_vs, which directly arborises these neurons, indicating M-cell synchrony of these neurons across conditions (Stoleru et al., 2005).

SGG expression in the E-cells leads to rhythmicity in constant white light (LL), a condition that usually generates arrhythmicity, though the effectiveness of SGG

overexpression on behaviour, or how SGG might mediate rhythmicity is disputed (Stoleru et al, 2007, Fischer et al, 2016). This is not the case in M cells, and E-cell specific CRY expression was the only subgroup required for full CRY-mediated rhythmicity, indicating that E-cells have a unique molecular network of photoentrainment. In LL, period is dictated by the E-cells, and it is the differing responses to light activation that explain the difference in M cell/E cell dominance in phase setting across LD (Stoleru et al., 2007). In this case, rhythms are present in DN1 cells, and this rhythmicity could also be rescued by PER overexpression in the TIM+ve, PDF-ve cells, supporting to an extent the findings of (Murad et al., 2007, Stoleru et al., 2007).

In white-light LD cycles, PDF expression in the PDF+ve cells is required to control evening peak activity when the visual pathway is the sole source of entrainment, yet not when CRY is the sole source of entrainment, indicating that PDF+ve cells mediate visual information to the rest of the circuit. The four evening oscillator cells cycled PER antiphase to the rest of the circuit in $pdf^{0}cry^{b}$ double mutants, indicating that the molecular rhythmicity of these cells are synchronised by other cells, mediated by PDF signalling (Cusumano et al., 2009). Low levels of CRY have been detected in cry^{b} mutants, indicating that despite several loss of function phenotypes it is not a true null, unlike subsequently produced cry^{01} and cry^{02} (Busza et al., 2004, Dolezelova and Hall., 2007).

s-LN_vs mediate the morning activity peak through interactions with other neurons. Ablation of PDF receptor (PDFR) in clock neuron subsets has defined CRY+ve cells as essential downstream targets, where PDFR function in this group is sufficient for normal M peak, whilst PDFR function in PDF+ve neurons is insufficient (Lear et al., 2009). PDF signalling from l-LN_vs to E cells is similarly required for correct E peak phase (Schichtling et al, 2016). Narrow Abdomen (*na*) is a sodium leak ion channel, which when knocked out leads to a loss of rhythmicity in DD and abolishment of morning and evening activity peaks in LD (Nash et al., 2002, Lear et al., 2005). Rescue of *na* specifically in the $DN1_p$s is sufficient to recover the morning peak, as is the case with PDFR rescue in $DN1_p$s, indicating that morning behaviour, controlled by the s-LN_vs, requires PDF signalling with the DN1s (Zhang et al., 2010a).

Evening oscillations can be driven purely by molecular rhythmicity in four CRY

expressing, PDF –ve cells, the 5th s-LN_v and three LN_ds. These cells are additionally thought to control rhythms in LL (Rieger et al., 2006, Stoleru et al., 2007, Cusumano et al., 2009). Expression of PER in either E cells or M cells in flies with cry^b mutation or ablation of cells using GMR-hid, which ablates the entire eye, led to full behavioural rhythmicity, indicating that both morning and evening cells were capable of driving the behavioural clock when acting as the sole neuronal groups capable of entrainment, and both could achieve this via CRY-dependent and CRY-independent entrainment pathways (Cusumano et al., 2009).

In constant light, the hierarchy of the clock changes such that the 5th s-LN_v and the CRY+ve LN_ds dorsal clock neurons desynchronise from the LN_vs, both displaying distinct molecular rhythmicities. Previous work has identified that cry^b flies exhibit complex behaviour in LL, controlled by 22hr and 25hr cycles of the M cells and E cells respectively (Yoshii et al., 2004, Rieger et al., 2006). That both activity periods occur purely when evening activity is intact indicates that both subsets may control evening activity and contrasts work of (Grima et al., 2004, Stoleru et al., 2004). This desynchrony in molecular rhythm is due to a combination of *cry* loss, and constant input through the visual pathway, but the mechanism accounting for rhythm splitting is unknown (Rieger et al., 2006). Light intensity is also a likely confounding factor in these experiments (Cusumano et al, 2009).

$Pdfr^{5304}cry^b$, comprising both a null PDFR mutant and loss of function CRY mutant, are arrhythmic in DD and in LD lack an evening peak, which contrasts to the loss of morning peak and maintenance of evening peak found in single $Pdfr^{5304}$ mutants, Pdf^{01} lines and lines with apoptosed PDF cells. In these lines, the molecular rhythms of the 5th s-LN_v and the LN_ds were antiphasic to the rest of the clock. As this double mutant line is PDF-independent it is unsurprising that it would lose synchrony of clock cells, and that these neurons remain rhythmic in $Pdfr^{5304}$ single mutants due to entrainment via CRY, yet it is unknown why a CRY-independent mechanism of entrainment would cause antiphase clock gene cycling. In the absence of CRY, the light-degradative component of the pathway is removed and the clock can in theory function in antiphase, yet would require an alternate mechanism of pacing the clock, potentially involving an alternate mechanism of entrainment via the visual pathway, unequally affecting different clock cell subsets on the basis of neuronal connectivity (Zhang et al., 2009, Cusumano et al., 2009). DN2 rhythms are naturally antiphasic, presumably a result of its lack of CRY, where

ectopic CRY expression leads to normal phasic oscillations in DD (Klarsfeld et al., 2004). The mechanism that renders other CRY-ve cells phasic in DD is not understood.

Recent studies have challenged the view of Master clocks controlling morning and evening oscillations, and contend instead that the clock is made from numerous independent oscillators (Yao and Shafer, 2014). Altering cell-specific periodicities via expression of a post-translational modifier showed that larger discrepancies between period length in PDF+ve neurons and other clock cells lead to lowered locomotor rhythmicity, and in certain cases the development of complex periodicities comprising the PDF and non-PDF rhythms. Notably, the prevailing locomotor rhythm in all manipulations stemmed from the neuron subset with a period closest to 24 hr (Yao and Shafer, 2014).

Whilst previous studies have demonstrated the requirement for PDF in synchronising rhythms, recent work demonstrates the requirement of PDF for PDF+ve cells in influencing the clock, in which *Pdfr*^{5304} flies possess a locomotor rhythm corresponding to the molecular rhythm of the non-PDF cells (Helfrich-Förster et al., 2000, Yao and Shafer, 2014). Where PDF signalling influences behaviour, only a subset of clock neurons express PDFR, meaning only part of the central clock can directly respond to PDF signalling, hence the PDF neurons cannot directly control the clock circuit, and must rely on other neuronal signalling mechanisms (Im and Taghert, 2010, Yao and Shafer, 2014). PDFR+ve LN_ds and the 5th s-LN_v can be influenced by PDF neurons, yet can also synchronised with the molecular clock of the two PDFR-ve LN_ds. Neuropeptides other than PDF have been demonstated to mediate s-LN_v effects on independent clock cell subsets, though synchronisation of molecular oscillators with other neuropeptides has yet do be demonstrated (Yao and Shafer, 2014). LN_vs are glycinergic and glycine loss effects electrical properties of the DN1ps and period length (Frenkel et al., 2017). sNPF similarly can influence the phase of LN_d and $DN1_a$ Ca^{2+} rhythms, which are independent of PDF signalling (Liang et al, 2016, Liang et al, 2017, Frenkel et al, 2017). Upon ligand binding of either PDF or DH31, another neuropeptide, PDFR, a G-protein coupled receptor, activates a signalling cascade, ultimately activating cAMP, which may explain the ability of PDF to phase-shift Ca^{2+} rhythms in downstream neurons (Duvall and Taghert, 2012, Goda et al., 2016). The manner in which PDF signalling can shift molecular oscillators in downstream neurons, however, remains unknown.

The functions of this diverse group of neurons have only been partially characterised, and in time further developments of the core clock will be realised. However, these core clock neurons are not the only clock bearing cells in the fly, and numerous other tissues, such as wings, legs, testes, compound eye, malpighian tubules, oenocytes, antennae and epidermis possess endogenous clocks, known as peripheral clocks (Plautz et al., 1997, Giebultowicz, 2001, Levine et al., 2002, Tanoue et al., 2004).

Behavioural rhythms are solely mediated by the neuronal clock circuit, which, in addition, can entrain and regulate timing in certain peripheral clocks, through cells expressing the full molecular complement of the clock. These clocks can operate in lieu of a functional central clock through cell-autonomous expression of CRY (Emery et al., 2000). Not only are many peripheral clocks independent, but in certain cases the peripheral clocks cycle with an earlier phase to central clocks, indicating a fundamental molecular difference; potential upstream regulatory mechanisms in the peripheral clocks not conserved with the central clock (Giebultowicz, 2001).

Induction of CLK expression in non-clock bearing neurons, via the *cry24-GAL4* driver, which targets regions of the ellipsoid body and several neurons throughout the dorsal protocerebrum, in addition to the CRY+ve clock neurons, led to transcription of *per, tim* and *cry* and ultimately, cycling clock components in some of the non-clock bearing neurons targeted by the driver, the creation of ectopic neural clocks. In females with ectopic clocks in three brain regions, behavioural profiles were altered, with a significantly shorter period and non-existent evening peak, a more intense phenotype than CLK-overexpression in the CRY+ve neurons, which have a weakened, though still present evening peak. Ectopic neural clocks, proximal to the central clock circuit may be able to innervate this circuit to regulate period length (Zhao et al., 2003).

Ectopic clocks could not be induced solely by other clock genes, and although these *Clk*-driven clocks were long-lived, with a loss of *Clk* the molecular rhythmicity damped after a couple of weeks, indicating that transgenic overexpression of *Clk* was not required, but boosted rhythmicity, a contrast to *Clk* overexpression lines in central clocks (Kilman and Allada, 2009). CYC, and presumably CLK/CYC dimer is required for ectopic clock formation. That these non-clock tissues require CYC to form clocks indicates either that *cyc* is somehow expressed in these non-clock cells, unknown due to a paucity of CYC

protein mapping, ectopic *Clk* can induce *cyc* expression in these cells by a currently unknown mechanism, or *cyc*-mediated rhythmicity in the nearby central clock is required for conferring rhythmicity to the ectopic clock (Kilman and Allada, 2009). Whilst central clock cells express CLK/CYC during embryonic and larval stages, CLK/CYC is undetectable in other tissues until late metamorphosis, potentially the result of a developmental repressor, though the identity of this repressor, it's mechanism of action, or the range of cells it is expressed in, are unknown. Bantam is a miRNA previously implicated in development through control of cell proliferation and apoptosis which has been shown to be under circadian regulation and limit development of ectopic PDF cells, and it is likely a CLK/CYC developmental repressor may act in a related post-transcriptional fashion (Brennecke et al., 2003, Zhao et al., 2003, Kilman and Allada, 2009, Kadener et al., 2009, Lerner et al., 2015).

The Rosbash and Ceriani groups have previously identified a divergence in CRY entrainment in the morning and evening cells, though failed to provide a mechanism (Stoleru et al., 2007). CRY-dependent TIM degradation has kinetic constraints, requiring approximately 120 minutes to become undetectable in response to a continued light pulse. cry^b flies failed to entrain to phase shifts of more than two-hours, revealing a mechanistic limitation to CRY-independent light response. Molecular oscillations of all clock cells bar the $DN1_p$s shifted phase to the same extent, whilst in cry^b flies, only the-LN_vs, the 5th-s-LN_v and the LN_ds were oscillating, and only the 5^{th}-LN_v and the LN_ds, which together control evening peak, shifted to phase. It therefore seems that the E cells are the site of CRY-independent light input. cry^b Pdf^{01} flies are less sensitive to light and 5^{th}-LN_v and LN_d molecular rhythms are damped in LD cycles, demonstrating that despite the importance of the E cells in entrainment, PDF-dependent signalling of visual information via the PDF+ve neurons appears a substantive input of CRY-independent E cell phase shifting (Yoshii et al., 2015).

Drosophila cryptochrome is predominantly sensitive to blue-light, wavelengths of less than 500nm, with an optimum peak at 450nm, yet *Drosophila* possess visual photoreceptors capable of responding to different wavelengths of light that allow CRY-independent pathways of input (Yamaguchi et al., 2010). The eight classes of rhodopsins in the eye are capable of detecting light from UV wavelengths to green spectra, with much lower sensitivity to wavelengths above 620 nm (Yamaguchi et al., 2010). However, whilst *Drosophila* do not respond in decision-making or phototaxic assays to red light,

they do readily entrain (Heisenberg, 1977). *norpA* mutants, which lack canonical visual transduction and are functionally blind, are unresponsive to red light, indicating a visual input, as were *rh1 rh6* double mutants, indicating that these rhodopsins mediate red light entrainment (Hanai et al., 2008).

Rhodopsin 6 is the only red-light sensitive photopigment in larvae, and exposure to constant red light in larvae disrupts PER oscillations in the LN_v, but no other clock neurons, a rhythmicity that can be regained by loss of RH6. This demonstrates that the LN_v responds to Red-light entrainment and is the sole larval clock neural subset that directly connects to the visual system (Klarsfeld et al., 2011). The consequence of LN_v-specific loss of molecular oscillations through development on adult behavioural rhythms has yet to be tested.

In adults, the Hofbauer-Buchner eyelet, a photosensitive organ, is connected to the LN_vs and is an important component for circadian entrainment (Veleri et al., 2007). However, red-light entrainment is partially PDF independent, so if the pathway between white light and the LN_vs is shared for red light entrainment, PDF independent pathways must be capable of synchronising clock cells, or another pathway may exist that connects clock neurons to the visual photoreceptors. However, Pdf^{01} flies have an altered waveform from wildtype (wt) in red light/dark cycles, indicating the neuropeptide continues to play a role in red-light behaviours (Cusumano et al., 2009).

The role of l-LN_v arbors, and arbors from several other clock neuron subsets, which are extensive throughout the optic lobe are less well understood (Helfrich-Förster, 2004). The larval optic nerve interacts with clock neurons from an embryonic timepoint and LN_vs are located near to the medulla and extensively arborise them, indicating a clear link between light-input and the clock neural circuit (Malpel et al., 2002). Both PDF-expressing cells, the 5^{th} PDF-ve LN_v and ITP+ve (Ion Transport Peptide) LN_d innervate the medulla, indicating that there are potentially multiple pathways for the clock to interact with the visual system, though these are poorly understood (Johard et al., 2009, Schubert et al, 2018).

1.4 – Output pathways: Connecting the molecular clock to rhythmic phenotypes

The most studied circadian output is the rest-activity rhythm, and thus work on the

complete output pathways for this is most advanced. GRASP analysis, studying reconsitution of pre- and post-synapse-tethered GFP fragments between known neural subsets, has been used to identify essential output neurons interacting with the core clock system (Feinberg et al., 2008). Dorsal projections of LN_vs were found to interact with DN1 through this system. Repeating the GRASP analysis for the DN1s, it was found that DN1 was able to interact with neurons throughout the Pars Intercerebralis (PI). In conjunction, DH44 expression, a neuropeptide, was found to be limited in a subset of six PI neurons interacting with DN1. DH44 knockdown leads to behavioural arrhythmia, confirming this route as a required output pathway for locomotor rhythms (Cavanaugh et al., 2014). Downstream of the DH44+ve cells are Hugin+ve neurons which project to the ventral nerve cord, and affecting Hugin cell function also affects rhythms, though arguably not sufficiently so to be considered core to behavioural output (King et al., 2017). Loss of Leucokinin neuropeptide or receptor additionally reduces behavioural rhythmicity, and Leucokinin+ve dendrites have been shown to arborise the dorsal brain and respond directly to changes in PDF cell firing (Cavey et al., 2016).

However, no rhythmic property contributing to behavioural rhythms has been identified as transducable through the DN1s, and any actual output role is assumed. It can be safely concluded that several neuronal cell groups in communication with the clock circuit have more general roles in mediating rest or arousal behaviour, yet the manipulations of these cells which lead to arrhythmia are not necessarily disrupting information transfer in which these cells are intermediaries of rhythmic information, but could reflect dominant control over behaviour elsewhere.

A range of clock outputs have been identified and the neurological pathways linking behaviour to the central clock are being elucidated. However, to focus purely on anatomical outputs ignores the extensive roles of the clock in regulating transcription, and numerous genes are under circadian regulation.

Modulation of any gene that alters behavioural rhythms without influencing molecular rhythmicity of clock genes is assumed to function downstream, in an output pathway, and impact rhythmic strength, but not period length, so a great number of output genes have been identified, though their proximity to the clock and their role in a complete mechanism for circadian output is not known.

Fly heads contain many transcripts with robust circadian oscillations, with peaks at multiple phases of the oscillation, revealing further levels of regulation for these output genes (Claridge-Chang et al., 2001, McDonald and Rosbach, 2001, Lin et al., 2002, Ceriani et al., 2002, Ueda et al., 2002, Wijnen and Young, 2006, Keegan et al., 2007, Kula-Eversole et al., 2010, Nagoshi et al., 2010, Hughes et al., 2012).

Multiple transcripts have stable expression levels, and show levels of oscillation purely when associated with the ribosome, indicating circadian intervention occurs in regulating translation, and that core elements of this machinery may be under circadian regulation (Huang et al., 2013). Multiple genes that do not oscillate at the mRNA level are found to oscillate in circadian phase as proteins, which may be partially explained by these translational mechanisms. Circadian proteomic work, whilst extensive in mouse models has not been well studied in *Drosophila*. In mammals, it has been determined that protein-specific oscillations stem from a circadian regulation of ribosome biosynthesis and polyadenylation, which may also be the case in *Drosophila* (Kojima et al., 2012, Jouffe et al., 2013, Price, 2014).

The role of PDP1 has been briefly described earlier, as a CLK/CYC target and potential transcriptional activator of *Clk*. The exact role of PDP1 is controversial, and whilst it is known to regulate output through rest-activity cycles, the point at which it acts is not fully established.

Pdp1ε RNAi results in ablated behavioural rhythms. PDP1ε protein is constitutively low in Clk^{Jrk} and cyc^{01} flies, and high in per^{01} and tim^{01}, indicating that PDP1ε is regulated by the clock. That Clk^{Jrk} and cyc^{01} flies have high levels of *Clk* mRNA remains problematic, as PDP1 levels in these mutants are low and the (Cyran et al., 2003) model would favour low *Clk* mRNA in response to low *Pdp1* levels. Neither overexpression nor knockdown of *Pdp1* in clock cells affects oscillations of core clock genes and as such the potential of PDP1-binding upstream of *Clk* demonstrated in-vitro either does not occur in-vivo, or is negligible to affecting clock rhythmicity (Benito et al., 2007). Expression of a dominant-negative version of PDP1 failed to alter molecular rhythmicity, supporting the (Benito et al., 2007) finding, yet displayed neuroanatomical defects, as did knockdown with a novel *Pdp1* RNAi line, suggesting additional functions of PDP1 (Lim et al., 2007).

This finding of PDP1 acting purely downstream of the core clock was contrasted by

work on a new PDP1 mutant, specific to the ε isoform, which demonstrated behavioural arrhythmia and showed a reduction of CLK expression in DD, in the s-LN_vs and the peripheral clocks, supporting the role of PDP1 in regulating CLK. Expression of *Clk* in *Pdp1*^{3135} mutants restored molecular oscillations, but not behavioural rhythms, confirming the role of *Pdp1* as both an output gene, and a regulator of the core molecular oscillation (Zheng et al., 2009). Unlike core clock mutants, *Pdp1* isoform specific mutant s-LN_vs have been shown to lack PDF, despite PDF+ve l-LN_vs, suggesting a secondary output function (Zheng et al., 2009). In support of this, ectopic *Clk* expression in *Pdp1*^{3135} mutants rescued molecular oscillaitons with the *cry-gal4* but not *pdf-gal4* driver, suggesting PDP1 is involved in PDF transcriptional control. Clock-cell specific loss of VRI comparably results in a loss of s-LN_v-specific PDF, at the mRNA level, and a loss of rhythmic fasciculation of second order s-LN_v processes (Gunawardhana and Hardin, 2017).

Knockdown of MEF2 and dominant-negative expression lead to behavioural arrhythmia and loss of PER expression in DD. Overexpression results in shorter period length, a slight delay in PER expression, resulting in complete desynchronisation by the 8th day of freerunning, when wt oscillations would remain synchronised. However, alteration of MEF2 expression levels did not affect LN_v morphology through development (Blanchard et al., 2010). MEF2 has additional circadian roles, present in the nucleus of LN_vs, LN_ds and the DNs. MEF2 is expressed rhythmically, with enriched expression in the PDF-neurons at night and expression is ablated in clock gene mutants, indicating a function downstream of the core clock (Sivachenko et al., 2013).

Whilst it has been shown that MEF2 does not affect development of the core s-LN_v cells, it is required for daily neuronal remodelling of LN_v projections. MEF2 knockdown leads to persistent axonal fasciculation, and overexpression leads to persistent axonal defasciculation, whilst wt flies exhibit rhythmic switching between these axonal states (Fernandez et al., 2008, Sivachenko et al., 2013). A pulldown of MEF2 targets in *Drosophila* heads identified numerous targets involved in axonal changes, including FAS2, a cell adhesion molecule rhythmically expressed in LN_vs, which had previously been shown to be involved in control of neuronal morphology. *Fas2* expression is negatively regulated by MEF2 and ectopic expression can alleviate the defasciculation phenotype of MEF2 overexpression. Knockdown of *Clk* in PDF neurons, which removes rhythms in PDF arbor complexity, can regain a wild-type phenotype by induced MEF2

expression, demonstrating MEF2 as the sole circadian output for this process (Sivachenko et al., 2013). FAS2 overexpression can inhibit axonal pruning through excessive cell adhesion, so a similar mechanism may prevent remodelling (Bornstein et al., 2015).

The lack of PER in *Mef2*-RNAi clock neurons indicates a potential mechanism exists where MEF2 is capable of feeding back onto the core clock. Overexpression of P38KB, the kinase that phosphorylates PER to mediate nuclear translocation, can ameliorate the arrhythmic phenotype of *Mef2* knockdown (Vrailas-Mortimer et al., 2014, Dusik et al., 2014).

PDP1 and MEF2 are BZip-containing transcription factors with related developmental roles, and they act synergistically as transcriptional activators, yet this requires the second exon of *Pdp1* not present in *Pdp1ε,* so a commonality of function cannot be seen (Lin and Storti, 1997, Reddy et al., 2000). *Pdp1* and *Mef2* are complex genes, which serves roles in the clock output pathways, which may also feed back into regulating the mechanism of the core clock. *Mef2* RNAi flies have disrupted molecular rhythms, indicating potential feedback to the core molecular clock (Blanchard et al., 2010).

Any experimental work studying the genetic control of rest/activity cycles relies on these unknown output pathways as a conduit to linking genotype and behaviour, and thus, an understanding of these pathways will lead to an understanding of the observed behavioural phenotypes in developmental circadian mutants.

1.5 - Clock output rhythms in sleep and nocturnality

The most obvious behavioural rhythm, of rest-activity cycles, highlights the crepuscular nature of *Drosophila*, with activity peaks at dawn and dusk. The majority of wt fly activity is in the presence of light, and in darkness there is comparably little activity. *Drosophila* undergo bouts of lethargy, with diminished responsiveness to stimuli, analogous to mammalian sleep, and the bulk of this occurs at night (Shaw et al., 2002). Like in humans, sleep is theorised to be governed by an interaction between the circadian clock, which initiates sleep on a circadian basis, and the sleep homeostat, which increases sleep demand as duration of wakefulness increases (Figure 5)(Borbely and Achermann, 1999).

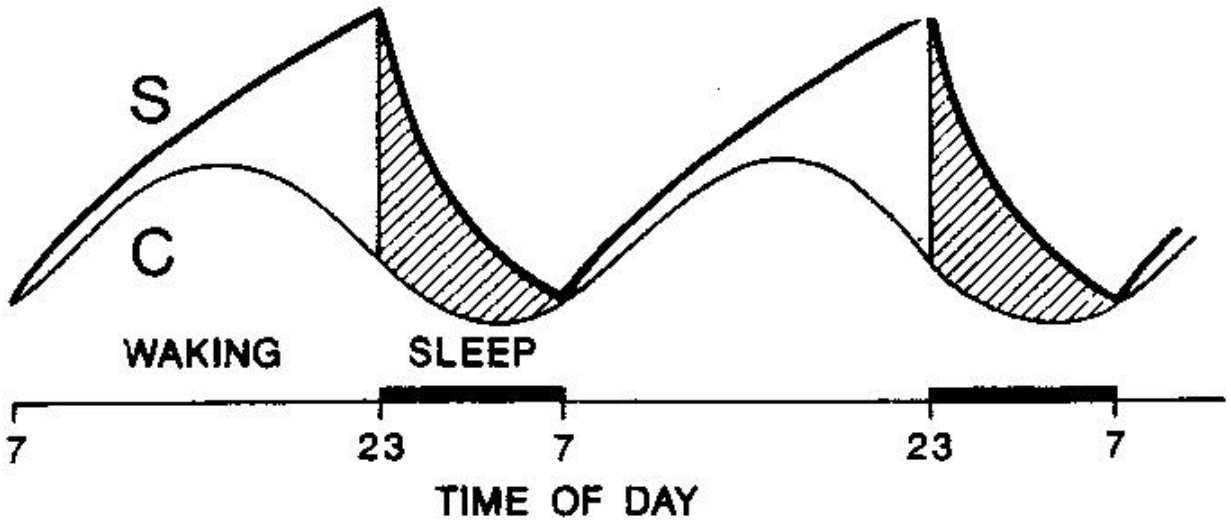

Figure 1.4 - Borbely-Achermann model of sleep*. Taken from (Borbely and Achermann, 1999), cartoon of the sleep homeostat model, demonstrating co-regulation by the circadian clock and the sleep homeostat. Sleep need progressively increases through wakefulness, which can be offset by circadian-controlled wake-promoting factors.*

Despite their crepuscular nature, *D. melanogaster* are mostly active during the light phase of a 12:12 hr LD cycle, dependent on temperature, and in freerunning conditions they maintain subjective diurnality. Intriguingly, Clk^{Jrk} flies and cyc^{01} flies, with mutations affecting the positive arm of the molecular clock are considered nocturnal in LD cycles, with greater overall activity during the dark phase. tim^{01} and per^{01} flies on the other hand remain active in the light, which demonstrates a potential competitive interaction between the two arms (Lee et al., 2013). That per^{01}/tim^{01} and Clk^{Jrk}/cyc^{01} are all arrhythmic but display differing activity patterns suggest a mechanism of action involving clock genes, yet independent from their 24hr oscillation in expression, potentially related to the arrest state of the clock.

A mechanism has been proposed to explain nocturnality in Clk^{Jrk} flies. l-LN_vs are required for light-mediated arousal and startle response and their firing rate is highest during the day, yet hyperexcitation by expression of *NaChBac* led to a reversal of this pattern, a higher nocturnal firing rate and a switch to nocturnal behaviour (Sheeba et al.,

2008b). CRY expression is required for nocturnal activity, and cry^{b}, cry^{01} and cry^{02} flies lack lights-off masking activity. Expression of CRY in l-LN_v specific drivers induced greater nocturnality, pinpointing the phenotype to light-mediated arousal determining cells. However, Clk^{Jrk} cry^{02} double mutant lacks the nocturnal phenotype of Clk^{Jrk}, indicating that this phenotype is dependent on CRY levels (Kumar et al., 2012).

fmn, a dopamine transporter mutant also shows increased nocturnality in LD, and has increased CRY levels. Clk^{Jrk} flies have increased levels of TH (*tyrosine hydroxylase*), a dopamine-synthesis enzyme. *fmn* and Clk^{Jrk} heterozygotes show diurnal activity patterns, and a *fmn*/Clk^{Jrk} heterozygote shows strong nocturnal activity, showing that dopamine signalling and CLK/CYC mutually regulate nocturnality. Loss of dopamine processing genes or *cyc* leads to a reduced startle response, indicating that CRY and dopamine may lower the baseline response for activity at night, prompting more activity with less stimuli (Kumar et al., 2012). Lower daytime activity may be due to an increased sleep debt or a reduction in CRY levels. This mechanism is intriguing as it proposes a function for the CLK/CYC dimer in the absence of circadian rhythms and an independent functional role. Potentially, this dimer regulates multiple processes, including clock cell development.

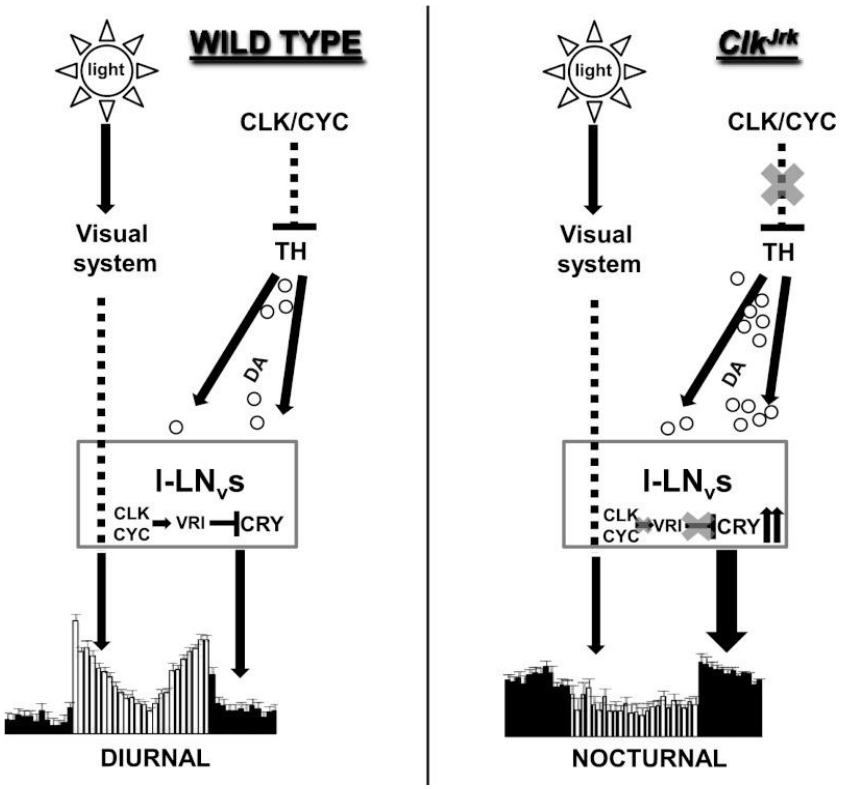

Figure 1.5 - Proposed mechanism of nocturnality following loss of Clock or cycle. *Taken from (Kumar et al., 2012), cartoon of a proposed CLK/CYC-dependent regulation of nocturnal activity via dopaminergic signalling and CRY levels. CLK/CYC is presumed to limit TH synthesis and dopaminergic cell activity by and unknown mechanism, whilst repressing CRY within the large lateral ventral neurons (l-LN$_v$s).Upregulation of CRY presumably represses activity during the day, whilst increased dopaminergic signalling promotes hyperactivity at night.*

Larvae with constitutively high CLK/CYC levels decrease LN$_v$ excitability, the larval light-responsive neurons, whilst increasing DN1 excitability. High CLK/CYC levels at lights-off is repressive to LN$_v$s, and results in a lowered light-avoidance response compared to other times of the day (Collins et al., 2012). This finding may support those of the Sehgal lab, as in both adult and larval systems CLK/CYC is a dusk-specific repressor of light-mediated arousal, and nocturnality results from a loss of CLK/CYC dimer at this stage (Collins et al., 2012, Kumar et al., 2012). *Clk^{Jrk}* and *cyc^{01}* mutant larvae have increased light avoidance activity (Collins et al., 2012). Increased dopamine activity through addition of bromocriptine, an agonist of dopamine receptor lead to increased nocturnal activity in all flies with the exception of *Clk^{Jrk}*, supporting this model (Lee et al., 2013).

A combination of poorly studied dopaminergic pathways, and feedback from the circadian clock appear to regulate this nocturnality-diurnality switching. The relationship between nocturnality and higher overall activity levels seems to indicate the sleep homeostat may regulate this pathway. Indeed, dopamine signalling has been heavily implicated in regulating wakefulness, though whether known dopaminergic neurons involved in sleep regulation also regulate nocturnality is unknown.

Arousal in *Drosophila* is controlled via dopamine signalling (Andretic et al., 2005). Activation of dopaminergic neurons leads to disturbances in sleep levels, and specifically activation of a pair of neurons projecting into the dorsal fan-shaped body (Liu et al., 2012).

Need for sleep is highest during development, where freshly eclosed flies sleep for longer with a higher arousal threshold. Sleep deprivation through dopaminergic hyperexcitation and external stimuli results in impaired adult behaviour, with disrupted

courtship, resulting from a malformation of the VA1v part of the dorsal fan-shaped body which controls courtship behaviours (Kayser et al., 2014). Thus, sleep at certain developmental timepoints is a determinant of behaviour. Early sleep deprivation additionally resulted in reduced aversive phototaxic behaviour, whereas sleep deprivation in mature flies (> 6 days old), did not differ from controls (Kayser et al., 2014). That dopaminergic pathways seem heavily involved in sleep supports the idea that the requirement of dopamine signalling in nocturnality is related to sleep.

Clk^{Jrk} and cyc^{01} flies have lower absolute levels of sleep (Shaw et al., 2002). CLK appears necessary for normal sleep patterns, and inhibition of CLK/CYC transcriptional activity via CLKGR, a CLK-glutocorticoid-receptor fusion which serendipitously decreases amplitude of rhythmic gene expression at the transcriptomic level, leads to more numerous sleep bouts during the dark phase of LD cycles, but of decreased duration, indicating that CLK/CYC may regulate the threshold for wakefulness, an additional function that may complement that in regulating CRY-mediated nocturnality (Kumar et al., 2012, Weiss et al., 2014). Clk^{Jrk} and cyc^{01} daytime sleep levels are lower than those of wt flies, but the difference is exaggerated at night, in which Clk^{Jrk} sleep is less than during the daytime. Clk^{Jrk} and cyc^{01} also have an increased sleep latency, resultant on downregulation of l-LN_v-specific WAKE in these mutants (Liu et al., 2014). This indicates an l-LN_v-specific mechanism regulating response to stimuli, which is reduced in both cyc^{01} and Clk^{Jrk}, and a potential link between sleep and nocturnality.

The regulation of the dynamics of rest-activity within a circadian period is poorly understood, yet it is known that core clock genes and the central clock circuit are involved in establishing this activity. Furthermore, it appears that diurnality-nocturnality switching is dependent on the presence of a CLK/CYC dimer and independent of rhythms, making this system ideal for the study of independent roles of CLK/CYC. Few other examples of CLK/CYC functions outside of maintaining rhythms have been recorded (Ito et al., 2008, Goda et al., 2011).

1.6 – Involvement of circadian rhythms in developmental timing in *Drosophila*

Drosophila development is a conserved process, consisting of several major stages. At 25ºC, the *Drosophila* embryo develops within twenty-four hours to form a larva, with an intact nervous system. The larvae undergoes several hormonally-controlled molts

commensurate with increases in body size, and the final molt, to become a third-instar larvae, is associated with a change in behaviour from feeding and burrowing, to seeking a pupation site, which occurs after approximately five days at 25ºC. Most larval structures, with the exception of the nervous system, are degraded during pupation, and several epithelial structures containing undifferentiated cells, termed imaginal discs, then develop to form many of the organs of the mature fly, in standardised stages (Bainbridge and Bownes., 1981). At 25ºC, mature flies eclose from the pupal case, approximately ten days after egg-laying.

Developmental timing is a tightly controlled process that pervades and regulates almost all processes in development, yet is mostly independent of circadian regulation. In flies, eclosion preferentially occurs at dawn, an event that occurs both under freerunning, LD and natural conditions and even when metamorphic development has been completed many hours prior, so is determined by circadian rhythms, in this case from the peripheral clock of the prothoracic gland (Myers et al., 2003).

That rhythms are temperature-compensated whilst development is not suggests an intrinsic disconnect between the two processes, whereby flies raised at different temperatures might show altered timing of circadian-influenced and circadian-independent developmental events, realised in developmental defects. Whilst this is not apparent, several studies have implicated molecular clock speed in developmental timing, though this may occur at checkpoints in which development can be delayed, such as the induction of pupation or eclosion (Kyriacou et al., 1990, Paranjpe et al., 2005, Yadav et al., 2014).

It has not been demonstrated that environmental changes in development can affect adult behavioural rhythms, but as mentioned in sections above, adult rhythms are responsive to environmental changes, and regulated by stress pathways (Kumar et al., 2014). Eclosion rhythm can be disrupted by hypoxia (Pittendrigh, 1954), though this is likely not due to an effect on the molecular clock.

1.7 - Development of circadian rhythms in *Drosophila*

Flies reared from egg-laying in constant darkness have functioning clocks in adulthood, though these are asynchronous, indicating that entrainment is not necessary for the clock

to function, and the phase of each clock is set by the completion of a developmental event in the absence of entrainment cues (Sehgal et al., 1992). Circadian rhythms are therefore not heritable through maternal effect, and as the central clock is neuronally based, the clock is non-functional until a base level of molecular and anatomical clock components are present.

The initial larval clock circuit is much reduced, consisting of eighteen clock neurons, the PDF+ve s-LN_vs and a pair of each the $DN1_a$s and DN2s. Input is controlled by CRY and the Bolwig organs, precursor groups of a dozen photoreceptors that form the extraretinal eyelet during metamorphosis (Kaneko and Hall, 2000). Larval DN1 processes connect to the DN2s, which associate with the presynaptic axons of the s-LN_vs and connect across the bilateral divide to the other DN2 pair, unifying the two hemispheres (Helfrich-Förster, 2003). s-LN_vs additionally arborise the precursor to the aMe, the optic neuropil (Helfrich-Förster, 1997).

In Clk^{Jrk}, LN_vs are undetectable in larvae, demonstrating a requirement for CLK in PDF and clock gene expression in these cells, as in adulthood (Park et al., 2000, Houl et al., 2008).

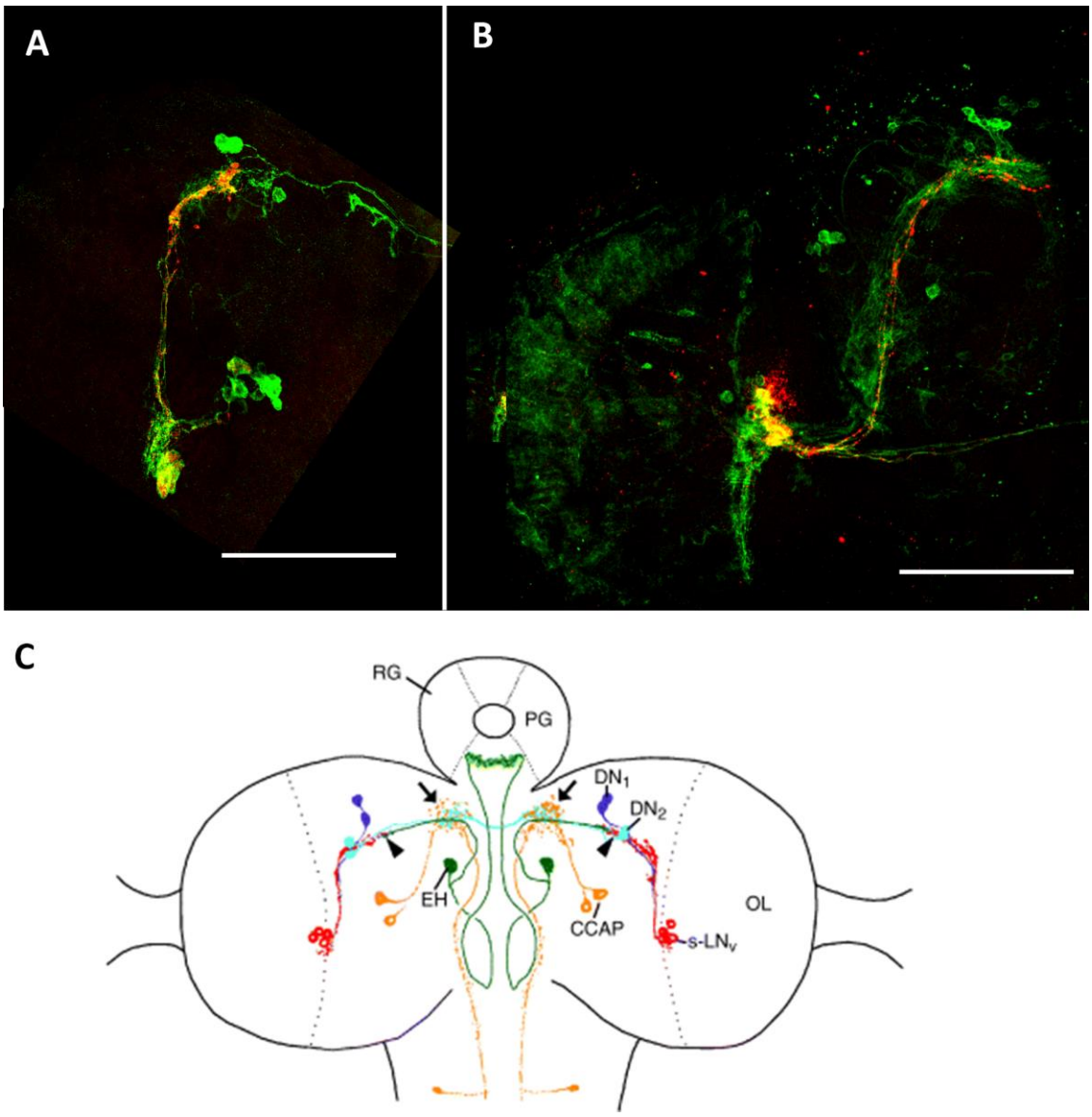

Figure 1.6 - Diagram of the larval neural clock circuit. *Panel A and B show a single hemisphere of the circadian clock circuit in the third-instar larva and adult respectively, with PDF labelled in red and membrane-tagged GFP in green, expressed in all clock cells. Scale bars in the bottom right correspond to 100μm. Panel C is reproduced from (Helfrich-Förster, 2004). PDF neurons, shown in red, cluster laterally and send axonal projections dorsally to interact with other clock cell groups, the DN1s (Dark blue) and the DN2s (Light blue), which similarly send projections near to neurons involved in steroid hormone regulation (Green and Yellow). The basic location of PDF neurons and their interaction with dorsal clock neurons may be conserved through development. OL = Optic Lobe, PG = Prothoracic gland. RG =Ring gland, EH =eclosion-hormone expressing neuron, CCAP = Crustacean Cardioactive peptide*

During metamorphosis, many structures of the larvae are extensively remodelled,

including the nervous system. The gross morphology of the brain remains similar, though a growth of the optic lobes and the differentiation of the prothoracic gland and subesophageal ganglia are observed, the overall presence and distribution of cell bodies remains similar. Within the first 12 hours of pupal formation, axons in the mushroom body decrease by 40% through axon pruning (Technau and Heisenberg, 1982). In the Peripheral nervous system (PNS), most observed structures demonstrate either an axonal retraction or a degradation of axonal and dendritic processes, initially minor processes 12 hrs post-pupariam formation (PPF), but ultimately large numbers of axons are pruned (Kuo et al., 2005). From 24 hours PPF, the re-emergence of axons is observable. These reconnect within a morphologically altered fly, and so the targets of motoneurons differ significantly, such that this PNS-wide loss of processes appears necessary to re-innervate the adult fly (Truman, 1990). This pruning occurs on a smaller scale throughout the fly brain, notably in the mushroom bodies and olfactory projection neurons (Watts et al., 2003, Kuo et al., 2005, Yaniv et al., 2012)

s-LN_v axonal pruning has not been observed, though molecular evidence exists that suggest it may occur, and re-extension may be dependent upon synaptic feedback (Helfrich-Förster, 1997, Gorostiza and Ceriani, 2013). In systems where remodelling does occur, projection patterning remains intact through metamorphosis, even if pre or post-synaptic partners are ablated, indicating a relative independence from synaptic signalling and network states on developmental circuit refinement in *Drosophila*, whilst this feature is an established part of mammalian neuronal refinement (Berdnik et al., 2006, Tessier, 2009). The altered composition of the clock circuit through development would favour s-LN_v remodelling to an extent, though this has not been shown in relation to changing post-synaptic targets.

PER expression is visible in larval and adult flies, but in early pupal stages PER expression was not identifiable (Kaneko, 1997), though the pedurance of phasic information from embryonic stages necessitates a continued CNS oscillation (Sehgal et al, 1992, Kaneko et al, 2000). *tim*-promotor-driven GFP expression could also be identified throughout puparium development. Initially this expression pattern was identical between larval and pupal brains, however by 9 hours post puparium formation, weak GFP expression was seen in cells nearby the known larval clock neuron clusters, first in locations corresponding to that of DN3 neurons and by 22 hours the cell bodies of clock gene expressing-neurons was identical to that of adults (Kaneko and Hall, 2000).

This demonstrates that the development of the cells composing the mature clock circuit is completed in early pupal stages, yet their molecular rhythms, axonal projections and mechanisms of synchronisation are not fully understood.

A further study identified large cell bodies in a location analogous to lateral neurons in late larval stage brains that expressed *tim*-driven GFP, but were not immunoreactive to clock protein or PDF antibodies. By 24 hours PPF these cells had extended processes into the aME and towards the dorsal neurons, and by 48 hours had clearly diverged into the l-LN_v subsets, showing that these neurons had a common precursor, though the pathway leading to their induction is unknown (Helfrich-Förster, 1997, Helfrich-Förster et al., 2007).

A more recent study utilised CLK-GFP and CYC-GFP, to study the timing of the development of clock cells, and the lapse between CLK/CYC expression, and rhythmic clock formation, In contrast to previous data, all clock cells, with the exception of the l-LN_vs, were present in 3rd-instar larvae, expressing CLK and CYC. Several DN1s, though not the full adult complement, appeared throughout 3rd-instar larvae brains, presumably extending into pupal stages. These cells had only been observed in pupae previously, by PER and seemingly less sensitive CLK antibody, demonstrating a lag between expression of CLK/CYC and rhythmic PER/TIM expression (Kaneko, 1997, Houl et al., 2008, Liu et al., 2015).

It is expected that CLK/CYC precedes PER/TIM expression, but a gulf of several days indicates that CLK/CYC alone is not sufficient to form a rhythmic clock, and additional cofactors, not expressed in 3rd-instar larvae, are required. This also does not demonstrate late-stage clock neuron genesis occurs in 3rd-instar larvae, merely that they do not express CLK/CYC prior to that (Liu et al., 2015).

The conditions required for triggering formation of a molecular oscillation within a clock cell are unknown, but as the majority of clock neurons only possess detectable oscillations upon pupation, it must be considered that a molecular signal during embryogenesis and during metamorphosis governs the start of daily timekeeping by these clocks. Ectopic *Clk* expression is sufficient to induce the formation of ectopic brain clocks, though their developmental emergence was not characterised (Zhao et al., 2003). When *Clk* is not subject to post-transcriptional modification: a difference occurs in the

development of the pacemaker neurons, with additional PDF-expressing LN_vs temporarily forming in *ClkSV40* flies during metamorphosis, which contain a control 3'UTR which decouples CLK from it's usual post-transcriptional regulation. These extra s-LN_vs were not present in larval flies, identifying a potential metamorphic role for CLK in clock cell neurogenesis (Lerner et al., 2015).

1.8 - Developmental requirements for CLK/CYC in behavioural rhythmicity

A conditional restoration of CYC specifically within adulthood of cyc^{01} flies could not restore behavioural rhythms, whilst expression of CYC throughout development could. Flies that conditionally overexpress PER in pupae also lose adult behavioural rhythms and show less rhythmic PER expression in adulthood (Goda et al., 2011). However, per^{01} flies do not possess this developmental requirement, as reintroduction of PER to adult per^{01} flies is sufficient to restore rhythms. PER overexpression results in low levels of functional CLK/CYC, whilst per^{01} flies have high levels of CLK/CYC, reflecting two separate arrest states of the clock. Thus, reduced CLK/CYC within clock neurons during development results in behavioural arrhythmia (Goda et al., 2011).

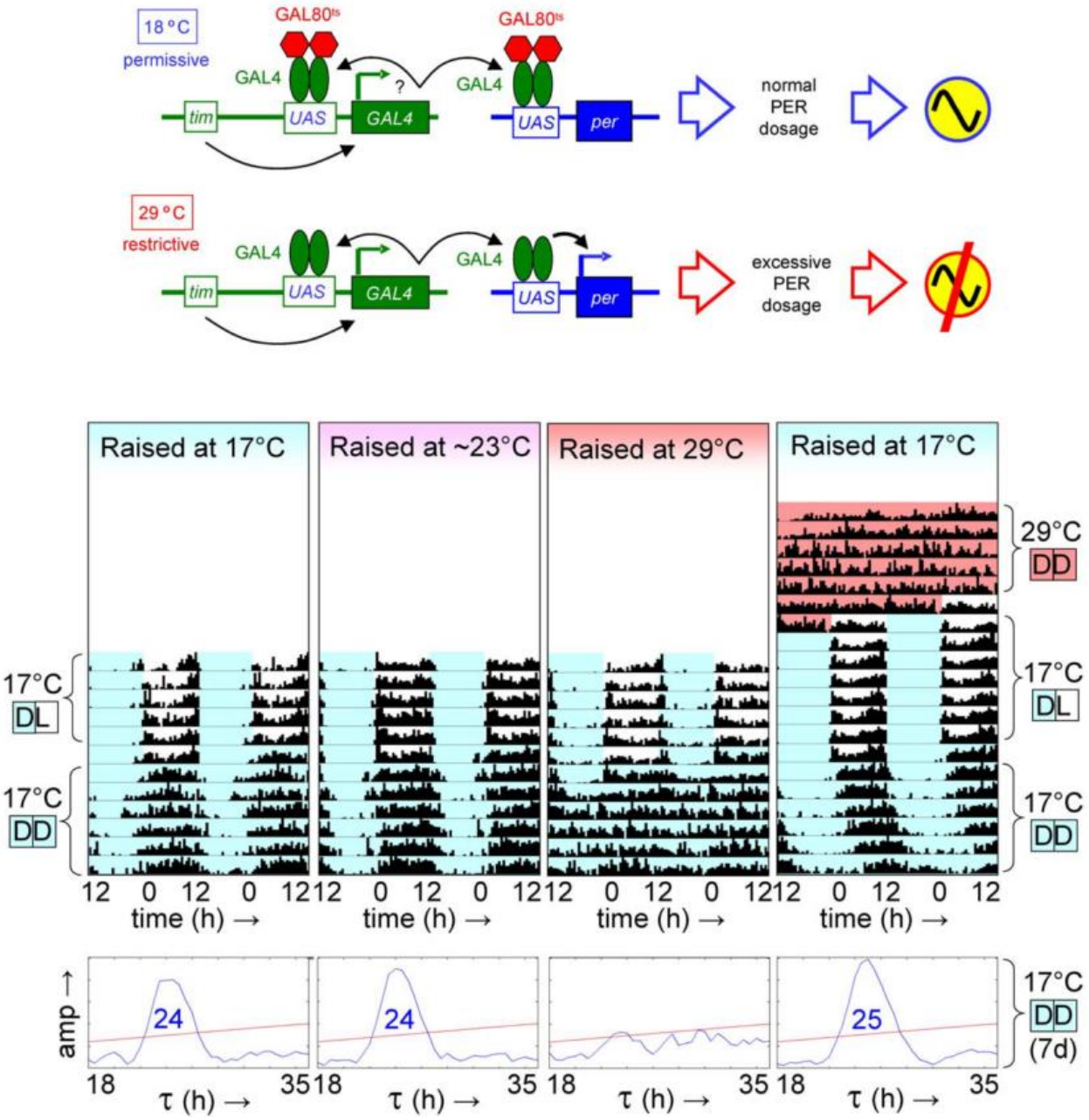

Figure 1.7 - Developmental overexpression of period results in adult behavioural arrhythmia. *Taken from (Goda et al., 2011), demonstrating the dynamics of conditional PER overexpression line, [timP.per]^{ts}, when raised at different temperatures. Above is a schematic of conditional PER overexpression, with repressive behavioural effects manifesting at 29C. Below are entrained and free-running actograms, alongside chi-squared periodograms, demonstrating developmental overexpression of PER results in behavioural arrhythmicity at subsequent permissive conditions, whilst adult-specific PER-overexpression is rescuable by subsequent permissive conditions.*

Deficient CLK/CYC activity due to restricted-expression of *cyc* or over-expression of *per* specifically from pre-pupal stages onward was sufficient to cause behavioural

arrhythmicity, indicating a pupal-specific role for CYC. As previously described, this timepoint includes activation of clock gene expression in several neuronal subsets, and subsequent integration into the remodelled clock circuit, providing a plethora of potential roles for CLK/CYC. Molecular rhythms in the s-LN_v of restrictively raised PER-overexpression lines were discovered to significantly damp, suggesting this may cause the behavioural arrhythmia (Appendix Figure 13).

The developmental defects observed in cyc^{01} and Clk^{Jrk} s-LN_v processes are not present in per^{01} or tim^{01} flies, yet these defects are observable in cyc^{01} and Clk^{Jrk} larval brains as well, suggesting that neuronal defects present in larvae are either not resolved upon metamorphic remodelling if CYC is reintroduced, are present in conditional CYC rescue larvae and simply do not effect behavioural rhythms, or the restrictive conditions of conditional CYC rescue line (Figure 1.8, Figure 3.1) allow sufficient basal CYC levels to rescue this defect (Park et al., 2000, Goda et al., 2011). The mechanistic basis of this, and developmental CLK/CYC targets are unknown.

The bulk of this project seeks to understand the cause of this development-specific defect and the developmental role of CYC that is required for rhythmic behaviour in adults.

Null PDF mutations lead to axonal defects, yet these are only apparent post-metamorphosis, with no anatomical defect in larval brains. Pdf^{01} mutants possess a distinct axonal pattern, where processes from one or two s-LN_vs extend towards the posterior optic lobe, occurring even when PDF expression is rescued from 1st instar larva onwards. $Pdfr^{5304}$ mutants exhibit the same phenotype, such that PDF signalling mediating fasciculation states may rely on communication with other neurons. Knockdown of BMP signalling ligands in developing PDFR+ve neurons lead to noticeably more severe defasciculation, implicating this pathway in correct formation of projections of these neurons. Overexpression of *Medea* (*Med*), a component of BMP signalling specifically in 3rd-larval or pupal stages led to a repeat of phenotype, suggesting s-LN_v remodelling during metamorphosis, potentially partially primed by connectivity between larval PDF and DN1 cells (Gorostiza and Ceriani, 2013).

Conditional overexpression of *lark*, regulator of the post-translational feedback loop, in PDF+ve neurons during development leads to a similarly altered s-LN_v morphology, in defasciculation and repressed axonal branching at the dorsal branching site, though the

severity is not comparable to misregulation of BMP signalling components (Huang et al., 2009). As adult LARK overexpression leads to behavioural arrhythmia, and loss of PDP1 rhythms, but not molecular arrhythmia or neuroanatomical defects, this finding indicates that LARK may function upstream of PDP1 in regulating output, and participate in a developmental output pathway of the clock (Sundram et al., 2012). Indeed, both LARK overexpression and PDP1 loss result in lower PDF within s-LN_vs (Zheng et al., 2009).

Another potential phenotype caused by developmental CYC loss is an alteration in molecular rhythms. An enduring change in the molecular composition of clock neurons as a result of CLK/CYC loss may result in an inability to generate oscillations.

Levels of 48-RELATED 2 (FER2), a transcription factor, are significantly higher in LN_vs compared to other clock cells, and PDF-specific misexpression leads to arrhythmia. FER2-ve lines lack PDF and PER from the 3rd-instar larva onwards, indicating this gene is involved in early clock cell specification (Nagoshi et al., 2010). *Fer2* mutant lines additionally have fewer LN_vs and LN_ds and lower, though still present levels of CRY and CLK expression in these cells, indicating potential developmental control over the clock, and indeed FER2-ve PAM neurons, a cluster of dopaminergic cellswidely studied in *Drosophila* models of Parkinson's disease, are more likely to be misformed or die in development (Nagoshi et al., 2010, Dib et al., 2014).

Loss of multiple, seemingly unassociated, genes upstream of the molecular oscillator within the PDF-cells during development, LARK, E75 and UNF, have all been shown to lead to adult arrhythmia, suggesting that clock-associated genes are required at this stage for adult rhythms, potentiating clock-control of developmental processes, or at the very least suggesting commonalities between molecular interaction networks of circadian physiology and developmental biology (Huang et al., 2009, Goda et al., 2011, Beuchle et al., 2012, Jaumouille et al., 2015).

1.9 - Advantages of *Drosophila* as a model organism

Drosophila have been used as a model organism for over a century, initially utilised in uncovering the basics of heritability and population genetics. *GAL4*-UAS is a widely used system facilitating the ectopic expression of genes. *GAL4*-UAS are a transcription factor and it's respective target activating sequence, components of the Leloir pathway,

metabolising galactose in yeast (Brand and Perrimon, 1993). This pathway is absent in *Drosophila*, and so tying *GAL4* expression to a tissue-specific promotor and a gene of interest to the UAS sequence allows the gene of interest to be expressed in the expression pattern of the desired promotor and ancillary upstream elements.

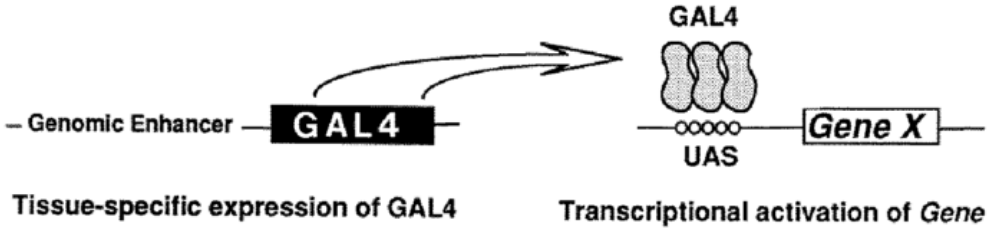

Figure 1.8 - Schematic of the Gal4-UAS system. *Taken from (Brand and Perrimon, 1993), displaying the basic principle of the Gal4-UAS system, in which a promotor region of choice can express gal4 in a tissue or timepoint of choice, which activates a transgene of choice downstream of the UAS promotor.*

An additional component of the Leloir pathway, *Gal80*, serves as a transcriptional repressor, preventing *GAL4*-UAS interacting, allowing the establishment of more complex phenotypes., (Brand and Perrimon, 1993, Duffy, 2002). A temperature-sensitive variant of *Gal80*, containing two point mutations was identified in a mutagenic yeast screen, in which mutant colonies could only grow on a galactose-containing medium at high temperatures. This *Gal80*ts becomes inactive at temperatures ~30°C and as such can be utilised as a tool to dynamically repress *Gal4*-UAS expression in a temperature dependent manner, providing a platform to isolate studies of gene function to specific developmental timepoints and locations (Matsumoto, 1978). The ability to rapidly create transgenics expressing multiple genetic elements in separate, characterised neuronal populations make *Drosophila* an adept tool to ask questions in behavioural neuroscience and circuit analysis.

1.10 - Study Aims

Despite longstanding awareness that developmental roles exist for CLK/CYC, the developmental timepoint, spatial location or ultimate function of these CLK/CYC requirements are unknown. In this thesis, I first aimed to exploit conditional CYC reintroduction lines previously generated by the lab to better characterise these developmental roles, alongside other known phenotypes of CYC loss in LD behaviour,

which has also been under-addressed in the literature.

- Characterise the behavioural consequences of conditional CYC manipulation, in DD and LD
- Characterise the effect of conditional CYC manipulation in development and adulthood on pacemaker cell molecular oscillators
- Describe clock cell morphology and connectivity through development following CYC loss
- Identify the spatial and temporal requirements for CYC expression, developmentally or otherwise, for adult behavioural rhythms

In studying development, we are confronted with a worryingly spartan, and in many places divided, literature of connectivity and interactions between clock cell subsets, and their respective roles in controlling behaviour. As such, my secondary aim revolved around gaining a deeper understanding of clock circuitry through behavioural analyses underscored by a combination of genetic and environmental manipulations. I wished to focus on a particular clock state in which the PDF cells are thought to lose dominance over the clock cell network, which was additionally dependent on poorly-understood CRY-independent light-input pathways (Rieger et al., 2006, Murad et al., 2007, Cusumano et al., 2009, Im et al., 2011).

- Define altered PDF cell requirements and functions in constant red light
- Identify the central pacemaking neuron subset required for behavioural rhythms in constant red light
- Define the contributions of different input pathways to pacemaker shift in constant red light
- Identify changes in clock network hierarchy, signalling and output pathways in constant red light
- Identify shifted clock network requirements and properties in nocturnal flies following CYC loss

Chapter 2 - Materials and methods:

2.1 - Fly culture

Flies were raised on BDSC (Bloomington Drosophila Stock Center) cornmeal diet, simply consisting of 1l water, 6g Agar, 17.5g soya flour, 7.3g yellow maize, 4.6g malt extract and 4.8g sucrose per liter of food. Unless suggested otherwise, flies were stored in 23°C environmentally-controlled room subject to a "12:12 LD" cycle, comprising 12 hours of light followed by 12 hours of darkness, with instantaneous changes between lights-on and off, without gradations in light levels, and with a relative humidity of ~50%. Flies raised or run in 29°C experienced a lower humidity of ~ 30% RH, a constraint of the environment, which may contribute to a lower overall activity at high temperature, but a constant humidity has not previously been shown to affect the daily distribution of activity.

Several experiments necessitated transfer of flies at certain developmental stages between temperatures, through movement to a separate environmentally controlled room (ECR). Third-instar-larvae which leave food to seek a pupation site on the side of the vial were individually transferred using forceps to a fresh food vial, pre-heated or chilled to the subsequent temperature condition. Pupae were transferred by gentle removal from the edge of their original vial with a wet paintbrush, and to a fresh food vial, pre-heated or chilled to the subsequent temperature condition. Pupae were selected at a defined stage, P6, on the basis of the relative longevity of the stage relative to other pupal stages, and were identifiable on the second day following pupation through the gradual greening of the Malpighian tubules, the invertebrate renal organ, and the absence of pigment in other developing structures (Bainbridge and Bownes, 1981). Adult flies were simply "flipped" into separate vials.

2.2 - Fly strains

A list of fly lines utilised throughout the thesis and their source, including where possible a Bloomington Stock Center number, and full genotype:

Experimental	
[tim.per]^{ts}:w* tubpgal80^{ts}; tim-UAS-gal4; UAS-per24	(Goda et al., 2011)
[cry.per]^{ts}: w* tubpgal80^{ts}; cry-gal4^{39}; UAS-per24	Wijnen Lab -

[Pdf.per]^{ts}: w*tubpgal80^{ts}; Pdf-gal4; UAS-per24	Wijnen Lab -
cyc^{01} [elav.cyc]^{ts}$_{\#7}$: elav::gal4 w*/+; UAS-myc-cyc$_{\#7}$/+; tubpgal80^{ts} cyc^{01}/cyc^{01}ry^{506}	Wijnen Lab -
cyc^{01} [elav-Pdf80.cyc]^{ts}$_{\#7}$: elav-gal4 w*/+; UAS-myc-cyc$_{\#7}$/Pdf-gal80; tubpgal80^{ts} cyc^{01}/cyc^{01} ry^{506}	Wijnen Lab -
cyc^{01} [Pdf.cyc]$^{ts\#7}$: Pdf-gal4 w*/Y; UAS-myc-cyc$^{\#7}$/+; tubpgal80^{ts} cyc^{01}/cyc^{01} ry^{506}	Wijnen Lab -
cyc^{01} [Pdf+Clk4.1M.cyc]^{ts}$_{\#7}$: Pdf-gal4 w*/Y; UAS-myc-cyc$_{\#7}$/+; tubpgal80^{ts} cyc^{01}/Clk4.1M-gal4 cyc^{01} ry^{506}	Wijnen Lab -
cyc^{01} [elav-VGlut.cyc]$^{ts\#7}$: elav-gal4 w*/+; UAS-myc-cyc$^{\#7}$/VGlut-gal80; tubpgal80^{ts} cyc^{01}/cyc^{01} ry^{506}	Wijnen Lab -
cyc^{01} [cry-pdf.cyc]$^{ts\#7}$: Y/+; UAS-myc-cyc$^{\#7}$/Pdf-gal80; tubpgal80^{ts} cyc^{01}/cry-gal4$_{13}$ cyc^{01} ry^{506}	Wijnen Lab -
cyc^{01} [c929+R78G02.cyc]$^{ts\#7}$: Y/+; UAS-myc-cyc$^{\#7}$/c929-gal4; tubpgal80^{ts} cyc^{01}/GMR78G02-gal4 cyc^{01} ry^{506}	Wijnen Lab -
cyc^{01} [R78G02.cyc]$^{ts\#7}$: Y/+; UAS-myc-cyc$^{\#7}$/+; tubpgal80^{ts} cyc^{01}/GMR78G02-gal4 cyc^{01} ry^{506}	Wijnen Lab -
Pdfr^{5304}[timP.per]^{ts}: Pdfr^{5304}; tim-UAS-gal4/ tubpgal80^{ts}; UAS-per24	Wijnen Lab
Pdfr^{5304}cyc^{01} [elav.cyc]$^{ts\#7}$: Pdfr^{5304}; UAS-myc-cyc$^{\#7}$/elav-gal4; tubpgal80^{ts} cyc^{01}/cyc^{01} ry^{506}	Wijnen Lab
Pdfr$^{EY11851\text{-}Gal4}$[P.per]^{ts}: Pdfr $^{EY11851\text{-}gal4}$; tubpgal80^{ts}; UAS-per24	Wijnen Lab
Pdfr $^{EY11851\text{-}Gal4}$cyc^{01} [.cyc]$^{ts\#7}$: Pdfr $^{EY11851\text{-}gal4}$; UAS-myc-cyc$^{\#7}$/+; tubpgal80^{ts} cyc^{01}/cyc^{01} ry^{506}	Wijnen Lab
Stocks	
w; tim-UAS-gal4/CyO ; tubpgal80^{ts}*	Wijnen Lab
w; UAS* cyc*Δ^{103}*	(Tanoue et al., 2004)
w; UAS-myc-cyc$^{\#7}$*	(Tanoue et al., 2004)
w; tim-UAS-gal4*	Gift from Mike Young Lab (Blau and Young, 1999)
w; cry-gal4^{13}*	(Stoleru et al., 2004)
w; Pdf-gal4*	(Renn et al., 1999)

w; Clk4.1M-gal4*	Gift from Hardin lab (Zhang et al., 2010a)
w; mai179-gal4*	Gift from Rouyer lab, (Siegmund and Korge, 2001)
w::Pdf-gal80*	(Stoleru et al., 2004)
y^{1} per^{01} w^{*}	(Konopka and Benzer, 1971)
w;;* cyc^{01} ry^{506}	(Rutila et al., 1998)
elav-gal4; UAS-myc-$cyc^{\#7}$*/CyO;* $tubpgal80^{ts}$ cyc^{01}	Wijnen Lab -
elav-gal4; UAS-myc-$cyc^{\#10}$*/CyO;* $tubpgal80^{ts}$ cyc^{01}	Wijnen Lab -
elav-gal4; UAS-myc-$cyc^{\#10}$*/CyO;* cyc^{01}	Wijnen Lab -
w;;UAS-pdp1*	(Benito et al., 2007)
w; tim-UAS-gal4/CyO; UAS-Pdp1/ TM6B-Tb*	Wijnen Lab -
w\; If^{1}*/CyO; UAS-Mef2(High)*	(Gunthorpe et al., 1999)
w\; If^{1}*/CyO; UAS-Mef2(10T4A)*	(Gunthorpe et al., 1999)
17230: w; UAS::Mef2*^{EP2002a} */CyO*	(Rorth, 1996)
43412: w; UAS::Mef2*^{EP321} */CyO*	(Rorth, 1996)
$Pdfr^{5304}$ *[tim.per]*^{ts}*:* $Pdfr^{5304}$*; tim-UAS-gal4/*$tubpgal80^{ts}$*; UAS-per24*	Wijnen Lab -
[Pdfr.per]^{ts}*: Pdfr-gal4; tubpgal80*^{ts}*; UAS-per24*	Wijnen Lab -
$Pdfr^{5304}$ cyc^{01} *[elav.cyc]*$^{ts\#7}$*:* $Pdfr^{5304}$*; UAS-myc-*$cyc^{\#7}$*/elav-gal4;* $tubpgal80^{ts}$ cyc^{01}*/* cyc^{01}	Wijnen Lab -
cyc^{01} *[Pdfr.cyc]*$^{ts\#7}$*: Pdfr-gal4; UAS-myc-*$cyc^{\#7}$*/+;* $tubpgal80^{ts}$ cyc^{01}*/* cyc^{01}	Wijnen Lab -
elav-gal4 (2^{nd}*) 8765 P{*w^{+mC}*=gal4-elav.L}2/CyO*	Bloomington, Peter Kolodziej
repo-gal4 7415 w^{1118}*; P{*w^{+m*}*=gal4}repo/TM3,* Sb^{1}	Bloomington, (Sepp et al., 2001)
Pdfr-gal4 P{GawB}$Pdfr^{EY11851\text{-}gal4}$ w^{67c23}	
dsPDF 4380GD	VDRC
dsITP 43848GD	VDRC
dsHairy : y^{1} sc w*; P{y[+t7.7]*	Bloomington, TRiP stock,

v[+t1.8]=TRiP.HMS01313}attP2	
dspdp1 1788R3	National Institute of Genetics, Japan
dsLar KK107996	VDRC
dsLeucokinin 25798 y^1 w; P{$y^{+t7.7}$ $v^{+t1.8}$=TRiP.JF01816}attP2*	Bloomington, TRiP stock
dsLKR 25936 y^1 w; P{$y^{+t7.7}$ $v^{+t1.8}$=TRiP.JF01956}attP2*	Bloomington, TRiP stock
*dsSFR 34947 y^1 sc*w*; P{$y^{+t7.7}$ $v^{+t1.8}$=TRiP.HMS00299}attP2*	Bloomington, TRiP stock
dsSFR 25831 y^1 w; P{ $y^{+t7.7}$ $v^{+t1.8}$=TRiP.JF01849}attP2*	Bloomington, TRiP stock
dsDH44 25804 y^1 w; P{ $y^{+t7.7}$ $v^{+t1.8}$=TRiP.JF01822}attP2*	Bloomington, TRiP stock
dsSF 60484 y^1 w; P{ $y^{+t7.7}$ $v^{+t1.8}$=TRiP.HMJ22876}attP40*	Bloomington, TRiP stock
dSIFa 29428 y^1 w; P{ $y^{+t7.7}$ $v^{+t1.8}$=TRiP.JF03364}attP2*	Bloomington, TRiP stock
y^1 w^*;;Pdf^{01}	(Renn et al., 1999)
5682: $disco^1$	Bloomington, (Steller et al., 1987)
Lkr^{C003}: 16250: y^1 w^{1118}; PBac{3HPy+}Lkr^{C003}	Bloomington, P-element insertion
Lk^{C275}: 16324: y^1 w^{1118}; PBac{3HPy+}	Bloomington, P-element insertion
Hdc^{JK910} BL64203	Bloomington, (Burg et al., 1993)
eya^2: 2285	Bloomington, (Bonini et al., 1993)
$norpA^7$: 5685	Bloomington, (Harris and Stark, 1977)
dv-Pdf-gal4	Park lab, (Bahn et al., 2009)
R6-gal4 P{?GawB}crc^{R6}	Gift from Taghert lab, (Hewes et al., 2000)
C929-gal4 25373 w; P{ $w^{+mW.hs}$ =GawB}dimm[929] crc[929]*	Bloomington, (O'Brien and Taghert, 1998)

ple-gal4 BL8848 w; P{ w^{+mC} =ple-gal4.F}3*	Bloomington, Birman lab (Friggi-Grelin et al., 2003)
UAS-Kir2.1/CyO; Sb^1'/TM3-Ser^1	Bloomington, (Nitabach et al., 2002)
UAS-hid(II)	Unknown provenance,
UAS-NaChBac; 9466 y^1 w; P{ w^{+mC} =UAS-NaChBac-EGFP}4*	Bloomington, Holmes lab (Nitabach et al., 2006)
UAS-TeTxLC(tnt) 28840 w; P{ w^{+mC} =UAS-TeTxLC.(-)V}A2*	Bloomington, (Sweeney et al., 1995)
UAS-TeTxLC 28838 w; P{ w^{+mC} =UAS-TeTxLC.tnt}G2*	Bloomington, (Sweeney et al., 1995)
UAS-TrpA1 26263 w; P{$y^{+t7.7}$ w^{+mC} =UAS-TrpA1(B).K}attP16*	Bloomington, (Hamada et al., 2008)
R42F08 CG17888(pdp1) w^{1118}; P{GMR42F08- gal4}attP2	Janelia Farm, Flylight stock
R19H11 CG18345(TrpA1) w^{1118}; P{GMR19H11- gal4}attP2	Janelia Farm, Flylight stock
R21G01 CG12598 (adar) w^{1118}; P{GMR21G01- gal4}attP2	Janelia Farm, Flylight stock
R43D05 CG7391(clk) w^{1118}; P{GMR43D05- gal4}attP2	Janelia Farm, Flylight stock
R14F03: w^{1118}; P{GMR14F03-gal4}attP2	Janelia Farm, Flylight stock
R54D11: w^{1118}; P{GMR54D11- gal4}attP2	Janelia Farm, Flylight stock
R78G02:w^{1118}; P{GMR78G02- gal4}attP2	Janelia Farm, Flylight stock
y^1 w; P{w^{+mC} =UAS-mCD8::GFP.L}LL5, P{UAS-mCD8::GFP.L}2*	Bloomington, (Lee and Luo, 1999)
w; P{w^{+mC}=UAS-syt.eGFP}3 BL6926*	Bloomington, Broadie lab (Zhang et al., 2002)
w;VGlut-gal80.V}attP40/CyO; TM6B, Tb^1/TM3, Sb^1*	Bloomington, Vosshall lab (Yapici et al., 2016)

Dh31$^{\#51}$	Gift from Fumika Hamada, University of Cincinnati (Head et al., 2015)
Pdfr^{5304}	Backcrossed, Gift from Fumika Hamada, University of Cincinnati (Head et al., 2015)
w; UAS-Pdp1; pdp1*^{3135}	Gift from Sehgal lab, courtesy of dechun chan (Zheng et al., 2009)
SIFa-gal4	Gift from Sehgal lab, unknown origin, presumed (Terhzaz et al., 2007)
Kurs58-gal4 P{GawB}Kurs58	Gift from Sehgal lab, courtesy of Dechun Chen
Dh44-gal4 R65C11	Gift from Sehgal lab, originally Flylight line, Rubin lab

UAS- overexpression lines for rescue screen were obtained from FlyORF stock center (Zurich), details listed in Appendix.

2.3 - Locomotor assay setup

As previously described (Goda et al., 2011), flies were placed in glass tubes containing diet composed of 5% sucrose, 1% agar, 0.07% tegosept, and were loaded into monitors from the DAM Trikinetics system at 2-7 days post-eclosion. Assays were conducted in modified waterproof marine boxes (SolentPlastic), sealed with blackout cloths and tape (Thorlab), and run in either 12:12 LD, 12:12 RD, LL, RR or DD conditions. Programmed switches between light and dark settings were instantaneous, with no gradations in light intensity. In subsequent freerunning conditions, CT0 (Circadian Time 0) corresponded to the lights-on time for the previous 12:12 LD light regimen, and CT12 (Circadian Time 12) corresponded to the lights-off time. A tray of water containing antimicrobial

substances (0.1% biocide [“Gerrards ASAB”, Fisher scientific], polyclean algaecide) was placed in the boxes to maintain humidity. All locomotor experiments were conducted in environmentally controlled rooms. When temperature changes were included within an experiment, experimental monitors were transferred within assay boxes between environmentally controlled rooms programmed at different temperatures. Activity was ideally recorded for seven days in each condition, excluding the first day of the experiment, although in isolated cases, LD experiments were conducted for five or six days.

As in Figure 2.1, red light excites at a single 630nm peak of intensity 0.57 µmol m^{-2} s^{-1} (approx 40 lux for fluorescent light), whilst white light shows a broad range of excitation with peaks at 441nm and 547nm of intensity 0.97 µmol m^{-2} s^{-1} (approx 70 lux for fluorescent light). Light intensity measurements were not conducted in DD boxes, but given the published exquisity of Drosophila light-sensitivity, the inability of otherwise arrhythmic flies to display driven rhythmicity to 12:12 LD cycles of the ECR in which the assay box is situated indicates light-impermability of the DD boxes (Vinayak et al., 2013). Both red light and white light intensities in this condition are sufficient to entrain flies lacking either *cryptochrome* or visual transduction pathways (Stanewsky et al., 1998).

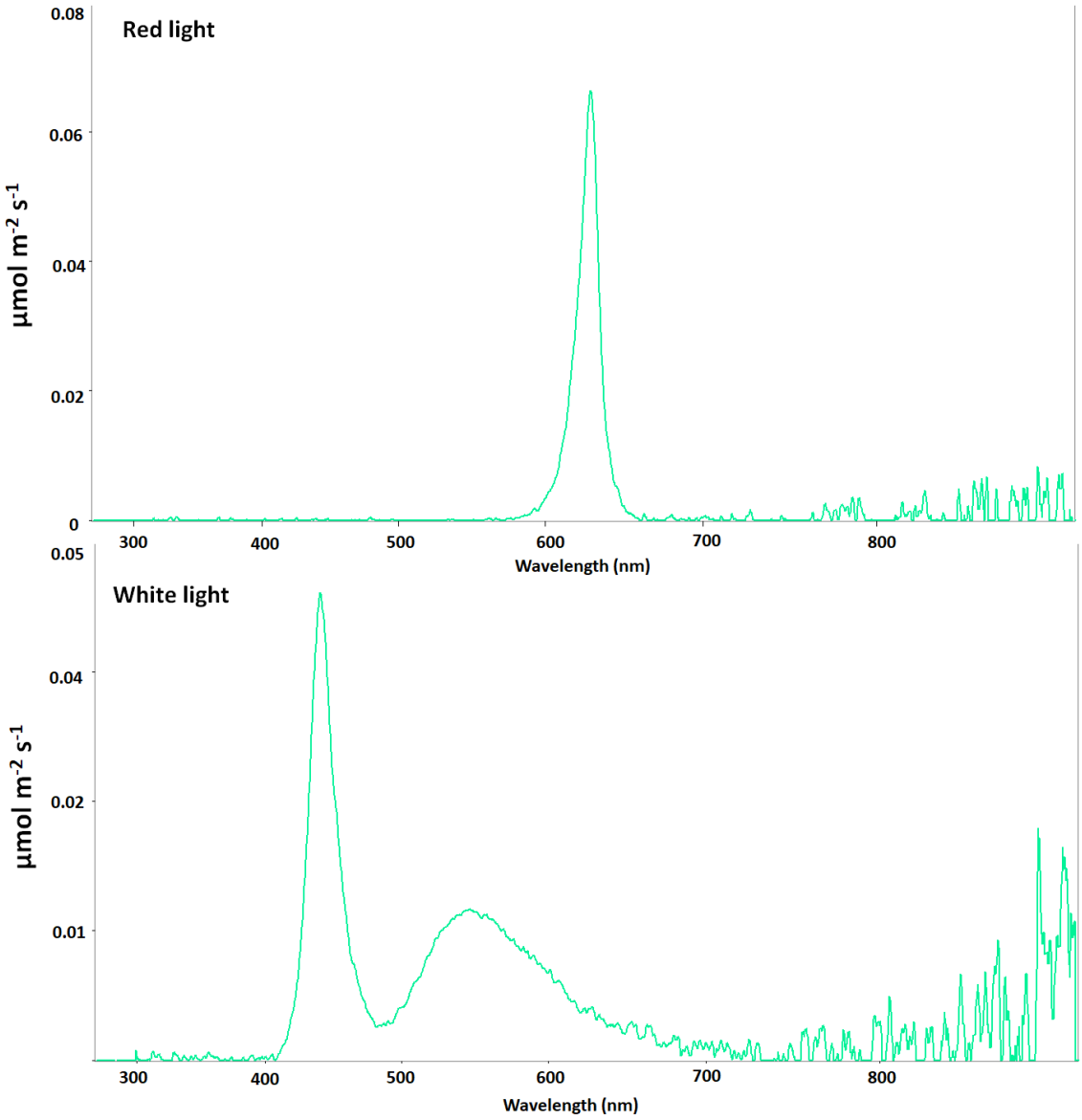

Figure 2.1 - Absorption spectra for different experimental light conditions. *Data gathered by other lab members, demonstrating absorption spectra for red light and white light conditions in which behavioural assays were conducted, demonstrating the fidelity of the red-light condition in excluding wavelengths which could activate CRY (Yamaguchi et al., 2010).*

Movement data was saved into five minute bins, and, for analysing circadian rhythms, was aggregated further into thirty minute bins. Data from 23ºC and 29ºC run-experiments were collected by a shared DAM system, whilst monitors in 17ºC were attached to a separate DAM system, and therefore datasets stemming from experimental monitors moved between 17ºC and other conditions had to be fused within an excel file before analysis.

Within the text, flies undergoing a temperature regimen are referred to first by their developmental temperature, and then an adult temperature, sometimes accompanied by a light-regimen. If flies undergo multiple developmental temperatures, the developmental stages at which temperatures are switched is noted. For instance, a fly raised at 17ºC from egg-laying through to eclosion, and subsequently experimentally assessed at 29ºC would be described as: 17 →29°C. A fly that was raised at 17ºC from egg-laying until the third-instar larval stage, and then transferred to 29ºC until eclosion, and run in a behavioural experiment at 29ºC would be referred to as: 17EL-L3-29 →29°C

2.4 - Locomotor data analysis

Relative rhythmic power (RRP) and period length were generated via Clocklab software (actimetrics), via the maximum height of an activity peak, relative to the heights of adjacent activity counts. Period length, sometimes referred to as TAU, was calculated by the spacing between these peaks over several days. Individual flies were classed as Strongly rhythmic (SR), Weakly rhythmic (WR) or Arrhythmic (AR) for RRP values >1.5, 1.5>n>1.0 and <1 respectively. Significance of the distribution of SR, WR and AR flies between conditions was analysed using a 2x3 Fisher's exact test in IBM SPSS. To study differences in RRP, AR flies were assigned an RRP of 1, the upper limit of arrhythmicity, and integrated into RRP datasets. Comparisons between RRPs for different populations was conducted using one-way ANOVA in IBM SPSS. Comparisons between period lengths for different populations was conducted using one-way ANOVA in IBM SPSS, following the exclusion of arrhythmic flies from the dataset. To present all statistics, for locomotor behaviour or otherwise, P values <0.05 were signified with a single asterisk (*), P values <0.01 were signified by dual asterisks (**), and P values <0.001 were signified by triple asterisks (***). Period length was assigned in a similar way.

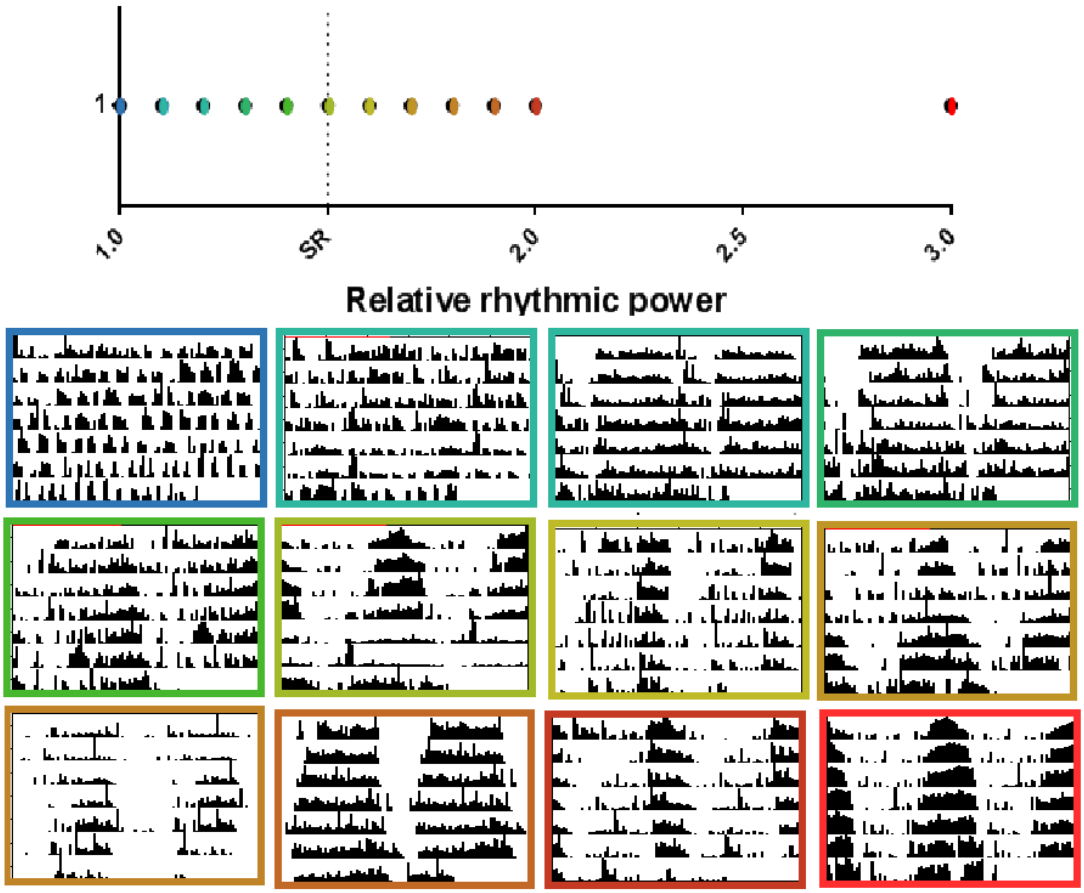

Figure 2.2 –Freerunning behavioural actograms corresponding to various Relative Rhythmic Power (RRP) values. *Example actograms of 24hr period of varying Relative Rhythmic Power, to visualise the rhythmicity at various RRP values shown on dotplots in cases where corresponding actograms are not shown. RRPs range from 1.0 to 3.0, in which 1.5 is deemed as strongly rhythmic. The border colour of the actogram corresponds to the similarly coloured RRP value on the dotplot.*

Images of actograms were obtained from median population data aggregated in thirty-minute bins, unless otherwise stated, whilst activity profiles were generated from median population data aggregated into five-minute bins. Activity profiles are presented as a default output from Clocklab, plotting mean counts per minute for each bin across a 24hr period for the duration of behavioural acquisition. These profiles were presented exclusively to convey relative population-wide changes across a 24hr period irrespective of overall activity, and so scale from Y-axes were removed in certain cases (Figure 2.3).

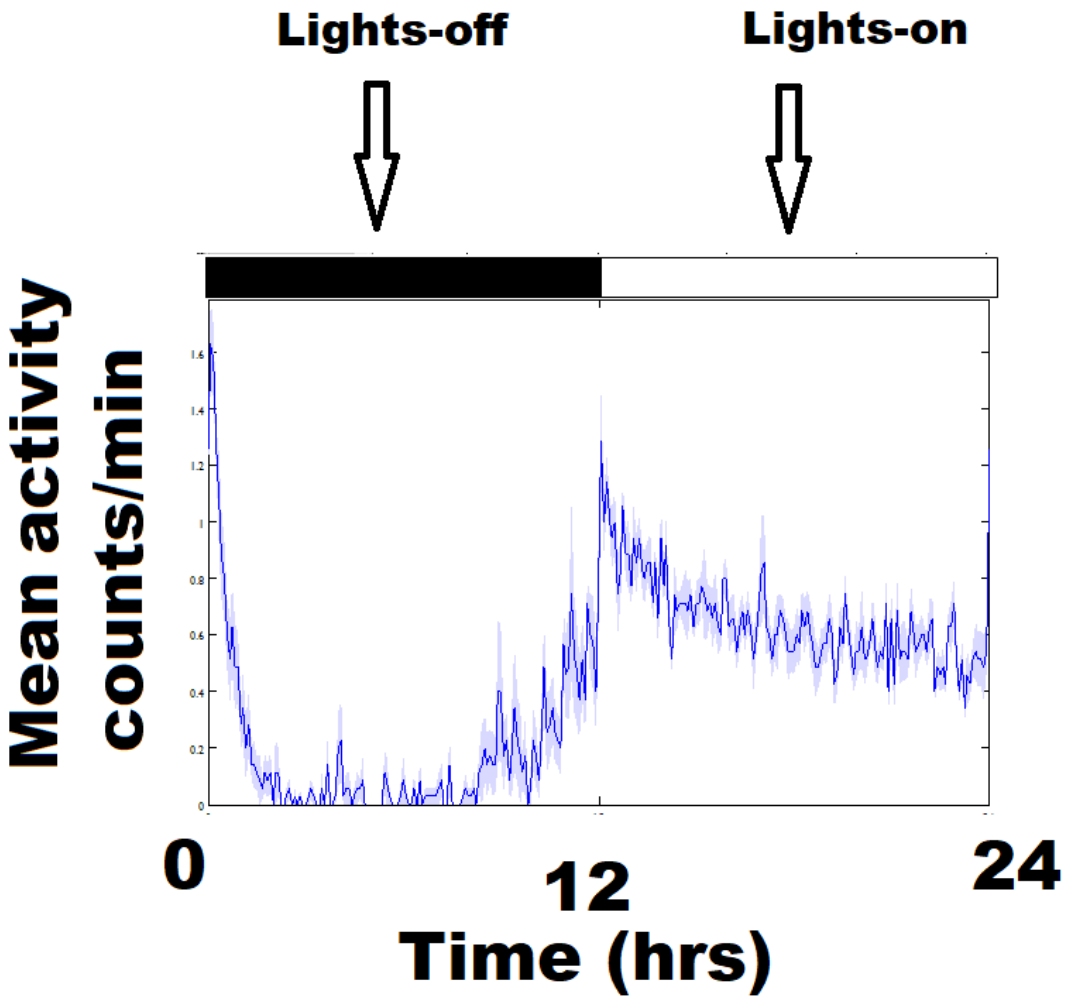

Figure 2.3 - Presentation of activity profile data*. Annotated activity profile generated in clocklab, displaying mean activity over a period of several days, with time of day on the X-axis, and mean counts on the Y-axis. Light-protocol is displayed above the graph. Time of day on the x-axis is relative, and not indicative of ZT, which initiates from time of lights-on. Each peak in the activity profile represents the median of a 5 minute bin over multiple days of a behavioural timecourse. Lighter blue colouration indicates standard error for each respective timepoint across a behavioural timecourse. Throughout the thesis, activity profiles are preented from median data rather than individual flies.*

For the analysis of nocturnality, Activity counts in LD were collected in five minute bins for up to seven days, excluding the first experimental day of a given LD condition, and Clocklab generated a .xls file containing counts within the Diurnality/Nocturnality (D/N) ratio was calculated for individual flies as previously described, as in example Figure 2.4 (Kumar et al., 2012):

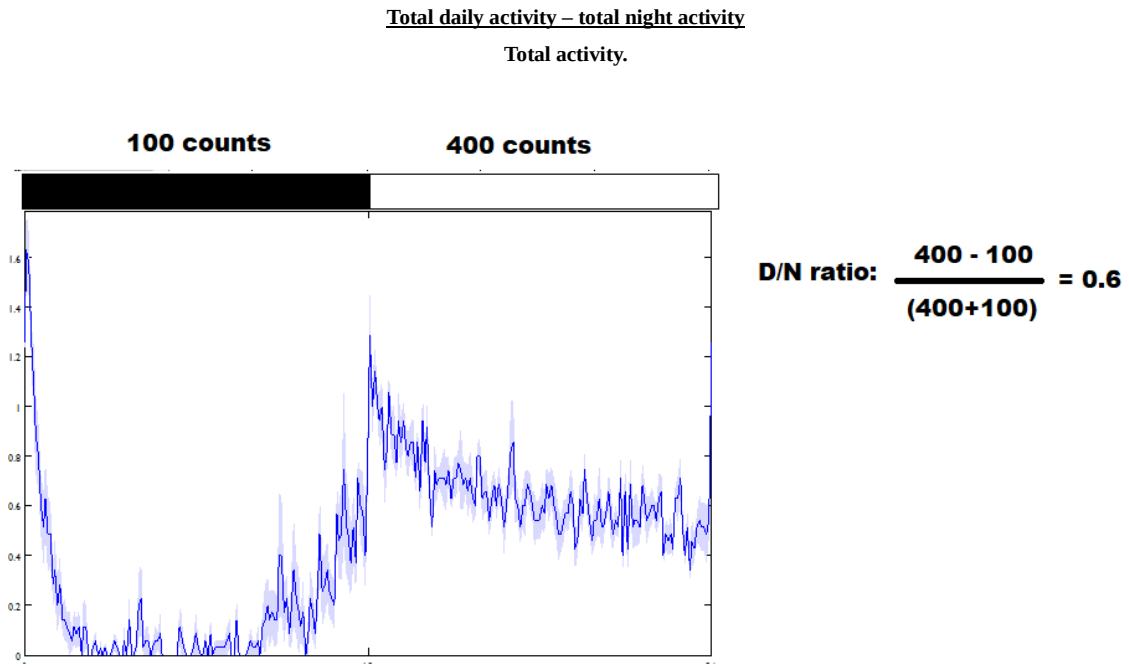

Figure 2.4- Diurnality/Nocturnality ratio calculation. *Example D/N ratio of a diurnal activity profile of D/N ratio: 0.6. Counts given are approximate rather than actual values.*

Statistics comparing D/N ratios between conditions were conducted using one-way ANOVA calculated in IBM SPSS.

As shown in Figure 2.5, evening anticipation was studied by collecting LD data in one hour bins for individual flies over seven days, excluding the first day in a given LD condition. Evening anticipation was quantified using a previously published evening anticipation index, which generates a value based on the consistency of incremental increases in activity bins in the hours preceding lights-off, in which a value of zero or less indicates a lack of quantifiable evening anticipation, and increasing positive values represents consistent or larger stepwise increases in activity counts in bins taken prior to lights-off (Stoleru et al., 2004). This strategy of quantification is more concerned with the waveform of evening anticipation rather than the relative levels of activity preceding lights-off.

Evening anticipation index was calculated by the (Stoleru et al., 2004) formula $AI = b_{-1}(b_{-1} - b_{-2})(b_{-2} - b_{-3})/b_{+1})$, in which b +/-I represents number of activity counts in a bin relative to lights-off. Activity counts for each individual fly were binned for each of the three hours preceeding light change, and the subsequent hour.

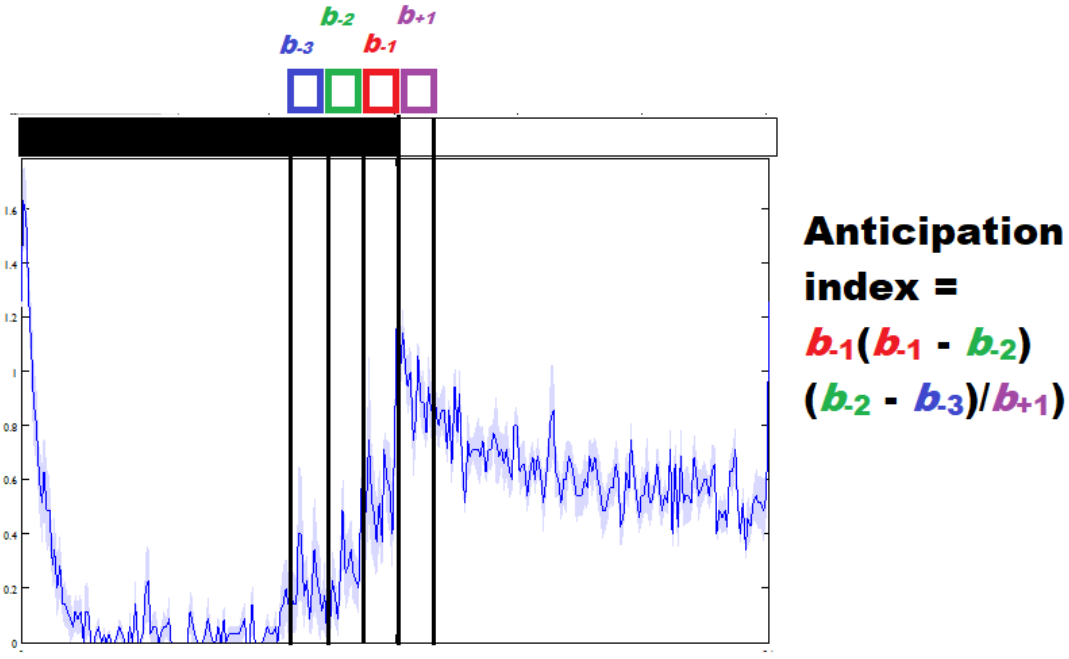

Figure 2.5 - Schematic of Evening Anticipation Index. *Example of the segregation of bins in order to calculate evening anticipation. Activity counts for the three hours before, and the hour after lights-off are collected for a behavioural timecourse. Calculation derived from (Stoleru et al., 2004).*

Evening peak (E-peak) phase (Figure 5.6) was determined by generating a median activity profile for seven days of LD data for individual flies, excluding the first day in a given LD condition, and calculated by the position of the thirty-minute bin with most activity counts prior to lights-off, and subsequent to the daytime nadir in activity, as shown in Figure 2.6. Comparisons between E-peak phase between different populations was calculated via one-way ANOVA in IBM SPSS.

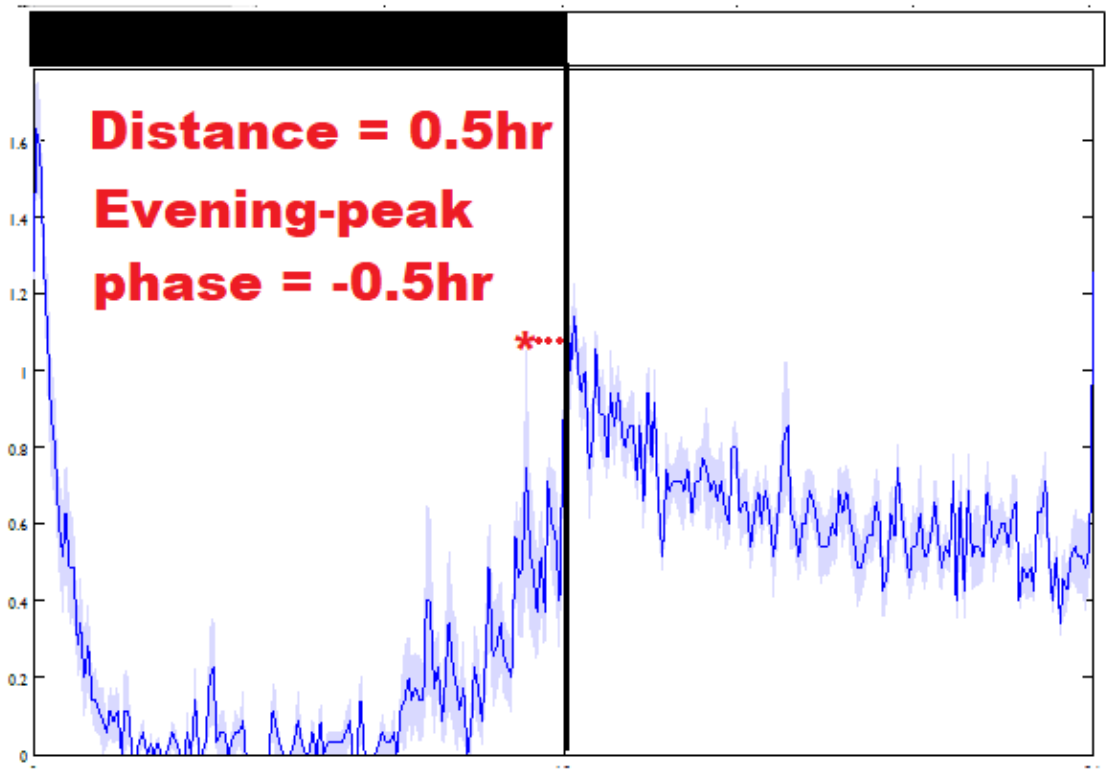

Figure 2.6 – Demonstration of E-peak phase calculation. *example of E-peak phase value, determined as the distance of the bin containing most activity counts prior to lights-off. Experimental E-peak phases were derived from 30 minute bin sizes rather than 5-minute bins as shown in the figure, to minimise noise*

2.5 - Pupariation assay

As adapted from (Yamanaka et al., 2013), 3rd instar larvae, defined by their climbing behaviour, were loaded at ZT10, in the evening shortly prior to lights-off, to the midpoint of an apparatus of two glass vials, joined with autoclave tape and partially and uniformly filled with 5% sucrose, 1% agar and 0.07% tegosept. One half of the apparatus was covered in black electrical tape and the apparatus was placed overnight in a LL box, and the following morning pupae were tallied based on location within the light or dark half of the apparatus. Non-pupated larvae, and pupae remaining at the midpoint of the apparatus were excluded from the analysis.

2.6 - Immunofluorescence

Unless another entrainment regimen was described, Flies were entrained to 12:12 LD cycles for three days in an assay box, transferred to DD during the dark phase of the third day and dissected on the second day of DD, followed by transferral to a glass vial on ice in DD. Once chilled on ice to anaesthetize the flies and slow the kinetics of light-induced

destabilisation of light-sensitive proteins, dissections were performed under ambient lighting, and limited to 10 minutes, in order to minimize the time between collection and sample fixation. For all staining of PDF-cell projections, or of morphology of GFP- or Ion transport peptide (ITP)-labelled clock neurons, experiments were conducted at CT2, two hours following subjective lights-on in the morning, in which PDF levels are anticipated to be highest (Park et al., 2000). For experiments studying the staining intensity and subcellular localisation of the clock gene PER, timepoints were taken at CT2, CT8, CT14 and CT20, encapsulating presumed low and high points in PER staining, with highest levels corresponding to the hours preceding lights-on, and lowest levels corresponding to the hours preceding lights-off.

Dissections for larval and pupal brains at all stages were conducted in a plastic tissue culture dish (Corning 60x15mm) on ice, partially filled with pre-chilled 1x Ringers solution (3mM $CaCl_2$, 182mM KCl, 46mM NaCl,10mM tris, pH 7.2). Following this, dissection protocols were conducted as previously described in (Wu and Luo, 2006).

Adult brains were dissected on a metal block, re-chilled at -20°C for 30 minutes and placed onto ice immediately prior to dissection. Adult heads were removed with a razorblade (0.12” single-edge, Fisherbrand) and the proboscis was removed with forceps (5 Inox, Idealtek). Brains were removed through the resulting cavity by applying pressure to the compound eyes, and residual eye remnants, cuticle, trachea and other detritus was removed. Brains were transferred to a 0.2ml PCR tube (Fisherbrand, polypropylene) by submergence in a drop of 4% paraformaldehyde and gentle pipetting to avoid damage.

Brains were subsequently incubated in 4% paraformaldehyde (in 1x PBS) on a nutator at room temperature for 20 minutes. Brains were then washed twice with 1x PBT (100mM Na_2HPO_4, pH7.2, with 0.4% triton-x 100) and then incubated on a nutator for 3x20 minute steps in PBT. Brains were then incubated in blocking buffer (5% Normal Goat Serum [sigma] in PBT) for 30 minutes, transferred to blocking buffer containing appropriate primary antibody and stored in this condition for two nights on a nutator. On the third day, brains were washed twice with PBT, incubated on a nutator for 3x20 minute steps in PBT and transferred to a blocking buffer containing secondary antibody, and placed on a nutator for two nights again, wrapped in aluminium foil to prevent fluor bleaching. On the fifth day, brains were washed again twice with PBT and 3x20 minute

washes in PBT on a nutator, to remove residual antibody. Brains were submerged in vectashield hardset mounting medium (Vectorlabs, H-1400) and transferred to a microscope slide (Menzel Gläser, 76x26mm, B57011/2), surrounded by raised ridges of dried nail polish, which prevents the coverslip (22x22mm, glass) squashing the brain and preserves sample integrity. Completed slides were stored at 4°C and imaged within a few days of mounting, and subsequent to imaging were stored at -20°C.

Antibodies were added at the following concentrations: For experiments on cyc^{01} *[elav.cyc]*^{ts}: monoclonal Mouse-anti-PDF (1:200), polyclonal rabbit-anti-PER (1:4000), 488-goat anti rabbit (1:200), 568-goat anti-mouse (1:200). For *CD8::GFP* imaging, chicken-anti-GFP primary antibody (1:1000) and 488-goat anti chick (1:200) was used. ITP staining was conducted with rabbit-anti-ITP (1:5000) and 488-goat anti rabbit (1:200) (Hermann-Luibl et al., 2014). Rabbit anti-CRY was used at (1:1000).

All antibodies were stored as aliquots at -20°C with sodium azide, with the exception of Mouse-anti-PDF which arrived as a supernatant and was stored at 4°C. Rabbit-anti-PER antibody was purified prior to use through incubation using the above protocol on per^{01} embryos and hence stored as a 1:100 or 1:300 dilution, whilst other antibodies were not diluted. Antibodies were obtained from:

Mouse-anti-PDF	PDF, C7, Iowa hybridoma bank
Rabbit-anti-PER	Dr Jeff Hall (Liu et al., 1992)
Chicken-anti-GFP	Abcam ab13970
Rabbit-anti-ITP	Gift from Dr Heinrich Dircksen, Stockholm University
Rabbit-anti-CRY	Gift from Dr Charlotte Helfrich-Förster, (Yoshii et al., 2008)
488-goat anti Rabbit	A-11034, Thermo-Fisher
568-goat anti-Mouse	A-11031, Thermo-Fisher
488-goat anti Chick	A-11039, Thermo-Fisher

Images were obtained on an SP8 Leica confocal microscope, at 40X in Leica type F immersion oil, with a stack thickness of 0.45µm in the case of quantifying soma intensity or 1µm stacks for characterising axonal projection morphology, or the presence of large

groups of cells. Settings were kept constant, 488nm secondary antibodies were encapsulated via excitatory wavelengths between 491-543nm, and 568nm secondary antibodies were excited with 589-653nm, and in cases of multiple secondary antibodies, the separate channels were scanned sequentially to prevent cross-excitation. In the interests of time constraints, captured z-stacks were limited to the region of interest and did not encapsulate other clock cells. Due to the magnification, hemispheres within a brain were imaged separately at 1024x1024 pixels. Images were saved into aggregate .lif files and named in order of acquisition without genotypic information, to ease blinding prior to quantification. Relevant sample information was compliled in excel files concurrent with imaging.

2.7 - Image analysis

Skeletons for PDF cell axons were generated using the Simple Neurite Tracer application, a standard segmentation plugin on Fiji, a version of ImageJ optimised for cell biology applications. Stained arbors were semi-automatically traced via the program to generate a skeleton representative of the entire projection. Tracing was conducted through a z-stack rather than a flattened image, to more accurately trace overlapping projections. Total Projection Disorder was calculated by dividing the sum length of branches traced within the projection, by the maximal length of the major neurite and the longest second-order terminal. Comparisons between total projection order for different populations was conducted using one-way ANOVA, generated in IBM SPSS.

Sholl analysis was performed as previously described in (Fernandez et al., 2008). Second-order processes of the s-LN_v dorsal projections were traced using simple neurite tracer, as above, initiating at the first dorsal branch point, which is readily identifiable in wt-like projections. In mutant projections, the point of dorsal branching was indistinct in certain cases, and estimated based on location and distribution of branches. Sholl analysis was automatically performed by Simple Neurite Tracer software, by generating concentric circles, increasing in radius by 10 µm from the initial branch-point of dorsal termini, and counting the number of sites at which the axonal skeleton breached each circle, as visualised in Figure 2.7c. For our purposes, the total number of breaks by one projection for all circles was pooled to give one integrated sholl value. Assaying sholl values of each concentric circle resulted in variability that prevented meaningful comparison between genotypes. Comparisons between sholl values for different populations was conducted using one-way ANOVA, generated in IBM SPSS. Projection

length was not normalised to brain size, which should not affect total projection disorder, a ratio, but may impact sholl analysis, where larger brains may have projections which intersect more circles.

Projection staining intensity was measured by taking a max-intensity z-stack encompassing the entire projection, tracing around the entire projection, thresholding to an integrated density value of 100, and subtracting the remaining mean staining intensity as background. All representative images presented, unless stated otherwise, were acquired via a max intensity projection of multiple slices of a z-stack encapsulating the projections or soma of interest. Comparisons between dorsal and basal staining intensity were conducted in the same manner, with the dorsal area of the projection defined from the point of second-order process branching, and the basal area encompassing the remainder of the major neurite, and the mean dorsal stain was divided by the mean basal stain, such that higher values reflected comparatively more dorsal distribution of staining. The demarcation of dorsal and basal projection is displayed in Figure 2.7d. The Posterior optic tract (POT) was not included in quantifcation.

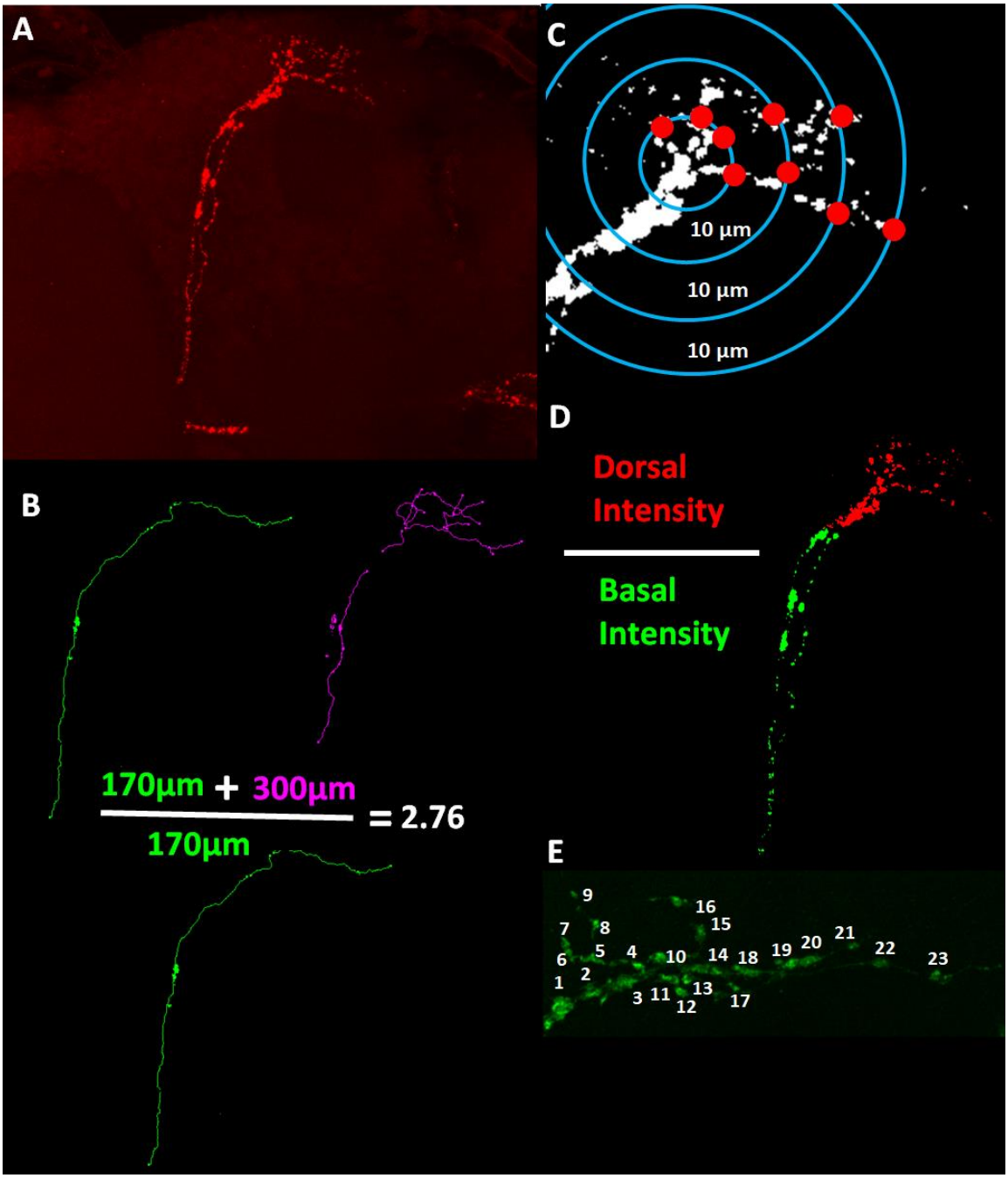

Figure 2.7 - Demonstration of quantification of axonal phenotypes. *Panel A is an example s-LN$_v$ projection stained with PDF antibody, representing a complete Z-stack at maximal intensity. Panel B shows example skeleton of traced processes in s-LN$_v$ dorsal projection, derived from the image on Panel A, created using the simple neurite tracer plugin. In green is the major neurite process, as determined by staining intensity, and in magenta are second-order processes and offshoots, as determined semi-automatically. Total projection disorder is calculated by dividing the total skeleton length by the length of the major neurite. Panel C shows the method of Sholl analysis quantification, in which axonal crosses of concentric rings spaced 10um apart are quantified and pooled, in this*

case giving a sholl value of nine. Panel D shows the division of basal and dorsal parts of the projection used to compare the distribution of PDF or synaptic markers in Chapter 4. Panel E shows an example of bouton counts, using Synaptotagmin-GFP as a marker. Individual puncta in the second order processes are counted by hand.

As shown in Figure 2.8, Quantification of oscillations within cell bodies was conducted by assessing the Mean fluorescence within the nucleus, relative to background, a subjectively-identified region of relatively uniform staining intensity surrounding or adjacent to the quantified cells. For each cell, an approximate max-intensity z-stack was taken spanning the entirety of the cell soma. N/C (Nuclear/cytoplasmic) ratio was measured by the CTCF (corrected total cell fluorescence) of the whole soma divided by that of the nucleus, using the cytoplasm-specific PDF stain as a guideline of nucleus location. The % nuclear quantification was determined subjectively by scoring the presence of a sole discrete spheroid staining pattern, significantly smaller than the PDF+ve soma. Background stain was also subtracted, using a randomly selected region adjacent to the cell. Sample information was excluded from image filenames and images were analysed several days after imaging in order to limit bias during quantification.

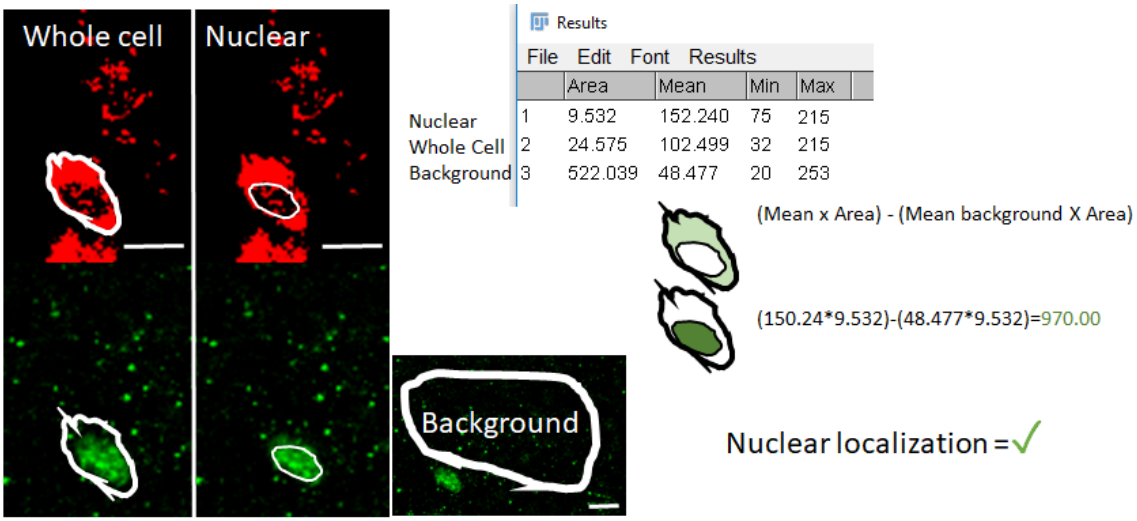

Figure 2.8 - Demonstration of quantification of clock protein levels and localization within the soma. *Image of oscillation quantification, showing the areas used to demarcate nuclear and cytoplasmic compartments, and the formula to calculate nuclear PER staining intensity. Scale bar in bottom right is 20µm.*

Bouton number was determined manually by the number of discrete *SYT::GFP* +ve puncta, and boutons on each projection were counted multiple times to ensure accuracy of results, as shown in Figure 2.7e. Quantified boutons were restricted to the dorsal part

of the projection as previously defined, although total bouton number across the entire projection was also quantified. Counts of cell soma were similarly conducted manually, on the basis of appropriate marker stain, soma position and, where possible, by the presence of canonical projections associated with the soma. In experiments involving CRY or ITP staining, or *CD8::GFP* expression in broader driver lines, numerous non-clock neurons were identifiable, and cells were excluded on the basis of morphology and location. This potentially means counts in which a lower number of clock cell soma are observable is due to a mis-localisation of these soma to a non-clock cell cluster, along with a loss of canonical projection trajectories, although this may fit into our conclusions of an altered cell specification.

Scale bars of 20, 50 or 100µm were generated for example images using measurements from the scale metadata.

Image quality: For quantification of stain intensity, imaging settings were standardised, such that samples could be compared. In slides focussed on axonal complexity or presence of clock cell groups, imaging settings were altered between setting intensities in order to maximally expose the extent of the projection or cell group, and were subsequently excluded from experiments concerning staining intensity. As for behavioural analyses, statistical analysis was performed using Microsoft Excel and IBM SPSS statistics. Comparisons between genotypes, gender or condition were made using one-way ANOVA. Graphs were produced either with Microsoft Excel or Graphpad Prism 7.1.

For bipartite correlation analysis in Appendix Figure 10 and 11, two-tailed test with Pearsons co-efficient was used.

Chapter 3: Behavioural analysis of conditional CYC modulation

Previous work in the lab, alongside an older study from the Hall lab, has established a developmental dispensability of PER, and thus a developmental dispensability of the molecular oscillator during development for adult behavioural rhythms, with a separate finding that CYC was required (Ewer et al., 1990, Goda et al., 2011). CYC, and presumably CLK/CYC therefore possess roles independent of their imparting rhythmicity to transcription. I first sought to replicate this result and further define the phenotypes resulting from developmental CYC loss to identify developmental CYC requirements.

3.1 - Validated *cyc^{01} [elav.cyc]^{ts}* lines become arrhythmic following developmental loss of CYC

The lab had previously created a fly line, named *cyc^{01} [elav.cyc]^{ts}*, summarised in Figure 3.1, which conditionally reintroduces CYC onto a *cyc^{01}* background in a temperature-specific manner. A development-specific restriction of CYC expression led to an irreversible adult arrhythmicity, suggesting a role for CYC at this stage. The line had to be reconstructed, as described in the methods, through crossing *cyc^{01} [elav.cyc]^{ts}* virgins with *cyc^{01}* males to give the final genotype *elav-Gal4/(+ or Y); UAS-myc-cyc$^{\#7}$/+; tubpgal80^{ts} cyc^{01}/cyc^{01} ry^{506}* (Goda et al., 2011).

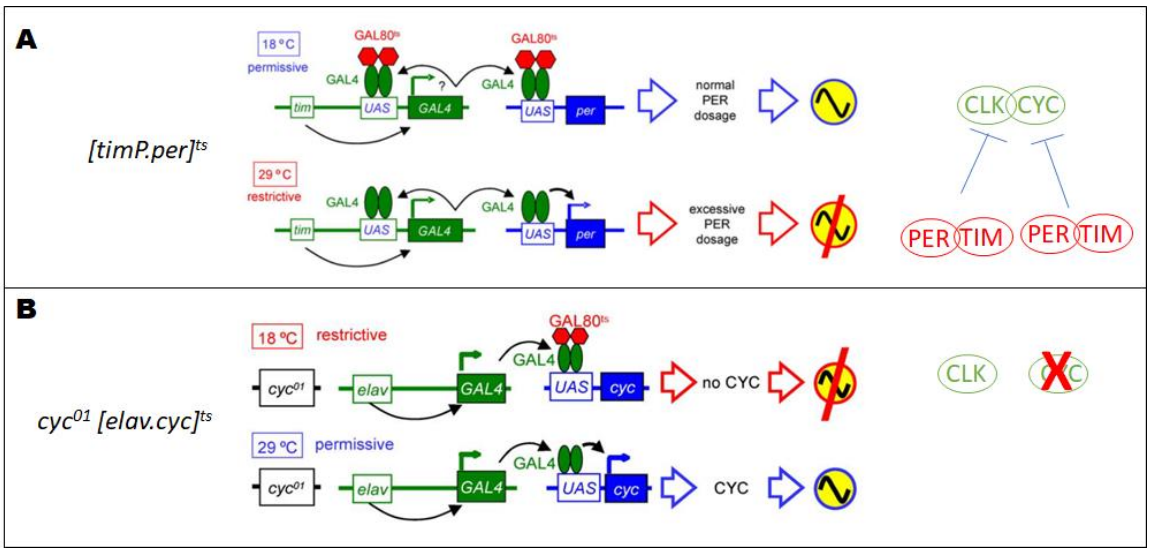

Figure 3.1 - A genetic scheme for conditional regulation of cycle levels. *Adapted from (Goda et al., 2011), schematic for restrictive and permissive tempratures, conditionally overexpressing PER, [timP.per]^{t}, shown in Panel A, or conditionally rescuing CYC on a mutant background, cyc^{01} [elav.cyc]^{ts,} shown in Panel B. For PER overexpression, low temperatures are permissive, whilst for ectopic rescue of CYC expression, low temperatures are restrictive.*

Hypothetically, lower temperatures would provide a restrictive condition in which *GAL80*^{ts} blocks CYC expression, whilst at high temperatures CYC expression should resume as *GAL80* is inactivated. In order to define restrictive and permissive conditions, *cyc*^{01} *[elav.cyc]*^{ts} progeny were raised from early larval stages to adulthood at 17°C, 23°C or 29°C in LD, and freerunning behavioural data was collected for 7 days at 17°C, 23°C and 29°C DD, as detailed in Table 3.1, and Figures 3.1 and 3.2. For brevity, throughout the text, temperature regimens for TARGET flies are given as (Developmental temperature → Adult temperature [experimental condition], for example flies raised at 17°C through development and moved to 23°C in adulthood were described as 17 →23°C).

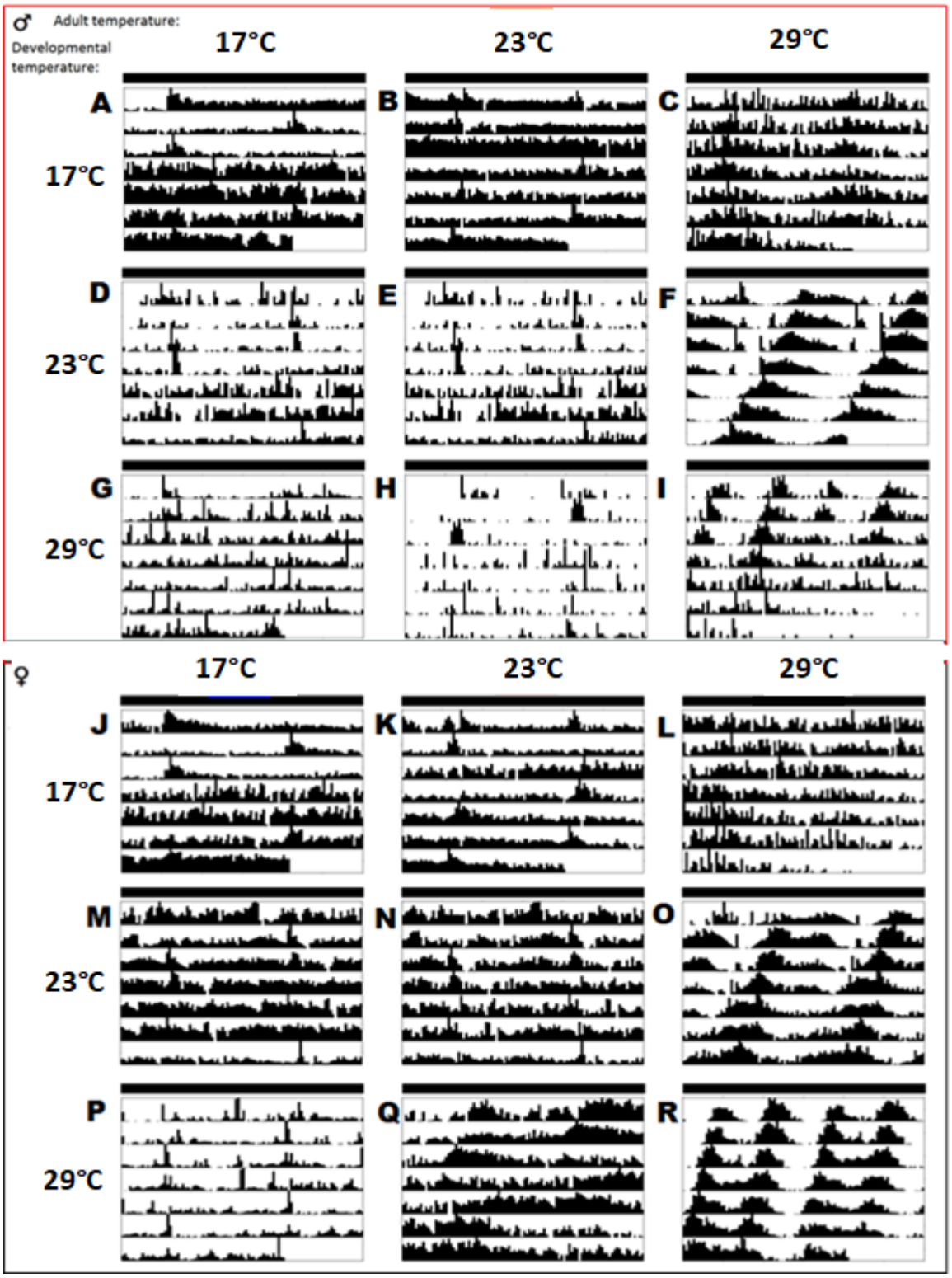

Figure 3.2 - Both developmental and adult cycle expression are required for behavioural rhythms in constant darkness. *Median freerunning actograms for cyc^{01} [elav.cyc]^{ts} males (Panels A-I) and females (Panels J-R), raised and run at 17°C, 23°C and 29°C. Numbers on the left indicate developmental temperature, and numbers at the top indicate adult temperature at which the behavioural assay was conducted. Clear rhythms are shown in Panels F, I, O and R, at a combination of high adult temperature and high or moderate developmental temperature. Accompanied in Table 3.1 is a summation of these values.*

Dev + adult temperature	n		% SR	% WR	% AR	TAU ± SEM	RRP ± SEM
M 17 →17°C	22		0.00	13.64	86.36	23.50±0.50	1.07±0.04
F 17 →17°C	22		0.00	4.55	95.45	19	1.11
M 17 →23°C	10		0.00	0	100	N/A	N/A
F 17 →23°C	7		0.00	28.57	71.43	24.00 ± 0.50	1.17 ± 0.055
M 17 →29°C	35		0.00	17.14	82.86	24.17 ± 0.69	1.09 ± 0.018
F 17 →29°C	43		0.00	11.63	88.37	22.70 ± 0.12	1.14 ± 0.039
M 23 →17°C	22		0.00	18.18	81.82	28.63 ± 5.35	1.09 ± 0.029
F 23 →17°C	23		0.00	34.78	65.22	25.44 ± 3.23	1.10 ± 0.035
M 23 →23°C	21		0.00	23.81	76.19	23.50 ± 0.22	1.44 ± 0.330
F 23 →23°C	18		0.00	22.22	77.78	24.88 ± 1.72	1.08 ± 0.041
M 23 →29°C	34	***	73.53	17.65	8.82	22.34 ± 0.44	1.99 ± 0.104 ***
F 23 →29°C	47	***	46.81	34.04	19.15	22.68 ± 0.30	1.78 ± 0.103 ***
M 29 →17°C	13		0.00	30.77	69.23	22.88 ± 0.83	1.22 ± 0.079
F 29 →17°C	16		0.00	6.25	93.75	23.50	1.21
M 29 →23°C	12		0.00	25.00	75.00	28.67 ± 0.08	1.15 ± 0.040
F 29 →23°C	15		0.00	0.00	80.00	21.00 ± 3.51	1.10 ± 0.038
M 29 →29°C	35	***	11.43	40.00	48.57	23.72±0.84	1.42±0.08 ***
F 29 →29°C	31	***	83.87	12.90	3.23	23.5 ± 0.37	2.48 ±0.121 ***

Table 3.1 - Freerunning behavioural rhythms following conditional manipulation of CYC levels across varied developmental and adult temperatures. *Supplement to Figure 3.2, detailing rhythmic behavioural properties of cyc^{01} $[elav.cyc]^{ts}$ flies raised and run at 17°C, 23°C and 29°C for 7 days in DD, in which flies Statistics comparing rhythmicity between conditions are detailed in Appendix Table 1, though significant differences in both the distribution of rhythms and rhythmic strength are observable between 17 →29°C and either 23 →29°C or 29 →29°C for both genders, as indicated by asterisks.*

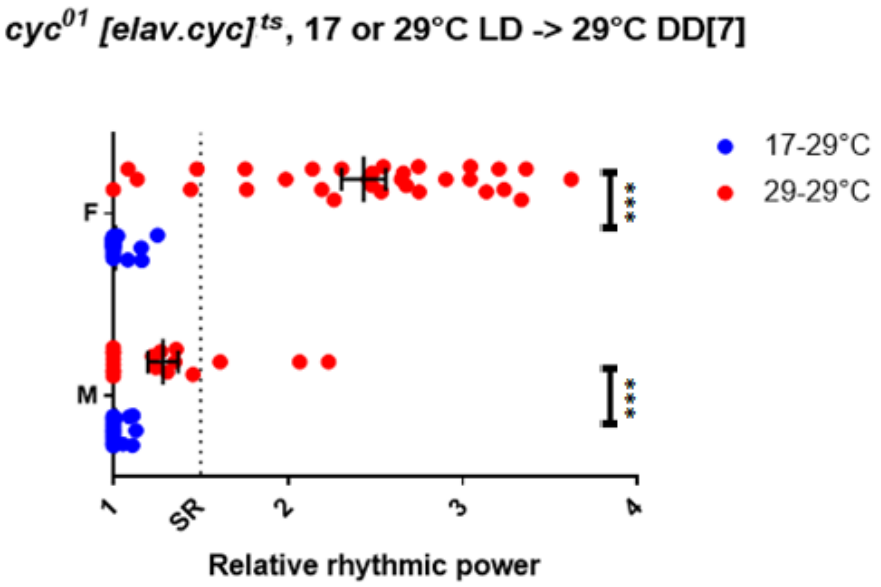

Figure 3.3 - Development-specific loss of cycle expression results in persistant behavioural arrhythmia. *Demonstrating distribution of rhythmic power in restrictively and permissively raised cyc^{01} [elav.cyc]$^{ts\#7}$, run permissively in DD. These conditions have been highlighted as the two temperature conditions repeatedly investigated in Chapters 3, 4 and 5. (F P<0.001***,* M *P<0.001***).*

cyc^{01} [elav.cyc]$^{ts\#7}$ run at 17°C as adults were broadly arrhythmic regardless of developmental condition, defining 17°C as a restrictive condition for adult CYC (Table 3.1)(Figure 3.2a-c, j-l). As CYC is a component of the molecular oscillator, adult-specific loss of CYC is expected to stall behavioural rhythms. Similarly, 23°C is a restrictive adult temperature, in which flies are majority arrhythmic regardless of developmental temperature (Table 3.1)(Figure 3.2d-f, m-o).

Adult temperatures of 29°C are conversely capable of sustaining behavioural rhythms, dependent on developmental temperature. 17 raised→29°C run *cyc^{01} [elav.cyc]^{ts}* are broadly arrhythmic, and have a significantly different distribution of rhythmicities to 23→29°C and 29→29°C raised flies, which appear majority rhythmic (Appendix Table 1)(Table 3.1) (Figure 3.2 f, i, o and r). The rhythmic strength of 17 raised→29°C run *cyc^{01} [elav.cyc]^{ts}* conversely do not differ to flies subsequently kept at 17°C as adults (Appendix Table 1). Thus, whilst 23°C is a restrictive temperature for behaviour during adulthood, it is a developmentally permissive temperature.

A gender specific difference emerges in rhythmic strength for permissively raised and

run 29→29°C flies, (P<0.001***), in which female rhythmicity appears to be stronger than male rhythmicity, although this is not the case at 23→29°C. Combined, our *cyc*^{01} *[elav.cyc]*^{ts} manipulation replicates the dynamics of that in (Goda et al., 2011), in which developmentally restrictive temperatures result in persistent behavioural arrhythmia, whilst developmentally permissive temperature does not cause arrhythmia. Similarly, an adult-specific restrictive temperature results in behavioural arrhythmia. Controls lacking CYC remain arrhythmic in 29→29°C DD (Figure 3.4a)

A short period length observable in 29→29°C flies re-emerges in a *cyc*^{01}/+ background, but disappears in CyO controls lacking *UAS-cyc* (Figure 3.4b,c). Thus, transgenic CYC expression contributes to shortened period (Figure 3.4b,c) irrespective of the presence of endogenous CYC. As CYC is expressed pan-neuronally, expression in non-clock cells may somehow shorten period, but it is more likely that artificially high CYC expression within clock cells is responsible. The Rosbash lab has previously demonstrated a CYC transgene tied to VP16, a viral transcriptional activator, is capable of shortening molecular and behavioural oscillations, and it is likely that the short period in *cyc*^{01} *[elav.cyc]*$^{ts\#7}$ arises via a conserved mechanism (Kadener et al., 2008).

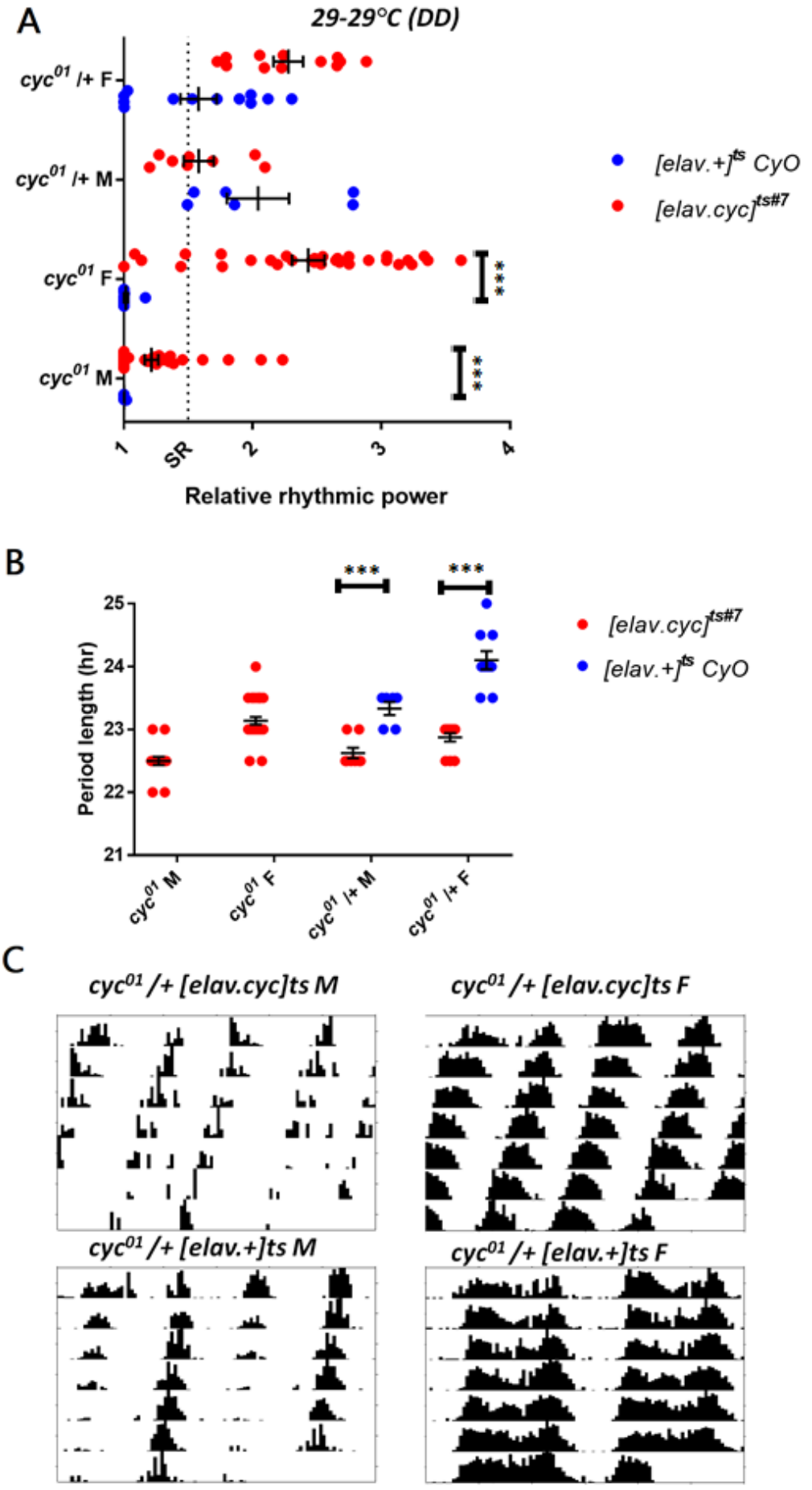
A
29-29°C (DD)
cyc01 /+ F
cyc01 /+ M
cyc01 F
cyc01 M
***
***
1
SR
2
3
4
Relative rhythmic power
[elav.+]ts CyO
[elav.cyc]ts#7
B
***
***
25
24
23
22
21
Period length (hr)
cyc01 M
cyc01 F
cyc01 /+ M
cyc01 /+ F
[elav.cyc]ts#7
[elav.+]ts CyO
C
cyc01 /+ [elav.cyc]ts M
cyc01 /+ [elav.cyc]ts F
cyc01 /+ [elav.+]ts M
cyc01 /+ [elav.+]ts F

Figure 3.4 - Expression of transgenic cycle results in shortened period length. *Panel A shows distribution of rhythmic power in permissively raised 29→29°C cyc^{01} $[elav.cyc]^{ts\#7}$ in DD. Compared are experimental flies (red), with responderless CyO controls (blue), alongside cyc^{01}/+ controls, between which significant differences emerge for both genders. Panel B shows period lengths of 29→29 °C raised cyc^{01} $[elav.cyc]^{ts}$, and Panel C displays median actograms of heterozygous and CyO controls in which divergent periods are evident. Asterisks in Panel B mark that cyc^{01}/+ heterozygous flies expressing UAS-cyc significantly differ in period length to flies which do not express UAS-cyc.*

We thus expand upon previous work with a revitalised cyc^{01} $[elav.cyc]^{ts}$ line, wherein a developmentally restrictive temperature results in persistent behavioural arrhythmia in adulthood.

3.2 – Expression of *cycle* conditionally alters nocturnality in an adult-specific manner

In addition to freerunning arrhythmia, loss of CLK or CYC is known to alter behaviour in LD profiles, though the mechanistic basis of this is not well understood. As cyc^{01} $[elav.cyc]^{ts}$ presents a resource to conditionally study CYC function, it can serve as a tool to give insights to the mechanism underlying nocturnality stemming from CLK/CYC loss. Previous work on the line by a former PhD student in the lab has suggested a stronger developmental repression results in increased nocturnality (Mirowska 2015 thesis), whilst high temperatures, inconveniently the cyc^{01} $[elav.cyc]^{ts}$ permissive state, have been shown to independently increase nocturnal behaviour (Majercak et al., 1999). A previous paper from the Sehgal lab presents a mechanism of indirect CLK/CYC regulation of dopamine, which subsequently interacts with constitutively high CRY in the l-LN_vs to mediate arousal in darkness (Kumar et al., 2012).

We thus studied cyc^{01} and cyc^{01} $[elav.cyc]^{ts}$ behavioural distribution throughout several days of 12:12 LD cycles at 17°C, 23°C or 29°C following a developmental temperature of 17°C, 23°C or 29°C, to determine any differences in nocturnal and diurnal behaviour that emerge (Figure 3.5). Activity counts in day and night phases were binned to generate D/N ratios (Figure 3.6)(Appendix Figure 1).

Most importantly, we demonstrate that 17→23°C and 23→17°C, both arrhythmic in

freerunning conditions (Figure 3.2), display strongly nocturnal (D/N ratio = -0.58±0.04) and strongly diurnal (D/N ratio = 0.44±0.03) profiles respectively, which significantly differ for both genders (P<0.001***) (Figure 3.5, 3.6a & b, Appendix Figure 1). This can be easily explained as only 17→23°C has a developmentally restrictive temperature, and hence development-specific loss of CYC, but not adult-specific loss of CYC is required for nocturnal behaviour. In support of this, 23→17°C cyc^{01} *[elav.cyc]*^{ts} significantly differ to 23→17°C cyc^{01} (P<0.001*** both genders), demonstrating the significance of a permissive developmental temperature on adult LD behaviour, even in the absence of adult CYC (Figure 3.6). All 17°C-raised cyc^{01} *[elav.cyc]*^{ts} demonstrate a mean nocturnal preference, irrespective of adult temperature (Figure 3.6a & b).

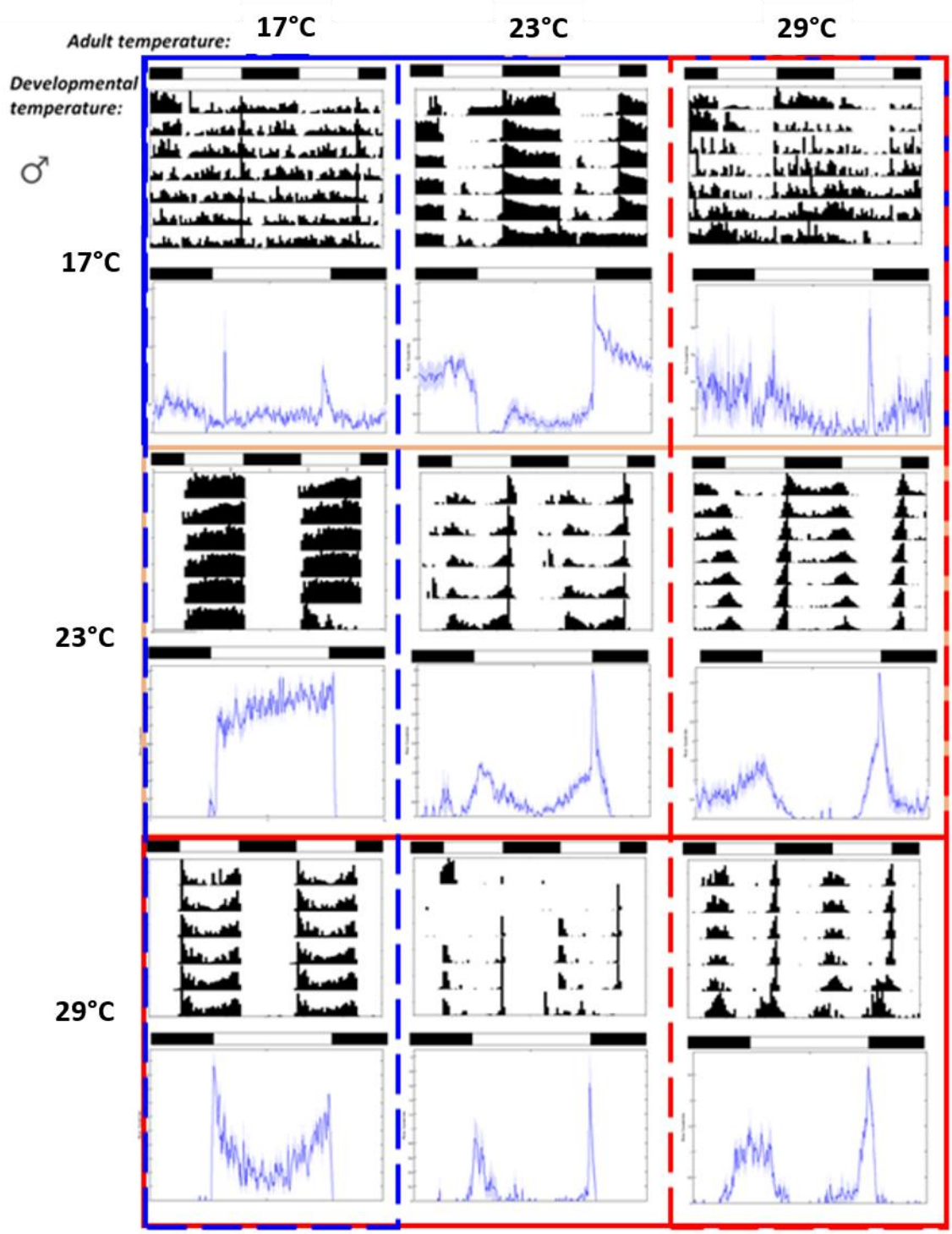

Figure 3.5 - Developmental and adult-loss of cycle expression result in distinct changes in day and night behavioural activity. *Displayed are 12:12 LD actograms and activity profiles for cyc^{01} $[elav.cyc]^{ts}$ males raised (Solid line) and run (Dotted line) at 17°C (Blue), 23°C (Orange) and 29°C (Red). Numbers on the left represent developmental temperature and numbers across the top represent adult temperature, at which the behavioural assay was conducted. Accompanied in Appendix Table 1 is a summation of these values, alongside a graphical representation in Appendix Figure 21. Accompanying females actograms and activity profiles are in Appendix Figure 1.*

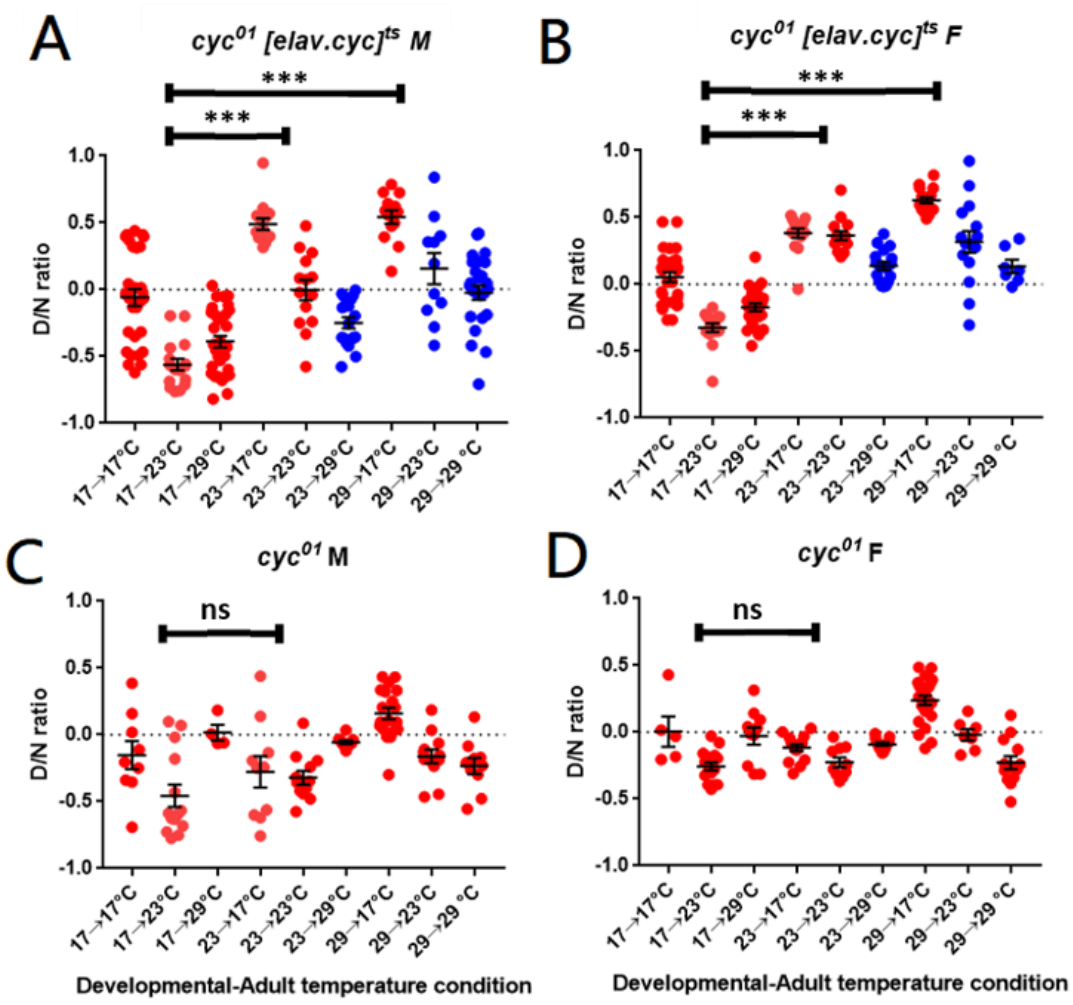

Figure 3.6 - Relative day and night activity differs dependent on temperature, and presence of cycle*. Panel A and B show 12:12 LD D/N ratio of cyc^{01} [elav.cyc]^{ts} for males and females respectively. Panels C and D show 12:12 LD D/N ratio of cyc^{01} for both genders raised and run at 17°C, 23°C or 29°C. Results are ordered first by developmental temperature, and then adult temperature. Blue reflects a behaviourally rhythmic freerunning condition, whilst red identifies conditions that were arrhythmic in freerunning conditions. Identifiable in cyc^{01} [elav.cyc]^{ts} is an increase in nocturnality with rising adult temperature, irrespective of developmental condition, and greater nocturnality correlating with a lower developmental temperature. This principle disappears in cyc^{01}, and is likely related to temperature regulation of ectopic CYC expression.*

The second point of note is crepusularity, the presence of distinct morning and evening components appears qualitatively more pronounced in rhythmic flies, as expected (Figure 3.5, Appendix Figure 1).

cyc^{01} demonstrate a nocturnal preference across many temperatures, however under certain conditions, such as 29→17°C, these can become strongly diurnal, and female *cyc*^{01} lack a notable D/N preference across temperatures (Figure 3.6c & d). Therefore,

assays of nocturnality utilising the TARGET system have to account for subtle to non-existant nocturnal phenotypes at certain temperatures.

cyc^{01} *[elav.cyc]*^{ts} D/N ratio trends strongly with adult temperature, irrespective of developmental temperature, appearing more nocturnal at higher temperatures. Qualitatively, this adult-responsiveness is more noticeable in *cyc*^{01} *[elav.cyc]*^{ts} than *cyc*^{01} (Figure 3.6). Raising at restrictive developmental temperature of 17°C appears to result in stronger nocturnal preference, relative to higher developmental temperatures, which is not evident in *cyc*^{01}, indicating an effect of development-specific CYC loss, and suggesting that nocturnality may correlate with freerunning arrhythmicity due to developmental CYC loss.

Combining our interpretation of LD data with DD phenotypes, *cyc*^{01} *[elav.cyc]*^{ts} flies which are arrhythmic due to development-specific CYC loss appear nocturnal, whilst flies which are arrhythmic due to adult-specific CYC loss appear diurnal, in some instances with siesta, but no anticipatory behaviour (Figures 3.1, 3.2, 3.4, 3.5). Rhythmic flies, 23→29°C and 29→29°C conversely do show morning and evening anticipatory behaviours, preceding changes in light condition, suggestative of function (Figure 3.5).

Unfortunately, the strong diurnality of 29→17°C *cyc*^{01}, and weak diurnal preference of some 17→17°C *cyc*^{01} *[elav.cyc]*^{ts} hampers the conclusion that developmental CYC loss is solely capable of causing nocturnality, as both lines should lack developmental CYC. It is parsimonious to say developmental CYC loss primes nocturnal behaviour whilst adult-specific CYC loss does not, though a potential for nocturnal behaviour through developmental CYC loss can be overridden by adult temperature.

3.3 - Developmental loss of *cycle* results in a *cyc*^{01}-like behavioural profile in light-dark cycles, even in cases of adult *cycle* re-introduction

The assessment of LD profiles (Figures 3.5, 3.6 & 3.7) suggest that a combination of developmental and adult CYC levels, alongside independent temperature effects, have influence on nocturnal behaviour, yet these experiments do not determine if the effect is due to a temperature change at a certain developmental timepoint, or a temperature change prior to the point of recording behaviour, where a prior temperature in adulthood may affect behaviour.

To further separate the effect of developmental temperature from the effect of the TARGET system, *cyc^{01} [elav.cyc]^{ts}* were restrictively raised at 17°C, moved to a 29°C permissive condition as adults, and moved back to a 17°C restrictive condition (Figure 3.9). Significant differences in D/N ratio uniformly occur between permissive and restrictive adult temperature for genotypes and conditions, independent of endogenous or ectopic CYC presence or absence (Appendix Table 3.2).

For the condition 17→29-17°C (Figure 3.7a), *cyc^{01} [elav.cyc]^{ts}* flies in the 17°C phase show a diurnal preference, like in 29→17°C (Figure 3.5, 3.6), and unlike the lack of overall light preference in 17→17°C (Figure 3.5, 3.6), suggests the influence of prior CYC expression, either developmental or adult, in promoting diurnality. Supporting this, in the absence of CYC expression, as in *cyc^{01}*, (Figure 3.7c), the inability to re-express CYC in adulthood correlates with a lack of subsequent diurnality at 17°C. (Figure 3.7c), as is the case with *cyc^{01} [elav.cyc]^{ts}* in 17→17°C (Figure 3.5, 3.6).

As the 29°C phase of 17→29-17°C hypothetically reintroduces CYC expression in *cyc^{01} [elav.cyc]^{ts}* flies, yet they show strong behavioural nocturnality (Figure 3.7a, Figure 3.8a), we can suggest that nocturnal behaviour of *cyc^{01}* is primed by developmental loss of CYC, but potentially modulated by adult CYC expression and temperature.

Despite superficial similarity of D/N ratio, activity profiles of restrictively raised *cyc^{01} [elav.cyc]^{ts}* are notably different to other permissively raised or heterozygous flies, lacking obvious morning and evening activity associated with normal clock cell function, and lacking an overall crepuscular preference (Figure 3.8). Thus, despite rescue of D/N ratio, adult-specific CYC re-introduction fails to rescue a wt-like activity profile, potentially due to developmental defects, and we can suggest developmental loss of CYC disrupts the mechanisms involved in generating anticipatory behaviours.

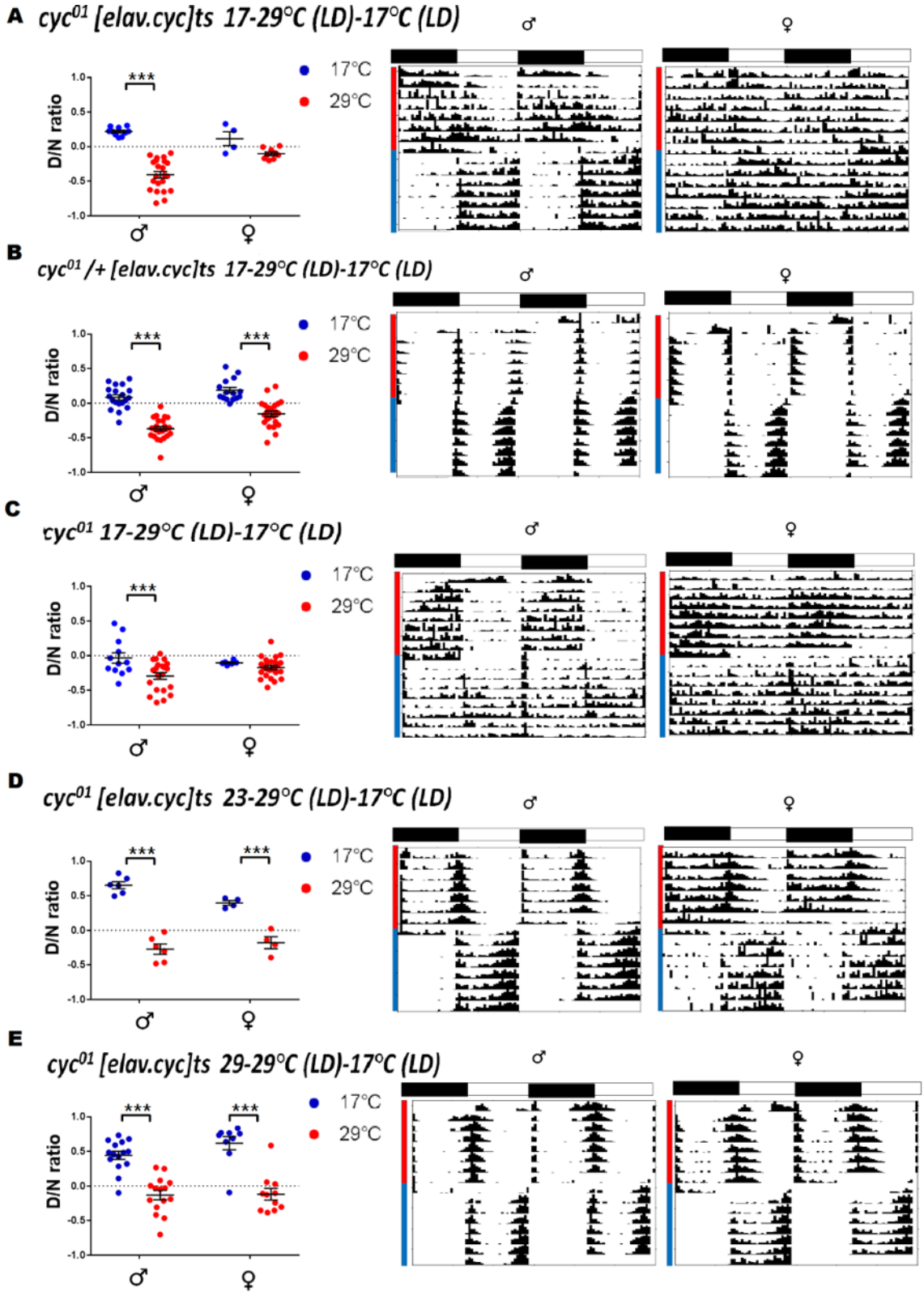

Figure 3.7 - Day and night behavioural activity levels are altered dependent on development- and adult expression of cycle. *D/N ratios and accompanying actograms for restrictively or permissively raised flies run permissively at 29°C LD, followed by restrictive 17°C LD. Accompanying statistics are found in Appendix Tables 2 and 3. Activity profiles for each respective condition are present in Figure 3.8. Panel A displays restrictively raised cyc^{01} $[elav.cyc]^{ts}$, Panel B displays it's heterozygous counterpart whilst Panel C displays cyc^{01}. Panels D and E show permissively-raised cyc^{01} $[elav.cyc]^{ts}$.*

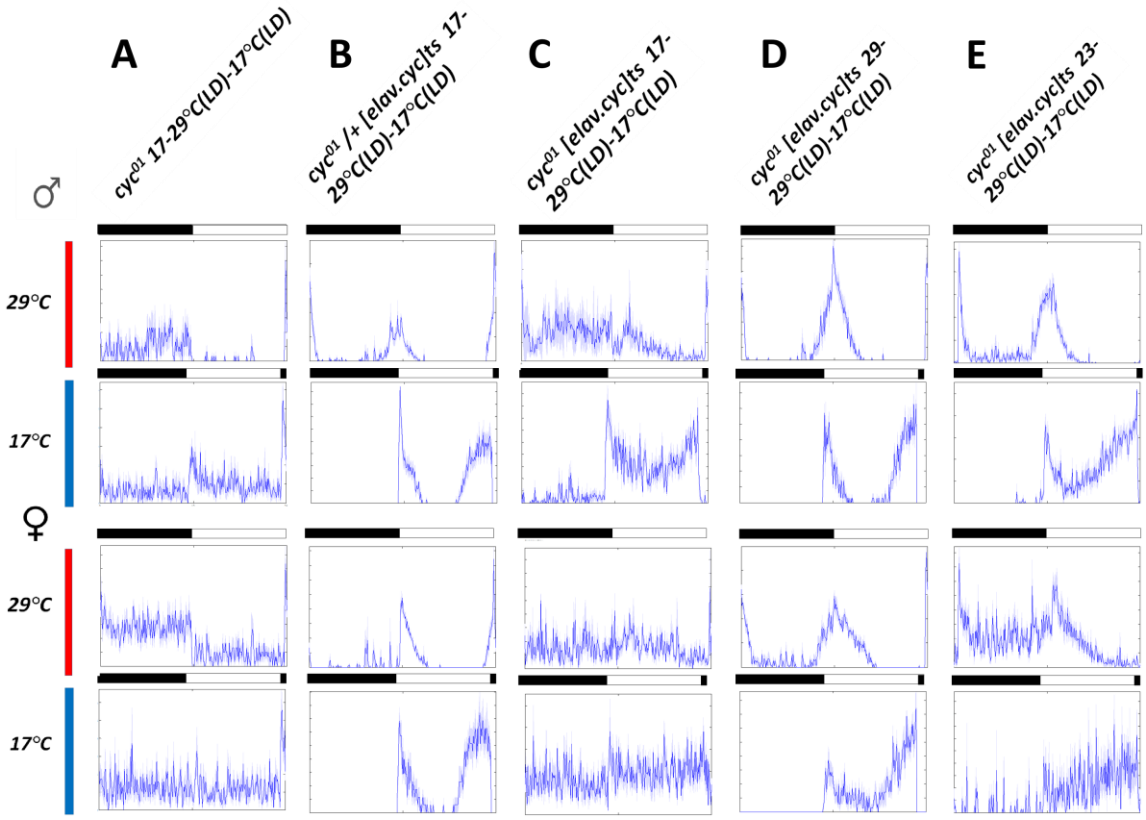

Figure 3.8 – Activity profiles in light-dark cycles following modulation of adult levels of cycle. *Activity profiles for each respective genotype and temperature condition from Figure 7. Panels A-E refer to analagous genotypes in Panels A-E of Figure 3.7*

3.4 - Spatial reintroduction of *cycle* in specific clock neuron clusters reveals expression within the PDF cells promotes diurnality, whilst loss within the PDF cells promotes nocturnality

We are thus aware that developmental depletion of CYC primes a state enabling nocturnal behaviour, without yet speculating on the underlying mechanism, and we therefore wished to spatially map the requirement for CYC loss in generating nocturnality, from which we could identify neurons composing, or contributing to the development of, a nocturnal behavioural circuit. Data from the Sehgal lab suggests that CLK/CYC loss may increase l-LN$_v$ CRY levels, but in addition, CLK/CYC loss within an unknown cell subset has a role in upregulating dopamine, so we hypothesised CYC rescue in either cluster may reduce nocturnal preference (Kumar et al., 2012). As raised above, the potential exists for developmental CYC to prime either CRY or dopamine levels.

At permissive conditions, 29→29°*C*, *cyc*^{01} remains relatively nocturnal, so this high

temperature condition can be used as a baseline to assay spatial CYC requirement, relative to the M-and E-peak possessing crepuscular behaviour of *cyc^{01} [elav.cyc]^{ts}* (Figure 3.6).

We first attempted rescue of *cyc^{01}* with *UAS-cyc* using the *Pdf-gal4* driver, either raised permissively at 29°C or restrictively at 17°C, and behaviour was then assayed in 29°C LD cycles. Permissively raised *cyc^{01} [Pdf.cyc]^{ts}* shows a crepuscular profile, with a strong and notable morning anticipation, but no evening anticipation, merely a lights-off startle response (Figure 3.9). Heterozygous controls with endogenous CYC similarly lack anticipation, but display a prolonged activity following lights-off. When restrictively raised, this morning anticipation disappeared, and the waveform was featureless save for a lights-off startle response (Figure 3.9).

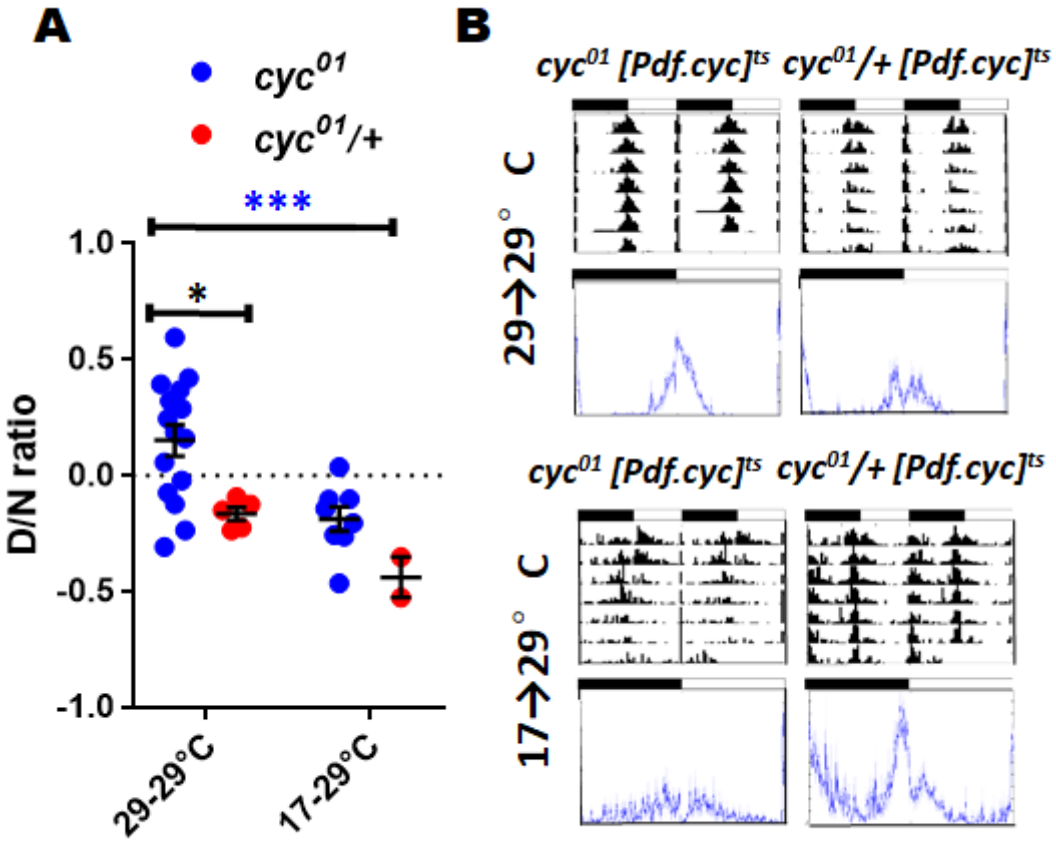

Figure 3.9 - Expression of cycle specifically within PDF cells is sufficient for anticipatory behaviours at night. *Panel A shows D/N ratio of cyc^{01} [Pdf.cyc]^{ts} flies raised restrictively or permissively and run at a permissive 29°C, alongside cyc^{01}/+ heterozygous controls, demonstrating that rescue of CYC rescues nocturnal preference.*

Panel B shows LD actograms and activity profiles for the above manipulation, with visible morning anticipation following PDF-cell specific rescue of CYC.

Spatial mapping with *elav-gal4* and *Pdf-gal4* drivers at restrictive and permissive developmental temperatures has established an important paradigm as to clock cell functionality. 29→29°*C* cyc^{01} *[Pdf.cyc]*^{ts} has morning anticipation but no evening anticipation, which is expected to require an oscillator in evening cells (Stoleru et al., 2004)(Figure 3.9), suggesting a developmental requirement for PDF+ve cell CYC for morning anticipation.

We performed the reverse manipulations, expressing CYC pan-neuronally whilst reducing transgene expression in PDF cells with *Pdf-gal80*, a genotype referred to as cyc^{01} *[elav-Pdf80.cyc]*^{ts}. In this manipulation, harbouring a rhythmic oscillator everywhere except the PDF cells resulted in similarly crepuscular behaviour in LD, but with mild nocturnal preference (Figure 3.10). In males, this significantly differs with the D/N ratio of cyc^{01} *[elav.cyc]*^{ts} (P=0.008**), but not cyc^{01} flies (P=0.939), whilst females are intermediate between the D/N ratio of either condition (Appendix Table 32). The crepuscular nature of the behaviour, including prominent morning anticipation suggests that although these flies are majority arrhythmic in DD (Chapter 4), an unknown property of the clock driving morning anticipation is still intact.

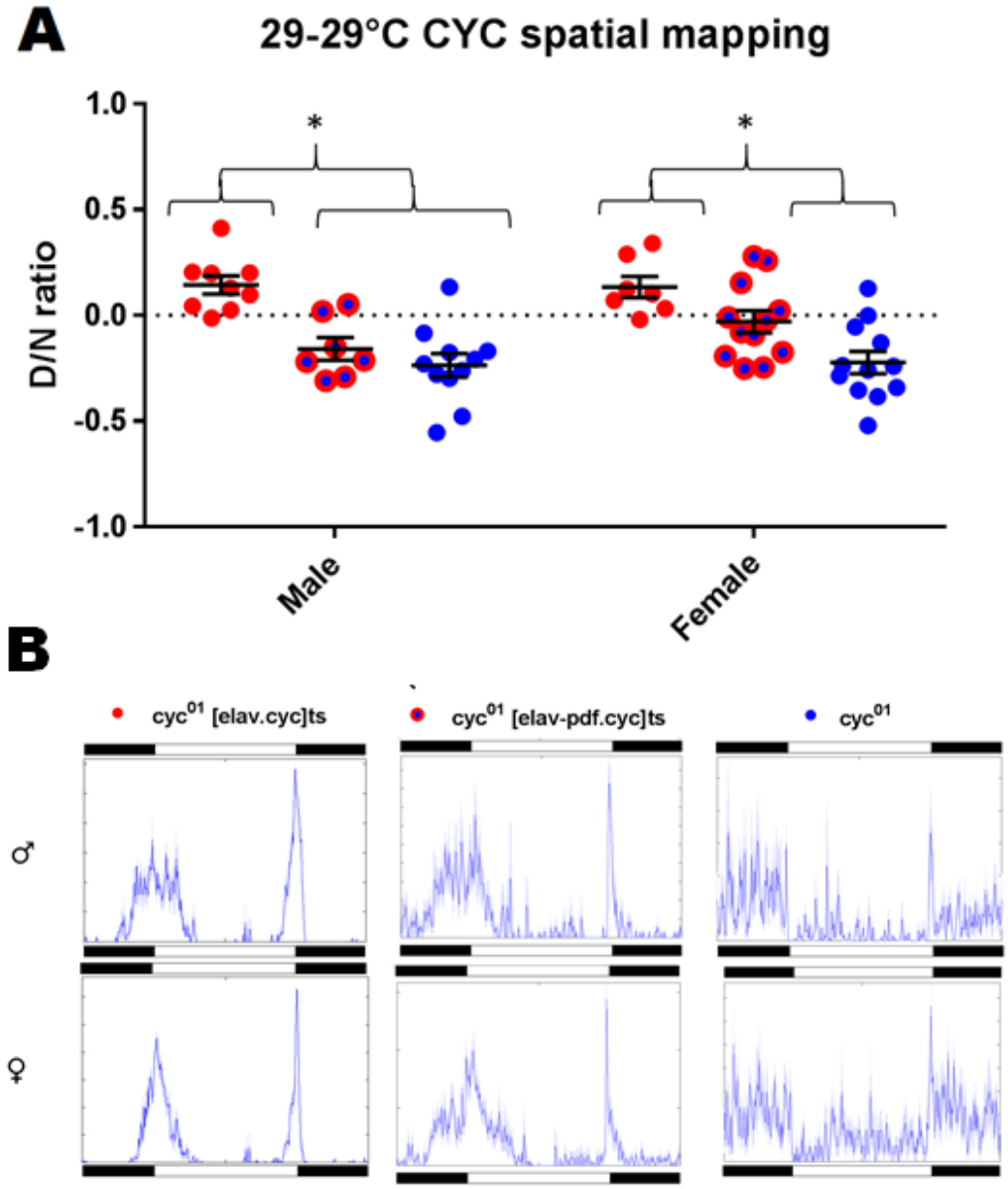

Figure 3.10 - Loss of cycle within the PDF cells impacts the distribution of day and night behavioural activity. *Panel A shows D/N spatial mapping 29→29 °C, demonstrating diurnal preference of cyc^{01} [elav.cyc]^{ts} is limited by abrogating CYC re-expression within PDF cells with Pdf-gal80, producing an intermediate phenotype to cyc^{01}. In males, cyc^{01} [elav.cyc]^{ts} significantly differs to cyc^{01} [elav-Pdf80.cyc]^{ts} and cyc^{01}, which do not differ between themselves. In females, cyc^{01} [elav-Pdf80.cyc]^{ts} doesn't significantly differ to either group. Panel B shows activity profiles to visualise relative differences between genotypes. Nocturnal activity in cyc^{01} [elav-Pdf80.cyc]^{ts} is clearly increased, yet much of this is weighted towards the morning.*

Attempts to further spatially map rescue with cyc^{01} [TUG.cyc]^{ts} were marred by the ineffectiveness of the *tim-UAS-gal4* driver on a cyc^{01} background, as *tim* transcription is directly regulated by CLK/CYC (Figure 3.11). Expression of CYC purely in the s-LN_vs with *R6-gal4*, or evening cells with the *R78G02-gal4* driver both failed to rescue

crepuscularity or activity profiles (Figure 3.11).

However, by comparison of the similarly crepuscular *cyc^{01} [elav-Pdf80.cyc]^{ts} and cyc^{01} [Pdf.cyc]^{ts}*, it is evident that loss of CYC within PDF cells results in higher nocturnal activity (P<0.001***) that does not significantly differ to *cyc^{01}*, whilst CYC expression solely within PDF cells results in a diurnal D/N ratio (Figure 3.11).

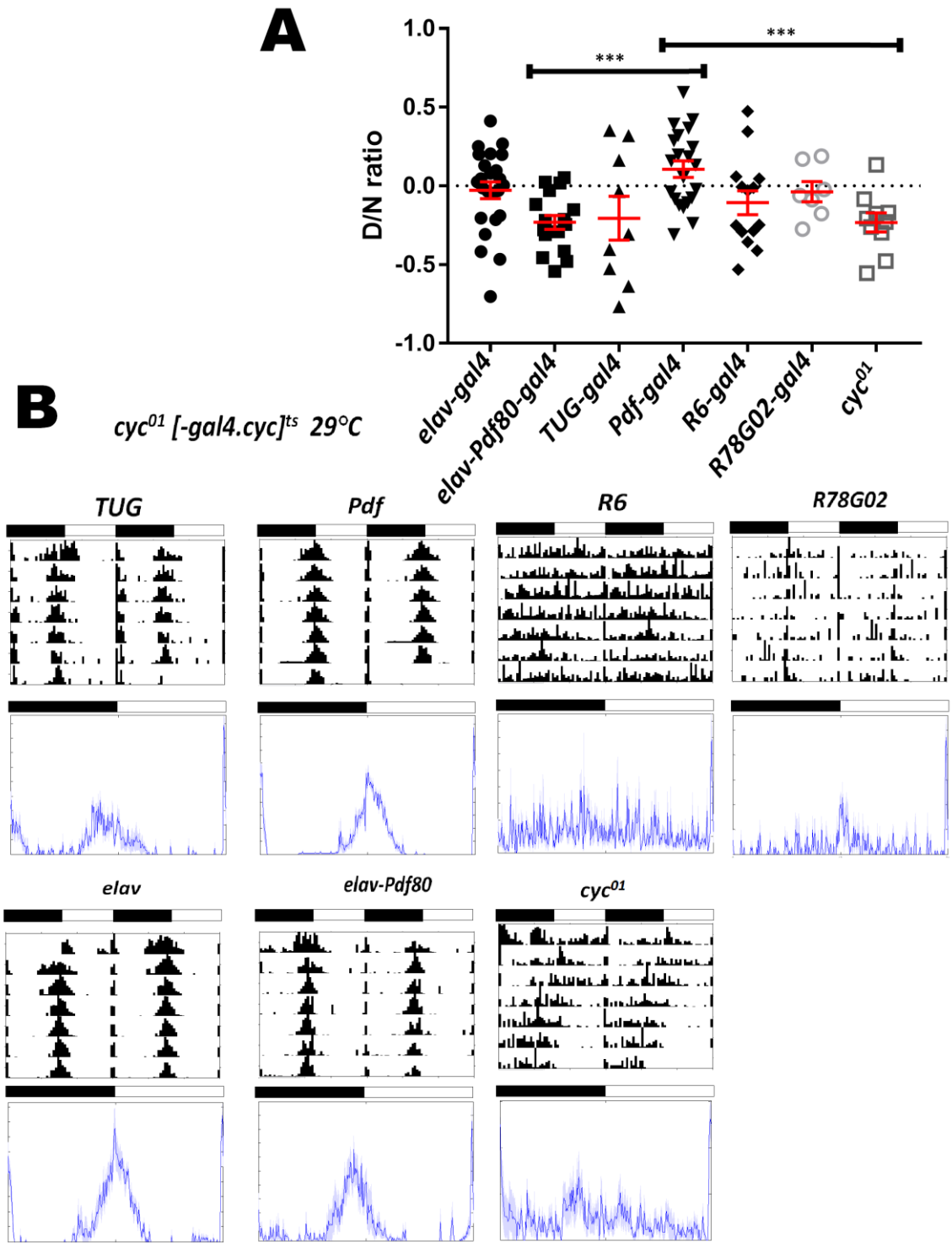

Figure 3.11 - cycle expression in either PDF-expressing or non-PDF cells can generate anticipatory behaviour, but result in altered distribution of day and night activity.

*Panel A shows D/N ratio and Panel B shows actograms and activity profiles at 29°C LD following spatial mapping re-introduction of CYC using cyc^{01} [n.cyc]^{ts} with various driver lines. Lines were consitutively raised and run at 29°C so as to assay purely the effect of different spatial patterns of CYC expression. Pan-neuronal or PDF-specific rescue of CYC trends towards diurnality, significantly differing elav-Pdfgal80 rescue (P<0.001***) or cyc01 (P<0.001***), which appear to trend towards nocturnality.*

In summation, we can state that CYC induction restricted to the PDF cells can induce a crepuscular profile with a mild diurnal preference, whilst loss of CYC specific to the PDF cells induces a crepuscular profile which leans towards nocturnality. The regulation of nocturnality by presence of CYC in other clock cell groups appears to be essential, but undefined. Development-specific CYC loss in both PDF and non-PDF cells is sufficient to cause nocturnal behaviour, whereas maintenance in one of these two subsets is sufficient to preserve a crepuscular adult activity profile

The influence of temperature, developmental CYC presence, and genetic background on nocturnality limits the interpretability of studies in this topic using conditional CYC expression, and thus we wished to use simpler genotypes to continue our investigation of the basis of nocturnality.

3.5 – Nocturnal behaviour of *cyc^{01}* flies is not due to aberrant PDF cell exciteability or signalling

In order to extend prior findings of (Kumar et al., 2012) regarding the nocturnality of *Clk^{Jrk}*, also observable in *cyc^{01}*, we studied the impact of dopaminergic signalling on *cyc^{01}* nocturnality, and identified that a "silencing" of dopaminergic neurons through tetanus toxin expression, of genotype *ple>TeTxLC; cyc^{01}* led to a decrease in nocturnality, and a loss of light preference in these arrhythmic flies, whilst dopamine silencing had comparably little effect in *cyc^{01}*/+ controls (Figure 3.12). Day activity counts do not significantly differ with *cyc^{01}* (M P=0.792, F P=0.166), and nightime activity is markedly lower (M P=0.140, F P<0.001 ***), demonstrating that dopamine release specifically influences nocturnal hyperactivity in *cyc^{01}* LD profile, but does not contribute to loss of day activity (Appendix Figure 9).

Though very similar to manipulations performed by the Sehgal lab, our replication of this work solidifies that dopaminergic signalling is increased at night, leading to greater arousal, and whilst their model suggests l-LN$_v$-specific CLK/CYC is necessary for upregulating CRY, the spatial requirement of CLK/CYC in silencing night-time DA contribution is unknown (Kumar et al., 2012). Certainly, our spatial mapping of CYC requirement indicates that genotypes with CYC within the PDF cells appear more

diurnal, though this is due largely to consolidation of activity within a morning-specific activity peak, and any change in intrinsic light responsiveness is masked by clock-driven activity (Figures 3.8 & 3.11 above). The Sehgal lab additionally states that an increase in dopaminergic signalling is solely capable of inducing a Clk^{Jrk}/cyc^{01}-like LD profile, though we failed to replicate this through exciting dopaminergic cells by expression of a bacterial sodium channel with the *Ple-gal4* driver, which includes the sequence upstream of the *Drosophila* tyrosine hydroxylase gene, to specifically drive expression in dopaminergic cells (Friggi-Grelin et al., 2003). This manipulation is termed *ple>NaChBac* (Figures 3.12 & 5.28)(Kumar et al., 2012).

To determine if PDF signalling input contributed to nocturnality, perhaps through signalling to dopaminergic PAM neurons, as has been established (Vaccaro et al., 2017), we studied nocturnality in $Pdfr^{5304}::cyc^{01}$ flies, incorporating a loss of function mutant in the sole PDF receptor. $Pdfr^{5304}::cyc^{01}$ flies remained nocturnal, and do not significantly differ compared to PDFR+ve controls in D/N ratio, eliminating a positive role of PDF signalling in maintaining nocturnality, potentially through dopaminergic misregulation (Figure 3.12).

The untested assumption of (Kumar et al., 2012), based on a substantial body of work relating to the l-LN_vs (Sheeba et al., 2008a, Shang et al., 2008), is that the l-LN_vs are inherently arousal promoting cells, and the mechanism of increased CRY at night will lead to an increase in nighttime firing of these cells. Indeed, the paper shows that l-LN_v specific CRY within Clk^{Jrk} is sufficient for loss of daytime activity, and it is known these cells are responsive to dopamine (Shang et al., 2011, Lee et al., 2013). The Rosbash and Holmes groups show that constitutive l-LN_v activation in LD cycles shifts the distribution of activity in wild-type flies to greater nocturnality (Sheeba et al., 2008a, Shang et al., 2008). To further determine the extent to which the nocturnality we observed in cyc^{01} flies was predicated by alterations in PDF cell firing due to CYC loss, we sought to manipulate these with *Pdf-gal4>UAS-Kir2.1;* cyc^{01}, *Pdf-gal4>UAS-TeTxLC;* cyc^{01} and *Pdf-gal4>UAS-NaChBac;* cyc^{01} (Figure 3.12).

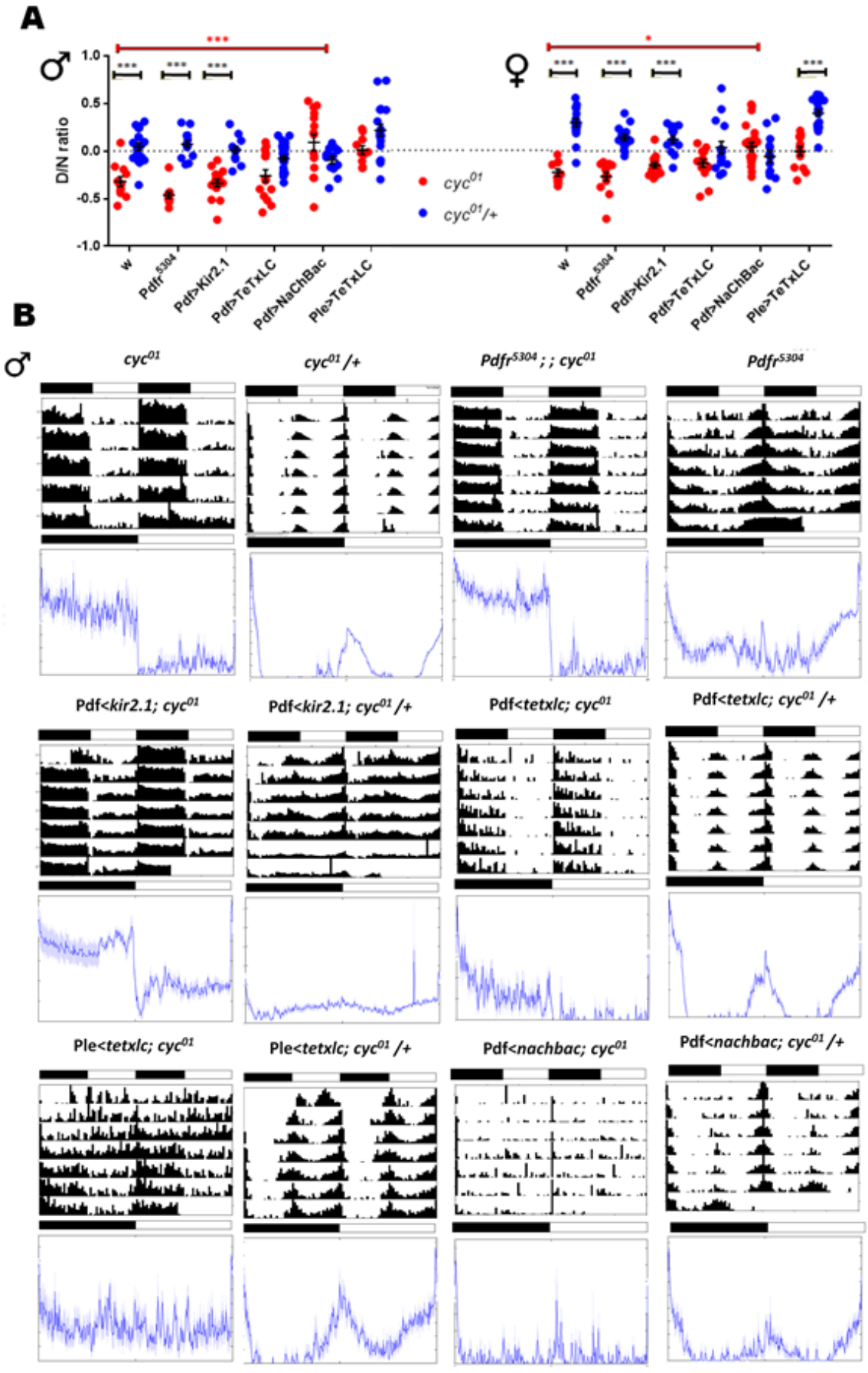

Figure 3.12 - Nocturnal behaviour in cycle mutants is independent from PDF signalling but dependent on dopaminergic neurons. *D/N ratios, actograms and activity*

profiles for cyc^{01} and cyc^{01}/+ lines compiled with disruptions to PDF cell function or signalling, or dopaminergic cell function. Panel A shows D/N ratios for various conditions. Loss of PDF signalling or silencing of PDF cells does not ameliorate the significant difference in nocturnality between cyc^{01} and heterozygous controls. The nocturnality of cyc^{01} can be significantly reduced by hyperexciting PDF neurons through expression of the NaChBac channel. Panel B shows median actograms and activity profiles for males. Full statistics are available in Appendix Table 4.

Whilst we do not dispute the molecular mechanism proposed by (Kumar et al., 2012), silencing PDF cells on a cyc^{01} background fails to significantly change D/N levels (Appendix Table 3)(Figure 3.12). *Pdf> TeTxLC* has underwhelming effects on freerunning rhythms, hypothetically as PDF secretion may involve tetanus-resistant SNARE complexes, so a lack of clear phenotype is not unexpected (Kaneko et al., 2000, Blanchardon et al., 2001). *Kir2.1,* which elicits dramatic phenotypes in other conditions (Figure 5.2), similarly does not alter the cyc^{01} behavioural profile, coalescing to the argument that excitation of these cells does not contribute either to bolstering nocturnal hyperactivities, or in repressing activity during the day (Figure 3.12). Potentially, though this is untested, PDF cell firing may be already lowered on a cyc^{01} background, hence a failure to generate an altered phenotype.

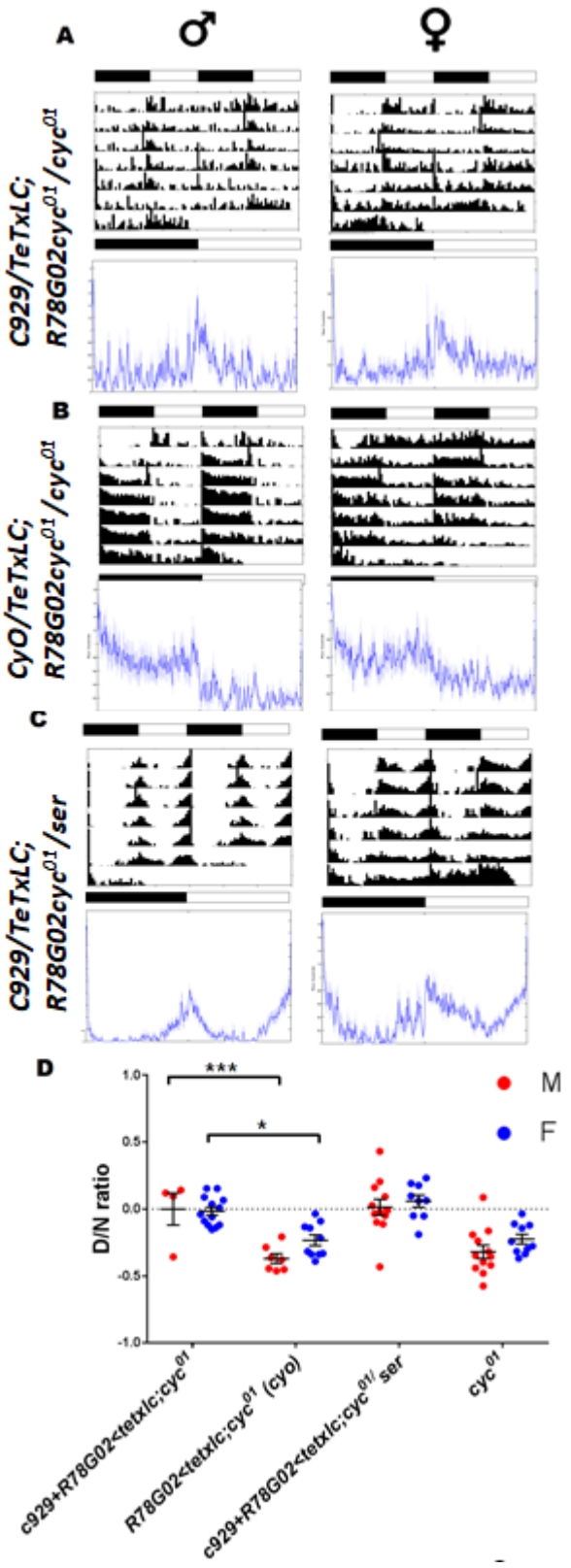

Figure 3.13 - Tetanus toxin expression within peptidergic neurons reduces nocturnal behaviour stemming from loss of cycle. *Panel A demonstrates actograms and activity profiles of cyc^{01} with concurrent silencing of peptidergic and evening cells of genotype c929-gal4/UAS-TeTxLC; R78G02-gal4cyc^{01}/cyc^{01}. Panel B shows undriven controls and Panel C shows lines with heterozygous cyc^{01}. Panel D shows D/N ratios for the*

respective conditions. Evident is a significant effect of silencing specifically peptidergic cells on nocturnal behaviour, which is not the case with Pdf-gal4 driver (Figure 3.12).

We were intrigued to further delineate this function. As previous studies show stronger phenotypes with the *c929-gal4* driver than the *Pdf-gal4* driver, which simultaneously bypasses the s-LN_vs, we wished to silence purely these cells, but found *Kir2.1* expression was lethal (Sheeba et al., 2008a)(Kumar et al., 2012). This was also the case when expressed in the s-LN_v specific *R6-gal4* driver (Data not shown).

We attempted *TeTxLC* expression with the *c929-gal4* driver, alongside *R78G02-gal4*, though it is clear from controls that *R78G02-TeTxLC* expression fails to alleviate nocturnal behaviour. *c929>TeTxLC* convincingly removes nocturnal preference from cyc^{01} flies, implicating peptidergic cell signalling in nocturnal hyperactivity (Figure 3.13). *c929-gal4* driven manipulations exhibit a much greater change in nocturnal preference than *Pdf-gal4*, which is apparent in phenotypes generated both by the Sehgal and Holmes labs, in hyperexcitation or CRY-reintroduction respectively (Sheeba et al., 2008a) (Kumar et al., 2012). Neither paper utilises a *Pdf-gal80* control to ensure *c929-gal4* phenotypes are purely l-LN_v mediated, and it is unfortunate our genotype would make such a control difficult. As PDF cell silencing fails to influence nocturnal hyperactivity, this data is hard to reconcile, and suggests that phenotypes we see, alongside those of other groups may involve clock-ve peptidergic cells. Peptidergic cells have been implicated in controlling light responses, so further study would be necessary to draw firm conclusions (McNabb et al., 2008, Yamanaka et al., 2014).

A more valuable experiment therefore is the opposing manipulation of constitutive PDF cell hyperexcitation, to identify if a repressive effect of increased PDF cell firing can prevent a nocturnal behavioural profile. D/N ratio following PDF cell hyperexcitation with *NaChBac* does not differ between cyc^{01} and cyc^{01}/+, and characteristic nocturnal preference is not attainable in homozygotes, suggesting a loss of PDF firing, likely at night, may contribute to nocturnal hyperexcitation (Figures 3.12 & 3.14). This would indicate PDF cells can function as an activity repressor, a novel function not observable following PDF cell hyperexcitation alone, but potentially CYC loss results in alterations at the circuit-level, allowing novel excitatory effects to manifest.

D/N ratio of *Pdf>NaChBac;* cyc^{01}/+ significantly differs to wild-type in females

(P<0.001***), but not males (P=0.093), and significant differences do not occur when compared to other heterozygote lines, so we cannot conclude if PDF-cell hyperexcitation alone is sufficient to make flies more nocturnal, in a mechanism independent of PDF-mediated nocturnality, as has been suggested by other groups (Sheeba et al., 2008).

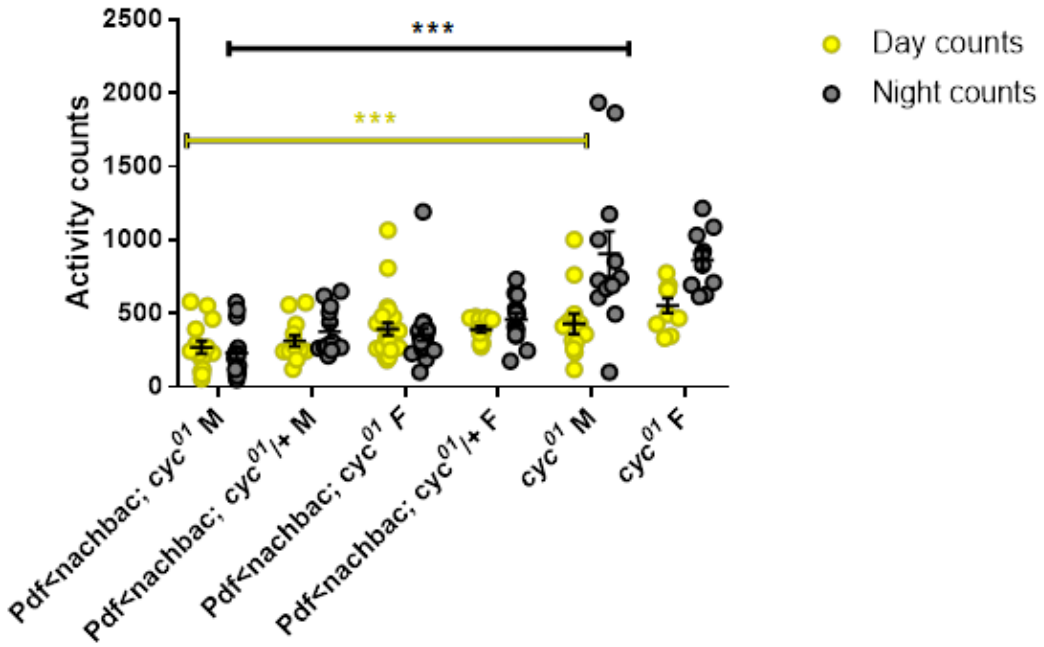

Figure 3.14 - PDF cell hyperexcitation reduces both day and night activity levels. *Relevant to Figure 3.12, comparing night and day activity counts following PDF cell hyperexcitation with NaChBac on a cyc^{01} background. PDF cell hyperexcitation significantly increases both day and night activity counts relative to cyc^{01} (M P<0.001 ***, F P<0.001***).*

We are confident in saying that neither PDF signalling, nor PDF cell excitation drives aspects of the nocturnal activity profile, though dopaminergic and potentially peptidergic inputs may be involved. Our data indicates PDF cell firing must be reduced in order to achieve a *cyc^{01}*-like LD profile.

3.6 – Nocturnal behaviour following loss of *cycle* is dependent on light wavelength during the day and persists following the ablation of PDF-expressing cells

It is also suggested that the nocturnality of *Clk^{Jrk}* is CRY-dependent, and we thus decided to run *cyc^{01}* flies in 12:12 Red-light dark cycles (RD), in which CRY would

hypothetically remain inactive (Kumar et al., 2012). *cyc*^{01} lose their nocturnal preference in RD (M: P<0.001***, F: P=0.027 *), confirming that red-light-specific visual system stimulation of the clock circuit cannot promote nocturnality in the manner that CRY activation, via white-light stimulation, can (RD data contributed by C. Hurdle, analysis performed by myself)(Figure 3.15). This data, paired with our results, suggests that CRY, in an unknown cell cluster, is somehow capable of exerting an effect on behaviour in a PDF independent manner. In mammals, diffusion neurotransmission is a possible mechanism, though this has not been reported in *Drosophila* (Bach-y-Rita, 1993).

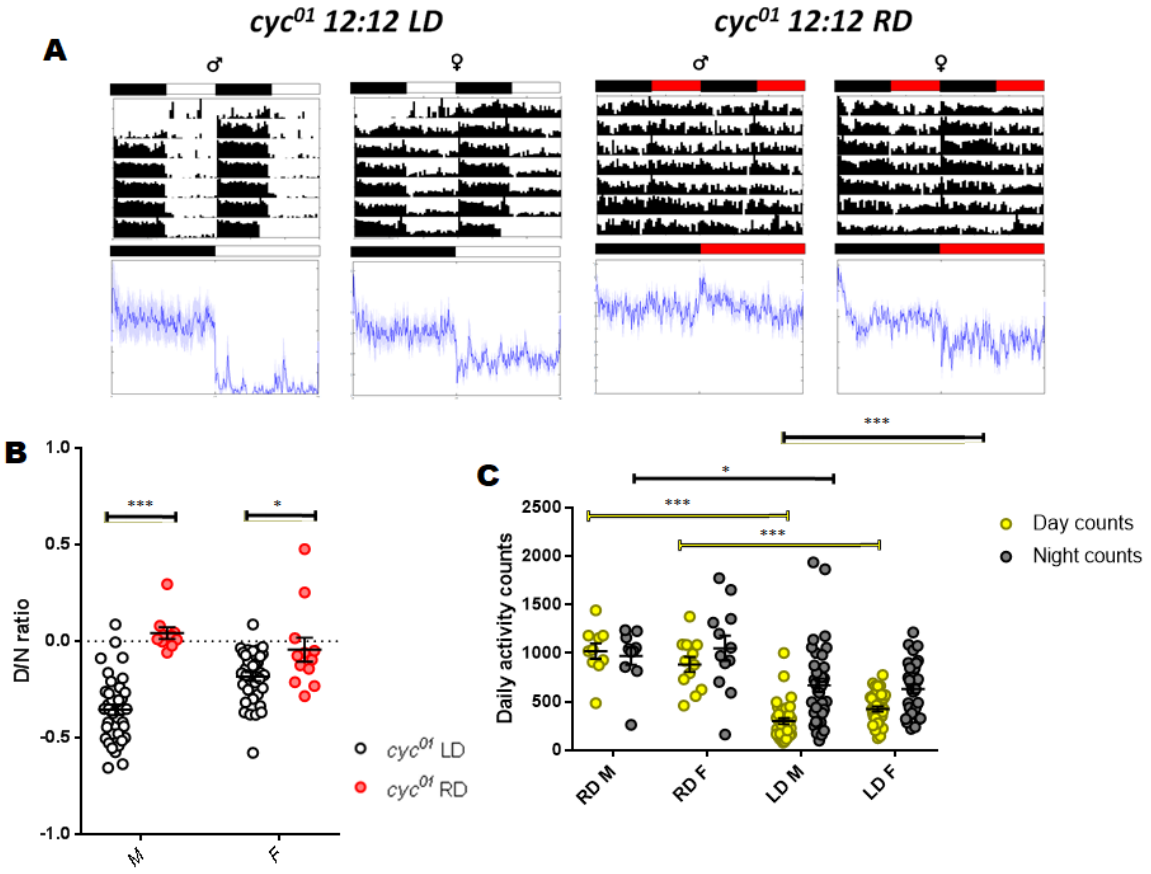

Figure 3.15 - Increased nocturnal behaviour following loss of cycle is primed by white-light exposure during the day*. Panel A shows median actograms for cyc*^{01} *males and females in 12:12LD and RD. Panel B shows D/N ratios for this dataset, in which significant differences emerge between conditions for both males (P<0.001***) and females (P=0.027 *). Panel C shows activity counts in light and dark, in which both night and day activity counts are significantly reduced in LD compared to RD. RD flies raised and run by Charlie Hurdle.*

Both night and day activity is lessened in LD relative to RD (Figure 3.15)(♀ day P<0.001***, ♂ day P<0.001***, ♀ night P<0.001***, ♂ night P=0.036 *). Taking this

result in conjunction with the evidence in (Kumar et al., 2012), we therefore conclude CRY activation is capable of exerting a repressive effect on locomotor activity behaviour in its active state which may indirectly repress nocturnal hyperactivity, a novel CRY function. We demonstrate in Appendix Figure 9 that limiting nocturnal hyperactivity does not result in increased daytime behaviour, suggesting there is no homeostatic response following a condtion that either represses activity or rest.

As PDF cell silencing does not impact cyc^{01} LD profile (Figure 3.12), we ablated PDF cells on a cyc^{01} background with *UAS-hid*, to determine if PDF cells contributed to nocturnality in a manner independent of electrical silencing. To our immense surprise, constitutive ablation with the *Pdf-gal4* driver lessened, but did not remove, an overall nocturnal preference (Figure 3.17). Notable lights-on inactivity was still exhibited, though nocturnal hyperactivity decreased throughout the night. Of 42 immunostained hemispheres, only 3 retained PDF+ve l-LN_vs, staining 1, 4 and 4 cells respectively, and no PDF+ve s-LN_vs were identifiable, confirming the effectiveness of the ablation.

This result suggests that nocturnal preference may be due in part to CYC loss in other cells, and suggests that nocturnal activity is seperable from intrinsic, immediate light-responses of l-LN_vs. Both PDF+ve and PDF-ve cell CYC rescue was capable of disrupting this phenotype (Figures 3.9 & 3.10), so we could hypothesise that functional l-LN_vs could override the intrinsic nocturnality of the CYC-ve remainder of the circuit, though an alteration of PDF cell firing due to CYC loss prevents this, and in the absence of information from the PDF cells, nocturnality is propagated by PDF-ve cells. The difference in D/N ratio significant between cyc^{01} and cyc^{01}/+ for both males (P=0.014*) and females (P<0.001***), and differences in activity profile are immeadiatly obvious.

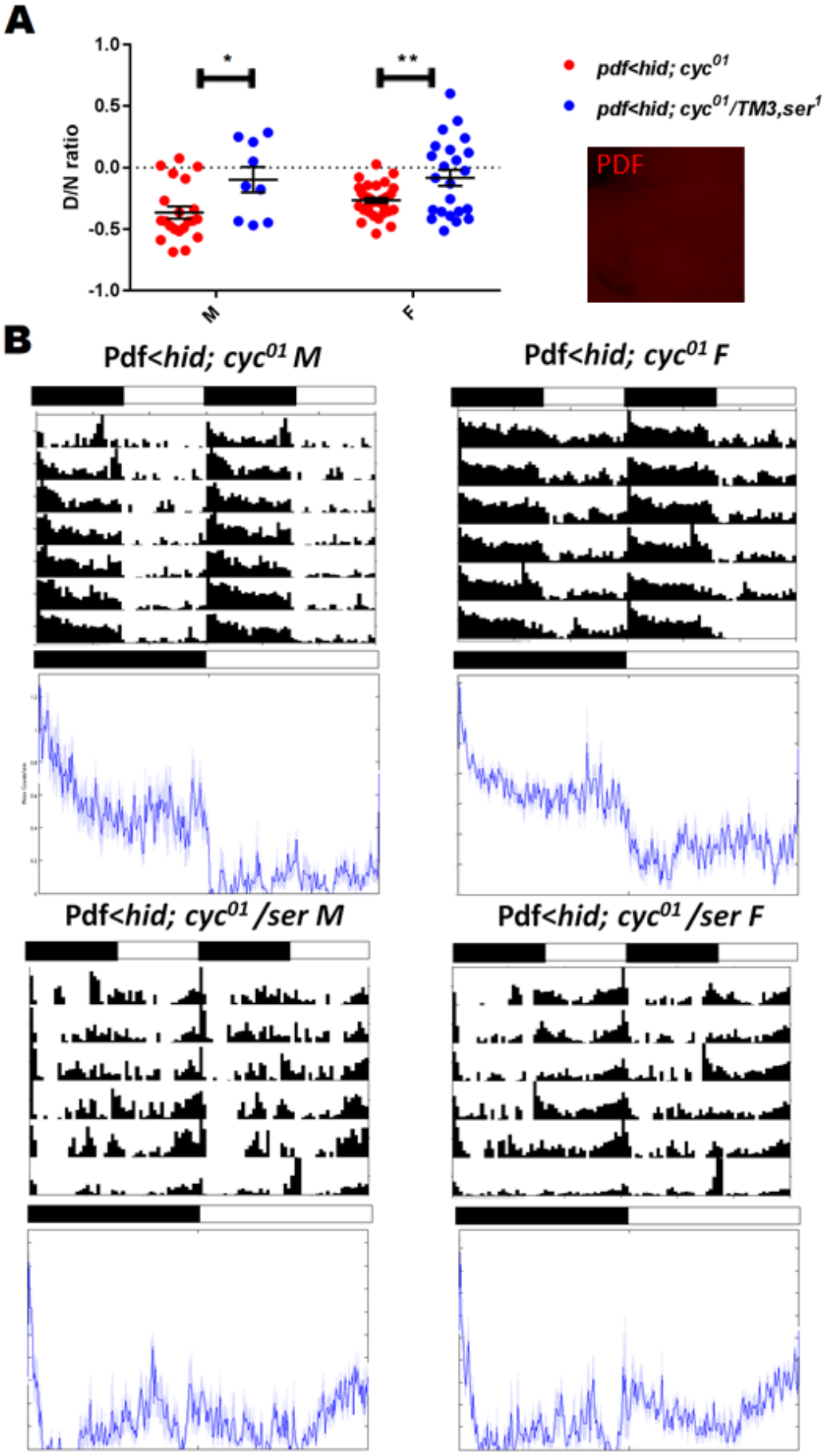
A
1.0
0.5
0.0
-0.5
-1.0
D/N ratio
*
**
M
F
pdf<hid; cyc01
pdf<hid; cyc01/TM3,ser1
PDF
B
Pdf<hid; cyc01 M
Pdf<hid; cyc01 F
Pdf<hid; cyc01 /ser M
Pdf<hid; cyc01 /ser F

Figure 3.16 - Ablation of PDF cells does not disrupt nocturnal behaviour caused by loss of cycle*: Panel A shows D/N ratio and Panel B shows behavioural profiles of Pdf>hid;cyc^{01} and Pdf>hid; cyc^{01}/+ in LD cycles, Statistical differences between heterozygous and homozygous lines were (♂ P=0.014 *, ♀ P=0.003 **). Subsequent to behavioural assay, brains were dissected from males and it was found that 39 of 42 PDF-stained hemispheres lacked visible PDF, confirming the effectiveness of the ablation, with an entire brain hemisphere shown in top-right..*

As we demonstrate *cyc^{01}* nocturnality persists in the absence of PDF cells, we wished to pursue the hypothesis that altered DN1p firing states contributed to nocturnality (Zhang et al., 2010a, Fluorakis et al., 2015). We attempted to increase DN1p neuronal signalling with *TrpA1*, *(Transient receptor potential cation channel A1),* which encodes a Ca^{2+} channel, normally expressed in sensory neurons and activated at higher temperatures (Viswanath et al., 2003). As pre-synaptic vesicle release depends upon Ca^{2+} influx, ordinarily via voltage-gated calcium channels, ectopic *TrpA1* expression within a targeted neuronal population hypothetically allows exuberant vesicle release at the synapse when the fly is placed into higher temperatures, and thus, increased signalling. As other groups have published, we used 29°C as an experimental condition of high *TrpA1* activity, and 23°C as a condition of low *TrpA1* activity (Cavanaugh et al., 2014).

We hypothesised DN1p activation by *TrpA1* expression could counteract potential firing defects that may be present on a *cyc^{01}* background.

UAS-TrpA1/+; Clk4.1M cyc^{01}/cyc^{01} displayed a quintessential *cyc^{01}*-like nocturnal profile at 29°C, suggesting enhanced DN1p firing does not cause nocturnality (Appendix Figure 6). We do however observe that DN1p excitation in *cyc^{01}*/+ appears to deepen the siesta activity trough in females, a finding previously published by the Rosbash lab, which has the side-effect of intensifying relative nocturnality, such that *UAS-TrpA1/+; Clk4.1M cyc^{01}/cyc^{01}* and *UAS-TrpA1/+; Clk4.1M cyc^{01}*/+ do not show significantly different D/N ratios (Appendix Figure 6)(Guo et al., 2016). Assuming that DN1p firing is restored by *TrpA1* expression, the behavioural nocturnality of *cyc^{01}* mutants appears to be distinct from that observed for *na^{har}* mutants (Nash et al., 2002). It is feasible that changes in ion channel type and number within DN1ps caused by CYC loss would render a silent state that could not simply be rescued by *TrpA1*. As expected, *TeTxLC* expression in the DN1ps with *UAS-TeTxLC/+; Clk4.1M cyc^{01}/cyc^{01}* has no noticeable effect on D/N ratio

or activity profile (Appendix Figure 8).

Our work on nocturnal behaviour is novel in several areas. First, the strongly nocturnal behaviour of cyc^{01} and presumably Clk^{jrk}/Clk^{out} flies is contingent upon both a developmental insult and an adult-specific loss. Secondly, nocturnal properties extend beyond the PDF cells. Manipulations affecting the firing properties of the l-LN_vs can alter overall D/N ratios, but cannot replicate a cyc^{01}-like state, suggesting a complex change in the molecular constitution following CYC loss.

3.7 - Conditional loss of *cycle* across developmental timepoints suggests post-larval developmental requirements for *cycle* in establishing adult behavioural rhythms

Our data thus far has defined a developmental requirement for CYC in multiple clock circuit cells for wt-like behaviour in LD and freerunning conditions, though the point of that developmental requirement is unknown, and it is possible that CYC requirement occurs at multiple developmental stages or may be plastic, and not confined to any one stage. There was little impact on adult behaviour of cyc^{01} *[elav.cyc]*^{ts} flies when egg-laying was conducted at a permissive temperature of 23°*C* for two-three days prior to transfer to the appropriate permissive or restrictive developmental condition (Figures 3.1-3.3). Though initially undertaken in order to increase numbers of progeny, this experimental approach is informative, as the significant segregation of behavioural rhythmicity is dependent on the subsequent developmental temperature (Figures 3.1-3.3), ruling out a CYC requirement within the embryonic and 1st-instar larval stages for adult circadian behaviour.

Though not tested, there is no evidence that maternal clock genes are present which can contribute to adult clock formation, and the many conditional rescue experiments and heterozygotes, with arrhythmic mothers and rhythmic progeny would rule out a maternal contribution.

Raising cyc^{01} *[elav.cyc]*^{ts} restrictively from egg-laying through to first-instar larvae (L1) and transferral to permissive conditions results in a majority rhythmic contingent of flies, such that if CYC is involved in initial clock circuit specification, this is rescuable with later developmental CYC expression (Figure 3.17, Appendix Table 6). It is unknown if larval clock function in circadian regulation of photophobicity is disrupted by this

(Mazzoni et al., 2005).

An experiment was performed where flies were raised from the first day of egg-laying at a restrictive temperature, and moved to a permissive temperature at L3 through to adulthood, to identify if behavioural defects occurred. Notably, these flies showed a spectrum of behavioural rhythms, in which a slim majority are behaviourally rhythmic in adulthood (Figure 3.17, Appendix Table 6). Therefore, larval CYC depletion is likely not the cause of behavioural arrhythmia seen in Figures 3.1-3.3. It is reasonable to assume that a gradual CYC accumulation occurs following inactivation of *GAL80*^{ts}, and persistently low levels of CYC abound before that; this supports a post-larval developmental requirement for CYC, as *cyc* transcription should rapidly increase through the late larval and early pupal stages, dependent on the age of individual larvae when moved, evidencing a requirement for CYC in early pupae.

Flies raised restrictively through larval stages are statistically less rhythmic than flies raised permissively throughout development, and is evidently not a full rescue, and whilst we ascribe this to the slow CYC accumulation at later stages, this is difficult to prove, and we cannot rule out the potential of a plastic time-frame for CYC requirement encapsulating the third-instar larval stage.

To support our hypothesis, we extended the restrictive phase into the P6 stage of pupation, ~approx one-two days PPF, on the basis that behavioural rhythmicity in these flies more similar to flies restrictively raised throughout development than larval-specific restriction would indicate an isolated developmental timepoint within early pupa where CYC is required (Figure 3.17). P6 was selected as a timepoint as it endures for a relatively long time, allowing the collection of greater numbers of stage-matched pupae, and is subsequent to ecdysone-mediated degeneration and regrowth of other projections (Watts et al., 2003). Though not significant, extending the restrictive phase into P6-stage did reduce rhythmic strength in both genders (Appendix Table 7).

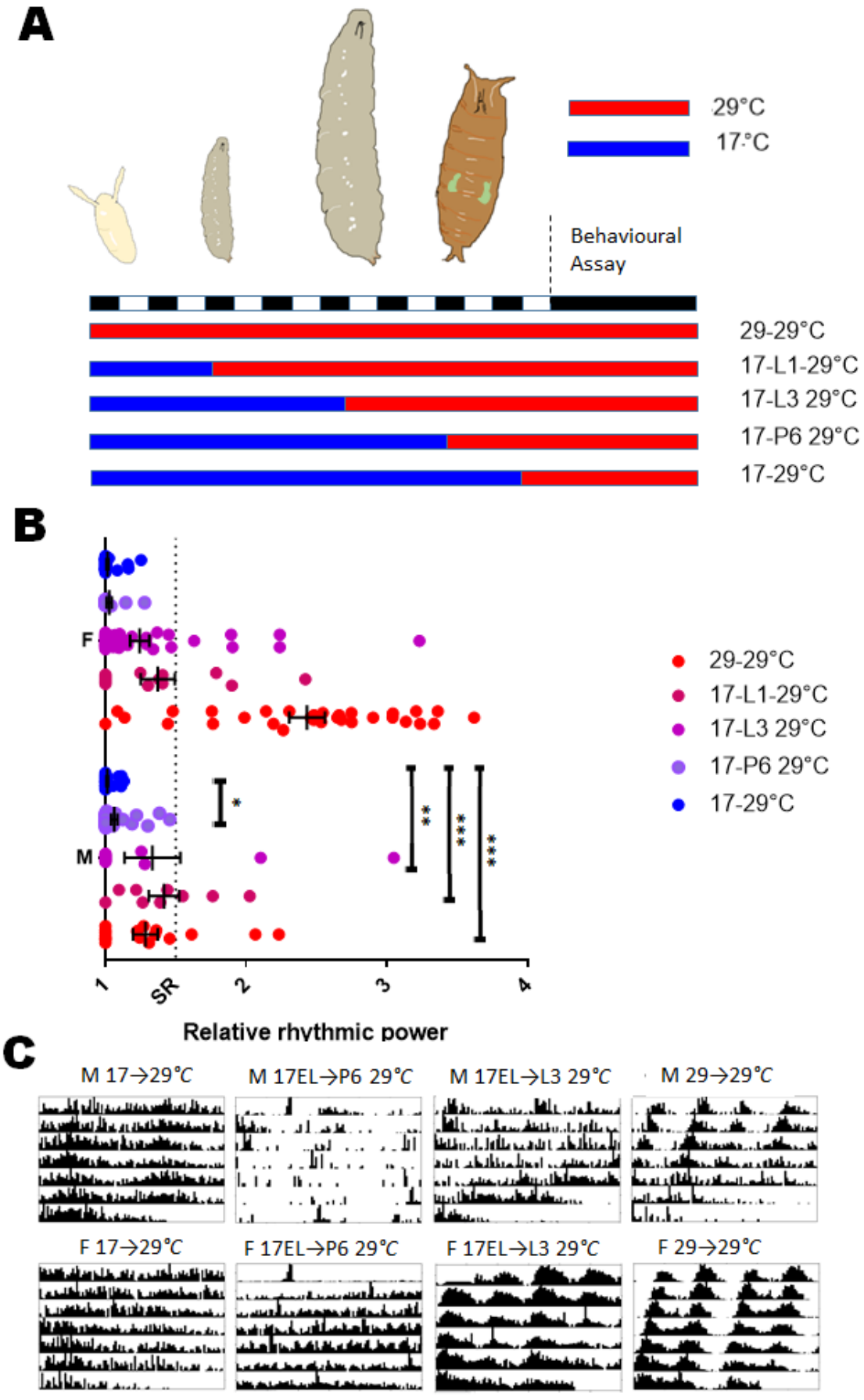

Figure 3.17 - Loss of cycle expression through later developmental stages progressively

weakens adult bejavioural rhythms. *behavioural data at 29°C DD incorporating cyc^{01} [elav.cyc]^{ts} flies raised at 17°C from egg-laying until P6 pupae, and transferral to 29°C until adulthood. Panel A shows a schematic of the various temperature regimens of different conditions, with 29°C demarcated in red, and 17°C in blue. LD cycles are approximate as developmental time differs dependent on temperature condition. Panel B shows rhythmic strength of genotypes raised at different temperatures, Panel C shows median actograms for the respective conditions, with a visible loss of rhythms commensurate with increased developmental time at a restrictive temperature.*

Unfortunately, the insensitivity of the TARGET system does not allow a rapid accumulation or inactivation of CYC, so a detailed mapping of CYC requirement is not feasible. Attempts to remove CYC specifically during pupal stages with a restrictive condition of 17°*C* and permissive condition throughout embryonic and larval stages of 29°*C* were unsuccessful, and flies displayed wt-like rhythmicity (data not shown). We repeated this experiment with a lower developmentally permissive temperature of 23°*C*, on the assumption that CYC levels, whilst sufficient for developmental function, would be lower than at 29°C, and thus easier to turn over during the restrictive pupal phase. Rhythmic strength is significantly lower in flies that experience a restrictive temperature from late third-instar to adulthood (♂ P<0.001 ***, ♀ P<0.001 ***), suggesting that CYC developmental function likely occurs during this timepoint (Figure 3.18, Appendix Tables 3 & 4). Period length also appears to differ. As has been previously mentioned, *cyc^{01} [elav.cyc]^{ts}* flies have a shorter period at high temperatures (23→29°*C* ♂ tau=22.34±0.44), compared to (23EL-L317→29°*C* ♂ tau=23.92±0.15) those incorporating a pupal-restrictive temperature (P<0.001 ***), which may be related to a build-up of CYC in the adult.

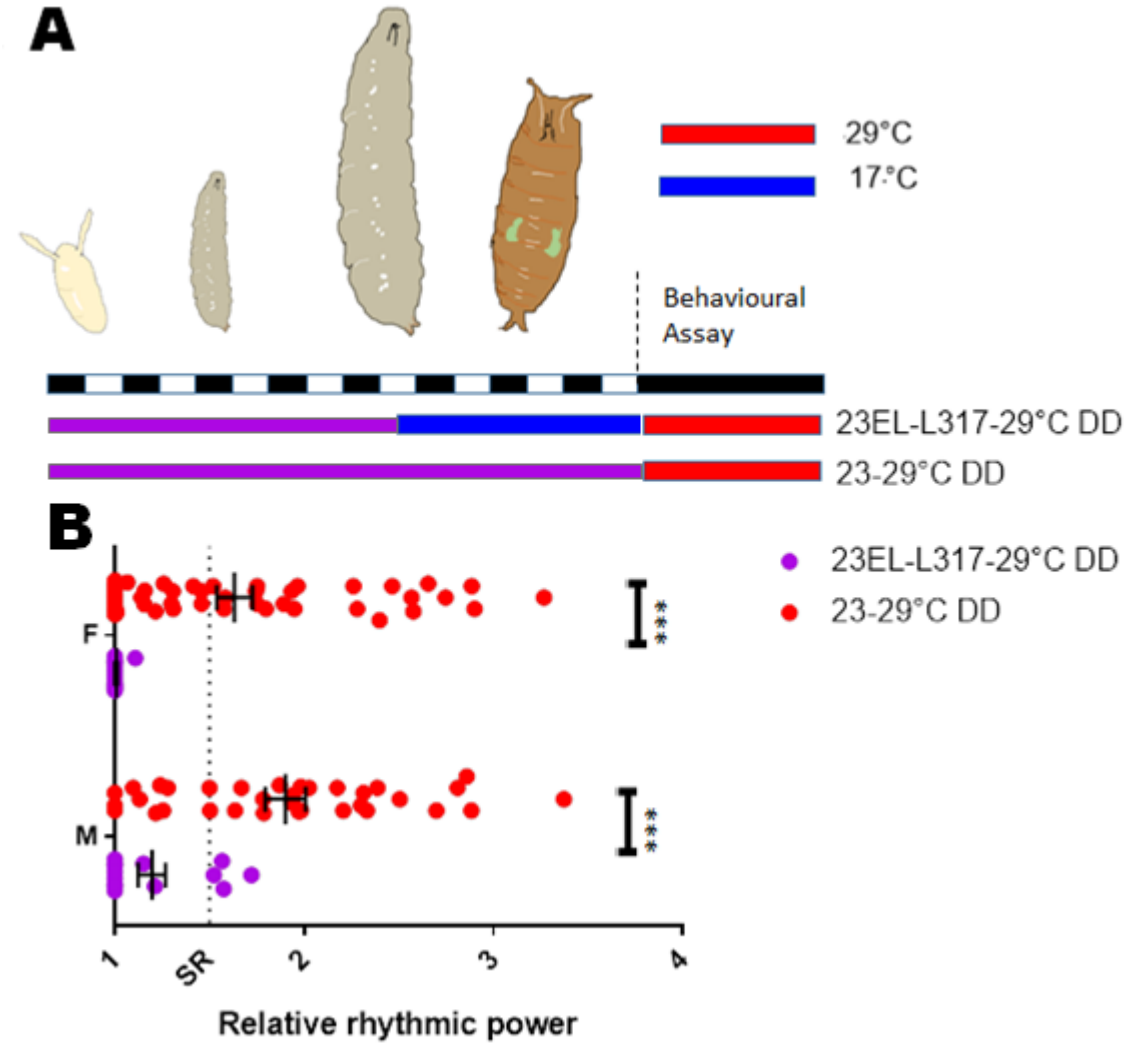

Figure 3.18 - Loss of cycle expression during pupation significantly lowers adult behavioural rhythmicity*. Panel A shows a schematic of the developmental temperatures employed in this experiment. Panel B shows rhythmic strength of* cyc^{01} *[elav.cyc]*^{ts} *flies raised at 23°C from egg-laying until third instar larvae, and consequently 17°C into adulthood, run at 29°C DD. Pupal restriction of CYC significantly reduces adult behavioural rhythmicity compared to flies raised at 23°C throughout development (P<0.001*** for both genders).*

Behavioural rhythmicity does not significantly differ to that of pan-developmentally restrictive 17→29°C in females, with mild differences emerging in males, suggesting that pupal-specific CYC restriction encompasses much of the developmental defect blocking rhythmicity.

Combined, temporal mapping of CYC developmental requirement for behavioural

rhythms suggests the requirement is largely pupal, though we are limited by resolution, and possibilities of a more plastic developmental requirement are feasible.

3.8 – Flies lacking adult expression of *cycle*, but not flies over-expressing *period* as adults, are able to entrain in light-dark cycles at adult restrictive temperature

As shown in Appendix Figure 29, previous work from the lab has studied the role of the older cyc^{01} *[elav.cyc]*^{ts} iteration, homozygous for the tub_P-*gal80*^{ts} transgene, in responding to phase shifts, the alteration of the phase of a zeitgeber to enforce re-entrainment of the molecular oscillator. Permissively raised cyc^{01} *[elav.cyc]*^{ts} were subject to phase-shifted light treatments, in an adult restrictive condition and then placed into permissive freerunning conditions. Across six different phase shift regimes, the freerunning phase corresponded to the phase of the restrictive light condition rather than the pre-existing LD cycle or shift into permissive conditions (Appendix Figure 29).

This indicates that the molecular oscillation is not phasically locked in the absence of CYC, and is capable of responding to entrainment cues (Appendix Figure 29). I wished to repeat this using *[timP.per]*^{ts}, but found that following adult restrictive conditions, flies were initially arrhythmic following introduction to permissive freerunning conditions (Figure 3.19). Previous published work with this line raises flies permissively, then places them in a restrictive adult condition before re-entraining them to an LD cycle at permissive conditions, after which they appear rhythmic (Figure 1.8, (Goda et al., 2011)). Repeating this, I found that flies were more rhythmic following a permissive LD cycle, though the mechanism for this is unknown (Figure 3.19).

On the suspicion that adult restrictive conditions led to a build-up of PER/TIM, I subjected flies to LL prior to a permissive freerunning state, ostensibly to degrade TIM and thus destabilise PER/TIM dimers. These flies subsequently were significantly more rhythmic in freerunning conditions, though phase was aligned with the cessation of LL (Figure 3.19). It is therefore difficult to draw conclusions from behavioural data as to the entrainability of oscillators experiencing PER overexpression, as the only strategy to restore behavioural rhythms is phase-resetting. However, this does suggest that the molecular oscillator states are qualitatively different between *[tim*$_P$*.per]*^{ts} and cyc^{01} *[elav.cyc]*^{ts} flies. Whether this reflects a different level of arrest or a mechanistic difference between arrests triggered by PER over-expression versus CYC depletion

remains unclear.

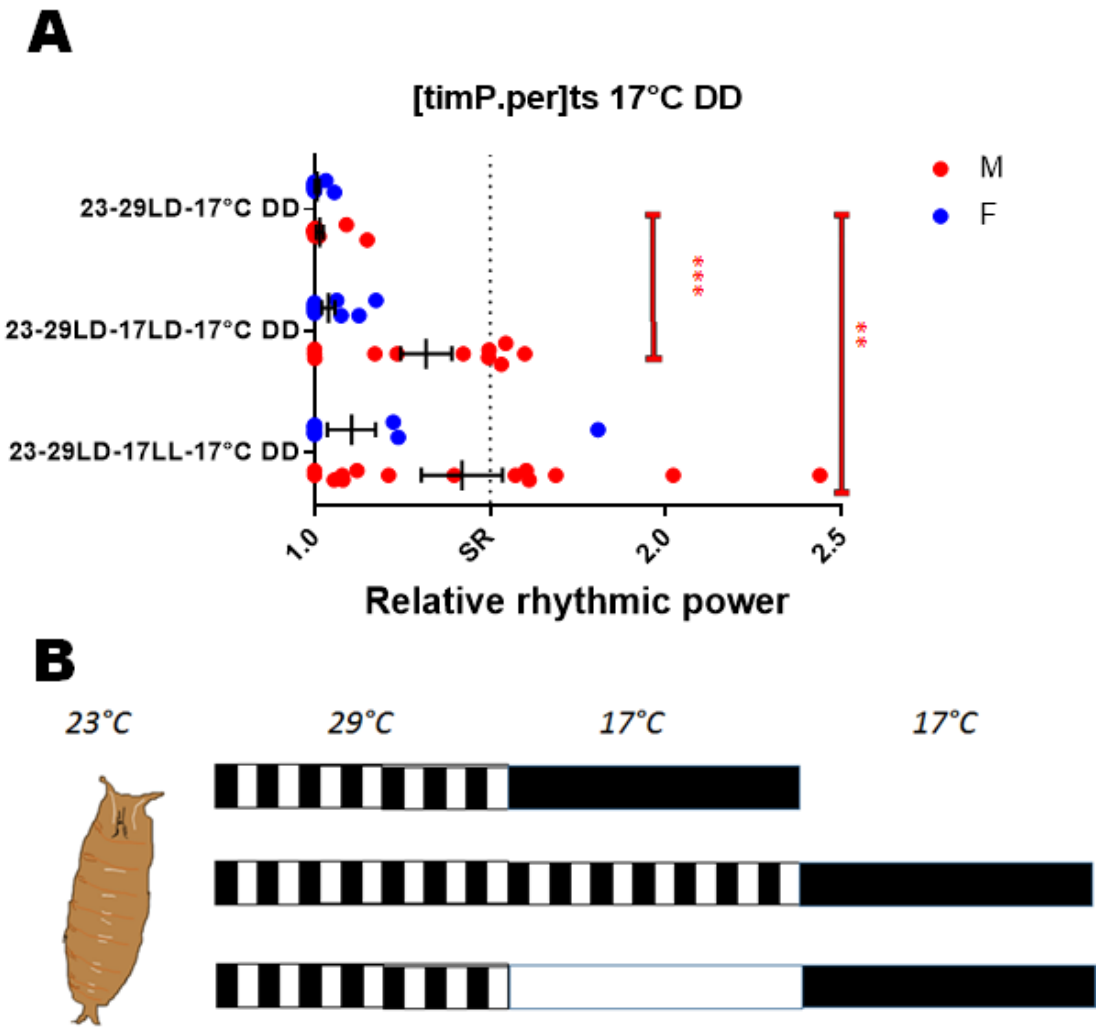

Figure 3.19 - Conditional overexpression of period during adulthood, unlike adult-specific loss of cycle, results in loss of behavioural rhythms, which can be rescued by exposure to light*. Panel A demonstrates different behavioural rhythmicities of permissively raised [timP.per]^{ts}, run at a restrictive 29°C LD cycle then moved either to a permissive freerunning condition, with an LD or LL intermediate. Behavioural rhythms are completely absent upon transferral to freerunning conditions, though this is significantly improved by exposure to light at a permissive temperature in males (LD P<0.001 ***, LL P=0.001**). This dataset is pursuant to Figure 1.8, in which flies can recover from adult-specific, but not development-specific PER overexpression, Panel B is a cartoon detailing the light conditions used in the three experiments, corresponding top to bottom. 17°C DD is the point at which behavioural rhythmicity was measured.*

3.9 - Molecular rhythms persist in *cyc^{01} [elav.cyc]^{ts}* sLN$_v$s following return to

permissive conditions during adulthood

Previous work in the lab has characterised the molecular dynamics of restrictively and permissively raised, permissively run *[timP.per]*^{ts} in DD (Goda et al., 2011)(Appendix Figure 28). It was discovered that developmental PER overexpression led to a loss of TIM oscillations in the s-LN$_v$s, and a significant damping in the LN$_d$s despite a return to permissive conditions, suggesting that stopping the oscillator in a low CLK/CYC, High PER state negatively impacts the resumption of molecular oscillations in adulthood, perhaps through a failure to prevent establishment of a factor that blocks oscillation (Appendix Figure 28). Oscillators can be induced in non-clock cells with relative ease, and there is no obvious candidate for an environment not conducive to oscillator formation if CLK/CYC is present, suggesting that if this is the case, a developmental change must allow the instigation of a factor that blocks the clock (Zhao et al., 2003, Kilman and Allada, 2009, Lerner et al., 2015). Initial conclusions were that this persistant molecular arrhythmicity was the result of developmentally low CLK/CYC, rather than a combination of low CLK/CYC and developmentally high PER. In light of differing responses to phase-shift experiments in restrictive conditions between *cyc*^{01} *[elav.cyc]*^{ts} and *[timP.per]*^{ts}, I was therefore curious to determine if a molecular oscillator was intact within the clock cells of adult flies following developmental CYC loss (Figure 3.19, Appendix Figure 29).

Flies raised either permissively at 29°C or restrictively at 17°C from embryonic stages and returned to a permissive temperature for three days were dissected at CT2, 8, 14 and 20 on the second day of DD and stained with PER and PDF. s-LN$_v$ and l-LN$_v$ nuclear PER was quantified. I additionally scored cells on the presence or absence of a distinct nuclear compartment marked solely by PER stain, as an assessment of localisation, as PER should be high and nuclear at CT20 and CT2, timepoints straddling the subjective dawn, and low and without nuclear preference at CT8 and 14, the subjective evening (Figure 3.20)(Shafer et al., 2002).

Unexpectedly, both permissively and restrictively-raised *cyc*^{01} *[elav.cyc]*^{ts} appeared to show oscillating PER levels, with peaks over CT20 and CT2, and lower levels at CT8 and CT14, suggesting that adult, but not developmental CYC is required for molecular rhythmicity. However, males of both developmental conditions possess high nuclear PER staining intensity at only one of the expected peaks. Restrictively raised nuclear PER

significantly differs between CT2 and CT14 for both males (P=0.008**) and females (P=0.030*), and between CT2 and CT8 for both males (P=0.003**) and females (P=0.048*), whilst CT8 and CT14 do not differ between themselves (Males P=0.081, Females P=0.251). As both CT8 and CT14 show low PER, and visualising PER localisation qualitatively suggests a rhythm in PER nuclear localisation, we are confident that rhythms exist in these cells, but may not possess a 24-hour period.

17→29°C flies are more than 80% arrhythmic in freerunning conditions and so we cannot predict an expected molecular oscillator period. However, 29→29°C flies have a slightly shortened period, and we could predict that the molecular period of the s-LN_vs would similarly be shortened, advancing the rapid loss of PER in the relative morning, such that levels at CT2 may be lower, as is observed. We could predict from this that high PER may precede CT20 and may be present at CT18, though we did not test at additional timepoints.

As mentioned in Figure 3.4, and in (Kadener et al., 2008), ectopic CYC expression may influence period length, which was not accounted for when designing this experiment, and it must also be noted that *cyc*^{01}/+ heterozygotes when first described showed an increased period, so a dosage effect of CYC may influence the oscillator, in which less CLK/CYC possibly corresponds to a slower accumulation of PER/TIM and thus a longer period (Rutila et al., 1998). *cyc* mRNA levels do not cycle (Rutila et al., 1998) and hence are not usually a limiting factor for the speed of oscillation. A recent study suggests that CYC protein is stabilised by CLK protein (Liu et al., 2017). Were CYC a rate-limiting component, low levels might be expected to lengthen the periodicity imparted by rhythmic *Clk* mRNA and protein. As ectopic CYC shortens period, it might be predicted that *Clk* mRNA would similarly possess a short period that is squandered by limited endogenous CLK/CYC dimerisation kinetics. If wild-type *Clk* mRNA and protein accumulation matched a 23.5 hr behavioural period, then an excess of ectopic CYC would be rate-limited to this accumulation and thus unable to shorten period. *Clk* mRNA oscillations have not been studied at suitable resolution to detect minor period changes (Glossop et al., 1999, Cyran et al., 2003).

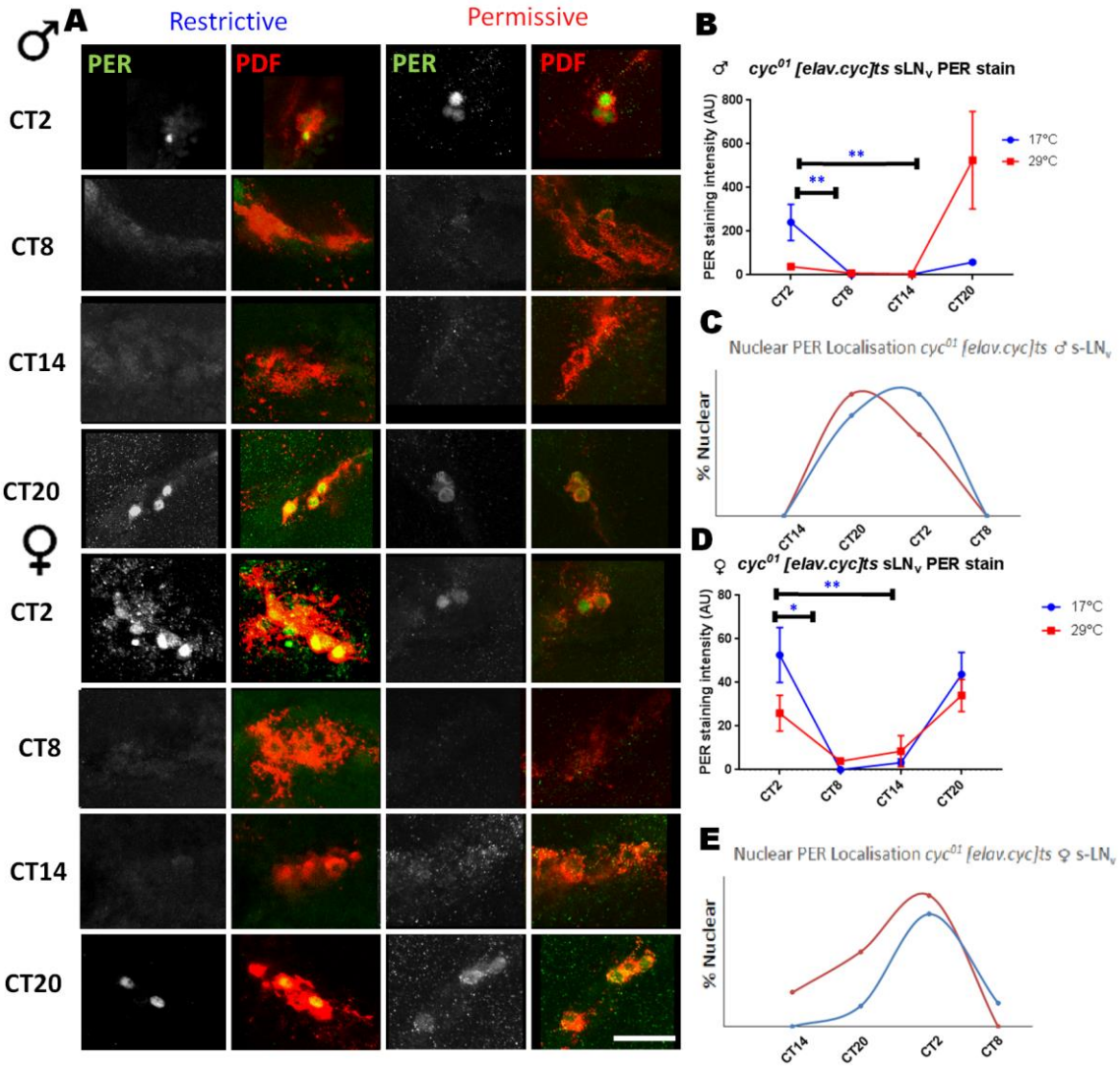

Figure 3.20 - Developmental loss of cycle expression does not prevent molecular rhythms re-emerging in adulthood*. Molecular PER rhythms in restrictively (Blue) and permissively (Red) raised cyc^{01} [elav.cyc]^{ts} flies, following 3 days LD at 29°C, and dissection at indicated timepoints on second day of DD. Panel A shows representative images of s-LN$_v$ PER staining, showing PER (Grayscale/Green) and merged with PDF (Red). The top sixteen windows are taken from males, and the bottom sixteen from females. Scale bar in the bottom right panel is 20 um and all windows are of the same scale. Panel B and D shows quantified levels of PER intensity within the nucleus for males and females respectively, relative to background. Panels C and E quantify the % of nuclear-located PER at each timepoint for males and females respectively. Similar figures in the appendix quantify these metrics within the l-LN$_v$s. Each timepoint contains data from a minimum of three brains.*

3.10- Loss of *cycle* expression in the adult is capable of damping the molecular oscillator in s-LN$_v$s

As restrictively-raised flies possess a molecular oscillator, to validate the function of our conditional CYC reintroduction we characterised the molecular oscillator in adult restrictive states, to ensure molecular oscillations could be lost.

To determine if our manipulation was capable of disrupting the molecular oscillator at all, restrictively and permissively raised flies were placed into restrictive conditions as adults for 3 days in LD, then 2 days in DD and PER levels were quantified within brains taken at CT2 and CT14, the expectation being that in the absence of CYC, PER levels should become constitutively low (Figure 3.21)(Rutila et al., 1998). Significant differences between trough and zenith timepoints persisted in the oscillation at 29→17°*C* in males, suggesting that the manipulation is too weak to immediately remove molecular oscillations (Appendix Table 9). From this perspective, the finding in Appendix Figure 29 that the molecular clock is entrainable in this condition is unsurprising, presumably containing PER/TIM as a substrate for entrainability. A sex-specific difference emerges in damping at this stage, which may be a result of driver strength, or an entirely independent defect. Conversely, male behavioural rhythms are weaker than females in permissive conditions, following development at 29°C, but this relationship reverses following prior development at 23°C (Table 3.1). Although a shorterned behavioural period does not manifest, this could be interpreted as a deleterious overexpression of CYC in males, similar to previous results that show loss of rhythmic strength following transgenic *Clk* over-expression (Zhao et al., 2003). Hence, turnover of accumulated CYC may take several days in 29°C-raised males (Figure 3.21). It is notable in the actograms of 29→17°*C* flies that a residual behavioural rhythm is observable that damps, and a significant fraction of these flies remain behaviourally rhythmic for some days, supporting the notion of a slow restrictive effect (Figures 3.1, 3.2).

A parsimonious interpretation of this data is that residual CYC feeds the oscillator for days afterwards due to limitations of *GAL80*^{ts} function or insufficient CYC turnover, and the oscillator can consequently sustain itself for several days with low CYC. However, CYC is rapidly degraded in the absence of CLK, itself independent from CYC-levels, so either *cyc* mRNA from developmental expression can endure for several days, or a resilient excess of CLK/CYC heterodimer is able to persist (Liu et al., 2017).

For 29→17°*C* females and 17→17°C of both genders, PER levels were low in both timepoints, suggesting that a damping does occur, and validating 17°*C* as a truly restrictive condition. As a developmentally restrictive temperature in isolation does not remove adult molecular oscillations, the stronger damping in 17→17°*C* compared with 29→17°*C* is likely not due to a developmental effect, but simply related to issues of

CYC turnover. Potentially, studying 23→17°C or storing 29→17°C flies at 17°C for a week rather than 2 days prior to dissection would produce more prominent damping.

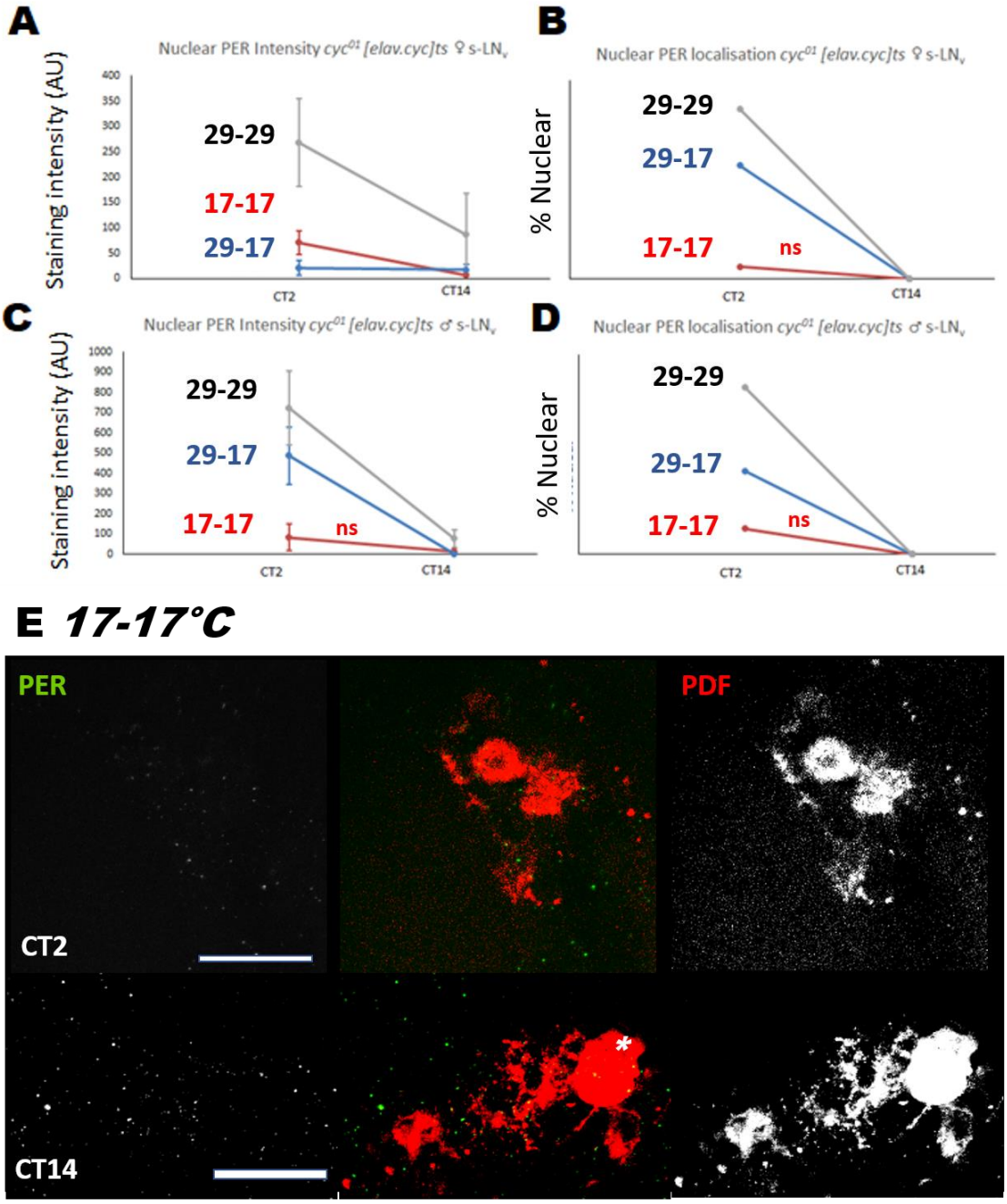

Figure 3.21 - Persistant lack of cycle expression in the adult results in loss of molecular period rhythms. *Molecular PER rhythms in s-LNvs run either permissively or restrictively, following 3 days LD at 17°C and dissection at indicated timepoints on second day of DD. Panels A+C quantify levels of PER intensity within the nucleus, relative to background and panels for females and males respectively. Panels B+D quantify the % of nuclear-located PER at each timepoint for females and males respectively. Panel E shows representative images for males in 17-17°C, with scale bars in bottom right corresponding to 20µm.White asterisk at CT14 represents an l-LNv intermingled with s-LNvs.*

Rhythms within the l-LN$_v$s appear more erratic, as has been previously published in DD (Appendix Figure 12). Though not formally quantified due to absence of a suitable cytoplasmic marker, PER+ve nuclei corresponding to LN$_d$s were visible in permissive but not restrictively-raised *cyc^{01} [elav.cyc]^{ts}* brains.

3.11 - Discussion – Chapter 3:

cyc^{01} nocturnality is dependent on blue-light input, is PDF-cell independent and can be rescued by either developmental or adult CYC, or PDF-cell CYC (Relevent to Sections 3.3-3.6)

The resurgence of s-LN$_v$ PER oscillations in 17→29°C *cyc^{01} [elav.cyc]^{ts}* suggests that CYC rescue is effective, and we can infer from this that CYC is rescued in these flies in LD, which display a featureless, *cyc^{01}*-like nocturnal profile (Figures 3.4, 3.5 and 3.20). Therefore we argue that developmental CYC loss primes *cyc^{01}*-like nocturnal behaviours. However, it is feasible that CYC levels, despite being sufficient to restart the molecular oscillator within a few days, are not sufficient to influence behaviour, and more time spent at 29°C LD might result in the emergence of wt-like activities. Additionally, the difference in *cyc^{01} [elav.cyc]^{ts}* and *cyc^{01}* activity profiles at 17°*C* LD may not be due to a failure to recreate a restrictive CYC condition (Figure 3.12). We demonstrate that 29°C-raised, 17°C run *cyc^{01}* shows a highly diurnal LD profile, such that strong diurnal behaviour is still attainable in the absence of CYC, although anticipatory behaviours are not observable (Figures 3.4, 3.5 and 3.7).

Broadly, we find that female *cyc^{01}* flies appear slightly less nocturnal than males across a variety of genotypes (Figures 3.6 & 3.12). To explain this, we show that virgin females do not differ to male D/N ratios, whilst significantly differing to mated females (Appendix Figure 2). It has been shown that sex peptide in mated females inhibits daytime sleep in LD, which would result in a relatively more diurnal D/N ratio in *cyc^{01}* (Isaac et al., 2010). (Guo et al, 2016) has demonstrated sex-differences in DN1p activation results in the striation of siesta phenotypes in males and females, a difference which is also known to occur in mated, but not virgin females (Isaacs et al., 2010). We can therefore interpret our finding that nocturnality, which appears to be related to mating status in females, may similarly be due to differences in DN1p function (Appendix Figure 2). Though this is untested, it lends credence to potential regulation of

nocturnality by DN1ps, as inferable from (Lear et al., 2005) and (Zhang et al., 2010). Similarly, the siesta in 17°C-raised *cyc^{01} [elav.cyc]^{ts}* appears qualitatively weaker than that of 23C or 29C at permissive temperatures, which could be interpreted that this DN1p-oriented circuit may be disrupted by developmental CYC loss (Figure 3.9)(Guo et al, 2016).

We initially hypothesised that *cyc^{01}* nocturnality may be the result of l-LN$_v$ hyperexcitation, which the Holmes group postulates drives nocturnal activity (Sheeba et al., 2008a). However in that paper, nocturnal activity was PDF signalling dependent, suggesting a separate mechanism to *cyc^{01}* nocturnality, which we demonstrate can be experimentally separated from PDF signalling (Figures 3.12 & 3.16)(Sheeba et al., 2008a). We used *Pdfr^{5304}* rather than *Pdf^{01}* but both should have the same effect, bar the potential existence of further uncharacterised PDF receptors.

One must consider that more general loss of PDF cell function has not been described to drive nocturnal behaviour, so an absence of normal l-LN$_v$ function is not the expected cause of this phenotype, and CYC loss may cause a novel aberrant function of the PDF cells. This raises the idea that l-LN$_v$s at night have an arousal-repressing role that is bypassed in the absence of CYC.

That nocturnality persists in *cyc^{01}* following PDF cell ablation melds well with our silencing dataset, and suggests that nocturnality is a latent state of *cyc^{01}* flies (Figures 3.12 & 3.16). Potentially PDF-cell CYC loss alters signalling from these cells, failing to repress a nocturnality induced by CYC loss in the remainder of the clock circuit. A lack of CYC in non-PDF cells is capable of inducing nocturnality as long as there is no signal emanating from the PDF cells, so it is interesting that PDF-cell specific CYC expression is capable of rescuing nocturnality (Figure 3.9). That PDF-cell excitation with *NaChBac* can decrease nocturnality supports this dataset, suggesting PDF cells can repress or override the circuit. This additionally suggests *cyc^{01}* PDF cell connectivity is existant, and likely interacts with other clock cells. Ca^{2+} imaging of *cyc^{01}* PDF cells would be an interesting future experiment, and an attractive hypothesis would be that firing is diminished in the absence of CYC, preventing PDF cells from halting the nocturnal behaviour promoted by the PDF-ve clock circuit.

The Shafer lab demonstrates a DN1p-specific repression of l-LN$_v$ firing, linking the two

prospective nocturnality-promoting clusters (Yao, 2016). However, our study of *Pdf>hid;cyc*^{01} precludes the idea that derepression of l-LN$_v$ firing is critical to *cyc*^{01} nocturnality (Figure 3.16). The idea that *na*^{har} mutant nocturnality might stem from repression of the l-LN$_v$s alone is hard to consider in light of our data, and we might expect CYC loss in other cell clusters influence light-response independently of the PDF cells (Fluorakis et al., 2015). Further manipulations of DN1p cells in particular would be of interest.

Pdf>TeTxLC cyc^{01}/+ appear less diurnal than other *cyc*^{01} heterozygote manipulations and the D/N ratio does not differ to it's homozygous counterpart, though this is chiefly due to a robust activity peak following lights-off and the activity profile demonstrates the ineffectiveness of this manipulation in altering aspects of typical *cyc*^{01} LD behaviour. This lack of significant difference between heterozygote and homozygote D/N cannot be considered evidence of PDF-cell silencing resulting in a *cyc*^{01}-like nocturnality (Figure 3.12). Since *Pdf>TeTxLC* is not thought to affect DD freerunning or LD behaviour, so this minor effect could be related to background, or it could be a legitimate phenotype (Kaneko et al., 2000, Blanchardon et al., 2001)(Figure 3.12).

Comparison of *Pdf>hid;cyc*^{01} in LD and *cyc*^{01} in RD is informative, as *Pdf>hid;cyc*^{01} appears mildly more nocturnal (Figures 3.15 and 3.16). Known visual photic input to the clock circuit occurs via the Hofbauer-Buchner eyelet signalling to PDF cells, so the inability of the red-light-responsive visual system to promote a nocturnal behavioural profile, and the dispensability of the PDF cells together points towards a sufficiency of CRY in PDF-ve cells to trigger daytime inactivity in *cyc*^{01} (Helfrich-Förster et al., 2002). An interpretation of this is that CRY outside the clock neurons in the central brain can drive flies more nocturnal, through activity repression, by an unknown mechanism. The Helfrich-Förster group additionally demonstrates that light-induced phase shifts in LD cycles are the result of either CRY or visual system reentrainment specific to the E but not M cell oscillator, supporting the capability of PDF-ve cell CRY in behavioural responses (Yoshii et al., 2015).

It could be hypothesised that nocturnal hyperactivity would cause sleep-deprivation and a homeostatic sleep rebound in light (Hendricks et al., 2001), although it is feasible that CRY-mediated inactivity causes a subsequent homeostatic hyperactivity response, potentially related to feeding. It is also likely that both nocturnal hyperactivity and

daytime inactivity are unrelated phenotypes in *cyc*^{01}, as we fail to alter both with any manipulation other than CYC-reintroduction. The relationship to sleep, which has yet to be distinguished from activity state in *Drosophila*, in both cases would be of interest.

CYC loss may modify CRY function at the cellular level or the network level, altering the molecular constitution so as to afford CRY a novel control over neuronal firing, or else changing the clock cell network such that CRY-activity in CRY+ve cells produces alternate behavioural patterns. To be discussed in Chapter 4 in more detail, CRY levels, whilst higher in whole fly heads following CLK/CYC loss, have not been confirmed to increase within clock neurons specifically (Kumar et al., 2012).

Future experiments mapping clock cells involved in nocturnality would also be informative, as it appears DN1p firing alone does not drive nocturnality (Figure 3.7)(Appendix Figure 6). A requirement for CRY activation in PDF-ve cells potentially points to the E cells, or CRY+ve DNs. As will be discussed in Chapter 4, CRY expression in low CLK/CYC brains, though expected, has remained theoretical, and if CRY levels are mis-regulated, mechanisms of nocturnality may radically differ to those hypothesised.

The electrical properties of the l-LN$_v$s differ between night and day, independent of CRY (Buhl et al., 2016). Other groups have suggested nocturnality appears to be CRY-dependent, suggesting mechanistic independence of this, even though it is likely altered l-LN$_v$ firing contributes to nocturnality (Figure 3.15)(Kumar et al., 2012). Furthermore, nightime CRY should be inactive, suggesting that maybe there is a latent function to the inactivated form of CRY, perhaps in binding or sequestering cell components, or preventing access to the cell membrane (Fogle et al., 2015). Structural studies do not support obvious secondary functions, nor have in-vitro studies identified binding partners for inactive CRY, though a complete proteomic analysis of CRY binding partners has not been performed (Peschel et al., 2009, Czarna et al., 2013).

It is known that in wt flies, l-LN$_v$s are depolarised and firing is higher during the day, one of the reasons why certain transgenics constitutively increasing firing show a night-specific increase in activity (Sheeba et al, 2008a, Sheeba et al., 2008b). The phenotype distinguishing our flies from the many hyperexcited l-LN$_v$ lines is not purely an increase in nighttime activity, but a loss of daytime activity. Manipulations altering the firing in

day but not nighttime may be beneficial, and in future work an optogenetic strategy may be employed.

Lights-on startle response is dependent on l-LN_v presence and is at a point of high l-LN_v firing (Sheeba et al., 2010), so it was expected that *$Pdfr^{5304}$* and *Pdf>Kir2.1* would not rescue the lights-on startle response. Notably, whilst these passive manipulations do not remove lights-on triggered inactivity in *cyc^{01}* flies, ablation appears to in males (Figures 3.12 & 3.16). It is likely l-LN_v firing rate is somehow decreased in the morning in *cyc^{01}*, though not a homeostatic consequence of suddenly alleviated firing pressure in darkness. Perhaps increased firing of another cell cluster due to CYC loss is able to repress l-LN_v firing. Since TeTxLC-mediated silencing of dopaminergic neurons does not bring back a notable lights-on peak, potential l-LN_v repressors will likely include non-dopaminergic cells.

Relevance of larval light avoidance circuitry to adult nocturnal preference

Strikingly, CLK and CYC mutants and knockdowns show a heightened, though ultimately quite minor, light-avoidance response as larvae, underpinned by a reduced DN1 firing and an increased PDF firing rate (Mazzoni et al., 2005, Collins et al., 2012). This is Bolwig organ mediated, CRY-independent and precedes l-LN_v circuit integration, so mechanistically distinct from adult nocturnal preference, which is CRY-dependent (Mazzoni et al., 2005).

It is unknown, however, why eye-mediated light avoidance disappears in the adult, as activity promoting s-LN_vs and inhibiting DN1s are still present (Guo et al., 2016). To this effect, (Keene et al., 2011) demonstrates light avoidance is PDF-cell independent, but clock-cell dependent. *TUG-crygal80>Kir2.1* disrupts larval avoidance, allegedly mediated by 5^{th}-LN and DN2s, which are CRY-ve in larvae, though apparently adult nocturnality appears to be CRY-dependent. E-cell rescue of CYC fails to rescue elements of behavioural architecture, but is not outright nocturnal, and may have influence in removing nocturnal hyperactivity (Figure 3.11).

Previous work has established a robust 70% of larvae will pupate in the dark when prompted with a light/dark preference assay, which can be altered via manipulation of certain cells (Yamanaka et al., 2013). We show *cyc^{01}* do not show a significantly different

pupariation site preference compared to wt (Appendix Table 5). Second-instar larval quiescence has been assayed, with no observable circadian rhythm, whilst third-instar activity rhythms have never been assayed, but the lack of an increased dark preference in pupation site suggests that photophobicity is not particularly stronger in the absence of CYC, and adult nocturnal preference may be entirely unrelated (Szuperak et al., 2018).

Spatial mapping of CYC reveals morning anticipatory behaviours are not driven by CYC expression in any one clock neuron cluster, but diurnal preference is enhanced by CYC expression in PDF cells (Relevant to Section 3.4)

cyc^{01} [elav-Pdf80.cyc]ts, specifically lacking CYC in PDF neurons, shows a crepuscular LD profile with an evident morning anticipation. This persistence of morning anticipation phenocopies previously described behaviour of *cyc^{01} [elav-Pdf80.cyc]* flies, a similar genotype lacking the *$gal80^{ts}$* element (Goda et al., 2011). A lack of evening anticipation is also conserved between the two genotypes in (Goda et al., 2011), and it is feasible that PDF-ve clock cells are capable of contributing to morning anticipation. *per^{01} [elav-Pdf80.per]*, rescuing PER in PDF-ve neurons, was shown by the Rosbash lab to fully rescue morning and evening anticipation, and it could be interpreted that developmental defects caused by CYC loss within the PDF cells could compound defects in evening anticipation (Stoleru et al., 2004).

Potentially, as will be discussed in other chapters, some CYC expression may be present in the PDF cells despite *Pdf-gal80*, resulting in a milder phenotype, despite a requirement for CYC in the PDF-cells. CYC loss is seperable from oscillator loss, and potentially defects extending beyond oscillator function in the PDF cells affects contribution of PDF-ve cells to morning anticipation.

It may be most parsimonious to suggest *Pdf-gal80* effectiveness is less than absolute, and residual developmental CYC expression within PDF cells contributes to crepuscularity. The waveform of restrictively raised *cyc^{01} [elav-Pdf80.cyc]^{ts}* shows a notable nocturnal preference, and no M or E-peak is visible, the same as all other restrictively raised *cyc^{01} [-gal4.cyc]^{ts}* (Appendix Figure 3). In order to determine the persistence of M peak following PDF-cell CYC loss, further work will be needed to characterise residual functionality in PDF cells.

The Allada lab has shown in several studies that narrow abdomen (*na*) mutants show nocturnal preference and loss of lights-on response, similar to cyc^{01}, which can be rescued by $DN1_p$-specific re-expression of *na* (Nash et al., 2002, Zhang et al., 2010a). Thus there is an implication that $DN1_p$s mediate light-responsiveness and potentially regulate dopamine synthesis, or at least functions downstream in the pathway controlling response to light. na^{har} mutants showed hyperpolarised $DN1_p$s, potentially indicating a contribution of hyperpolarised $DN1_p$s to nocturnal behaviour (Flourakis et al., 2015). Wild-type $DN1_p$ firing is lowest following lights-off, so likely does not directly inhibit night-time activity-promoting cells, though any mechanism would be highly speculative. We attempted CYC rescue concurrently with *Pdf-gal4* (PDF cells) and *Clk4.1M-gal4* (DN1p) cell subsets, which did not alter the morning-specific behavioural rescue of cyc^{01} *[Pdf.cyc]*^{ts} (Appendix Figure 4,6).

cycle is developmentally required during pupation for adult behavioural rhythmicity (Relevent to Section 3.7)

Our results above demonstrate that a developmental loss of CYC using cyc^{01} *[elav.cyc]*^{ts} results in persistent behavioural arrhythmia (Table 3.1, Figures 3.2, 3.3 & 3.4). As we are reproducing old data from (Goda et al., 2011) with a reconstituted line, our findings should not be a surprise. The level of temporal mapping is an elaboration upon (Goda et al., 2011) results, and is potentially mitigated by the limits of conditionally altering CYC functionality purely through transcriptional regulation. We argue for a pupal-specific requirement on this basis, and downplay the mild defect of a larval-restrictive, pupal-permissive state on the basis that CYC may not accumulate rapidly (Figures 3.17 and 3.18). Timecourse qPCR of clock genes over early pupal stages would validate our hypothesis, to track increases in *cyc* mRNA and subsequent initiation of rhythms. Similar caveats exist in moving from a larval-permissive to pupal-restrictive state, requiring an intermediate permissive temperature of 23°C, and even then failing to completely remove rhythms (Figure 3.18). It is arguable that CYC is required over a longer period of time, perhaps in the specification of multiple clock cell subsets spanning late larval and early pupal stages, and intermediate permissive/restrictive states produce intermediate defects (Liu et al., 2015).

Restrictive temperatures encompassing egg-laying in addition to larval stages demonstrates that low CYC levels in embryonic phases does not remove adult rhythms

(Figure 3.17). As CLK/CYC have long been assumed to have roles in cell specification, this initial dispensability is unexpected, and shifts back the initiation of the CLK/CYC developmental window. Tubulin is certainly abundant in the embryo, so it is assumed, though not proven, that *GAL80*^{ts} expression is not weaker at this stage (Kellogg et al., 1988). Whether clock cell specification is an aspect of neuronal identity encoded within early development, or a plastic property that can be induced in mature neurons is unknown.

Pupal-specific CYC loss within *cyc*^{01} *[elav.cyc]*^{ts} does not result in period shortening evident in more strongly rhythmic *cyc*^{01} *[elav.cyc]*^{ts} raised at higher temperatures (Figure 3.18). If period shortening is due to CYC transcriptional effect on the molecular oscillator, as posited by (Kadener et al., 2008), developmental CYC loss may impact accumulation of CYC in the adult. This idea of minor peturbations may be relevant to Figure 3.20 and Figure 3.21, and may suggest lowered developmental *cyc* expression levels have a long-term impact that extends into adulthood.

Our dataset demonstrates a requirement for pupal CYC, but not neccesarily larval CYC. Geneswitch is an alternative to TARGET that similarly regulates gene expression at a transcriptional level featuring a conditional mifepristone-activated transcriptional driver, as opposed to temperature-regulated control. Utilising Geneswitch would be particularly informative during nocturnality experiments, in which temperature is clearly a confounding influence. However, it is impossible to regulate during pupal stages due to a food-borne delivery (Roman et al., 2001, Osterwalder et al., 2001).

Adult-specific expression of *cycle* is sufficient for molecular rhythms within the small lateral ventral neurons (Relevent to Sections 3.9 and 3.10)

Our data also shows that following developmental CYC depletion, behaviourally arrhythmic flies possess a molecular rhythm within the s-LN$_v$s, demonstrating first that only adult-specific CYC is required for the instigation of a molecular rhythm, supporting the previous finding that adult-specific inducible oscillators through conditional PER rescue is sufficient for resumption of molecular rhythms (Goda et al., 2011). Secondly this data suggests that a developmental requirement for CYC must occur downstream of the molecular oscillator in controlling behaviour (Figure 3.20).

Similarly, study of LD profiles reveals that developmental and adult CYC restriction produce separate defects, in which wild-type-like morning behaviour is rescued by developmental CYC expression in either PDF or non-PDF clock neurons, whereas adult CYC rescue may further modify daily activity profiles. Evening locomotor activity in anticipation of dusk is compeletely absent if CYC is only expressed in either PDF or non-PDF neurons (Figures 3.9 & 3.10). Thus, developmental CYC expression in both cell types may contribute to this feature.

We saw rapid damping of PER oscillations within l-LN_vs in DD, as has been published elsewhere (Stoleru et al., 2004)(Appendix Figure 12). We did not study l-LN_v rhythms in LD, so feasibly a defect in oscillator production occurs in these cells following developmental CYC loss, which may influence LD activity profiles separately to freerunning, and may be an opportunity for future work.

Phase of the average s-LN_v molecular oscillation in cyc^{01} *[elav.cyc]*^{ts} was not entirely as predicted, which may be due to n number, and also as the dataset is neccesarily an aggregate (Figure 3.20). With immunofluorescence, we can only measure PER levels for one timepoint per fly, and in doing we assume commonalities of phase between flies. Feasibly every fly we test may possess a strong 24hr rhythm, but if a heterogeneity of phase is evident, which may be the case if developmental CYC loss does not remove the molecular oscillator but somehow limits the effectiveness of entrainment mechanisms, a dataset similar to the one we observe would be feasible. A strategy for live-imaging molecular oscillations, rather than collecting timepoints would clarify our data, as has been recently developed (Sabado et al., 2017). Similarly, repeating the dataset with more timepoints, and on multiple days throughout the freerun period, would be a highly desirable experiment for the lab to pursue in future work, and confirm is there are period changes following developmental CYC reduction.

Purely qualitatively, PER at locations representative of the LN_ds and 5^{th}-s-LN_v were readily identifiable in permissively raised flies, though not in restrictively raised flies, suggesting not all rhythms can be re-established. However, the complexity of the genetic background prevented a neat secondary marker to delineate cell groups, so we avoided a formal quantification.

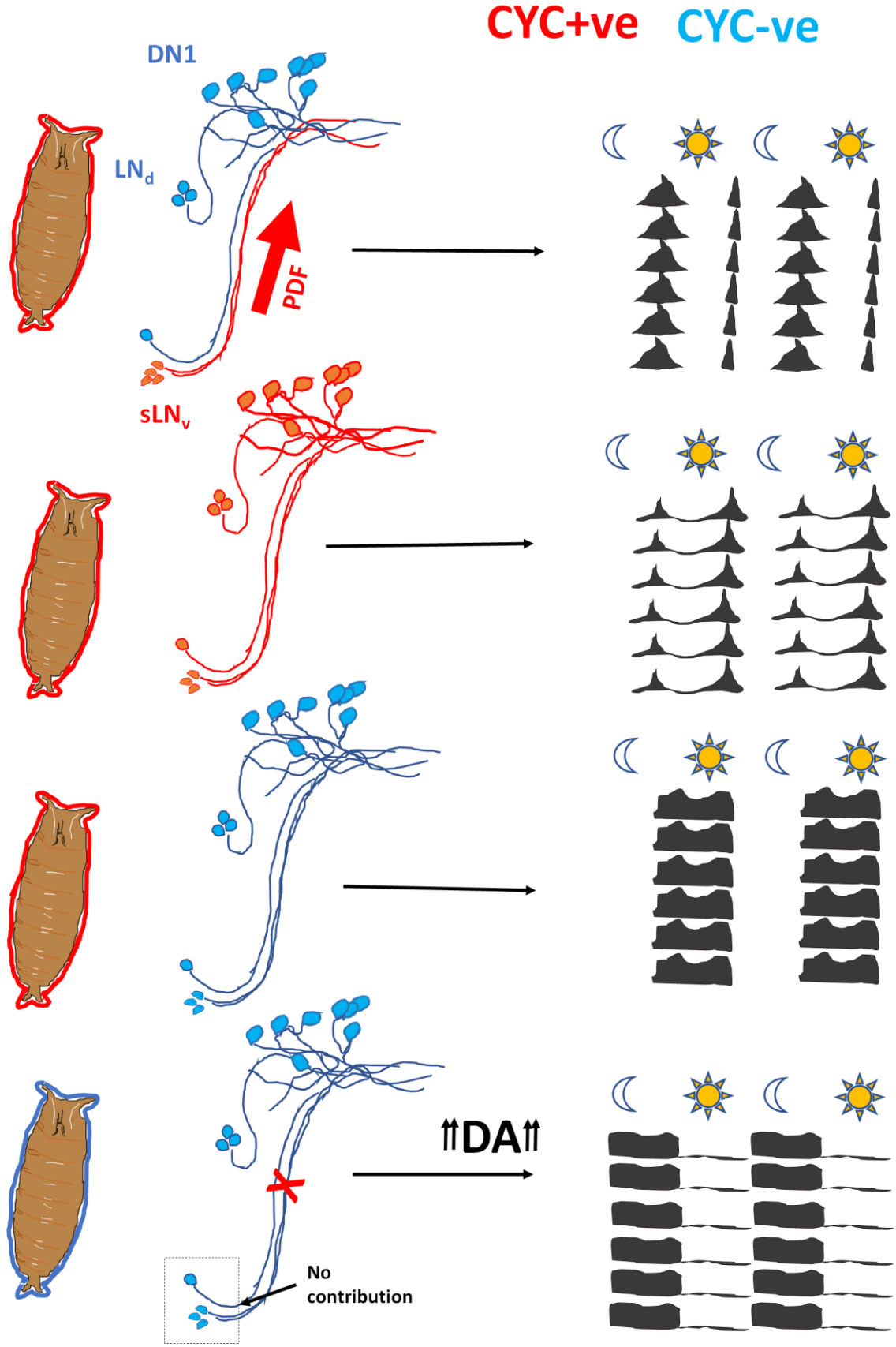

Figure 3.22 - Model for developmental and adult roles for cycle in behaviour during light-dark cycles. *Wild-type flies possessing normal levels of CYC exhibit a crepuscular profile in LD cycles, with mild diurnal preference. This general trend is retained when*

CYC expression is limited to the PDF-expressing neurons, although evening anticipatory behaviour is limited. Loss of either developmental or adult CYC eliminates a crepuscular profile and limits anticipatory behaviour. Loss of both developmental and adult CYC results in nocturnal preference, contingent on CRY activation during the day, dopaminergic cell signalling at night, which occurs irrespective of the presence of PDF-expressing neurons.

Chapter 4: Clock cell network morphology following developmental CYC loss

The previous chapter has defined the behavioural consequence of developmental CYC loss and uncoupled this phenotype from defects in molecular rhythms. The logical next step was to study aspects of the clock circuit downstream of the s-LN_v molecular oscillation, to identify defects that emerge following developmental CYC loss, primarily through neuroanatomical study.

4.1 - *cyc^{01}* flies, lacking functional *cycle*, possess dorsal PDF+ve projections that exhibit defasciculation and misrouting defects

Previous work has suggested a minority of *cyc^{01}* flies lack PDF+ve dorsal projections, both at larval and adult stages, suggesting a potential developmental role at larval stages or earlier, in initial projection formation (Park et al., 2000). This is similar to the observed *Clk^{Jrk}* projection phenotype in which PDF+ve fibers are uniformly absent from the dorsal brain, *Pdp1* RNAi phenotypes and PDF-specific CYC loss, (Park et al., 2000, Lim et al., 2007, Zheng et al., 2009, Goda et al., 2011). Another study from the Hall lab, though not an in-depth look, disagrees, suggesting that though projections between the s-LN_vs and DN1s are absent in *Clk^{Jrk}*, they are present and weaker in *cyc^{01}* (Kaneko and Hall, 2000). A paper from the Birman and Klarsfeld labs presents a similarly conflicting view, of "altered", though present dorsal projections in *cyc^{01}* (Vaccaro et al., 2017). A further study from the Park lab, also presents images of *cyc^{01}* dorsal projections, though it refers to them as l-LN_v derived deviations of the posterior optic tract (POT) (Bahn et al., 2009).

We first wanted to properly characterise the *cyc^{01}* dorsal projection phenotype, not purely by a qualitative approach as is the case with other labs, but by using the simple neurite tracer plugin in Fiji and analysing the resultant axonal skeleton map. Imaging and subsequent quantification of dorsal PDF+ve projections in 23°C raised adult *cyc^{01}*, dissected on the second day of DD at CT2, revealed projections were present and projected dorsally in a majority of cases (Figures 4.1, 4.2). A small minority appeared stunted, which are likely l-LN_v derived (Figure 4.4), potentially reflecting a complete absence of s-LN_v dorsal projections, or an inability to transport PDF. Of dorsally

projecting axons, few appeared akin to wt, a minority arborised the pars intercerebralis region and some would fail to arborise and form visible synaptic boutons at the correct site. In a majority of cases misrouted projections would emerge from the s-LN_v projections, the POT or the l-LN_vs, and in all cases the major neurite of the dorsal projection would show a strong defasciculated phenotype, potentially composed of overbranching, a loss of axonal bundling and in some cases arborisation of a misrouted projection around the dorsal projection.

As we utilise temperature-specific manipulations, we were intrigued to see if developmental temperature could affect this phenotype. We therefore raised *cyc*^{01} flies at 17°C, 23°C and 29°C, dissected as before and quantified the resultant phenotype, seeing no difference in PDF+ve cell or projection number, or projection complexity (Figure 4.1).

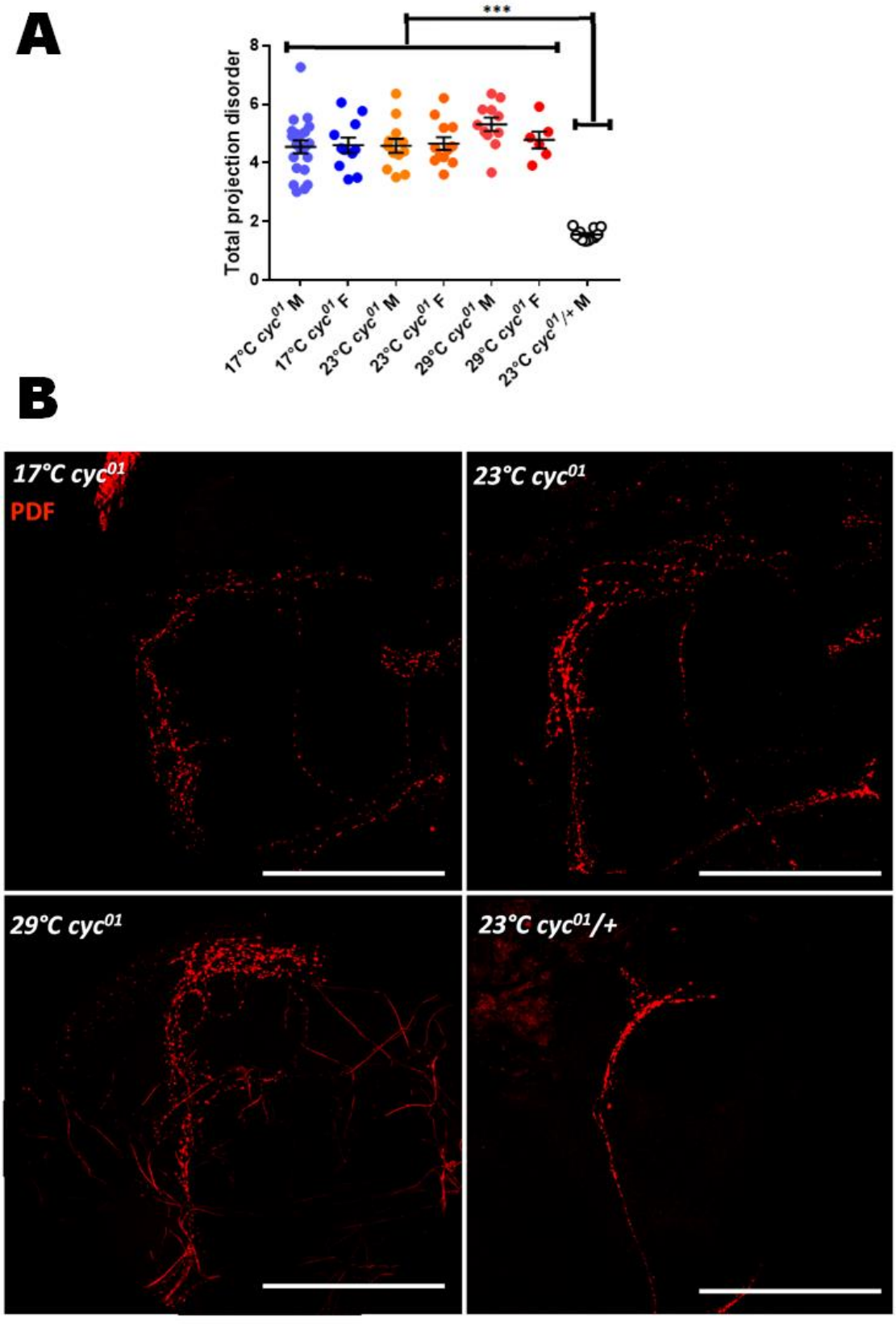

Figure 4.1 - Loss of cycle expression results in increased axonal complexity of PDF cells. *Panel A shows cyc^{01} projection complexity when raised at different developmental temperatures and dissected in DD at CT2. Complexity does not significantly differ between any two cases, relevant statistics by One-way ANOVA are presented in Appendix*

Table 8. A control for females 23°C cyc^{01}/+ was not conducted.Panel B shows representative images for each temperature, with scale bars in bottom right corresponding to 100µm.

We additionally studied projections expressing membrane-tethered of the genotype *Pdf-gal4>CD8::GFP;cyc^{01}* to confirm any differences between this and PDF stain, and, particularly as PDF stain is punctate, to strengthen our quantitative approach. Whilst there was extensive colocalisation between GFP and PDF, GFP expression appeared much weaker towards the dorsal part of the projection, and based purely on GFP stain, a chronic underestimate of PDF-projection completeness would be likely.

In certain cases, GFP is only expressed in the soma of l-LN_vs, and in these cases GFP is restricted to basally terminating projections, whilst dorsal PDF-expressing arbors are seperable (Figure 4.4). In these cases, we can infer GFP-ve projections originate from the s-LN_vs, and thus, both s-LN_vs and l-LN_vs innervate dorsally, but l-LN_vs terminate earlier, resulting in the "stunted" projections identified by other groups (Figure 4.4)(Park et al., 2000, Goda et al., 2011).

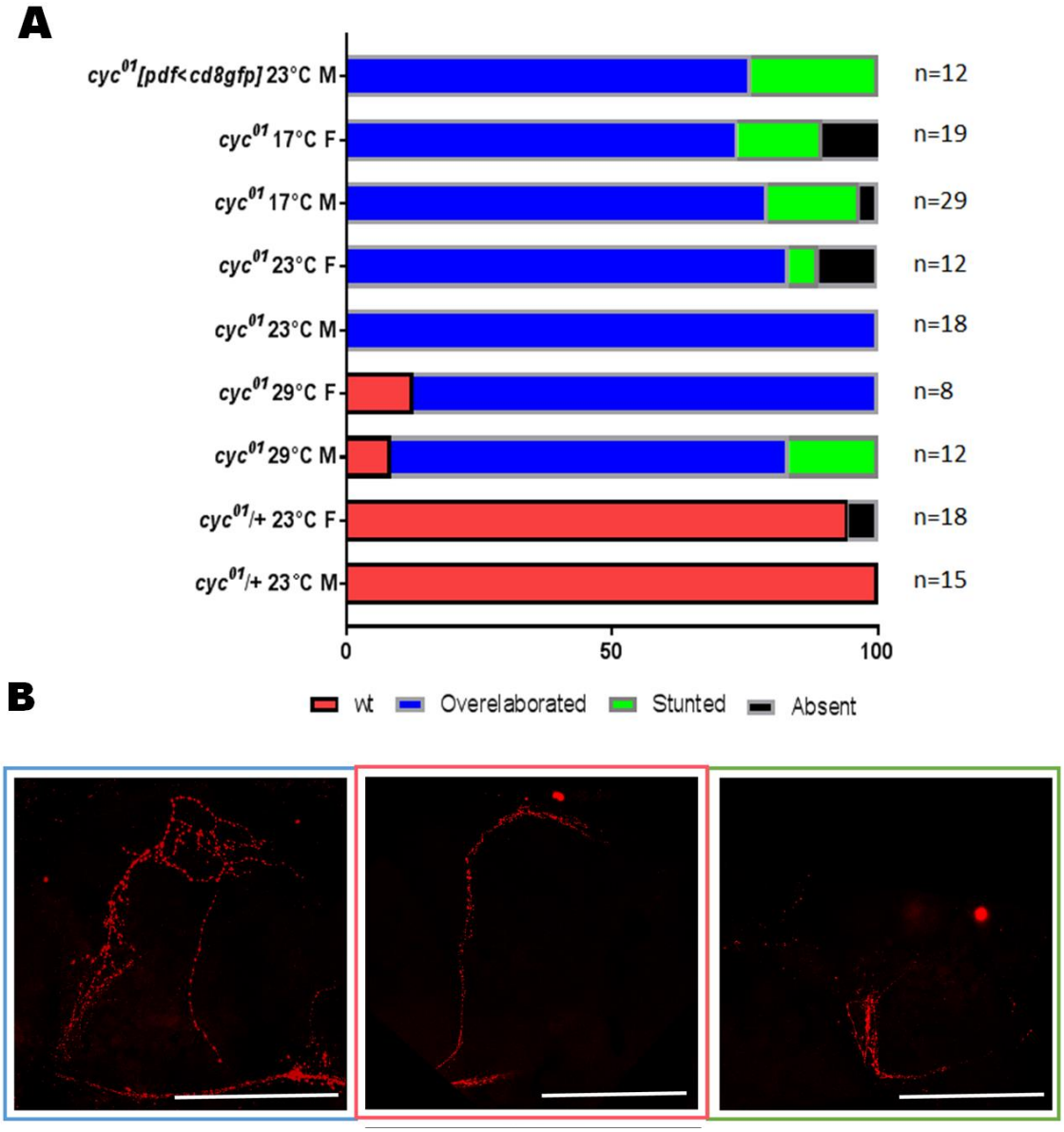

Figure 4.2 - Temperature has a negligible effect of PDF cell axonal complexity following loss of cycle. *Distribution of cyc^{01} s-LN_v dorsal projection morphologies at different temperatures, alongside % stunting, % misrouted, % wt-like. Panel B show representative overelaborated (Blue border), wt-like (Red border) and stunted (Green border) projections respectively. White scale bar in bottom right is 100μm.*

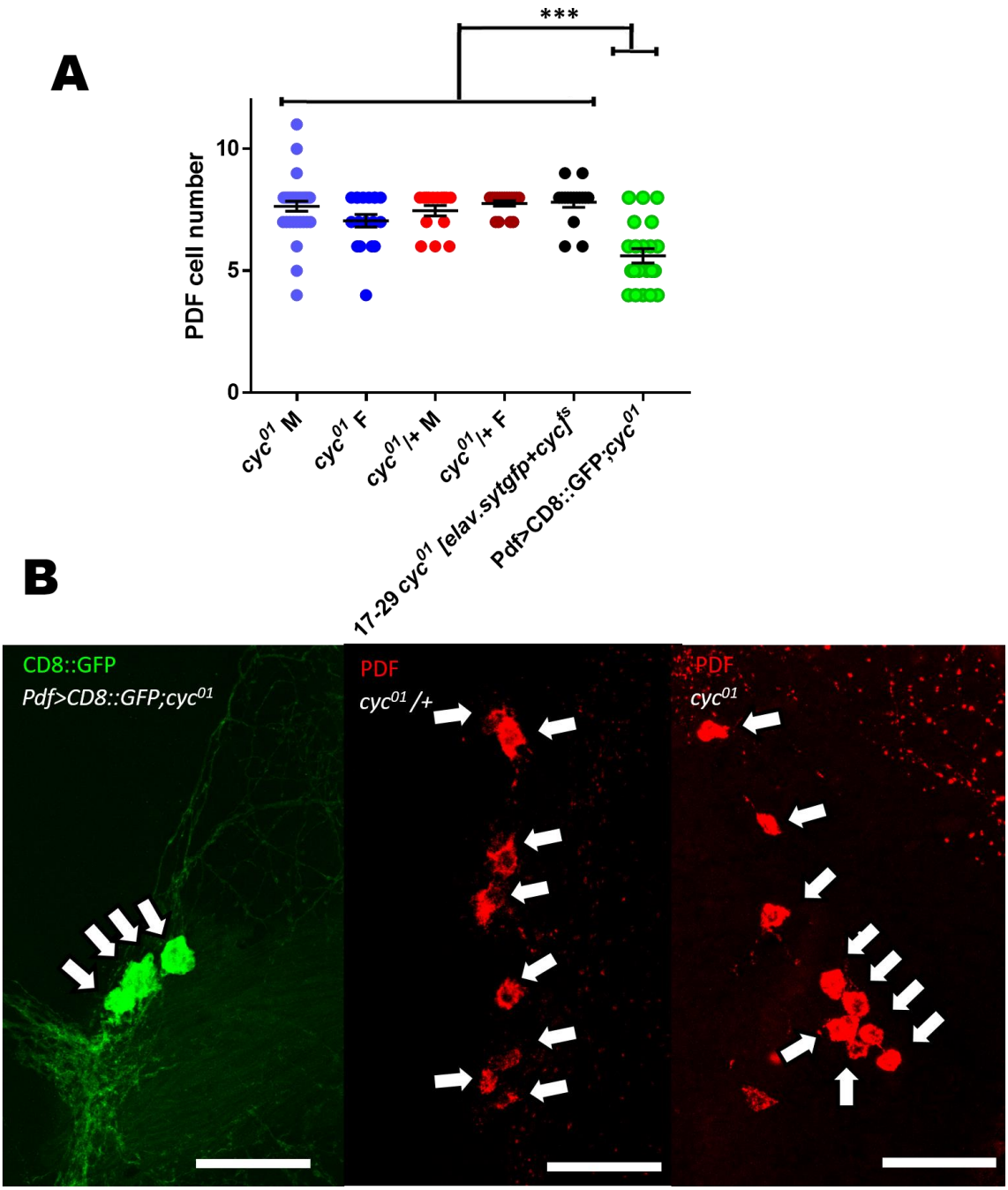

Figure 4.3, Panel A shows PDF cell counts in cyc^{01} and control flies, assessing the (Park et al., 2000) idea that observable PDF+ve soma, purely s-LN$_v$s, are reduced. Significant differences do not occur between cell groups quantified by PDF stain, regardless of genotype (Appendix Table 33). However, quantification of CD8-GFP cell number in genotype Pdf>CD8::GFP; cyc^{01} significantly differed to all other groups. Panel B shows example images of cell counts, with an additional PDF+ve soma visible in cyc^{01}, and no s-LN$_v$s visible in Pdf>CD8::GFP; cyc^{01}. Scale bar in bottom right is 50µm.

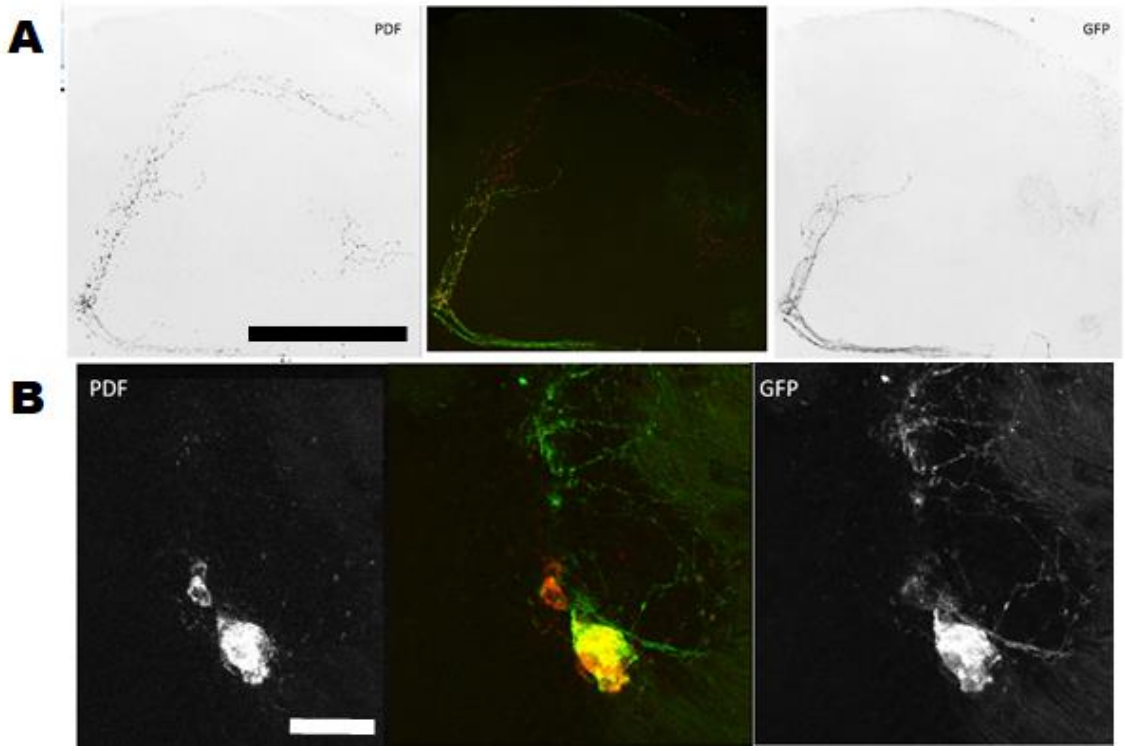

Figure 4.4 - Axons from both small and large lateral ventral neurons are misrouted dorsally following loss of cycle expression. *Panel A shows a maximum projection of a projection stained with PDF and GFP from a projection of genotype Pdf>CD8::GFP;cyc^{01}. Black scale bar in bottom right is 100µm. Panel B shows a single slice from a z-stack for Pdf>CD8::GFP;cyc^{01}, demonstrating representative differing staining patterns of PDF and CD8::GFP in soma, commensurate with that in axons. White scale bar in bottom right is 25µm. It must be stressed, in the majority of cases, GFP is visible along the length of the s-LN$_v$ dorsal projection, though in certain cases, weaker GFP presence in the s-LN$_v$s creates a visible divide between s-LN$_v$ and l-LN$_v$ projections.*

Unfortunately, staining GFP with *R6> CD8::GFP* and *c929> CD8::GFP* was unsuccessful (data not shown), which could have seperately highlighted s-LN$_v$ and l-LN$_v$ -derived projections.

4.2 – Developmental, but not adult loss of *cycle* expression phenocopies *cyc^{01}* projection phenotype

Dorsal projections were imaged and quantified at CT2 as previously described, on *cyc*^{01} *[elav.cyc]*^{ts} flies raised permissively for three days, moved to 17°C following egg-laying until adulthood, entrained in LD for three days at 29°C and dissected on the second day of DD at 29°C. This was repeated with flies raised permissively throughout development. As evident, the complexity of these projections is increased relative to those raised and run in permissive conditions, comprising a loss of axonal bundling, defasciculation and misrouting, similar defects to those of *cyc*^{01} flies (Figure 4.5). Permissively-raised flies appear to broadly phenocopy wild-type projection morphology, with a single fasciculated neurite and second order processes. No difference is observable between PDF cell size in either case, nor are additional PDF+ve cells common, as CLK misregulation has previously been shown to produce during metamorphosis (Lerner et al., 2015)(Appendix Figure 22).

cyc^{01} *[elav.cyc]*^{ts} flies raised permissively at 29°*C*, and moved into restrictive adult conditions at 17°*C* for five days prior to dissection were stained with PDF and dorsal projections were observed. In these flies, dorsal projections appeared intact, with very low levels of axonal elaboration or misrouting. Permissively raised, restrictively run flies do not significantly differ to permissively raised, permissively run flies at CT2, either pre or post-branching (♂: P=0.433, ♀: P=0.620), though a minority of brains do display an overelaborated phenotype (Figure 4.4). Post-branching site, it may be expected that loss of oscillations through loss of CYC would result in a static fasciculation state across circadian timepoints. One potential caveat we have identified is the presence of entrainable molecular oscillations in this condition (Figure 3.21), suggesting we do not create a truly restrictive condition in the adult, though projection complexity remains low in both males and females, despite the differing levels of molecular rhythmicity in these genders.

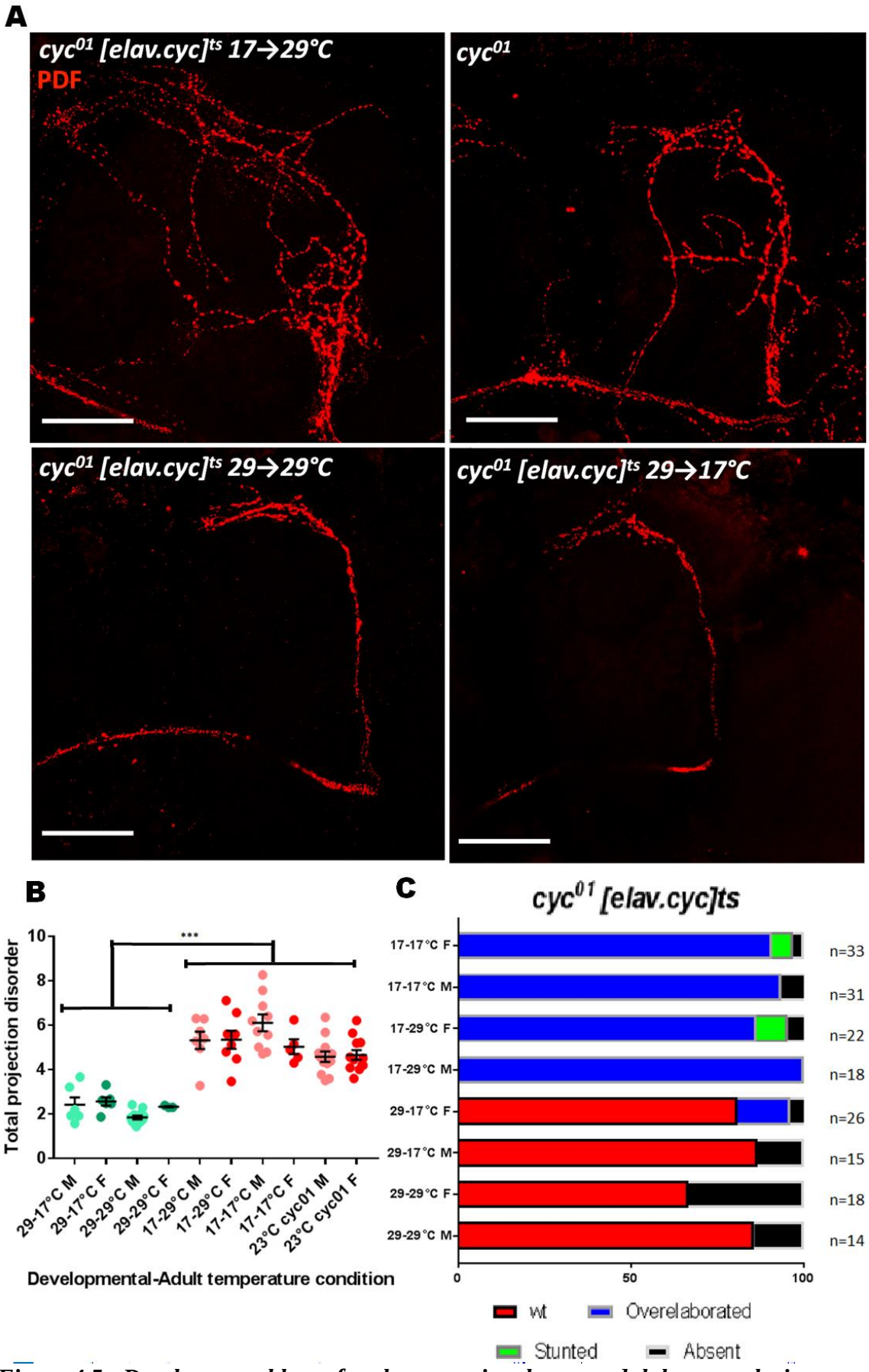

Figure 4.5 - Developmental loss of cycle expression, but not adult loss, results in increased axonal complexity of PDF cells. *Panel A shows representative images of s-LN$_v$ dorsal projection morphology in permissively and restricitvely raised, restrictively*

run cyc^{01} [elav.cyc]^{ts} flies and 23°C raised cyc^{01}. Scale bar in bottom left corresponds to 50µm. Panel B shows quantification of total axonal length relative to major neurite length, with significant differences between all flies possessing developmental CYC (Green), and all flies lacking developmental CYC (Red). Panel C shows the number of projections catagorised as wt (red), overelaborated (blue), stunted (green) or absent (black), with examples in Figure 4.2.

Conditional developmental PER overexpression, as expected, results in significantly more complex projections, relative to permissively raised controls. Though marred by low sample number, the projection complexity in these flies is not as severe as most low-CYC manipulations (Figures 4.5, 4.6), suggesting that inhibition via TIM/PER overexpression does not match levels of CYC knockdown. This additionally lends credence to the idea that the more severe damping of molecular rhythms following developmental PER overexpression is not due to a more effective abrogation of CLK/CYC function than *cyc^{01} [elav.cyc]^{ts}*, but is a separate byproduct of high PER levels.

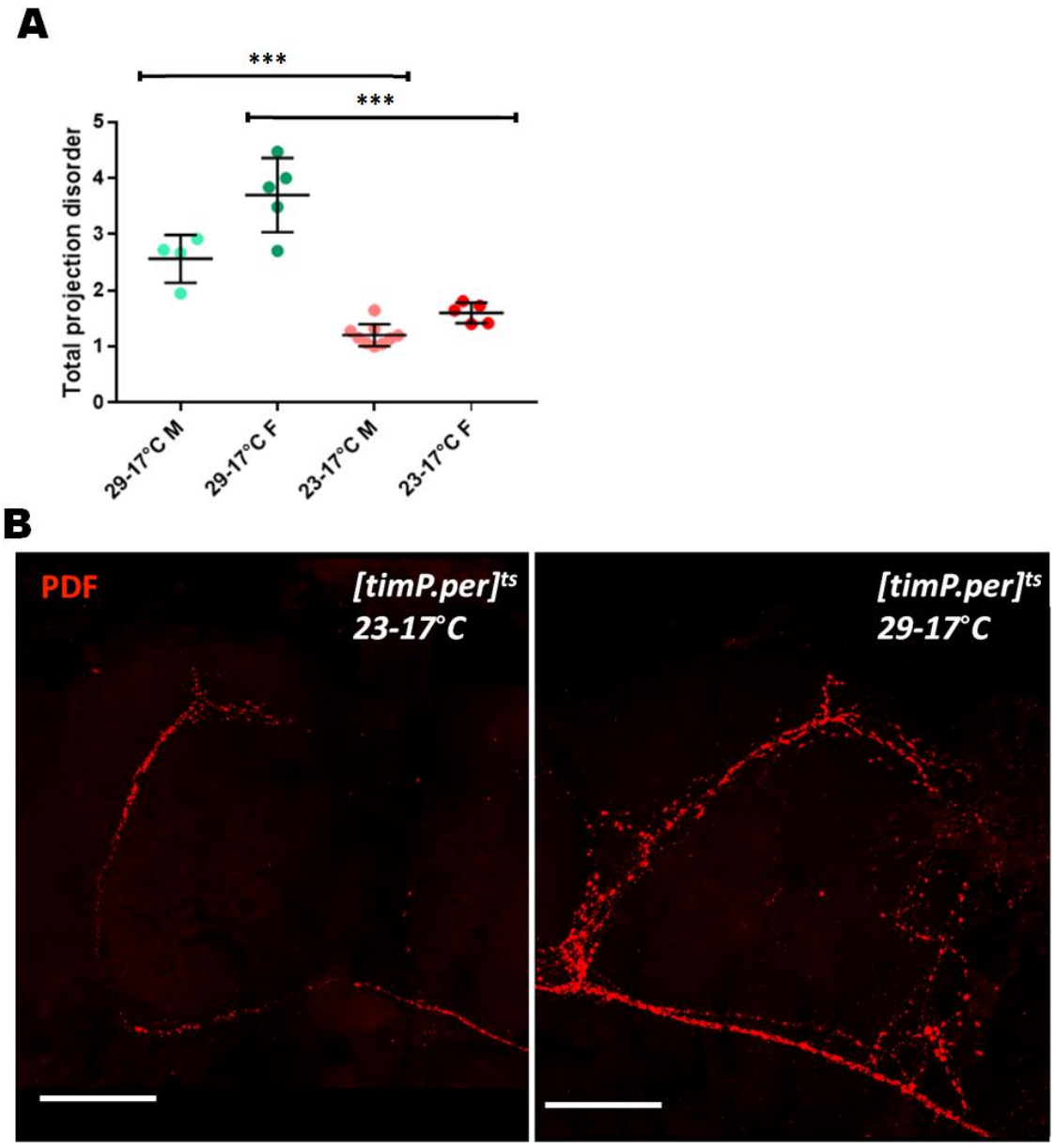

Figure 4.6 - Developmental overexpression of period increases the axonal complexity of PDF cells. *Panel A shows a dotplot of projection complexity of restrictively and permissively raised [timP.per]^{ts} PDF projections, in brains dissected at CT2 in 17°C DD. Restrictively raised flies appear noticeably more complex (P<0.001*** for both genders), in alignment with cyc^{01} [elav.cyc]^{ts} data. Panel B shows representative images of projections from restrictively (29°C) and permissively (17°C) raised male brains. Scale bar in bottom left is 50µm.*

4.3 – Following loss of *cycle*, increased branching complexity is observable within PDF-expressing neurons from third-instar larvae onwards

We further studied projection complexity in developmental stages, to identify where this

defect first arises, if this predates l-LN_v formation, and if this compliments our behavioural data suggesting a largely metamorphic requirement for CYC. (Park et al., 2000) contends that *cyc*^{01} and *cyc*^{02} larvae showed weaker PDF staining overall, and though cell bodies were visible, axonal projections could not be visualised in any brain. We therefore chose to stain *cyc*^{01} *[elav.cyc]*^{ts} 3rd-instar larvae, raised either at 17°*C* or 29°*C* from egg-laying, hypothesizing that some level of defect would be present in these brains.

Surprisingly, no significant differences arise between complexity of restrictively and permissively raised 3rd-instar larvae projections (Figure 4.7). In spite of this, we additionally quantified projection complexity in *cyc*^{01} and *cyc*^{01}/+ brains, in which PDF+ve projections were present, in this case *cyc*^{01} did not significantly differ to permissively and restrictively raised controls, but *cyc*^{01}/+ possessed a significantly lower complexity than all other groups (vs 17°*C cyc*^{01} *[elav.cyc]*^{ts} P=0.001 **, vs 29°*C cyc*^{01} *[elav.cyc]*^{ts} P=0.005 **, vs *cyc*^{01} P=0.014 *). One explanation is that ectopic CYC expression in the larvae is weak enough to result in a CYC deficit and defects in 29°*C cyc*^{01} *[elav.cyc]*^{ts}, which are then rescuable, resulting in the less-complex adult projection state, and suggestive of a corrective developmental remodelling.

(Park et al., 2000) suggests a minor reduction in s-LN_v cell number in third-instar larval *cyc*^{01} brains, and that the majority are present, but fewer are visible into adulthood. We do not see significant differences in cell number at this stage, which seem independent of CYC-regulation (Figure 4.7). PDF staining in 1st-instar larvae was too sporadic and weak to formally quantify, so we could not determine if projection defects coincided with original larval projection formation, or were due to a later developmental event.

As the beginning of pupation is a state of ecdysone-induced neuronal remodelling, and an increase in complexity of the clock neural network, it is not unexpected that PDF projections would be required to prime adult connectivity at this time. Indeed it is known that the dorsal cells identifiable by the *Clk4.1M-gal4* driver, which directly interact with the s-LN_vs are absent in the larval clock circuit (Zhang et al., 2010a, Guo et al., 2016).

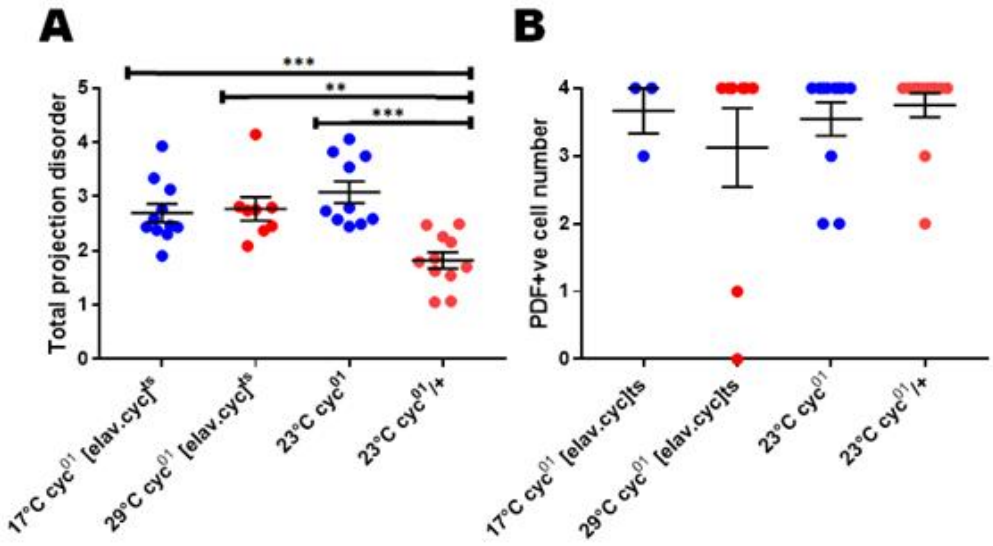
A
B
Total projection disorder
PDF+ve cell number
***
**
***
17°C cyc01 [elav.cyc]ts
29°C cyc01 [elav.cyc]ts
23°C cyc01
23°C cyc01/+

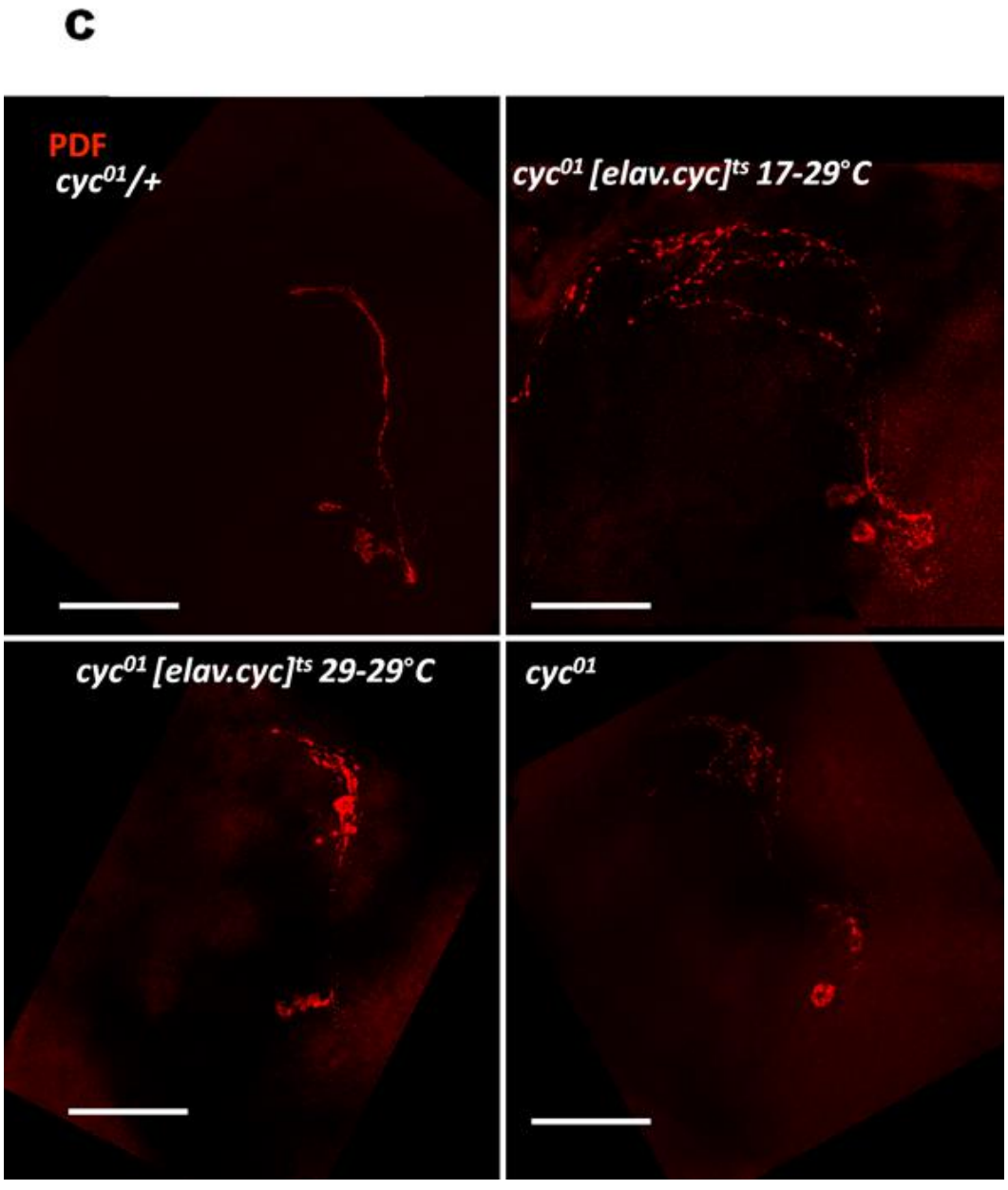
C
PDF
cyc01/+
cyc01 [elav.cyc]ts 17-29°C
cyc01 [elav.cyc]ts 29-29°C
cyc01

Figure 4.7 - Loss of cycle expression results in increased axonal complexity of PDF cells in larval brains*. Comparison between complexity of PDF+ve dorsal projections in 3rd-instar larvae, in restrictively and permissively raised cyc^{01} $[elav.cyc]^{ts}$ and cyc^{01} , dissected at CT2. Panel A shows projection disorder, in which wt-like heterozygotes significantly differ to cyc^{01} and both experimental genotypes. Panel B shows PDF+ve cell number. Panel C shows representative images for each condition, where it is observable that PDF projections for cyc^{01}/+ appears strongly fasciculated, whilst others do not. Scale bar shown in bottom left is 50μm.*

This raises several hypotheses as to the function of CYC. CYC expression may be required to mediate either pruning, if it exists, leading to exuberant structures which disrupt subsequent sites of growth cone formation and result in defasciculation, or as a negative regulator of regrowth or branching of axons, in the absence of which we see an increase in complexity. The implication is that this signalling may take place within the s-LN_v cells, though as these communicate extensively with other clock cell clusters, perhaps CYC in other clock cells mediates this phenotype. More than one hundred clock-bearing neurons are identifiable throughout 3rd-instar and pupal stages, yet do not form a part of the larval clock circuit, and, as CYC has previously been shown as required in the formation of ectopic clocks, it may be involved in integration of these cells into the circuit (Zhao et al., 2003, Liu, 2015).

We have suggested that l-LN_v projections, absent in third-instar larvae, through similarities in molecular constitution with the s-LN_vs are able to follow s-LN_v axonal guidance cues and aberrantly innervate the dorsal area in an s-LN_v-like way, contributing to the defect, as has been suggested by others, and been observed in Clk^{Jrk} mutants (Park et al., 2000, Wulbeck et al., 2008). On the basis of staining intensity, it seems likely that these stunted projections are l-LN_v derived, and likely contribute to projection disorder.

Though we have focussed on the dorsal s-LN_v projections, misrouting is also regularly identifiable around the l-LN_v-derived POT, particularly at the midpoint, as has previously been published in cyc^{01} (Park et al., 2000). As an l-LN_v-based neurite, it is unknown if this misrouting is l-LN_v-specific, or very extensive misrouting of s-LN_v axons which respond to POT cues. *Pdf>CD8::GFP;*cyc^{01} staining of projections which have completely deviated from a canonical neurite appear generally GFP-ve, suggesting these

are not l-LN_v-derived (Figure 4.4).

One paper suggests, without crucial morphological evidence that the larval s-LN_vs likely degenerate through pruning and a reformed adult projection extends in the early pupal stages (Gorostiza and Ceriani, 2013). Synaptic degeneration is expected to occur so the dorsal projections can respond to find targets in a rapidly altering CNS, though the extent of this, or whether pruning is induced, is unknown, and to characterise the CYC loss defect it is necessary to define if, and how, the s-LN_vs remodel during early metamorphosis.

If pruning and re-extension does occur during this early pupation, it is not unreasonable we might struggle to identify projections. A rapid inspection of wt brains at 18 hours post-puparium formation (hpf), the timepoint at which pruning is reliably identifiable and studied in the mushroom bodies, intact s-LN_v projections were visible in 50/54 hemispheres. The projections were not individually imaged, so were not traced or quantified, but no obvious morphological changes from larvae were apparent. Our inability to identify pruning is consistent with observations from other groups (Helfrich-Förster, 1997).

Projections were visible in 17/28 cyc^{01} hemispheres at 18hpf, though in these cases there were no obviously stunted or retracted projections, suggesting that if CYC does prevent pruning, this may be restricted to a minority of projections, or more likely relates to PDF levels. This does not preclude a more widespread pruning occurring at a later stage, though such a phenotype would not coincide with the metamorphic ecdysone pulse.

We then looked at the projections of cyc^{01} and cyc^{01}/+ at P6 developmental stage (25-40 hpf) (Figure 4.8), a developmental stage identifiable by a gradual greening of Malpighian tubules in the absence of other pigmented structures. The decision to use (Bainbridge and Bownes., 1981) developmental stages rather than % pupation as in previous circadian studies was founded on the condition that we might need to distinguish developmental states in TARGET-containing flies raised at different temperatures, where morphological assessment of development may be more informative than temporal, and secondly to allow a broader window in which to dissect pupae (Bainbridge and Bownes., 1981, Helfrich-Förster, 1997, Liu, 2015). Unfortunately, we struggled to collect sufficient TARGET-flies at the permissive temperature, and looked instead at cyc^{01} and cyc^{01}/+

projections. *cyc*^{01} projections were significantly more complex than *cyc*^{01}/+ at this stage, remarkably so, demonstrating that CYC loss results in increased axonal complexity (Figure 4.8).

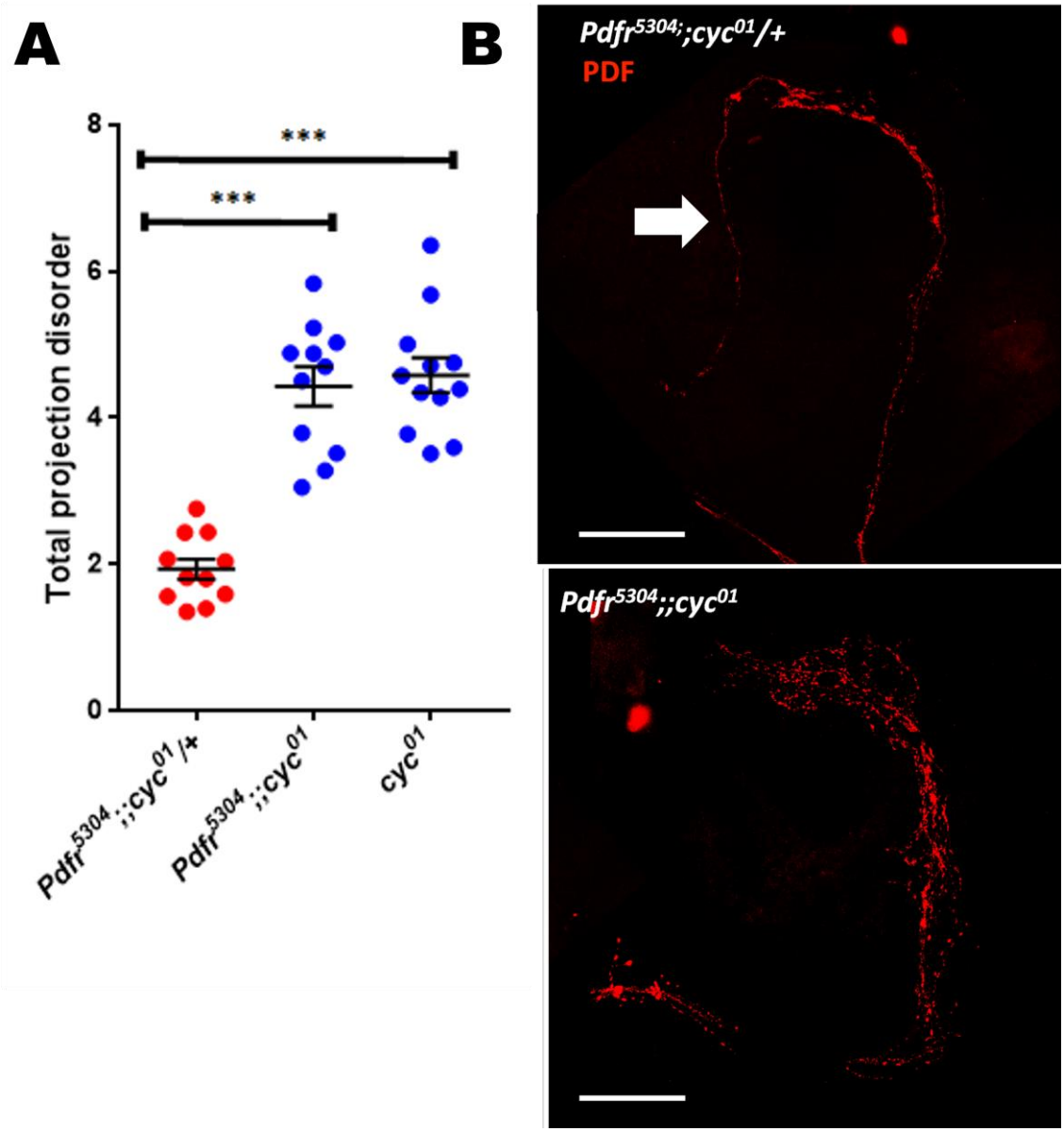

Figure 4.8 - Loss of cycle expression results in increased axonal complexity in mid-pupal brains*. Panel A shows projection disorder of s-LN*$_v$ *dorsal projections in 23°C-raised stage P6 pupae, possessing or lacking CYC, dissected at CT2, demonstrating significant differences in projection complexity are observable during pupal remodelling. Panel B shows representative images for cyc*^{01} *and cyc*^{01}*/+ pupal s-LN*$_v$ *projections, scale bar shown in bottom left is 50μm.*

In the vast majority of these flies (10/12 *cyc*^{01}/+ and 12/14 *cyc*^{01}), l-LN$_v$+ve soma or projections were not visible, and the literature suggests they do not develop until late

metamorphosis, adding to our belief that increased complexity is largely not the result of l-LN_v misrouting. As our quantification of projection complexity is inversely related to length of the major neurite, we demonstrate significant differences in complexity between genotypes is not due to neurite length, and indeed there is a significant correlation between greater axonal length and overall projection complexity (Appendix Figures 10 & 11).

We have thus demonstrated that developmental CYC loss results in increased projection complexity, although in the case of permissively raised *cyc^{01} [elav.cyc]^{ts}*, high larval complexity is not indicative of adult projection complexity, suggesting CYC can regulate complexity during metamorphosis. A functional s-LN_v dorsal projection is required for freerunning behaviour, and though morphological defects opens the possibility to altered function, it is unknown if this projection defect is capable of causing behavioural arrhythmia, though this would be hypothesised (Fernandez et al., 2008, Agrawal and Hardin, 2016).

4.4 - Increased complexity of PDF-expressing dorsal projections is not solely indicative of projection dysfunction and can occur in behaviourally rhythmic populations

Whilst low CYC genotypes resulting in majority aberrant dorsal projections are also majority arrhythmic, despite restarting the molecular oscillator, it is preferable to demonstrate a segregation of the two phenotypes, on a population of mixed behavioural rhythmicities. Raising flies at 17°*C* from egg-laying and transferring 3rd-instar larvae to a permissive condition into adulthood results in a distribution of rhythmicities with significant strongly rhythmic and arrhythmic fractions (Figure 3.17), and flies raised in this manner were sorted into AR and SR categories before dissecting and staining for PDF. To our surprise, Sholl and projection disorder metrics did not significantly differ between AR and SR groups. Both groups showed a high-level of defasciculation and, though at the cusp of significantly differing in complexity to 17→29°*C cyc^{01} [elav.cyc]^{ts}* females, significant differences do not emerge when compared with other low-CYC genotypes (Appendix Table 12). Whilst this does not detract from our finding of a novel requirement for CYC during projection formation, it appears that increased projection complexity alone does not cause behavioural AR in *cyc^{01} [elav.cyc]^{ts}* flies. It is likely that defasciculation is not the sole phenotype of metamorphic CYC loss, purely the most

easily observable of a litany of defects present within the projection. Whilst the AR and SR populations cannot be distinguished solely by PDF-cell morphology, whether both groups are forming functional synapses with the dorsal clock cells is unknown.

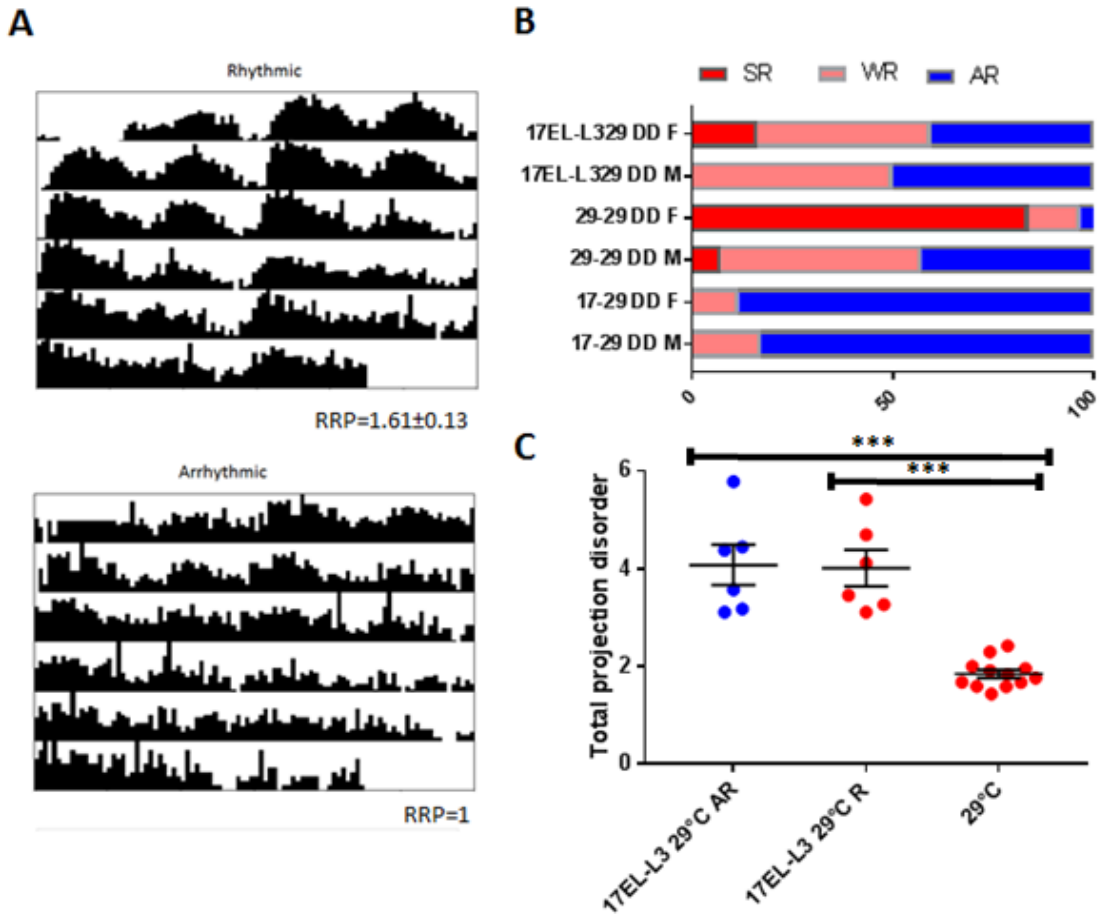

Figure 4.9 - Mild increases in axonal complexity are observable in both behaviourally rhythmic and arrhythmic flies*. Panel A demonstrates the intermediate behavioural rhythmicity of flies raised restrictively through to larval stages, compared with those raised restrictively throughout development or permissively throughout development. Panel B shows average actograms of rhythmic and arrhythmic fractions of 17°C EL-L3 29°C* cyc^{01} *[elav.cyc]*^{ts} *flies. Panel C shows total projection disorder of AR and R fractions, compared to permisively raised* cyc^{01} *[elav.cyc]*^{ts}*, in which arrhythmic and rhythmic fractions significantly differ to permissively raised brains, but not to each other.*

One could argue that the threshold of CYC reached in rhythmic flies is sufficient for certain roles, but not for others, for instance CYC levels may be too low for correct projection routing, but high enough for wt connectivity. Developmental CYC loss therefore results in a state of increased projection complexity, itself not neccesarily

causative of arrhythmia, and intact molecular oscillations, so the reason for behavioural arrhythmia is not straightforward.

4.5 – Bouton number and localization in PDF-expressing dorsal projections is altered in the absence of *cycle*.

In order to uncover other defects associated with the cyc^{01} dorsal projections, we expressed synaptotagmin-tagged GFP, a presynaptic marker, with the *Pdf-gal4* driver in order to visualise and quantify mature synaptic boutons. WT synapse number at CT2 in our experiment is similar to that in other published work, validating our approach (43.57±2.20), clustering around the projection termini with few or no boutons at the base of the projection (Figure 4.10) (Gatto and Broadie, 2009, Gorostiza et al., 2014). Surprisingly, repeating this experiment on a cyc^{01} background, we saw considerably more GFP+ve puncta at the second order processes (Figure 4.10)(Appendix Table 13). Though we excluded basal synapses from our analysis, many morphologically correct synapses appeared on misrouted projections around the base. As the bulk of this is likely l-LN_v derived, it is interesting that l-LN_vs are not merely misrouting but aberrantly attempting to form synaptic connections in this region of the brain, with potential functional implications.

In both wt and cyc^{01}, GFP staining is evident in the soma of the LN_vs, demonstrating that mature synapses, whilst well represented, are not the sole site of synaptotagmin-GFP localisation, and a secondary argument might contend that GFP accumulation along the projection may be due to trafficking defects.

In many cases, GFP and PDF puncta colocalise, suggesting mild blebbing in which proteins accumulate, or aberrantly-developing synapses. Uniformly, staining at the lower neurite is relatively stronger than staining in the dorsal part of the projection, in contrast to wt, which shows the opposite effect. Our staining experiment with *CD8::GFP* (Figures 4.2,4.4) suggests that in many cases, *Pdf-gal4* driven expression differs between s-LN_vs and l-LN_vs, demarcating projections from each respective cell type, thus giving the illusion of stronger basal stain. *SYT::GFP* appears to be expressed and trafficked to the s-LN_v second order-processes more reliably than *CD8::GFP*, though we are unsure why.

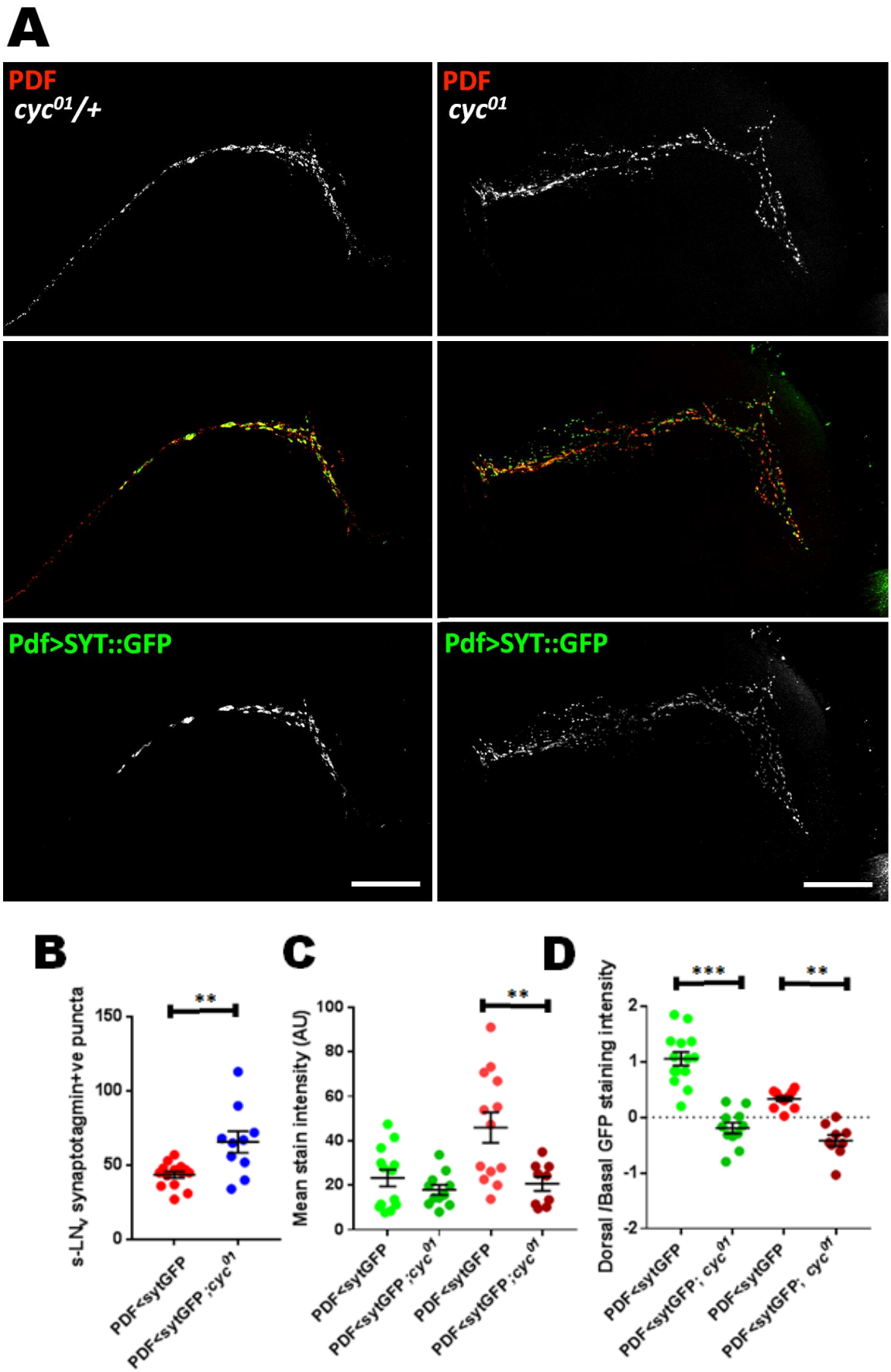
A
PDF
cyc01/+
PDF
cyc01
Pdf>SYT::GFP
Pdf>SYT::GFP
B
s-LNv synaptotagmin+ve puncta
150
100
50
0
**
PDF<sytGFP
PDF<sytGFP ;cyc 01
C
Mean stain intensity (AU)
100
80
60
40
20
0
**
PDF<sytGFP
PDF<sytGFP ;cyc 01
PDF<sytGFP
PDF<sytGFP ;cyc 01
D
Dorsal /Basal GFP staining intensity
2
1
0
-1
-2
***
**
PDF<sytGFP
PDF<sytGFP; cyc 01
PDF<sytGFP
PDF<sytGFP; cyc 01

Figure 4.10 - PDF cell synapses are more numerous and mis-localised following loss of cycle expression. *Panel A shows representative co-staining of PDF (Red) and Pdf>SYT::GFP (Green) in cyc^{01} and cyc^{01}/+ flies, dissected at CT2. Scale bar in bottom right is 50μm. Panel B shows quantification of bouton number in the dorsal projection, where, despite greater numbers of puncta, cyc^{01} puncta appear smaller and weaker, and are perhaps not indicative of mature pre-synapses. Panel C displaying values of Mean GFP staining intensity in the dorsal part of the projection. Panel D shows Ratio of PDF or SYT-GFP staining between the dorsal and basal part of the projection, where wild-type flies show an increase in PDF and SYT staining at the dorsal termini, which is lost in cyc^{01}. Green represents GFP, and red represents PDF. Statistics are available in Appendix Table 13.*

We additionally performed Sholl analysis on s-LN$_v$ termini in order to determine differences in complexity. Second-order-processes appear consistently more complex in flies lacking developmental CYC, indicating that the difference in complexity is not solely the result of basal l-LN$_v$ innervation, but also at the point of presumed local connection formation. This increase in complexity correlates with an increased bouton number, suggesting targets are altered at this time (Figure 4.11, Appendix Table 10).

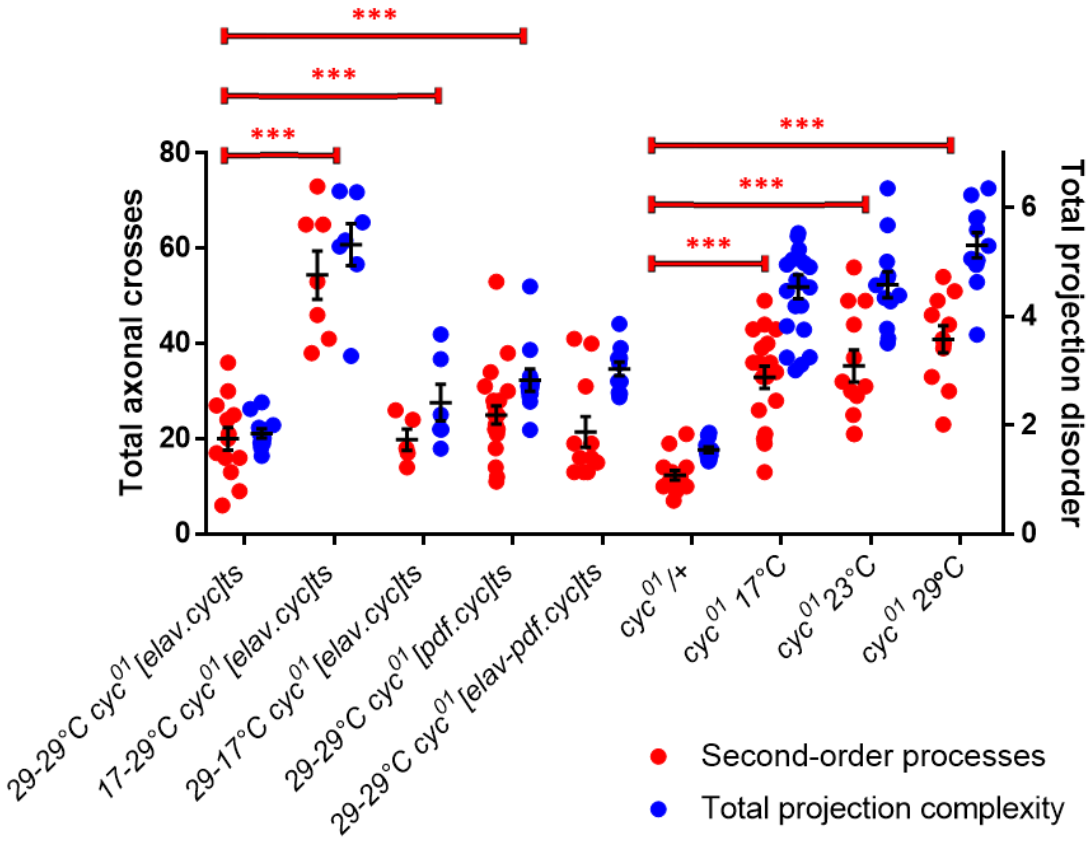

Figure 4.11 - Loss of cycle expression alters the morphology of dorsal synapse-forming termini of pacemaker neuron axons. *Sholl analysis of second-order processes in various cyc^{01} and CYC rescue lines at CT2, in comparison with total projection complexity. Sholl*

analysis of restrictively raised cyc^{01} $[elav.cyc]^{ts}$ and cyc^{01} differ to control conditions, rescue of CYC in either PDF cells or non-PDF neurons results in a sholl value which does not significantly differ to pan-neuronal rescue of CYC.

4.6 –Post-synaptic targets of PDF-expressing neurons in the dorsal brain appear altered in the absence of *cycle*.

We also studied projection morphology of PDF-ve clock neurons in cyc^{01} flies to determine connective states. A previous paper, (Kaneko and Hall, 2000) failed to identify significant losses in cell projection or soma number in cyc^{01} brains, however, this study was cursory and we strove to re-test this.

A recent study showed loss of LAR, a transmembrane axon guidance gene, which results in loss of s-LN_v dorsal projections, does not prevent molecular rhythms, and in doing so demonstrates the presence of PER-positive nuclei segregated to expected regions of the brain in wt-like numbers, suggesting that these cells, but not necessarily their projections, develop normally without s-LN_v input (Agrawal and Hardin, 2016). We can infer from this, and our other data that reduced identifiable dorsal clock cells is not the result of projection phenotypes caused by CYC-loss.

We first studied presence of a purported s-LN_v target, the DN1ps, via *CD8::GFP* expression with *Clk4.1M-gal4* driver, the strength of which hypothetically should not be tied to CLK/CYC levels. However, the *Clk4.1M*+ve cluster of DNs was never fully visible in cyc^{01} flies. Isolated soma and weak projections could be identified, in which some residual connectivity could be assessed. In the majority of cyc^{01} brains, there was no hint of dorsal staining and from that we infer a general disrupted connectivity. In wild-type brains, *Clk4.1M*+ve DN1ps and PDF cells form distinct connections, as exemplified by colocalisation in Figure 4.12a, and previously published elsewhere (Zhang et al., 2010a , Guo et al., 2016). This could be a result of reduced driver strength, but may also be due to a developmental effect influencing DN1 formation and specification. As these cells become clock+ve during metamorphosis, it is feasible that metamorphic cues dependent on CYC are necessary for their specification. Indeed, the DN1p cells may be present, but simply do not fall under the purvue of the *Clk4.1M-gal4*

driver without CYC, and cannot be visualised.

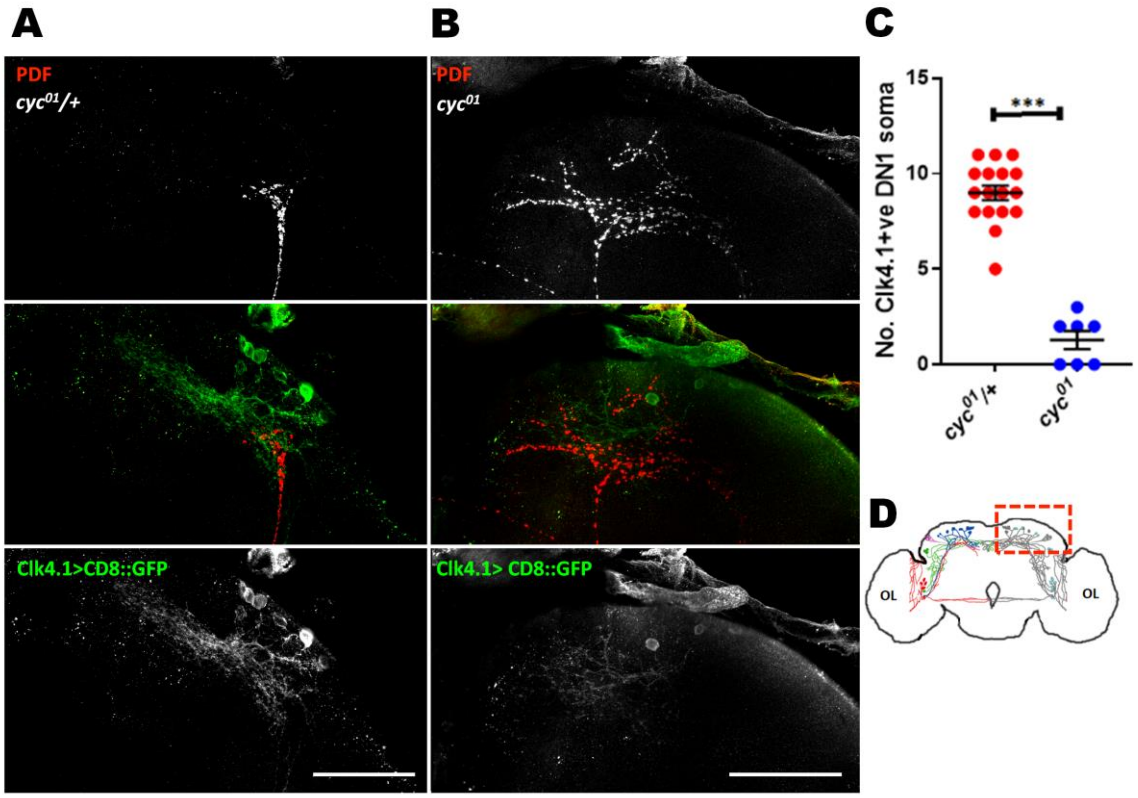

Figure 4.12 - Loss of cycle expression results in a decrease in identifiable dorsal clock neurons*. Comparison between Clk4.1M>CD8::GFP staining in cyc^{01} and cyc^{01}/+ at CT2. Panel A shows an example image from cyc^{01}/+, with wt-like s-LN_v projections (Red) interacting stably with GFP+ve DN1p dendrites (Green). Panel B shows a cyc^{01} brain, with misrouted PDF arbors (Red) and a reduction in identifiable DN1ps (Green). Scale bars in bottom right are 50μm. Panel C quantifies the number of visible Clk4.1M+ve DN1p cells in cyc^{01} heterozygote and homozygote backgrounds. Evident is a loss of identifiable cells on a homozygous background (P<0.001***). Panel D highlights the imaged dorsal region of the brain.*

Unfortunately, we found *Clk4.1M>UAS-hid* to be lethal, so the requirement of these cells in establishing PDF-cell morphology is unknown. Expression of Δcyc^{103} with *Clk4.1M-gal4* driver in DN1ps fails to impact behaviour, suggesting a limited requirement for DN1p CYC in behavioural circuit formation, however Δcyc^{103} may not remove all CYC function (Chapter 5).

Though caveats, outlined above, are present, we identify differences in clock circuit

connectivity in the absence of CYC, and suggest that *cyc*^{01} does not possess an intact circuit. Principles of axon guidance state that separate cues regulate growth cone targeting to a certain region and synaptic connectivity, and the absence of dorsal projection in the dorsal region combined with the defasciculated s-LN$_v$ projections entering this region suggests that response to cues in multiple clock cell subsets may be defective.

4.7 - The projection and behavioural phenotypes caused by developmental loss of *cycle* are not due to aberrant PDF signalling

The lack of *Pdf*^{01}-like LD phenotypes suggests PDF signalling is not defective, though this is likely related to l-LN$_v$ PDF levels rather than s-LN$_v$ PDF levels, which are involved in freerunning rhythms. Whilst PDF levels may be present in *cyc*^{01}, it is unknown if the accumulation of PDF in the dorsal terminals in low CYC manipulations is sufficient for PDF-signalling driving behavioural rhythms, and cannot be ruled out as a cause for behavioural arrhythmia. Tethered ectopic PDF, resulting in constitutive PDF signalling improves *Pdf*^{01} rhythmicity, though rendering complex rhythms, so cyclical PDF accumulation in the s-LN$_v$ termini is not required for behavioural rhythms, but potentially phase (Kula et al., 2006, Choi et al., 2009).

As previously mentioned, (Gorostiza and Ceriani, 2013) characterised a misrouting phenotype in s-LN$_v$s through developmental loss of PDF signalling. The defect of PDF signalling appears milder and stereotypic compared to that of CYC loss, though we deemed quantification via our methodology was necessary to rule out a potential dominant role of PDF signalling in worsening the defect. We studied *Pdfr*^{5304} and *Pdfr*^{5304}*::cyc*^{01} projection complexity in order to conclusively state that A) the s-LN$_v$ misrouting phenotype previously characterised in PDF signalling mutants is milder and distinct from *cyc*^{01} defect, and B) Aberrant and exuberant PDF signalling stemming from a loss of developmental CYC does not cause projection defects (Figure 4.13).

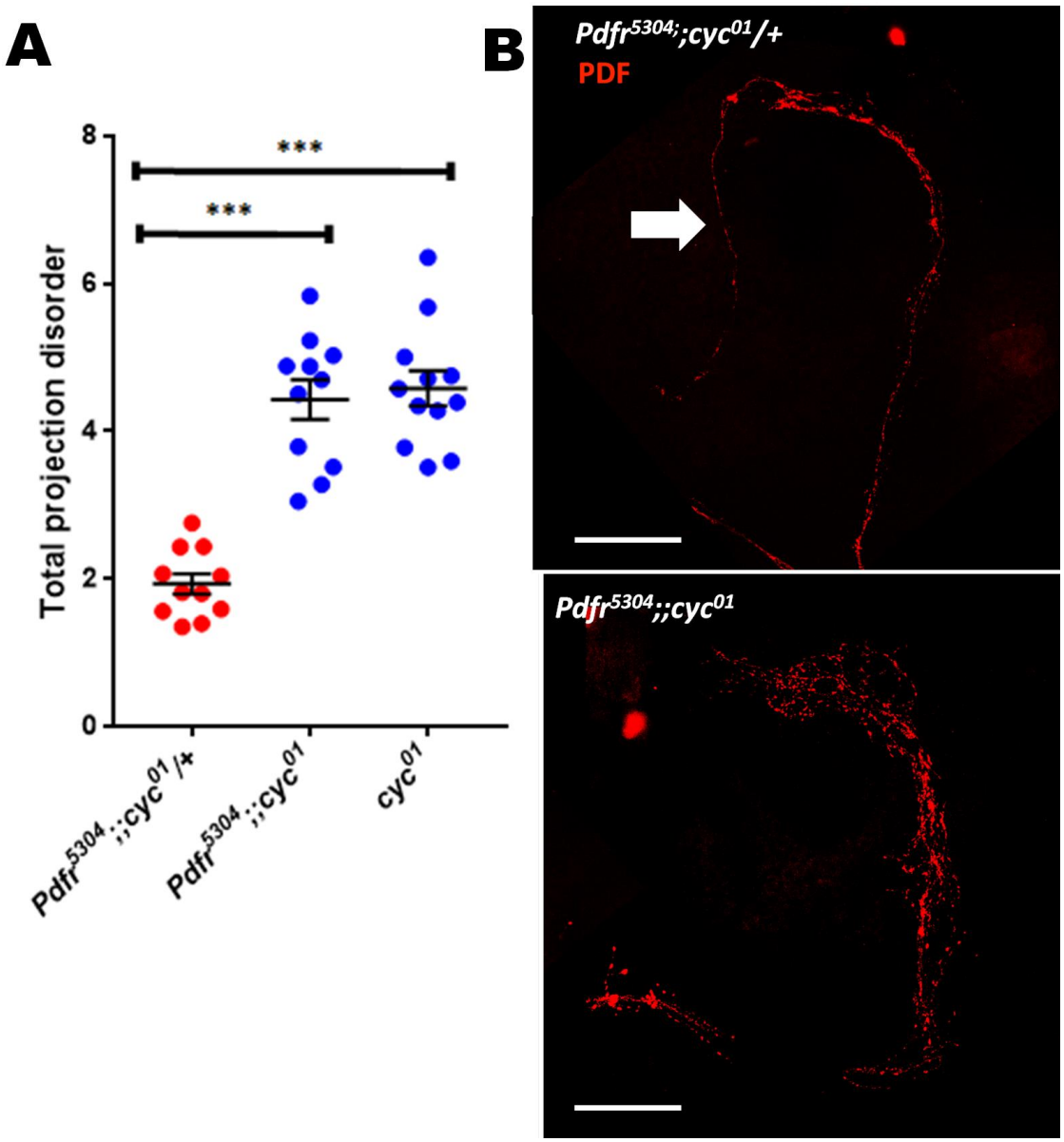

Figure 4.13 - PDF receptor is required for correct PDF axon termini morphology, but loss of PDF receptor is distinct from loss of cycle expression. *Comparison of s-LN$_v$ dorsal projection complexity between Pdfr^{5304} and Pdfr^{5304}::cyc^{01}, demonstrating that loss of PDF signalling has only mild effects on overall projection complexity. Panel A shows a dotplot of projection disorder demonstrating that Pdfr^{5304}::cyc^{01} and cyc^{01} do not significantly differ (P=0.905), whilst both significantly differ with Pdfr^{5304} (P<0.001***). Panel B displays a representative Pdfr^{5304} projection, with a single misrouted arbor (white arrow), as has been published previously (Gorostiza and Ceriani, 2013). Scale bars in bottom left are 50μm.*

Though the misrouting defect, of a single arbor, is present in a number of *Pdfr^{5304}* projections, the overall projection complexity is low and comparable to wt, demonstrating independence of the defects. *Pdfr^{5304}::cyc^{01}* projections appeared complex

and *cyc*^{01}-like, showing that a deranged but active PDF signalling is not responsible for the *cyc*^{01} phenotype. This is not entirely unexpected, as the Ceriani group has previously shown electrical activity is not required in the clock circuit during development for adult rhythms, suggesting the projection defect and neuronal remodelling is seperable from conventional s-LN$_v$ signalling (Depetris-Chauvin et al., 2011). However, PDF trafficking and secretion may occur in states of low electrical activity, so ours is a novel finding.

The Ceriani lab additionally demonstrated loss of BMP-signalling during pupation caused a defasciculated phenotype more evocative of *cyc*^{01} than *Pdfr*^{5304} projections, which they ascribe to retrograde trans-synaptic BMP signalling, as has been characterised in the larval neuromuscular junction (McCabe et al., 2003), and potentially BMP regulates s-LN$_v$ metamorphic decisions (Gorostiza and Ceriani., 2013).

Combined, manipulations resulting in loss of synaptic vesicle release, loss of PDF signalling and electrical silencing cannot produce comparable defects, and though there are feasibly other mechanisms of signalling between dorsal projections, or dorsal active zones in establishing adult connectivity, it is beyond our means to study this in greater detail (Kaneko et al., 2000, Nitabach et al., 2002, Depetris-Chauvin et al., 2011). Our work faces the uncomfortable dichotomy, wherein (Gorostiza and Ceriani, 2013) shows loss of the pruning initiation pathway increases axonal complexity, but pruning is not evident.

4.8 – Expression of *cycle* within PDF-expressing neurons is required, but not neccesarily sufficient, for PDF projection formation

Our data above suggests s-LN$_v$ signalling and connectivity is affected by, but not causative of, neuroanatomical defects in the s-LN$_v$s, and phenotypes may be present in other clock cells. We have thus far focussed on a pan-neuronal CYC rescue, so sought to use more restricted driver patterns to identify the required developmental expression pattern of CYC for wild-type-like projection morphology and behaviour.

Previous work from the lab has identified projection defects in *elav-gal4; UAS--myc-cyc*$^{\#10}$*/Pdf-gal80; cyc*^{01} flies, in this case demonstrating a stunting of projections (Goda et al., 2011). We repeated this projection-staining experiment using the 29°C- raised transgenic *elav-gal4; UAS-myc-cyc*$^{\#7}$*/Pdf-gal80; tubpgal80*^{ts}*cyc*$^{01/}$ cyc^{01}, *cyc*^{01} *[elav-*

Pdf80.cyc]^{ts} . Despite being raised permissively, these brains exhibited mild, though statistically significant misrouting defects (P<0.001***), but not stunting (Figure 4.15). As *cyc*^{01} *[elav.cyc]*^{ts} rescues projection morphology, we have therefore defined a requirement for CYC expression in PDF+ve cells for correct s-LN$_v$ projection formation (Figure 4.5). Notably, complexity at the second-order processes, as assessed by sholl analysis, did not significantly differ between *cyc*^{01} *[elav-Pdf80.cyc]*^{ts} and *cyc*^{01} *[elav.cyc]*^{ts}, suggesting neuronal connectivity does not differ between these manipulations (Figure 4.11).

The projection phenotype of *cyc*^{01} *[elav-Pdf80.cyc]*^{ts} was significantly less severe than *cyc*^{01} or restrictively-raised *cyc*^{01} *[elav.cyc]*^{ts} projections, suggesting that loss of CYC in other cells may contribute to the defect, or else may be the result of residual CYC in the s-LN$_v$s due to limitations of *Pdf-gal80*. PDF levels are indirectly regulated by the clock, at the transcriptional level, so it is feasible that *Pdf-gal80* indirectly represses it's own expression, resulting in a relatively mild CYC loss phenotype (Blau and Young, 1999, Park et al., 2000).

cyc^{01} *[elav-Pdf80.cyc]*^{ts} shows behavioural arrhythmia, as would be expected in the light of loss of a molecular oscillator within the PDF cells (Figure 4.18). In particular, as the introduction of the *Pdf-gal80* element in this genotype triggers the observed behavioural arrhythmia in DD, it can be assumed that the *cyc*^{01} state of the PDF cells is responsible. However, our understanding of this genotype prompts two potential interpretations. Both morning anticipation and freerunning rhythms require a PDF-cell oscillator, though freerunning rhythms depends upon the s-LN$_v$ dorsal projections, whilst morning anticipation does not (Agrawal and Hardin, 2016). The LD profile of these flies reveals a residual morning anticipation (Figure 3.11), suggesting functional PDF signalling, potentially stemming from the l-LN$_v$s. In contrast, the free-running arrhythmicity may be due to a predicted loss of the s-LN$_v$ molecular oscillator or a block of output from this oscillator, possibly due to dysfunctional dorsal s-LN$_v$ projections.

We studied s-LN$_v$ rhythms in PER to characterise oscillator function in these cells, demonstrating a notably weakened rhythm in which only a minority of cells possessed nuclear PER at CT2, and significantly lower nuclear intensity than pan-neuronal controls (P=0.039*)(Figure 4.14). Nonetheless, differences in nuclear staining intensity between CT2 and CT14 were significant in s-LN$_v$s (P=0.007**) and l-LN$_v$s (P<0.001***),

demonstrating that though amplitude was reduced, *Pdf-gal80* does not completely remove rhythms, which must measure any interpretation of behavioural data gleaned from this genotype (Appendix Table 9). The phenotype of behavioual arrhythmia in DD is particularly interesting, which may result from an insufficient rhythmic strength of the s-LN_v oscillator, or else a secondary defect caused by developmental CYC loss. As the remainder of the clock circuit possesses CYC, and it is known that CYC expression with the *elav*-driver is sufficient for behavioural rescue without *Pdf-gal80*, it can be assumed any dysfunction lies within the PDF cells, and provides further evidence of a disruption to PDF cell function.

The presence of residual molecular rhythms, and hence residual CYC function, can be interpreted as limiting the extent of the projection phenotype in this genotype, and it is likely that a more effective lowering of CYC in the PDF cells may result in greater projection disorder.

Though not formally quantified due to lack of a cytoplasmic stain, nuclear PER corresponding to the LN_ds was regularly detectable at CT2 but not CT14, as was the case with cyc^{01} *[elav.cyc]*^{ts}, indicating CYC expression in other clock cells.

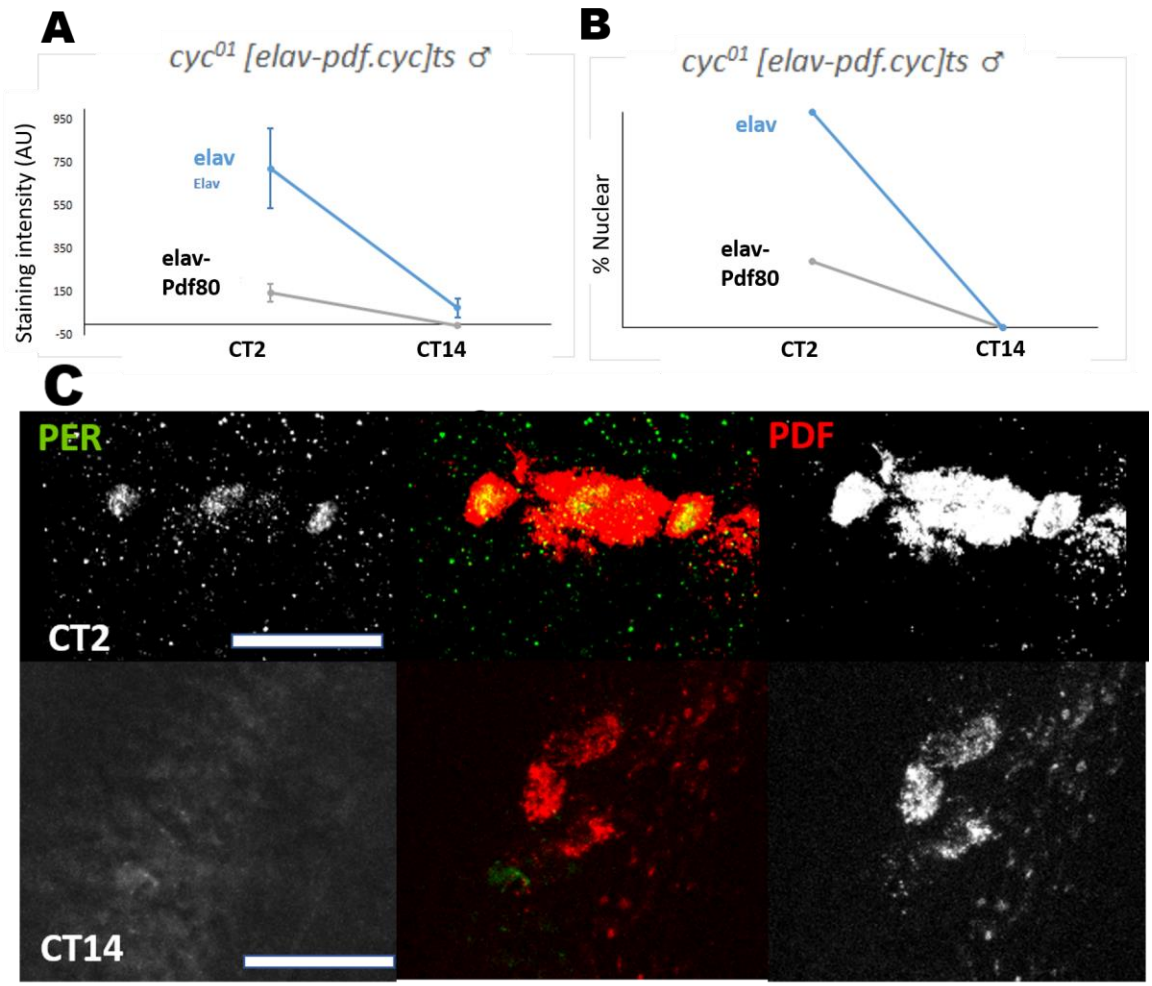

Figure 4.14 - Inhibition of ectopic cycle rescue within PDF cells results in a decrease in molecular period rhythms. *Panel A shows PER staining intensity within s-LN$_v$s at CT2 and CT14 on the second day of DD, of genotype cyc^{01} [elav-Pdf80.cyc]^{ts}. Panel B shows respective nuclear localisation. Significant differences emerge between staining intensity at CT2 and CT14 for the experimental condition (P=0.007**), but not localisation (P=0.082). Nuclear PER staining intensity and localisation appears weaker than cyc^{01} [elav.cyc]^{ts}. Panel C shows example images at CT2 and CT14. Scale bars in bottom right corresponding to 20µm*

Whilst we show that PDF cell CYC is required for correct s-LN$_v$ formation, we have not yet shown it is sufficient. The spatial requirement for CYC in s-LN$_v$ projection formation may not be limited to the PDF cells, instead relying on CYC for specification or signalling in other cell subsets. As post-synaptic targets of the s-LN$_v$ projections, CYC-regulated signalling stemming from the DN1s may also be involved. *Pdf-gal4(X); UAS--myc-cyc$^{\#7}$/+; tubpgal80^{ts}cyc^{01}/cyc^{01}*, referred to as *cyc^{01} [Pdf.cyc]^{ts}*, was raised at 29°C and dissected, to verify projection complexity. Projection complexity of these flies,

though not wt-like, was notably and significantly lower than that of cyc^{01}s, suggesting, like the cyc^{01} *[elav-Pdf80.cyc]*^{ts} dataset, that CYC loss within these cells is the primary mediator of the defasciculation defect (Figure 4.15). We can say that PDF-cell CYC makes a contribution to correct projection formation, but we cannot definitively say it is sufficient. It is arguable that if *Pdf-gal4* expression is compromised in a cyc^{01} background that wt-like levels of CYC may not be attainable by third-instar stages, contributing to the defect, but this is unknown.

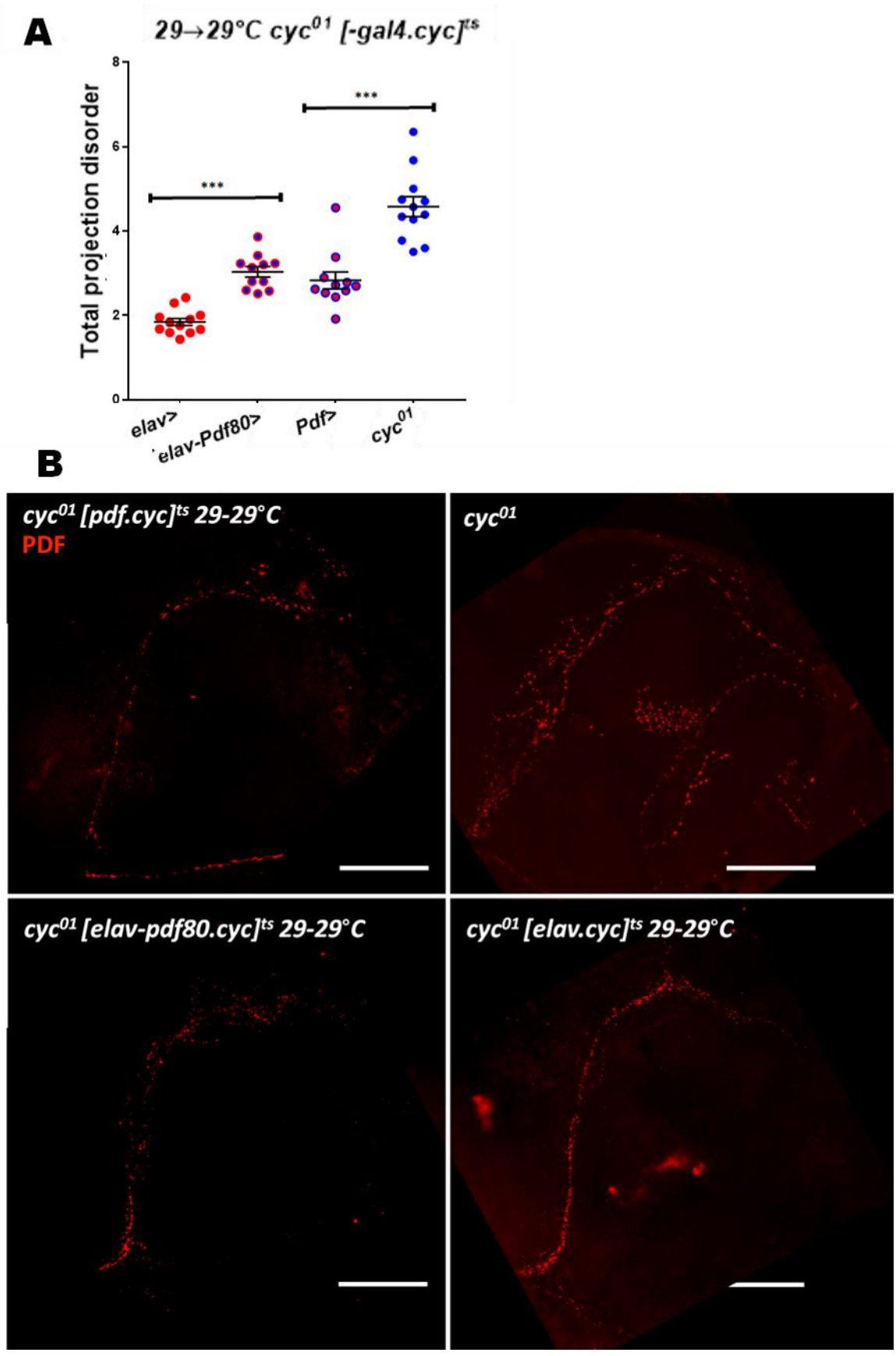

Figure 4.15 - Loss of cycle within PDF cells increases their axonal complexity, and expression of cycle only within PDF cells decreases their axonal complexity.

Panel A shows projection disorder metric of permissively raised-and-run cyc^{01} [Pdf.cyc]^{ts}

and cyc^{01} [elav-Pdf80.cyc]^{ts}, compared to permissively run cyc^{01} [elav.cyc]^{ts} and cyc^{01}.Panel B shows representative images for each condition. Scale bar in bottom right is 50µm.

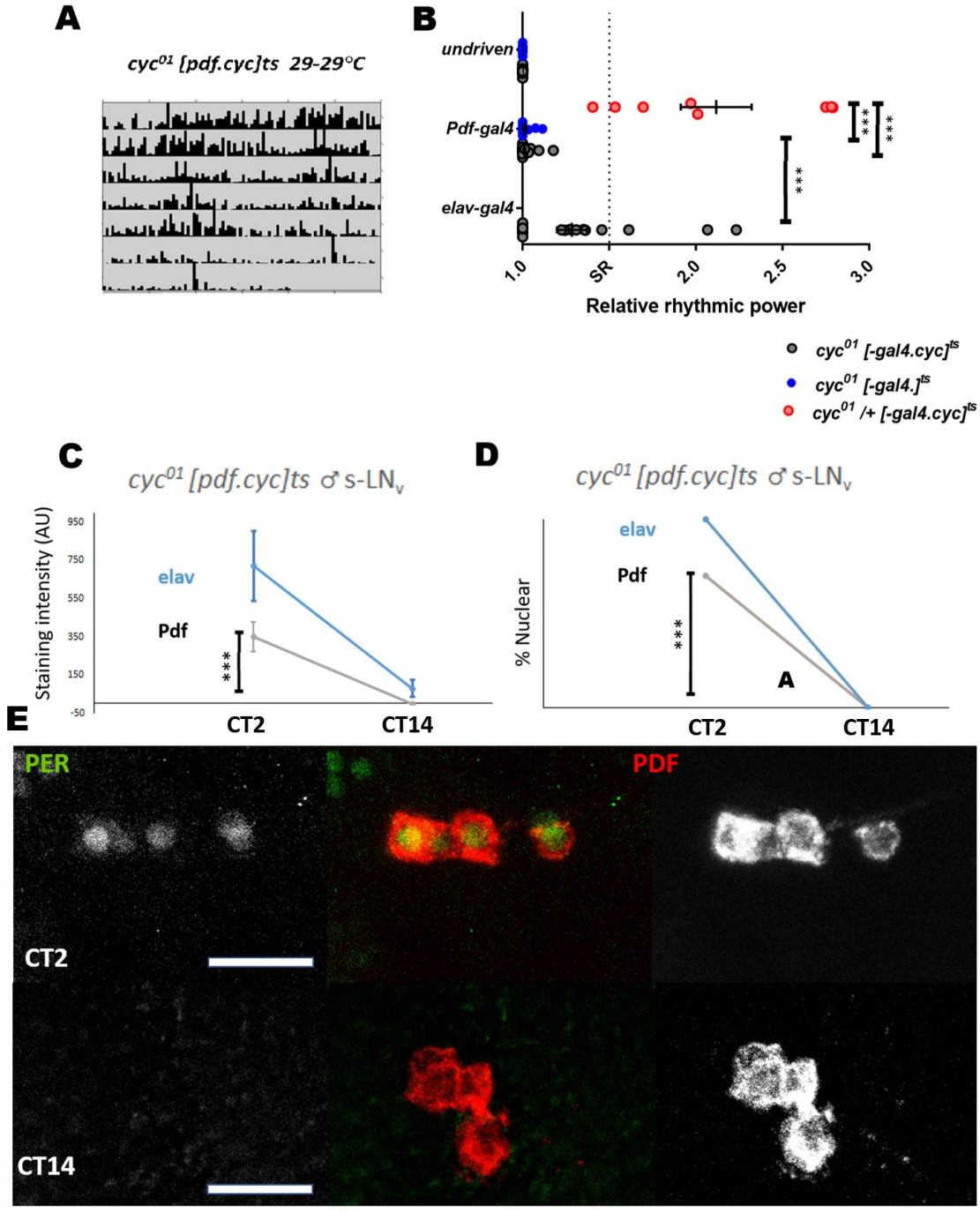

Figure 4.16 – Constitutive rescue of cycle expression within PDF cells is sufficient for molecular period rhythms, but not behavioural rhythms. *Panel A shows a median actogram of fly behaviour in freerunning conditions following PDF-cell specific rescue of CYC expression. Panel B shows Relative rhythmic power of cyc^{01} [Pdf.cyc]^{ts} and appropriate controls, demonstrating that PDF-cell specific rescue of CYC significantly*

*differs to pan-neuronal rescue (P<0.001***) and cyc^{01}/+ heterozygous controls (P<0.001***). Panel C shows PER staining intensity and Panel D shows nuclear localisation at CT2 and CT14 in 29°C-raised, 29°C run cyc^{01} $[Pdf.cyc]^{ts}$, which significantly differ by both metrics, (P<0.001***), demonstrating existance of a molecular rhythm. Statistics in Panels B and C are generated by One-way ANOVA, and staistics in Panel D are from 2x2 Fisher's exact test. Panel E shows example images of PER staining intensity at CT2 and CT14. Scale bars in bottom right corresponding to 20µm*

We quantified the resumption of molecular rhythms in these flies, on the understanding that this would indicate appropriate CYC rescue and constitute a sufficient oscillatory quotient for behavioural rhythmicity. Though the peak staining intensity is lower than rescue with *elav* driver, a significant difference emerges in nuclear PER staining intensity between CT2 and CT14 (P<0.001 ***), demonstrating an oscillation (Figure 4.16c)(Appendix Table 9). In spite of the weak stain, a marked nuclear demarcation of PER is visible in the majority of s-LN_vs at CT2 demonstrating this oscillation is reasonably intact. A significant rhythm is also identifiable in l-LN_vs (Figure 4.16d, Appendix Figure 15)(Appendix Table 9). Though not formally quantified, PER staining was never identified in PDF-ve cells, as would be expected. It is therefore interesting that this molecular rhythm, in conjunction with lessened projection defects is incapable of restoring behavioural rhythms.

However, as suggested elsewhere, it is assumed that defects exist outside the PDF cells, which may disrupt signalling downstream of the projection, even if overall complexity is reduced. *UAS-SYT::GFP* and *UAS-myc-cyc* were co-expressed with the *Pdf-gal4* driver on a $tubpgal80^{ts}cyc^{01}/cyc^{01}$ background, raised permissively or restrictively and quantified, to identify if *SYT::GFP* was strongly aggregated in dorsal puncta as in wt, or if trafficking defects persisted. Developing the experiment of (Figure 4.10), we can study the effect of adult CYC restoration on signal intensity, with a potentially bolstered driver strength, and compare any deficiencies between permissively-raised phenotype and wild-type flies, which is suggestative of PDF-ve cell requirements for CYC in correct dorsal projection function.

Permissively-raised PDF-specific CYC expression led to an intermediate phenotype, in which the dorsal/basal ratio of both PDF and GFP was restored to wt-like levels and PDF

staining intensity was increased, but bouton number was akin to *cyc*^{01}, worryingly suggesting that certain aspects of dorsal projection physiology are not being restored with PDF-specific CYC (Figure 4.17). An increase in bouton number in particular indicates altered synaptic connectivity, potentially related to loss of post-synaptic partners.

Restrictively raised *cyc*^{01} *[pdf.cyc+SYT::GFP]*^{ts} , expressing CYC purely in the PDF cells in adulthood, appeared *cyc*^{01}-like in bouton-number, morphology, PDF and GFP staining intensity, suggesting adult-specific CYC could not rescue these aspects (Figure 4.17). Developmental defasciculation and presynaptic misorganisation of restrictively raised *cyc*^{01} *[-gal4.cyc]*^{ts} processes may not be easily reversible in adult brains, while restoration of PDF and GFP staining levels would have appeared more likely. However, it is possible that three days at 29°C may not be sufficient for restrictively-raised *cyc*^{01} *[pdf.cyc+SYT::GFP]*^{ts} to recuperate GFP and PDF levels comparable to that of it's permissively-raised counterpart.

Whilst we infer that molecular rhythms are rescuable in these s-LN$_v$s from data in 17→29°C *cyc*^{01} *[elav.cyc]*^{ts} and 29→29°C *cyc*^{01} *[Pdf.cyc]*^{ts}, it is difficult to conclude if developmental CYC loss results in long-term changes to adult PDF and SYT::GFP levels, which may be restored to a greater extent following longer incubation at 29°C

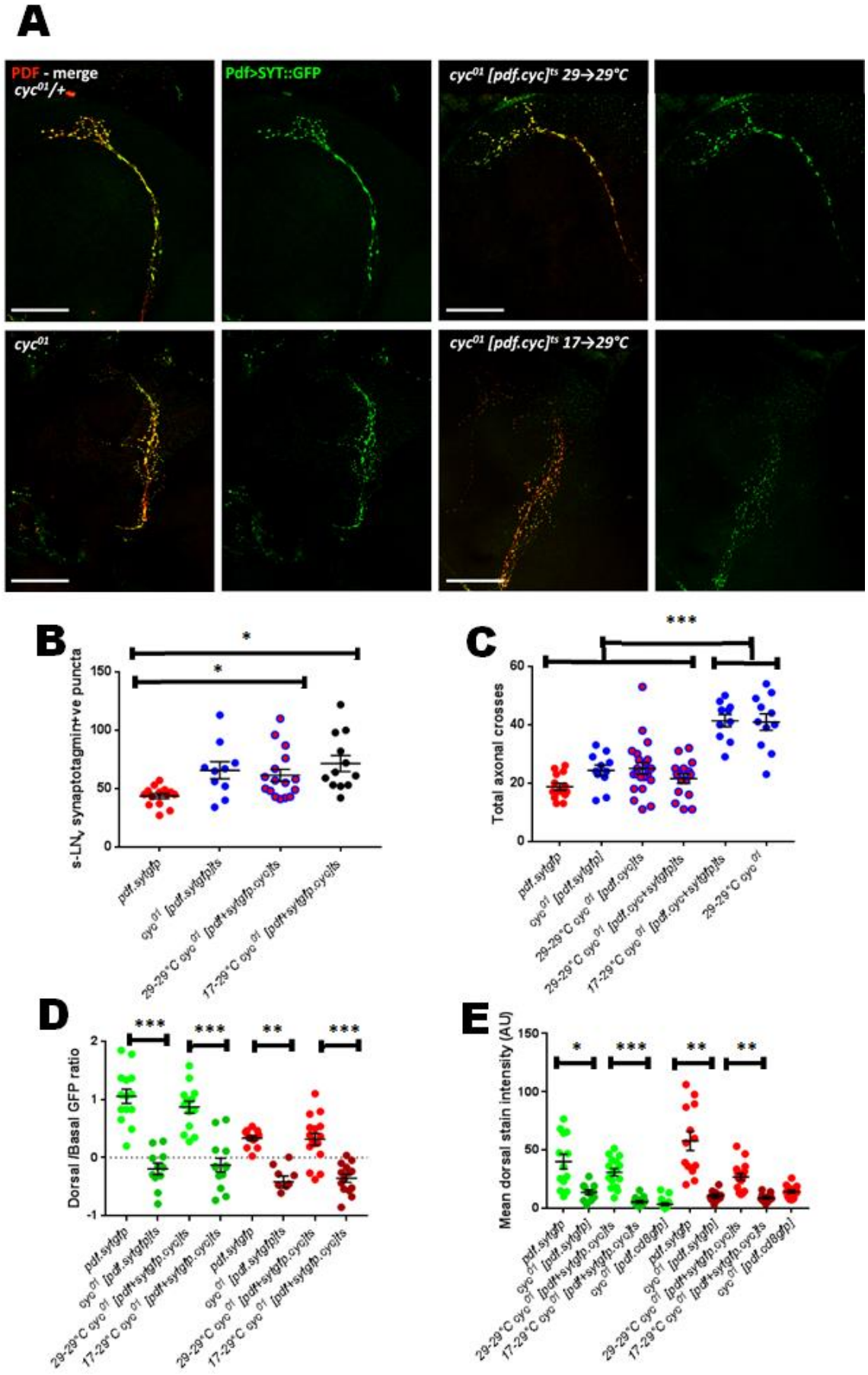
A
PDF - merge
cyc01/+
Pdf>SYT::GFP
cyc01 [pdf.cyc]ts 29→29°C
cyc01
cyc01 [pdf.cyc]ts 17→29°C
B
s-LNv synaptotagmin+ve puncta
pdf.sytgfp
cyc 01 [pdf.sytgfp]ts
29-29°C cyc 01 [pdf+sytgfp.cyc]ts
17-29°C cyc 01 [pdf+sytgfp.cyc]ts
C
Total axonal crosses
pdf.sytgfp
cyc 01 [pdf.sytgfp]
29-29°C cyc 01 [pdf.cyc]ts
29-29°C cyc 01 [pdf.cyc+sytgfp]ts
17-29°C cyc 01 [pdf.cyc+sytgfp]ts
29-29°C cyc 01
D
Dorsal /Basal GFP ratio
E
Mean dorsal stain intensity (AU)
cyc 01 [pdf.cd8gfp]
29-29°C cyc 01
17-29°C cyc 01

Figure 4.17 - Rescue of cycle expression within PDF cells fails to fully rescue synapse number and morphology within PDF axonal projections*. SYT::GFP bouton number, staining intensity and localisation in 29→29 °C and 17→29 °C Pdf; UAS-cyc#7/+; tubpgal80^{ts}cyc^{01}/UAS-SYT::GFP cyc^{01} Pdf>SYT::GFP vs others = P=0.062, 0.023*, 0.10*. 17 vs 29 cyc^{01} [pdf.cyc+SYT::GFP]^{ts} = 0.655. Panel A shows representative images for each condition, labelled with (Green) or merged with PDF (Red). Scale bars in bottom left are 50µm, with a noticeable divergence in brain size between conditions. Panel B shows bouton number, Panel C shows defasciculation of second-order s-LN$_v$ processes as determined by Sholl analysis, for various PDF-specific CYC rescue and SYT::GFP -expressing lines. Panel D shows dorsal/basal ratio and Panel E shows dorsal stain intensity of PDF and SYT::GFP within intact s-LN$_v$s. In Panel D and E, green corresponds to GFP stain, and red corresponds to PDF stain*

As discussed in Chapter 3, the *cyc^{01} [Pdf.cyc]^{ts}* LD phenotype displays an M peak but no E peak, indicative of PDF-cell oscillator function, but no oscillator in the E cells, as would be assumed (Figure 3.11). This restores confidence in the lacklustre molecular data for this genotype.

Whilst only the 150 core clock neurons express all core clock genes including TIM, PER, CLK, CYC, VRI and PDP1 (Figure 1.3), it is known that CLK is expressed in non-clock neurons, and though no effective CYC antibody has been developed, it can be assumed that expression extends beyond the pacemaker clock cells. This opens the potential of uncharacterised CYC+ve cells regulating the clock, potentially via guidance cues.

Numerous other driver combinations, as expected, fail to rescue DD behavioural rhythms, such as, *Clk4.1M-gal4*, *Pdf+Clk4.1M-gal4*, *R78G02-gal4* or *crygal4-Pdfgal80*, aligning with the *elav-Pdfgal80* result suggesting a PDF-cell requirement for CYC in DD behaviour (Figure 4.18). TUG -specific rescue in this context showed a partial, though incomplete restoration of adult circadian behaviour, which may be attributable to the CLK/CYC-dependence of the *tim* promoter (Figure 4.18). The failure of *Pdf* and *Clk4.1-gal4* to combinatorially improve freerunning rhythmicity demonstrates defects in the DN1ps due to CYC loss, as has been characterised, are not the cause of behavioural arrhythmia following *Pdf-gal4*-mediated rescue of s-LN$_v$ molecular oscillations. This suggests defects lie in other cells and disputes the hypothesis that PDF→DN1p signalling is an output route for freerunning rhythms (Cavanaugh et al., 2014). However, a

potentially limited expression strength of *Clk4.1-gal4* in cyc^{01} brains may hamper sufficient CYC rescue within DN1ps.

We additionally created a line, termed cyc^{01} *[elav-VGlut.cyc]*^{ts}, which rescues CYC pan-neuronally, bar glutamatergic cells. The major connective clock-cell partner of the s-LN_vs during development, the $DN1_a$s, are glutamatergic in larvae and adults and we can assay requirement of CYC in these cells (Hamasaka et al., 2007, Collins et al., 2012). Males do not significantly differ in rhythmicity to pan-neuronal rescue, whilst significantly differing to driverless controls (Appendix Tables 22, 23), suggesting that CYC is not required in $DN1_a$s for functional connectivity in either circuit.

We can therefore narrow down the spatial requirement for developmental CYC expression as extending beyond the PDF cells, though we fail to precisely define the subsets.

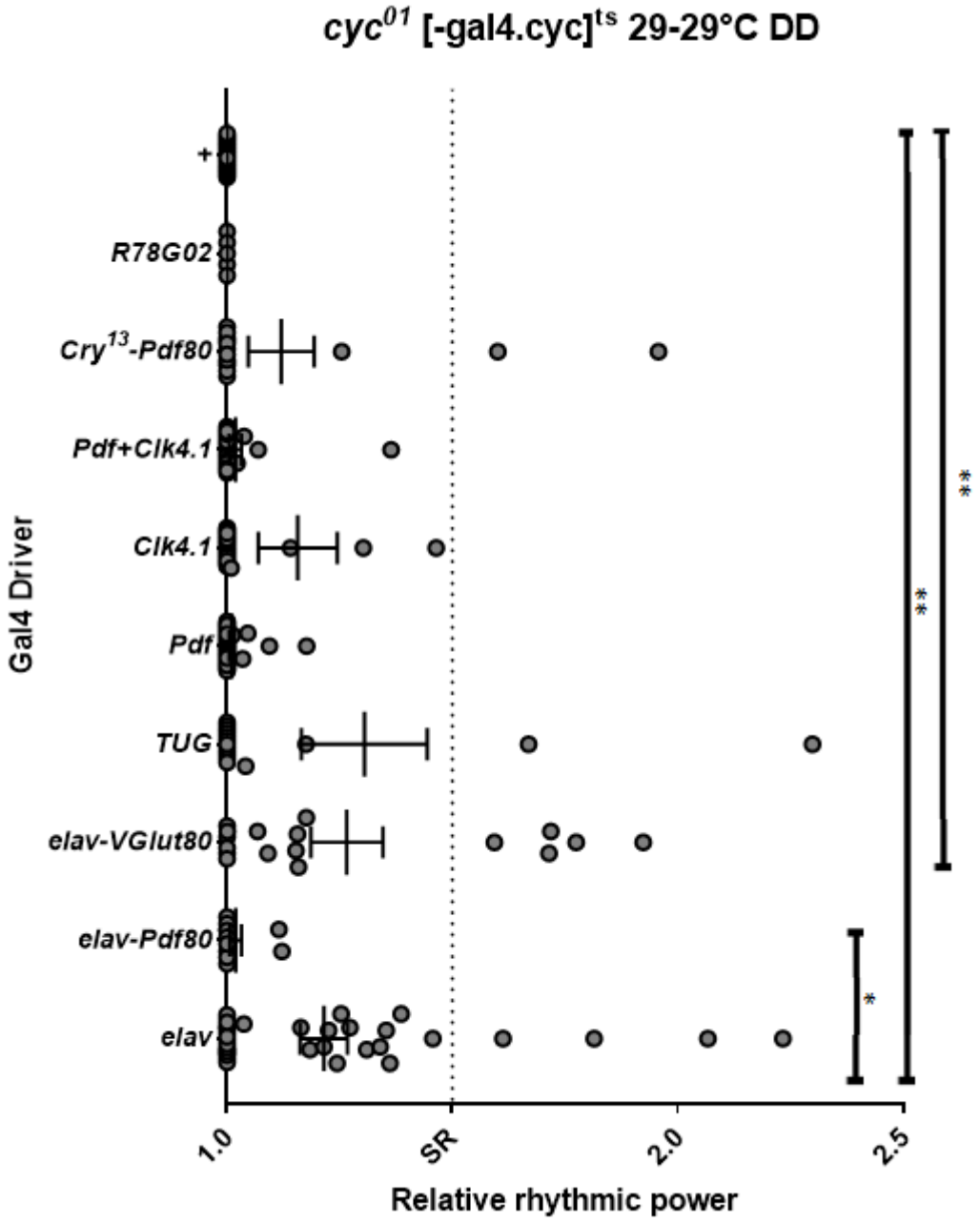

Figure 4.18 - Robust behavioural rhythms are only achievable when cycle is expressed across multiple clock cell groups. *Behavioural rhythmicities for conditional CYC rescue with various drivers, raised at 29°C and run at 29°C DD for 7 days. All flies were male, due to experimental constraints. Not shown are CyO negative controls lacking UAS-cyc#7 and cyc^{01}/+ heterozygote positive controls, which are available in Appendix Tables 30, with additional statistics in Appendix Table 31. Evident is a broad inability of drivers, with the exception of elav, to rescue behaviour.*

4.9 - Adult-specific expression of *cycle* is required for ITP neuropeptide expression within clock neurons, and loss of *cycle* reduces expression of multiple clock-neuron drivers.

cyc^{01} and cyc^{01} /+ flies were stained with an antibody for ITP, a neuropeptide with alleged minor roles in the clock circuit (Hermann-Luibl et al., 2014). In addition to expression within four insulin-producing cell clusters (IPCs), ITP is expressed within the 5th s-LN_v and one LN_d, composing half the E cell cluster, and ITP staining reveals extensive projections from these cells heading to the medulla and dorsally to meet at the pars intercerebralis. Notably, clock cell ITP was unidentifiable in nearly all analysed cyc^{01} brains, despite other ITP+ve cells appearing normal (Figure.4.19). To determine if this was a result of defective cell specification during development or an adult-specific control of CLK/CYC in ITP expression, we looked at ITP in 17→29°*C* cyc^{01} *[elav.cyc]*^{ts} brains, identifying the stereotypic ITP projections in most cases, such that significant differences manifest compared to cyc^{01}, but not heterozygous controls (Appendix Table 14), suggesting that CYC was required specifically in adulthood for ITP expression. *itp* mRNA has been shown to oscillate, and lower levels of ITP had previously been found in Clk^{AR}, so this direct regulation of expression by CLK/CYC is not unexpected (Hermann-Luibl et al., 2014). Though not formally quantified due to a more variable morphology than s-LN_v projections, ITP projections appeared wt-like, successfully innervating the pars intercerebralis, suggesting these cells develop normally in the absence of CYC, and are capable of finding output targets. $Pdp1^{3135}$ also demonstrates present, though apparently fewer ITP+ve cells, likely due to an upstream effect on CLK/CYC levels (Figure 4.19).

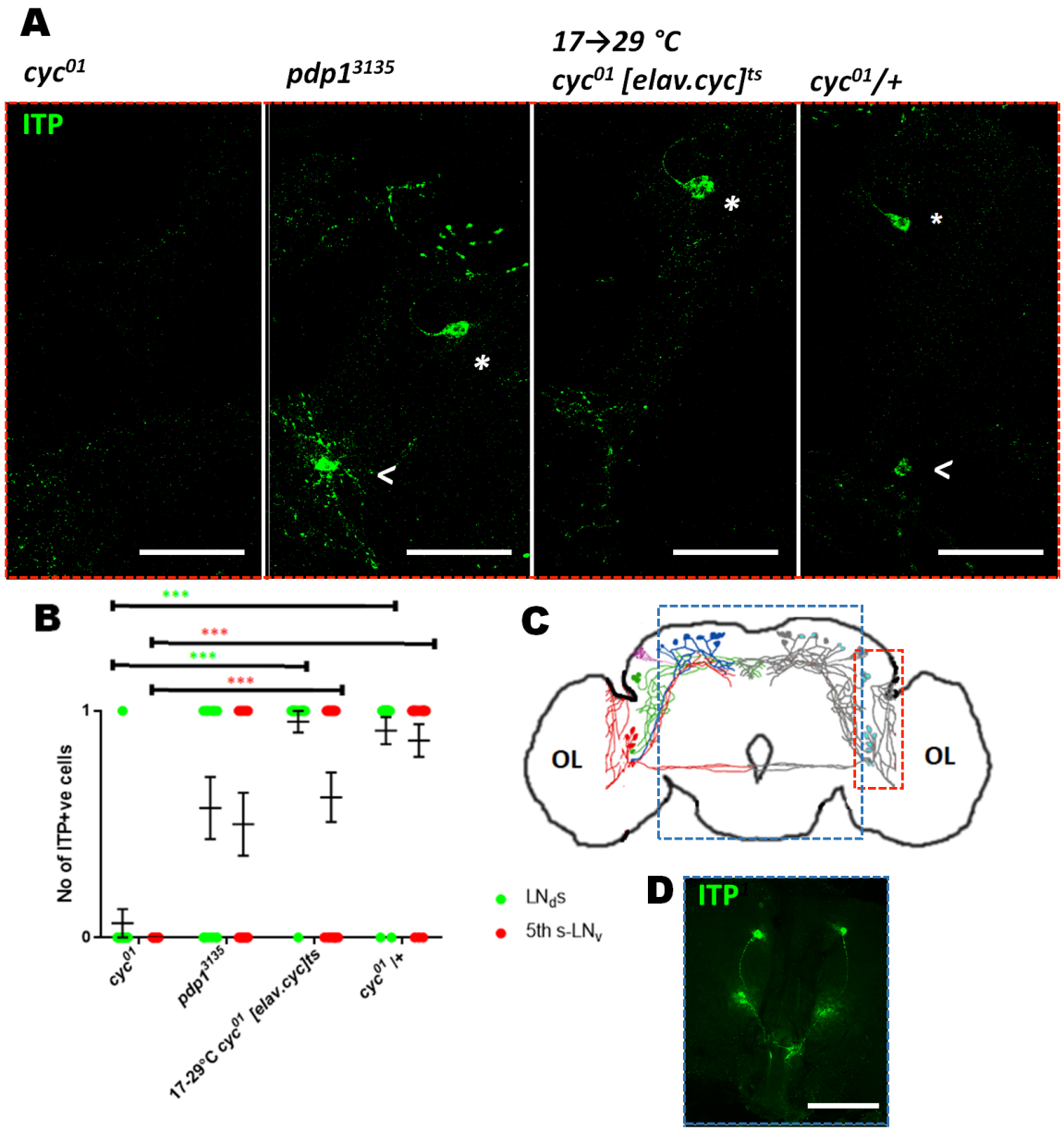

Figure 4.19 - Loss of cycle expression results in fewer ITP-expressing clock cells. *Panel A shows representative images of ITP-stained brains of flies with or without CYC function, * identify ITP+ve LN_ds and < identify ITP+ve 5th s-LN_vs. Scale bars in bottom right represent 50µm. Panel B shows quantification of ITP+ve cell number in cyc^{01}, $Pdp1^{3135}$ and 17→29 °C cyc^{01} $[elav.cyc]^{ts}$, assayed from brains with normal ITP staining within IPC cells. cyc^{01} n=17 , $pdp1^{3135}$ n=14, 17→29 °C cyc^{01} $[elav.cyc]^{ts}$ n=21, cyc^{01}/+ n=23 . As detailed in Appendix Table 14, cyc^{01} significantly differs in ITP cell number to 17→29 °C cyc^{01} $[elav.cyc]^{ts}$ (P<0.001***) and cyc^{01}/+ (P<0.001***), though cyc^{01}/+ and 17→29 °C cyc^{01} $[elav.cyc]^{ts}$ do not significantly differ. Panel C shows the approximate areas of the brain imaged, with the ares imaged in Panel A outlined in Red, and the areas imaged in Panel D outlined in blue. Panel D shows non-clock cells stained with ITP, which were ITP+ve irrespective of genotype and used to mark correctly stained brains, scale bar in bottom right is 100µm.*

We stained cyc^{01} flies expressing *R78G02>CD8::GFP* to identify if the other three CRY+ve LN_ds were present and projecting normally. ITP+ve IPC cells, an unknown pair

of cells extensively innervating the lobula, and a selection of dorsal neurons, potentially clock cells, were visible in all brains, though many other cells were variably present or absent (Figure 4.20). Brains were co-stained with PDF such that *cyc*^{01} defect was confirmable via s-LN$_v$ projection morphology, though we did not stain with another clock cell marker, and our quantification is based on soma localisation and neuroanatomy. The stereotypic "loop" arborisation pattern of the LN$_d$s was absent in all *cyc*^{01} brains, although 5th-s-LN$_v$ soma and projections were occasionally visible.

It is possible that E cells are present in *cyc*^{01} brains with an altered neuroanatomy, and could not be reliably identified. Inferring from our ITP staining data, it is also possible that *R78G02-gal4* driver strength is affected by loss of CYC specifically within the clock cells, though as this driver is taken from a flanking region of Sex Peptide Receptor (SPR), like *Clk4.1M-gal4* driver we struggle to explain why driver expression may be weakened.

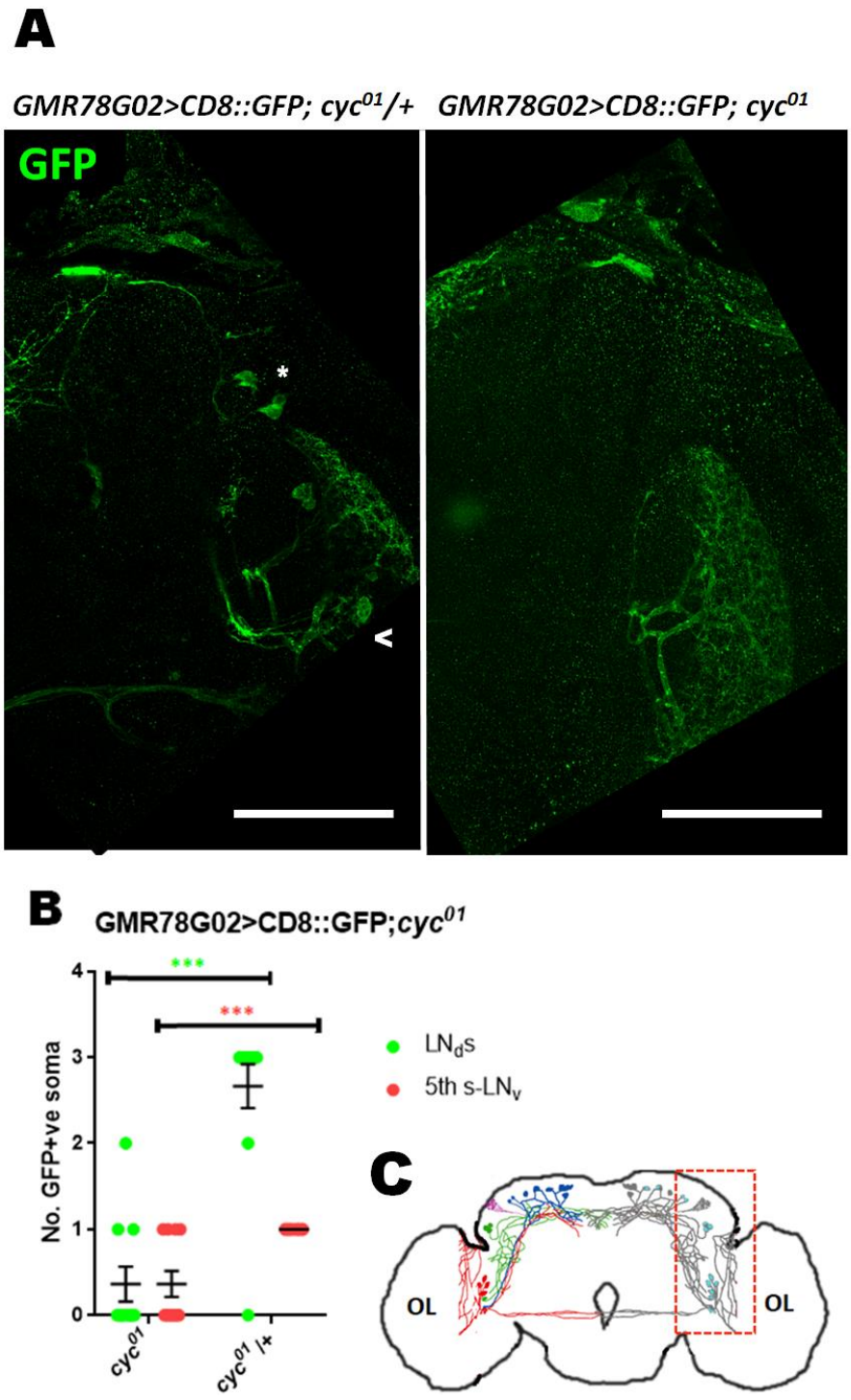

Figure 4.20 - An evening cell driver line, R78G02-gal4, expresses in fewer cells following loss of cycle expression. *Panel A shows example images of CD8::GFP expression with the R78G02-gal4 driver in cyc^{01} and cyc^{01}/+ control brains. Scale bars in bottom right are equivalent to 50µm. * sign marks the location of LN_ds, and < marks the location of LN_vs. Panel B shows number of visible clock cell soma in R78G02>CD8::GFP;cyc^{01} and cyc^{01}/+ control, detailing the three LN_ds and sole PDF-ve s-LN_v, selected from brains with identifiable staining in IPC cells and the optic lobe. Panel C shows the location of brain from which images were taken, outlined by a red*

box.

We additionally expressed *CD8::GFP* with *cry-gal4-13 + Pdf-gal80*, hypothesised to target all LN_ds, the 5^{th} s-LN_v and two $DN1_a$s. This manipulation was remarkably clean with little PDF costaining, although DN1s and CRY-ve LN_ds were not uniformly visible in cyc^{01}/+ controls, and thus targeted the same cells as *R78G02* without non-clock cells. In this case, GFP+ve cells were uniformly absent in cyc^{01}, but not heterozygotes (Figure 4.21). *cry* mRNA levels are constitutively high in cyc^{01} and CRY protein is high in Clk^{Jrk}, though both of these were largely derived from peripheral clocks, so *cry-gal4* driver strength may again be limited in cyc^{01}, but like *R78G02-gal4* and *Clk4.1M-gal4*, this is not predicted (Emery et al., 1998, Kumar et al., 2012). As ectopic CLK expression induces CRY in the CNS, it is feasible CLK/CYC regulation of CRY differs between peripheral and central clocks, which may be an interesting avenue of future research.

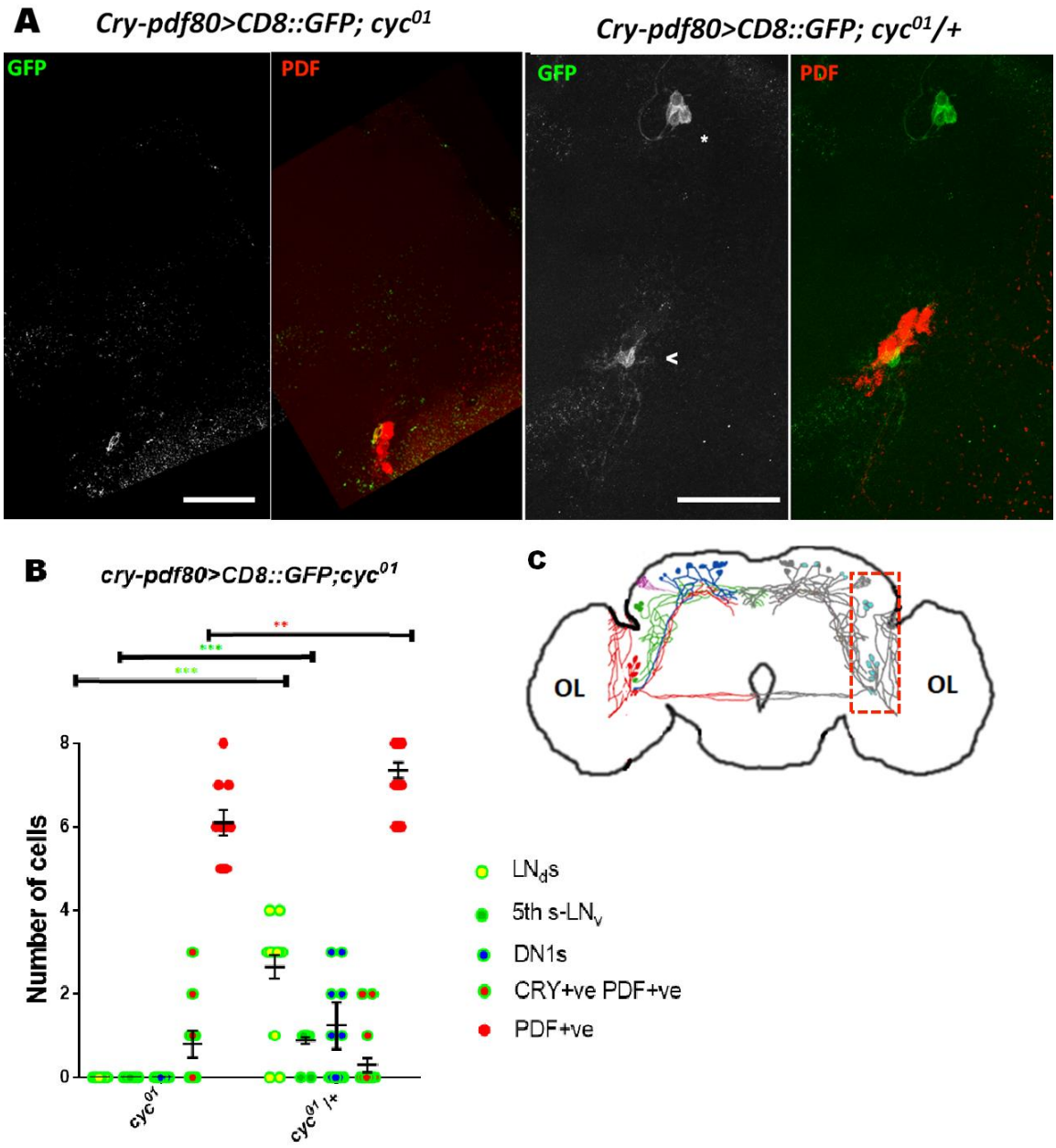

Figure 4.21 - Fewer cells induce transcription from the cry-promotor region following loss of cycle*. Panel A shows example images for GFP expression with cry-gal413/pdfgal80 on cyc^{01} and heterozygote backgrounds, alongside merged images with PDF stain. Scale bars in bottom right are equivalent to 50µm. * sign marks the location of LN_ds, and < marks the location of LN_vs, not shown were DN1s. Panel B quantifies cell counts of GFP or PDF+ve cell groups. cyc^{01} n=10, cyc^{01}/+ n=17. Statistics are detailed in Appendix Table 14, although LN_d, 5^{th}-sLN_v and PDF cell counts significantly differ between genotypes (P<0.001***), whilst DN1 number does not (P=0.057). Panel C shows the region of brain imaged, outlined in red.*

We can infer from the correct morphology of the ITP+ve E cell and 5^{th}-sLN_v, that though

adult-specific CYC is required for E cell functionality, in ITP synthesis, developmental CYC loss does not appear to disrupt this, nor is morphology disrupted. Thus, despite becoming clock-positive during metamorphosis, CYC is seemingly not required for ITP+ve cell morphological specification. GFP-expression in ITP+ve cells with *R78G02* and *cry-gal4-13* consistently fails despite presence in cyc^{01} *[elav.cyc]*^{ts}, and we cannot infer that other GFP-ve cells are thus absent.

To stain for CRY we placed brains of genotypes cyc^{01}/+ and cyc^{01} in DD for 3 days in order to allow CRY accumulation. cyc^{01}/+ demonstrated visible cell bodies corresponding to LN_vs and LN_ds, and in line with published data, which were uniformly not identifiable in cyc^{01} (Yoshii et al., 2008)(Figure 4.22). Restrictive and permissively raised cyc^{01} *[elav.cyc]*^{ts} bore an intermediate phenotype, in which a minority of CRY+ve cells were visible, though staining intensity may have contributed to this.

$pdp1^{3135}$ mutants, which disrupt a positive regulation of *clk* transcription, as will be discussed later in Chapter 4, similarly lacked visible CRY+ve clock cells, unlike heterozygotes, further validating that loss of CLK/CYC may lower CRY levels (Cyran et al., 2003)(Figure 4.22).

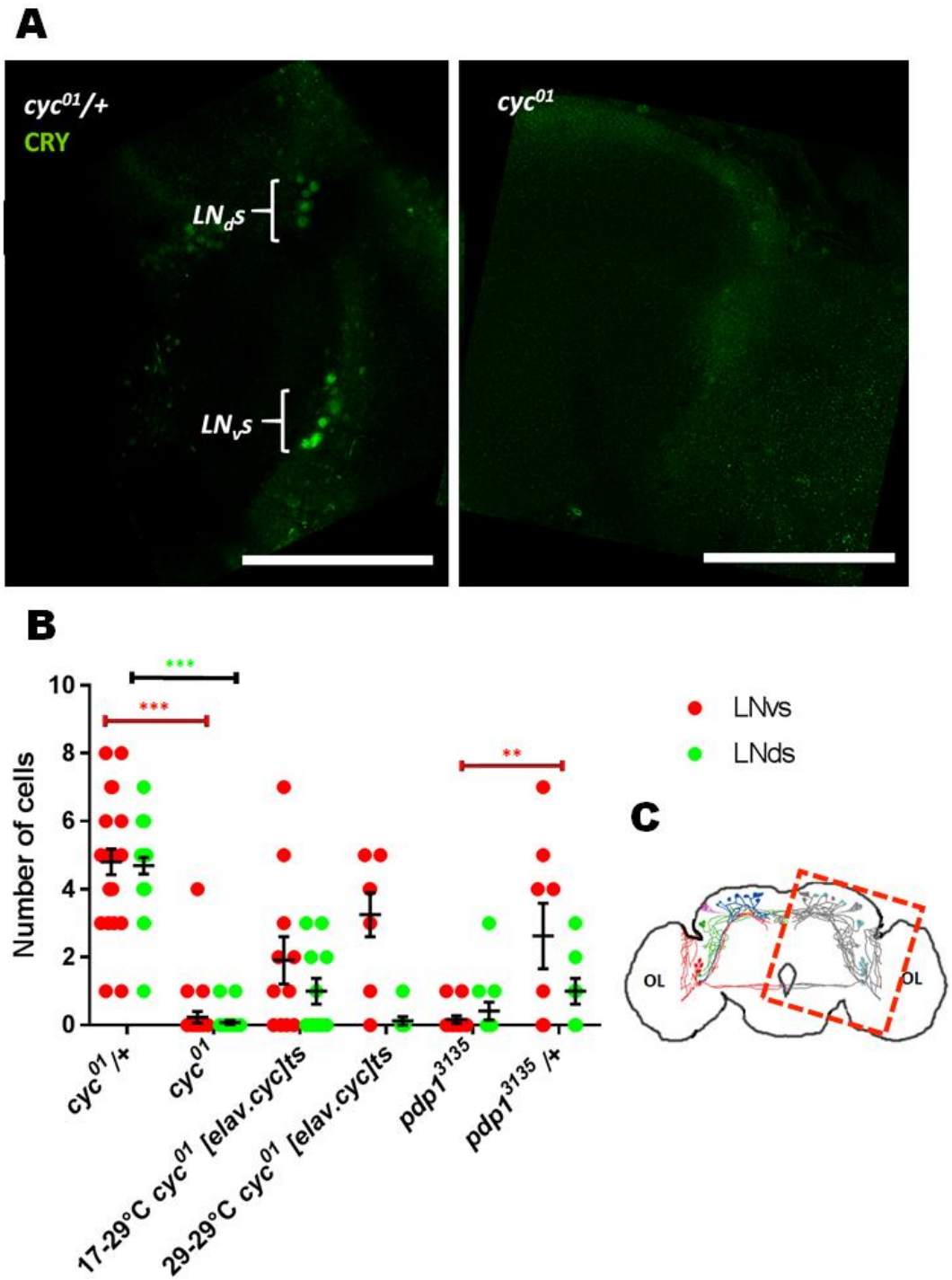

Figure 4.22 - Fewer CRY-expressing cells are identifiable following loss of cycle. *Panel A displays a hemisphere stained with CRY antibody for cyc^{01} and cyc^{01}/+ heterozygotes, revealing certain mutants lack identifiable CRY. Scale bar in bottom right is 100µm. Panel B is a graph quantifying number of observable CRY+ve clock neurons for cyc^{01}, cyc^{01}/+, $pdp1^{3135,}$ $pdp1^{3135}$/+ and cyc^{01} $[elav.cyc]^{ts}$, demonstrating certain genotypes lack visible CYC in multiple clock neuron subsets. cyc^{01}/+ n=26, cyc^{01} n=25, 17→29 °C cyc^{01} $[elav.cyc]^{ts}$ n=11, 29→29 °C cyc^{01} $[elav.cyc]^{ts}$ n=8, $pdp1^{3135}$ n=12, $pdp1^{3135}$/+ n=8. Statistics calculated by one-way ANOVA are detailed in Appendix Table 14, in which*

restrictively and permissively raised cyc^{01} $[elav.cyc]^{ts}$ do not significantly differ in cell counts, whilst cyc^{01} and cyc^{01}/+, and $pdp1^{3135}$ and $pdp1^{3135}$/+ do. Panel C demonstrates the area of brain imaged, outlined in red.

Differences in staining intensity precluded effective quanitifcation beyond visible cell numbers, and the incompleteness of CRY expression within control cell bodies suggests in the absence of an optimised stain, CRY+ve cells are being underestimated. However, this data tentatively coalesces around a novel reduction in CRY levels within CYC mutant brains. Though no molecular data directly disagrees with this, it is unexpected and clashes with models of nocturnal behaviour, and thus will require additional experiments if it is to be believed. qPCR or western blots on dissected brains would be insufficient, as CRY+ve non-clock cells are identifiable (Yoshii et al., 2008).

4.10 – Loss of *pdp1* or *Clock*, which regulate levels of each other, results in related phenotypes to loss of *cycle*, but ectopic expression of either fails to rescue phenotypes caused by loss of the other

In our work so far we have characterised a series of defects within flies lacking developmental or adult CYC, yet the functional basis of this is unclear. CYC is a transcription factor driving expression of hundreds of circadian-regulated transcripts, has a poorly characterised expression pattern and thus has numerous potential output genes which could regulate the phenotypes we observe. In spite of this, no known developmental role for CYC has been characterised, and we sought to understand the mechanism by which CYC regulates developmental clock circuit formation via study of known and predicted CLK/CYC targets.

A previous lab member conducted a small conditional knockdown screen to identify circadian-related genes which are developmentally required for adult behavioural rhythmicity, identifying *Fer2, Mef2, Smi35a* and *Pdp1*. FER2 is known to function upstream of the oscillator, and has an established early developmental role in clock cell formation (Nagoshi et al., 2010). MEF2 has been studied in-depth and, whilst regulating rhythms in dorsal projection fasciculation, *Mef2* mutants do not display PDF-projections akin to those of cyc^{01} flies following constitutive MEF2 loss (Blanchard et al., 2010, Sivachenko et al., 2013). Thus, we have limited candidates with known developmental roles for further study. I conducted a visual screen through overexpression of CLK/CYC

targets involved in neuronal remodelling, on a *cyc*^{01} background, in a bid to ameliorate the defect. As detailed in the appendix, no obvious rescue was attained (Appendix Figure 16).

Clk^{Out} is a recently published CLK null mutant, though projection morphology has not been published. In a bid to characterise similarities to *cyc*^{01} projections, we stained these brains with PDF at CT2. In line with the literature for *Clk*^{Jrk}, no PDF+ve s-LN$_v$s are visible at all, and consequently dorsal projection morphology is not quantifiable (Figure 4.23). *cyc*^{01} is a nonsense mutation resulting in a truncated protein which includes the DNA-binding BHLH domain, and as such may possess residual function, resulting in a less severe phenotype than CLK mutants, though it is feasible CLK is capable of restoring residual function with unknown binding partners, or the truncated protein present in *cyc*^{01} (Rutila et al., 1998).

In *Clk*^{out} brains we also observed innervations of l-LN$_v$ processes into the dorsal protocerebrum, indicative of an l-LN$_v$ dysfunction (Figure 4.23). Though we have previously shown CYC loss results in increased projection complexity prior to l-LN$_v$ PDF immunoreactivity, it is likely and arguable that the increased projection complexity of adult *cyc*^{01} and *cyc*^{01} *[elav.cyc]*^{ts} flies stems in part from elision between s-LN$_v$ and l-LN$_v$ projections. However, the maximal length of l-LN$_v$ projections precludes their contribution to increased second-order process complexity visible in dorsal PDF projections in low CYC lines.

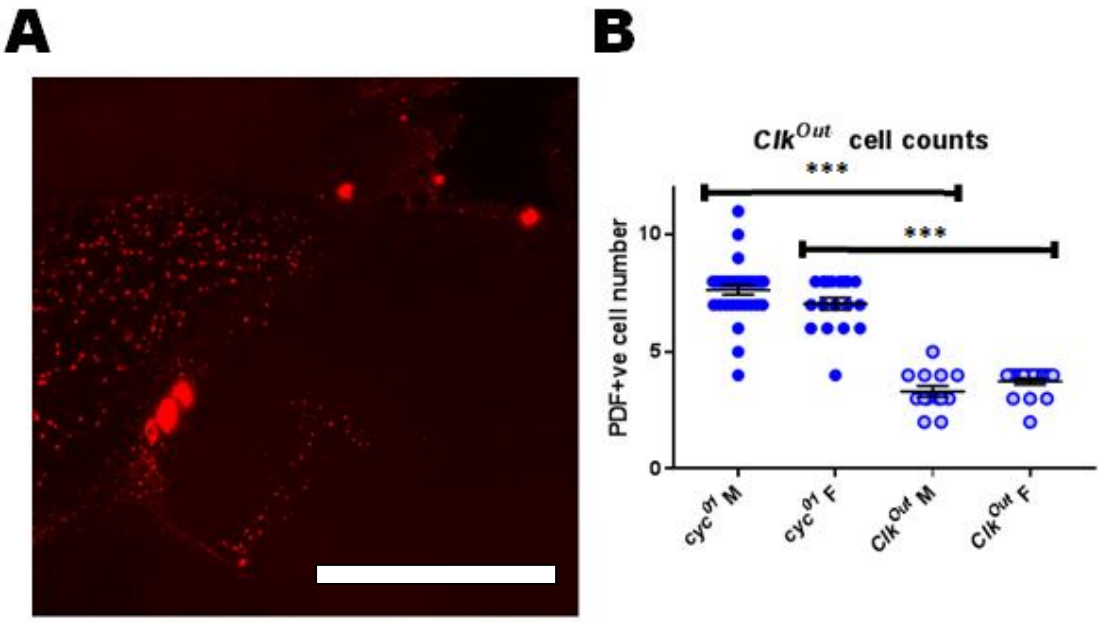

Figure 4.23 - Fewer PDF cell soma are identifiable in following loss of CLK than loss of CYC. *Panel A shows representative image of a Clk^{out} brains, stained with PDF, exhibiting first an absence of PDF+ve s-LN_v soma or dorsal projections, and demonstrating a stunted innervation, with scale bar in bottom right of 100µm. Panel B shows quantification of PDF+ve cell number in from the l-LN_vs projecting into the dorsal protocerebrum. ($P<0.001$***) between cyc^{01} and Clk^{Out} PDF+ve cell number for both genders, as compared by one-way ANOVA.*

A substantial proportion of Clk^{Jrk}/+ are behaviourally arrhythmic and lack characterised projections, so we were eager to observe if disrupted projection morphology might contribute to this (Allada et al., 1998). We show that s-LN_v dorsal projections and cell bodies are PDF+ve and projections appear intact and progress dorsally in all observed cases (Figures 4.23 & 4.24). Notably, a minority of these brains possess a cyc^{01}-like defasciculated morphology. The enduring reasons for Clk^{Jrk}/+ arrhythmicity are unknown, though rhythms in PER protein failed to oscillate in western blots in (Allada et al., 1998), characterisation of oscillations in pacemaker cells was never performed, and the weak behavioural rhythms identified in a majority of Clk^{Jrk}/+ indicates intact pacemaker rhythms. Potentially, defasciculation phenotypes observed in a minority of Clk^{Jrk}/+ are relevant to cyc^{01} arrhythmia and indicative of graduated dosage effects of CLK/CYC loss, in which residual function results in defasciculation, and total loss of function results in loss of s-LN_v PDF.

The function of PDP1 within the circadian clock is somewhat controversial, in which multiple papers argue for roles both upstream and downstream of CLK/CYC. Previous PDP1 mutants demonstrate a neuroanatomical defect similar to Clk^{Jrk}/Clk^{Out}, in which dorsal projections, and in many cases s-LN_v cell bodies were not PDF+ve (Lim et al., 2007, Zheng et al., 2009). Other manipulations with RNAi and dominant negative loss of PDP1ε isoform results in a milder defect in which PDF+ve s-LN_v cell bodies are present, but over-complex projection defects emerge, resembling our cyc^{01} *[elav.cyc]*^{ts} projections (Lim et al., 2007). Either PDP1 functions developmentally upstream of CLK/CYC, and both defects represent different severities of CLK/CYC dysfunctionality, or an isoform-specific role in projection specification occurs downstream from CLK/CYC, masked by the defects of upstream PDP1 loss.

A mutant of PDP1 which disrupts only the function of the circadian isoform, epsilon, $pdp1^{3135}$, specifically preventing expression of the circadian-relevant epsilon isoform, has previously been generated by the Sehgal lab, with existant but PDF-ve s-LN_vs, and the projection morphology of these is unknown (Zheng et al., 2009). We imaged $pdp1^{3135}$ brains stained with PDF and demonstrated the vast majority of brains lacked PDF+ve dorsal projections and s-LN_v cell bodies, corroborating previous data (Figure 4.23). In addition, we identified a *Pdp1* RNAi line from Kyoto stock center which exhibited the same low-PDF phenotype when driven in clock cells (Figure 4.23). In all cases, PDF+ve l-LN_v cell bodies were identifiable.

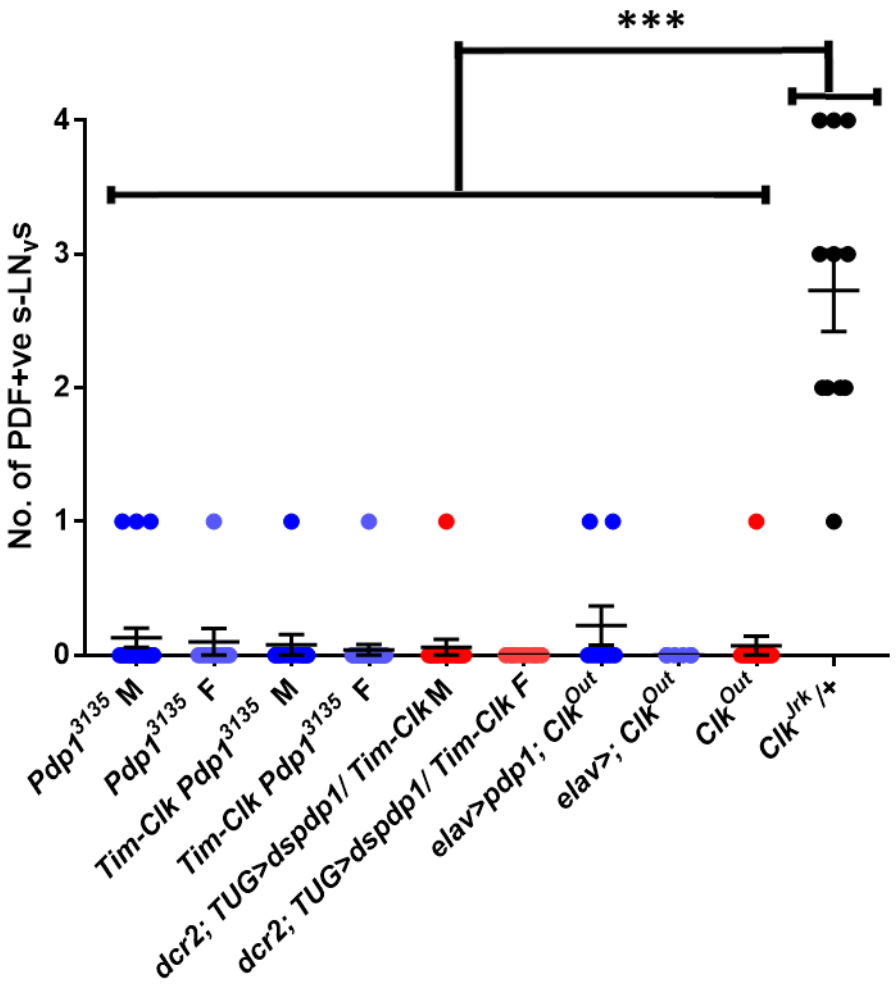

Figure 4.24 - Loss of either PDP1 or CLK results in fewer PDF cell soma. *We fail to rescue PDF+ve s-LN$_v$ soma with Pdp1 reintroduction to CLK mutants, or CLK reintroduction to PDP1 mutants. Pdp1^{3135} ♂ n= 22, Pdp1^{3135} ♀ n= 12, timClk Pdp1^{3135} ♂ n= 15, Pdp1^{3135} ♀ n= 24, dcr; TUG; timClk/dsPdp1 ♂ n=18, dcr; TUG; timClk/dsPdp1 ♀ n=10, elav>pdp1; Clk^{Out} ♂ n=9, elav>+; Clk^{Out} ♂ n=6, Clk^{Out} ♀ n=14, Clk^{Jrk}/+ n=11.*

As *Pdp1^{3135}* projections were uncharacterised, we attempted to identify these projections with *cry^{13}>CD8::GFP;Pdp1^{3135}*, *Pdf>CD8::GFP;Pdp1^{3135}* and *Pdf>Tub::GFP; Pdp1^{3135}* but failed to adequately stain s-LN$_v$ soma or projections (data not shown). As suggested in (Cyran et al., 2003), PDP1 may regulate PDF at the transcriptional level, so it is likely that *Pdf-gal4* driver requires functional PDP1. The projection phenotype of these brains thus remained inconclusive.

To identify potential downstream roles of PDP1, we first attempted to rescue the *cyc^{01}* projection phenotype through pan-neuronal expression of PDP1. PDP1 failed to noticeably rescue projection morphology, resulting in either stunted or defasciculated

projections (Appendix Figure 18). Repeating this at 29°C with genotype *elav; UAS-Pdp1/CyO; tubpgal80^{ts}cyc^{01}/cyc^{01}* was uniformly pupal lethal, for unknown reasons, but hints to aberrant effects of high PDP1 expression (data not shown). CLK overexpression in many broad neuronal drivers results in lethality (Zhao et al., 2003), but not CYC (Chapter 3), though we cannot state if this is CLK or PDP1-mediated. Attempts to conditionally re-introduce PDP1 with genotype *elav-gal4;UAS-Pdp1ϵ/tubpgal80^{ts};pdp1^{3135}* similarly resulted in a line with prohibitively high lethality, and as such conditional PDP1 re-introduction could not be performed, though would be an interesting future experiment, potentially utilising Geneswitch.

However, CLK/CYC function and CLK function are not neccesarily the same, as the variable phenotypes of *cyc^{01}* and *Clk^{Jrk}/Clk^{Out}* attest, and PDP1 could be required for s-LN$_v$ PDF expression. In support of this hypothesis, the Sehgal group showed that *Cry-gal4-24* driven PDP1 re-introduction was capable of rescuing behaviour, demonstrating driver functionality in this mutant, whilst *Cry-gal4-24>UAS-Clk* reintroduction to *pdp1^{3135}* rescued molecular rhythms, but not PDF expression (Zheng et al., 2009). As mentioned above, we failed to show CRY stain in *pdp1^{3135}* mutants, and failed to adequately express *CD8::GFP* with *Cry-gal4-13*, so could not repeat this result (Figure 4.22).

We defined a series of experiments to interrogate if roles for PDP1 existed both upstream or downstream of the oscillation, by uncoupling CLK expression from PDP1, similar to earlier studies (Zheng et al., 2009). To circumnavigate the assumed dual roles of PDP1 we generated *Pdp1* RNAi lines expressing a *tim-Clk* construct and *tim-Clk pdp1^{3135}* recombinants, voiding the potential of direct PDP1 regulation of *Clk* transcription through ectopic CLK expression, looking at dorsal projections and behavioural rhythms (Kim et al., 2002). Essentially repeating (Zheng et al., 2009) findings, we fail to see PDF+ve s-LN$_v$s (Appendix Figure 14, Figure 4.23), however *tim-Clk* does not result in identifiable PER (Appendix Figure 17), so may not be an effective CLK rescue, potentially due to altered phase of CLK, or due to weakness of TIM-driver in the low CLK/CYC *pdp1^{3135}* (Zheng et al., 2009).

We performed the reverse manipulation, of expressing *UAS-Pdp1* with the *elav* driver on a *Clk^{out}* background, and stained with PDF. PDF was not obviously restored and brains remained *Clk^{out}* -like. We therefore cannot build upon (Zheng et al., 2009) experiments

and conclude PDP1 has an output role in s-LN$_v$ PDF production or projection morphology.

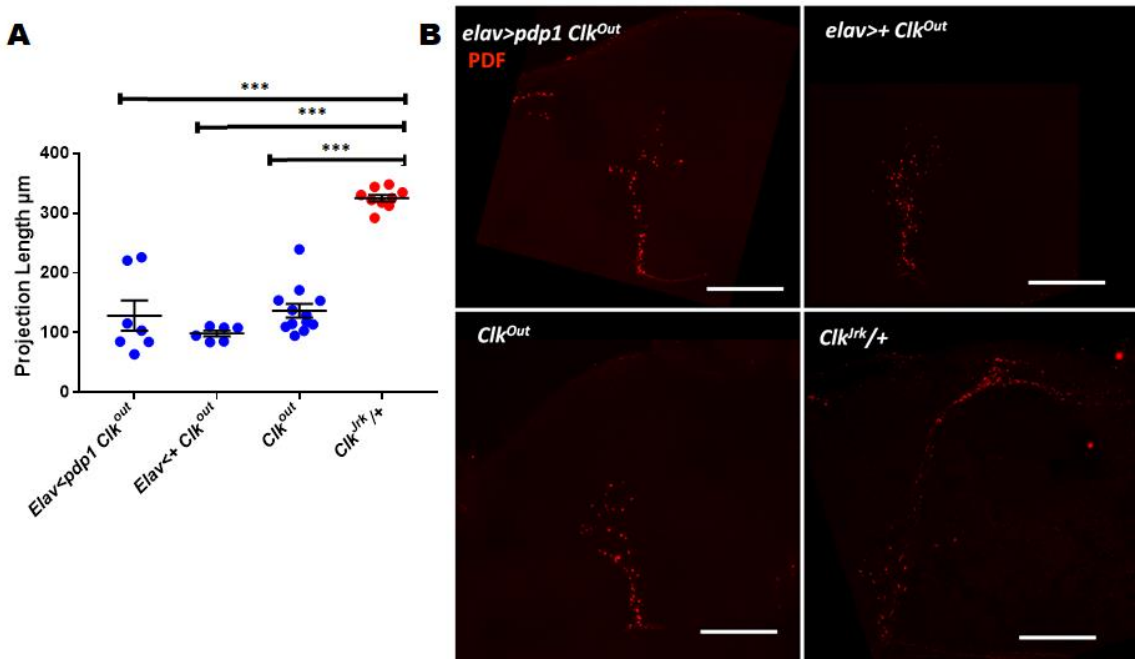

Figure 4.25 - PDP1 expression fails to rescue the PDF projection stunting identified in CLK mutants. *Panel A shows measurements of PDF dorsal projection length and Panel B shows example images for each genotype, demonstrating stunting following loss of Clk, which cannot be rescued by ectopic PDP1 expression, with scale bar of 50μm. PDF+ve projections appear mostly l-LN$_v$-derived and stunted. Clk^{Jrk}/+ projection length, stemming from visible s-LN$_v$ soma, significantly differs to all three (P<0.001***), whilst elav>pdp1 Clk^{out} does not differ in projection length to responderless and driverless counterparts (P=0.669 vs elav>+; Clk^{out}, P=0.990 vs Clk^{out})*

Summarily, we have further defined defects in both s-LN$_v$ and l-LN$_v$ projection morphology after developmental CYC loss, although attempts to find CLK/CYC targets that produce a similar phenotype was unsuccessful. Similarly we have identified purported changes in gene expression within clock cell groups in the absence of CYC, though these are not neccesarily developmental.

4.11 - Discussion- Chapter 4

We thus have a greater understanding of neuronal defects induced by loss of

developmental CYC, which potentially disrupts outflow of rhythmic information from the s-LN$_v$s, l-LN$_v$s and other clock cells.

Developmental loss of *cycle* results in defects in morphology of PDF-harbouring axons of small and large-lateral-ventral neurons (Relevent to Sections 4.1 -4.8)

Our characterisation of s-LN$_v$ projections places a greater emphasis on morphological changes in the absence of CYC, which appear significantly more complex than wt-like projections, wheras previous studies have focussed instead on reduced PDF levels. One simple explanation emerges, in antibody use (Figures 4.1 and 4.5). The original Hall lab paper characterising stunted projections utilises the original fly PDF antibody, now largely superseded in use by the Blau hybridoma antibody used in our study (Park et al., 2000). The robustness of our phenotype across multiple genotypes and experimental conditions, our quantitation of projection complexity and length, prompts us to consider the idea that these projections are absent or PDF-ve is overly reductive, and incorrect.

We posit that l-LN$_v$s misroute in the dorsal brain, with additional s-LN$_v$ projection defects, though unfortunately *CD8::GFP* stains with the *c929* and *R6* drivers did not provide adequate resolution to test this (Figure 4.4). An experiment we regrettably did not conduct would knockdown PDF with the *c929-gal4* on a cyc^{01} background, to remove l-LN$_v$ contribution to the l-LN$_v$ stain and allow quantification of the s-LN$_v$s alone. Additionally, conditional s-LN$_v$ ablation (Figures 5.5 & 5.6) could be integrated onto a cyc^{01} background, with the expectation of a $Clk^{Jrk/Out}$-like phenotype. It is initially tempting to suggest that l-LN$_v$ innervation of the dorsal brain occurs in the same fashion as s-LN$_v$ due to molecular similarities between the two clusters, enabling them to follow related guidance cues. However, this raises a new question, in that s-LN$_v$ projections terminate far more dorsally than l-LN$_v$s, hinting at differences in their receptivity to guidance cues, or synaptic organisers. It would be interesting to profile the surfaceome of l-LN$_v$s and s-LN$_v$s to assay differences in expression of cell-adhesion proteins mediating synaptogenesis.

It is demonstrable that changes in projection morphology due to CYC loss are visible throughout development, though as high larval complexity does not indicate high adult complexity, and high adult complexity does not preclude behavioural rhythms, larval defects are potentially rescuable by later CYC expression and may not neccesarily indicate dysfunction (Figures 4.7, 4.8 & 4.9). In either case, it appears CYC may have

developmental roles both before and after 3rd-instar larval stage. Nevertheless increased pupal and adult PDF projection complexity associates with behavioural arrhythmia with the understanding that similar intermediate projection phenotypes can occur in the context of residual behavioural rhythms.

Notably, s-LN_v dorsal projections and aberrant innervations of the l-LN_vs into the dorsal brain arise following developmental CYC loss, forming novel synaptic connections (Figures 4.10 & 4.17). Whether this disrupts rhythmic information transfer along the s-LN_vs is unknown, in part as an in-depth characterisation of post-synaptic targets contributing to rhythmic behaviour has not been performed. Low PDF levels of CYC mutants, though present, do not appear to be rescued in second-order proceses following adult CYC re-introduction, which may contribute to arrhythmia, although other behavioural quirks of low-PDF mutants, discussed in Chapters 3 and 5 do not arise in these flies, though this may be masked by more severe defects. It is clear that lessened or aberrant PDF signalling cannot cause the established *cyc^{01} [elav.cyc]^{ts}* projection phenotype. We also demonstrate that PDF-specific CYC rescue significantly improves projection morphology, but cannot rescue dorsal pre-synaptic bouton number, indicating that whilst PDF cell CYC controls aspects of axonal formation, CYC in post-synaptic clock cells may be required for correct connectivity. (Gorostiza et al,. 2013) introduces the concept of retrograde signalling in remodelling PDF projection morphology, which we might suggest involves CYC expression in post-synaptic cells. Identification of CYC-regulated effectors of retrograde signalling, which may encompass BMP signalling pathway components, would be an obvious subsequent step.

Chapter 3 introduces the idea that strong morning anticipation is evident in both *cyc^{01} [elav-Pdf80.cyc]^{ts}* and *cyc^{01} [Pdf.cyc]^{ts}* despite freerunning arrhythmicity in both. (Agrawal and Hardin, 2016) suggests morning anticipation is s-LN_v projection independent whilst freerunning arrhythmicity is projection dependent, so under this model, incomplete s-LN_v projection connectivity in both lines would result in the observed behavioural data. Other groups report associations between a PDF cell oscillator and morning anticipation, although there is, arguably, a stronger link between PDF signalling from l-LN_vs and morning anticipation, though whether the residual rhythm in *cyc^{01} [elav-Pdf80.cyc]^{ts}* can account for an extant morning peak is unknown (Stoleru et al., 2004, Agrawal and Hardin, 2016).

Behavioural spatial mapping of CYC reintroduction suggests that PDF-ve cells require CYC for adult behavioural rhythms, with little resolution of specific subsets (Figure 4.18). Early-developing DN1s do not appear to require CYC as glutamatergic-cell-specific CYC inhibition does not readily produce behavioural defects, an unsurprising finding, as these cells are not known to influence adult behaviour. However, they do constitute the major clock cell target of larval PDF cells, and a dispensability of their function (Collins et al., 2012). Though it was not tested, it would be interesting to study larval PDF projection complexity in this genotype, to identify if DN1 CYC was required for larval, but not adult projection formation. Post-larval DN1s are harder to visualise, and, though we cannot definitively state these cells are absent, a failure to specify relevant clock cell subsets in development due to CYC loss could cause adult arrhythmia (Figure 4.12).

In future work, GRASP would be utilised to better study synaptic connections between clock cell groups lacking CYC. To our knowledge, no group has published GRASP studies on mutant lines, instead utilising the technology predominantly to trace wt-connections, so such a dataset would be of interest. The awkwardness of integrating GRASP's genetic elements with cyc^{01}, alongside several inexplicably unsuccessful fly lines prevented our completion of this dataset. Indeed, drawing conclusions of connectivity without GRASP is highly speculative and likely to be disregarded. Marking post-synaptic dendrites with UAS-Denmark would also be helpful in establishing potential connections, especially combined with a technique such as expansion microscopy to increase resolution of synapse structure. As *CD8::GFP* staining has proven particularly weak in certain key projections, namely the DN1p dendrites, it is impossible for us to directly assess connectivity. It is difficult to acertain DN1p cell number in cyc^{01}, and potentially DN1ps persist in wt-like numbers, form functional connections with the s-LN_vs, but are simply not *Clk4.1M*+ve, due to changes in gene expression.

The possibility of a post-synaptic CYC requirement in regulating synapse number in the s-LN_vs has been discussed, and it is clear that loss of CYC within the sole known CYC+ve larval post-synaptic partner, the $DN1_a$s, does not influence rhythms, as shown by cyc^{01} *[elav-VGlut80.cyc]*^{ts} (Figure 4.18). Feasibly CYC loss in $DN1_a$s could alter s-LN_v synapse number without impacting rhythms, or even disrupt larval circadian behaviours, but not adult and it is unfortunate we lacked a *UAS-SYT::GFP* element which

could be readily integrated into the *cyc^{01} [elav-VGlut80.cyc]^{ts}* genotype. Even more unfortunately, we cannot easily study s-LN$_v$ bouton number for *cyc^{01} [elav-Pdf80.cyc]^{ts}*, in which we might predict bouton number was similarly decreased from a wt-like second-order branching complexity in spite of a significantly higher overall complexity (Figures 4.11 & 4.15).

Co-rescue of *cyc^{01}* through concurrent CYC expression in the *Pdf* and *Clk4.1M* drivers completely fails to rescue freerunning behaviour. As we have argued that *Clk4.1M*-driven expression may be weaker in the absence of CYC, and that a post-synaptic cell type may require CYC to regulate s-LN$_v$ synapse number, it is interesting that *Clk4.1M-gal4* CYC rescue, in conjunction with rescue of the pacemaker oscillator (Figuress 4.15 & 4.18), fails to rescue behavioural rhythms. Future work would express *SYT::GFP* and *CD8::GFP* in these subsets to identify DN1p cell presence and bouton number following CYC reintroduction, though this was not feasible within the timeframe of the thesis. Though PDF-ve clock cells are required for freerunning rhythms, there is no comprehensive dataset addressing which ones are required or not, which would assist in our mapping.

In numerous other models, bouton size and number is plastic, and both correlate with increased neuronal activity. Developmental CYC loss may alter adult electrical activity within the s-LN$_v$s, although this has not been explored.

The *VGlut-gal80* element utilised in *cyc^{01} [elav-VGlut80.cyc]^{ts}* has not been published in relation to the clock circuit, so although it is known DN1$_a$s are glutamatergic, it is assumed, but not verified that *GAL80* would be expressed in these cells, opening the door to a harmful false-negative. Were *cyc^{01} [elav-VGlut80.cyc]^{ts}* more intrinsic to the conclusions we draw, *tim-UAS-gal4-VGlut80>CD8::GFP* and PER immunofluorescence would need to be conducted to establish this.

Another caveat of our dataset is the dependence on two timepoints to assess a peak and trough of PER stain. As CYC reintroduction demonstrably results in a shortened behavioural period, molecular period may not be best represented in such a form (Figures 3.20, 4.14 & 4.16). Indeed, the assessment of molecular rhythms in Chapter 3 relies on more timepoints, and a direct comparison between CT2 and CT14 would not be significant in certain cases. Whilst we are reasonably confident that the significant

differences between CT2 and CT14 for *cyc^{01} [elav-Pdf80.cyc]^{ts}* and *cyc^{01} [Pdf.cyc]^{ts}* can be used to demonstrate the presence of an oscillation, this experiment is poorly suited to demonstrating the absence of an oscillation (Figures 4.14 & 4.16).

Expresssion of clock cell markers is disrupted in mutants lacking functional *cycle* (Relevant to Section 4.9)

Expression of numerous driver lines appears to be reduced in clock cells in *cyc^{01}*, suggesting many genes are dysregulated in these mutants (Figures 4.12, 4.20 & 4.21). NPF neuropeptide, important for courtship and expressed in the LN_ds is absent exclusively within clock cells in *Clk^{Jrk}* and *cyc^{01}* mutants, and retained elsewhere (Lee et al., 2006). Our data supports the literature in suggesting CLK/CYC controls ITP and PDF neuropeptide levels, and it is feasible that the net effect of CYC loss is a widespread lowering of gene expression in clock cells, affecting many driver lines. *cyc^{01} [elav.cyc]^{ts}* are ITP+ve, yet ITP clock neurons cannot be visualised via GFP expression with *crygal4-13* or *R78G02* drivers, so it is difficult to assess clock neuron presence via known driver lines (Figures 4.19, 4.20 & 4.21). A comprehensive series of staining experiments with more drivers may ultimately map clock cell presence, though the extent of CYC defects remains unknown in the absence of reliable markers.

The finding that CRY stain appears lower in clock neurons in cyc^{01}, whilst validating *cry-gal4-13* driver weakness in *cyc^{01}*, is problematic, and relevant to models of nocturnality discussed in chapter 3. CRY levels in whole heads of *cyc^{01}* and *Clk^{Jrk}* flies are higher, though this is largely composed of CRY in peripheral clocks, and pacemaker CRY levels have never been quantified in CLK/CYC mutants (Emery et al., 1998). However, two pieces of evidence contradict this result: *cyc^{01}* nocturnality occurs in LD but not RD cycles, from which we conclude blue-light input, likely mediating CRY activation, contributes to loss of daytime behaviour, which is supported by data from (Kumar et al.,2012), in which *Cry^{01}Clk^{Jrk}* mutants lack nocturnal preference, which can be regained through rescue with UAS-CRY. This discrepancy could be clarified through isolation of central clock specific *cry* mRNA and protein (Abruzzi et al.,2015).

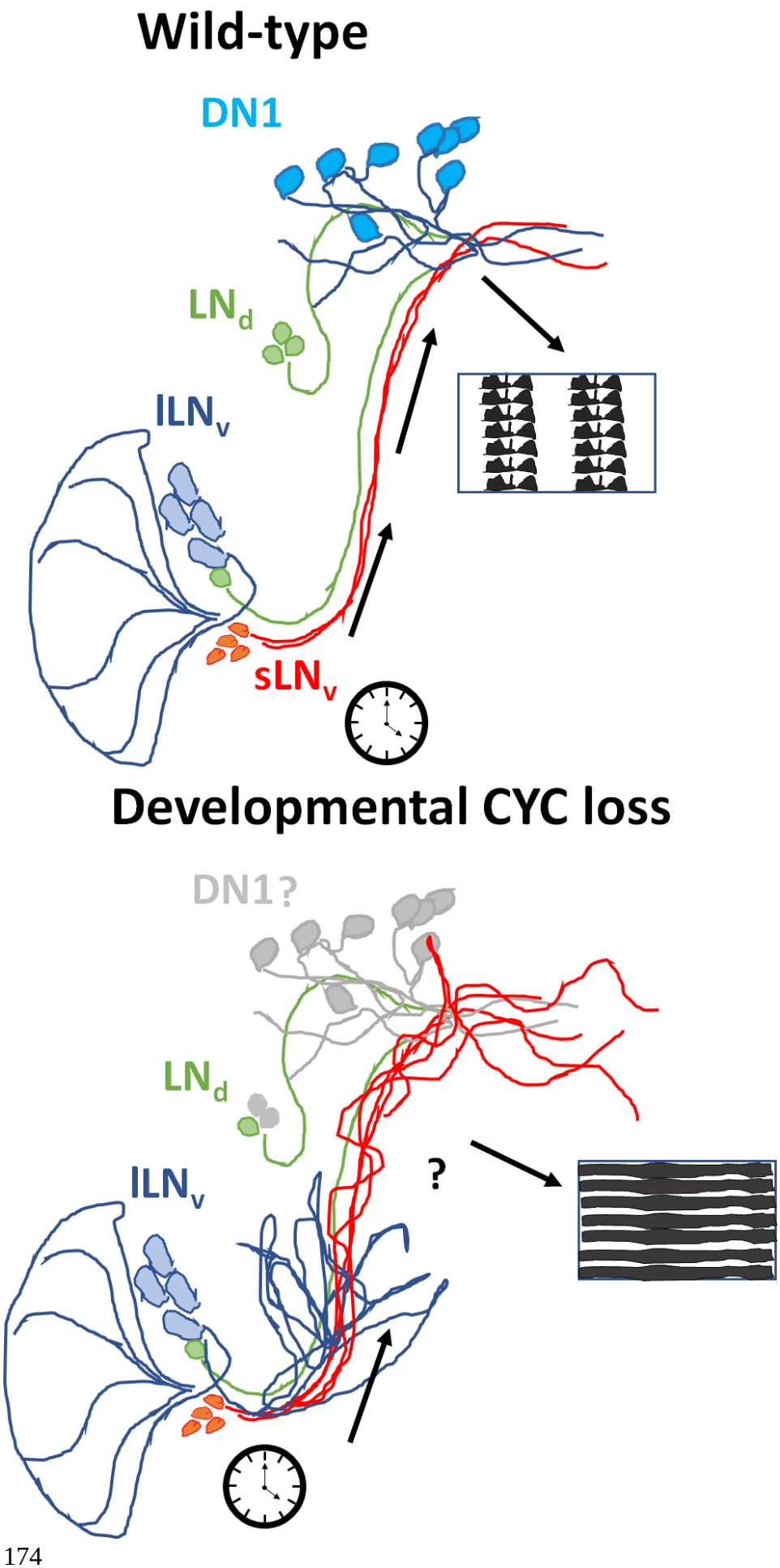
Wild-type
DN1
LNd
lLNv
sLNv
Developmental CYC loss
DN1?
LNd
lLNv
?

Figure 4.26 – Model for effect of developmental loss of cycle on the adult clock circuit. *Molecular oscillations within the s-LNvs usually propagate rhythmic information to dorsal clock cells and output circuits through rhythms in neuronal signalling. Loss of developmental CYC fails to disrupt molecular oscillations within the s-LN_vs, but rhythms in behaviour are disrupted. Axonal projections of both s-LN_vs and l-LN_vs are misrouted and display altered connectivity. Expression of CYC within PDF-expressing neurons partially rescues neuroanatomical phenotypes and molecular rhythms of PER, but not behavioural rhythms. The presence of DN1 and LN_d neurons, or at least their markers, is compromised following CYC loss, which may contribute to behavioural defects.*

Chapter 5: Characterisation of red-light mediated clock circuit network changes and relevance to developmental CYC requirement

Our findings in previous chapters tentatively coalesce around potential developmental CYC functions in both PDF+ve and PDF-ve clock cells. Our assays have been predominantly behavioural, and freerunning behaviour is broadly orchestrated by PDF+ve s-LN_vs. In imaging the clock circuit, many labs will focus purely on PDF cells for the ease of staining, and, as we encountered repeated challenges in imaging other clock cells, the PDF-ve clock circuit remains a relatively unexplored area. It is therefore prefereable for us to exploit and develop instances in which we can interrogate the PDF-ve clock cells with a behavioural readout without dependence on the state of the s-LN_vs.

As multiple studies have suggested that the arrhythmicity of flies in constant white light (LL) is entirely CRY-dependent, we attempted to study this PDF-independent clock network state, as an otherwise uncharacterised circuit state with unique dynamics (Stoleru et al., 2007, Murad et al., 2007). Red light has been used intermittently as a means to examine freerunning flies, on the assumption that the clock is unresponsive to red light, an assumption partially reliant on the insensitivity of CRY to blue/green light, and we thus sought to study if the cry^{01}/cry^{b} LL phenotype could be simplified by simple exposure of CRY+ve flies to constant red light, removing a recessive mutant from the genotype and facilitating more complex genetic backgrounds to be employed in circuit delineation (Helfrich and Engelmann, 1983).

5.1 - PDF cell firing states are dominant, yet dispensable for behavioural rhythms in constant red light

In collaboration with other lab members, I looked at the freerunning behaviour of Pdf^{01} mutants in constant red light (RR) and constant darkness (DD), identifying that despite disruption of PDF signalling, behavioural rhythms persist in RR, significantly stronger than in DD (Figure 5.1)(Appendix Table 25). These rhythms notably were of a uniformly short period, whilst wt flies retain a ~24 hr period in RR, supporting previous publications that a PDF-cell independent rhythm could be generated in such cases, with a

divergent period, reflecting either a molecular period within a pacemaker cell or a period emergent of the network, which is incapable of generating the 24 hr period of the PDF cells (Cusumano et al., 2009).

In support of Pdf^{01} data provided by other lab members, I studied $Pdfr^{5304}$ in RR and DD, identifying a statistically significant resurgence of weak rhythms in RR, with a similar short period rhythm, which bolsters our conclusions (Figure 5.1c).

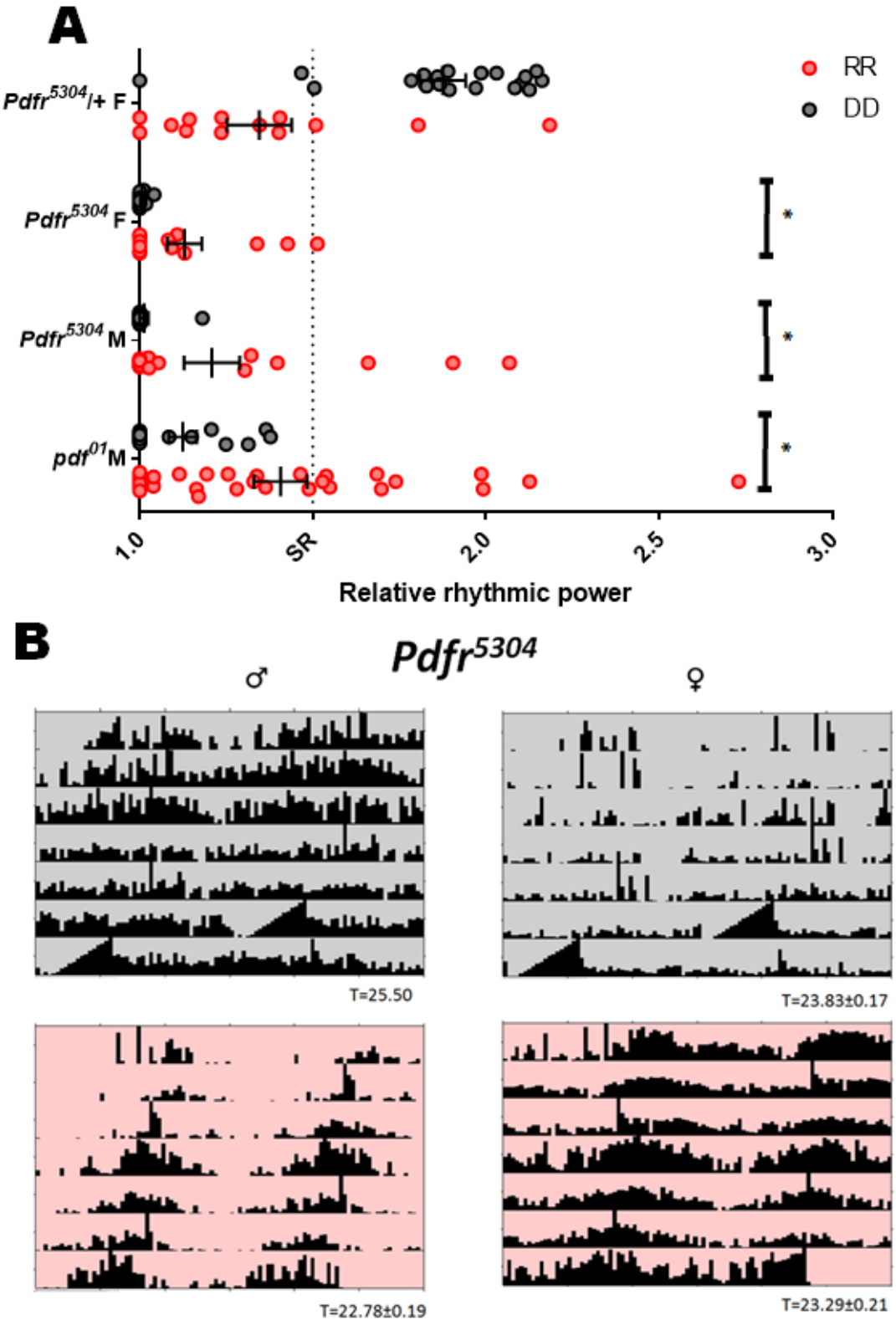

Figure 5.1 - PDF signalling is required for freerunning behavioural rhythms in constant darkness, but not in constant red light. *Panel A shows behavioural datasets generated by Charlie Hurdle, Ines Lin and myself, demonstrating relative rhythmic power in RR and DD of* Pdf^{01}*, in which males are significantly more rhythmic in RR (P=0.018*). Panel B shows median actograms of* $Pdfr^{5304}$ *mutant and heterozygous*

female controls in RR and DD. Full data and statistics are presented in Appendix Tables 18 and 19, wherein significant differences emerge between RR and DD rhythmicity for both genders. Panel C shows median actograms demonstrating the emergent short period rhythm in RR for Pdfr^{5304} mutants.

I endeavoured to continue investigation into PDF cell function in RR. Preventing vesicle release from the PDF cells with *Pdf>TeTxLC* fails to reduce rhythmicity in RR or DD (Figure 5.2), as has been shown in DD elsewhere (Kaneko et al., 2000, Blanchardon et al., 2001), though *TeTxLC* expression within a broader driver such as TUG has been shown to disrupt DD rhythmicity, suggesting, as will be discussed elsewhere, that fast synaptic transmission has roles in clock output that diverge from PDF signalling. I then attempted to electrically silence the PDF cells using *Kir2.1* (Figure 5.2)(Nitabach et al., 2002), demonstrating in this case a severe loss of rhythms in DD and RR which did not significantly differ between conditions (♂ P=0.538, ♀ P=0.410), and was significantly less rhythmic than responderless controls across conditions (Appendix Table 26). Therefore, there appears to be a contribution of PDF cell electrical activity to RR rhythmicity, though this activity may have effects other than release of the PDF neuropeptide.

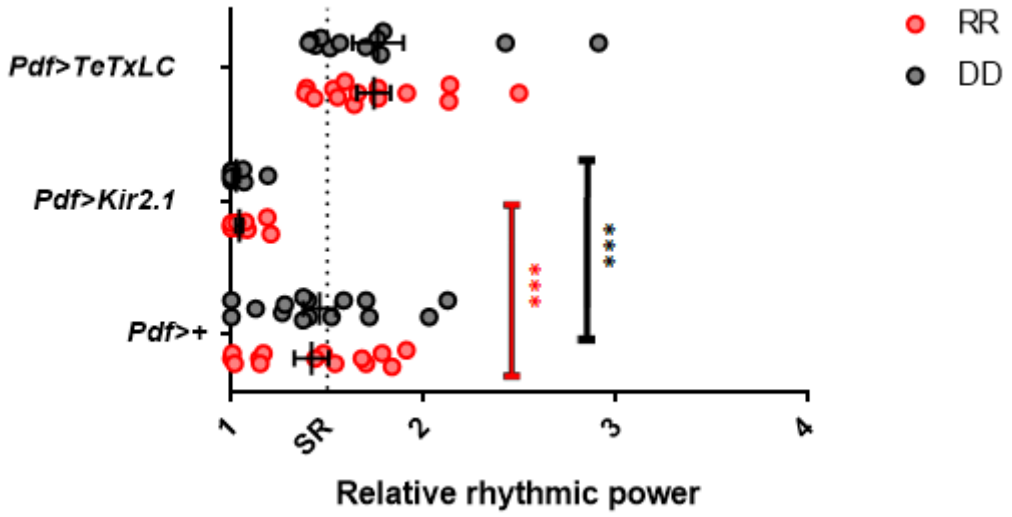

Figure 5.2 - PDF-cell silencing through ectopic expression of Kir2.1 potassium channel decreases behavioural rhythmicity in constant red light and constant darkness. *Limited effect of PDF-cell TeTxLC expression. In light of strong rhythms, which did not significantly differ in either case, we elected not to repeat the experiment with inactive tetanus toxin. Pdf>Kir2.1 conversely shows a phenotype of strong arrhythmia in both RR and DD*

I additionally studied the behaviour of flies following hyperexcitation of the PDF cells with *NaChBac* and *TrpA1*, driven by the finding that excitation with *NaChBac* is known to induce split rhythms, with multiple periods derived from oscillators in several separate clock neuron groups (Nitabach et al., 2006)(Figure 5.3). Either loss or retention of this phenotype would have important ramifications for our understanding of clock circuitry, in which emergent effects may be observable in RR. Hyperexcitation reduces rhythmic power in RR, commensurate with that in DD, demonstrating a level of dominance of the PDF cells in this state (Figure 5.3). The phenotype of multiple complex rhythmicities attainable in previous studies does not immediately arise (Nitabach et al., 2006, Sheeba et al., 2008b), and was unfortunately not discernible within the 7 days of experimental recording, though this may be the case with a longer behavioural experiment (Figure 5.3).

Pdf>TrpA1 had no effect on rhythmic strength in RR or DD, and we did not see any rhythm splitting, even following three weeks in constant conditions (data not shown).

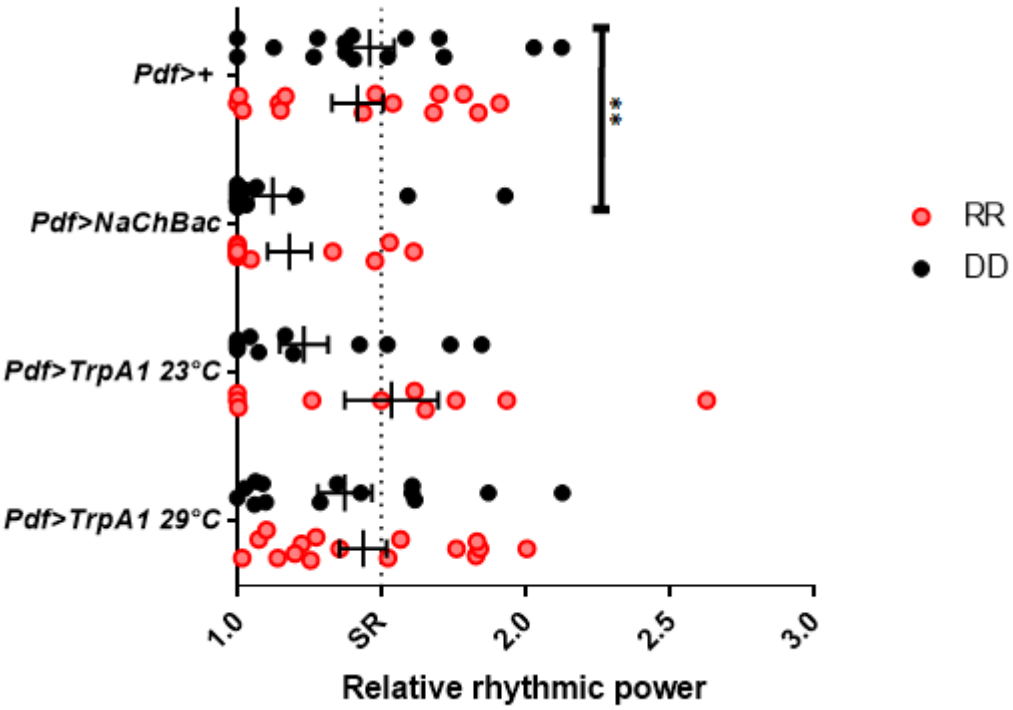

Figure 5.3 - Hyperexcitation of PDF-cells fails to impact freerunning rhythmicity in

***constant red light**. Behavioural rhythmicities for lines and controls hyperexciting the PDF cells, Pdf>NaChBac and Pdf>TrpA1. Pdf>TrpA1 does not significantly reduce rhythmicity, whilst NaChBac lowers rhythmic strength relative to undriven controls in DD (P=0.005**) and in RR females (P=0.035*), but not RR males (P=0.062), though median rhythms are lower.*

In all cases, *NaChBac* is constitutively active, whilst TRPA1 is placed at higher temperatures in an adult-specific manner, resulting in less TRPA1 activation during developmental stages, so we raised *Pdf>TrpA1* flies at 29°C to see if this affected behavioural rhythmicity. Our assumption was the failure of other groups to publish this was indicative of a negligible effect, or even a compensatory homeostatic effect that negated adult TRPA1 activation, but to our surprise, whilst development-specific excitation did not differ to permissive controls, continued developmental and adult excitation had a deleterious effect on rhythmicity, though with a potential contribution of prolonged exposure to high temperature (Appendix Figure 20)(Appendix Table 28, 29).

The Ceriani lab showed that whilst adult-specific silencing results in arrhythmicity without affecting the oscillator, prolonged alteration of cell firing through development and adulthood can have an effect on molecular oscillations, and prolonged hyperexcitation may have a similar effect (Depetris-Chauvin et al., 2011).

5.2 - s-LN$_v$s are dispensable for behavioural rhythmicity in constant red light, contingent upon l-LN$_v$ presence

Preliminary lab data has suggested that ablation of PDF-cells through expression of apoptotic gene *hid* resulted in a loss of both RR and DD rhythms, a finding I replicated (Figure 5.4). This supports our finding that *Pdf>Kir2.1* results in RR arrhythmicity and suggests that although PDF signalling in these cells is dispensable for RR rhythms, the cells themselves, and their electrical activity, are required.

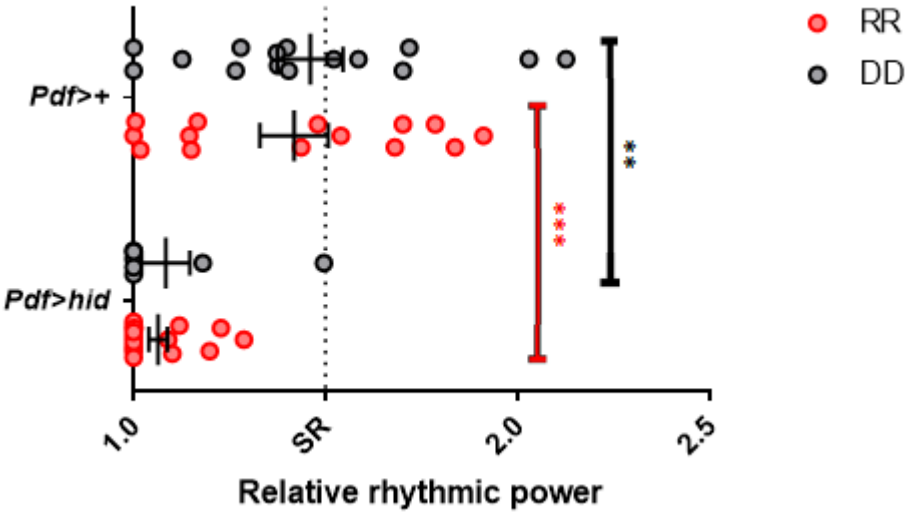

Figure 5.4 - Ablation of PDF cells reduces behavioural rhythmicity in constant darkness and constant red light. *Behavioural profile demonstrating non-significant difference between Pdf>hid flies in DD and RR Significant differences do not emerge between DD and RR, but Pdf>hid is significantly less rhythmic than undriven controls in both genders and conditions. Full behavioural data and statistics are available in Appendix Tables 18 and 19*

As *R6>hid, c929>hid* and *R78G01>hid*, drivers which segregate s-LN$_v$ and l-LN$_v$s, are lethal (data not shown), we wanted a manipulation to isolate the PDF cell subset responsible for the relative severity of the *Pdf>hid* phenotype. We raised *Pdf-gal4; UAS-hid/+; tubpgal80^{ts}/+* at 29°C from egg-laying until the 3rd instar larval stage, before transferral to 17°*C*, where they remained through adulthood. As l-LN$_v$s become PDF+ve in mid-pupal stages, we hypothesised we could ablate first-instar larval s-LN$_v$s, and re-activate *GAL80^{ts}* prior to *hid* transcription within the l-LN$_v$s, rendering s-LN$_v$-specific ablation.

Ambitious though this experiment seemed, s-LN$_v$s were ablated in all cases, with no visible soma or projections, whilst l-LN$_v$s remained broadly intact (Figure 5.5). We saw broad arrhythmia in DD, as would be expected by s-LN$_v$ ablation, but also a marked increase in RR rhythmicity, suggesting that ablation of the s-LN$_v$s alone did not result in RR arrhythmia, and clarifying that their presence, in pacemaker function or as network intermediaries, was dispensable. We can suggest, by process of elimination, that the l-LN$_v$s must be present for strong RR rhythms. As l-LN$_v$ molecular oscillations are too weak for pacemaker function in DD, their role is likely related to their affiliation with

red-light responsive photic input pathways, though rhythms are observable following silencing of these cells.

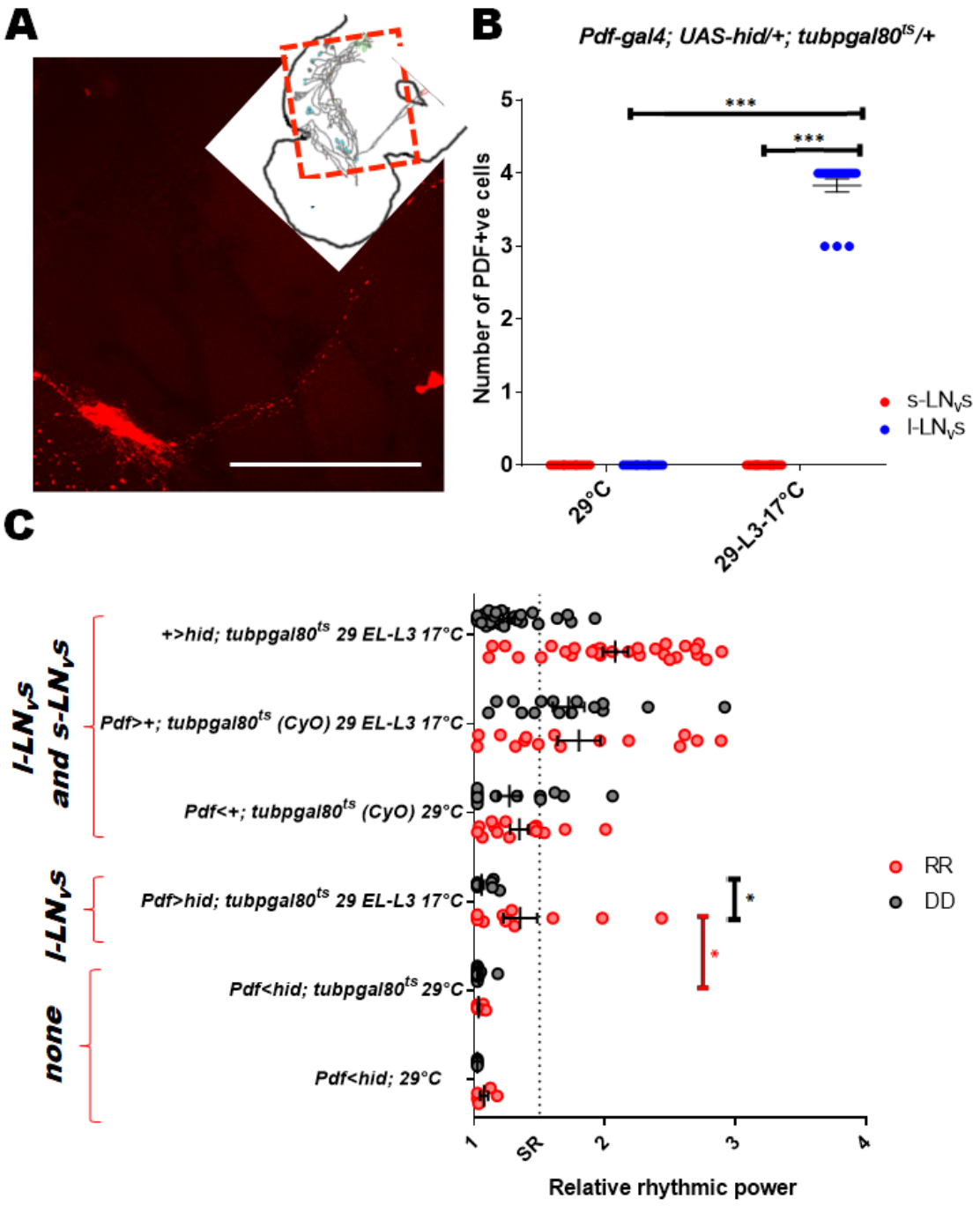

Figure 5.5 - Conditional ablation of small lateral ventral neurons does not remove behavioural rhythms in constant red light, so long as large lateral ventral neurons are intact. *Panel A shows a representative image of a PDF-stained brain with posterior optic tract and l-LN$_v$s visible, without s-LN$_v$ cells or projection. Inset is a schematic of the*

*orientation of the image, and in the bottom right is a scale bar of 100µm. Panel B shows relative cell counts (Imaged 29°C raised brains n=16, imaged 29-L3→17°C brains n=18). l-LN$_v$ number significantly differs between conditions (P<0.001***), as calculated by one-way ANOVA. Panel C shows Relative rhythmic power for Pdf-gal4(x)/Y; UAS-hid/+; tubpgal80^{ts}/+raised either at 29°C from egg-laying into adulthood, or from egg-laying to third-instar larval stages, subsequently moved to 17°C RR and DD. Accompanied are driverless, responderless and constitutive ablation controls. Due to a generalized lower rhythmicity, females were excluded from the figure. Full behavioural data is available in Appendix Table 36, and statistics are available in Appendix Table 16.*

The period of conditional s-LN$_v$-ablated flies approximates 26 hr in both RR and DD, longer than the short period observed in other manipulations, potentially due to a combination of temperature and genetic background, which persisted in unablated controls. It is arguable that the short-period observable in RR in *Pdf^{01}/Pdfr^{5304}/Pdf>Kir2.1* etc does not stem from s-LN$_v$ dysfunction, as s-LN$_v$-specific ablation does not shorten period, and, if pacemaking function is shifted to another clock neuron cluster, short period may not solely be a property of an unshackled secondary pacemaker, but may potentially be influenced by l-LN$_v$ input. Our data demonstrates that l-LN$_v$ cell presence is required for RR rhythms in the absence of s-LN$_v$s, but the purpose of l-LN$_v$s in this process can only be speculated on.

We wished to exploit s-LN$_v$-specific ablation as a novel assay for separating s-LN$_v$ and l-LN$_v$ function, and studied the behaviour of flies in 12:12 LD. A controversy exists in the literature. The Taghert lab showed morning anticipation required PDF-expression in the s-LN$_v$s, but not l-LN$_v$s (Shafer and Taghert, 2009), though other groups show that loss of s-LN$_v$ projections does not remove morning anticipation (Agrawal and Hardin, 2016). Additionally, there are multiple arguments for the emergence of an advanced E-peak in *Pdf^{01}*, *Pdfr^{5304}* and *Pdf>hid* flies, with potential s-LN$_v$ or l-LN$_v$ contributions (Renn et al., 1999). A recent study demonstrates a PDF knockdown specific to the l-LN$_v$s results in advanced E-peak, and PDFR rescue within the E-cells rescues the advanced E-peak of *Pdfr^{5304}*, arguing for an l-LN$_v$→E cell link influencing evening emergence, without an s-LN$_v$ contribution. Conditional s-LN$_v$ ablation can thus be used to clarify these differences (Schlichting et al., 2016).

We identify ablation of both s-LN_vs and l-LN_vs results in the previously-published advanced E peak, whilst ablation of the s-LN_vs alone fails to do so, resulting in a phase equivalent to unablated controls (Figure 5.6a,b). This data supports published data that l-LN_v PDF signalling delays the E peak in the absence of s-LN_v PDF signalling, though we extend this finding to suggest s-LN_vs are not required in any capacity (Schlichting et al., 2016).

Morning anticipation was limited as our flies were neccesarily run at 17°C to preserve l-LN_vs, with the side-effect of promoting diurnality and severely limiting morning anticipation, and thus we could not address s-LN_v and l-LN_v contributions to morning anticipation.

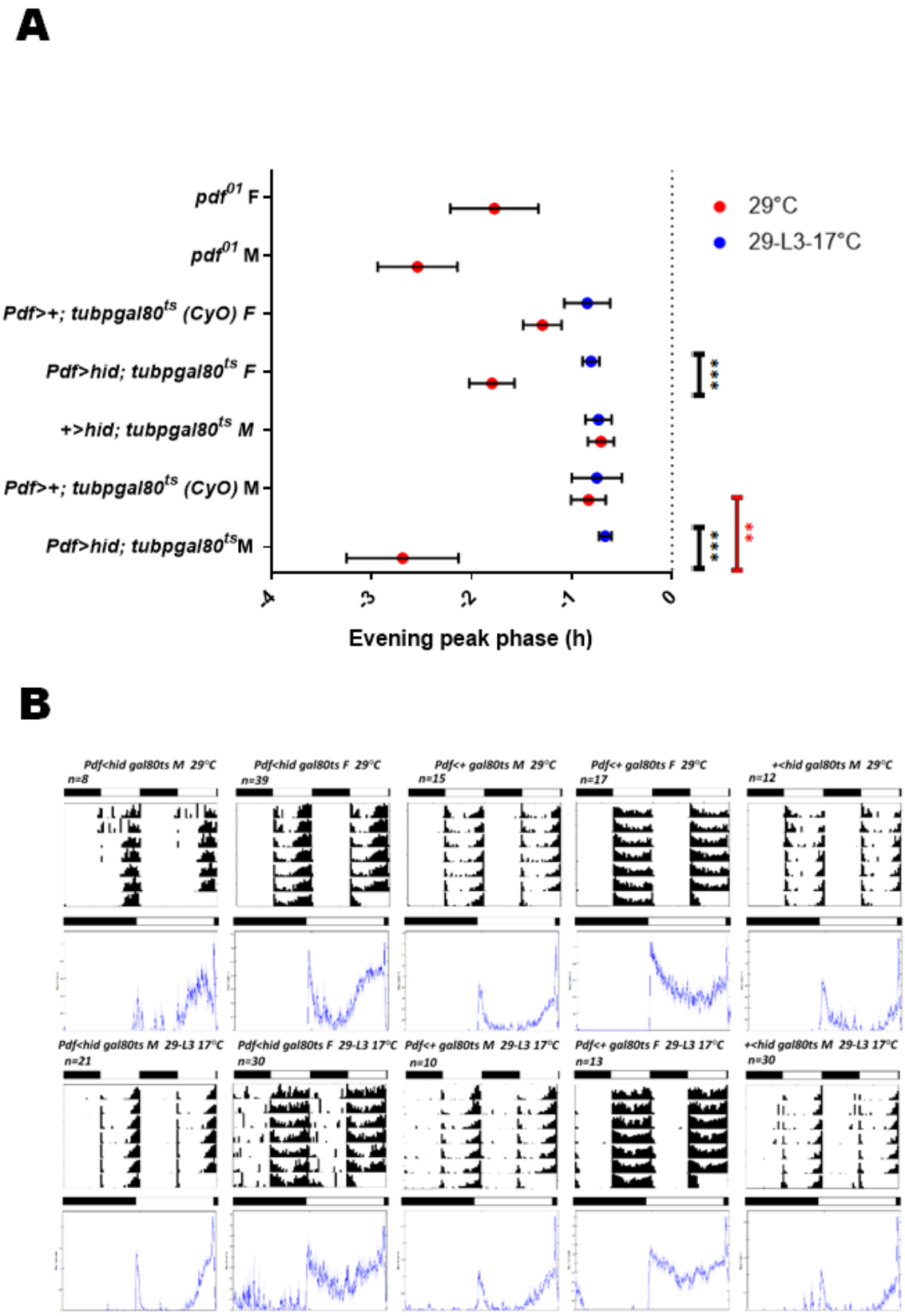

Figure 5.6 - Conditional ablation of small lateral ventral neurons does not affect evening anticipation, suggesting PDF control of evening anticipation timing is derived from large lateral ventral neurons. *Panel A shows E-peak phase quantification of Pdf; hid/+; tubpgal80^{ts}/+ and various controls run in 17°C LD following either a 29°C*

*development or a transferral from 29 to 17°C during the third-instar larval stage. Significant differences occur between restrictively and permissively raised E-peak for experimental flies of both genders (P<0.001***). Panel B shows median actograms and activity profiles for the respective conditions. Full statistics are available in Appendix Table 17.*

Behavioural analysis following PDF cell manipulation has thus identified that whilst PDF cells are capable of exerting dominant effects in RR, their firing and PDF signalling are dispensible for behaviour in RR, and s-LN_vs can be ablated entirely without removing rhythms. Instead, we suggest l-LN_vs possess a role in minimising s-LN_v pacemaker function in the presence of red light.

Attempts to extend the potential of conditional apoptosis to other constitutive-lethal drivers was unfortunately unsuccessful, and viable adults of genotype *c929/hid; tubpgal80^{ts}/+* and *hid/+; R78G02/tubpgal80^{ts}* failed to lose relevant cell groups, as identified by staining with PDF or ITP respectively (data not shown). An attempt to ablate the entire larval clock circuit, whilst leaving the adult-specific circuit intact with *tim-UAS-gal4* was similarly unsuccessful and ablation failed. However, there is undoubtably potential in extending this technique to other drivers, or in studying other circuits.

5.3 - Spatial mapping of pacemaker function confirms the importance of CRY+ve but not PDF+ve cell molecular oscillators for behavioural rhythmicity in constant red light

We have thus defined a condition in which pacemaker function is no longer confined to the s-LN_vs, and instead resides in a separate group of cells. We sought to remove molecular rhythms from clock neuron subsets via expression of a dominant-negative *cyc* allele, *cyc*$\Delta^{103,}$ to identify cells required for RR pacemaker function (Tanoue et al., 2004). I additionally contributed to a related project in the lab which sought to reintroduce oscillations in cell subsets within an arrhythmic line, to identify which cells were sufficient for rhythms in RR.

As a driven control, we first demonstrated *repo>* cycΔ^{103}, expressing in glial cells, had no significant effects on rhythms (Appendix Figure 23). A glial oscillator is not required

for behavioural rhythms, and non-glial driver *ela*v-gal4 rescues cyc^{01} *[elav.cyc]*^{ts} behavioural rhythms, so we are sure loss of glial CYC does not contribute to the defects discussed in Chapters 3 and 4.

As expected, *TUG> cyc*Δ^{103}, which hypothetically disrupts all oscillations, appeared severely arrhythmic with no strongly rhythmic flies in DD (Figure 5.7). In RR, these flies are also majority arrhythmic, and there is no statistically significant difference between RRP in either lighting condition. Likewise, *cry> cyc*Δ^{103} flies, affecting the s-LN_vs, l-LN_vs, 5^{th}-s-LN_v, 3-LN_ds and several DN1s are strongly AR in both DD (♀ = 92.3%, ♂ = 72.7%), and RR (♀ =85.7%, ♂ = 50%), suggesting in both cases that the molecular oscillator is present within these cells. This covers both putative oscillators, in the E cells and the DN1s, and from both these datasets we can map a required RR pacemaker function, to cells targeted by the CRY+ve driver.

Pdf> cycΔ^{103} flies appeared weakly rhythmic in DD and strongly rhythmic in males in RR, though in RR, pronounced split rhythms occur and RRP is significantly higher in males (P<0.001***)(Figure 5.7)(Appendix Table 18, 12).

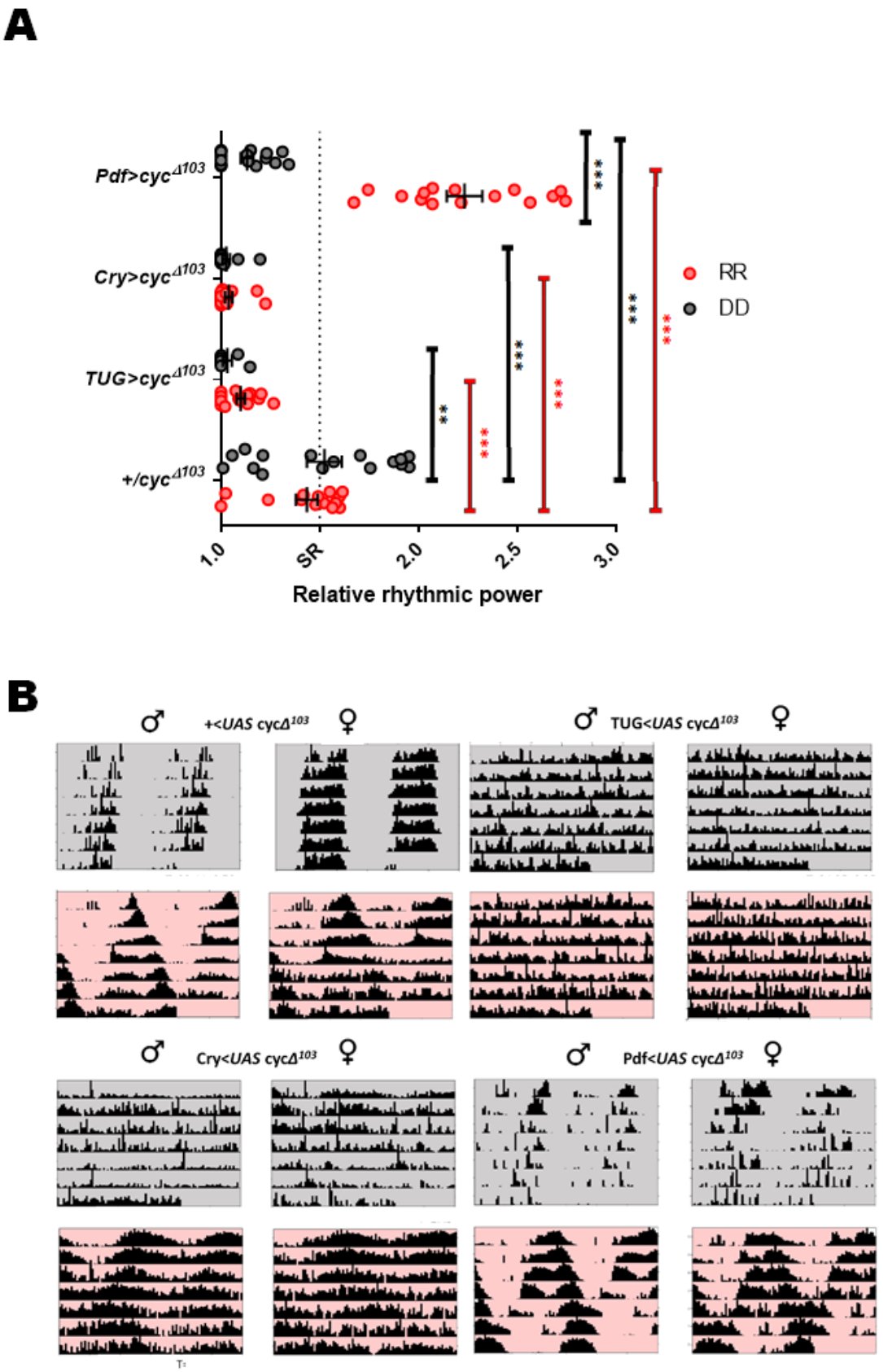

Figure 5.7 - Inhibition of molecular oscillations in CRY-expressing, but not PDF-expressing clock neurons, results in a loss of behavioural rhythmicity in constant red light. *Panel A shows Relative rhythmic power of UAS* cycΔ^{103} *expressed with Tim-(UAS)-*

Gal4, cry_{13}-Gal4, Pdf-Gal4 and undriven respectively in RR and DD conditions. Expression with cry_{13}-Gal4 or Tim-(UAS)-Gal4 driver results in significant loss of rhythmicity in both RR and DD. Expression with the Pdf-Gal4 driver demonstrates significant differences between DD and RR rhythmicity. Panel B shows average actograms for both genders. Due to a generalized lower rhythmicity, females were excluded from the quantification in Panel A, although trends were the same.

The literature has identified split rhythms on multiple occasions, in all cases stemming from desynchronised oscillators in the morning and evening cells, suggesting A) that the M-cell oscillator in RR is not completely disrupted by PDF-cell specific Δcyc^{103} expression, a concept backed up by the continuation of rhythms in DD, and B) that E oscillator independence in RR implies a greater participation from these cells and a possible RR pacemaker function (Yoshii et al., 2004, Nitabach et al., 2006, Rieger et al., 2006, Sheeba et al., 2008). It is unknown how Δcyc^{103} would promote a desynchrony, we can suggest from our data and previous work that reduced PDP1 through loss of CLK/CYC may lead to weaker PDF expression, and a potential scenario in which PDF levels are insufficient to mediate synchronisation of clock cell oscillators, whilst sufficient that s-LN_v rhythmic information can still be passed to output circuits.

To confirm the PDF cell oscillator drives one of the split rhythms, we ran *$Pdfr^{5304}$; Pdf> $cyc\Delta^{103}$*, with the hypothesis that this would eliminate the longer period component in RR. Indeed, this is the case, and these flies appeared AR in DD, with a weak short-period rhythm in RR (Figure 5.8). We can thus conclude that the long-period component stems either directly from a PDF-cell oscillator, or another downstream oscillator dependent on PDF signalling to exert its effects.

We utilised a second *Pdf-gal4* driver, located on the X-chromosome, to support this data. Again, we see a significant difference in the distribution and rhythmic power of male flies in RR and DD, with stronger rhythms in RR ($P<0.001$***)(Figure 5.8). This again demonstrates, contingent on the idea that PDF cell oscillator activity is abrogated, a reduced contribution of this oscillator in RR. Once again, rhythm splitting is evident, suggesting a dual pacemaker function, though long period rhythmic strength is consistently stronger than the short-period rhythm in RR.

It is important to consider, that in both instances of Δcyc^{103} expression with a *Pdf-gal4*

driver, rhythmicity in RR is significantly stronger in males than in DD, whilst this is not the case with controls. It could be suggested that attempts to constrain a secondary pacemaker to a fully functional M cell oscillator may create a level of noise in the workings of the secondary pacemaker cells and in other parts of the clock circuit that declarifies rhythmic information from that pacemaker. We interpret this to mean that RR pacemaker function is at least partially independent from molecular oscillator function in the s-LN_vs, whereas DD pacemaker function is not.

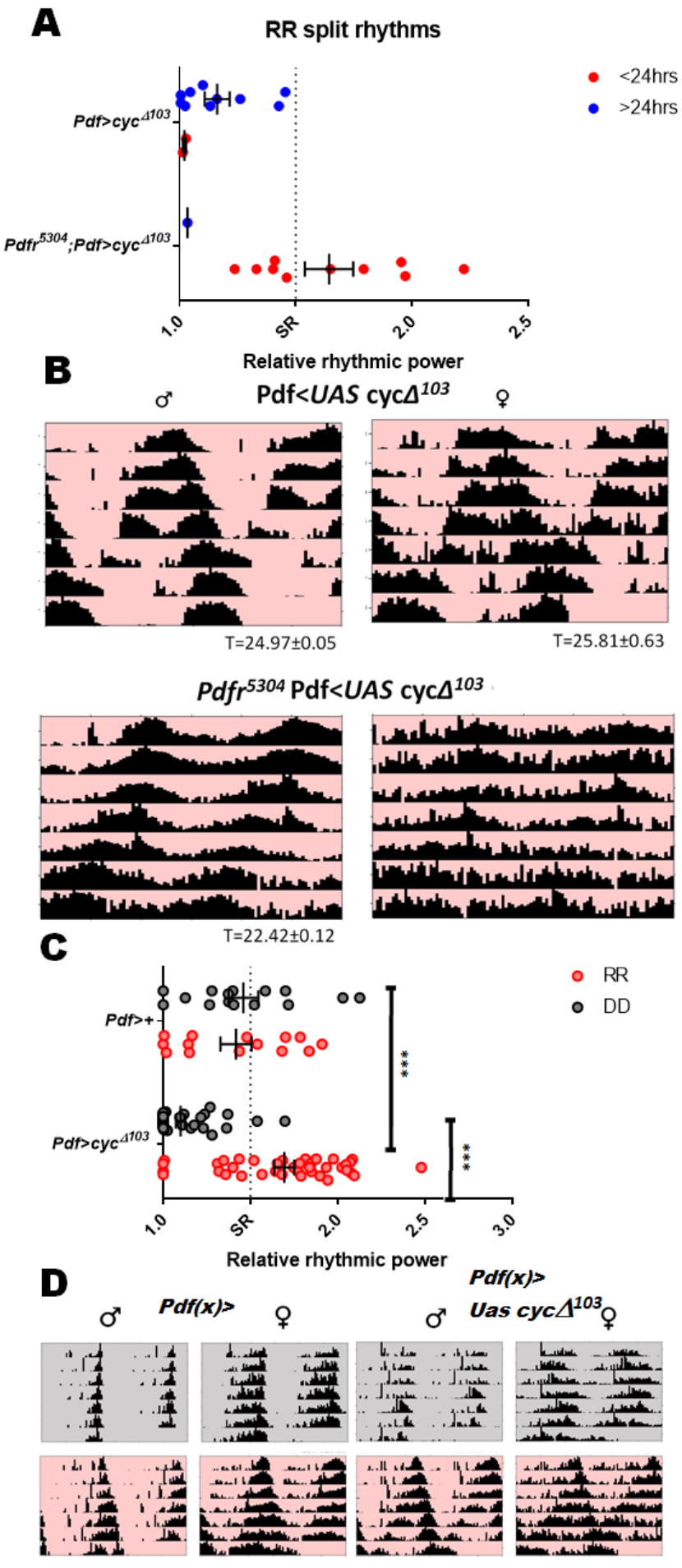
A
RR split rhythms
<24hrs
>24hrs
Pdf>cyc^Δ103
Pdfr^5304;Pdf>cyc^Δ103
1.0
SR
2.0
2.5
Relative rhythmic power
B
♂
Pdf<UAS cycΔ^103
♀
T=24.97±0.05
T=25.81±0.63
Pdfr^5304 Pdf<UAS cycΔ^103
T=22.42±0.12
C
RR
DD
Pdf>+
Pdf>cyc^Δ103
***
***
1.0
SR
2.0
2.5
3.0
Relative rhythmic power
D
♂
Pdf(x)>
♀
♂
Pdf(x)>
Uas cycΔ^103
♀

Figure 5.8 - Loss of PDF cell molecular oscillations results in split behavioural rhythms in constant red light, with a short-period component which is independent of PDF signalling. *Panel A shows Pdf> cycΔ^{103} rhythmic power of split rhythms with integration of Pdfr^{5304} null mutant. Panel B shows average actograms for the above condition, with an accompanying loss of long period component following loss of PDF signalling. Statistics were not conducted for Panel A due to the low n-number.*
*Panel C shows Relative rhythmic power and Panel D shows average actograms of Pdf-gal4; Δcyc^{103}/+, ostensibily removing moleclular rhythms within the PDF cells, in RR and DD. Significant differences emerge between RR and DD conditions (P<0.001***) and control/experimental genotypes in DD alone (P<0.001***). Due to a generalized lower rhythmicity, females were excluded from the figure.*

With assistance from a student under my tutelage, we then ran (*TUG-Pdf80)> cyc*Δ^{103} flies, expressing everywhere except the PDF cells, in RR and DD. Rhythmicity does not differ in DD or RR compared to driver-line controls, and is far milder than *TUG>* Δcyc^{103}, demonstrating that blocking the molecular oscillator within the secondary pacemaker, whilst retaining an oscillator in the s-LN_vs, allows a behavioural rhythm to manifest (Figure 5.9). This is founded upon a split rhythm in RR, similar to that of *Pdf> cyc*Δ^{103} with a dominant long oscillation, and suggesting a similar effect, that a partial though incomplete inhibition of one oscillator promotes desynchrony, though in this case the effect would have to be PDF-independent, and may exhibit downstream, at whatever abstract point of the circuit first exhibits a behavioural period. Limitation of CYC has been previously reported to mildly lengthen period, although the more salient effect of Δcyc^{103} expression may be a weakening of rhythmic power allowing the uncoupling of s-LN_vs from RR pacemaker neuron (Rutila et al., 1998).

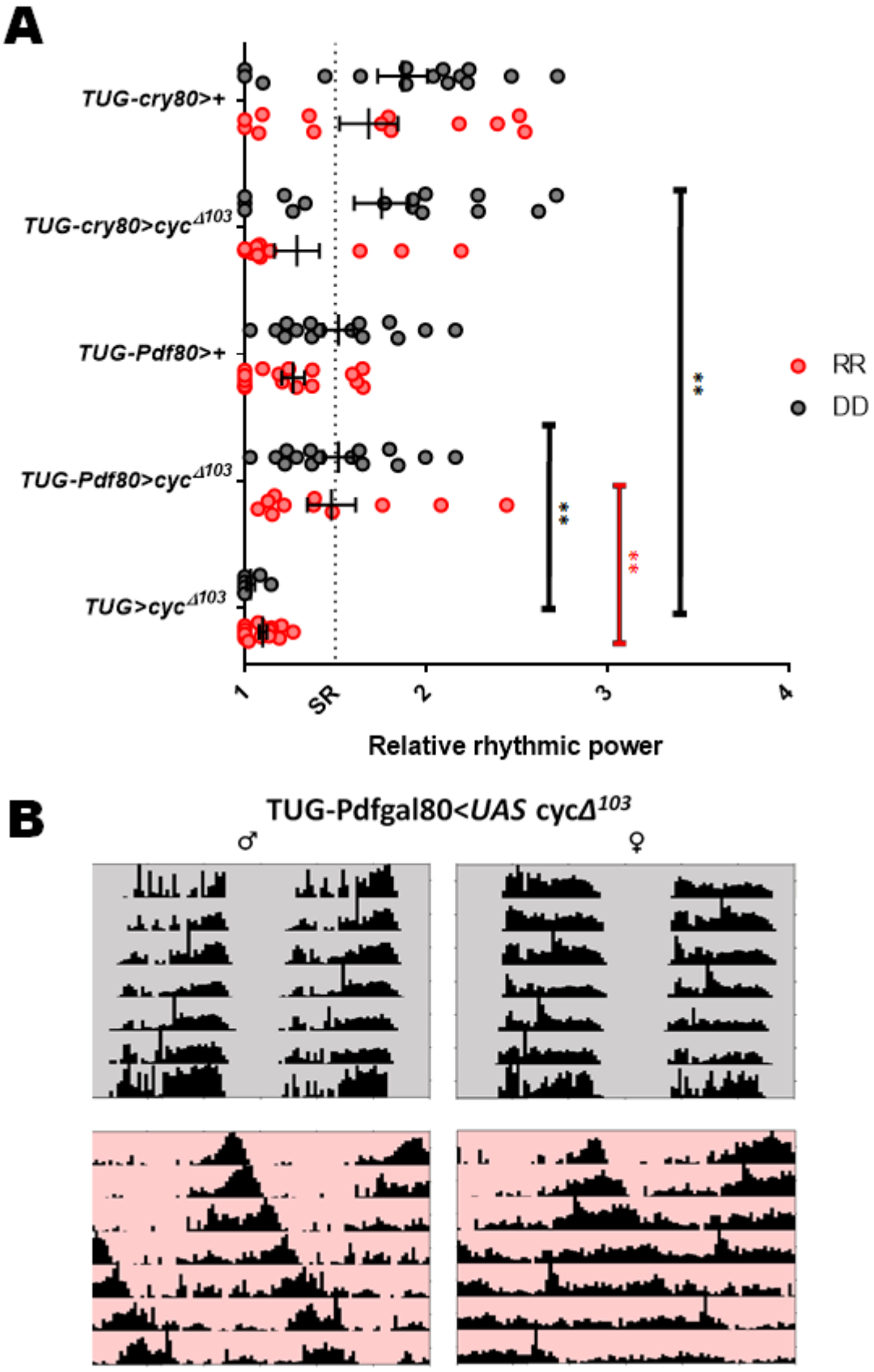

Figure 5.9 - Molecular oscillator function within CRY-ve clock cells in the dorsal brain can influence rhythms in constant red light. *Panel A shows behavioural rhythmicity of flies following ostensible removal of clock function everywhere bar the PDF or CRY cells*

through expression of a dominant-negative CYC transgene. RR control data courtesy of summer student Ana de costa. Panel B shows average actograms of TUG-Pdf80> Δcyc^{103}. Due to a generalized lower rhythmicity, females were excluded from the figure.

We are thus confident that a functional PDF cell oscillator is capable of dictating period information to the secondary CRY+ve pacemaker, dependent on PDF signalling. This CRY+ve pacemaker could involve a combination of three LN_ds, the 5th s-LN_v, a selection of two $DN1_a$s and several $DN1_p$s, very arguably with varying, redundant contributions (Yoshii et al., 2008, Zhang et al., 2010b).

cry13-gal4 expresses in two $DN1_a$s and two $DN1_p$s, but not all CRY+ve DNs, and we are confident that both marked and unmarked DN1s can be excluded from pacemaker function (Stoleru et al., 2004, Helfrich-Förster et al., 2007). In support of this, expression of Δ*cyc*^{103} with *Clk4.1M-gal4*, a driver specifically targeting the DN1ps show no noticeable alteration in period (Appendix Table 19 + 14), and RR rhythms appear strongly rhythmic. Thus, the CRY+ve subset of $DN1_p$s can be safely ruled out as required RR pacemakers, though they may have redundant function with other clock cells.

Whilst DN1as could contribute, (Murad et al., 2007) focusses on hypothetically CRY+ve $DN1_p$s, as a *cry*^{b} LL pacemaker, however their behavioural data shows resurgence of rhythms via PER or MORGUE expression with *TUG-Pdfgal80*, and a complete loss of rhythms with *TUG-crygal80*, which supports an LN_d/5th s-LN_v pacemaker championed by the Rouyer group (Picot et al., 2007, Cusumano et al., 2009), rather than the molecular data from which they draw their later conclusions. We are therefore confident in rejecting the DN1 cells as major contributors to the RR pacemaker.

(TUG-cry80)> cyc*Δ*^{103} does not significantly differ in rhythmic power to responderless controls in DD (P=0.577) or RR (P=0.072) in males, though significant differences occur in both conditions for females (Figure 5.9). The molecular oscillators of TIM+ve, CRY-ve cells have no prior established role in timekeeping for freerunning behaviour, so this result is not unexpected. (Murad et al., 2007) suggests, despite behavioural evidence implicating the CRY+ve PDF-ve clock cells in *cry*^{b} LL pacemaker function, that TIM+ve CRY-ve DN1s are the sole molecularly rhythmic clock cell subset in this state. This paper additionally measured aggregated molecular rhythms from all six LN_ds, which are molecularly distinct and can be divided into arrhythmic and rhythmic subsets in this

condition (Picot et al., 2007). Our dataset thus far supports a requirement for CRY+ve cell oscillators in RR, though in a male-specific fashion.

Δ*cyc*^{103} expression with the *VGlut-gal4* driver, which expresses in a subset of DN1$_a$s and DN3s (Hamasaka et al., 2007), resulted in strongly rhythmic males in RR, again ruling out these cells from contention in an RR pacemaker role (Appendix Figure 24)(Appendix Table 33).

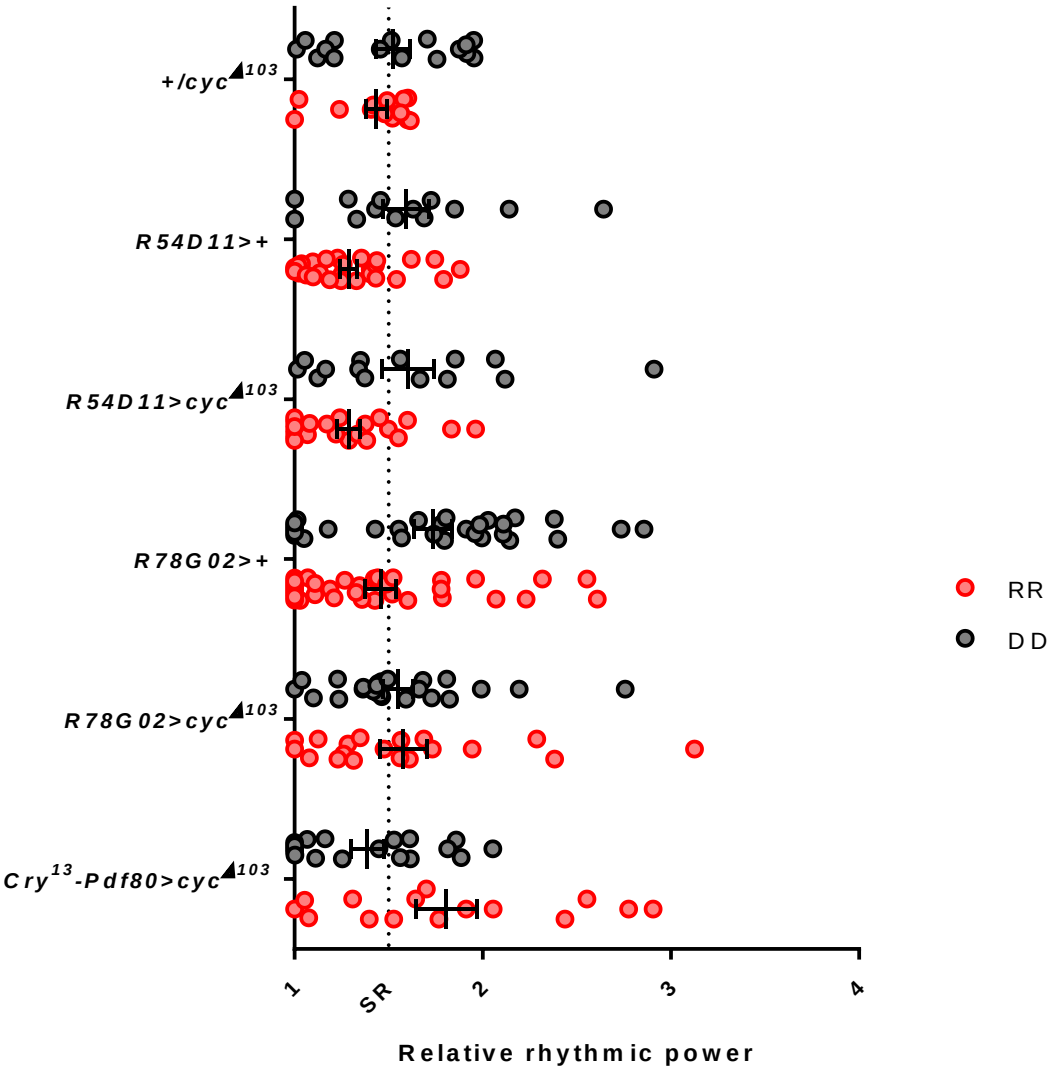

Figure 5.10 - Molecular oscillations are not required in CRY-expresssing evening cells for behavioural rhythms in constant red light*. behavioural data following dominant-negative CYC expression within the CRY+ve PDF-ve cells, through genotypes Cry-gal4-Pdf80> Δcyc*^{103}*, R54D11> Δcyc*^{103} *and R78G02> Δcyc*^{103}*. Significant differences do not emerge between RR and DD rhythmicity, nor do experimental rhythmicities signficiantly*

differ to that of responderless or driverless controls. Due to a generalized lower rhythmicity, females were excluded from the figure.

Cry-gal4-Pdf80> Δcyc^{103}, hypothetically stopping the oscillation in these cells alone, fails to cause a noticeable loss of rhythms in RR or DD (Figure 5.10). This argues that the presence of an oscillator within the M cells is capable of sustaining a rhythm in RR without using CRY+ve PDF-ve cells as an intermediary. In males, relative rhythmic power signficiantly differs between *Cry-gal4-Pdf80>* Δcyc^{103} and *Cry-gal4>* Δcyc^{103} in both RR (P<0.001***) and DD (P=0.003**), demonstrating that *Pdf-gal80* is specifically improving rhythms in both cases, and suggesting PDF-cell molecular oscillations are capable of contributing to behavioural rhythms despite limitation in other cells.

A recently produced flylight line, *GMR78G02*, has been developed by the Rubin lab which expresses, alongside numerous non-clock cells, in the 5^{th}-sLN_v and the three CRY+ve LN_ds, the minimum purported E cell pacemaker, allowing manipulation of the same cells as *mai179-gal4/ Pdf-gal80* on a simpler genotype (Schichtling et al, 2016)(Figure 4.20, Appendix Figure 32). Indeed, *mai179-gal4* and *dv-Pdf-gal4* failed to produce measurable effects in our hands, regardless of what was expressed, so *GMR78G02* was a necessary tool to continue investigation (data not shown). *R78G02>* $cyc\Delta^{103}$ males had broadly intact behavioural rhythms in both RR and DD, which did not significantly differ despite milder lower rhythmicity in RR, suggesting that an oscillator in the E cells is not required for RR behaviour (Figure 5.10). This does not mean that the E cells cannot control RR behaviour, and they may be sufficient, but they are not required if a functioning clock is present in the M cells.

Though we lost the recombined stock before we could finish experimentation, repeating this phenotype with a recombined Pdf^{01} background resulted in significantly lower RRP in RR males compared to single Pdf^{01} mutants, indicating that intact PDF signalling renders the *R78G02*-cell oscillators dispensible for RR control of rhythms, but required in the absence of PDF (Appendix Figure 19, Appendix Table 20). It is also important to note that whilst rhythm splitting is observable in several other lines with alterations in PDF oscillator strength, we cannot identify it in this manipulation, arguing perhaps that intact PDF cells, alongside PDF-mediated entrainment of the clock circuit can dominate control of rhythmic output.

In addition, a flylight line exists, GM*R54D11*, which targets an even smaller subsection of cells, approximating one CRY+ve LN_d and the 5^{th}-sLN_v, both of which are ITP+ve (Appendix Figure 31)(Yoshii et al., 2015). Of interest, this driver arises from a fairly barren section of genome with no association with ITP or clock cell function, potentially related to ITP lineage formation. *R54D11> cyc*Δ^{103} is relatively rhythmic in both RR and DD, though RR females are less rhythmic than controls, even though both are weakly rhythmic. We do not see a significant difference in rhythmicity in males, which as discussed appear to be the more robust gender for genetic dissection of the clock circuit, though females are significantly less rhythmic than controls (Figure 5.10).

A recent study suggests Ion Transport Peptide (ITP) neuropeptide function is limited, and only appears to play a role in the behavioural rhythms of flies with desynchronised, fairly weak clocks lacking PDF, a result which appears peripherally similar to the effect we see on the weakened behaviour of females in RR (Hermann-Luibl et al., 2014).

To study a potential increased role for ITP in the RR circuit, we knocked down *Pdf* and *Itp* simultaneously with *TUG* driver in the presence of *UAS-Dicer-2*. As expected, *Pdf* knockdown appears more severe in DD than RR (Figure 5.11)(Appendix Table 34). *Itp* knockdown alone has very limited effect on DD rhythms, and again only limited effect in RR, suggesting that in a state of shifted pacemaker function to the E cells, ITP is not a required neuropeptide for output. Like (Hermann-Luibl et al., 2014), we found co-knockdown of *Pdf* and *Itp* resulted in strong AR in DD, though in this case it was not significantly weaker than knockdown with *Pdf* RNAi alone (Appendix Table 35). We do not dispute the idea that *Itp* has a minor role in propagating weak freerunning rhythms in low PDF states, as (Hermann-Luibl et al., 2014) has suggested, as the significant difference they see discriminates between already very weak rhythms, and our failure to replicate this may simply be an issue of n number.

In RR, dual knockdown females appeared broadly arrhythmic, as is common in RR, but males possessed a majority rhythmic population, equivalent to responderless controls, and comparable, if not non-significantly more rhythmic than knockdown of PDF alone (Figure 5.11)(Appendix Table 34,35). Once again, we cannot see a recessive involvement in rhythmicity exposed by loss of PDF signalling, it certainly is not exacerbated in RR, and in conjunction with our previous data we have to conclude that ITP has no marked influence on behaviour in either RR or DD. Whether the ITP-cell oscillator, in analogy to

the *R78G02-gal4* oscillator can complement a loss of PDF signalling in RR remains to be determined (Appendix Figure 19).

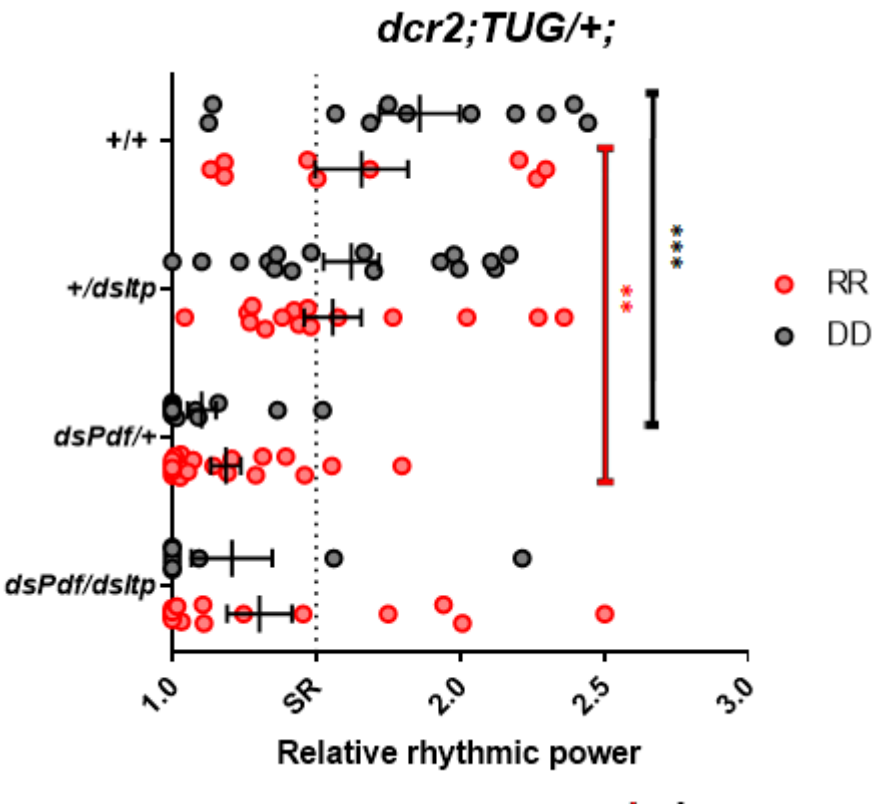

Figure 5.11 - ITP neuropeptide is not required for behavioural rhythms in the presence or absence of PDF signalling in constant darkness or constant red light. *Relative rhythmic power of dcr2; TUG/+; dsItp/dsPdf flies, and associated controls, run in RR and DD, to assess the effect of loss of combined neuropeptides. Statistics are in Appendix Table 35, demonstrating ITP knockdown does not significantly reduce RRP alone, or additively following PDF knockdown. Due to a generalized lower rhythmicity, females were excluded from the figure.*

An alternative argument for a minor increase in rhythmicity is one of expression strength, in which *UAS-dsPdf*, though heterozygous in all tested genotypes, is weakened by the provision of a secondary UAS-site in *UAS-dsItp*, which competes for a limited *Gal4* resource and limits PDF knockdown. As a control, we co-expressed *Pdf* RNAi with an RNAi validated by a previous lab member to have no effect on freerunning rhythmicity, *hairy*, which showed equivalent rhythmicity to the dual knockdown, significantly stronger than *dsPdf* heterozygotes, suggesting the increase in rhythmicity caused by ITP expression is not due to rescue by ITP (Appendix Figure 25).

The period lengths in this set of experiments in RR do not differ between genotypes with or without PDF, in contrast to earlier data which show period shortening following PDF loss (Appendix Table 25, 26). Potentially short period rhythmicity is limited by residual PDF function from an incomplete knockdown.

We screened six other flylight lines targeting subsets of clock cells in RR and DD, and identified non-significant effects (Appendix Tables 14, 15). Some of the putative targeted cells we suspect have no role in RR or DD pacemaker function (*R21G01-gal4* – *TRPA1*+ve DN2s and *R42G08-gal4* – PDP1-associated and expressed in dorsal clock cells). Others such as *R14F03-gal4* and *R43D05-gal4*, upstream of PER and CLK respectively, which should hit all clock-bearing cells, and *R19H11-gal4* which hits LN_ds and DN1s, generate no phenotype with $cyc\Delta^{103}$ expression in either RR or DD, and have been disregarded on the basis of weak driver strength (Kunst et al., 2014). The generation of phenotypes with well-established driver lines targeting these cells trumps the lacklustre phenotypes of uncharacterised drivers.

Red light rhythmicities summarily differ to DD freerunning rhythmicity, though both require molecular oscillators in CRY+ve cells, DD freerunning rhythms are more dependent upon an oscillator within PDF cells. Further characterisation of RR pacemaker function has been elusive, and suggests that no single CRY+ve subset is required for behavioural rhythms, instead multiple subsets control rhythms, and stress within one results in period desynchrony in another.

5.4 - Spatial reintroduction of PER onto per^{01} maps oscillator requirement in constant red light to the Evening cells.

In addition to the approach of removing oscillator function, other group members attempted to reintroduce *UAS-per16* to certain cell subsets on a per^{01} background, to identify if oscillations in the E cell pacemaker were solely capable of driving rhythms (Appendix Figure 30). Restoration of PER in the PDF cells led to rhythmic behaviour in DD and, as suspected, arrhythmic behaviour in RR, suggesting this freerunning oscillator, whilst capable of driving rhythms alone, cannot sustain behaviour in RR. It is notable that PDF-specific PER is sufficient for behavioural rhythms in DD, as

Pdf>specific CYC is not (Chapter 4)(Peng et al., 2003), meaning that though PDF-ve cells do not require oscillations for behaviour, they require CYC in the establishment of rhythms, presumably, though not necessarily, a developmental role.

per^{01}*; Cry13>per16* rescues rhythms in RR and DD, whilst *per*^{01}*; R78G02>per16* and *per*^{01}*; R54D11>per16* both appeared rhythmic in RR, supporting our notion that a CRY+ve PDF-ve clock cell group had pacemaker function specifically in RR. *per*^{01}*; R78G02>per16* bizarrely showed a weak rhythm in DD as well as RR (Appendix Figure 30). Indeed this dataset is significantly neater than mapping with Δ*cyc*^{103}, and whilst I suggest that the E cell clocks are not required for RR behavioural rhythms, it appears they are sufficient. It is also suggested that PDF-cell specific PER rescue cannot rescue RR rhythms, which suggests that the weakened and split RR rhythms of *TUG-Pdf80>* Δ*cyc*^{103} are likely due to a failure to fully remove oscillations in those cells. *per*^{01}*; R78G02*-specific rescue of CYC fails to remotely restore behavioural rhythms in RR, which may be due to lack of specification of *R78G02-gal4* clock neurons in the *cyc*^{01} background (Figure 4.20).

I repeated *per*^{01}*; R78G02>per16* and *per*^{01}*; Cry-Pdf80>per16* to solidify these results (Figure 5.12)(Appendix Table 23). To my surprise the weak DD rhythm found by other lab members was exhibited in *per*^{01}*; R78G02>per16* and significantly differed to driverless controls (DD P=0.009** RR P=0.037*) but not RR, either suggesting, as we cannot see *R78G02*-driven GFP in clock cells (Figure 4.20), that canonical ideas of a PDF cell oscillator for freerunning behavioural rhythms is not neccesarily true (Figure 5.12).

No other group has published this manipulation, though the cacophony of experiments rescuing rhythms exclusively within the E cells without DD rescue should enforce caution in our interpretation. Nonetheless, *Δcyc*^{103} expression with this driver has little effect, from which we have suggested a redundancy in PDF cell and E cell pacemaker function. Thus while, the *R78G02-gal4*-marked cells harbour oscillators sufficient for pacemaking free-running behaviour in DD and RR, they are not strictly required for this in either condition.

per^{01}*; Cry-Pdf80>per16* appears to improve rhythms in RR, though the effectiveness of

the *Pdf-gal80* is debateable, as weak rhythms occur through DD. However, rhythms are significantly stronger in RR than DD (P<0.001***), supporting the idea of a CRY+ve PDF-ve cell subset control of behaviour, which compliments the PER rescue dataset nicely (Appendix Table 23, 24). Similtaneously, *per^{01}; Cry-Pdf80>per16* is significantly stronger than driverless controls in RR (P<0.001 ***), but not in DD (P=0.116), demonstrating a red-light specificity to this phenotype. Rescue with the *cry-gal4* driver without *Pdfgal80* results in higher mean RRP in DD and RR, though differences are not significant (Appendix Table 24). That DD rhythms are not significantly improved by loss of *Pdfgal80* is disheartening, though these appear majority, and are similar to results of *per^{01}; Cry>per16* obtained by another lab member (RRP for RR = 1.70±0.09, DD =1.29±0.07, Appendix Figure 30, Ramirez thesis 2017). We additionally show a general failure of the partially CRY+ve DN1ps to rescue RR rhythms with *Clk4.1M-gal4*, though a very weak, residual rhythm is achievable in DD (Figure 5.12).

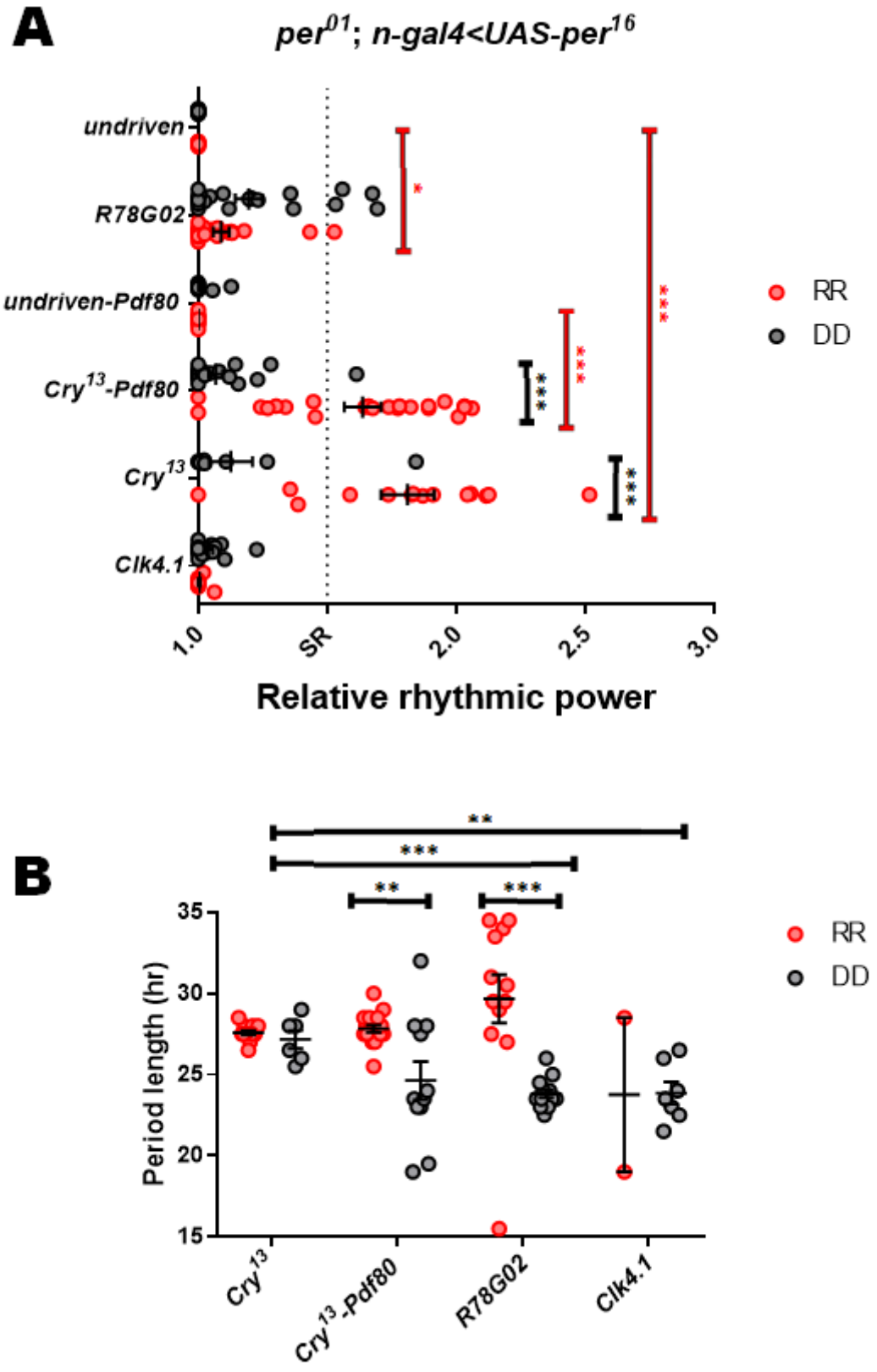

Figure 5.12 - PER expression solely within evening cells is sufficient for behavioural rhythmicity in constant red light. *Panel A shows behavioural rhythmic strength*

following PER rescue with the crygal4 13, crygal4 13-Pdfgal80 or R78G02-gal4 driver on a per^{01} background in RR or DD. Significant differences emerge between RRP for RR and DD when PER is expressed in evening cells, which also significantly differs to undriven controls in RR. Panel B shows period length under these conditions, in which significant differences emerge between period in RR and DD when PER is rescued only in evening cells. Expression of PER in morning and evening cells significantly increases period length in DD compared to PER expression in evening cells alone.

Period changes are additionally observable following PER introduction (Figure 5.12b)(Appendix Table 23). PER overexpression can slow the oscillator, validating the divergent pacemakers of DD and RR (Goda et al., 2011, Beckwith et al., 2013). Expression in both M and E cells with *cry-gal4-13* results in increased period in both RR and DD, as would be expected by PER overexpression. Likewise, expression of PER specifically within E-cells with *Cry-Pdf80* or *R78G02* results in an increased period in RR (Figure 5.12b). However, in DD, the period is normal, approximating 24hrs. This may be an artifact of increased period variability due to the lower rhythmic strength, or potentially the long period of a pacemaker cell can manifest itself in behaviour, whilst the residual long-period rhythmicity conferred by E cells in DD is mitigated at the circuit level as period length becomes a transient network property, despite a lack of competing oscillators.

Nevertheless, our data convincingly coalesces around a dispensability of oscillatory function or connectivity of the M cell cluster for RR rhythms alongside sufficiency of an E-cell oscillator but not an M cell oscillator for RR rhythms, alongside a novel weak control of freerunning rhythms by the E cells. The resolution with which we dissect clock cell circuitry is not at the single-cell level, so simple manipulations may have simultaneous contradictory effects on the circuit which may go underappreciated with behavioural readouts.

cyc$^{\Delta 103}$ and PER reintroduction do not merely test required and sufficient oscillators for RR rhythms alone, and though both should result in arrhythmia, they leave the oscillator stalled in different arrest states, one of low CLK/CYC and one of high CLK/CYC, with consequently divergent gene expression profiles, potentially impinging on neuronal function (Claridge-Chang et al., 2001). Though investigated and discussed below (Figures 5.23 & 5.25), a complimentary approach using conditional CYC reintroduction,

which measures oscillator sufficiency rather than requirement in a low CLK/CYC state, is confounded by likely developmental defects, though this dataset is useful in mapping oscillatory requirements in RR.

We have previously defined a requirement for the l-LN_vs in RR rhythmicity, and this experiment makes it clear that not only are l-LN_v molecular oscillations insufficient for pacemaker function, but neither are they required in conjunction with an E cell pacemaker subset, suggesting the l-LN_v role in RR occurs at the circuit level, likely in altering circuit properties that allow the E cells to control rhythms.

5.5 - Behavioural rhythms in constant red light are dependent upon compound eye signalling in the absence of PDF signalling

Several photoreceptive organs possess the necessary photoreceptors to respond to red light, the Hofbauer-Buchner (H-B) eyelets which interact directly with the s-LN_vs, the compound eye and the ocelli. s-LN_v-cell ablated flies behave differently in RR, but not DD, but not l-LN_v-cell ablated flies, suggesting photic information can reach the clock circuit via the extensive arborisation of the l-LN_vs into the optic medulla (Figure 5.5). Feasibly, photic information via the H-B eyelet can also induce a hierarchical shift, though we lacked an experiment to adequately test this.

We studied *norpA*^{7} mutants, lacking the phospholipase C visual transduction pathway, to identify the relevance of this system to RR-mediated hierarchical shifts. We demonstrate a requirement for this pathway in phototransduction, as *norpA*^{7}*::Pdf*^{01} double mutants are relatively arrhythmic upon shift to constant red light in addition to freerunning conditions (Figure 5.14). In addition, we looked at *eya*^{2}*;Pdf*^{01} mutants, in which signalling from the H-B eyelet and ocelli remains intact, whilst the compound eye does not generate (Bonini et al., 1993). RR rhythmicity does not significantly differ to DD rhythms in these flies, remaining majority arrhythmic, demonstrating that hierarchy-shifting photic information must stem from the compound eye (Figure 5.14)(Appendix Table 37, 38). The severity of the *eya*^{2}*;Pdf*^{01} phenotype is slightly, though not significantly greater compared to that of *norpA*^{7}*::Pdf*^{01}, suggesting that whilst the compound eye is clearly required, *norpA*-independent input may be capable of rescuing this network shift to a minor extent. For RR males, both *norpA*^{7}*::Pdf*^{01} (P=0.003**) and *eya*^{2}*;Pdf*^{01} (P<0.001 ***) significantly differed to the more rhythmic *Pdf*^{01}, whilst significant differences did not emerge in

females or in DD (Appendix Table 38).

Similarly, E cell specific rescue of the oscillator in *cry*^{b} flies in constant light has been shown to be blocked by addition of GMR-hid, ablating the compound eyes, likely via a shared mechanism (Cusumano et al., 2009).

Of note, students under my supervision studied *disco*^{1} mutants. These mutants have previously been extensively characterised to display defects in both s-LN$_v$ presence and in visual system connectivity (Steller et al., 1987, Hardie, 1989, Helfrich-Förster, 1997). These were uniformly AR in DD, and remained majority AR in RR, with a minor, weakly rhythmic contingent (Figure 5.13)(Appendix Table 37). This result can be interpreted in various ways, though it may be most parsimonious to say that as *disco*^{1} mutants lack s-LN$_v$s, a mild increase in RR rhythms strengthens our argument of a dispensable s-LN$_v$ pacemaker in RR, and variable defects in the visual system will limit, and in some cases completely block light-induced network changes facilitating RR rhythmicity. This difference is not significant, unfortunately, and we cannot neatly say that loss of the s-LN$_v$s is fully rescuable in this mutant, though the conditional *Pdf>hid* experiment above neatly accounts for this (Figure 5.5). In future work, it might be interesting to dissect and stain RR rhythmic and arrhythmic *disco*^{1} to assess changes in connectivity or number of l-LN$_v$s and LN$_d$s.

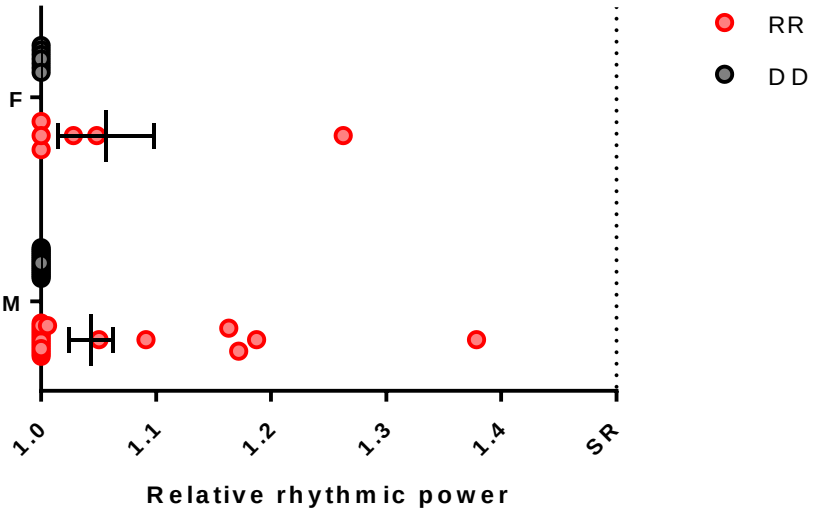

Figure 5.13 - disco*^{1} *mutants, lacking small lateral ventral neurons and visual connectivity, are broadly behaviourally arrhythmic in constant darkness and constant

***red light**. Data provided by Ana de Costa, Rhianna Davies and Leighton Osborne. Behavioural dataset for disco[1] mutants in RR and DD. Though both are characterised by low rhythmicity, rhythms are noticeably, though not significantly, stronger in RR than DD.*

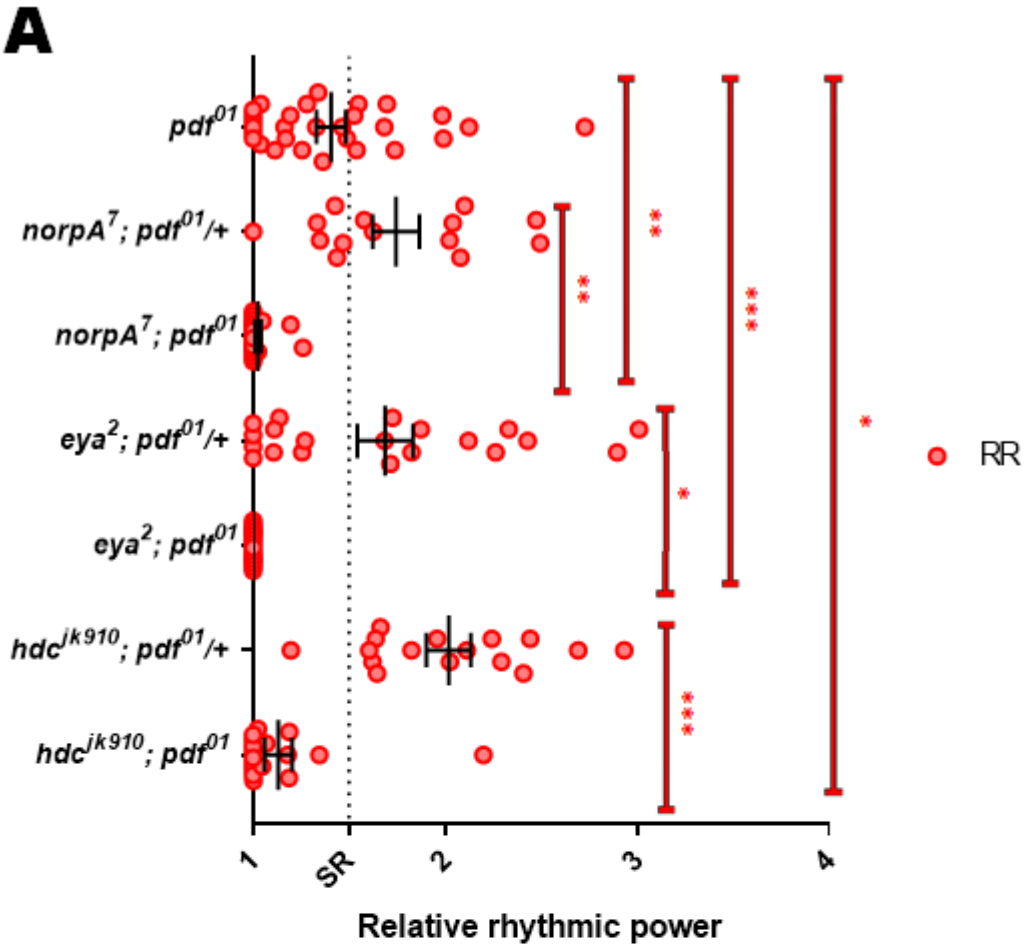
A
pdf01
norpA7; pdf01/+
norpA7; pdf01
eya2; pdf01/+
eya2; pdf01
hdcjk910; pdf01/+
hdcjk910; pdf01
RR
1
SR
2
3
4
Relative rhythmic power

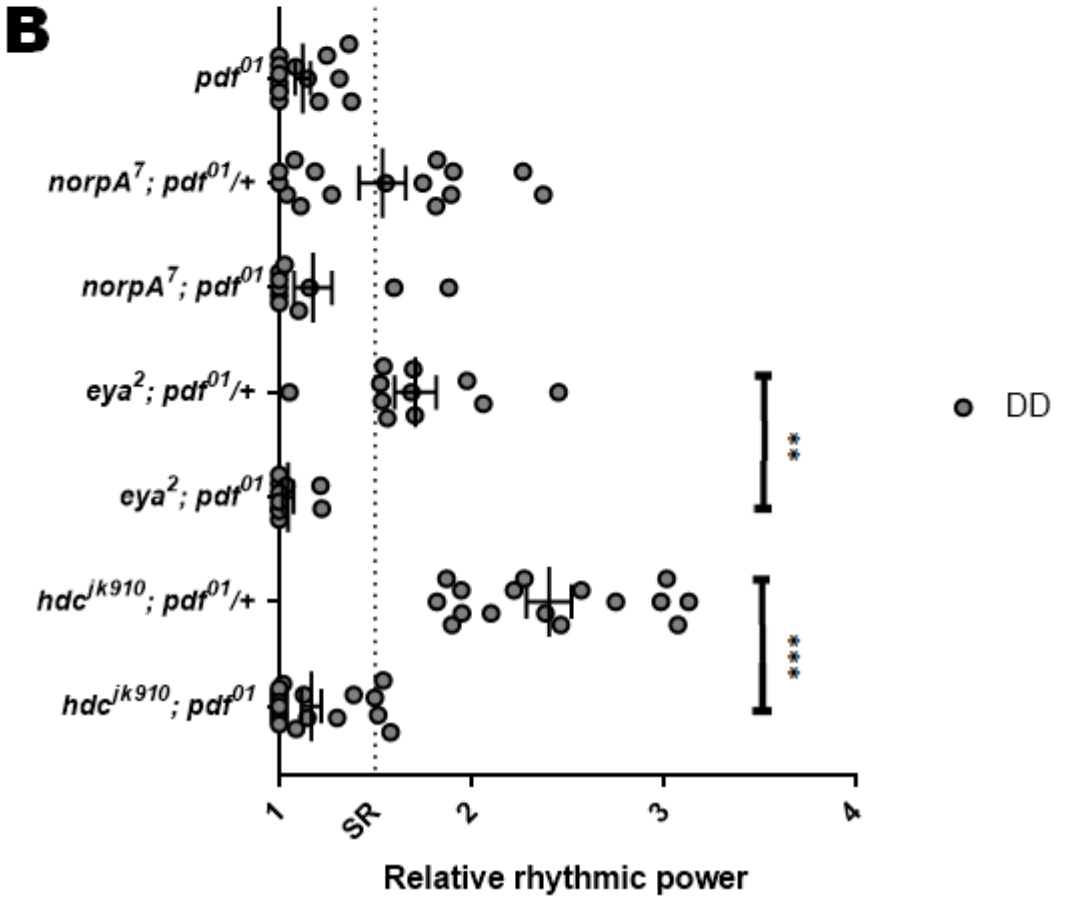
B
pdf01
norpA7; pdf01/+
norpA7; pdf01
eya2; pdf01/+
eya2; pdf01
hdcjk910; pdf01/+
hdcjk910; pdf01
DD
1
SR
2
3
4
Relative rhythmic power

Figure 5.14 - Loss of both visual system function and PDF signalling completely removes behavioural rhythmicity in constant red light. *Behavioural dataset for various visual system mutants, with or without pdf signalling, via Pdf^{01}. Full statistics are detailed in Appendix Table 38. Panel A shows RRP of flies run in RR, whilst Panel B shows RRP of flies run in DD. Addition of visual system mutation significantly reduces pdf^{01} rhythmicity in RR, but in no cases for DD, which differ only between pdf^{01} homozygotes and heterozygotes. Due to a generalized lower rhythmicity, females were excluded from the figure.*

Previous data has shown Pdf^{01} flies possess a short period in RR. We do not see this short period materialise in the weakly rhythmic contingent of the visual system and Pdf^{01} double mutant flies, though this is likely due in part to the variability induced by low rhythmic power (Appendix Table 25). Potentially visual-system-mediated changes, rather than a loss of PDF-signalling, are responsible for period shortening, potentially occurring within the molecular oscillator of E-cells.

The major phototransductive neurotransmitter is histamine, so we studied mutants in histaminergic signalling to identify if this pathway was required (Hardie, 1989). $Hdc^{jk910};Pdf^{01}$ flies, incorporating hypomorphs of histidine decarboxylase, required for correct histamine synthesis, do not significantly differ in rhythmicity between RR and DD, suggesting as expected that histamine signalling is required for mediating this network shift (Figure 5.14). In both RR and DD, flies appeared majority rhythmic, higher than expected for a Pdf^{01} mutant, however LD profiles confirm a Pdf^{01}-like advanced evening activity, suggesting this mutant indeed lacks PDF, and flies are significantly less rhythmic than $Hdc^{jk910};Pdf^{01}/+$ in both genders and conditions (Appendix Figure 26). $Hdc^{jk910};Pdf^{01}$ males in RR are less rhythmic than Pdf^{01} (P=0.021*), supporting an additive role for histamine in this process.

Histaminergic signalling is a major part of visual transduction in the compound eye, and though only a hypomorph, Hdc^{jk910} appear functionally blind in behavioural assays (Chaturvedi et al., 2016) and histamine has been shown to influence the clock circuit through the PDF cells (Oh et al., 2013). Notably the behavioural loss of rhythmicity is not as severe as eya^{2} and $norpA^{7}$ mutants, maybe due to residual function of the hypomorph, or potentially other signalling pathways can have minor effects.

In light of this phenotype, we sought other histamine mutants in the hopes of a more definitive answer. We hypothesised histamine signalling, stemming from the histamine-receptive l-LN$_v$s (Hong et al., 2006) rather than optic histamine could improve rhythmicity. Interestingly histamine has been found to be repressive to l-LN$_v$s, suggesting that its restoration of rhythmicity might be associated with provision of periodic suppression of l-LN$_v$ activity (Schichtling et al., 2016). *Drosophila* possess two histamine receptors, HISCL1 (Zheng et al., 2002) and ORT (Gengs et al., 2002), of which ORT is known as the only receptor postsynaptic to photoreceptors, so is an expected downstream candidate, whilst HISCL1 is the sole clock-cell +ve histamine receptor, from which a phenotype would be noteworthy (Hong et al., 2006, Oh et al., 2013). Whilst RR rhythms may be slightly weakened by *hisCl1* RNAi in clock cells, this loss is not significant, and we must therefore conclude that histamine signalling from the compound eyes does not directly interact with the clock circuit (Figure 5.15).

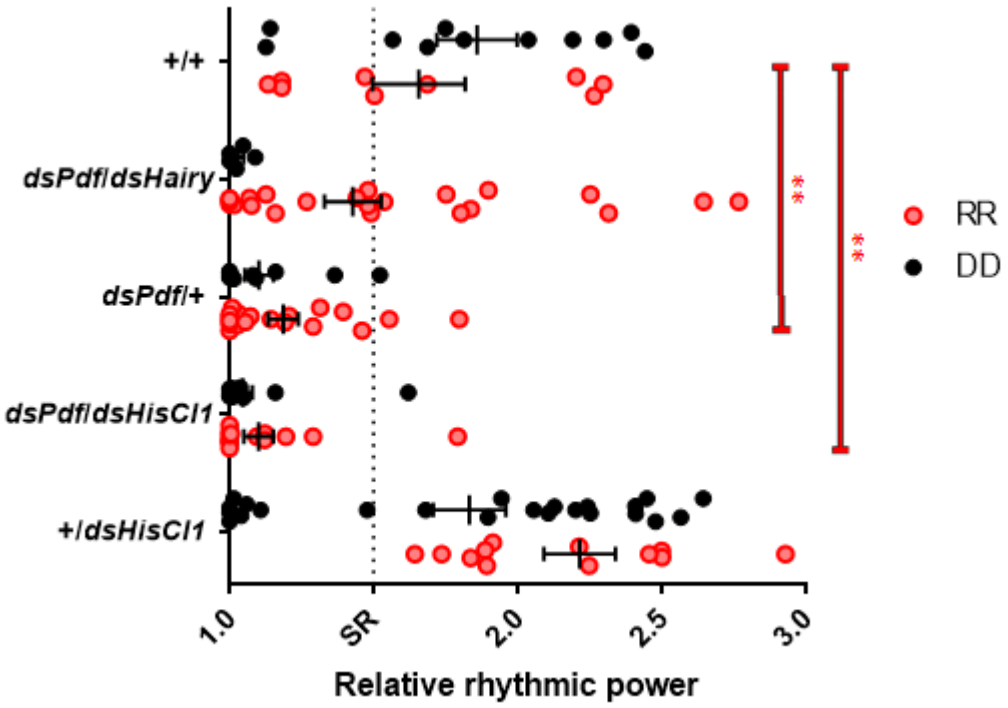

Figure 5.15 - Histamine receptor HisCl1 is not required within clock cells for behavioural rhythms in constant red light in the absence of PDF signalling. *Behavioural rhythmicities of flies expressing shRNAs for PDF, hisCl1 or hairy within the clock circuit with dcr; TUG/+; RNAi/RNAi. Significant differences do not emerge between RRP of dsPdf knockdown alone compared to dual knockdown of dsPdf and dsHisCl1 or dsHairy in RR or DD. Due to a generalized lower rhythmicity, females were excluded from the figure.*

We have thus defined inputs for red-light rhythmicity, in conjunction with conditional ablation experiments suggesting a requirement of compound eye signalling and l-LN_vs to facilitate a network change bolstering E-cell control of rhythms. Notably, hyperexcitation of both PDF cells with *TrpA1* does not disrupt RR rhythms, suggesting l-LN_v excitability can be misregulated (Figure 5.2). The effect of l-LN_v excitation on a Pdf^{01} background in freerunning conditions has not been tested, but would be interesting as an assay of a more generalised output that shifts pacemaker states.

Light-induced hierarchical shifts reliant on histamine may be mediated by signalling through ort to an intermediary cell cluster, which then interacts with the clock circuit, a hypothesis which will be addressed in future work. We conclude l-LN_vs have a role in inducing the red-light hierarchical shift, and though they have not been shown to directly receive histaminergic-mediated photic information, they may still be the sole clock cells capable of integrating information from the compound eye and initiating network changes.

5.6 - Interrogation of red light clock cell hierarchy reveals new insights into circuit layout and plasticity

Inhibition of a molecular oscillator within a cell prevents the emanation of intrinsic rhythmic information from its oscillator, yet a cell with a disrupted oscillator may still impart rhythmic information through conveyance of rhythm derived from interactions with its neighbours within a circuit. Indeed, it is likely that red light rhythms in wt flies, whilst maintaining behaviour corresponding to the period of the s-LN_v oscillator, may be dependent upon the presence of a phase-matched E cell oscillator. We suggest RR behaviour requires an E-cell derived rhythm in neuronal signalling that can be bolstered by the E cell molecular oscillator, but not solely through rhythmic information conveyed from other cells.

Locating RR pacemaker function is, given the literature in support of our conclusions, a fairly unambitious endeavour, yet the flow of information, and requirement for signalling and connections between other clock cell subsets in RR is unknown. The inconvenience of integrating *cry* mutants into already complex genotypes has limited attempts to study

this network in LL, and the transience of the state supporting E-driven activity in LD cycles prevents genetic interrogation of the network in an evening-specific context. We thus chose to hyperexcite or silence clock cell subsets with expression of *UAS-NaChBac*, *UAS-TrpA1*, *UAS-Kir2.1* or *UAS-TeTxLC* to identify differences in the robustness of behavioural rhythms between RR and DD, and from this infer alterations in the signals and interactions of components of the clock cell network in generating rhythmic behaviour.

An example of an established interaction within the clock cell network, a recent study shows excitation of *TUG-crygal80* cells with *NaChBac* results in behavioural arrhythmia within DD (Dissel et al., 2014). Likely related, (Guo et al., 2016) suggests partially CRY-ve DN1s repress M cell activity promotion to create a daytime siesta. *TUG-crygal80* hyperexcitation may have a direct repressive effect on s-LN_vs, or an indirect effect disrupting output signals, though the consequence of this manipulation in RR interested us regardless of mechanism.

We repeat this phenotype, of a general arrhythmia in DD, significantly different to responderless controls ($P<0.001$***) but then show a residual behavioural rhythm is rescued by transferral to RR, which does not differ to responderless controls ($P=0.117$)(Figure 5.16). In this manipulation. PDF signalling is presumably intact, which E cells are responsive to, inviting the interpretation that, if TUG+ve CRY-ve cell hyperexcitation directly represses s-LN_vs, the consequences of a network-mediated repression of output information does not dominate to repress E-cell activity. Neither does this repression act to silence the l-LN_vs, which have an unknown RR function.

Suggested output pathways use CRY+ve and potentially CRY-ve dorsal clock cells as an intermediary, and feasibly excitation of these cells could disrupt output rhythms. Another possibility is that E cell output pathways differ to s-LN_vs, and are thus independent of TUG+ve CRY-ve cells in output.

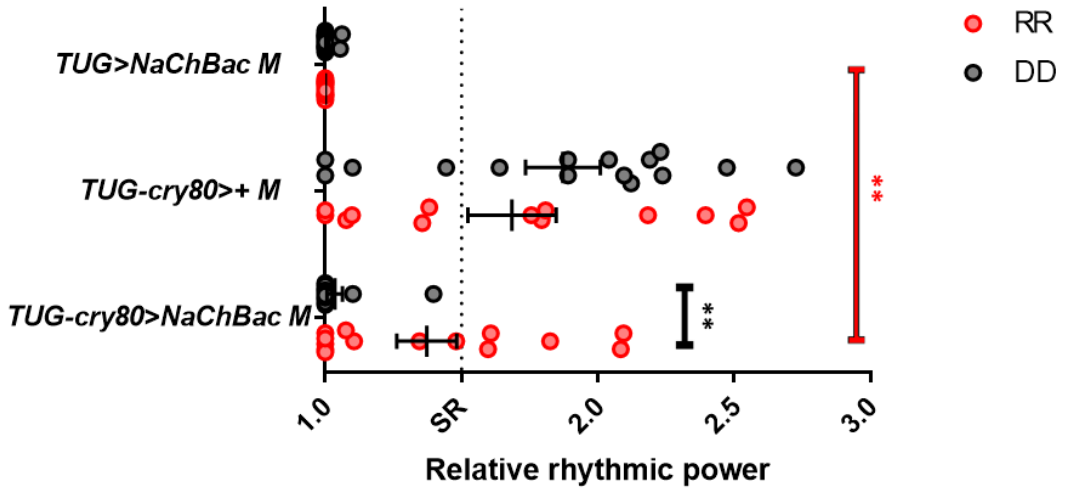

Figure 5.16 - Hyperexcitation of CRY-negative clock neurons represses rhythmic behaviour in constant darkness, but not in constant red light. *Behavioural rhythmicity data for hyperexcitation of TIM+ve CRY-ve clock cells with NaChBac. Significant differences emerge between RRP for experimental flies in RR and DD, and differences emerge compared to whole-clock-circuit excitation in RR, but not in DD. Due to a generalized lower rhythmicity, females were excluded from the figure. Full statistics are in Appendix Table 27.*

We wanted to study the effect of manipulating E cell excitation levels on behavioural rhythmicity in RR or DD, as this is a question that has not been directly asked in the literature.

It is known that increases in electrical activity of the s-LN$_v$ cells with *NaChBac*, but not *TrpA1* is able to alter normal rhythmicity, but does not necessarily override rhythms, so in light of secondary pacemaker roles in *cry*+ve cells, we were interested if excitation of these cells could similarly influence behaviour (Nitabach et al., 2006). *NaChBac* or *TrpA1*-expression with *R54D11* has no noteworthy effect on rhythms (Figure 5.17a)(Appendix Table 26). One could hypothesise that whilst electrical activity can propagate pacemaker rhythms into circuit, through rhythmically stimulating vesicle release, constitutive increased firing rate from evening cells is not sufficient to disrupt information transfer from the s-LN$_v$s. Thus, limitation of ITP cell firing is not a component of network generation of rhythmic behaviour.

Increasing E cell electrical activity with *R78G02*-driven expression of *NaChBac* results

in lower RR than DD rhythmicity (P<0.001***), though this does not differ to undriven responderless controls (P=0.623)(Figure 5.17b, Appendix Table 26). Excitation of these cells with *TrpA1* however results in a very significant loss of rhythmicity in 29°C RR compared to DD (♂ P=0.002**, ♀ P=0.001 **) and 23°C (♂ P=0.011*), suggestive of a role of firing within these clock cells on behaviour (Figure 5.17b, Appendix Table 26). Supplementing this data set with an undriven control 29ºC may further strengthen this interpretation

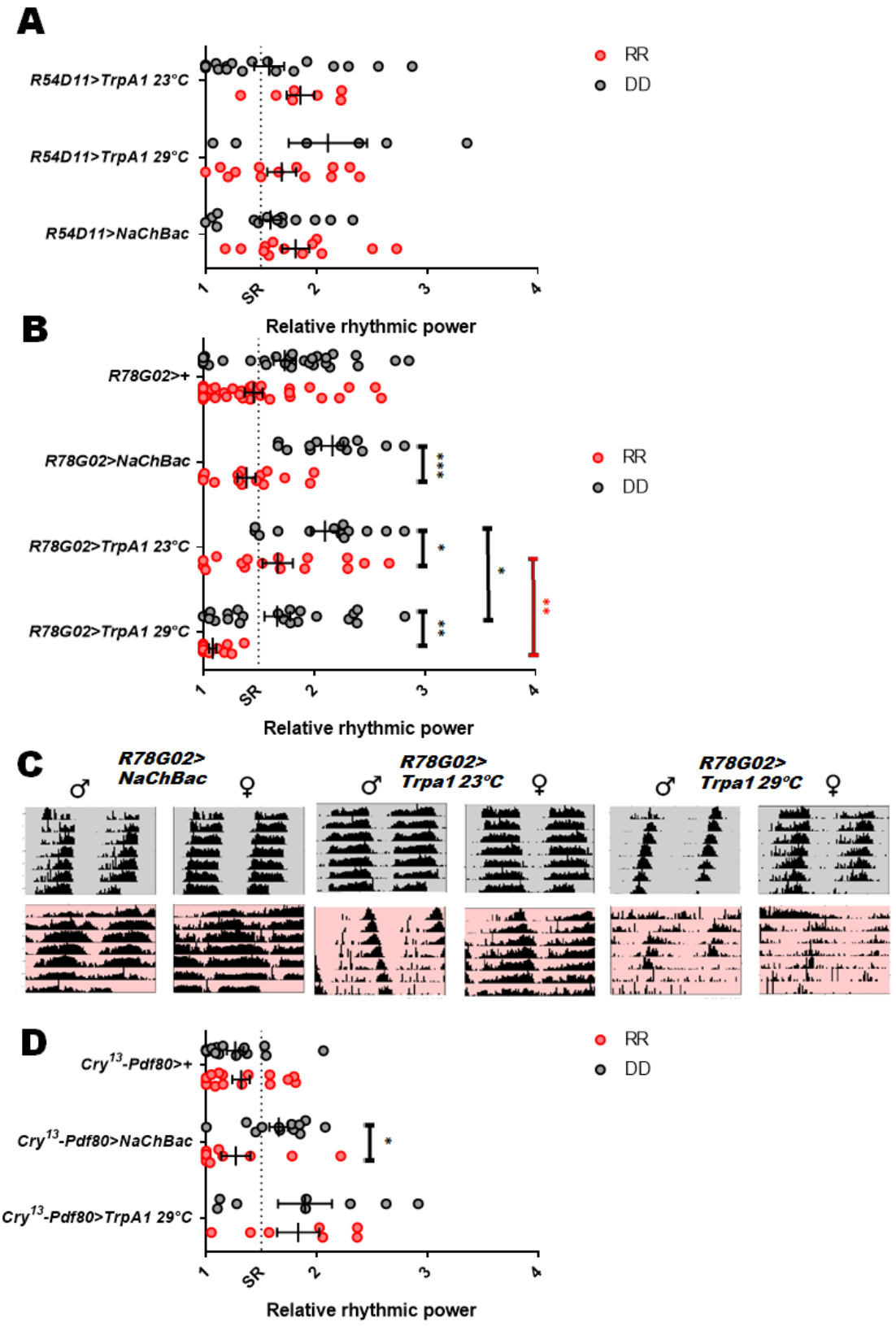

Figure 5.17 - Hyperexcitation of CRY-expressing evening cells results in decreased behavioural rhythmicity in constant red light relative to constant darkness. *Panel A shows behavioural rhythmicity data demonstrating ITP cell excitation with TrpA1 or NaChBac does not induce differences in rhythmic power between RR and DD. Panel B*

shows behavioural rhythmicity data and Panel C shows average actograms for lines expressing TrpA1 within the E cells, inactive at 23°C or active at 29°C. Panel D shows behavioural rhythmicity data for Pdf-gal80/UAS-(TrpA1 or NaChBac); crygal4^{13}/+. Due to a generalized lower rhythmicity, females were excluded from the figure.

This data is interesting, as, within the PDF cells, *NaChBac* affects rhythms whilst TRPA1 does not, whilst we see TRPA1 appears more severe, although effects of high temperature could also contribute (Nitabach et al., 2006)(Figure 5.4). It is worth noting that potentially other cells are excited in this manipulation, and in the absence of convincing results in the more restrictive ITP cell driver, we could only very tentatively speculate that this phenotype is robust. *TUG>NaChBac* and *Pdf>NaChBac* are both arrhythmic in DD and RR, reflective of a potential dominant effect of PDF cell signalling on the red-light circuit, and from this we cannot decipher if hyperexcitation of other clock cells impacts rhythms.

Though I did not have time, it would be interesting to see if behavioural phenotypes differed in RR on a *Pdf^{01}* background, where it could be suggested E cell firing may have a greater influence on rhythms, as loss of E cell oscillators has an effect on RR rhythms only on a *Pdf^{01}* background. Simultaneous loss of oscillator and hyperexcitation in the E cells may have more potent combinatorial effects in DD and RR.

Variable rhythm splitting emerges through *Pdf>NaChBac* in DD (Nitabach et al., 2006, Sheeba et al., 2008b). In our hands, the DD behavioural phenotype of this line approaches arrhythmia while splitting is discernible in RR (Figures 5.3, 5.17c). However, *R78G02>NaChBac* or *R78G02>TrpA1* at 29°C do not cause such dissociation of rhythmic components in RR in spite of the strong effect of the latter manipulation on rhythmicity. The implication is that whilst PDF cells are upstream of slave-clocks that can manifest in behaviour, the E cells are not, thus limiting splitting.

The effect of hyperexciting CRY+ve PDF-ve clock cells has not been published in the past in relation to behavioural rhythms, so we attempted expressing both *NaChBac* and *TrpA1* in these cells, which fails to manifest a phenotype (Figure 5.17d). It is therefore difficult to conclude the arrhythmia we see following *R78G02*-cell excitation is the result of clock cell excitation, but potentially a misregulation of other behaviours that overrides clock control of activity. Whether of not combination of *R78G02>TrpA1* with *cry-gal80*

would ameliorate the phenotype might provide clarity to our dataset, and is a potential future experiment. We thus have a conflicting dataset, which largely suggest E cell excitation fails to disrupt red light behavioural rhythms.

Conversely, we attempted to silence the E cells, to see if this had any deleterious effect on RR behavioural rhythms. *R78G02>Kir2.1* and *hid* were lethal in nearly all cases, likely reflective of the many non-clock cells encompassed. *R54D11>Kir2.1* and hid were also lethal, limiting the depth of our interrogation.

Attempting to limit vesicle release at E cell synapses, we expressed tetanus toxin with E-cell driver lines. For males, *R78G02>TeTxLC* is less rhythmic than negative controls in RR ($P<0.001$***) demonstrating that E cell signalling is integral to RR rhythms (Figure 5.18)(Appendix Table 26). However, overall DD rhythmicity is still significantly decreased in males ($P=0.003$** *TeTxLC* vs *TeTxLC* (NEG)), suggesting that E cell firing has an effect on bolstering latent freerunning rhythms in DD as well (Appendix Table 26).

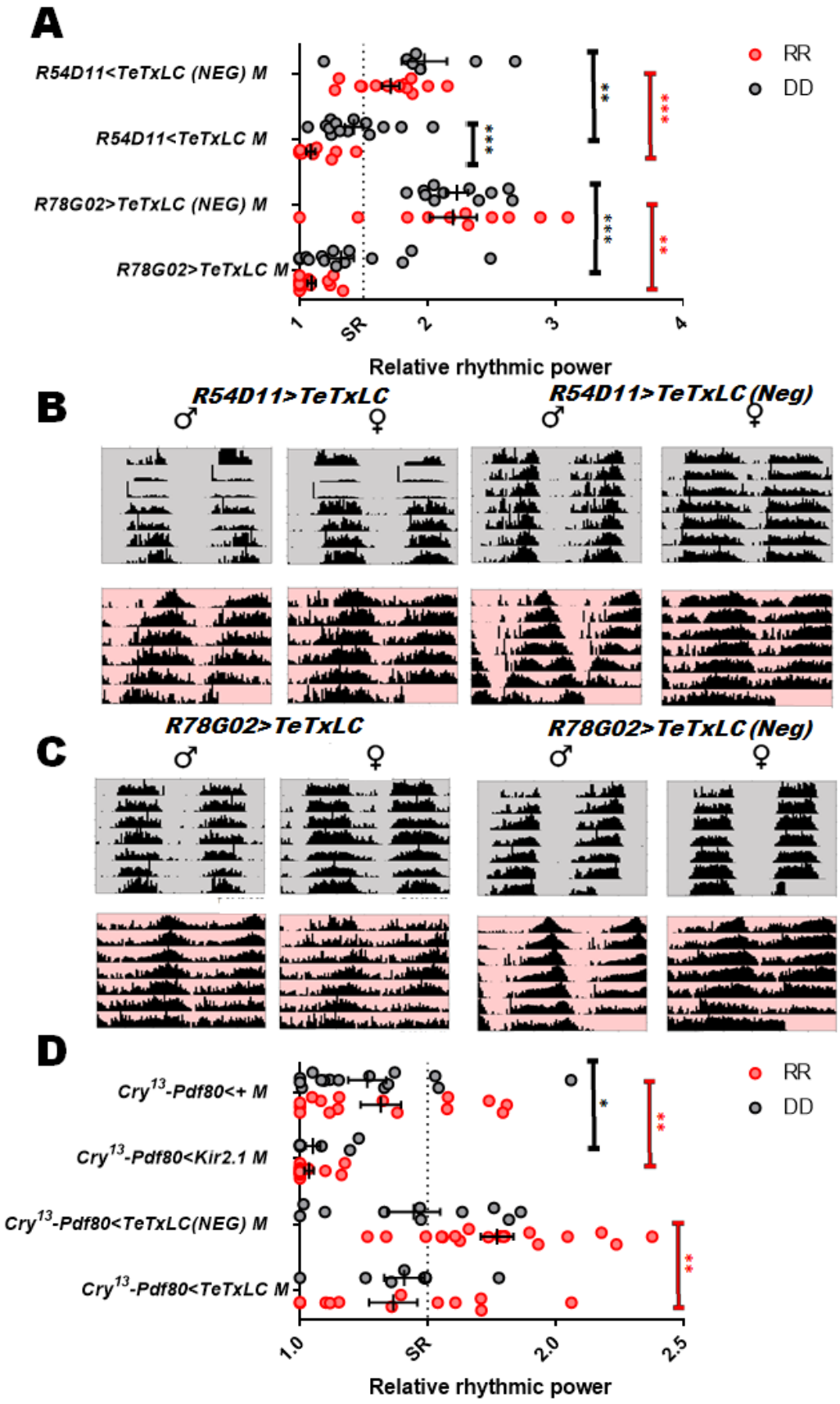

Figure 5.18 - Reduction of signalling from CRY-expressing evening cells results in decreased behavioural rhythmicity in constant red light. *Panel A shows behavioural rhythmicity data for flies with disrupted synaptic function within E cells, in either RR or*

DD. Panel B and C show average actograms for flies with silenced ITP cells, of genotype UAS-TeTxLC/+; R54D11-gal4/+ or UAS-TeTxLC/+; R78G02-gal4/+, in either RR or DD. Panel D shows behavioural rhythmicities for pdfgal80/(UAS-Kir2.1 or UAS-TeTxLC); crygal4 13/+ in RR and DD. Observable is a significant loss of rhythmicity following Kir2.1 expression in both light conditions, and an RR-specific loss of rhythmicity following TeTxLC expression. Due to a generalized lower rhythmicity, females were excluded from the figure.

Of interest, we expressed *TeTxLC* with the ITP+ve cells of the *R54D11* driver, from which we had previously ascribed no function. We observe similar phenotypes to that of *R78G02*, decreased rhythmicity in both conditions, which is arguably more severe in RR than DD (Figure 5.18a). *R78G02* expresses in many non-clock cells, see Appendix Figure 32, and it is tempting to argue the reduction in rhythms for that genotype is not the result of E cell silencing specifically. *R54D11* possesses a relatively limited spatial pattern, comparatively, and the only cells which both drivers definitively hit are the ITP+ve s-LN_v, LN_d and several ITP+ve IPCs. Silencing results in a shorter period in males in RR, relative to (NEG) controls, in which the long-period element resultant of a rhythm splitting is diminished (♂ P=0.010 *, ♀ P=0.839)(Appendix Table 26). We could suggest that the clock cell group promoting longer-period behaviour is repressed by ITP cell silencing, though if this is through mitigation of E cell output or an indirect effect on PDF cell signalling is unknown.

Expression of *Kir2.1* in CRY+ve PDF-ve clock cells did not result in lethality as may have been predicted, but very severe arrhythmia in both RR and DD (Figure 5.18d). The literature is spartan and unhelpful regarding this manipulation: PDF-cell silencing with *Kir2.1* results in arrhythmia, but a later study showed attempts to silence with *crygal4-13* had little effect, though the failure of others groups to publish this obvious experiment in DD, or other E-cell manipulations perhaps indicates unpublished negative results (Nitabach et al., 2002, Dissel et al., 2014). *TeTxLC* expression in the CRY+ve PDF-ve cells resulted in a far more subtle phenotype than *Kir2.1*, potentially a result of driver strength, so it is difficult to directly compare this phenotype to *R78G02* and *R54D11* silencing (Figure 5.18). *Pdf-gal80* may not completely neutralise *Kir2.1* expression in the PDF cells, and *Cry-Pdf-gal80>Kir2.1* may effect the PDF cells to an extent which would reduce DD rhythmicity. Feasibly this result is not due to silencing of four E cells specifically, but other CRY+ve DNs involved in propagation of output rhythms.

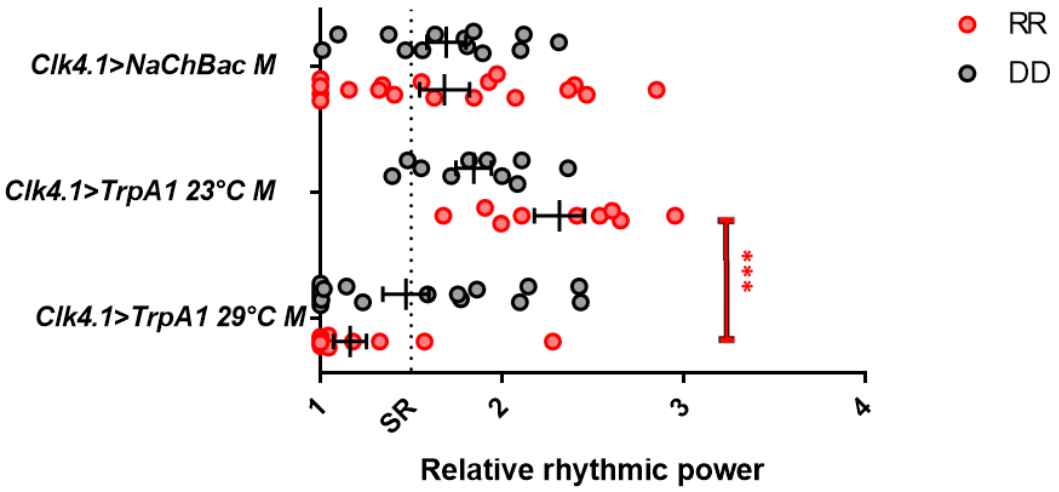

Figure 5.19 - Hyperexcitation of downstream clock neurons, DN1$_p$s, has limited effect on behavioural rhythms in both constant red light and constant darkness. *Rhythmic strength of flies expressing either TrpA1 or NaChBac with the Clk4.1M-gal4 driver, run in RR or DD at 23 or 29°C. Hyperexcitation with NaChBac remains strongly rhythmic, whilst TrpA1 activation lowers rhythmicity in RR (P<0.001***). Due to a generalized lower rhythmicity, females were excluded from the figure.*

The signalling dynamics of other clock cell subsets is poorly studied, particularly relevant to freerunning rhythmicity. The previously mentioned red-light mediated neutralisation of TUG+ve CRY-ve hyperexcitation as a behavioural-rhythm-repressing manipulation suggests excitation of these cells does not influence rhythms independent of the PDF cells. Additionally, DN1s potentially function both in regulating the clock circuit, and serving as a part of an output pathway, so the position of these cells in the red-light circuit is important to establish (Cavanaugh et al., 2014, Guo et al., 2016).

We hyperexcited the DN1ps using *TrpA1* and *NaChBac*, and whilst we failed to generate notable loss of rhythms in either condition with *NaChBac*, a loss of both DD and RR rhythms was noticeable with *TRPA1* (Figure 5.19)(Appendix Table 26). Unfortunately no group has published DD arrhythmia stemming from any ectopic expression with the *Clk4.1M*-driver, incidentally straining credulity of theories of a requirement of these cells in output, so a neat assay of DN1p control over output cannot be attempted.

The literature shows pan-clock *TeTxLC* expression leads to severe behavioural arrhythmia in DD, but PDF silencing does not, and the strong arrhythmia of these results

is more severe than our E-cell *TeTxLC* expression, suggesting fast-synaptic transmission is required in another subset (Kaneko et al., 2000, Blanchardon et al., 2001). *TeTxLC* expression in DN1ps also has little effect on freerunning rhythms, suggesting a broad independence of DN1p firing from freerunning behaviour (Guo et al., 2016).

Clk4.1M demarcated DN1ps and ITP+ve clock cells both project to the PI to form connections, so the possibility exists of redundant pathways within the clock network extending into output, potentially favoured in a time-of-day specific manner, but also means E cell-derived RR rhythms may pass directly to non-clock neurons (Cavanaugh et al., 2014, Hermann-Luibl et al., 2014). Unfortunately the uncertainty of how DNs handle rhythmic information, and lack of assayable lines prevent our interrogation of these cells in RR.

From this study, we have identified new potential modalities in clock cell interconnectivity, in both RR and DD. Notably, we suggest for the first time the importance of E cell signalling in the propagation of freerunning activity in both conditions, though we do not see different impacts of clock cell firing manipulations between the two conditions, suggesting that the hierarchical shift mediated by RR does not radically shift the clock cell network. Potentially more interesting effects would arise were we to combine these manipulations with a loss of PDF signalling, and functional s-LN_vs in RR may inhibit network changes that might otherwise occur.

5.7 - Interrogating known output signalling pathways required for behavioural rhythms during constant darkness reveals certain output pathways are required under constant red light conditions, whlist others are marginalised.

Several papers demonstrate the connectivity of the clock circuit to pathways relevant to rhythmic behaviour, for instance the signalling of PDF-cells to Leucokinin-cells, and the connection between DN1s and neurons within the pars intercerebralis (Cavanaugh et al., 2014, Cavey et al., 2016). We sought to replicate the behavioural experiments from these publications in RR as well as DD, to identify if changes to the red-light circuit hierarchy were confined to the established clock circuit, or if circuit changes allowed the activation of altered, or otherwise redundant output pathways. Ablation of *SIFa*+ve cells, a small group of cells in the PI which express SIFamide neuropeptide and have been shown to interact with $DN1_p$s via GRASP, was previously shown to very mildly reduce

freerunning behavioural rhythms, and we replicate this very mild phenotype in RR, suggesting that these cells are no more relevant in RR behavioural output, but neither does RR provide an alternative output mechanism unreliant on *SIFa*+ve cells (Cavanaugh et al., 2014)(Figure 5.20).

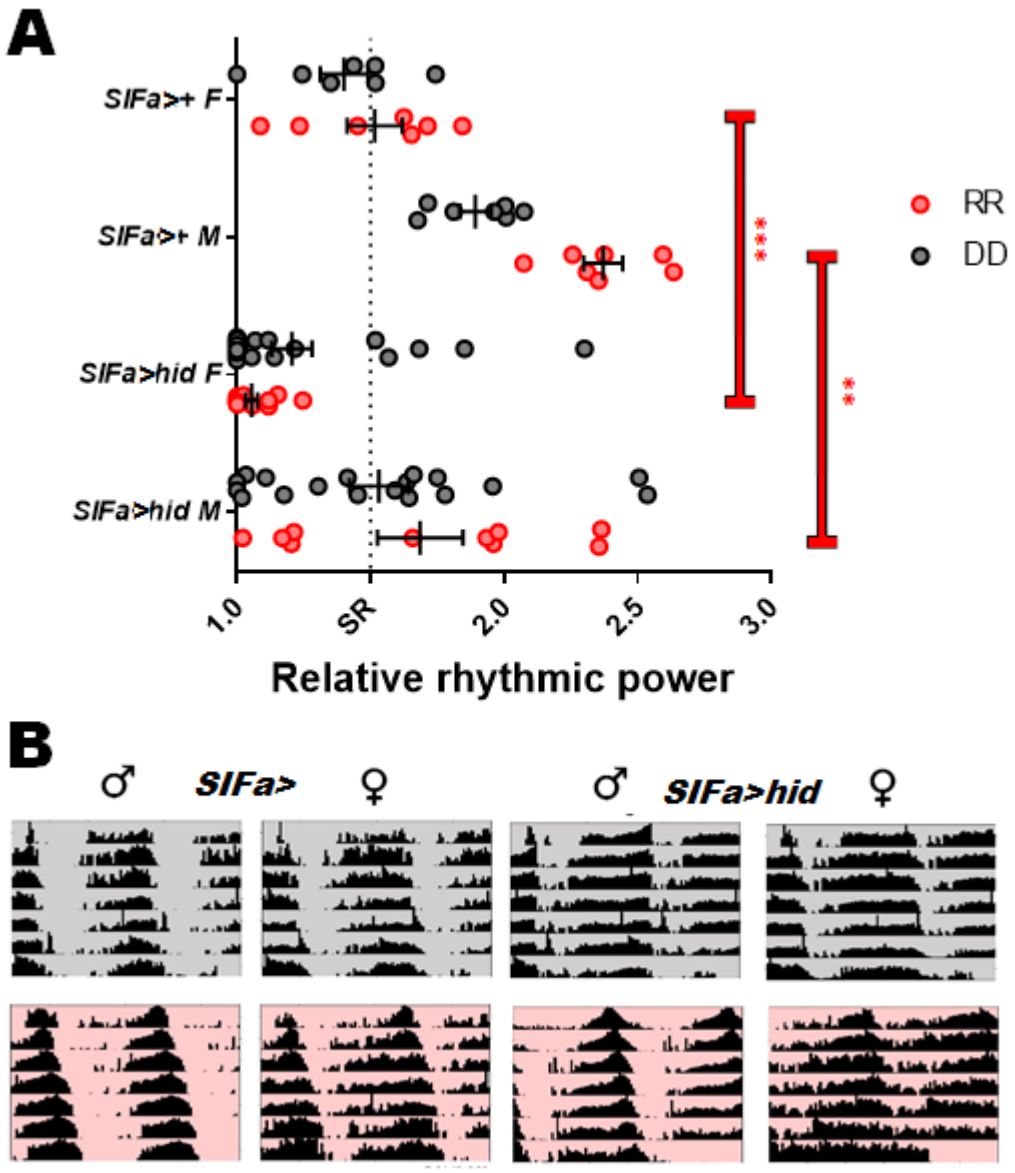

Figure 5.20 - Ablation of SIFamide-expressing neurons results in decreased behavioural rhythmicity in constant red light*. behavioural profiles of SIFa->hid and responderless controls in RR and DD. Panel A shows RRP, and significant differences between control and experimental lines in RR (M = 0.004** and F<0.001***), but not in DD (M=0.061, F=0.310). Due to a generalized lower rhythmicity, females were excluded from the figure. Full statistics are available in Appendix Table 40.*

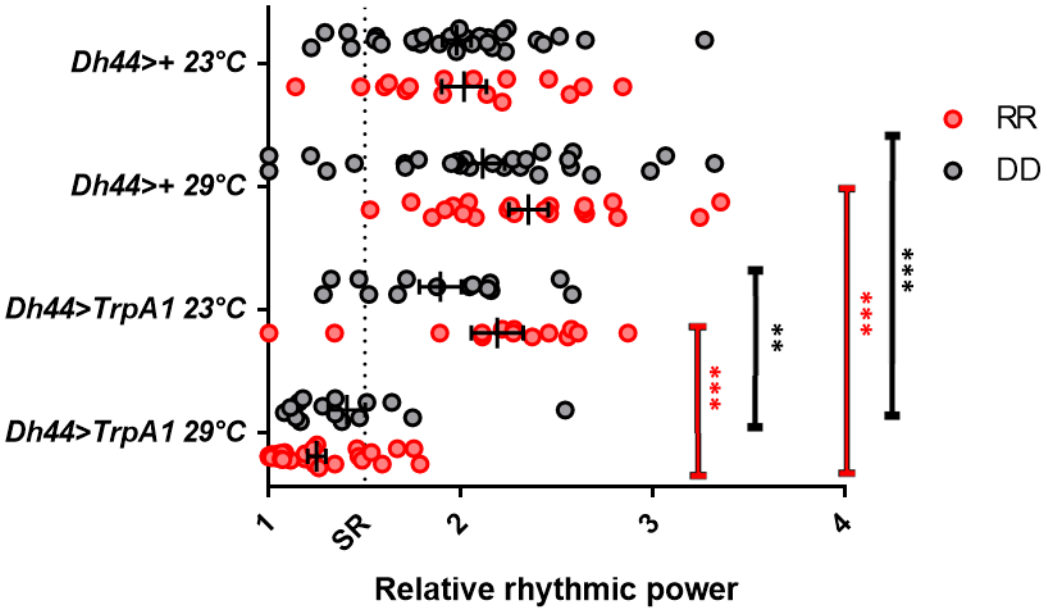

Figure 5.21 - Increased signalling from Dh44-neuropeptide-expressing neurons results in decreased behavioural rhythmicity in constant red light and constant darkness. *behavioural profiles for Dh44-gal4>UAS-TrpA1 and responderless controls raised at 23°C and run at 23°C or 29°C in RR or DD. Full statistics are available in Appendix Table 40. Due to a generalized lower rhythmicity, females were excluded from the figure.*

More severe phenotypes are allegedly attainable via hyperexcitation of a broader subsection of PI cells using the *kurs58-gal4* driver, though in our many, many attempts to replicate this we found lethality in all flies within two-three days of instigating the assay. Similarly, we found silencing with *Kir2.1* or *TeTxLC* resulted in lethality, and it is expected many other PI-mediated behaviours such as feeding may be disrupted. *Dh44^{vt}-gal4>hid,* targeting six Dh44+ve cells, was similarly unviable in our hands, whilst (Cavanaugh et al., 2014) suggests a strong decrease in rhythmicity.

(Cavanaugh et al., 2014) showed *Dh44-gal4* cell hyperexcitation with *TrpA1* was supposed to mildly reduce rhythms in DD compared to responderless 29°C controls, whilst bafflingly not differing with the inactivated 21°C experimental result, from which they suggest an effect of these cells in output. Surprisingly, we see a reduction at 29°C for males in both RR ($P<0.001$ ***) and DD ($P=0.004$ **) relative to responderless controls, suggesting there is a common output route through these cells (Figure 5.21, Appendix Tables 39 & 40).

These manipulations weaken rhythms, but the majority of flies appear rhythmic, suggesting a redundancy with other output pathways, likely thus-far uncharacterised.

In light of these lacklustre phenotypes, which seem to plague all output-related research (Cavanaugh et al., 2014, Kunst et al., 2014, Cavey et al., 2016, King et al., 2017), we elected a different strategy to uncover output phenotypes, through targeted knockdown of neuropeptides. Relevant neuropeptides for the PI region are *SIFa*mide and Dh44, and we knocked down both the neuropeptide and the receptor, where *Dh44* RNAi has shown mild reduction in rhythms (Cavanaugh et al., 2014, Cavey et al., 2016), and *SIFa*mide knockdown, though not analysed in more detailed, showed a stronger loss of rhythms than PDF knockdown (Cavey et al., 2016). We failed to observe a notable loss of rhythms in DD or RR for any neuropeptide, though we also failed to generate adequate phenotypes in our positive control line, expressing *dsPdp1*, limiting our interpretation of this data (Appendix Figure 21).

For the most part, out failure to replicate *Dh44*-output pathway results in DD must temper any conclusions we have, but we do not see a thematic greater or weaker sensitivity to these manipulations between light conditions, and the few instances of mild behavioural effect (*SIFa>hid* and *Dh44>TrpA1*) we see are common to RR and DD, so we very tentatively suggest a Dh44+ve output pathway contributes to both RR and DD rhythms, but is required for neither.

Dh31 in the dorsal clock cells is shown to directly increase cAMP levels in all PDF+ve cells, suggestive of upstream function, and additionally serves as a ligand for PDFR (Shafer et al., 2008, Kula-Eversole et al., 2010, Kunst et al., 2014, Goda et al., 2016). As has previously been published, we show $Dh31^{\#51}$ nonsense mutants have mildly weakened rhythms in DD, and this is the case in RR as well, though unfortunately heterozygous controls appear similarly less rhythmic (Figure 5.22)(Appendix Table 39). $Dh31^{\#51}$ flies in RR have a slightly long period (M =24.42±0.37, F= 24.71±0.79), arguing that this is separable from the short-period phenotypes associated with loss of PDF signalling.

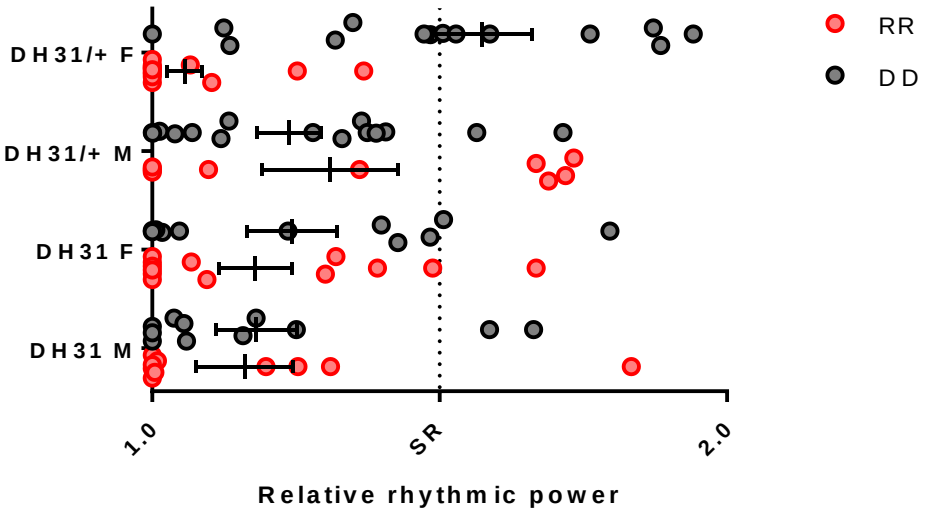

Figure 5.22 - Loss of Dh31 neuropeptide does not alter behavioural rhythmicity in constant red light or constant darkness. *Behavioural rhythmicity profile for Dh31 and Dh31/+ flies in 23°C RR and DD, in which significant differences do not arise between heterozygotes and homozygotes due to a weak rhythmicity in both cases*.

Thus, *Dh31* and *Dh44* may have mild roles in influencing behavioural output in both RR and DD.

Two mutants in Leucokinin (Lk) and Leucokinin receptor (Lkr), respectively, were previously shown to reduce freerunning behavioural rhythms (Cavey et al., 2016). We repeated this finding, showing very few of these flies were strongly rhythmic in DD, however a significant fraction did become strongly rhythmic upon exposure to RR conditions, suggesting that leucokinin signalling is less integral to RR output (Figure 5.23).

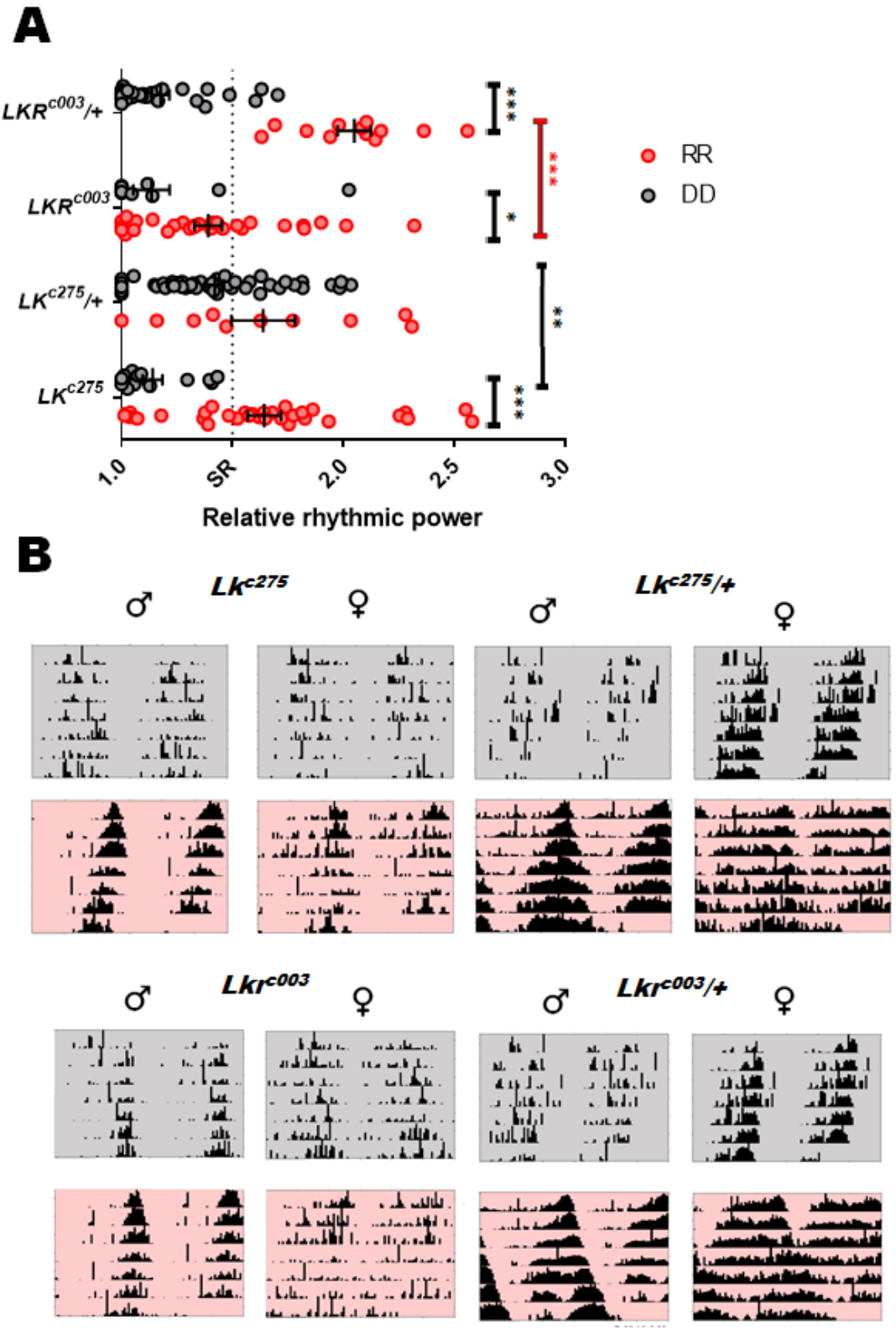

Figure 5.23 - Loss of leucokinin signalling results in decreased behavioural rhythmicity in constant darkness, but not constant red light. *Panel A shows behavioural profiles for homozygous and heterozygous mutants of leucokinin and leucokinin receptor in RR and DD. Panel B shows median actograms for the respective conditions. Due to a generalized lower rhythmicity, females were excluded from the figure. Full statistics are*

available in Appendix Table 40.

Leucokinin signalling is required for output and leucokinin neurons appears to contact PDF+ve cells; thus it is feasible that this output avoids the rest of the clock circuit. However, LHLK dendritic arbors are localised near, and potentially interact with LN_d and DN1p cells as well, providing potential RR circuit connections (Cavey et al., 2016). s-LN_v signalling, but not direct PDF neuropeptide inhibit LHLK firing, and LHLK hyperexcitation leads to AR, whilst LHLK silencing had no effect on behaviour. For rhythmicity in RR, another clock cell subset must be able to repress leucokinin signalling, or else this output can be excluded completely. LK cells show a firing rhythm dependent on the clock circuit, there is no evidence that the propagation of this rhythm is required for rhythmic behaviour. For s-LN_v-independent rhythmicity in RR, another clock cell subset must be able to repress LK neuron signalling or else the need for such repression may be bypassed under this condition (Cavey et al., 2016).

Whilst our dataset is not fully conclusive, a potential marginalisation of leucokinin in output may arise in RR, which will be addressed in future work with LK RNAi lines, and manipulation of Leucokinin cells with *LK-gal4*.

5.8 - Network requirements for behavioural rhythms in constant red light appear separable, and more stringent than requirements for evening anticipation in 12:12hr light-dark cycles

As the E cell oscillator has a dual role, in red light rhythms and in promoting evening arousal, and both conditions are at a state of low active CRY levels, it is worth making a comparison between them. Do manipulations altering RR rhythmicity impact the evening peak, and vice versa? One hypothesis founded upon the two observations above, is that the RR network state can be considered the perduring form of a transient evening state. If manipulations that abrogate behavioural rhythms in RR through circuit disruption can maintain the E peak in LD or vice-versa, then this hypothesis would be weakened

(Cusumano et al, 2009) shows the RR activity peak seems phasic to the evening peak when PDF cell function is challenged whilst freerunning phase seems balanced between M an E peaks when PDF cells are functional, indicating E cell activity may determine the initiation of RR freerunning activity alongside evening peak.

A confirmed l-LN_v→ E cell connection controls E peak timing in a PDF-dependent manner (Schichtling et al, 2016, Figure 5.6) and both subsets are involved in RR rhythms in a PDF-independent manner (Figure 5.5), suggesting a similar control of these processes. *Pdf^{01}* and *$Pdfr^{5304}$* combine an early E peak with a short RR period (Figure 5.1).

Numerous lines with lessened RR rhythmicity, namely *R78G02>TeTxLC, R78G02>TrpA1* and *R78G02>$cyc^{\Delta 103}$* were run in 12:12 LD cycles, in all cases demonstrating crepuscular activity patterns and quantifiable, if variable evening anticipation. None of these manipulations completely remove RR rhythms, however, so an extant E peak would not be a surprise (Figure 5.24). Unfortunately, *cry-Pdfgal80>Kir2.1*, in which we see severe arrhythmia in RR, appears to possess an intact evening peak. Thus, despite dependence on an E-cell oscillation, it appears the two processes are regulated differently, and an evening-peak can manifest in cases of low RR rhythmicity, potentially contributed by signalling from another clock cell subset (Appendix Figure 27).

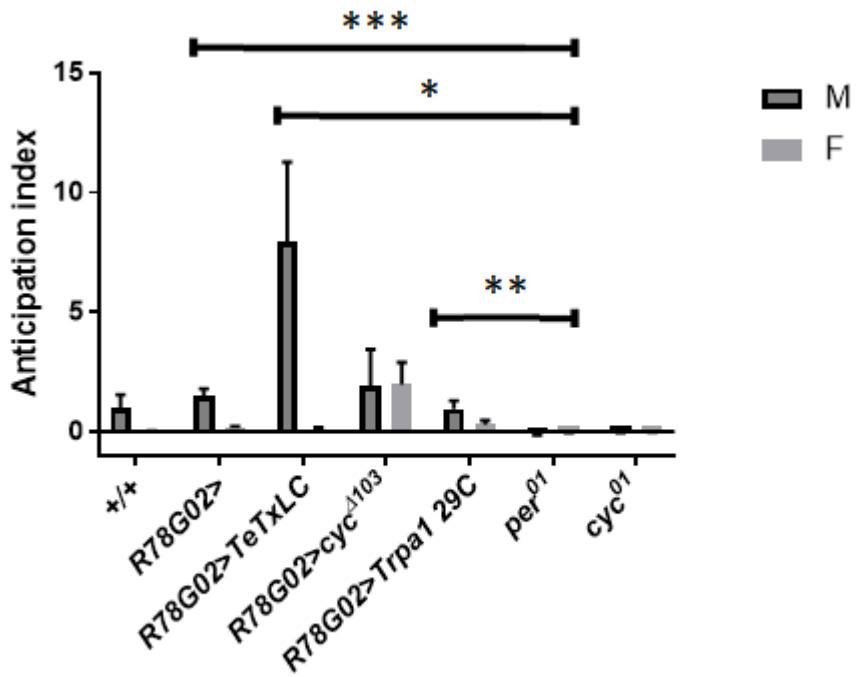

Figure 5.24 - Loss of behavioural rhythmicity in constant red light does not result in a

loss in evening anticipatory activity. *Evening anticipation index for R78G02>TeTxLC, $cyc^{\Delta 103}$ and TrpA1 in LD, revealing the presence of a distinct evening peak. Calculations were performed as described in methods section and (Stoleru et al., 2004). Any positive value represents an existent evening anticipation, neither of which is present in the case of per^{01} or cyc^{01}.*

One must acknowledge that the reasoning behind this experiment conflates purveyance of rhythmic information across a daily cycle with purveyance of arousal information at a fixed timepoint, potentially regulated by other cells in the network at all other times. Potentially E-cell hyperexcitation results in wt-like activity in LD as the evening is the only time the circuit state permits E-cell arousal-mediating influence on behaviour, a high excitation point of LN_ds which is dependent upon intact PDF signalling from the l-LN_vs (Schichtling et al, 2016, Liang et al, 2017). This hypothesis supports the limits to arrhythmia from E cell hyperexcitation, suggesting behaviour-promoting activity of the E cells is limited at other timepoints, regardless of excitability. In Pdf^{01} flies, LN_d firing is naturally phase-advanced, result in an early E peak, whilst in DD, LN_d firing does not correlate with the phase of residual rhythms, but is notably rhythmic (Liang et al, 2017).

As discussed in Chapter 3, we replicated a finding of (Kumar et al, 2012), that dopaminergic silencing with *TeTxLC* reduces nocturnality in CLK/CYC mutants. The paper then claimed that dopaminergic hyperexcitation with *NaChBac* was sufficient to create the Clk^{Jrk} LD profile, which we fail to replicate. Instead, *ple>NaChBac* is diurnal with noticeable morning and evening anticipation, (Figure 5.25). This manipulation similarly demonstrates that E-anticipation requirements are seperable from RR rhythmicity, though it is unknown whether dopaminergic requirement lies upstream or downstream of the clock network. As with all phenotypes, it is unknown the effectiveness of *NaChBac*-induced hyperexcitation in our hands, but both driver and responder have individually produced LD phenotypes (Figure 5.8).

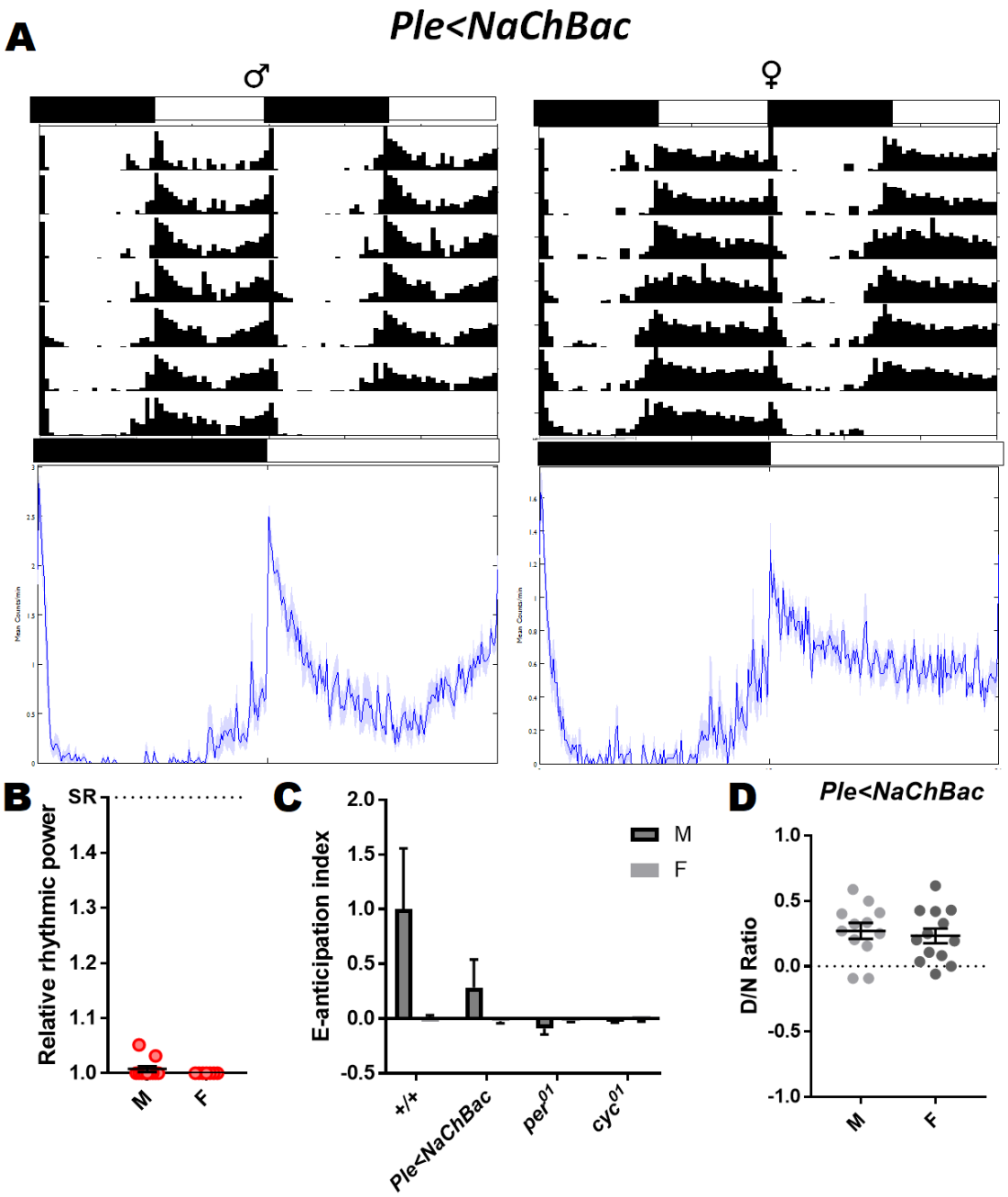

Figure 5.25 - Dopaminergic hyperexcitation does not remove anticipatory behaviours in light-dark cycles, despite loss of behavioural rhythmicity in constant red light. *Panel A) Actograms and activity profiles, Panel B) LD D/N ratios, Panel C) evening anticipation index and Panel D) RR rhythmicity for ple-gal4>NaChBac, hypothetically hyperexciting dopaminergic neurons. A positive evening anticipation value indicates an existant peak. ♂ n=12, ♀ n=13.*

In summation, we conclude RR comprises a network state, separable from transient network states in LD cycles, and though this state does not demonstrably occur during

any point of a natural cycle, it is relevant to characterise in understanding the mechanistic basis of rhythm generation within the circuit, and is serviceable as a tool to assay the functionality of a clock circuit in behavioural control where PDF cells are somehow compromised.

5.9 – The behavioural arrhythmia induced by developmental loss of *cycle* is not rescued by exposure to constant red light, nor does developmental expression of *cycle* within putative red-light pacemaker cells allow behavioural rhythms in constant red light.

The LD profile of 17→29°C cyc^{01} *[elav.cyc]*^{ts} flies suggests a residual E peak in behaviour, indicating functional E cells, though as described in the section above this is not necessarily the case (Stoleru et al., 2004, Grima et al., 2004). Though not formally quantified, high nuclear PER was never identified in locations corresponding to the LN_ds following developmental CYC loss (Chapter 3). ITP staining of these flies shows an approximately normal morphology following developmental CYC loss. Our characterised defect is limited to projection morphology of the s-LN_v cells, which control freerunning rhythms, but not M or E peak emergence (Agrawal and Hardin, 2016), so we studied 17→29°*C* and 29→29°*C* cyc^{01} *[elav.cyc]*^{ts} flies run in RR, as a freerunning state independent of PDF-cell presence. Conditional loss of CYC resulted in behavioural arrhythmia, with conditions statistically aligning across gender and temperature condition with the experiment when run in DD (Figure 5.26).

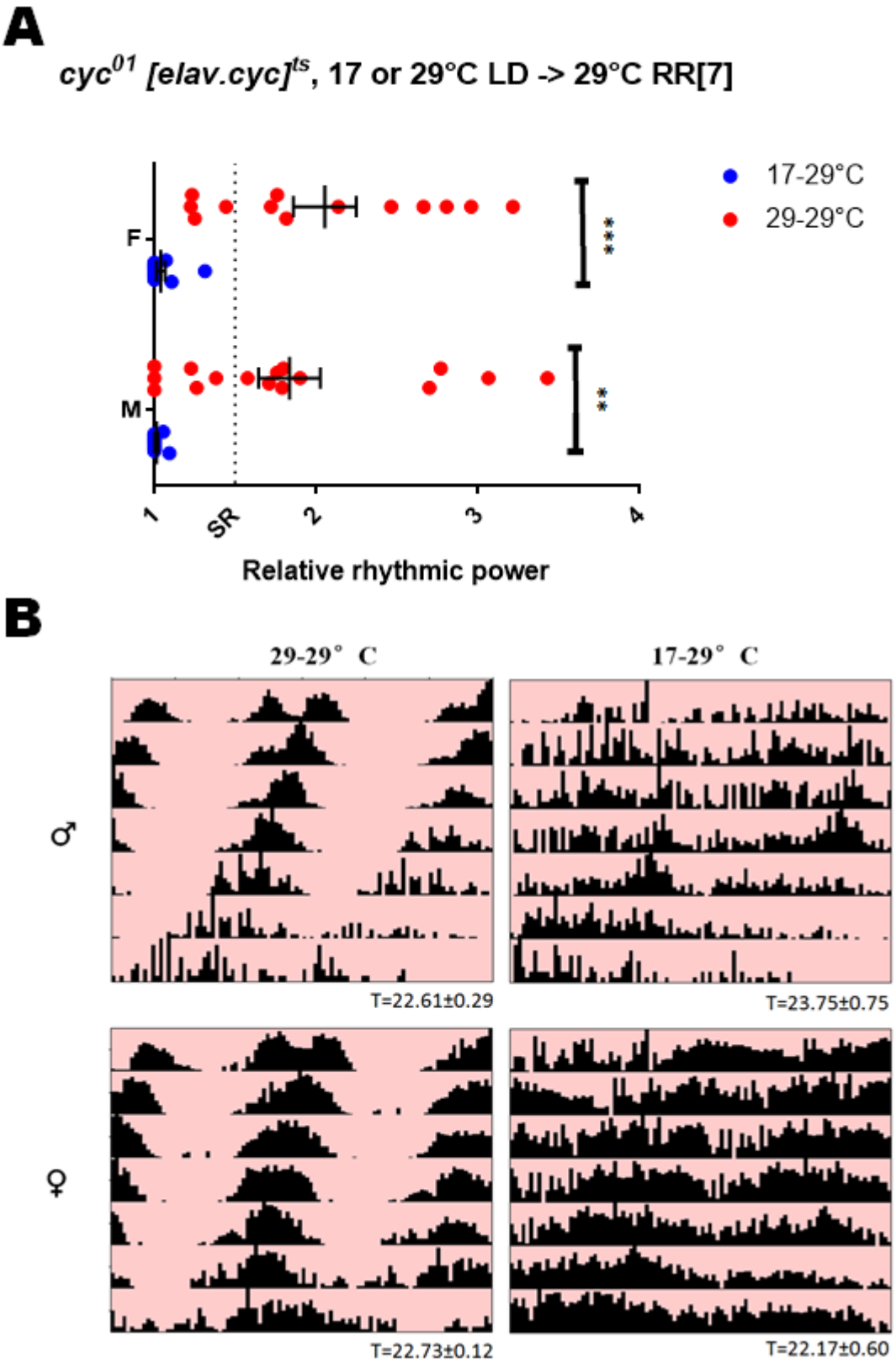

Figure 5.26 - Loss of developmental CYC expression results in behavioural arrhythmia in constant red light. *Panel A demonstrating behavioural rhythmicity in RR at a permissive temperature for permissively and restrictively raised* cyc^{01} *[elav.cyc]*^{ts}*. Panel B demonstrates median actograms for permissively and restrictively raised* cyc^{01} *[elav.cyc]*^{ts} *in RR. Full statistics are in Appendix Table 42.*

Once again permissively raised *cyc*^{01} *[elav.cyc]*^{ts} flies of both genders have circadian periods >23hrs due to ectopic CYC expression. Notably, permissively-raised males show stronger rhythms than 29→29°C DD, more similar to 23→29°C males in DD, though an explanation for this is difficult to procure.

The Hardin lab recently demonstrated PDF-cell-specific loss of Leukocyte antigen receptor (LAR), a tyrosine phosphatase protein involved in axon guidance, completely removed dorsal projections. We studied *Pdf>lar* RNAi, to study if these projections had any requirement in RR, representing a PDF-cell specific LAR knockdown was overwhelmingly AR in DD, as described by (Agrawal and Hardin, 2016), but became rhythmic in RR, confirming that loss of PDF projections did not damage the RR circuit (Figure 5.27).

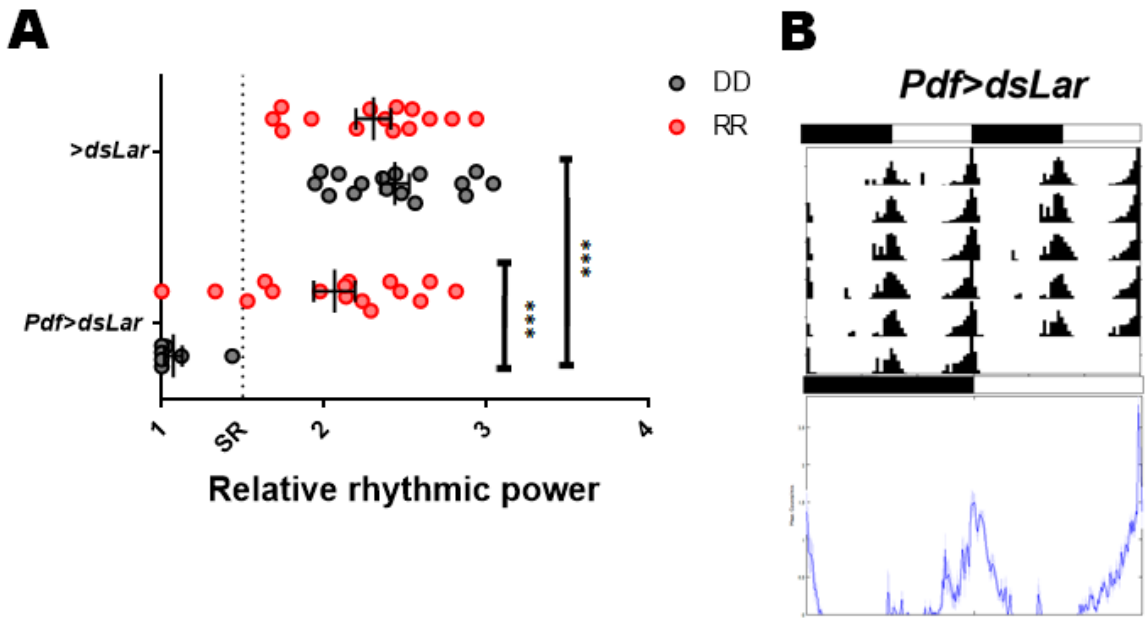

Figure 5.27 - Loss of Lar within PDF cells results in lowered behavioural rhythmicity in constant darkness, but not constant red light, and evening anticipation is maintained*. Panel A shows behavioural rhythmicity of lar RNAi lines in DD and RR. Evident is a significant loss of DD, but not RR rhythmicity. LD ♂ n=11, LD. Panel B shows median actograms and activity profiles for 12:12 LD cycles, demonstrating ongoing morning and evening anticipatory activity, as published in (Agrawal and*

Hardin, 2016).

$Lar^{13.2}/Lar^{DF}$, despite extensive use in (Agrawal and Hardin, 2016) was largely lethal in our hands, resulting in n numbers too low for serious analysis. However, the five experimental flies we obtained were all AR in RR. Beyond the clock circuit, it is assumed these flies would possess visual defects (Clandinin et al., 2001), though notably intact l-LN_v innervation of the accessory medulla, which in conjunction with disrupted s-LN_v signalling may prevent instigation of an RR network state.

It has been published that following *Lar* RNAi with either the *Pdf* or *TUG* driver, LD rhythms appeared wt-like with morning and evening anticipation activity, a result that we replicate (Figure 5.27)(Agrawal and Hardin, 2016). Similar data has been produced by the lab in affecting PDF-cell function through knockdown of *Rho1*, in which morning and evening anticipation is present in spite of arrhythmia in freerunning conditions (Ramirez thesis, 2017).

We studied permissively raised and run cyc^{01} *[elav-Pdf80.cyc]*^{ts} flies in RR and DD, as these flies possess defasciculated projections, yet presumptive pacemaker E cells should develop normally. It was necessary to use the conditional line for this manipulation, as pre-existing constitutive CYC reintroduction lines appeared arrhythmic (data not shown). As expected, cyc^{01} *[elav-Pdf80.cyc]*^{ts} were majority AR in DD, whilst significant weakly rhythmic population existed in RR (Appendix Table 43)(Figure 5.28). As RR rhythms without PDF cell input are usually relatively weak, this result can be considered evidence that the RR circuit remains intact in the absence of *Pdf>*specific CYC. This does not rule out the idea that increased s-LN_v projection complexity can have dominant effects on the RR circuit properties, either in aberrant connections or aberrant firing, as projections of this genotype, though significantly more complex than in wt, are milder than projections following than pan-neuronal CYC loss, and behaviourally rhythmic flies can exhibit this amount of complexity (17°*C* EL-L3 29°*C* AR).

Raising cyc^{01} *[elav-Pdf80.cyc]*^{ts} restrictively through development and permissively during adulthood results in severe behavioural AR in RR and DD (Figure 5.28). Though this is the case with cyc^{01} *[elav.cyc]*^{ts} too, we have demonstrated that CYC expression within PDF-ve cells alone is sufficient for a functional red-light circuit to develop, and we show the behavioural arrhythmia in RR following loss of developmental CYC is due

to a loss specifically in PDF-ve cells.

RR period length was short, (M=22.70±0.30, F=23.32±0.30), not noticeably different to *cyc*^{01} *[elav.cyc]*^{ts} (Figure 5.26). It would be tempting to draw parallels to the short period of PDF signalling mutants in RR, and attest that PDF-cell CYC loss and accompanying defects lead to period shortening as the E cell oscillator gains influence over behaviour, though if this occurs it is likely masked by other period effects.

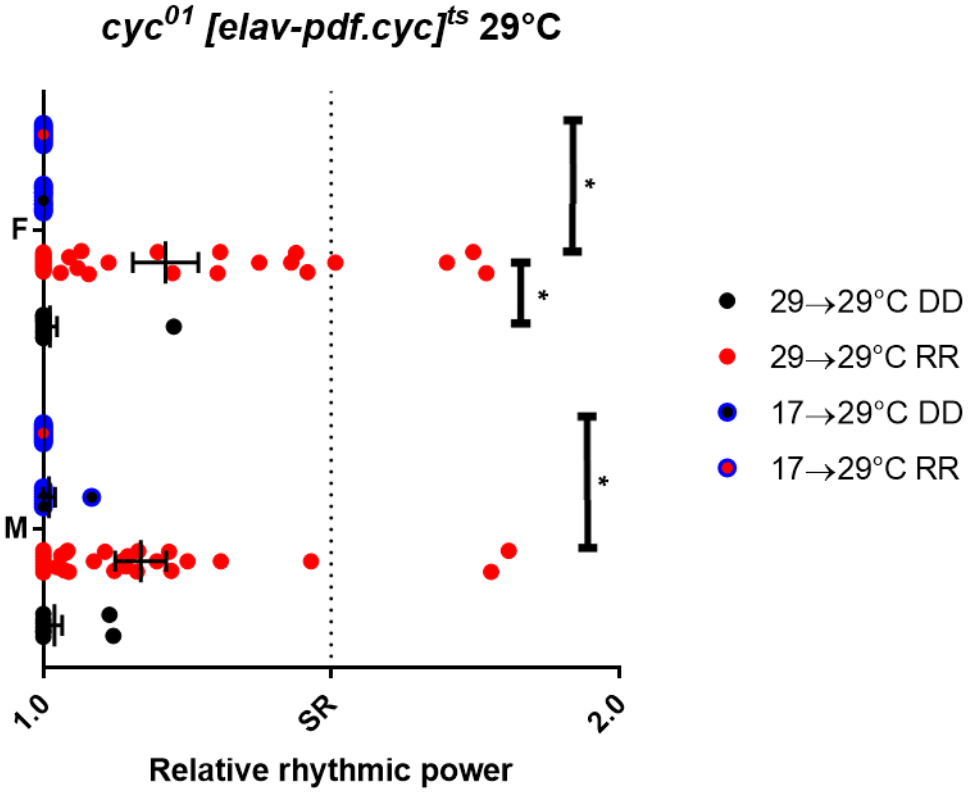

Figure 5.28 - Behavioural arrhythmia in constant darkness caused by adult loss of cycle within PDF cells can be partially rescued in constant red light. *behavioural profiles for cyc*^{01} *[elav-Pdf80.cyc]*^{ts} *in 29°C RR or DD. Notable is a significant difference in RRP between permissively and restrictively raised flies in RR, for both genders.*

It is expected from gross morphological defects in *cyc*^{01} *[elav-Pdf80.cyc]*^{ts} within the l-LN$_v$s, CYC loss within PDF cells may lead to defects in l-LN$_v$ function (Chapter 4).

Our previous conditional PDF-cell ablation data has demonstrated developmental s-LN$_v$

absence does not affect the red light rhythms, and likewise, *Pdf>dslar* suggests no developmental requirement for the s-LN_v dorsal projections in the clock circuit, so we can confidently state that s-LN_v projection defects should not adversely affect the RR circuit, though it is feasible that l-LN_v misrouting may disrupt l-LN_v→E cell connections.

We attempted to rescue CYC purely within the E cells using *R78G02* and *Crygal4-Pdf-gal80* drivers. In this case, flies were uniformly arrhythmic in RR (Figure 5.30). This can be contrasted to PER-rescue with these drivers, both rhythmic in RR, demonstrating that although molecular oscillator resumption with PER is sufficient for RR rescue, associated defects due to CYC loss in other cells are still capable of blocking behaviour (Figure 5.12). One argument would suggest that CYC loss generates a defect in the l-LN_vs for this genotype which blocks a hierarchical shift favouring the E cells. To address this we co-rescued CYC with *c929* and *R78G02*-drivers, which still resulted in persistant behavioural arrhythmia, hypothetically ruling out l-LN_v defects as causing arrhythmia.

It is likely driver strength may be reduced in E-cells on a cyc^{01} background, as *R78G02>CD8::GFP* and *Cry-Pdf80>CD8::GFP* spatial pattern appears altered, with fewer visible LN_ds. Thus, we may be unable to adequately rescue in these cells. We can also interpret from this data that E-cells may require dorsal clock cells as downstream mediators of behaviour, which do not require their own oscillator, but are compromised by developmental CYC loss. The lack of visible $DN1_p$s following CYC loss (Figure 4.12) may also cause RR arrhythmia, assuming that E cell projections to the PI cannot sustain RR behaviour.

cyc^{01} *[elav-VGlut80.cyc]*^{ts} males, lacking CYC rescue within the glutamatergic $DN1_a$s, do not significantly differ in rhythmicity to pan-neuronal rescue in either RR or DD, whilst significantly differing to driverless controls (Figure 5.29)(Appendix Table 31), suggesting that a $DN1_a$ oscillator, despite inclusion in CRY+ve PDF-ve dataset, is not a required component of the red light pacemaker. It could also be argued that if $DN1_a$ developmental defects arose in the absence of CYC, this would not disrupt RR rhythms. However, it is still feasible that CRY+ve $DN1_a$s have redundant functions in RR pacemaking and are sufficient if not required.

Unsurprisingly, cyc^{01} *[Pdf.cyc]*^{ts} is completely AR in RR, as is the case in DD, reflecting

that in addition to absence of an E cell oscillator, the ambiguous PDF-ve cell requirement persists (Figure 5.29).

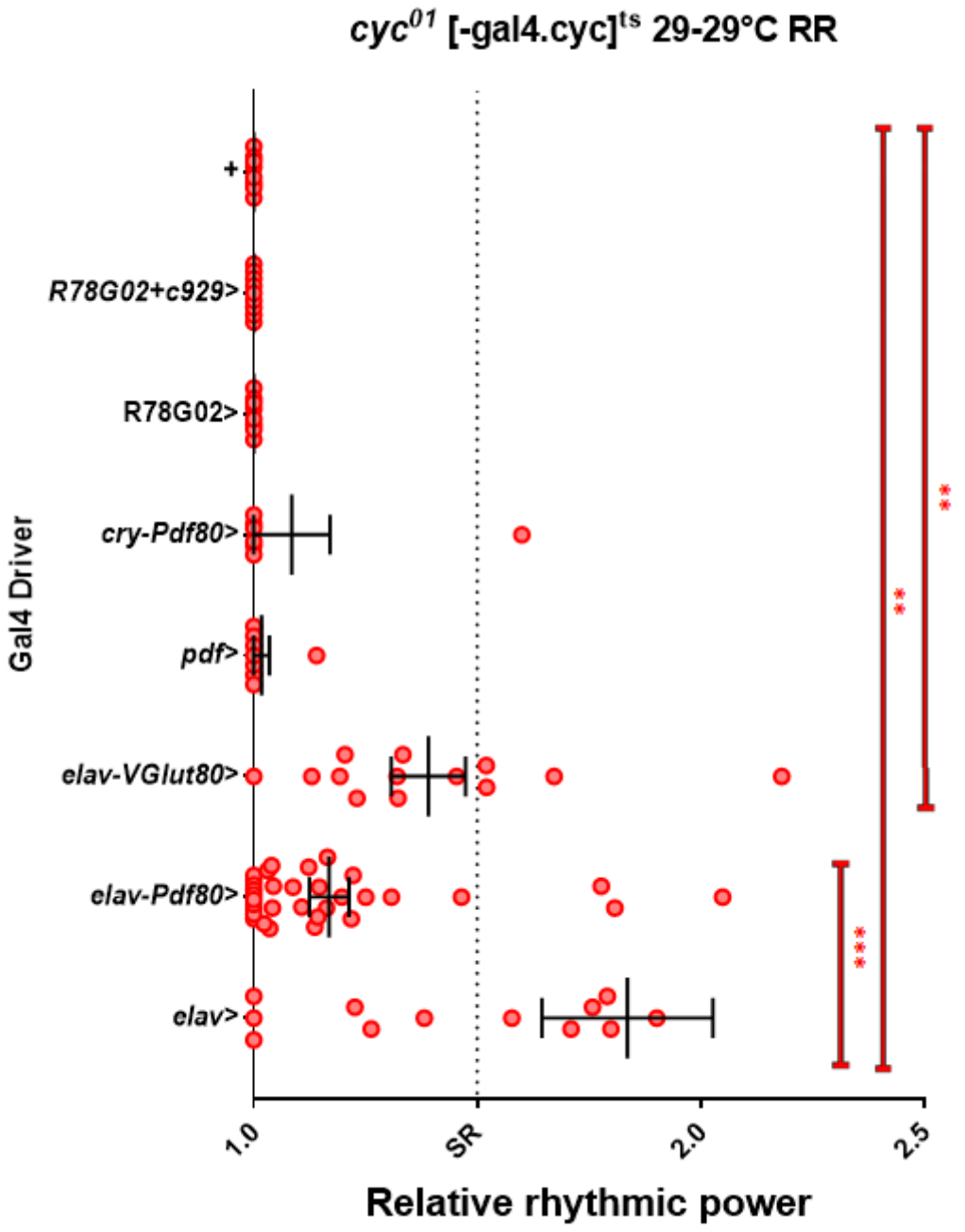

Figure 5.29 - Rescue of behavioural rhythmicity through ectopic expression of cycle is only achievable through pan-neuronal expression. *Behavioural rhythmicities for conditional CYC rescue with various drivers, raised at 29°C and run at 29°C DD for 7 days. All flies were male, due to experimental constraints. Evident is that E-cell specific drivers are not capable of establishing RR rhythms, whilst PDF or glutamatergic cell CYC is not required for an RR rhythm. CyO negative controls lacking UAS-cyc$^{\#7}$ and cyc^{01}/+ heterozygote positive controls are available in Appendix Table 30. Statistics are*

available in Appendix Table 31.

A secondary interpretation of our conditional PDF-cell ablation dataset (Figure 5.5), related to our study of developmental CYC requirement, is that a red-light specific circuit is capable of forming correctly and functioning in the absence of guidance cues emanating from s-LN_vs. Thus, RR arrhythmia following developmental CYC loss is likely not due to loss in the s-LN_vs, but instead a PDF-ve cell subset. It is also interpretable that l-LN_v dysfunction contributes to RR arrhythmia, through failure to induce network changes prioritising E cell pacemaker function, though it is known that adult-specific CYC can rescue nocturnal phenotypes, suggesting some l-LN_v function. Morning anticipation, likely l-LN_v mediated, however, is removed by developmental CYC loss, suggestative of l-LN_v dysfunction.

As has previously been published in (Goda et al., 2011), we demonstrated that conditional PER overexpression during development results in persistant behavioural arrhythmia, initially ascribed to be due to PER repression of CLK/CYC and supporting data in the *cyc^{01} [elav.cyc]^{ts}* line. However, these showed a more severe molecular phenotype, of damping in the s-LN_vs, and a mild damping in the LN_ds. To support our dataset, we attempted to determine if rhythms were rescuable in these flies in RR.

Like in DD, the 29°C-raised *[timP.per]^{ts}* were majority AR (♂=58.62%, ♀=89.66%), whilst the 23°C-raised flies were not (♂=0%, ♀=33.33%). In most cases, rhythmicity did not significantly differ between DD and RR run flies.

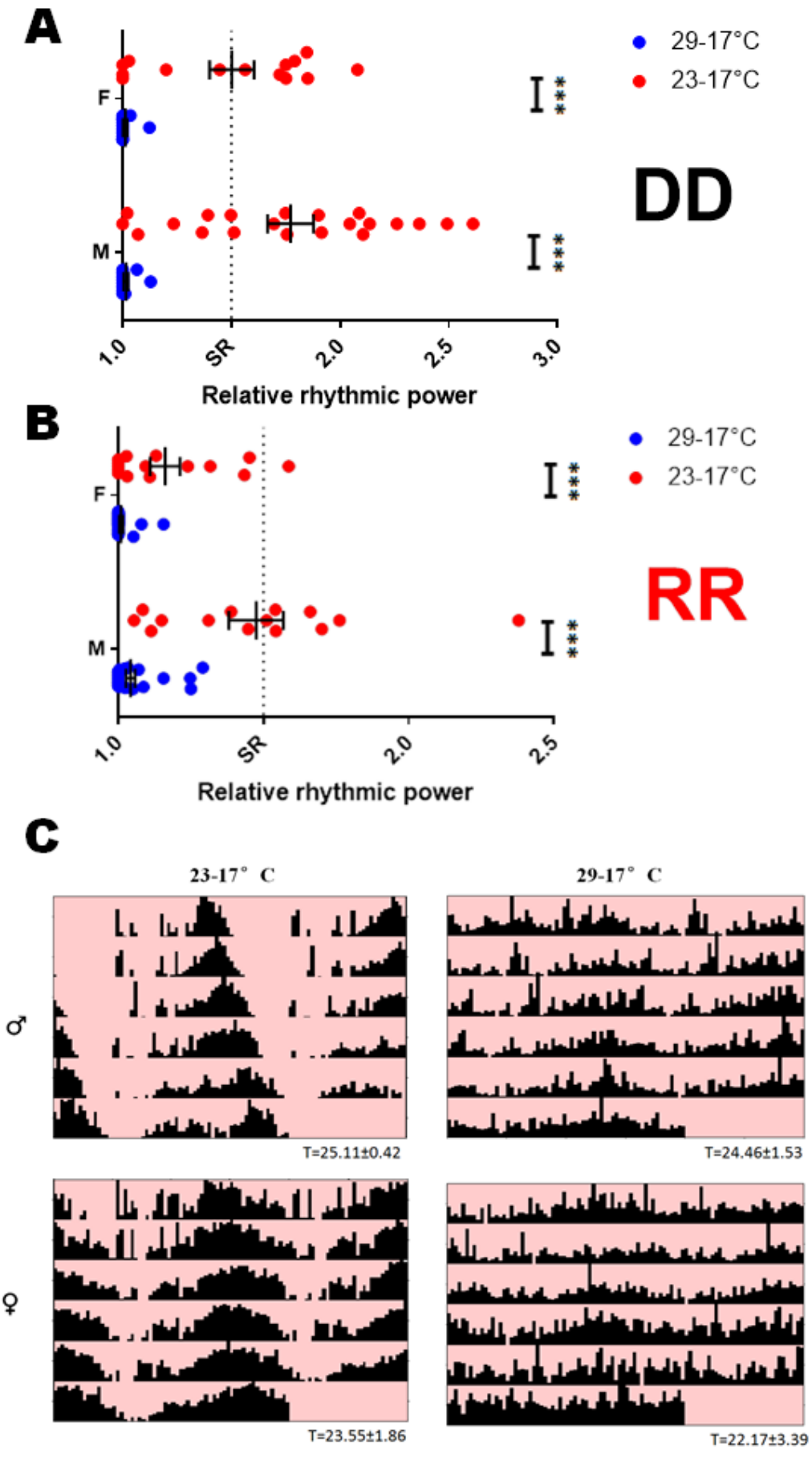
A
29-17°C
23-17°C
DD
F
M
1.0
SR
2.0
2.5
3.0
Relative rhythmic power
B
29-17°C
23-17°C
RR
F
M
1.0
SR
2.0
2.5
Relative rhythmic power
C
23-17° C
29-17° C
♂
♀
T=25.11±0.42
T=24.46±1.53
T=23.55±1.86
T=22.17±3.39

Figure 5.30 - Developmental overexpression of PER results in adult behavioural arrhythmia in both constant darkness and constant red light. *Displaying distribution of rhythmicities and median actograms of [timP.per]^{ts}, raised at 23 or 29°C and run at 17°C in RR or DD. Panel A shows distribution of RRP in DD, with significant differences emerging by developmental temperature (P<0.001***), Panel B shows distribution of RRP in RR, with significant differences emerging by developmental temperature (P<0.001***) and Panel C shows median actograms for both genders and developmental conditions in RR. Data is included in Appendix Table 44.*

A prior PhD student in the lab identified a partial damping in LN_d PER oscillations in *[timP.per]^{ts}*, which could account for a loss of RR rhythmicity, alongside ancillary defects pursuant to developmental CYC loss, as discussed earlier. These results, agglomerated with CYC loss data supports other findings throughout Chapter 5.

Thus, we can conclude that developmental loss of CYC disrupts red-light behavioural rhythms, suggestative of defects in PDF-ve clock cells, but with potential for a dominant repressive role of novel connections identifiable in PDF+ve cells. We can conclude from a partial behavioural red light rescue in *cyc^{01} [elav-Pdf80.cyc]^{ts}* that CYC in PDF-ve cells may have a separate developmental role, as suggested by other data in Chapter 4.

5.10 - Discussion – Chapter 5

Previous work has implicitly suggested a marginalisation for PDF cells in contributing to rhythms in RR (Cusumano et al., 2009), though our work builds upon this to characterise requirements for the l-LN_vs (Figure 5.6) and their electrical activity (Figure 5.4).

PDF-independent requirements for l-LN_v presence and electrical activity in red-light circuits (Relevant to Section 5.1 and 5.2)

This work is the first case of selective ablation of the s-LN_vs without ablating l-LN_vs, and the persistence of red-light rhythmicity following s-LN_v ablation, but not ablation of all PDF cells, demonstrates a novel role for l-LN_vs in maintaining behavioural rhythms, and to our knowledge is the first case of a fly exhibiting a robust behavioural rhythm whilst

lacking s-LN$_v$s.

An assumption of the experiment in Figure 5.6 is that conditional s-LN$_v$ ablation is that l-LN$_v$ function is required rather than redundant with s-LN$_v$s (Figure 5.6). As we lack a manipulation to specificially ablate the l-LN$_v$s, redundant effects may emerge between the clock cell subsets, seperable from pacemaker or PDF cell signalling function. This experiment may be feasible in the near future using Split-*gal4* lines (Dionne et al,, 2018). In any case, this requirement for the l-LN$_v$ in maintenance of rhythmic behaviour is a novelty.

The mechanism of action by which l-LN$_v$s shift the clock network following red-light exposure is harder to explain, though we can state that l-LN$_v$s may serve as an intermediary for CRY-independent photic input to the clock, and thus be required for initiating a hierarchical shift. l-LN$_v$s signal to the s-LN$_v$s via PDF secretion, whilst synaptic connections between the cells have not been identified, so a direct marginalisation of the PDF cells is feasible, as is communication between clock cell subsets.

We additionally have to contrast this finding with the dispensability of PDF signalling in red-light rhythms, and query which PDF-independent signalling pathways are utilised by l-LN$_v$s to contribute to a hierarchical shift. A known direct signalling pathway from the l-LN$_v$s to s-LN$_v$s requires PDFR in the s-LN$_v$s (Parisky et al., 2008). This pathway is a thus unfeasible mode of repression in RR, as RR rhythmicity persists in the absence of PDF signalling. The simplest explanation is that photic input via the visual pathways alleviates a repressive effect of l-LN$_v$s that prevents E-cell control of behaviour, even in the case of s-LN$_v$ defects, though testing this hypothesis will be an avenue of future work.

Future experiments could address the effect of combined pdf-cell hyperexcitation on a *Pdf*^{01} background, to see if this either bolsters or limits RR rhythms. Future experiments could also utilise the split-GFP GRASP system to validate putative connections between the l-LN$_v$s and LN$_d$s/ 5th-s-LN$_v$ as a potentially required link, and split-*Gal4* lines to manipulate l-LN$_v$s connections alone (Feinberg et al., 2008, Dionne et al., 2018).

CRY has been shown to be unresponsive to red light, however these experiments limited exposure to several minutes (Yamaguchi et al., 2010). To formally exclude an unconventional active role for CRY, as raised in (Im et al., 2011), a $cry^{01}Pdf^{01}$ double mutant may be a useful future experiment. Equally feasible is a biological function for inactive CRY, which would result in differences between *cry* mutants in LL and wt flies in DD, though no such role has been posited. Co-Immunoprecipitation of CRY in DD, followed by proteomic analysis would give insight into potential functions.

Sex specific differences emerge in behavioural rhythmic strength in constant red light (Relevant to Section 5 and Appendix):

A recurrent theme, evident in Figure 5.1, which occurs repeatedly throughout the RR chapter is that female rhythmicity in RR is comparably fragile in response to genetic interrogation, and several manipulations which leave the clock circuit unperturbed results in relatively weaker rhythms. The segregation of rhythmic or arrhythmic female genotypes is not particularly enlightening, and does not uncover an obvious required cell or process specific to females. Weakened DN1 firing is one of few established sex-dependent differences, and whilst we fail to show $DN1_p$ firing affects RR or DD rhythms, it is feasible that firing dynamics differ in other cells between gender. Relative evening anticipation is lower in females, which may be related to weakened siesta, but may indicate a weakness of the E cell oscillator in these flies, with relevance to RR rhythms (Figures 5.24 & 5.25).

It is likely that a combinatorial effect of x-chromosome background and sex-dependent wiring differences is responsible for the effect, though this could not be confirmed within this study. *Pdf>dsLar* shows a particularly compelling segregation of rhythmic strength in male vs female flies in RR, reflective of the idea that s-LN_v dorsal projection signalling is essential for female behaviour but dispensable for male behaviour, and circuit dimorphism must exist which allows only the male PDF-ve cell network to control rhythmic behaviour (Figure 5.27).

PDF levels appear consistently higher in males than females, a sex-dependent difference within the s-LN_vs, which may provide clues as to the increased reliance on these cells in rhythm generation in females, as potentially residual PDF cell function in males will have a comparably broader effect on rhtyhmicity (Park and Hall, 1998). (Lee et al., 2006)

shows NPF expression within the LN_ds differs between sex, though they fail to demonstrate rhythmic consequences of this, though as NPF regulates aspects of behaviour, this may only be unmasked in certain conditions, such as RR. Our work is immediately unhelpful in dissecting sex-specific differences in rhythm generation, though such an approach is necessary to tackle differences in network properties. A future experiment of interest could attempt to feminise male brains through expression of *transformer*, and identify changes in RR rhythmicity (Butler et al., 1986). Spatial mapping could further dissect the cellular basis of sex-specific differences.

Conditional mapping of shifted pacemaker function in constant red light (Relevant to section 5.3 and 5.4)

Unfortunately, *UAS-cyc*Δ^{103} flies, lacking a driver do not show consistently strong rhythms, suggesting either leaky expression or other defects associated with this line. Attempts to perform this analysis with another dominant-negative responder, *UAS-ClkΔ*, were unsuccessful (data not shown).

Firstly, whilst we demonstrate no behavioural phenotype in *repo> cyc*Δ^{103} (Appendix Figure 23), a recent publication shows *repo> cyc*Δ^{103} removes rhythms in PDF axonal remodelling. As multiple behaviourally rhythmic lines lack glial rhythms, including all rescue experiments utilising the elav driver, either glial clocks do not control this rhyhtmic remodelling, or this rhythmic remodelling is not required for behavioural rhythms (Ng et al., 2011, Herrero et al., 2017).

TUG> cycΔ^{103} and *cry$_{13}$> cycΔ^{103}* are majority arrhythmic in DD and RR, demonstrating that cells within this cluster influence behavioural rhythms (Figure 5.7). It would be expected that *(TUG-Pdf80)> cyc*Δ^{103} would be the most rhythmic of the experimental lines in DD, as PDF neurons are both necessary and sufficient for freerunning behavioural rhythms. *(TUG-Pdf80)> cycΔ^{103}* has non-significantly more rhythmic flies and a higher RRP than TUG, not only in DD, but in RR, indicating that the PDF neurons are not entirely marginalised in red light (Figure 5.9). Undriven *UAS*-cycΔ^{103} RRPs are generally higher than *(TUG-Pdf80)> cycΔ^{103}*, though the difference is not significant for any sex and condition (Figure 5.9).

The Shafer lab has studied period length changes in clock neuron subsets to suggest

behavioural period length is an emergent property, an integrated value comprised of rhythmic information from a variety of subsets, though the point where this final behavioural period first manifests, in a molecular or neuronal rhythm, is unknown (Yao and Shafer, 2014). It must be considered that the myriad evidence of desynchronised rhythms stemming from molecular changes in clock cell subsets must disrupt this coalescence of information, or else signal in such a pattern to compete with an emergent period. These converge on the concepts of dysfunctional intercellular communication and/or the emergence of irreconcilable differences in local periodicity or phase. Where others have manifested this through neuroanatomical defects (Yoshii et al., 2004, Wulbeck et al., 2008) or altering neuronal firing properties (Nitabach et al., 2006, Sheeba et al., 2008b) we show this can be achieved in RR simply through impacting oscillator function.

The phenomenon of split rhythms exemplified in *Pdf> cyc*Δ^{103}, composed of a short ~22 hr rhythm and ~25 hr rhythm have been identified by other groups following changes to PDF cell neuroanatomy or electrical activity (Dolezelova et al., 2007, Rieger et al., 2006, Yoshii et al., 2004, Wulbeck et al., 2008, Yoshii et al., 2009). These are tied to an internal desynchrony in molecular rhythms, potentially related to a loss of PDF signalling, or through differing responses to LL input in different neurons. In *cry*^{b} flies in LL, M cells possess a shorter molecular rhythm and E-cells control the longer rhythm (Rieger et al., 2006). However, *Pdf*^{01} flies in RR only possess a single shorter rhythm, indicating that network desynchrony and constant visual pathway input does not result in multiple rhythms (Cusumano et al., 2009). (Nitabach et al., 2006) demonstrates rhythm splitting can occur concurrent with an increased molecular oscillation period length in the s-LN_vs, so potentially a partial loss of CYC results in slower accumulation of functional TIM/PER and a longer period, contributing to the desynchrony. Demonstrably, excessive CYC has the opposite effect, of shoterened period, as seen in *cyc*^{01} *[elav.cyc]*^{ts} lines (Figures 3.1 and 3.2). It is notable, however, that less severe rhythm splitting can occur on control lines, suggesting that this is an intrinsic effect of RR hastened by alterations to period length. It has been shown that deviant period lengths can disempower an oscillator, which may contribute to rhythm splitting (Yao and Shafer, 2012)(Beckwith and Ceriani, 2015)(Yao et al., 2016).

Pdf>Kir2.1, Pdf^{01} and *Pdfr*^{5304} flies have a single short period, supporting the role of a dominant E-cell driven ~22 hr molecular rhythm defining behaviour in RR (Figures 5.1,

5.2 and 5.5). In contrast, s-LN_v-specific ablation results in a long period of ~26 hrs in both RR and DD, though this may be related to low temperature. The long-period component of the split rhythms of *Pdf> cycΔ^{103}* flies are lost following addition of *Pdfr^{5304}* , and we would expect residual PDF cell oscillator function produces the long-period component, which may even be lengthened by lowered, but existant CYC levels. Potentially the period of the molecular oscillations in individual neurons in RR differs to that of *cry^{b}* flies in LL, perhaps suggesting that RR differentially affects molecular rhythms to other wavelengths. A ~22 hr molecular oscillation in the E-cells has not been observed and would require timecourse immunofluorescence experiments. An immunofluorescence timecourse in the split rhythm genotypes *Pdf> cyc*Δ^{103} and *TUG-Pdf80> cyc*Δ^{103} would also be interesting to define respective subsets controlling behaviour.

PDF-specific defects may still be detrimental to rhythms in this condition, if flies developmentally resemble the case of *Pdf>cycΔ^{103}*, in which split rhythms emerge, suggesting an influence of either AR or low-CYC-containing PDF neurons on the red-light circuit (Figure 5.8). Comparison of the *Pdf>cycΔ^{103}* split rhythms with a line exhibiting PDF-specific repression of the negative arm of the oscillator, such as PER or TIM RNAi would determine if split rhythms are the result of the arrest state or general arrhythmia.

Spatial PER re-introduction neatly points to insufficiency of a PDF cell oscillator for RR rhythms, alongside sufficiency of an E cell oscillator (Appendix Figure 30, Figure 5.12). CYC re-introduction requires broad driver expression for RR rescue, potentially as many specific driver lines appear to lose expression strength in E cells, or E cells themselves may be absent, though suggests other parts of the RR circuit may require CYC, if not oscillations. (Goda et al., 2011) has demonstrated PER-reintroduction only needs to be adult-specific for wt behaviour, so RR mapping has additionally allowed us to define CYC requirement.

Essential future work is a characterisation of molecular phase within E cells in this condition, as (Cusumano et al., 2009) demonstrates antiphase cycling, aligned with evening-to-morning shifted behaviour of *Pdf^{01}* mutants, manifests in RD, whilst (Im et al., 2011) says E cell oscillations are deranged in *cry^{b}* flies in LD and LL, and it is imperitive we demonstrate E cells are capable of pacemaker function through existence

of a robust molecular oscillation in the absence of M cell input, such as in Pdf^{01}. (Im et al., 2011) stands in contravention to our data and (Cusumano et al., 2009), in arguing the short period behaviour in LL cry^{b} $Pdfr^{5304}$ mutants is due to control by a PDF cell oscillator.

Network properties of photic input, clock cell interconnectivity and output pathways differ in constant red light and constant darkness, relevant to Sections 5.5-5.8.

Despite demonstration of a requirement for l-LN_vs and the compound eye in RR rhythms, the link between these is surprisingly poorly understood, and the hope of a direct link to photoreceptors may be over-optimistic. l-LN_vs are known integrators of photic input in a CRY-dependent manner, resulting in altered membrane exciteability (Sheeba et al., 2008a, Fogle et al., 2011, Fogle et al., 2015), and extensively innervate the optic lobes, but response to visual system signalling is poorly studied. The l-LN_v circadian shift from tonic to burst firing is mediated by cholinergic inputs from L2 lamina neurons, rather than directly from photoreceptors, and L2 neurons themselves do not directly connect to the l-LN_vs (Muraro and Ceriani, 2015). It is likely that l-LN_v input from RR may be subsequent to visual processing from lamina to medulla neurons. As flies appear to lack cognition of red light, the pathway linking red light and the l-LN_vs may not be intuitive.

However, the l-LN_vs are not neccesarily the sole source of visual system input. The larval PDF-ve 5^{th} LN_v, part of the adult E cell pacemaker, is directly responsive to visual system inputs following combined CRY loss and PDF cell ablation, though bizarrely retains molecular oscillations in LL whilst CRY is present within these cells (Picot et al., 2007, Klarsfeld et al., 2011). Such a connection extending into adulthood is feasible, is suggested to exist from neuroanatomical data and may suggest l-LN_v play an alternate role in RR (Johard et al., 2009). The effectiveness of *hisCl1* knockdown was not tested, so whilst we might surmise that a direct link from photoreceptors to the l-LN_vs via histamine signalling is not occurring, further work is required to manipulate HISCL1 and ORT levels in clock neurons and known neurons downstream of the visual pathway (Figure 5.15).

Study of neuronal activity of clock cell groups on freerunning rhythms is surprisingly

limited compared to sleep and LD studies, in part due to the difficulty of conducting electrical recordings in DD, so although our reliance on behavioural data is a severe limitation, our work remains relatively comprehensive. Manipulation of electrical activity in further driver lines, such as DN-specific drivers *Clk4.5*, *Clk9* or split-*gal4* lines targeting smaller numbers of clock cells could be useful future experiments (Zhang et al., 2010). Our mapping provides us novel insight into DD rhythmicity, demonstrating that E-cell silencing reduces both DD and RR rhythmicity (Figures 5.17 & 5.18). (Liang et al., 2017) suggests E cell Ca^{2+} activity is rhythmic and highest in relative evening, dependent on PDF signalling, and a failure to produce this peak of firing may disrupt behaviour. Potentially this requirement for PDF signalling may be alleviated in RR, potentially changes in l-LN_v firing associated with light input can induce this peak independent of PDF. Feasibly, *TeTxLC* expression in IPC cells, which occurs in both *R54D11* and *R78G02* drivers may have an independent effect on rhythmicity, which could be addressed in the future with split-*gal4* lines. Though never independently published, (Johard et al., 2009) mentions, with the "data not shown" caveat, that *mai→179*-driven *TeTxLC* blocks RR rhythmicity, supporting our findings.

It appears that silencing of evening cells with tetanus toxin or *Kir2.1* can remove behavioural rhythms in constant red light, whilst hyperexcitation does not (Figures 5.17 & 5.18). Though not performed due to time constraints, the effect of silencing *R78G02* or *R54D11* with the addition of *Cry-gal80* would be informative in mapping this recurrent defect to the E cells.

The requirement for E cell firing in the mediation of rhythms in RR is not unexpected, as to have pacemaker function necessitates a propagation of rhythmic information. It is surprising then, that E cell firing would have such an important role in DD rhythmicity, in which E cell oscillators are not required at all (Figure 5.18, Section 5.4)(Stoleru et al., 2004). Any hypothesis we could propose is wildly speculative, but the effect of PDF cell and dorsal cell firing rates in cases of E cell silencing would be of immense interest.

A requirement for electrical activity in the manifestation of rhythmic information is established for pacemaker function in the s-LN_vs, so such results for E cell silencing in RR are not unexpected, but in DD are novel (Nitabach et al., 2002, Depetris-Chauvin et al., 2011). However, *Pdf>TeTxLC* does not result in particularly weak behaviour, and these do not differ between RR and DD, (Figure 5.2), suggesting that slow chemical

synaptic transmission has a greater relevance in E cell control over behaviour. Tetanus-insensitive SNARE-dependent exocytosis may also be utilised. A preponderance of dense-core-vesicles at non-synaptic sites in the s-LN_v dorsal projections suggests non-synaptic communication is important in s-LN_v signalling, likely involving PDF (Yasuyama and Meinertzhagen, 2010).

Loss of ITP signalling or ITP cell oscillator function has little effect on RR behaviour, so other synaptobrevin-dependent signals are involved in E cell signal transduction. Hence E cell molecular rhythms and signalling are important for behavioural rhythms in RR, with potentially redundant or non-existent function of the ITP cells.

The Rosbash lab demonstrates, as a supplemental figure and without further comment, that *TeTxLC* and *Kir2.1* expression in *dv-Pdf*+ve PDF-ve cells, encompassing the 5^{th} s-LN_v and four LN_ds results in reduced rhythmicity in DD (Guo et al., 2014). This complements our dataset nicely and reassures our conclusion suggesting a requirement for E-cell firing in promoting freerunning rhythmicity.

We have established differential requirements of leucokinin signalling in RR and DD, which will be consolidated with knockdown experiments in future work (Figure 5.23). The influence of leucokinin signalling on LD profiles has surprisingly not been published either, and an impact on morning, but not evening anticipation would be noteable. The (Cavey et al., 2016) paper independently shows a PDF-responsive rhythm in the Dh44+ve cells, hypothesised to exist in (Cavanaugh et al., 2014), though we do not see differences between RR and DD rhythmicity across a range of PI cell manipulations, unlike with leucokinin signalling. Dh44 cell Ca^{2+} rhythms are shown to be entirely dependent on PDF signalling, and as such cannot majorly contribute to RR rhythms, which persist in the absence of PDF (Cavey et al., 2016). It is likely that multiple, time-of-day specific output circuits exist, though our dataset would argue that the PI pathway is only a minor output pathway. Indeed, that the PI controls many behaviours would argue that ablation or altering firing of PI cells may blunt behavioural rhythms through asserting an independent behavioural imperative that overrides rhythms, rather than by disrupting a daily rhythm in PI neuron firing (Terhzaz et al., 2007, Sellami and Veenstra, 2015, Martelli et al., 2017). Dh44 neurons are LKR+ve, suggesting further interactions may occur between these output pathways (Cannell et al., 2016).

Leucokinin signalling pathways may be directly downstream of PDF cells, with the contribution of PDF-ve clock cells to the DD circuit consisting solely of signalling back to s-LN_vs, potentially involving axo-axonal connections. Our conditional CYC rescue data argues that PDF-ve cell CYC is required for DD rhythms, arguing either that other cells are involved, or they contribute to basic PDF cell function (Figure 4.18). The dispensability of LK for RR rhythmicity necessitates RR-specific-pathway outputs, though the reason this output is limited in DD is unknown (Figure 5.23). LN_ds are known to send projections dorsally to the PI, though specific targets are unknown (Hermann-luibl et al., 2014).

A loss of CYC in PDF cells alone does not prevent an emergent E-cell rhythm (Figure 5.28). As s-LN_vs are not required for RR rhythms, it is not controversial to argue that neither is s-LN_v CYC (Figure 5.6). PDF cell oscillators similarly are not required, yet manipulations that electrically silence or ablate l-LN_vs, diminish RR rhythms. l-LN_vs may have a function in gating RR-mediated network changes despite lowered CYC. However, the inability of E-cell specific CYC reintroduction to generate rhythmic phenotypes, in drivers where PER reintroduction is sufficient, suggests CYC is required in other cell groups for E cell pacemaker function to manifest, possibly a developmental role rather than one in sustaining molecular oscillations. We have not studied if the molecular oscillator is re-established in the E-cells in the case of adult-specific CYC rescue, which may be necessary to strengthen our conclusions, as a range of clock cell drivers may be weakened in cyc^{01}, limiting rescue. CYC rescue in both l-LN_vs and E cells, the two known subsets required for RR rhythmicity, fails to rescue RR rhythms, suggesting either that the drivers employed are not efficient in cyc^{01} background or that another clock cell cluster requires CYC for output specification (Figure 5.28). No published work has looked downstream of the E cells, so in hypothesising additional CYC+ve cells are required suggests rhythmic signalling from the E cells may pass to other clock cells, likely DNs, or potentially l-LN_vs, which then contact output neurons. Alternately, E cells may be capable of propagating rhythmic information to output neurons, but signalling from other clock cells requiring developmental CYC may be required to make output neurons amenable to E cell signalling. Unfortunately, or excitingly, the questions we ask exceed our knowledge of the clock circuit, and future work would require a detailed analysis of network structure and electrical activity using Ca^{2+} imaging, trans-tango and GRASP.

We appear to decouple RR rhythms from LD evening anticipation. The Rouyer lab has published that E-cell CRY is required in the absence of PDF-cells or signalling for E peak (Cusumano et al., 2009). This highlights a CRY-dependent and a CRY-independent function of the E cells, wherein the activity peak of RR is CRY-independent, yet CRY activation still mediates the E peak. There is a suggestion that CRY is required for the maintenance of robust rhythms in the LN_ds in the absence of PDF signalling (Im et al., 2011), maybe akin to findings that cry^M , a truncated light-insensitive *cry* mutant, is capable of transcriptional repression in the eye, yet cannot be light-activated (Collins et al., 2006). The Blau lab only studied peripheral and s-LN_v CRY, so a function in the LN_d oscillator is feasible (Collins et al., 2006). A requirement for inactive CRY would be supported by reduced RR rhythmicity in $Pdfr^{5304}::cry^{b/01/02}$ relative to $Pdfr^{5304}$, suggesting E cell rhythms require inactive CRY and CRY is thus supporting the E oscillator. 12:12 RD cycles may alter evening anticipation in these lines, and could be an avenue of future research.

A previous study has shown tetanus toxin expression in the E cells with *mai179-gal4, Pdf-gal80* abrogates evening anticipation and RR rhythmicity, which may partially support our results with *R78G02-gal4* and *R54D11-gal4* driving TETXLC. (Johard et al., 2009)(Figure 5.18). However, a link between synaptobrevin-mediated signalling in the E cells in RR and LD supports an expected role of these cells in activity promotion in both conditions.

We must consider that the 12:12 LD cycle does not faithfully replicate natural conditions, and in the wild, red-light wavelengths will dominate the available light spectra during dawn and dusk. However, in the context of an environmental light and temperature profile the timing of E peaks will be complexly regulated (Vanin et al., 2012, De et al., 2013, Green et al., 2015).

We repeat findings from the Shafer lab, demonstrating that the advanced E-peak observable in LD following a loss of PDF signalling is due to loss of PDF signalling within the l-LN_vs (Schichtling et al., 2016). Morning anticipation however is not so well understood, and it is unfortunate that at the low temperature we conducted our conditional PDF-cell ablation experiments, 17ºC has reduced activity prior to lights-on, as has been discussed in Chapter 3. In future work we could run short day cycles, with a 10 or 8 hour light-phase to attempt to maximise morning anticipatory activity, from

which we could then study the effect of s-LN_v-specific ablation on morning anticipation.

The shifted behavioural circuit in constant red light is disrupted by developmental loss of *cycle*, which is not rescued by developmental expression in isolated clock-cell subsets (Relevant to Section 5.9)

RR arrhythmia in cyc^{01} *[elav.cyc]*^{ts} and *[timP.per]*^{ts} following developmental CYC loss is not unexpected, as evening anticipation is not evident and we failed to identify PER+ve nuclei corresponding to the LN_ds following developmental CYC loss, and molecular arrhythmicity in these cells may very neatly explain arrhythmia beyond developmental defects.

The greater rhythmicity of 29→29°C cyc^{01} *[elav.cyc]*^{ts} males in RR than DD must be acknowledged, though is difficult to explain (Figures 3.3 & 5.26, Appendix Tables 22 and 23). CYC overexpression does not have aberrant effects beyond period increase, as highlighted by the rhythmicity of heterozygous cyc^{01} *[elav.cyc]*^{ts} controls (Figure 3.4). Spatial mapping of CYC requirement in RR cannot be mapped with the detail of PER re-introduction due to identified issues with driver strength in cyc^{01}, though an abstract PDF-ve cell requirement can be confirmed.

per^{01} *[elav-Pdf80.per]* in (Stoleru et al., 2004) fully rescues both morning and evening anticipation in LD cycles. Similarly, PDF-cell ablation fails to remove evening anticipation (Figure 3.16), whilst cyc^{01} *[elav-Pdf80.cyc]* ^{ts} lack evening anticipation (Figures 3.10 & 3.11), so potentially dominant defects caused by PDF-cell CYC loss disrupt Evening anticipation. In spite of this, a residual rhythm emerges in cyc^{01} *[elav-Pdf80.cyc]* ^{ts} in RR, suggesting, RR rhythms cannot be considered a perduring form of evening behaviour, and furthermore, that a developmental PDF cell defect blocking evening anticipation fails to commensurately block RR rhythms, suggesting that separate output pathways exist, either in signalling downstream of the E cells, or else via secondary oscillator function.

We can definitively state from this work that we have isolated several novel properties of the clock circuit resulting from photic stimulation via the visual pathway, comprising an initial characterisation of a readily inducible network state, and an interrogation that informs us of the underlying machinery of this network. Assaying developmental CYC

loss flies in this condition has informed us both of the severity of the defect, the cellular basis of CYC requirement in PDF-ve cells.

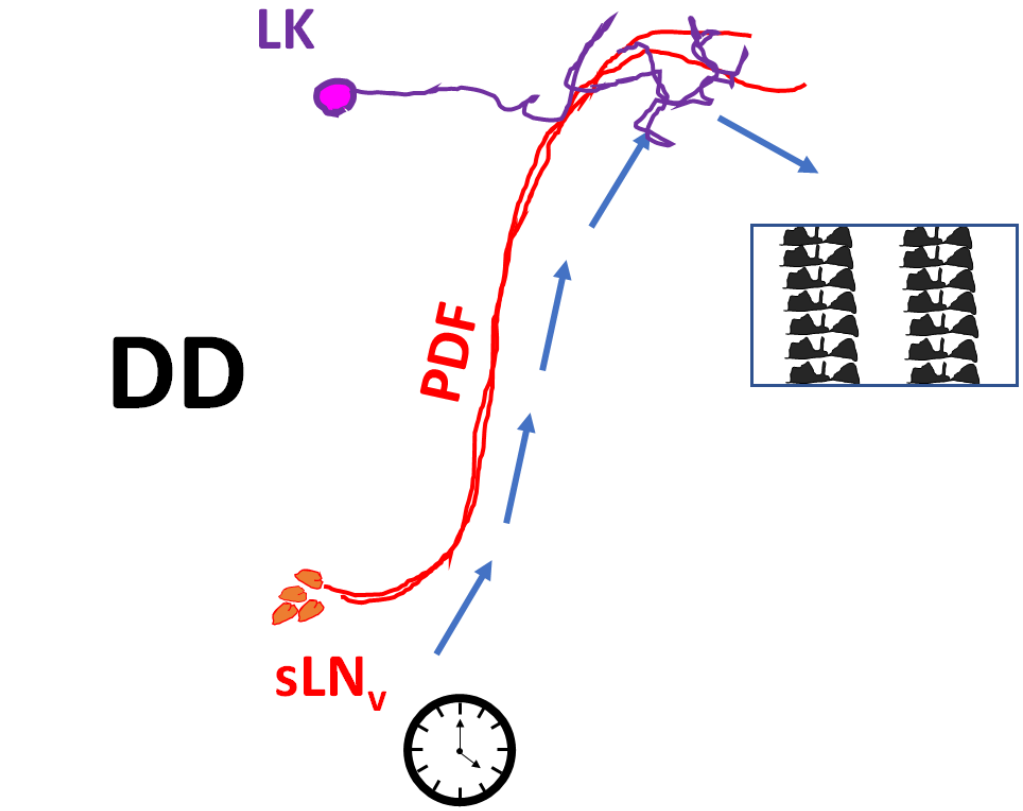

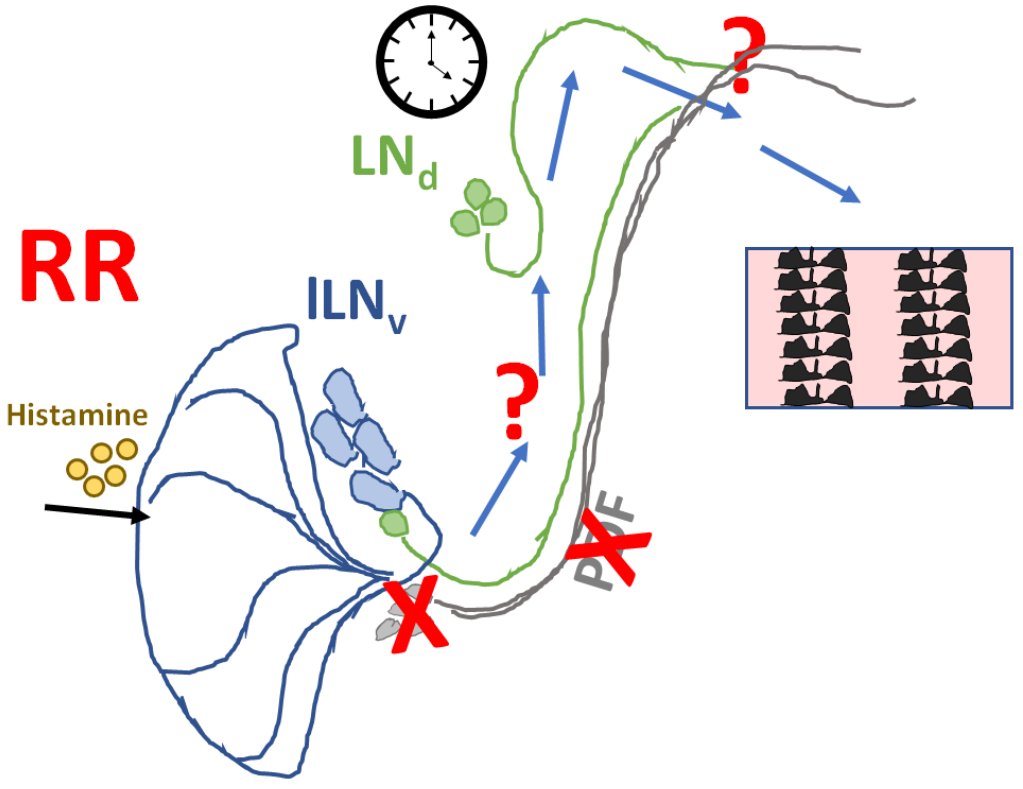

Figure 5.31 - Summary model of differing networks of rhythmic behavioural generation in constant darkness and constant red light. *In the absence of light information, molecular oscillations in the s-LN_vs, co-ordinate the rhythmic release of PDF neuropeptide to Leucokinin neurons, amongst others, resulting in rhythms in behaviour. Both Leucokinin peptide and receptor, PDF and the s-LN_vs are dispensible for behavioural rhythms upon constitutive exposure to constant red light. Electrical activity, and presence of the l-LN_vs is required, as is the visual transduction pathway, the neurotransmitter Histamine and a molecular oscillation within 3 LN_ds and one PDF-ve 5^{th} s-LN_v.*

Chapter 6 - Conclusions

With the caveats discussed in the chapters above, the major conclusions of this thesis are:

- **Developmental CYC is required for adult behavioural rhythms**
  Restriction of ectopic CYC on a *cyc*^{01} background to adult-specific expression using the TARGET system results in persistant arrhythmic majority of adults in free-running conditions, which statistically differs to flies of the same genotype run at a permissive temperature with presumed ectopic CYC expression during development.
- **Pupal-specific CYC-loss results in significant behavioural defects**
  Significant loss of adult behavioural rhythmicity can occur even when restrictive conditions are limited to late-third instar larvae through to eclosion. Furthermore, the later the developmental stage to which flies are restrictively raised, the weaker the resulting adult behavioural rhythms are. Restriction through early embryonic and 1st-instar larval phases do not result in adult bheavoiural arrhythmicity.
- **Adult-reintroduction of CYC is sufficient to restart molecular oscillations within the s-LN$_v$s**
  Peaks of nuclear PER are identifiable at predicted times of high PER during freerunning conditions in behaviourally arrhythmic flies with developmentally low CYC, following multiple days in permissive conditions as adults, suggesting first that adult-specific CYC re-expression is capable of restarting the molecular oscillator. Whilst this oscillator may not appear fully wt-like, the dynamics are not disrupted enough to account for the severity of behavioural arrhythmia observable
- **Flies lacking CYC during development possess defasciculated s-LN$_v$ processes**
  Developmental CYC loss results in significantly more complex PDF processes, comprised both of an increased complexity within the s-LN$_v$ processes, and an aberrant dorsal innervation by the l-LN$_v$s, which uniformly form synapses and terminate earlier than the s-LN$_v$s. s-LN$_v$ bouton number also appears increased. s-LN$_v$s can display a level of intermediate defasciculation within a behaviourally rhythmic population, though it is unproven if greater defasciculation can cause behavioural arrhythmia.
- **CYC loss within the PDF cells results in increased s-LN$_v$ projection**

complexity, though not to the extent of a pan-neuronal loss of CYC

Addition of *Pdf-gal80* to the conditional CYC rescue line partially damped s-LN_v rhythms, suggesting a measurable decrease in CYC levels. Concurrently, intermediate increases in projection complexity were observable, indicating CYC within the PDF cells contributed to correct PDF cell formation

- **PDF-specific CYC expression partially rescues projection com**plex**ity, though is insufficient for behavioural rescue**

  CYC re-introduction specifically within the PDF cells significantly improved molecular rhythms, indicating a resumption of CYC, which again significantly decreased projection complexity relative to cyc^{01} flies. That these were not fully wt-like may be the result of PDF-ve cell requirements for CYC

- **CYC is required for ITP protein production, whilst PDP1 is required for PDF protein production, which is non-overlapping, despite interweaving roles**

  ITP is detectable within IPC cells, but not clock cells, in cyc^{01} mutants, corroborating with previously published work that CLK/CYC regulates ITP synthesis. Expression strength of numerous drivers is reduced in these cells in cyc^{01}, suggesting broad transcriptional changes, however, adult-specific CYC reintroduction results in visible ITP+ve clock cells, in numbers not significantly differing to wt, suggesting developmental CYC loss does not affect specification of these post-embryonic cells. We also demonstrate ITP fails to significantly contribute to rhythmicity, even, as previously suggested, in controlling behaviour in a PDF-independent circuit

- **Constant red light represents a state in which PDF cells and associated functions, whilst still dominant in control of behavioural rhythms, can be removed without resulting in widespread arrhythmia, as is the case in a freerunning condition**

  Pdf^{01} and $Pdfr^{5304}$ display weak short-period rhythms in RR, comparably stronger than in DD, as has been previously suggested in cry^{b} in LL. However, PDF-cell silencing with *Kir2.1*, or ablation with *hid* results in RR arrhythmia, a result which indicates PDF cells, but not PDF, is required for RR rhythms. s-LN_v specific ablation, despite freerunning arrhythmicity, does not disrupt RR rhythms, meaning l-LN_v presence and firing, but not PDF signalling is an integral component of RR behavioural rhythm generation.

- **Behavioural rhythms in constant red light appear to be disproportionately**

dependent upon the molecular rhythms and firing state of the 4-cell E pacemaker, though not the ITP+ve half of the E-cell cluster

Constitutive reduction in CYC function within CRY+ve cells results in a loss of RR and DD rhythmicity. Conditional PER re-introduction in M cells were insufficient for RR rhythms, whilst E-cell re-introduction, encompassing multiple drivers, appeared to do so, demonstrating a clear pacemaker function for E cells in RR. The molecular state of E cells when dominating behaviour in RR, however, has not been characterised and is likely phasically unique, according to the literature.

- **RR-induced network shift is dependent upon the presence of the compound eye and intact histamine signalling**

  Loss of visual transduction or an intact compound eye or histamine signalling, the primary signal of visual output to the brain, eliminated the residual short-period phenotype of Pdf^{01} flies in RR. However, knockdown of the only characterised clock cell histamine receptor did not, suggesting that RR stimuli passes through the compound eye, and reaches the clock circuit via histamine signalling and an unknown intermediate. Either the E cells or l-LN_vs could be sources of RR input.

- **Developmental CYC loss is not rescued by RR**

  On the auspices that only PDF cell defects had been identified in behaviourally arrhythmic flies following developmental CYC restriction, RR was used as an assay to marginalise potentially defective PDF-centric outputs, however this failed to appreciable improve rhythms. Uncharacterised PDF-ve cell defects may cause enduring arrhythmicity in RR.

- **CYC expression everywhere except the PDF cells results in intact RR rhythms**

  Developmental CYC reduction abrogates RR rhythmicity, whilst developmental (and adult) loss solely in the PDF cells results in a weak yet significant RR rhythmicity, demonstrating PDF-ve clock cells require developmental CYC. This also indicates that developmental CYC loss within the l-LN_vs due to *Pdf-gal80*, which increases projection disorder, is not sufficient to disrupt the remainder of the RR circuit

- **Development-specific, but not adult-specific CYC loss is required for cyc^{01}-like nocturnal activity**

  cyc^{01}-like nocturnality is differentially effected by environmental temperature, limiting interrogation with the TARGET system. However, manipulations with

developmentally low CYC are a pre-requisite for nocturnal hyperactivity and light-induced inactivity.

- **PDF-cell specific CYC is sufficient to halt *cyc^{01}* nocturnality and initiate morning anticipation behaviour**

  Morning anticipation behaviour is known to be dependent on an oscillator within the M cells. Whilst adult-specific PDF-cell CYC rescue results in a featureless LD activity profile, constitutive CYC expression through development and adulthood results in a crepuscular activity profile with anticipatory behaviours, suggesting the CYC-ve portion of the circuit is overridden by PDF-cell CYC, which is notably not the case in freerunning conditions, reflecting divergent output mechanisms downstream of PDF cells.

- ***cyc^{01}* nocturnality persists in the absence of PDF cells**

  Despite the dominance of PDF cell CYC mentioned above, nocturnality is not predicated by CYC loss within the PDF cells, as PDF-cell ablation with hid results in a *cyc^{01}*-like profile, provoking the hypothesis that PDF-cell CYC loss primes a state in which PDF cells cannot override nocturnality intrinsic in a CYC-less PDF-ve clock cell circuit, which is supported by the ability of PDF cell hyperexcitation to limit nocturnality in *cyc^{01}*. Similarly, restriction of PDF-cell CYC rescue with *Pdf-gal80* results in a crepuscular LD profile, though it is likely residual CYC is functional in PDF cells in this manipulation.

The wider context of this work within the literature is in some cases complementary, and in other cases more controversial. The re-evaluation of s-LN$_v$ morphological defects in *cyc^{01}* flies, whilst contradicting the originally published results, argue the same point, that functional connections are disrupted in these flies, which, as *cyc^{01}* flies lack a source of rhythmic information to propagate, is noteworthy regarding behaviour only following an ectopic CYC rescue, but lends to a reappraised view of CYC functions. The mapping of this phenotype to an early pupal developmental function rather than an early-developmental lineage function is novel, and perhaps less expected, as is the potential seperability of CLK and CLK/CYC functions. The resumption of molecular rhythms following developmental CYC loss may also be considered controversial, as our groups original study, (Goda et al., 2011), shows a dampening of rhythms following developmental PER overexpression, which has been replicated since, with the assumption that developmental low CYC results in this phenotype. In other senses, this result is pleasing as many non-clock cells have been able to host molecular oscillators

following the ectopic expression of CLK and CYC, and adult-specific CLK-expression has been shown to initiate oscillations (Zhao et al., 2003, Killman et al., 2009, Liu et al., 2017).

The red light condition has been used sparingly in the past, and the general principle of constant photic stimulation resulting in a shift in hierarchy away from the PDF cells is generally agreed upon in the literature. Discrepancies emerge in the site of the secondary pacemaker, though our results of an E-cell function agree with those of the Rouyer lab. The litany of approaches we use, in driver lines and transgenes, are the most comprehensive yet, for studying this condition: the variability of results we receive reflects the danger of drawing concrete conclusions based on single manipulations, and it is only cautiously that we draw the conclusions we have. We suggest that the network hierarchy of the red-light circuit differs to the DD freerunning circuit, with RR specific bypass of the s-LN_vs as well as PDF and LK signalling. Instead, the E cells, or only the ITP-expressing subset take on a prominent role as pacemakers. Although many of the functions governing RR rhythmicity are also required for evening anticipation under LD conditions, there are distinctions that can be made between these two clock-associated functions including dependence on the combined role of CRY and PDF signalling.

Our spatial mapping of developmental CYC requirement to PDF-ve cells has not been tested in-depth, but is not unexpected, though advanced morphological characterisation unfortunately was not successful. In hindsight, a complementary approach with conditional CLK rescue, which faces more severe defects, may have aided this characterisation.

Our suggestions that PDF negative cells may contribute to nocturnality has been demonstrated before by the Allada lab, though it was not interpreted as such. Attempts within the thesis to manipulate nocturnality through alteration of firing rate within the $DN1_p$s were unsuccessful, but also limited, and there are many potential genetic configurations at our disposal that could address this. Cloning and creation of an effective *Clk4.1M-gal80* element would also be of tremendous help in this regard. The finding that a cyc^{01} circuit promotes nocturnality in the absence of PDF cells is a novel experiment, and to our standards, robust, as nocturnal flies were dissected immediately following the behavioural assay and effectiveness of ablation was confirmed. This data cannot be reconciled with the model of (Kumar et al., 2012), and requires a new model of

nocturnality.

Another interesting result lies in conditional CYC rescue experiments, which demonstrate that PDF-cell specific rescue of CYC is capable of restoring crepuscularity and morning anticipation, but not freerunning rhythmicity. The suggestion therefore, is that neural circuits in the output of morning anticipation must differ to those of freerunning rhythms, in which defects caused by CYC loss in PDF-ve cells only disrupts freerunning output. It is conceivable that this is not a wiring or specification defect, as may be the case of development-specific CYC loss: It is predicted that adult CYC loss results in a static oscillator of a certain arrest state, potentially causing a subsequent arrest state of membrane excitability, culminating in signalling from PDF-ve cells which disrupt DD behavioural rhythms. A manipulation in which PDF-ve cell CYC could be reduced specifically in adulthood would address this, although this would require the creation of new reagents.

Chapter 7 - APPENDIX – Supplemental Figures and Results

List of Appendix Tables

Table 1 - P-values comparing relative rhythmic power of of *cyc^{01} [elav.cyc]^{ts}* and cyc^{01} raised and run at various temperatures, pursuant to Table 3.1 265

Table 2 - Statistics concerning behavioural rhythmicity of *cyc^{01} [elav.cyc]$^{ts\#7}$* controls 266

Table 3 - Statistics in support of nocturnality levels following conditional manipulation of CYC levels across varied developmental and adult temperatures 269

Table 4 -Statistics in support of nocturnality levels following various manipulations affecting PDF cell function on a *cyc^{01}* background 272

Table 5 – Comparison of Light-dark pupariation preference of *cyc^{01}* and *y^{1}w** 277

Table 6 - Dataset demonstrating freerunning behavioural rhythms of *cyc^{01} [elav.cyc]^{ts}* flies raised and run at different temperatures for select periods of larval development – dataset employed in Figure 3.18 and 3.19. 277

Table 7 – Statistics pursuant to Appendix table 6, displaying P-value of signficiant differecnes between *cyc^{01} [elav.cyc]^{ts}* shifted between temperatures uring development 278

Table 8 – Statistics showing significant difference in total PDF+ve axonal complexity of *cyc^{01}* flies raised at 17, 23 or 29°C. 280

Table 9 – Statistics comparing intensity of PER stain and localisation between CT2 and CT14 for various genotypes 283

Table 10 – Statistics comparing complexity of PDF+ve s-LN$_v$ second-order processes across various genotypes 283

Table 11 - Statistics comparing s-LN$_v$ dorsal complexity between various genotypes with conditionally altered CYC levels across varied developmental and adult temperatures 284

Table 12 - Statistics comparing s-LN$_v$ dorsal complexity between rhythmic and arrhythmic subpopulations of *cyc^{01} [elav.cyc]$^{ts\#7}$* 284

Table 13 - Statistics comparing staining intensity of GFP and PDF in cyc^{01} $[pdf.cyc]^{ts\#7}$ and various controls 285
Table 14 - Statistics comparing number of clock cells in cyc^{01}, cyc^{01}/+ and cyc^{01} $[elav.cyc]^{ts}$ lines 286
Table 15 – Behavioural rhythmicities of CLK/CYC target overexpression with *elav*:: Uas-N/+ 288
Table 16 - Statistics comparing behavioural rhythms of conditional PDF cell ablation lines 292
Table 17 - Statistics comparing evening peak phase of conditional PDF cell ablation lines in 12:12 LD 292
Table 18 – Raw data for behavioural rhythmicities following spatial mapping of oscillator requirement with $cyc\Delta^{103}$ in RR or DD 295
Table 19 – Statistics pursuant to behavioural rhythmicities following subset specific CYC loss with $cyc\Delta^{103}$ in RR or DD 297
Table 20 – Behavioural data and statistics following dominant-negative CYC expression in E cells concurrent with loss of PDF signalling in 23°C RR and DD with $cyc\Delta^{103}$/+; $R78G02Pdf^{01}/Pdf^{01}$ 298
Table 21 – Continued spatial mapping of spatial mapping of oscillator requirement with $cyc\Delta^{103}$ in RR or DD 302
Table 22 – Statistics pursuant to behavioural rhythmicities following subset specific CYC loss with $cyc\Delta^{103}$ in RR or DD 304
Table 23 – Raw data for behavioural rhythmicities following spatial mapping of minimal pacemaker requirement using PER re-introduction in RR or DD 305
Table 24 – Statistics pursuant to behavioural rhythmicities following spatial mapping of minimal pacemaker requirement using PER re-introduction in RR or DD 306
Table 25 – Raw data for behavioural rhythmicities following manipulation of clock cell electrical or signalling properties in RR or DD 313
Table 26 - Statistics pursuant to behavioural rhythmicities following manipulation of clock cell electrical or signalling properties in RR or DD 319
Table 27 - Statistics comparing behavioural rhythms of *TUG-crygal80>NaChBac* in RR and DD 319
Table 28 – Behavioural data for *Pdf>TrpA1* raised and run at 23°C or 29°C RR or DD 321
Table 29 - Statistics comparing Rhythmic power for *Pdf>TrpA1* between temperature and light conditions 321
Table 30 – Raw data for behavioural rhythmicities of cyc^{01} $[n.cyc]^{ts}$ in 29°C RR or 29°C 327

DD, utilising a variety of driver lines
Table 31 – Statistics pursuant to spatial mapping of CYC requirement with *cyc^{01} [-gal4.cyc]^{ts}* in 29°C RR or 29°C DD 328
Table 32 – Statistics comparing D/N ratio of sptail CYC reintroduction between various lines in 29°C LD 329
Table 33 –Statistics comparing rhythmicity of lines following loss of glutamatergic cell oscillator function with *VGlut>cyc*Δ^{103} in RR or DD 333
Table 34 - Raw data for behavioural rhythmicities of various ITP and PDF RNAi lines in RR or DD 335
Table 35 – Statistics pursuant to behavioural rhythmicities of various ITP and PDF RNAi lines in RR or DD 336
Table 36 – Raw data for behavioural rhythmicites for conditional s-LN$_v$ ablation and controls in 17°C RR or DD 338
Table 37 - Raw data for behavioural rhythmicities of various histamine-signalling and visual system mutants in RR or DD 339
Table 38 - Statistics pursuant to behavioural rhythmicities of various histamine-signalling and visual system mutants in RR or DD 341
Table 39 - Raw data for behavioural rhythmicities of various manipulations allegedly compromising clock output functions in RR or DD 343
Table 40 - Statistics pursuant to behavioural rhythmicities of various manipulations allegedly compromising clock output functions in RR or DD 344
Table 41 - Statistics comparing number of PDF cell soma between various genotypes with manipulated CYC values 345
Table 42 - Statistics comparing behavioural rhythms of *cyc^{01} [elav.cyc]$^{ts\#7}$* across varied developmental and adult temperatures in RR and DD 345
Table 43 - Statistics comparing behavioural rhythms of *cyc^{01} [elav-Pdf80.cyc]$^{ts\#7}$* across varied developmental and adult temperatures in RR and DD 346
Table 44 - Statistics comparing behavioural rhythms of *[timP.per]^{ts}* across varied developmental and adult temperatures in RR and DD 346
Table 45 - Dataset of *cyc^{01}* behavioural rhythms 347

List of Appendix Figures

Figure 1 - Activity profile and actograms of *cyc^{01} [elav.cyc]^{ts}* females across temperature conditions 267
Figure 2 - D/N ratio of virgin and mated *cyc^{01}* females in 12:12 LD 268
Figure 3 - Activity profile and actograms of restrictively raised *cyc^{01} [elav-Pdf80.cyc]^{ts}* 269
Figure 4 – D/N ratio of 29°C LD raised *cyc^{01} [pdf+clk4.1.cyc]^{ts}* raised at various temperatures 270
Figure 5 - 12:12 LD actograms and activity profiles of *Pdfr^{5304}cyc^{01} [elav.cyc]^{ts}* raised in a variety of developmental temperatures 270
Figure 6 - 12:12 LD actograms and activity profiles of DN1$_p$-excitation with *Clk4.1M>TrpA1;cyc^{01}* or *cyc^{01}*/+ at 29°C 274
Figure 7 - 12:12 LD actograms and activity profiles of concurrent PDF and DN1$_p$-excitation with Pdf+*Clk4.1M>TrpA1;cyc^{01}* or *cyc^{01}*/+ at 29°C 275
Figure 8 -12:12 LD actograms and activity profiles of DN1$_p$-silencing with *Clk4.1M>TeTxLC;cyc^{01}* or *cyc^{01}*/+ 275
Figure 9 - day and night activity counts for 12:12 LD dopaminergic silencing of *cyc^{01}* with *ple>TeTxLC*; *cyc^{01}* or *cyc^{01}*/+ 276
Figure 10 - scatterplot demonstrating the relationship between s-LNv projection length, total projection disorder *in cyc^{01} and cyc^{01} [elav.cyc]^{ts}* 278
Figure 11 - scatterplot demonstrating the relationship between s-LNv projection length, total projection disorder *in cyc^{01} and cyc^{01} [elav.cyc]^{ts}* pupal brains 279
Figure 12 - Nuclear staining intensity and localisation of PER in l-LNvs for restricitively or permissively raised, permissively run *cyc^{01} [elav.cyc]^{ts}* 280
Figure 13 - Nuclear staining intensity and localisation of PER in l-LNvs for *cyc^{01} [elav.cyc]^{ts}* across various developmental and adult temperatures 281
Figure 14 - Nuclear staining intensity and localisation of PER in l-LNvs for permissively raised and run *cyc^{01} [elav-Pdf80.cyc]^{ts}* 281
Figure 15 - Nuclear staining intensity and localisation of PER in l-LN$_v$s for permissively raised and run *cyc^{01} [Pdf.cyc]^{ts}* 282
Figure 16 – PDF+ve dorsal projection complexity and example images of MED overexpression on a low CYC background, with 29→29°C *cyc^{01} [elav.med]^{ts}*. 289
Figure 17 – Representative image of PDF and PER staining in *tim-Clk pdp1^{3135}* recombinants at CT2 290
Figure 18 – s-LN$_v$ dorsal projection morphology following ectopic PDP1 expression on a *cyc^{01}* background 291
Figure 19 – Behavioural rhythmicity of dominant-negative CYC expression in E cells 297

concurrent with loss of PDF signalling in 23°C RR and DD with *cyc*Δ^{103}/+; *R78G02Pdf^{01}/Pdf^{01}*.

Figure 20 – Behavioural rhythmicities for *Pdf>TrpA1* raised and run at 23°C or 29°C RR or DD 320

Figure 21 – Behavioural rhythmicity following knockdown of various neuropeptides with *dcr; elav/+;* +/RNAi in 23°C RR and DD 322

Figure 22 – Mean cell size of s-LN$_v$s and l-LN$_v$s in *cyc^{01} [elav.cyc]^{ts}* across temperature conditions 329

Figure 34, Relative rhythmic strength of conditional PDF ablation lines raised and run permissively and subsequently transferred to restrictive conditions as adults 330

Figure 23 – Average actograms of dominant-negative CYC expression in glia with *repo-gal4/* cyc*Δ^{103}* in 23°C RR and DD 331

Figure 24 – Average actograms of dominant-negative CYC expression in glutamatergic cells with *VGlut-gal4/ cyc*Δ^{103} in 23°C RR and DD 332

Figure 25 – Behavioural rhythmicities of ITP, HAIRY and PDF knockdown within clock cells in 23°C RR and DD 333

Figure 26, 12:12 LD actograms of *hdc^{jk910};Pdf^{01}* males and females, demonstrating advanced Evening peak 336

Figure 27, Average actograms and activity profiles for *Cry-gal4 Pdfgal80>Kir2.1*, in 12:12 LD. 341

Figure 28, taken from Karolina Mirowska thesis (2015), studying TIM oscillations in various clock cell subsets in permissively or restrictively raised *timP.per]^{ts}* 348

Figure 29, taken from Karolina Mirowska thesis (2015), entrainability of *cyc^{01} [elav.cyc]^{ts}* at 17°C 349

Figure 30, taken from Miguel Ramirez-Moreno thesis (2017), showing average actograms of condtional PER reintroduction in various clock cell subsets in RR and DD 350

Figure 31, taken from flylight website, displaying staning pattern of GFP driven by GM*R54D11-gal4* 351

Figure 32, taken from flylight website, displaying staning pattern of GFP driven by GM*R78G02-gal4* 352

.

Appendix

	Distribution of rhythms	**RRP**
17→29 °C ♀ *cyc^{01}[elav.cyc]^{ts}* vs 29→29 °C ♀ *cyc^{01}[elav.cyc]^{ts}*	*>0.001***	*>0.001***
23→29 °C ♀ *cyc^{01}[elav.cyc]^{ts}* vs 29→29 °C ♀ *cyc^{01}[elav.cyc]^{ts}*	*0.004***	*>0.001***
17→17°C ♀ *cyc^{01}[elav.cyc]^{ts}* vs 17→29 °C ♀ *cyc^{01}[elav.cyc]^{ts}*	*0.656*	*0.455*
29→17°C ♀ *cyc^{01}[elav.cyc]^{ts}* vs 29→29 °C ♀ *cyc^{01}[elav.cyc]^{ts}*	*>0.001***	*>0.001***
17→29 °C ♂ *cyc^{01}[elav.cyc]^{ts}* vs 29→29 °C ♂ *cyc^{01}[elav.cyc]^{ts}*	*0.045 **	*>0.001***
23→29 °C ♂ *cyc^{01}[elav.cyc]^{ts}* vs 29→29 °C ♂ *cyc^{01}[elav.cyc]^{ts}*	*>0.001***	*>0.001***
	Distribution of rhythms	**RRP**
17→17°C ♂ *cyc^{01}[elav.cyc]^{ts}* vs 17→29 °C ♂ *cyc^{01}[elav.cyc]^{ts}*	*0.998*	*0.773*
29→17°C ♂ *cyc^{01}[elav.cyc]^{ts}* vs 29→29 °C ♂ *cyc^{01}[elav.cyc]^{ts}*	*0.185*	*0.095*
17→29 °C ♀ *cyc^{01}[elav.cyc]^{ts}* vs 17→29 °C ♀ *cyc^{01}*	*0.999*	*0.475*
29→29 °C ♀ *cyc^{01}[elav.cyc]^{ts}* vs 29→29 °C ♀ *cyc^{01}*	*>0.001***	*>0.001***
17→17°C ♀ *cyc^{01}[elav.cyc]^{ts}* vs 17→17°C ♀ *cyc^{01}*	*0.999*	*0.767*
23→29 °C ♀ *cyc^{01}[elav.cyc]^{ts}* vs 23→29 °C ♀ *cyc^{01}*	*>0.001***	*>0.001***
17→29 °C ♂ *cyc^{01}[elav.cyc]^{ts}* vs 17→29 °C ♂ *cyc^{01}*	*0.999*	*0.524*
29→29 °C ♂ *cyc^{01}[elav.cyc]^{ts}* vs 29→29 °C ♂ *cyc^{01}*	*>0.001***	*0.003***
17→17°C ♂ *cyc^{01}[elav.cyc]^{ts}* vs 17→17°C ♂ *cyc^{01}*	*0.999*	*0.196*
23→29 °C ♂ *cyc^{01}[elav.cyc]^{ts}* vs 23→29 °C ♂ *cyc^{01}*	*>0.001***	*>0.001***

Appendix Table 1, showing P-values of probable significant difference between cyc^{01}[elav.cyc]^{ts} nocturnality in different developmental and experimental conditions in LD. Pursuant to data in Figures 3.2, 3.3 & 3.4, Table 1.

	Period length	Distribution of rhythms	RRP
cyc^{01} [elav.cyc]$^{ts\#7}$ vs cyc^{01} /+[elav.cyc]$^{ts\#7}$ M	0.261	0.011*	0.005**
cyc^{01} [elav.cyc]$^{ts\#7}$ vs cyc^{01} /+[elav.cyc]$^{ts\#7}$ F	0.015*	0.501	0.480
cyc^{01} [elav.cyc]$^{ts\#7}$ vs cyc^{01} [elav.+]$^{ts\#7}$ CyO M	N/A	0.015*	>0.001***
cyc^{01} [elav.cyc]$^{ts\#7}$ vs cyc^{01} [elav.+]$^{ts\#7}$ CyO F	N/A	>0.001***	>0.001***
cyc^{01} /+ [elav.cyc]$^{ts\#7}$ vs cyc^{01} /+[elav.+]$^{ts\#7}$ CyO M	>0.001***	0.300	0.087
cyc^{01} /+ [elav.cyc]$^{ts\#7}$ vs cyc^{01} /+ [elav.+]$^{ts\#7}$ CyO F	>0.001***	0.037*	0.001**

Genotype	n	% SR	% WR	% AR	TAU ± SEM	RRP ± SEM
cyc^{01} [elav.cyc]$^{ts\#7}$ M	35	11.43	40.00	48.57	23.72±0.84	1.42±0.08
cyc^{01} [elav.cyc]$^{ts\#7}$ F	31	83.87	12.90	3.23	23.5 ± 0.367	2.48 ±0.121
cyc^{01} /+[elav.cyc]$^{ts\#7}$ M	8	50	50	0	22.63±0.08	1.58±0.12
cyc^{01} /+[elav.cyc]$^{ts\#7}$ F	12	100	0	0	22.88±0.07	2.28±0.12
cyc^{01} [elav.+]$^{ts\#7}$ CyO M	13	0	7.69	92.31	26.50	1.02
cyc^{01} [elav.+]$^{ts\#7}$ CyO F	11	0	18.18	81.81	23.75±8.25	1.08±0.08
cyc^{01} /+ [elav.+]$^{ts\#7}$ CyO M	6	83.33	16.67	0	23.33±0.11	2.04±0.24
cyc^{01} /+ [elav.+]$^{ts\#7}$ CyO F	12	58.33	25	16.67	24.10±0.15	1.70±0.14

Appendix Table 2: A: P-values comparing data in Figure 3.4. Distribution of rhythmicity was generated using 2x3 Fisher's exact test, and all other values by one-way ANOVA. B:

Behavioural data displayed in Figure 3.4, demonstrating rhythmic strength and period length of various genders and genotypes in 29→29 °C freerunning conditions.

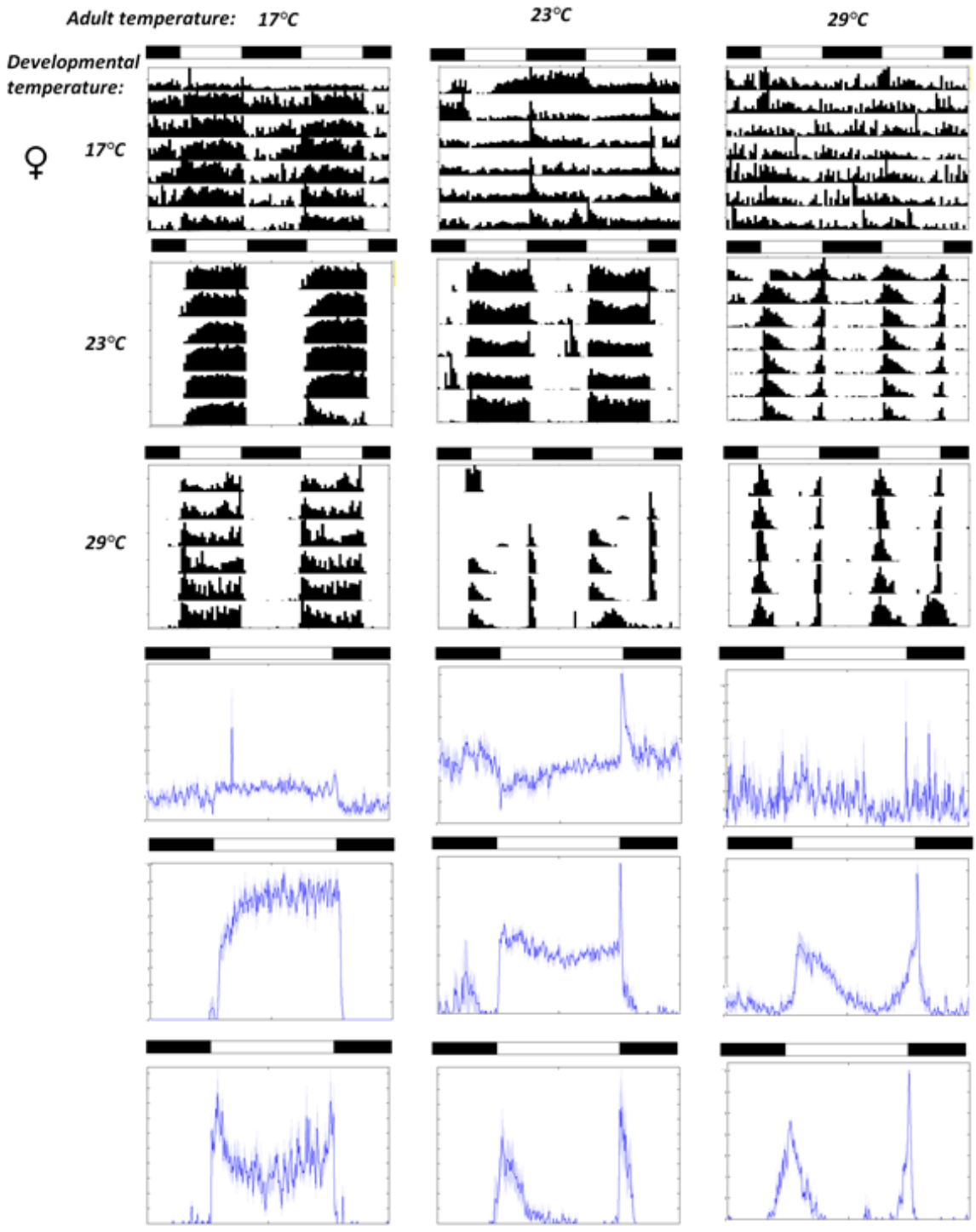

Appendix Figure 1 – 12:12 LD actograms and activity profiles for cyc^{01} [elav.cyc]^{ts} Females raised and run at 17°C, 23°C and 29°C. Accompanied in Appendix Table 1 is a summation of these values.

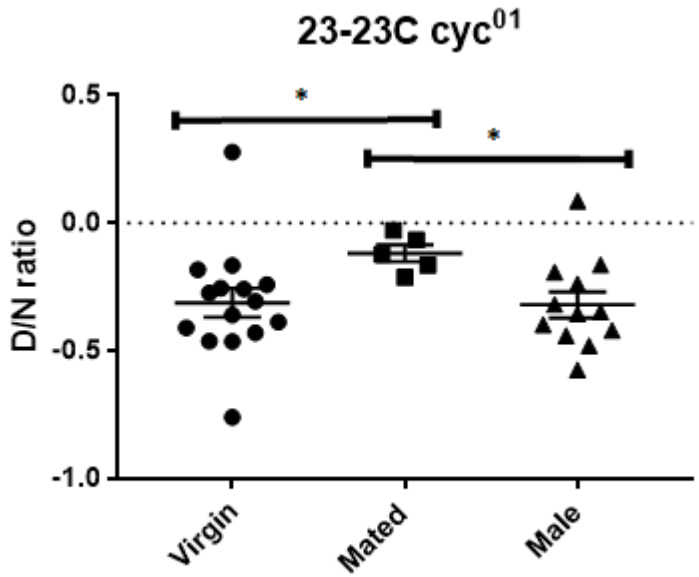

*Appendix Figure 2, Mating reduces Nocturnal preference in cyc^{01} females. Freshly eclosed females were placed in female-only or mixed-sex vials for 7 days before initiation of a 12:12 LD behavioural assay. Mated females significantly differ to virgin females (P=0.023 *) and males (P=0.013 *), which do not significantly differ (P=0.993)*

D/N ratio	**P-value**
cyc^{01}/+ [elav.cyc]^{ts} **17→29 →17 ♂ (17 vs 29)**	>0.001***
cyc^{01}/+ [elav.cyc]^{ts} **17→29 →17 F (17 vs 29)**	>0.001***
cyc^{01} [elav.cyc]^{ts} **17→29 →17 ♂ (17 vs 29)**	>0.001***
cyc^{01} [elav.cyc]^{ts} **17→29 →17 F (17 vs 29)**	0.289
cyc^{01} [elav.cyc]^{ts} **23→29 →17 ♂ (17 vs 29)**	>0.001***
cyc^{01} [elav.cyc]^{ts} **23→29 →17 F (17 vs 29)**	0.001 **
cyc^{01} [elav.cyc]^{ts} **29→29 →17 ♂ (17 vs 29)**	>0.001***
cyc^{01} [elav.cyc]^{ts} **29→29 →17 F (17 vs 29)**	>0.001***
cyc^{01} **17→29 →17 ♂ (17 vs 29)**	0.005**
cyc^{01} **17→29 →17 F (17 vs 29)**	0.258
cyc^{01}/+ [elav.cyc]^{ts} **vs** ***cyc^{01} [elav.cyc]^{ts}*** **17→29 →17 ♂ (17)**	0.559
cyc^{01}/+ [elav.cyc]^{ts} **vs** ***cyc^{01} [elav.cyc]^{ts}*** **17→29 →17 F (17)**	0.157
cyc^{01}/+ [elav.cyc]^{ts} **vs** ***cyc^{01} [elav.cyc]^{ts}*** **17→29 →17 M (29)**	0.519
cyc^{01}/+ [elav.cyc]^{ts} **vs** ***cyc^{01} [elav.cyc]^{ts}*** **17→29 →17 M (29)**	0.437
cyc^{01} [elav.cyc]^{ts} **29→29 →17 vs 17→29 →17 M (17)**	>0.001***
cyc^{01} [elav.cyc]^{ts} **29→29 →17 vs 17→29 →17 F (17)**	0.002**

***cyc*^{01} *[elav.cyc]*^{ts} 29→29 →17 vs 17→29 →17 M (29)**	0.002**
D/N ratio	**P-value**
***cyc*^{01} *[elav.cyc]*^{ts} 29→29 →17 vs 17→29 →17 F (29)**	0.865
***cyc*^{01} vs *cyc*^{01} *[elav.cyc]*^{ts} 17→29 →17 M (17)**	0.082
***cyc*^{01} vs *cyc*^{01} *[elav.cyc]*^{ts} 17→29 →17 F (17)**	0.382
***cyc*^{01} vs *cyc*^{01} *[elav.cyc]*^{ts} 17→29 →17 M (29)**	0.101
***cyc*^{01} vs *cyc*^{01} *[elav.cyc]*^{ts} 17→29 →17 M (29)**	0.181

Appendix Table 3 - P-values determined by One-way ANOVA comparing D/N ratios of various genotypes and conditions displayed in Figure 3.7

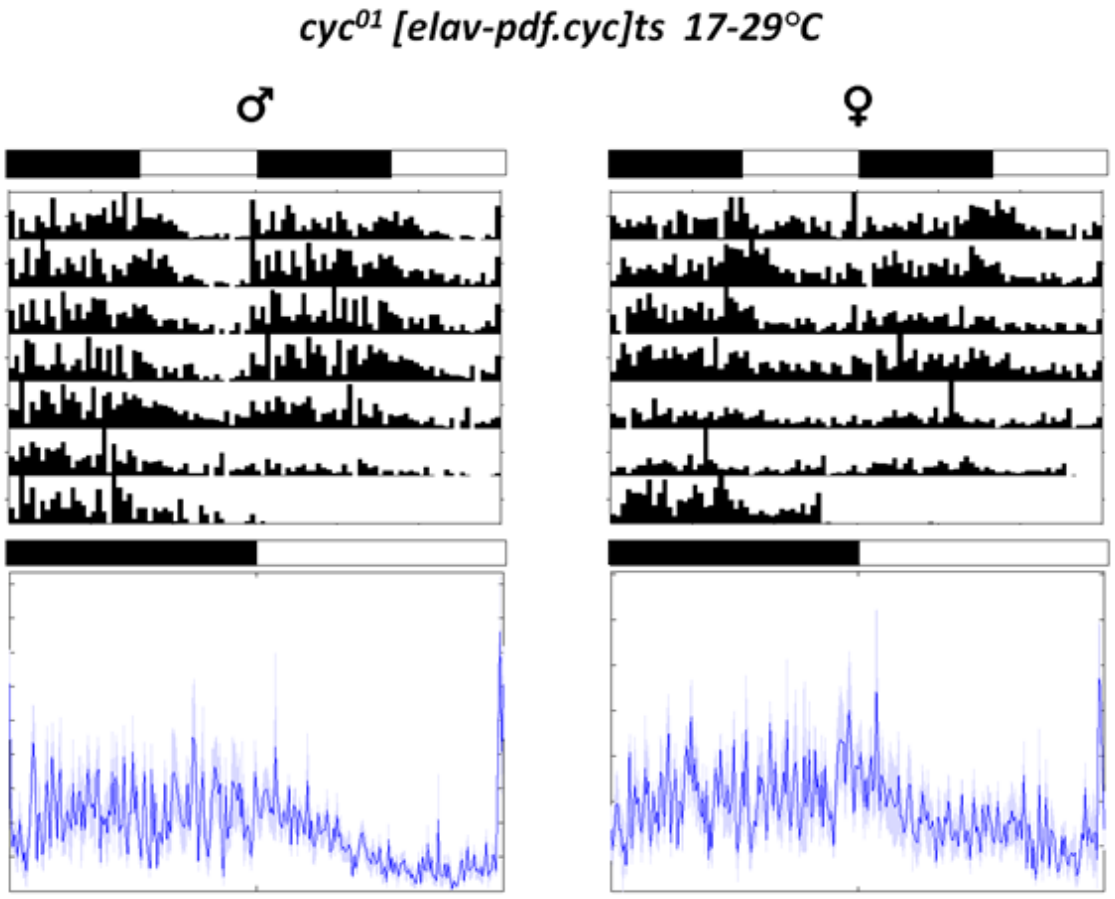

Appendix Figure 3, actograms and activity profile of 17→29 °C cyc^{01} *[elav-Pdf80.cyc]*^{ts} *in LD, reintroducing CYC into PDF-ve neurons in an adult-specific fashion. A broad nocturnal preference is observable, though this is not as severe as cyc*^{01}*, and inactivity response following lights-on is not apparent. Male n=12, Female n=10.*

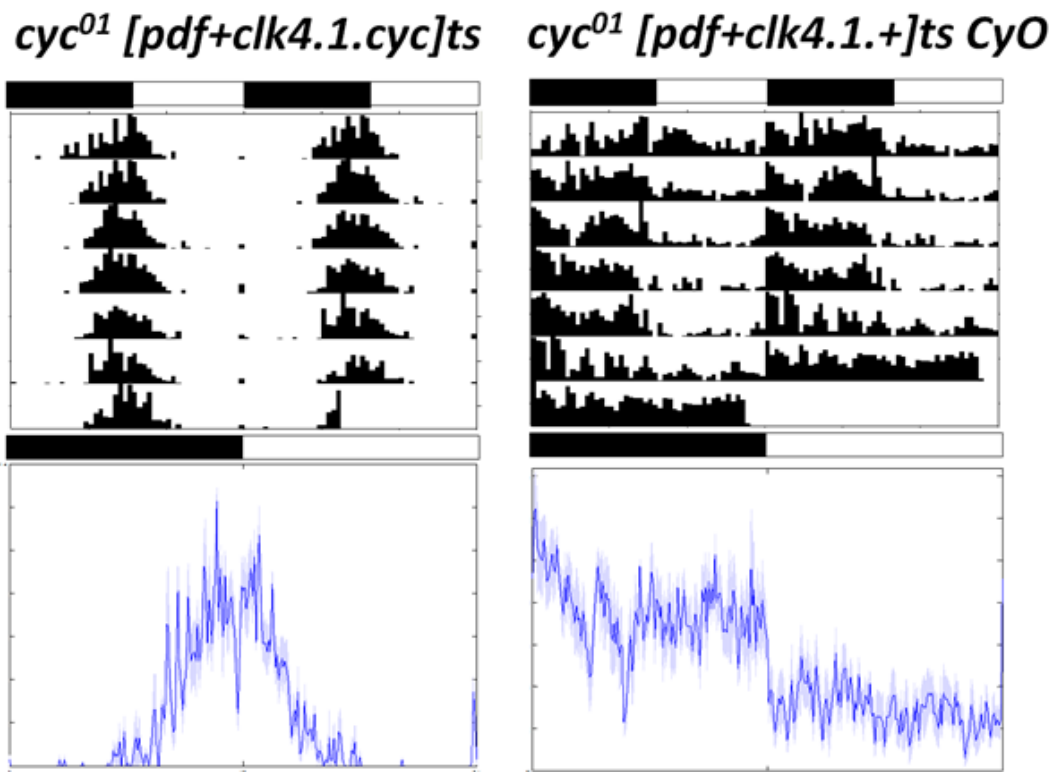

Appendix Figure 4: Behavioural data for concurrent CYC rescue within PDF+ve and CLK4.1M+ve cells of genotype cyc^{01} [pdf+Clk4.1M.cyc]^{ts} raised permissively at 29°C and run permissively at 29°C LD. Experimental n = 5, responderless control n=10.

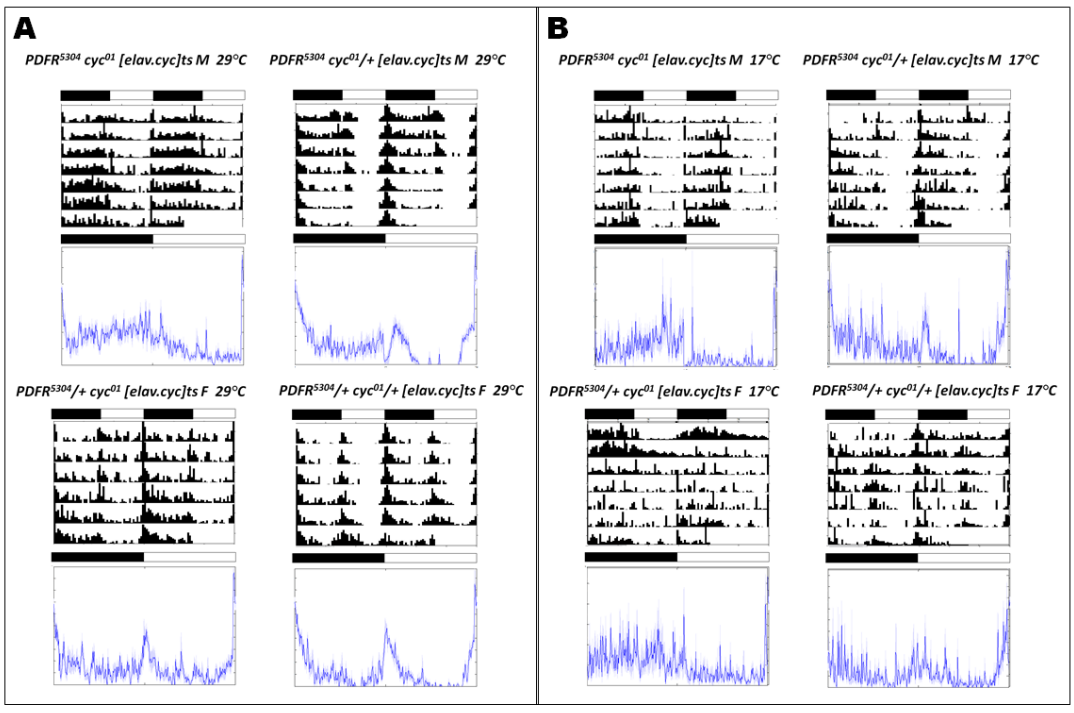

Appendix Figure 5: Panel A shows Activity profiles of permissively raised (Left four

sections) cyc^{01} [elav.cyc]^{ts} with $Pdfr^{5304}$ mutant. Panel B shows restrictively raised (Right four sections) cyc^{01} [elav.cyc]^{ts} with $Pdfr^{5304}$ mutant, disrupting PDF signalling. The upper two sections of each panel show homozygous $Pdfr^{5304}$, whilst the lower two sections show heterozygous $Pdfr^{5304}$, with presumably intact PDF signalling. The left-most two sections of each panel have elav-driver had to be moved to the 2nd chromosome for this manipulation, which we presume to have weak and largely insufficient rescue, as waveform fails to replicate cyc^{01}/+ controls. Though nocturnality is lower, Relative to 23°C $Pdfr^{5304}$;cyc^{01} in Figure 4.13, due to higher temperature, the advanced E-peak evident in cyc^{01}/+ controls is removed, and nocturnal preference dominate, regardless of PDF signalling. Notably, restrictively run females lose many aspects of the waveform, morning and evening anticipation, present in permissively raised females, suggesting 29°C is a partially permissive state. That the general architecture does not differ between permissively and restrictively raised $Pdfr^{5304}$-containing males therefore suggests independence from PDF-signalling in the defect. n numbers clockwise at 29°C=10, 5, 13, 7. For restrictively raised n-numbers clockwise were 6, 3, 6 and 3.

D/N ratio	**P=**
***cyc^{01}* vs *cyc^{01}*/+ M**	>0.001 ***
***cyc^{01}* vs *cyc^{01}*/+ F**	>0.001 ***
***$Pdfr^{5304}$; cyc^{01}* vs *$Pdfr^{5304}$; cyc^{01}*/+ M**	>0.001 ***
***$Pdfr^{5304}$; cyc^{01}* vs *$Pdfr^{5304}$; cyc^{01}*/+ F**	>0.001 ***
ple> *TeTxLC*; ***cyc^{01}* vs** ple> *TeTxLC*; ***cyc^{01}*/+ M**	0.18
ple>***TeTxLC*; cyc^{01}* vs** ple>***TeTxLC*; cyc^{01}*/+ F**	>0.001 ***
***Pdf>Kir2.1; cyc^{01}* vs *Pdf>Kir2.1; cyc^{01}*/+ M**	>0.001 ***
***Pdf>Kir2.1; cyc^{01}* vs *Pdf>Kir2.1; cyc^{01}*/+ F**	>0.001 ***
***Pdf>TeTxLC; cyc^{01}* vs *Pdf>TeTxLC cyc^{01}*/+ M**	0.136
***Pdf>TeTxLC; cyc^{01}*vs *Pdf>TeTxLC cyc^{01}*/+ F**	0.282
***Pdf>NaChBac; cyc^{01}* vs *Pdf>NaChBac cyc^{01}*/+ M**	0.073
***Pdf>NaChBac; cyc^{01}* vs *Pdf>NaChBac cyc^{01}*/+ F**	0.183
***cyc^{01}* M vs *$Pdfr^{5304}$; cyc^{01}* M**	0.308
***cyc^{01}* F vs *$Pdfr^{5304}$; cyc^{01}* F**	0.994
***cyc^{01}* M *vs* *ple>TeTxLC; cyc^{01}* M**	0.002**
***cyc^{01}* F *vs* *ple>TeTxLC; cyc^{01}* F**	0.023 *
***cyc^{01}* M vs *PDF>Kir2.1; cyc^{01}* M**	1

D/N ratio	**P=**
***cyc*^{01} F vs *PDF>Kir2.1; cyc*^{01} F**	0.67
***cyc*^{01} M vs *PDF>TeTxLC*; *cyc*^{01} M**	0.973
***cyc*^{01} F vs *PDF>TeTxLC*; *cyc*^{01} F**	0.483
***cyc*^{01} M vs *PDF>NaChBac*; *cyc*^{01} M**	0.001**
***cyc*^{01} F vs *PDF>NaChBac*; *cyc*^{01} F**	0.001**

Appendix Table 4 – P-values following One-way ANOVA comparing D/N ratios of various manipulations affecting PDF signalling on a cyc^{01} background, related to Figure 3.12

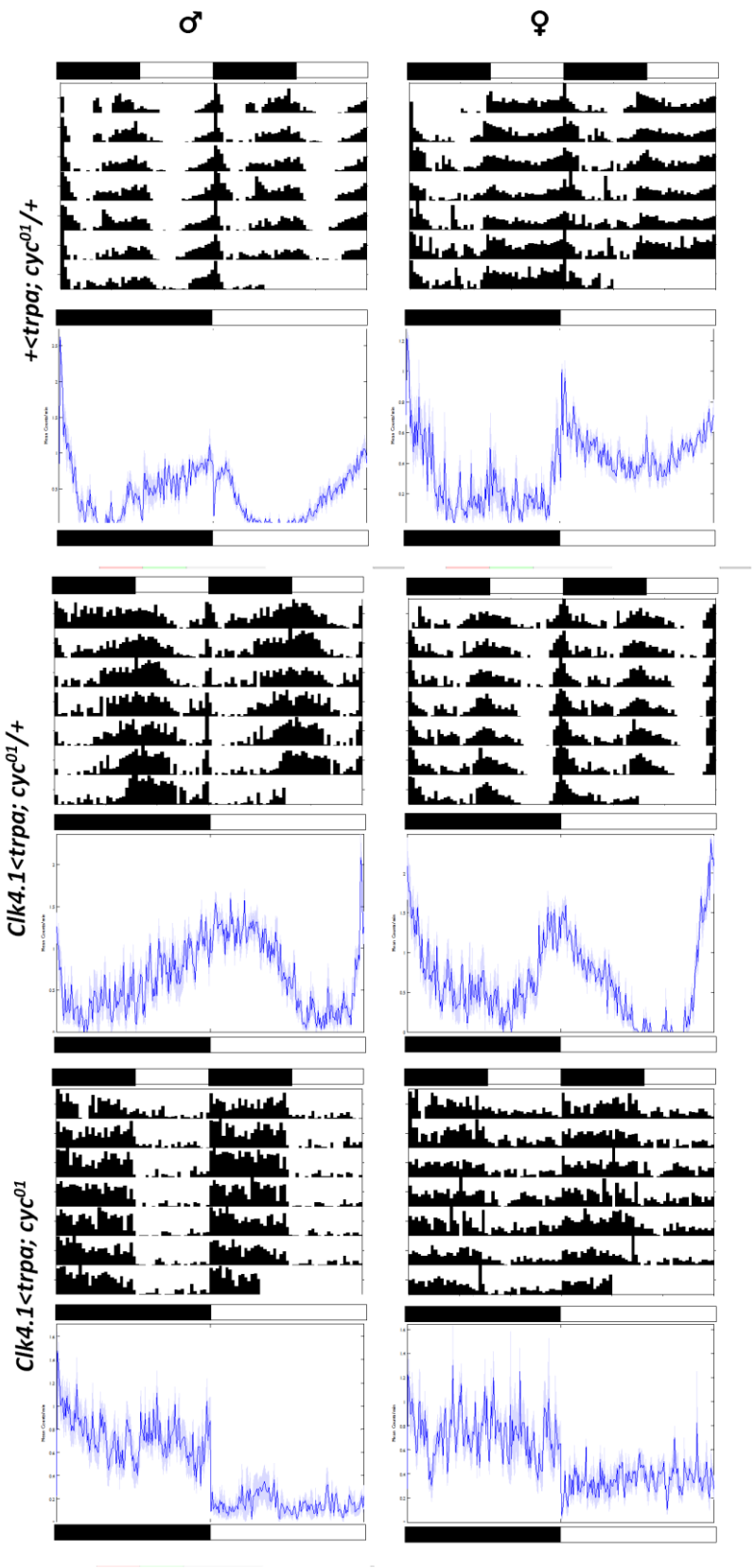
♂
♀
+<trpa; cyc01/+
Clk4.1<trpa; cyc01/+
Clk4.1<trpa; cyc01

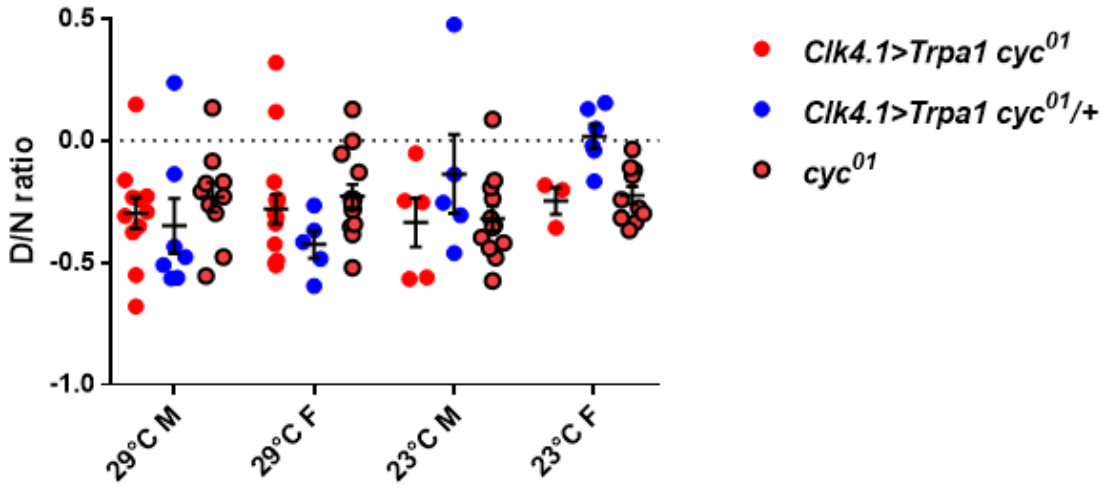

*Appendix Figure 6: D/N ratio and activity profiles of 29°C run Clk4.1M hyperexcitation flies on a cyc^{01} or cyc^{01}/+ background. Demonstrable is the obligate dark-induced hyperexcitation attainable in cyc^{01} flies in certain conditions, not noticeably ameliorated by $DN1_p$ excitation. Heterozygote controls show crepuscularity, with high light activity, as expected by high-temperature experiments, whilst driverless heterozygotes show an even more wt-like profile. Few significant differences are present. Significant differences are 29°C F vs 23°C F Clk4.1M>TrpA1; cyc^{01}/+(P=0.07**),*

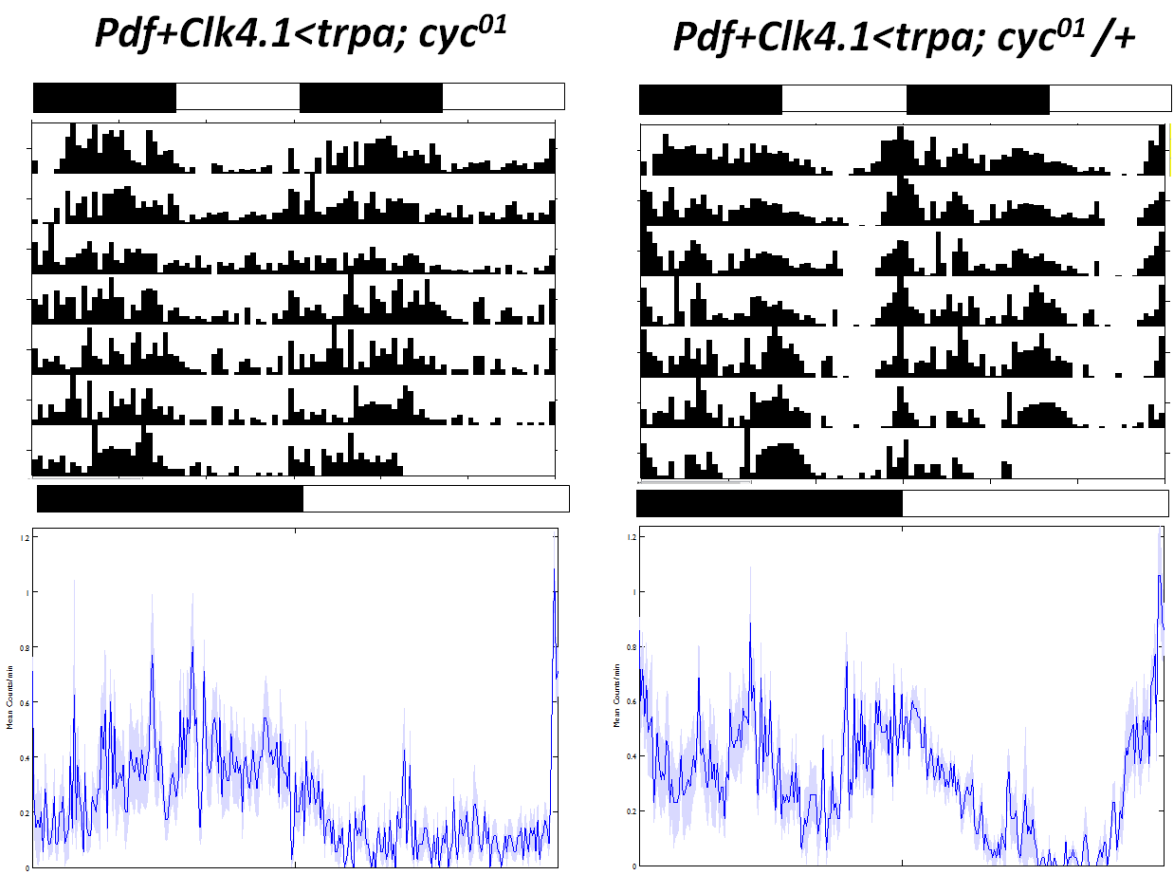

Appendix Figure 7: Female flies in 29°C LD, concurrently hyperexciting PDF and DN1ps with TrpA1. Activity profiles do not notably differ to sole excitation of Clk4.1M+ve DN1ps. N=5 for both experimental and control

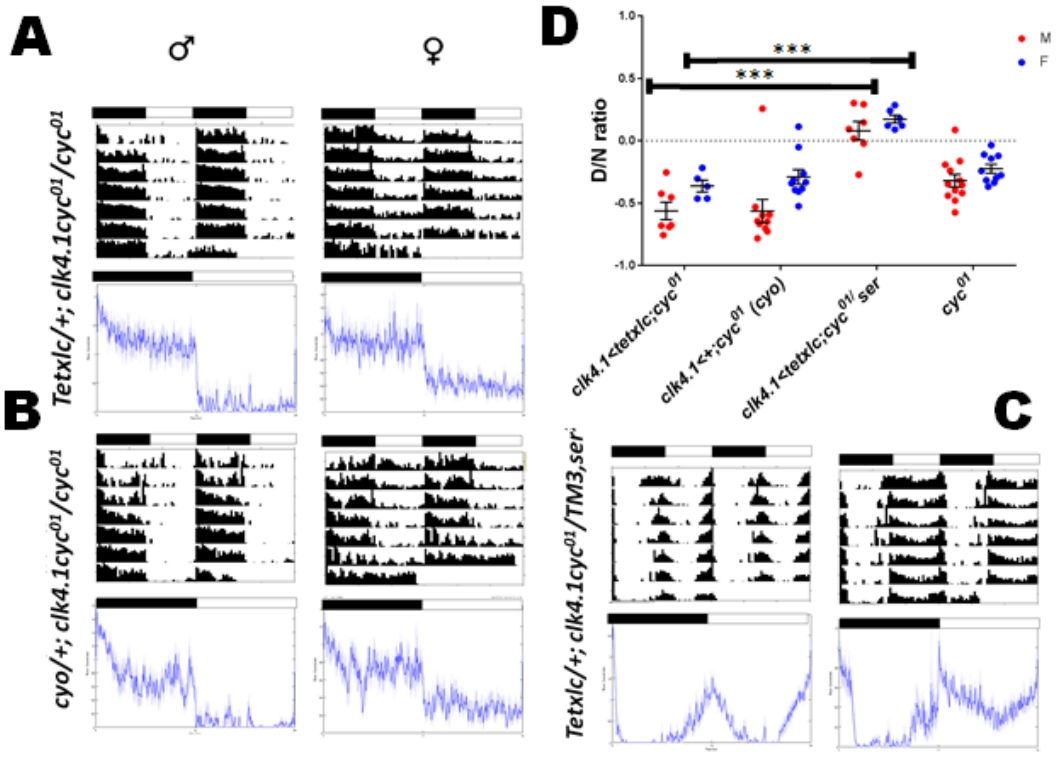

Appendix Figure 8: Panels A-C show Activity profiles and Panel D shows D/N ratio determining the effect of DN1p silencing on cyc^{01} nocturnal phenotype, using TeTxLC/+; Clk4.1Mcyc^{01}/cyc^{01} and controls. D/N ratio does not differ between experimental flies

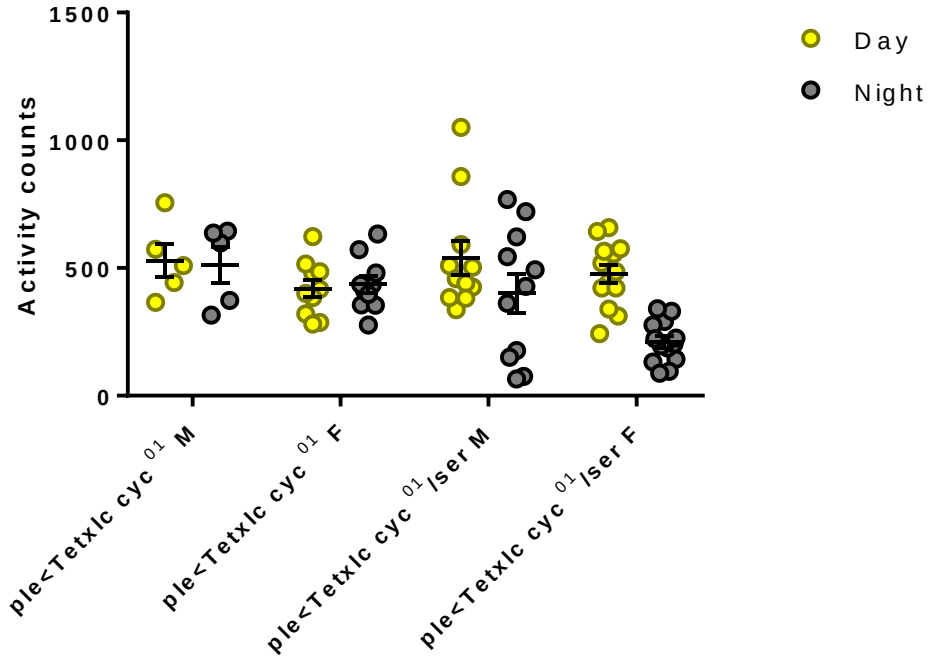

*and CyO controls (M P=0.990, F P=0.440), but does differ with TM3,ser^{1} +ve heterozygotes (M P<0.001***. F P<0.001***.)*

Appendix figure 9: Pursuant to Figure 3.12, activity counts for silenced dopaminergic neurons on cyc^{01} or cyc^{01}/+ backgrounds. Day counts do not significantly differ between any groups

	L	*D*	*%D*
cyc^{01}	21	75	78.125
cyc^{01}/+	17	42	71.18644

Appendix Table 5: Numbers of cyc^{01} and cyc^{01}/+ larvae pupating in the light or dark side of pupariation assay. Previous studies suggest approx. 70% of larvae pupate in darkness, and cyc^{01} do not significantly differ as assessed by 2x2 Fisher's exact test (P=0.343).

Dev + adult temperature	**n**	**% SR**	**% WR**	**% AR**	**TAU ± SEM**	**RRP ± SEM**
23EL-L3→17→29°C M	14	28.57	14.29	54.17	23.92 ± 0.15	1.46 ± 0.09
23EL-L3→17→29°C F	14	0.00	7.14	92.86	25.5	1.11
23→29°C M	34	73.53	17.65	8.82	22.34 ± 0.44	1.99 ± 0.104
23→29°C F	47	46.81	34.04	19.15	22.68 ± 0.30	1.78 ± 0.103
17→29°C M	35	0.00	17.14	82.86	24.17 ± 0.69	1.09 ± 0.018
17→29°C F	43	0.00	11.63	88.37	22.70 ± 0.12	1.14 ± 0.039
17-L1→29°C M	9	33.33	55.55	11.11	22.56 ± 0.15	1.47 ± 0.11
17-L1→29°C F	13	23.08	38.46	38.46	23.13 ± 0.13	1.56 ± 0.16
17-L3→29°C M	11	18.18	18.18	63.64	22.63 ± 0.13	1.92 ± 0.425
17-L3→29°C F	43	13.95	41.86	44.19	23.75 ± 0.75	1.44 ± 0.108
17-P6→29°C M	30	0.00	46.67	53.33	22.85 ± 0.98	1.14 ± 0.040
17-P6→29°C F	17	0.00	17.65	82.35	23.50 ± 0.76	1.15 ± 0.070

Appendix Table 6, Behavioural rhythmicities for cyc^{01} $[elav.cyc]^{ts}$ raised at multiple temperatures throughout development, Data is presented in Figures 3.18 and 3.19

	Distribution of rhythms	RRP
17EL-L3 29°C vs 17EL-P6 29°C M	0.141	0.803
17EL-L3 29°C vs 17EL-P6 29°C F	0.07	0.103
17EL-L1 29°C vs 17- 29°C M	>0.001***	>0.001***
17EL-L1 29°C vs 17→29 °C F	>0.001***	>0.001***
17EL-L1 29°C vs 29- 29°C M	0.178	0.373
17EL-L1 29°C vs 29- 29°C F	>0.001***	>0.001***
17EL-L3 29°C vs 17- 29°C M	0.047 *	0.73
17EL-L3 29°C vs 17→29 °C F	>0.001 ***	0.035 *
17EL-L3 29°C vs 29- 29°C M	0.526	0.794
17EL-L3 29 °C vs 29→29 °C F	>0.001 ***	>0.001 ***
17EL-P6 29°C vs 17- 29°C M	0.089	0.896
17EL-P6 29°C vs 17→29 °C F	0.639	0.992
17EL-P6 29 °C vs 29- 29°C M	0.096	0.004**
17EL-P6 29°C vs 29→29 °C F	>0.001 ***	>0.001 ***
17→29 °C vs 23EL-L3→17→29 °C M	0.005 **	0.107
17→29 °C vs 23EL-L3→17→29 °C F	0.999	0.907
23→29 °C vs 23EL-L3→17→29 °C M	>0.001***	>0.001***
23→29 °C vs 23EL-L3→17→29 °C F	>0.001***	>0.001***

Appendix Table 7 – P-values for statistics of behavioural rhythmicities for cyc^{01} [elav.cyc]^{ts} flies covering restrictive temperatures at certain developmental periods

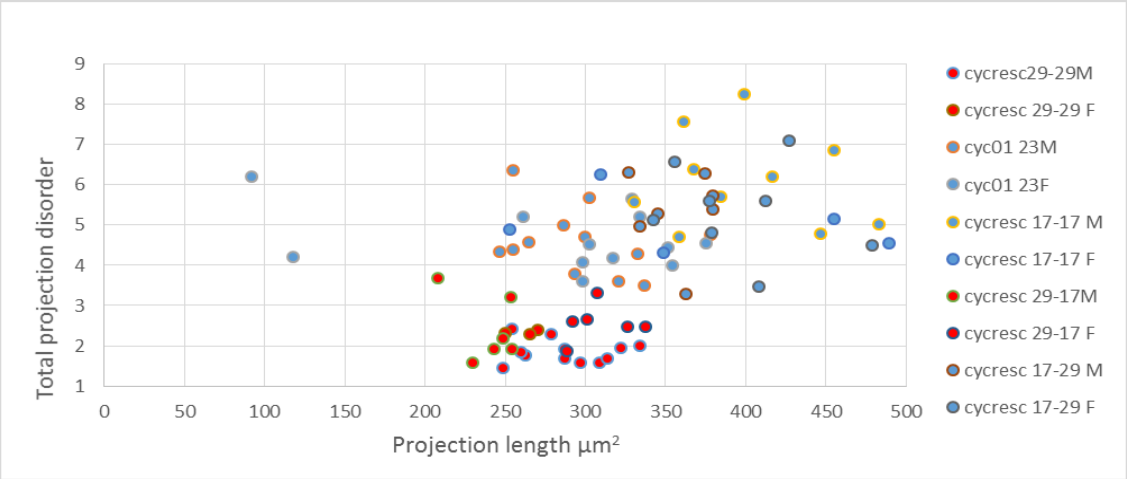

Appendix Figure 10, scatterplot demonstrating the relationship between projection length, total projection disorder, and genotype, with datapoints corresponding to flies possessing low developmental CYC labelled with a blue center, compared to a red center

for flies possessing high developmental CYC. Stunted projections, when occurant, have been excluded. Here we show that high CYC projections appear marginally shorter on average, perhaps due to the tendency of low CYC projections to over-extend dorsally.

We show that projection disorder correlates with major neurite length, (r=0.437**, P<0.001 ***) despite length having an inverse effect on projection disorder, showing that the disparity in low CYC and high CYC data is not artificially increased by our method of quantification, In projections exclusively from flies with low developmental CYC, length again correlates with projection disorder (r=0.319**, P=0.009 **), as may be expected, with a greater contribution of misrouted projections. For datapoints with high developmental CYC, there is no significant correlation between disorder and length (r=-0.119, P=0.553), suggesting this correlation emerges entirely only in populations with developmentally low CYC. The nature of misrouting may prevent us from accurately gauging the endpoint of a projection, thus artificially reducing disorder in projections with disorder.

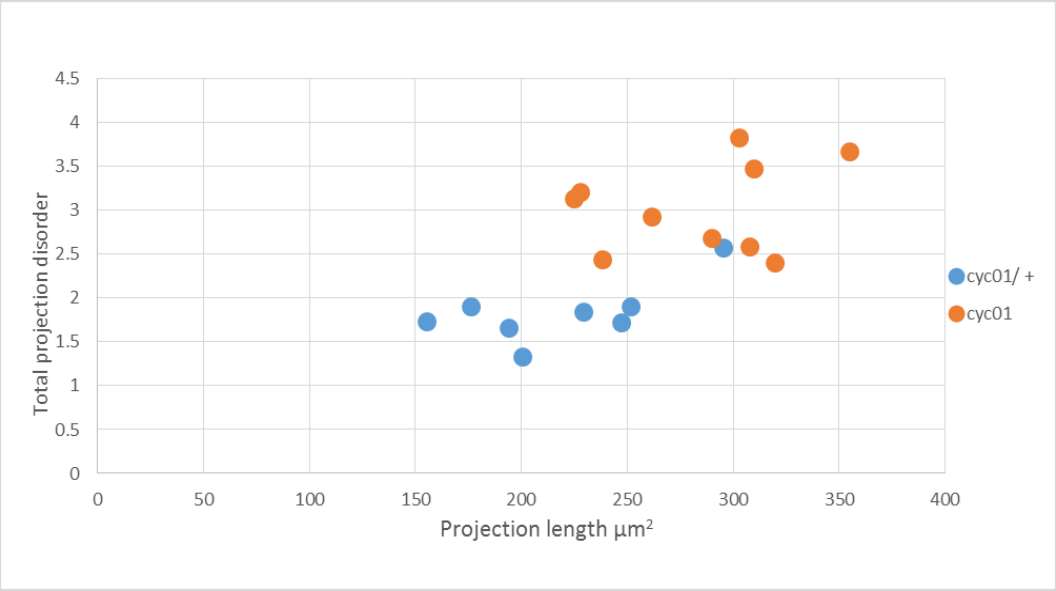

*Appendix Figure 11, demonstrating the same principle of Appendix Figure 10 in P6 pupae (25-40 hpf), that cyc^{01} results both in increased complexity and projection length, a significant correlation (r=0.672**, P<0.001***).*

P-value	17°C M	17°C F	23°C M	23°C F	29°C M	29°C F	cyc^{01}/+ M
17°C M		1	0.999	1	0.187	0.982	>0.001 ***
17°C F	1		1	1	0.355	0.996	>0.001 ***
23°C M	0.999	1		1	0.280	0.992	>0.001 ***
23°C F	1	1	1		0.351	0.999	>0.001 ***
29°C M	0.187	0.355	0.280	0.351		0.819	>0.001 ***
29°C F	0.982	0.996	0.992	0.999	0.819		0.001 **
cyc^{01}/+ M	>0.001 ***	>0.001 ***	>0.001 ***	>0.001 ***	>0.001 ***	0.001 **	

Appendix Table 8, P values comparing the complexity of cyc^{01} PDF+ve dorsal projections in 17°C, 23°C and 29°C raised flies, all kept as adults for 2-7 days at their developmental temperature. In no case are there significant differences in complexity

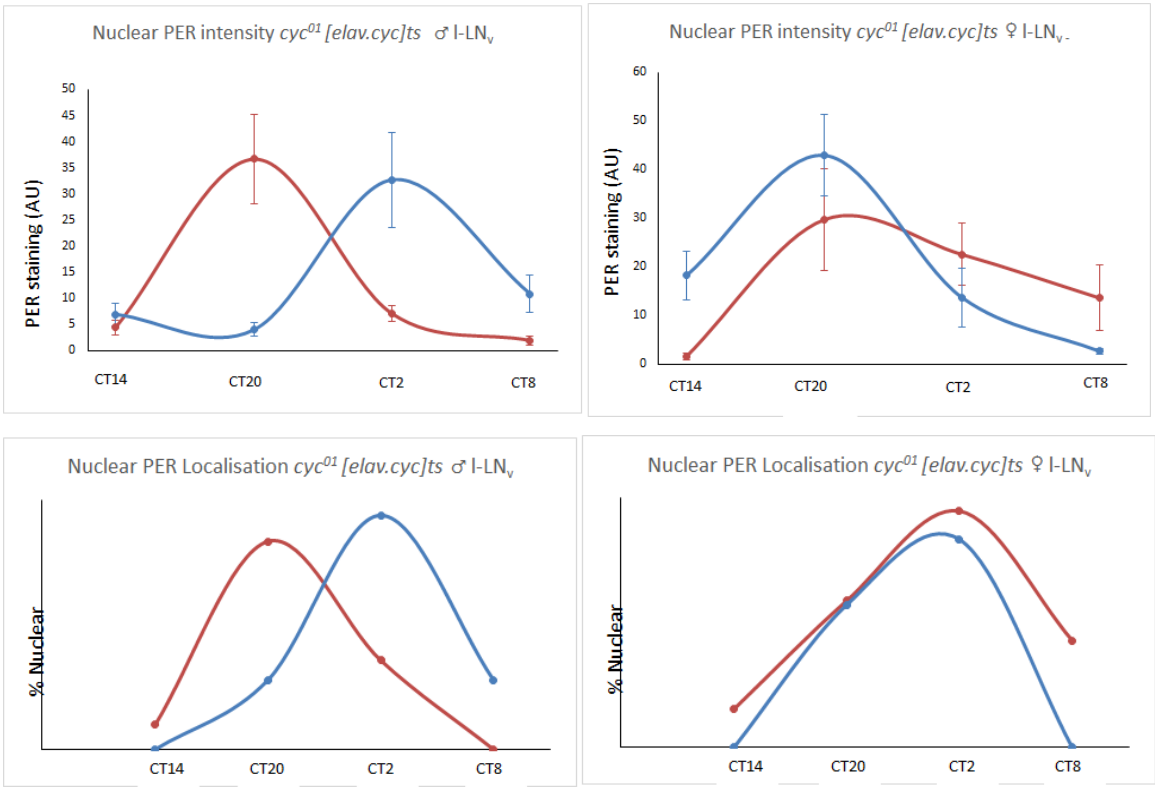

Appendix figure 12, nuclear staining intensity and localisation of PER within l-LNvs of 17→29 °C or 29→29 °C cyc^{01} [elav.cyc]^{ts} males and females at CT2, CT8, CT14 and

CT20. Identifiable is an oscillation with uniform troughs at CT8 and CT14. The variability of peak at CT2 and CT20 may be reflective of an altered periodicity, and the manifestation of a defect, but is more easily explained as the rapid degeneration of rhythms in these cells in freerunning conditions, as has been reported elsewhere (Stoleru et al., 2005).

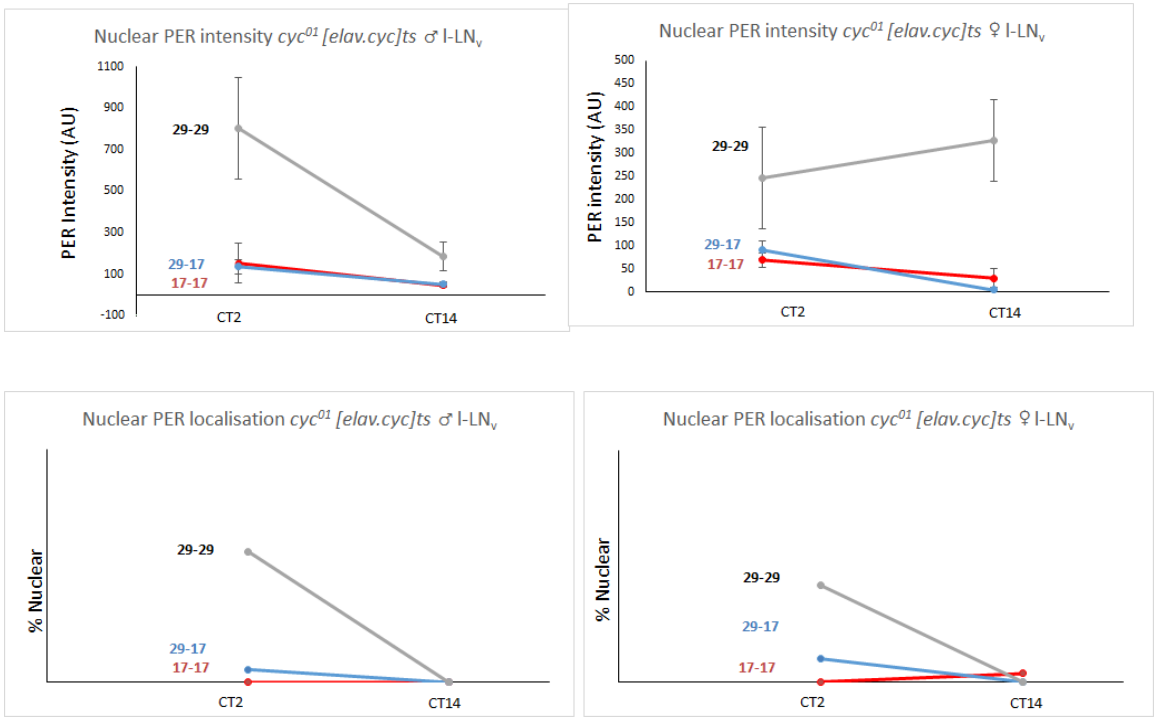

Appendix Figure 13, nuclear localisation of PER in 17→17°C, 29→17°C and 29→29 °C cyc^{01} [elav.cyc]^{ts} l-LN$_v$s at CT2 and CT14. Identifiable is a loss of nuclear PER in restrictively run flies, irrespective of developmental condition, which is present in permissively raised, permissively run flies. However, staining intensity does not match up with localisation, indicative of the degeneration in l-LN$_v$ rhythms in this condition. 29→29 °C significantly differs between timepoints for both genders, whilst no other conditions do (Appendix Table 9).

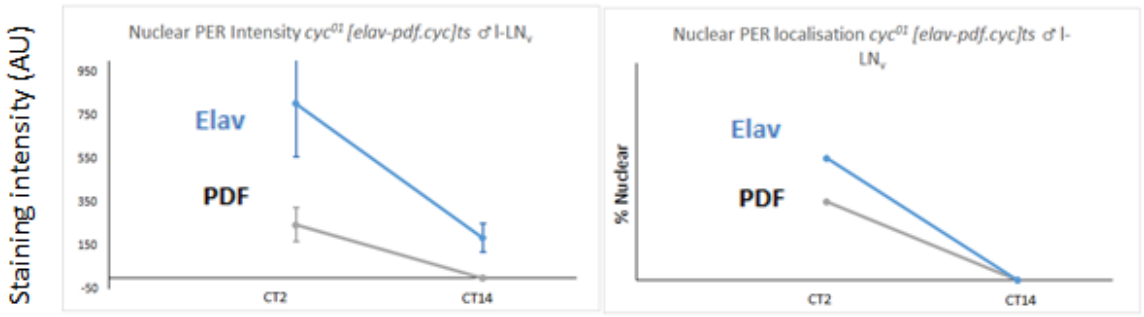

Appendix Figure 14: Nuclear staining intensity and localisation of PER in 29→29 °C

*cyc^{01} [elav-pdf.cyc]^{ts} l-LN$_v$s at CT2 and CT14. Demonstrated is a weak though significant rhythm (P<0001***) despite transferral to DD. It is expected that l-LN$_v$ rhythms will damp rapidly in DD, though these persist.*

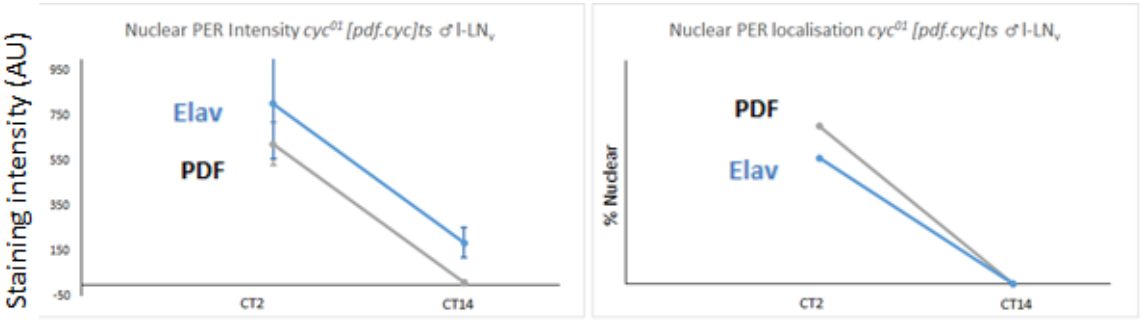

*Appendix Figure 15: Nuclear staining intensity and localisation of PER in 29→29 °C cyc^{01} [pdf.cyc]^{ts} l-LN$_v$s at CT2 and CT14. Demonstrated is a weak though significant rhythm (P<0001***) despite transferral to DD. It is expected that l-LN$_v$ rhythms will damp rapidly in DD, though these persist.*

CT2 vs CT14	**Staining intensity**	**Nuclear localisation**
M s-LNv 29→29 °C	0.038 *	>0.001 ***
M s-LNv 17→17°C	0.947	0.486
M s-LNv 29→17°C	0.331	0.231
F s-LNv 29→29 °C	0.368	0.034 *
F s-LNv 17→17°C	1	1
F s-LNv 29→17°C	0.348	1
M l-LNv 29→29 °C	0.137	0.004 **
M l-LNv 17→17°C	0.034 *	1
M l-LNv 29→17°C	0.397	1
F l-LNv 29→29 °C	0.952	0.003 **
F l-LNv 17→17°C	0.289	1
F l-LNv 29→17°C	0.289	0.54
M s-LNv *[pdf.cyc]* 29→29 °C	0.001 ***	>0.001 ***
M s-LNv *[elav-pdf.cyc]* 29→29 °C	0.007 **	0.082
M l-LNv *[pdf.cyc]* 29→29 °C	>0.001 ***	>0.001 ***
M l-LNv *[elav-pdf.cyc]* 29→29 °C	0.001***	>0.001 ***
M s-LNv 17→29 °C	0.212	>0.001 ***

CT2 vs CT14	Staining intensity	Nuclear localisation
M l-LNv 17→29 °C	0.991	0.304
F s-LNv 17→29 °C	0.014 *	0.030 *
F l-LNv 17→29 °C	0.024 *	0.024 *

Appendix Table 9, P-values for statistics comparing nuclear PER localisation between CT2 and CT14 for various cell groups for cyc^{01} [elav.cyc]^{ts} via 2x2 Fisher's exact test. Also included are cyc^{01} [elav-Pdf80.cyc]^{ts} and cyc^{01} [pdf.cyc]^{ts}

P-value	17→29 °C M	17→29 °C F	29→29 °C M	29→29 °C F	29→17°C M	29→17°C F	17→17°C M	17→17°C F	23°C cyc^{01} M	23°C cyc^{01} F
17→29 °C M		1	0.001 ***	0.004 **	0.004 **	0.003 **	0.890	1	0.815	0.873
17→29 °C F	1		0.001 ***	0.003 **	0.003 **	0.003 **	0.920	1	0.817	0.874
29→29 °C M	0.001 ***	0.001 ***		0.003 **	0.798	0.132	0.001 ***	0.005 **	0.001 ***	0.001 ***
29→29 °C F	0.004 **	0.003 **	0.003 **		1	0.930	0.001 ***	0.013 *	0.001 ***	0.001 ***
29→17°C M	0.004 **	0.003 **	0.798	1		1	0.001 ***	0.008 **	0.008 **	0.007 **
29→17°C F	0.003 **	0.003 **	0.132	0.930	1		0.001 ***	0.009 **	0.001 ***	0.001 ***
17→17°C M	0.890	0.920	0.001 ***	0.001 ***	0.001 ***	0.001 ***		0.543	0.076	0.095
17→17°C F	1	1	0.005 **	0.013 *	0.008 **	0.009 **	0.543		0.972	0.989
23°C cyc^{01} M	0.815	0.817	0.001 ***	0.001 ***	0.008 **	0.001 ***	0.076	0.972		1
23°C cyc^{01} F	0.873	0.874	0.001 ***	0.001 ***	0.007 **	0.001 ***	0.095	0.989	1	

Appendix Table 11, supporting statistics for Figure 4.5, comparing s-LN_v dorsal projection complexity in the presence or absence of developmental CYC. Red squares represent comparisons between developmentally low-CYC flies, green squares represent comparisons between developmentally high-CYC flies, and unfilled squares are P-values between high-CYC and low-CYC populations.

	Sholl analysis P-value
cyc^{01} /+ vs cyc^{01}17°C	>0.001 ***
cyc^{01} /+ vs cyc^{01} 23°C	>0.001 ***
cyc^{01} /+ vs cyc^{01}29°C	>0.001 ***
cyc^{01} [elav.cyc]^{ts} 29→29 °C vs 17→29 °C	0.004 **
cyc^{01} [elav.cyc]^{ts} 29→29 °C vs 29→17°C	1
cyc^{01} [elav.cyc]^{ts} 29→29 °C vs cyc^{01} [pdf.cyc]^{ts} 29→29 °C	0.765
cyc^{01} [elav.cyc]^{ts} 29→29 °C vs cyc^{01} [elav-Pdf80.cyc]^{ts} 29→29 °C	1
cyc^{01} [elav.cyc]^{ts} 29→29 °C vs cyc^{01}/+	0.134
cyc^{01} [elav.cyc]^{ts} 29→17°C vs cyc^{01}/+	0.225

Appendix Table 10, statistics pursuant to Figure 4.11, comparing radiation of second-order processes in various CYC-loss lines via Sholl analysis. Stats were conducted via one-way ANOVA.

Projection complexity of 17°C EL-L3 29°C *cyc^{01} [elav.cyc]^{ts}*	**Statistical significance**
Vs 17→29 °C *cyc^{01} [elav.cyc]^{ts}*	P=0.038 *
Vs 17→17°C *cyc^{01} [elav.cyc]^{ts}*	P=0.078
Vs 17°C *cyc^{01}*	P=0.169
Vs 23°C *cyc^{01}*	P=0.130
Vs 29°C *cyc^{01}*	P=0.132

Appendix Table 12 – P-values following one-way ANOVA comparing projection complexity following larval-specific CYC loss in cyc^{01} [elav.cyc]^{ts} compared to other temperature conditons and cyc^{01}

	Dorsal/Basal ratio		**Mean stain intensity**		**Bouton number**
	GFP	PDF	GFP	PDF	
pdf.SYT::GFP x cyc^{01} [pdf.SYT::GFP]	>0.001 ***	0.001 **	0.033 *	0.002 **	0.062
pdf.SYT::GFP x 29→29 °C cyc^{01} [pdf.cyc+SYT::GFP]^{ts}	0.938	1	0.945	0.060	0.023 *

	Dorsal/Basal ratio		**Mean stain intensity**		**Bouton number**
	GFP	PDF	GFP	PDF	
pdf.SYT::GFP* x *17→29 °C cyc^{01} [pdf.cyc+SYT::GFP]^{ts}	>0.001 ***	>0.001 ***	0.004 **	0.002 **	0.010 *
cyc^{01} [pdf.SYT::GFP]* x *29→29 °C cyc^{01} [pdf.cyc+SYT::GFP]^{ts}	>0.001 ***	0.001 **	0.004 **	0.003 **	0.881
cyc^{01} [pdf.SYT::GFP]* x *17→29 °C cyc^{01} [pdf.cyc+SYT::GFP]^{ts}	1	0.999	0.076	0.995	0.836
29→29 °C vs 17→29 °C cyc^{01} [pdf.cyc+SYT::GFP]^{ts}	>0.001 ***	>0.001 ***	>0.001 ***	0.001 **	0.487
cyc^{01} [pdf.CD8::GFP]* vs *pdf.SYT::GFP	N/A	N/A	0.002 **	0.004 **	N/A
cyc^{01} [pdf.CD8::GFP]* vs *cyc^{01} [pdf.SYT::GFP]	N/A	N/A	0.017 *	0.790	N/A
cyc^{01} [pdf.CD8::GFP]* vs *29→29 °C cyc^{01} [pdf.cyc+SYT::GFP]^{ts}	N/A	N/A	>0.001 ***	0.020 *	N/A
cyc^{01} [pdf.CD8::GFP]* vs *17→29 °C cyc^{01} [pdf.cyc+SYT::GFP]^{ts}	N/A	N/A	0.964	0.060	N/A

Appendix Table 13: Statistics display P-values for comparisons of GFP and PDF staining when SYT::GFP or CD8::GFP is expressed on a cyc^{01}, wt or cyc^{01} [Pdf.cyc]^{ts} background

	P-value
ITP cyc^{01} vs cyc^{01}/+ 5^{th} s-LN_v	>0.001 ***
ITP cyc^{01} vs 17→29 °C cyc^{01} [elav.cyc]^{ts} 5^{th} s-LN_v	>0.001 ***
ITP cyc^{01}/+ vs 17→29 °C cyc^{01} [elav.cyc]^{ts} 5^{th} s-LN_v	0.057
GFP R78gG02cyc^{01} vs R78G02cyc^{01}/+ 5^{th} s-LN_v	>0.001 ***
GFP cry-pdf cyc^{01} vs cry-pdf cyc^{01}/+ 5^{th} s-LN_v	>0.001 ***
ITP cyc^{01} vs cyc^{01}/+ LN_d	>0.001 ***
ITP cyc^{01} vs 17→29 °C cyc^{01} [elav.cyc]^{ts} LN_d	>0.001 ***
ITP cyc^{01}/+ vs 17→29 °C cyc^{01} [elav.cyc]^{ts} LN_d	0.615
GFP R78gG02cyc^{01} vs R78G02cyc^{01}/+ LN_d	>0.001 ***
GFP cry-pdf cyc^{01} vs cry-pdf cyc^{01}/+ LN_d	>0.001 ***
GFP Clk4.1Mcyc^{01} vs Clk4.1Mcyc^{01}/+	>0.001 ***
GFP cry-pdf cyc^{01} vs cry-pdf cyc^{01}/+ DN1	0.056
PDF cry-pdf cyc^{01} vs cry-pdf cyc^{01}/+ LN_v	0.001 **
CRY cyc^{01} vs cyc^{01}/+ LN_v	>0.001 ***
CRY cyc^{01} vs cyc^{01}/+ LN_d	>0.001 ***
CRY 17→29 °C vs 29→29 °C cyc^{01} [elav.cyc]^{ts} LN_v	0.081
CRY 17→29 °C vs 29→29 °C cyc^{01} [elav.cyc]^{ts} LN_d	0.076
CRY $Pdp1^{3135}$ vs $Pdp1^{3135}$/+ LN_v	0.004**
CRY $Pdp1^{3135}$ vs $Pdp1^{3135}$/+ LN_d	0.204

Appendix Table 14, statistics comparing significance of E cell number and ITP staining between various manipulations of CYC, one-way ANOVA

Attempted rescue of *cyc^{01}* functions with CLK/CYC targets

It is predicted that three developmental factors predict wiring decisions, basic neuronal fate specified during differentiation, molecular guidance cues, and selection of synaptic specificity. Of *cyc^{01}* defasciculated projections, the majority project dorsally and show a stereotypical pattern of arborisation in the dorsal regions, suggesting that interactions do occur between these and other cells.

Numerous databases of CLK/CYC targets have been generated, either the results of pulldowns or in silico analysis. One study, utilises ChIP-seq to study CLK, CYC and

CLK/CYC pulldowns in head tissues, the first such ‘omics-based study to discriminate between the TFs (Meireles-filho et al., 2014). The potential instability of monomeric CYC results in a limited set of CYC specific targets, and the defect is likely the failure to express a CLK/CYC heterodimeric target (Gunawardhana et al., 2017).

Of these, numerous CLK/CYC targets are potentially required for the defect, with functions in axonal pathfinding and synaptic formation. For example, multiple CLK/CYC targets exist in the pathway mediating the initiation of axonal pruning during metamorphosis.

In finding a minimum driver sufficient for rescue, one can assay output genes with the same driver in expectation of rescue. Phenotypic rescue via other drivers may not be the result of transcriptional regulation of the UAS-gene by CLK/CYC, but high levels altering signal of another cell cluster or rescue via partially redundant factor to that lost alongside CYC, leading to a phenotypic rescue via another avenue. Following the rescue of cyc^{01} defects with *elav>UAS-myc-cyc*, the following UAS lines, obtained from flyorf (Zurich) were expressed with *elav* driver on a cyc^{01} background and PDF projections were imaged.

First, UAS-lines were crossed with *elav-gal4* driver line, to A) ensure viability and B) Identify rhythmic defects. The rationale for the screen could have used multiple driver lines, but as the spatial mapping of CYC requirement for correct neuroanatomy had not been mapped at the initiation of the screen, a broader driver was more suitable, and cyc^{01} *[elav.cyc]*^{ts} flies could be easily repurposed for the screen. As demonstrated in Appendix Table 15, no defects were identified following *elav-gal4* driven overexpression of these genes, in viability or behavioural rhythmicity. This should be a point of concern as candidate genes are fundamental to development, however to our knowledge, in no cases has overexpression of candidate genes been documented to generate a phenotype.

elav-gal4>UAS-N	**n**	**% Rhythmic**	**% Arrhythmic**	**RRP + SEM**
LOLA	12	91.7	8.3	1.70±0.15
KRH1	11	90.9	9.1	2.35±0.19
CG8765	9	100.0	0	2.41±0.23

elav-gal4>UAS-N	**n**	**% Rhythmic**	**% Arrhythmic**	**RRP + SEM**
BUN	1	100.0	0	3.08
DL	4	50.0	50.0	1.53±0.02
NET	11	90.9	9.1	2.02±0.18
MED	12	100.0	0	2.03±0.13
MAD	11	100.0	0	1.81±0.17
EMC	11	90.9	9.1	2.33±0.15
HTH	11	100.0	0	2.01±0.17
FTZ-F1	10	80.0	20.0	1.59±0.15
BRK	7	100.0	0	1.44±0.14
E75	17	100.0	0	1.54±0.07

Appendix Table 15: Rhythmic distribution of FLYORF UAS lines under the control of elav-gal4

Necessarily, UAS-elements had to be recombined with cyc^{01}, and positive recombinants were selected for eye colour and arrhythmicity when crossed with $cyc^{01}ry^{506}$. Molecular confirmation for recombination was not sought unless a rescue was identified. Slides were visually inspected, and if no obvious rescue was identified, detailed complexity quantification was not performed in the interests of time.

Initially the screen was tested using MED, a gene of interest, but not a CLK/CYC target. As a proof of principle that the recombination process does not abrogate the cyc^{01} phenotype through alteration of potentially involved chromosomal markers, homozygote axonal complexity was quantified, with a high disorder index (4.61±0.18). Were rescue to occur in the screen, this is thus not neccesarily the result of the recombination process, and lends credence to the idea that the cyc^{01} projection phenotype segregates with behavioural arrhythmicity of the cyc^{01} homozygote, and is indepdent of the background of the cyc^{01} ry-containing 3rd chromosome.

As mentioned above, it was a perennial worry that recombination would induce context-specific PDF-ve s-LN_vs, as other groups have occasionally posited cyc^{01} to possess, which appears to manifest in this manipulation.

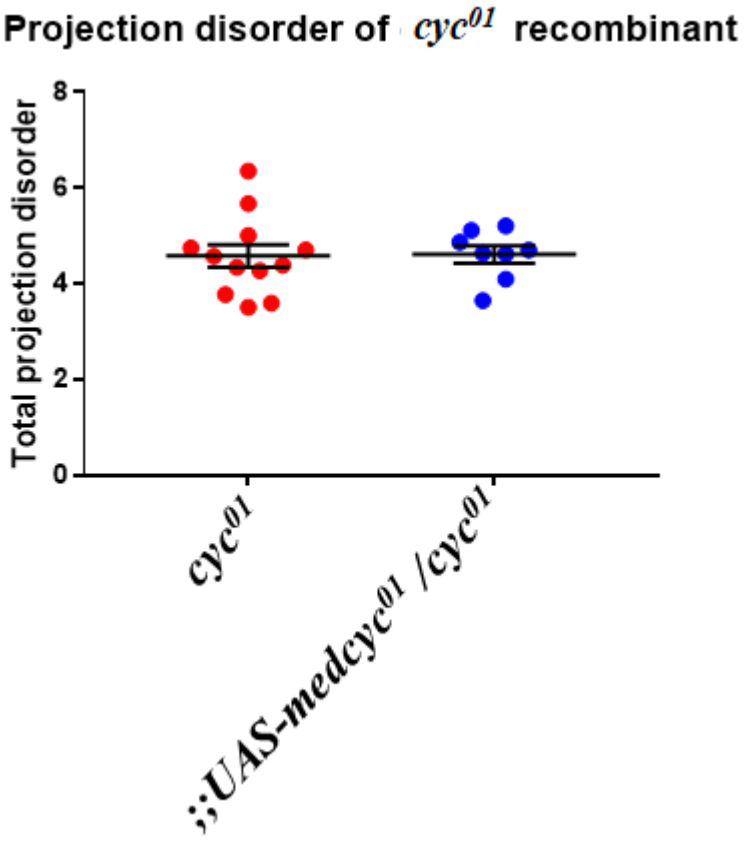

Appendix Figure 16: Panel A) Projection disorder of cyc^{01} and undriven UAS-Med cyc^{01}/cyc^{01} recombinants, demonstrating that the recombination process does not unduly influence projection morphology. As only cyc^{01}-mutants so far have been shown to produce this phenotype, with the potential of phenotypic contributions from the cyc^{01}-containing chromosome, the survival of this phenotype following recombination is reassuring.

For other screen candidates, homozygotes were inspected visually rather than fully imaged and quantified, to save time, and flies without a notable proportion of wt-like projections were rejected.

Notably, no other screen members demonstrated the stunting of *elav>med;*cyc^{01}, appearing defasciculated in most cases, arguing stunting is an emergent phenotype and not a quirk of pan-neural overexpression of factors. Screen members visually inspected as unsuccessful were: PDP1, SLOW, BUN, CRC, E75, NET, DL, IMPL3, MEF2, FTZf1, KR-H1, CROL, SMI35A , MAD and ESG.

Our small-scale screen failed to find an appropriate rescue of the defasciculation phenotype, and time constraints prevented any further study into downstream CLK/CYC targets. Indeed, it is unknown if the output gene(s) controlling s-LN_v dorsal projection formation are involved in other clock cells. Our failure to identify pruning or exuberant projection phenotypes during development of wt flies, in unison with the literature, suggests the *cyc*^{01} defect is not a failure to initiate or complete a certain developmental event, but rather an entirely aberrant response. We can say that elements of MB pruning pathways, in ecdysone and BMP signalling, are not the missing element in *cyc*^{01} flies.

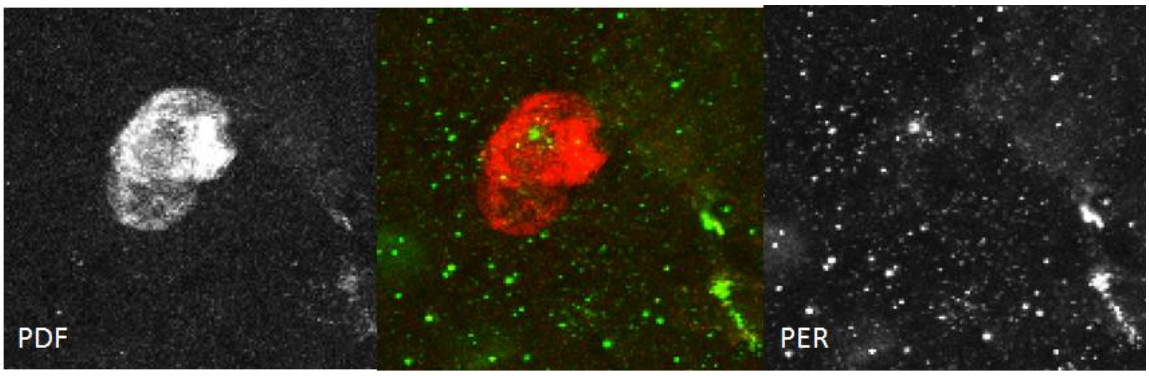

Appendix Figure 17, Example image of tim-Clk pdp1^{3135}*, in which l-*LN_v*s are PDF+ve and PER-ve in ZT2, whilst s-*LN_v*s are not visible. PDF is marked in red and PER in green. Ectopic CLK expression in the CRYgal4 driver results in a similar PDF phenotype, alongside PER rhythms in s-*LN_v*s and l-*LN_v*s (Zheng et al., 2009).*

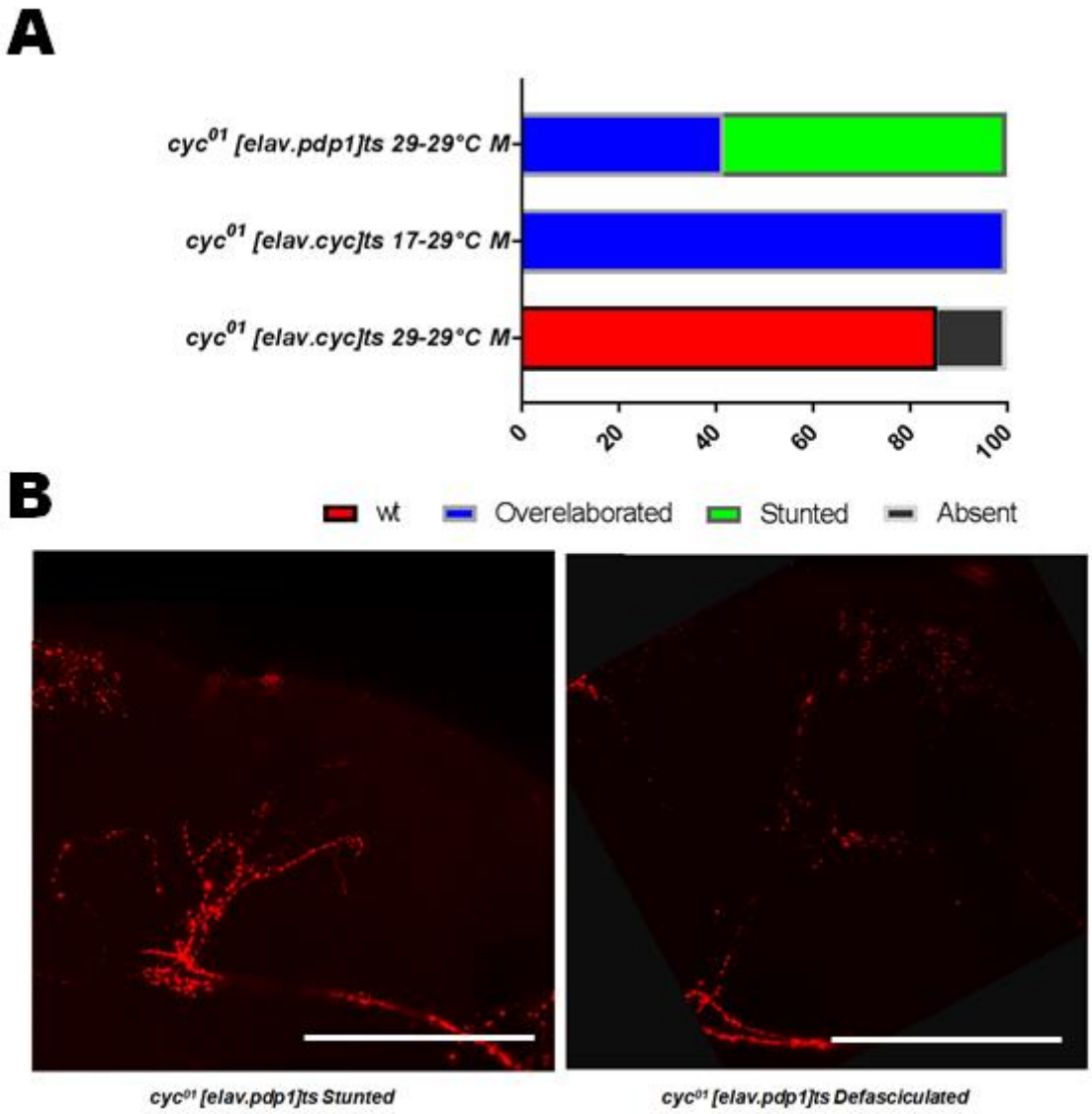

Appendix Figure 18, Panel A shows catagorisation of s-LN$_v$ projections following panneuronal PDP1 overexpression on a cyc^{01} background, n=12. Significant proportions are stunted, similar to pdp1^{3135}, and all others exhibit misrouted projections, similar to cyc^{01}. Panel B shows example images of defasciculated or stunted projections, scale bar in bottom-right is 100µm.

statistics	**Distribution of rhythms**	**RRP**
29 vs 29EL-L3 17		
***Pdf*>hid; *gal80*^{ts} M RR**	0.017 *	0.010 *
***Pdf*>hid; *gal80*^{ts} F RR**	>0.001***	0.002 **
***Pdf*>hid; *gal80*^{ts} M DD**	1	0.309
***Pdf*>hid; *gal80*^{ts} F DD**	0.309	0.257
***Pdf*>CyO; *gal80*^{ts} M RR**	0.181	0.017 *

statistics	Distribution of rhythms	RRP
***Pdf*>CyO; *gal80*^{ts} F RR**	0.021 *	0.005 **
***Pdf*>CyO; *gal80*^{ts} M DD**	0.003 **	0.005 **
***Pdf*>CyO; *gal80*^{ts} F DD**	0.001 **	>0.001***
RR vs DD		
***Pdf*>hid; *gal80*^{ts} 29 M**	0.999	0.779
***Pdf*>hid; *gal80*^{ts} 29 F**	0.603	0.174
***Pdf*>hid; *gal80*^{ts} 29EL-L3 17 M**	0.055	0.017 *
***Pdf*>hid; *gal80*^{ts} 29EL-L3 17 F**	>0.001***	0.001 **
***Pdf*>CyO; *gal80*^{ts} 29 M**	0.012 *	0.502
***Pdf*>CyO; *gal80*^{ts} 29 F**	0.138	0.353
***Pdf*>CyO; *gal80*^{ts} 29EL-L3 17 M**	0.999	0.7
***Pdf*>CyO; *gal80*^{ts} 29EL-L3 17 F**	0.7	0.152

Appendix Table 16, Statistics comparing conditional PDF-cell ablation between developmental temperatures and behavioural conditions. Significant differences emerge between temperature conditions for experimental genotypes in RR but not DD.

	P=
Pdf*>hid *gal80*^{ts} M 29°*C* vs 29-L3 17°*C	>0.001 ***
Pdf*>hid *gal80*^{ts} F 29°*C* vs 29-L3 17°*C	>0.001 ***
Pdf*>+ *gal80*^{ts} M 29°*C* vs 29-L3 17°*C	0.78
Pdf*>+ *gal80*^{ts} F 29°*C* vs 29-L3 17°*C	0.143
29°*C* M *Pdf*>hid *gal80*^{ts} vs *Pdf*>+ *gal80*^{ts}	0.001 **
29°*C* F *Pdf*>hid *gal80*^{ts} vs *Pdf*>+ *gal80*^{ts}	0.176

Appendix Table 17, P-values for one-way ANOVA comparing E peak phase between Pdf; hid/+; tubpgal80^{ts}/+ and controls raised under different condition in 17°C LD

	n	% SR	% WR	% AR	RRP(±SEM)	TAU(±SEM)
UAS *cyc*Δ^{103} RR M	7	42.86	57.14	0.00	1.722±0.236	23.357±0.237
UAS *cyc*Δ^{103} RR F	6	0.00	66.67	33.33	1.115±0.053	24.5±0.816
UAS *cyc*Δ^{103} DD M	14	14.29	64.29	21.43	1.422±0.127	22.410±0.783
UAS *cyc*Δ^{103} DD F	13	53.85	38.46	7.69	1.637±0.124	23.458±0.114

	n	% SR	% WR	% AR	RRP(±SEM)	TAU(±SEM)
***repo-gal4>UAS cycΔ*^{103} RR M**	13	92.31	7.69	0.00	2.45±0.141	27.35±0.09
***repo-gal4*>UAS *cycΔ*^{103} RR F**	12	16.67	58.33	25.00	1.30±0.06	26.33±0.20
***repo-gal4>UAS cycΔ*^{103} DD M**	15	26.67	66.67	6.67	1.46±0.07	25.04±0.85
***repo-gal4>UAS cycΔ*^{103} DD F**	6	50.00	83.33	16.67	1.46±0.11	24.44±0.38
***tim-UAS-gal4*/UAS *cycΔ*^{103} RR M**	16	0	75	25	1.135±0.167	22.458±1.677
***tim-UAS-gal4*/UAS *cycΔ*^{103} RR F**	15	0	40	60	1.079±0.309	24±1.979
***tim-UAS-gal4*/UAS *cycΔ*^{103} DD M**	7	0	71.429	28.571	1.077±0.046	24±0.988
***tim-UAS-gal4*/UAS *cycΔ*^{103} DD F**	16	0	75	25	1.090±0.017	24.542±0.135
***tim-UAS-gal4*/ UAS *cycΔ*^{103}; Pdf-*gal80*/+ RR M**	16	25	31.25	43.25	1.379±0.120	25±0.878
***tim-UAS-gal4*/ UAS *cycΔ*^{103}; Pdf-*gal80*/+ RR F**	15	26.667	26.667	46.667	1.412±0.095	23.687±0.687
***tim-UAS-gal4*/ UAS *cycΔ*^{103}; Pdf-*gal80*/+ DD M**	7	0	71.429	28.571	1.111±0.040	22.3±1.617
***tim-UAS-gal4*/ UAS *cycΔ*^{103}; Pdf-*gal80*/+ DD F**	14	14.286	50	35.714	1.371±0.081	24.5±0.905
***cry13-Gal4*/ UAS *cycΔ*^{103} RR M**	14	0	50	50	1.079±0.033	21.786±0.448
***cry13-Gal4*/ UAS *cycΔ*^{103} RR F**	14	0	14.286	85.714	1.151±0.006	25.75±0.25

	n	% SR	% WR	% AR	RRP(±SEM)	TAU(±SEM)
***cry13-Gal4*/ UAS *cycΔ*^{103} DD M**	11	0	27.272	72.727	1.100±0.053	27.167±1.481
***cry13-Gal4*/ UAS *cycΔ*^{103} DD F**	13	0	7.692	92.308	1	27.5
UAS *cycΔ*^{103}/+; *R78G02-gal4*/+ RR M	19	47.37	42.11	10.53	1.65±0.13	24.79±1.34
UAS *cycΔ*^{103}/+; *R78G02-gal4*/+ RR F	22	0.00	22.73	77.27	1.10±0.02	20.40±1.53
UAS *cycΔ*^{103}/+; *R78G02-gal4*/+ DD M	24	37.50	58.33	4.17	1.57±0.08	23.30±0.06
UAS *cycΔ*^{103}/+; *R78G02-gal4*/+ DD F	24	54.17	33.33	12.50	1.76±0.10	23.48±0.05
***Pdf-gal4*; UAS *cycΔ*^{103}/+; RR M**	38	71.05	21.05	7.89	1.75±0.05	24.97±0.05
***Pdf-gal4*; UAS *cycΔ*^{103}/+; RR F**	16	0.00	50.00	50.00	1.07±0.02	25.81±0.63
***Pdf -gal4*; UAS *cycΔ*^{103}/+; DD M**	39	5.13	38.46	56.41	1.23±0.04	23.26±0.04
***Pdf -gal4*; UAS *cycΔ*^{103}/+; DD F**	17	11.76	47.06	41.18	1.30±0.11	24.20±0.11
tim-UAS-gal4/ UAS *cycΔ*^{103}; cry-*gal80*/+ RR M	11	27.27	54.55	18.18	1.35±0.14	23.89±0.63
tim-UAS-gal4/ UAS *cycΔ*^{103}; cry-*gal80*/+ RR F	24	4.17	41.67	54.17	1.21±0.09	24.18±0.70
tim-UAS-gal4/ UAS *cycΔ*^{103}; cry-*gal80*/+ DD M	15	60.00	20.00	20.00	1.95±0.14	24.08±0.15
tim-UAS-gal4/ UAS *cycΔ*^{103}; cry-*gal80*/+ DD F	13	76.92	23.08	0.00	1.97±0.14	23.96±0.12

	n	% SR	% WR	% AR	RRP(±SEM)	TAU(±SEM)
tim-UAS-gal4/ **CyO;** ***cry-gal80*/+ RR M**	13	53.85	30.77	15.38	1.81±0.16	22.64±0.54
tim-UAS-gal4/ **CyO;** ***cry-gal80*/+ RR F**	15	40.00	53.33	6.67	1.50±0.10	23.89±0.15
tim-UAS-gal4/ **CyO;** ***cry-gal80*/+ DD M**	15	73.33	13.33	13.33	2.01±0.12	23.92±0.11
tim-UAS-gal4/ **CyO;** ***cry-gal80*/+ DD F**	13	23.08	53.85	23.08	1.35±0.11	24.80±1.03

Appendix Table 18: Behavioural rhythmicities of cyc$^{\Delta 103}$-expressing flies of various driver lines in RR and DD.

Comparison	**Distribution of rhythms**	**RRP**
***cyc*Δ^{103} ♂ RR vs DD**	*0.225*	*0.405*
***cyc*Δ^{103} ♀ RR vs DD**	*0.065*	>0.001 ***
***TUG*> cyc*Δ^{103} ♂ RR *vs* DD**	*0.067*	*0.063*
***TUG*> cyc*Δ^{103} ♀ RR *vs* DD**	*0.113*	*0.104*
***Cry*> cyc*Δ^{103} ♂ RR *vs* DD**	*0.414*	*0.709*
***Cry*> cyc*Δ^{103} ♀ RR *vs* DD**	*0.999*	*0.191*
***Pdf*> cyc*Δ^{103} ♂ RR *vs* DD**	*>0.001* ***	>0.001 ***
***Pdf*> cyc*Δ^{103} ♀ RR *vs* DD**	*0.048* *	*0.025**
***(TUG-Pdf)*> cyc*Δ^{103} ♂ RR *vs* DD**	*0.585*	*0.802*
***(TUG-Pdf)*> cyc*Δ^{103} ♀ RR *vs* DD**	*0.791*	*0.017**
***Clk4.1M*> cyc*Δ^{103} ♂ RR *vs* DD**	*0.002* **	>0.001 ***
***Clk4.1M*> cyc*Δ^{103} ♀ RR *vs* DD**	*0.294*	*0.320*
***(TUG-cry)*> + ♂ RR *vs* DD**	0.639	0.384
***(TUG-cry)*> + ♀ RR *vs* DD**	0.442	0.152
***(TUG-cry)*> cyc*Δ^{103} ♂ RR *vs* DD**	0.17	0.026 *
***(TUG-cry)*> cyc*Δ^{103} ♀ RR *vs* DD**	>0.001 ***	>0.001 ***
♂ RR cyc*Δ^{103} vs TUG*> cyc*Δ^{103}	*0.020* *	>0.001 ***
♀ RR cyc*Δ^{103} vs TUG*> cyc*Δ^{103}	*0.361*	*0.349*
♂ RR cyc*Δ^{103} vs Cry*> cyc*Δ^{103}	*0.007* **	>0.001 ***

Comparison	Distribution of rhythms	RRP
♀ **RR cycΔ^{103} *vs Cry*> cycΔ^{103}**	*0.037 **	*0.198*
♂ **RR cycΔ^{103} *vs Pdf*> cycΔ^{103}**	*0.004 ***	>0.001 ***
♀ **RR cycΔ^{103} *vs Pdf*> cycΔ^{103}**	*0.228*	*0.010 **
♂ **RR cycΔ^{103} *vs (TUG-Pdf)*> cycΔ^{103}**	*0.118*	*0.614*
♀ **RR cycΔ^{103} *vs (TUG-Pdf)*> cycΔ^{103}**	*0.164*	*0.067*
♂ **RR cycΔ^{103} *vs Clk4.1M*> cycΔ^{103}**	*0.021 **	>0.001 ***
♀ **RR cycΔ^{103} *vs Clk4.1M*> cycΔ^{103}**	*0.539*	*0.183*
♂ **DD cycΔ^{103} *vs TUG*> cycΔ^{103}**	*0.111*	*0.002***
♀ **DD cycΔ^{103} *vs TUG*> cycΔ^{103}**	*>0.001 ****	>0.001 ***
♂ **DD cycΔ^{103} *vs Cry*> cycΔ^{103}**	*0.024 **	>0.001 ***
♀ **DD cycΔ^{103} *vs Cry*> cycΔ^{103}**	*>0.001***	>0.001 ***
♂ **DD cycΔ^{103} *vs Pdf*> cycΔ^{103}**	*0.215*	>0.001 ***
♀ **DD cycΔ^{103} *vs Pdf*> cycΔ^{103}**	*0.013 ***	>0.001 ***
♂ **DD cycΔ^{103} *vs (TUG-Pdf)*> cycΔ^{103}**	*0.301*	*0.958*
♀ **DD cycΔ^{103} *vs (TUG-Pdf)*> cycΔ^{103}**	*0.029 **	>0.001 ***
♂ **DD cycΔ^{103} *vs Clk4.1M*> cycΔ^{103}**	0.318	0.282
♀ **DD cycΔ^{103} *vs Clk4.1M*> cycΔ^{103}**	>0.001 ***	>0.001 ***
♂ **RR *(TUG-cry)*> cycΔ^{103} *vs (TUG-cry)*>+**	0.431	0.072
♀ **RR *(TUG-cry)*> cycΔ^{103} *vs (TUG-cry)*>+**	0.001 **	>0.001 ***
♂ **DD *(TUG-cry)*> cycΔ^{103} *vs (TUG-cry)*>+**	0.761	0.723
♀ **DD *(TUG-cry)*> cycΔ^{103} *vs (TUG-cry)*>+**	0.108	>0.001 ***
♂ **RR *(Cry-Pdf80)*> cycΔ^{103} *vs Cry*>cycΔ^{103}**	-	>0.001 ***
♀ **RR *(Cry-Pdf80)*> cycΔ^{103} *vs Cry*>cycΔ^{103}**	-	0.215
♂ **DD *(Cry-Pdf80)*> cycΔ^{103} *vs Cry*>cycΔ^{103}**	-	0.003**
♀ **DD *(Cry-Pdf80)*> cycΔ^{103} *vs***	-	0.014*

***Cry*>cycΔ^{103}**

Appendix Table 19, relevant to Appendix Table 18, P-values for significance of rhythmicities in various lines expressing cycΔ^{103} in RR and DD. Distribution of rhythmicities was calculated using 2x3 Fisher's exact test, and differences between RRP using one-way ANOVA.

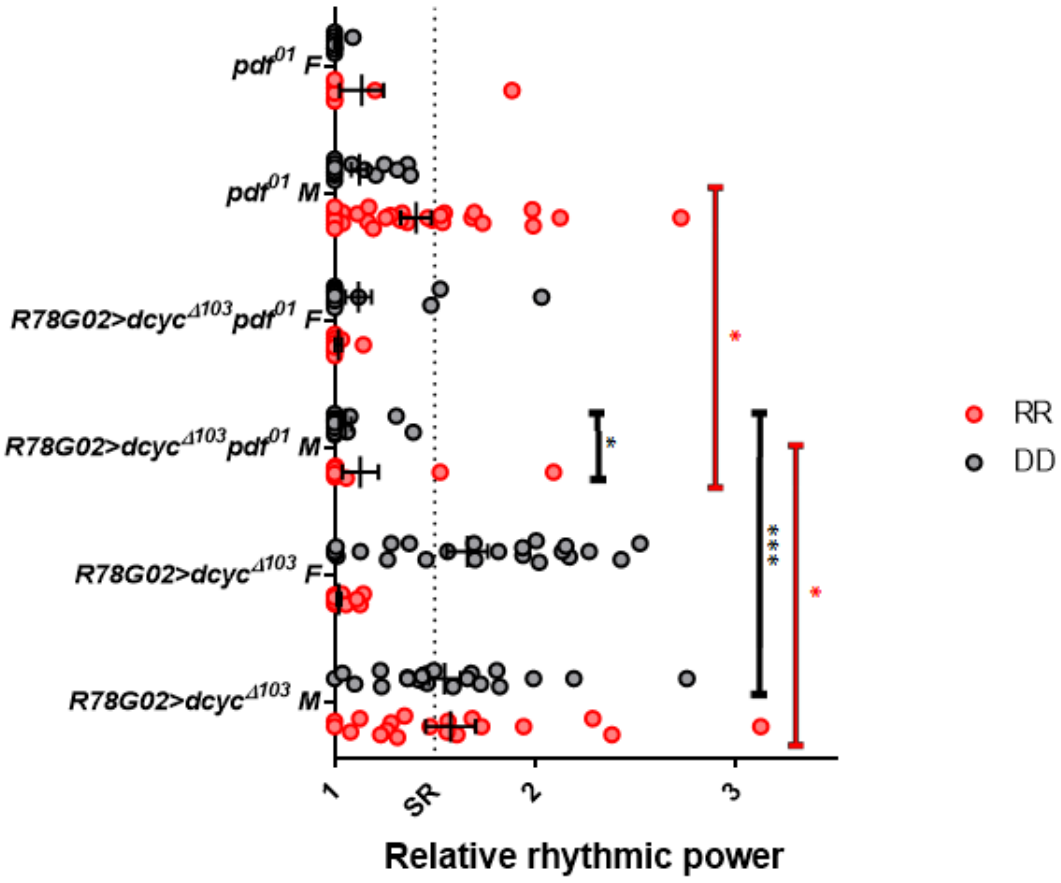

Appendix Figure 19, behavioural rhythmicities of R78G02- Δcyc^{103} in conjunction with Pdf^{01}. The lack of an obvious short period in the rhythmic minority, alongside a lack of controls limit our interpretation of this, though R78G02> Δcyc^{103} only has a significant effect on RR male rhythmicity in conjunction with Pdf^{01}.

Genotype	n	% SR	% WR	% AR	TAU + SEM	RRP + SEM
cyc$^{\Delta 103}$/+; GMR78G02-gal4 Pdf^{01}/Pdf^{01} RR M	12	25.00	16.67	58.33	25.00±2.07	1.34±0.21
cyc$^{\Delta 103}$/+; GMR78G02-gal4 Pdf^{01}/Pdf^{01} RR F	9	0.00	22.22	77.78	24.75±1.25	1.09±0.05
cyc$^{\Delta 103}$/+; GMR78G02-gal4 Pdf^{01}/Pdf^{01} DD M	16	0.00	37.50	62.50	26.25±1.82	1.14±0.06
cyc$^{\Delta 103}$/+; GMR78G02-gal4 Pdf^{01}/Pdf^{01} DD F	18	11.11	11.11	77.78	23.50±0.20	1.54±0.19

RR vs DD	distribution of rhythms	RRP
cyc$^{\Delta 103}$/+; GMR78G02-gal4 Pdf^{01}/Pdf^{01} M RR vs DD	0.123	0.012 *
cyc$^{\Delta 103}$/+; GMR78G02-gal4 Pdf^{01}/Pdf^{01} F RR vs DD	0.627	0.301
cyc$^{\Delta 103}$/+; GMR78G02-gal4 Pdf^{01}/Pdf^{01} vs Pdf^{01} RR M	0.062	0.039 *
cyc$^{\Delta 103}$/+; GMR78G02-gal4 Pdf^{01}/Pdf^{01} vs Pdf^{01} RR F	0.999	0.285
cyc$^{\Delta 103}$/+; GMR78G02-gal4 Pdf^{01}/Pdf^{01} vs Pdf^{01} DD M	0.713	0.159
cyc$^{\Delta 103}$/+; GMR78G02-gal4 Pdf^{01}/Pdf^{01} vs Pdf^{01} DD F	0.999	0.290
cyc$^{\Delta 103}$/+; GMR78G02-gal4 Pdf^{01}/Pdf^{01} vs cyc$^{\Delta 103}$/+; GMR78G02-gal4/+ RR M	0.022*	0.012 *
cyc$^{\Delta 103}$/+; GMR78G02-gal4 Pdf^{01}/Pdf^{01} vs cyc$^{\Delta 103}$/+; GMR78G02-gal4/+ RR F	0.999	0.923
cyc$^{\Delta 103}$/+; GMR78G02-gal4 Pdf^{01}/Pdf^{01} vs cyc$^{\Delta 103}$/+; GMR78G02-gal4/+ DD M	>0.001***	>0.001 ***
cyc$^{\Delta 103}$/+; GMR78G02-gal4 Pdf^{01}/Pdf^{01} vs cyc$^{\Delta 103}$/+; GMR78G02-gal4/+ DD F	>0.001***	>0.001 ***

Appendix table 20, Relevent to Appendix Figure 19, Overall rhythmicity values and P-values for comparison of behavioural rhythmicities for CYC knockdown in E cells on a Pdf^{01} background in RR and DD, with associated controls

RRP of *Clk4.1M>Δcyc*^{103} RR males, (2.104±0.14) significantly differs to males in DD (1.420±0.085) (P=0.001), whilst mean RRP of females in RR (1.272±0.102) is not significantly higher than DD (1.195±0.046). *Clk4.1M-Gal4* drives in a set of ~8-10 DN1s including the $DN1_p$s.

Genotype	**n**	**% SR**	**% WR**	**% AR**	**TAU + SEM**	**RRP + SEM**
cyc*$^{\Delta 103}$*/+; GMR14F03-Gal4/+ RR M	14	28.57	64.29	7.14	24.68±0.26	1.56±0.13
cyc*$^{\Delta 103}$*/+; GMR14F03-Gal4/+ RR F	19	5.26	47.37	47.37	25.60±0.31	1.26±0.05
cyc*$^{\Delta 103}$*/+; GMR14F03-Gal4/+ DD M	15	73.33	20.00	6.67	23.54±0.06	2.12±0.15
cyc*$^{\Delta 103}$*/+; GMR14F03-Gal4/+ DD F	15	66.67	26.67	6.67	23.82±0.12	1.64±0.08
cyc*$^{\Delta 103}$*/+; GMR54D11-Gal4/+ RR M	21	19.05	52.38	28.57	24.03±0.29	1.40±0.07
cyc*$^{\Delta 103}$*/+; GMR54D11-Gal4/+ RR F	23	0.00	4.35	95.65	24.50	1.07
cyc*$^{\Delta 103}$*/+; GMR54D11-Gal4/+ DD M	14	50.00	50.00	0.00	23.50±0.10	1.60±0.14
cyc*$^{\Delta 103}$*/+; GMR54D11-Gal4/+ DD F	16	31.25	62.50	6.25	23.50±0.22	1.40±0.07
cyc*$^{\Delta 103}$*/+; GMR43D05-Gal4/+ RR M	15	6.67	80.00	13.33	24.73±0.22	1.28±0.05
cyc*$^{\Delta 103}$*/+; GMR43D05-Gal4/+ RR F	10	20.00	20.00	60.00	25.13±0.80	1.67±0.28
cyc*$^{\Delta 103}$*/+; GMR43D05-Gal4/+ DD M	15	26.67	40.00	33.33	26.20±0.68	1.43±0.08
cyc*$^{\Delta 103}$*/+; GMR43D05-Gal4/+ DD F	16	31.25	56.25	12.50	26.14±0.28	1.44±0.10

Genotype	n	% SR	% WR	% AR	TAU + SEM	RRP + SEM
cyc$^{\Delta 103}$/+; GMR21G01-Gal4/+ RR M	12	75.00	8.33	16.67	24.85±0.15	2.16±0.14
cyc$^{\Delta 103}$/+; GMR21G01-Gal4/+ RR F	13	15.38	38.46	46.15	26.14±1.32	1.23±0.12
cyc$^{\Delta 103}$/+; GMR21G01-Gal4/+ DD M	15	53.33	40.00	6.67	23.50±0.05	1.56±0.07
cyc$^{\Delta 103}$/+; GMR21G01-Gal4/+ DD F	16	12.50	62.50	25.00	26.75±0.25	1.35±0.09
cyc$^{\Delta 103}$/+; GMR19H11-Gal4/+ RR M	29	72.41	17.24	10.34	25.08±0.08	1.83±0.08
cyc$^{\Delta 103}$/+; GMR19H11-Gal4/+ RR F	32	3.13	43.75	53.13	25.17±0.19	1.21±0.04
cyc$^{\Delta 103}$/+; GMR19H11-Gal4/+ DD M	16	50.00	31.25	18.75	23.88±0.14	1.52±0.10
cyc$^{\Delta 103}$/+; GMR19H11-Gal4/+ DD F	15	6.67	60.00	33.33	24.35±0.17	1.37±0.03
cyc$^{\Delta 103}$/+; GMR42F08-Gal4/+ RR M	16	50.00	50.00	0.00	24.84±0.14	1.57±0.08
cyc$^{\Delta 103}$/+; GMR42F08-Gal4/+ RR F	15	33.33	40.00	26.67	26.41±0.26	1.41±0.08
cyc$^{\Delta 103}$/+; GMR42F08-Gal4/+ DD M	12	75.00	16.67	8.33	24.23±0.45	1.65±0.12
cyc$^{\Delta 103}$/+; GMR42F08-Gal4/+ DD F	13	15.38	46.15	38.46	26.75±0.25	1.35±0.09
yw::GMR14F03-gal4/+ RR M	8	50.00	50.00	0.00	25.50±0.23	1.45±0.09
yw::GMR14F03-gal4/+ RR F	8	25.00	25.00	50.00	24.13±0.31	1.49±0.23
yw::GMR14F03-gal4/+ DD M	8	50.00	25.00	25.00	23.33±0.11	1.52±0.09
yw::GMR14F03-gal4/+ DD F	8	12.50	87.50	0.00	23.75±0.23	1.39±0.07
yw::GMR54D11-gal4/+ RR M	29	17.24	72.41	10.34	24.50±0.20	1.24±0.05
yw::GMR54D11-gal4/+ RR F	32	0.00	37.50	62.50	25.33±0.67	1.08±0.03
yw::GMR54D11-gal4/+ DD M	13	53.85	30.77	15.38	23.36±0.07	1.70±0.12

Genotype	n	% SR	% WR	% AR	TAU + SEM	RRP + SEM
yw::GMR54D11-gal4/+ DD F	16	100.00	0.00	0.00	23.50±0.05	2.10±0.09
yw::GMR43D05-gal4/+ RR M	8	87.50	12.50	0.00	25.06±0.18	2.06±0.15
yw::GMR43D05-gal4/+ RR F	8	0.00	25.00	75.00	22.25±4.75	1.09±0.01
yw::GMR43D05-gal4/+ DD M	8	12.50	50.00	37.50	22.90±0.86	1.27±0.10
yw::GMR43D05-gal4/+ DD F	8	12.50	50.00	37.50	27.50±0.22	1.37±0.05
yw::GMR21G01-gal4/+ RR M	8	50.00	37.50	12.50	24.14±0.26	1.55±0.16
yw::GMR21G01-gal4/+ RR F	8	0.00	87.50	12.50	28.79±0.34	1.17±0.07
yw::GMR21G01-gal4/+ DD M	8	0.00	75.00	25.00	23.17±0.11	1.11±0.04
yw::GMR21G01-gal4/+ DD F	8	0.00	62.50	37.50	26.80±0.34	1.26±0.06
yw::GMR19H11-gal4/+ RR M	8	75.00	25.00	0.00	24.19±0.23	1.64±0.14
yw::GMR19H11-gal4/+ RR F	8	12.50	25.00	62.50	24.17±0.17	1.41±0.10
yw::GMR19H11-gal4/+ DD M	8	0.00	25.00	75.00	23.50±0.00	1.09±0.08
yw::GMR19H11-gal4/+ DD F	8	0.00	75.00	25.00	22.42±0.90	1.15±0.04
yw::GMR42F08-gal4/+ RR M	8	50.00	37.50	12.50	24.64±0.24	1.55±0.12
yw::GMR42F08-gal4/+ RR F	8	0.00	25.00	75.00	22.75±2.25	1.07±0.06
yw::GMR42F08-gal4/+ DD M	8	0.00	75.00	25.00	23.75±0.21	1.22±0.03
yw::GMR42F08-gal4/+ DD F	7	0.00	85.71	14.29	23.50±0.26	1.17±0.04
w; Clk4.1M-gal4/Uas cyc$^{\Delta 103}$ RR M	15	93.33	6.67	0.00	2.10±0.14	23.57±0.15
w; Clk4.1M-gal4/Uas cyc$^{\Delta 103}$ RR F	16	18.75	37.50	43.75	1.27±0.10	22.78±0.74
w; Clk4.1M-gal4/Uas cyc$^{\Delta 103}$ DD M	14	35.71	57.14	7.14	1.42±0.09	23.54±0.14
w; Clk4.1M-gal4/Uas cyc$^{\Delta 103}$ DD F	15	0.00	40.00	60.00	1.20±0.05	24.58±0.44
w; mai179-gal4/Uas cyc$^{\Delta 103}$ RR M	12	75.00	25.00	0.00	25.79±0.11	1.99±0.19
w; mai179-gal4/Uas cyc$^{\Delta 103}$ RR F	12	0.00	33.33	66.67	26.00±0.35	1.24±0.06
w; mai179-gal4/Uas cyc$^{\Delta 103}$ DD M	12	83.33	16.67	0.00	24.17±0.13	1.91±0.08

Genotype	n	% SR	% WR	% AR	TAU + SEM	RRP + SEM
w; mai179-gal4/Uas cyc$^{\Delta 103}$ DD F	11	18.18	63.64	18.18	24.50±0.17	1.39±0.15
w; dvpdf-gal4/Uas cyc$^{\Delta 103}$ RR M	16	100.00	0.00	0.00	24.94±0.10	2.55±0.11
w; dvpdf-gal4/Uas cyc$^{\Delta 103}$ RR F	14	21.43	42.86	35.71	24.33±0.26	1.38±0.11
w; dvpdf-gal4/Uas cyc$^{\Delta 103}$ DD M	16	75.00	12.50	12.50	24.50±0.13	1.82±0.09
w; dvpdf-gal4/Uas cyc$^{\Delta 103}$ DD F	16	37.50	56.25	6.25	24.43±0.08	1.41±0.07
w; R6-gal4/Uas cyc$^{\Delta 103}$ DD M	12	41.67	58.33	0	23.96±0.16	1.47±0.08
w; R6-gal4/Uas cyc$^{\Delta 103}$ DD F	12	33.33	41.67	25	23.78±0.22	1.44±0.10

Appendix Table 21: Behavioural rhythmicities of cyc$^{\Delta 103}$-expressing flies of various driver lines in RR and DD.

driven vs undriven	distribution of rhythms	RRP
cyc$^{\Delta 103}$/+; GMR14F03-Gal4/+ RR M	0.774	0.689
cyc$^{\Delta 103}$/+; GMR14F03-Gal4/+ RR F	0.292	0.332
cyc$^{\Delta 103}$/+; GMR14F03-Gal4/+ DD M	0.469	
cyc$^{\Delta 103}$/+; GMR14F03-Gal4/+ DD F	0.016 *	X
cyc$^{\Delta 103}$/+; GMR54D11-Gal4/+ RR M	0.223	0.276
cyc$^{\Delta 103}$/+; GMR54D11-Gal4/+ RR F	>0.001 ***	0.092
cyc$^{\Delta 103}$/+; GMR54D11-Gal4/+ DD M	0.321	0.968
cyc$^{\Delta 103}$/+; GMR54D11-Gal4/+ DD F	>0.001 ***	>0.001 ***
cyc$^{\Delta 103}$/+; GMR43D05-Gal4/+ RR M	>0.001***	>0.001***
cyc$^{\Delta 103}$/+; GMR43D05-Gal4/+ RR F	0.613	0.236
cyc$^{\Delta 103}$/+; GMR43D05-Gal4/+ DD M	0.858	0.336
driven vs undriven	**distribution of rhythms**	**RRP**

cyc$^{\Delta 103}$/+; GMR43D05-Gal4/+	***DD F***	0.372	0.297
cyc$^{\Delta 103}$/+; GMR21G01-Gal4/+	***RR M***	0.834	0.066
cyc$^{\Delta 103}$/+; GMR21G01-Gal4/+	***RR F***	0.121	0.800
cyc$^{\Delta 103}$/+; GMR21G01-Gal4/+	***DD M***	0.025 *	>0.001***
cyc$^{\Delta 103}$/+; GMR21G01-Gal4/+	***DD F***	0.828	0.351
cyc$^{\Delta 103}$/+; GMR19H11-Gal4/+	***RR M***	1	0.063
cyc$^{\Delta 103}$/+; GMR19H11-Gal4/+	***RR F***	0.324	0.094
cyc$^{\Delta 103}$/+; GMR19H11-Gal4/+	***DD M***	0.013 *	0.007 **
cyc$^{\Delta 103}$/+; GMR19H11-Gal4/+	***DD F***	0.999	0.086
cyc$^{\Delta 103}$/+; GMR42F08-Gal4/+	***RR M***	0.462	0.569
cyc$^{\Delta 103}$/+; GMR42F08-Gal4/+	***RR F***	0.063	0.016 *
cyc$^{\Delta 103}$/+; GMR42F08-Gal4/+	***DD M***	0.002 **	0.138
cyc$^{\Delta 103}$/+; GMR42F08-Gal4/+	***DD F***	0.291	0.606

RR vs DD	**distribution of rhythms**	**RRP**
cyc$^{\Delta 103}$/+; GMR14F03-Gal4/+	***M***	0.02 *	0.010 *
cyc$^{\Delta 103}$/+; GMR14F03-Gal4/+	***F***	>0.001 ***	>0.001 ***
cyc$^{\Delta 103}$/+; GMR54D11-Gal4/+	***M***	0.043 *	0.029 *
cyc$^{\Delta 103}$/+; GMR54D11-Gal4/+	***F***	>0.001 ***	>0.001 ***
cyc$^{\Delta 103}$/+; GMR43D05-Gal4/+	***M***	0.113	0.640
cyc$^{\Delta 103}$/+; GMR43D05-Gal4/+	***F***	0.054	0.203
cyc$^{\Delta 103}$/+; GMR21G01-Gal4/+	***M***	0.224	0.017 *
cyc$^{\Delta 103}$/+; GMR21G01-Gal4/+	***F***	0.401	0.160
RR vs DD		**distribution of rhythms**	**RRP**

cyc$^{\Delta 103}$/+; GMR19H11-Gal4/+ M	0.333	>0.001 ***
cyc$^{\Delta 103}$/+; GMR19H11-Gal4/+ F	0.342	0.194
cyc$^{\Delta 103}$/+; GMR42F08-Gal4/+ M	0.114	0.850
cyc$^{\Delta 103}$/+; GMR42F08-Gal4/+ F	0.632	0.441
yw::GMR14F03-gal4/+ M	0.641	0.702
yw::GMR14F03-gal4/+ F	0.018 *	>0.001 ***
yw::GMR54D11-gal4/+ M	0.021 *	0.007 **
yw::GMR54D11-gal4/+ F	>0.001 ***	>0.001 ***
yw::GMR43D05-gal4/+ M	0.001 **	>0.001 ***
yw::GMR43D05-gal4/+ F	0.216	0.016 *
yw::GMR21G01-gal4/+ M	0.099	0.027 *
yw::GMR21G01-gal4/+ F	0.569	0.866
yw::GMR19H11-gal4/+ M	>0.001 ***	0.001 **
yw::GMR19H11-gal4/+ F	0.131	0.637
yw::GMR42F08-gal4/+ M	0.099	0.030 *
yw::GMR42F08-gal4/+ F	0.04 *	0.012 *

Appendix Table 22; Relevant to Appendix Table 21, P-values for comparing rhythmicities between RR and DD light conditions for flylight> cyc$^{\Delta 103}$ *and flylight>+. Comparisons between distributions of rhythmicity were calculated using 2x3 Fisher's exact test, and RRP using one-way ANOVA.*

Genotype	**n**	**% SR**	**% WR**	**% AR**	**TAU + SEM**	**RRP + SEM**
per^{01};+/+; R78G02/uasper16 RR M	21	4.76	52.38	42.86	29.67±1.50	1.50±0.05
per^{01};+/+; R78G02/uasper16 DD M	21	19.05	47.62	33.33	23.82±0.24	1.29±0.06
per^{01};+/+; ser/uasper16 RR M	11	0.00	0.00	100.00	N/A	N/A
per^{01};+/+; ser/uasper16 DD M	11	0.00	0.00	100.00	N/A	N/A
per^{01} pdfgal80/+; ser/uas-per16 RR M	20	0.00	0.00	100.00	N/A	N/A
per^{01} pdfgal80/+; ser/uas-per16 DD M	16	0.00	12.50	87.50	23.75±4.25	1.09±0.04
per^{01} pdfgal80/+; crygal4/uas-per16 RR M	24	62.50	29.17	8.33	27.93±0.20	1.66±0.06
per^{01} pdfgal80/+; crygal4/uas-per16 DD M	25	4.00	40.00	56.00	24.64±1.17	1.16±0.05
Genotype	**n**	**% SR**	**% WR**	**% AR**	**TAU +**	**RRP +**

					SEM	SEM
per^{01} CyO/+; crygal4/uas-per16 RR M	14	78.57	14.29	7.14	27.58±0.14	1.87±0.09
per^{01} CyO/+; crygal4/uas-per16 DD M	10	10.00	50.00	40.00	27.17±0.56	1.21±0.13
per^{01} +/+; Clk4.1Mgal4/uas-per16 RR M	19	0.00	10.53	89.47	24.00±4.50	1.04±0.02
per^{01} +/+; Clk4.1Mgal4/uas-per16 DD M	15	0.00	46.67	53.33	23.86±0.69	1.09±0.03
per^{01} +/+; chagal4/uas-per16 RR M	10	40	60	0	26.80±0.19	1.60±0.16
per^{01} +/+; chagal4/uas-per16 DD M	11	0	9.09	90.91	23.50	1.02

Appendix Table 23, behavioural rhythmicities for PER-rescue lines within various E cell drivers and controls, in RR and DD

RR vs DD	**distribution of rhythms**	**RRP**
per^{01};+/+; R78G02/uasper16 M	0.502	0.090
per^{01};+/+; ser/uasper16 M	1	1
per^{01} pdfgal80/+; ser/uas-per16 M	0.19	0.153
per^{01} pdfgal80/+; crygal4/uas-per16 M	>0.001 ***	>0.001 ***
per^{01} CyO/+; crygal4/uas-per16 M	>0.001 ***	0.001 **
per^{01} +/+; Clk4.1Mgal4/uas-per16	0.025*	0.021*
per^{01} +/+; chagal4/uas-per16	>0.001 ***	0.001 **
per^{01} pdfgal80/+; crygal4/uas-per16 vs per^{01} CyO/+; crygal4/uas-per16 RR	0.739	0.096
per^{01} pdfgal80/+; crygal4/uas-per16 vs per^{01} CyO/+; crygal4/uas-per16 DD	0.594	0.394
per^{01} pdfgal80/+; crygal4/uas-per16 vs per^{01} pdfgal80/+; ser/uas-per16 RR	>0.001 ***	>0.001 ***
per^{01} pdfgal80/+; crygal4/uas-per16 vs per^{01} pdfgal80/+; ser/uas-per16 DD	0.107	0.109
RR vs DD	**distribution of rhythms**	**RRP**

per^{01};+/+; R78G02/uasper16 vs per^{01};+/+; ser/uasper16 RR	0.001 **	0.046 *
per^{01};+/+; R78G02/uasper16 vs per^{01};+/+; ser/uasper16 DD	>0.001 ***	0.009 **
per^{01} CyO/+; crygal4/uas-per16 vs per^{01};+/+; ser/uasper16 RR	0.003 **	>0.001 ***
per^{01} CyO/+; crygal4/uas-per16 vs per^{01};+/+; ser/uasper16 DD	>0.001 ***	0.091
per^{01};+/+; cha/uasper16 vs per^{01};+/+; ser/uasper16 RR	>0.001 ***	0.001**
per^{01};+/+; cha/uasper16 vs per^{01};+/+; ser/uasper16 DD	0.999	0.329

Appendix Table 24, P-values comparing significance of rhythmicity shown in Appendix Table 23, assessing various spatial PER reintroduction lines in RR and DD. Comparisons between distributions of rhythmicity were calculated using 2x3 Fisher's exact test and RRP using one-way ANOVA.

Genotype	**n**	**% SR**	**% WR**	**% AR**	**TAU + SEM**	**RRP + SEM**
Pdfr^{5304} RR M	18	16.67	33.33	50.00	22.78±0.19	1.42±0.13
Pdfr^{5304} RR F	13	7.69	46.15	46.15	23.29±0.21	1.24±0.07
Pdfr^{5304} DD M	14	0.00	7.14	92.86	25.5	1.18
Pdfr^{5304} DD F	10	0.00	30.00	70.00	23.83±0.17	1.02±0.01
Pdf^{01} RR M	29	34.48	44.83	20.69	22.56±0.11	1.51±0.08
Pdf^{01} RR F	8	12.5	12.5	75	22.25±0.25	1.54±0.34
Pdf^{01} DD M	14	0	50	50	24.29±0.73	1.25±0.04
Pdf^{01} DD F	8	0	12.5	87.5	23	1.09
Dh31$^{\#51}$ RR M	10	10.00	50.00	40.00	24.42±0.37	1.27±0.12
Dh31$^{\#51}$ RR F	13	7.69	46.15	46.15	24.71±0.79	1.33±0.08
Dh31$^{\#51}$ DD M	11	18.18	54.55	27.27	25.31±0.65	1.25±0.09
Dh31$^{\#51}$ DD F	12	16.67	58.33	25.00	24.06±0.84	1.32±0.09
Dh31$^{\#51}$/+ RR M	16	31.25	12.5	56.25	25.36±0.09	1.71±0.18
Dh31$^{\#51}$/+ RR F	14	0	28.57	71.43	25.13±0.31	1.20±0.07
Genotype	**n**	**% SR**	**% WR**	**% AR**	**TAU +**	**RRP +**

					SEM	SEM
Dh31$^{\#51}$/+ DD M	16	12.5	75	12.5	24.64±0.56	1.27±0.06
Dh31$^{\#51}$/+ DD F	16	56.25	37.5	6.25	23.60±0.05	1.61±0.08
PDF>LarKD RR M	16	87.50	6.25	6.25	25.23±0.19	2.14±0.11
PDF>LarKD RR F	15	0.00	26.67	73.33	22.63±2.13	1.09±0.03
PDF>LarKD DD M	7	0.00	42.86	57.14	23.50±0.29	1.20±0.12
PDF>LarKD DD F	12	0.00	25.00	75.00	20.67±2.84	1.13±0.11
Pdf>hid RR M	16	0.00	43.75	56.25	24.64±1.67	1.15±0.04
Pdf>hid RR F	16	6.25	31.25	62.50	22.67±0.42	1.21±0.09
Pdf>hid DD M	8	0.00	25.00	75.00	22.5	1.34±0.16
Pdf>hid DD F	8	0.00	37.50	62.50	23.83±4.97	1.08±0.02
Pdf/+;+;+ RR M	14	42.86	50.00	7.14	25.58±0.80	1.45±0.09
Pdf/+;+;+ RR F	28	17.86	50.00	32.14	24.76±0.13	1.44±0.06
Pdf/+;+;+ DD M	12	50.00	50.00	16.67	25.92±0.10	1.66±0.08
Pdf/+;+;+ DD F	16	62.50	37.50	0.00	23.78±0.10	1.66±0.12
Pdf; TeTxLC/+ RR M	14	78.57	21.43	0	25.25±0.72	1.74±0.09
Pdf; TeTxLC /+ RR F	15	40	53.33	6.67	25.68±1.19	1.57±0.10
Pdf; TeTxLC /+ DD M	12	66.67	33.33	0	24.75±0.36	1.77±0.13
Pdf; TeTxLC /+ DD F	16	50	50	0	27.00±0.83	1.57±0.08
Pdf; Kir2.1 /+ RR M	15	0	40	60	22.25±0.28	1.11±0.03
Pdf; Kir2.1 /+ RR F	14	0	14.29	85.71	22.50±0.50	1.03±0.03
Pdf; Kir2.1 /+ DD M	12	0	25	75	21.67±1.17	1.11±0.04
Pdf; Kir2.1 /+ DD F	20	0	5	95	19	1.02
Pdf; NaChBac/+ RR M	10	20.00	30.00	50.00	25.10±0.33	1.40±0.10
Pdf; NaChBac/+ RR F	22	0.00	18.18	81.82	26.13±1.23	1.19±0.06
Pdf; NaChBac/+ DD M	15	13.33	26.67	60.00	23.92±0.35	1.31±0.15
Pdf; NaChBac/+ DD F	16	0.00	18.75	81.25	25.83±1.69	1.03±0.02
Pdf; uas-TrpA1/+ 29°C M RR	16	43.75	56.25	0.00	22.41±0.22	1.44±0.08
Pdf; uas-TrpA1/+ 29°C F RR	12	25.00	58.33	16.67	22.90±0.19	1.41±0.09
Pdf; uas-TrpA1/+ 29°C M DD	14	35.71	57.14	7.14	22.50±0.18	1.40±0.10
Pdf; uas-TrpA1/+ 29°C F DD	14	42.86	42.86	14.29	22.71±0.74	1.51±0.09
Pdf; uas-TrpA1/+ 23°C M RR	10	60.00	20.00	20.00	24.06±0.33	1.67±0.17

Genotype	n	% SR	% WR	% AR	TAU + SEM	RRP + SEM
Pdf; uas-TrpA1/+ 23°C F RR	12	50.00	33.33	16.67	23.45±0.49	1.67±0.13
Pdf; uas-TrpA1/+ 23°C M DD	13	23.08	38.46	38.46	25.00±0.78	1.38±0.11
Pdf; uas-TrpA1/+ 23°C DD	14	35.71	42.86	21.43	23.73±0.54	1.46±0.08
ds lar/ + RR M	14	100.00	0.00	0.00	24.61±0.16	2.31±0.11
ds lar/ + RR F	15	26.67	46.67	26.67	25.23±0.25	1.43±0.10
ds lar/ + DD M	16	100.00	0.00	0.00	23.47±0.06	2.44±0.09
ds lar/ + DD F	15	80.00	20.00	0.00	23.77±0.08	1.91±0.11
Uas-TeTxLC/+; GMR78G02-gal4/+ M RR	15	0.00	53.33	46.67	23.63±0.25	1.17±0.04
Uas-TeTxLC/+; GMR78G02-gal4/+ F RR	13	0.00	38.46	61.54	25.20±1.62	1.13±0.03
Uas-TeTxLC/+; GMR78G02-gal4/+ M DD	17	23.53	47.06	29.41	24.42±0.38	1.46±0.12
Uas-TeTxLC/+; GMR78G02-gal4/+ F DD	29	27.59	55.17	17.24	24.13±0.09	1.33±0.05
Uas-NaChBac/+; GMR78G02-gal4/+ M RR	16	37.50	56.25	6.25	23.57±0.35	1.46±0.08
Uas-NaChBac/+; GMR78G02-gal4/+ F RR	16	0.00	25.00	75.00	25.63±0.13	1.19±0.10
Uas-NaChBac/+; GMR78G02-gal4/+ M DD	14	87.50	6.25	6.25	23.53±0.03	2.04±0.11
Uas-NaChBac/+; GMR78G02-gal4/+ F DD	16	100.00	0.00	0.00	23.56±0.04	2.45±0.09
Uas-TrpA1/+; GMR78G02-gal4/+ 29°C RR M	7	0.00	42.86	57.14	22.67±0.83	1.18±0.03
Uas-TrpA1/+; GMR78G02-gal4/+ 29°C RR F	6	0.00	0.00	100.00		1.00
Uas-TrpA1/+; GMR78G02-gal4/+ 29°C DD M	22	54.55	40.91	4.55	23.17±0.08	1.70±0.12
Uas-TrpA1/+; GMR78G02-gal4/+ 29°C DD F	24	29.17	50.00	20.83	23.58±0.09	1.41±0.08
Uas-TrpA1/+; GMR78G02-gal4/+ 23°C RR M	16	56.25	31.25	12.50	24.93±0.09	1.77±0.14
Uas-TrpA1/+; GMR78G02-	16	0.00	31.25	68.75	24.50±0.22	1.09±0.02

gal4/+ 23°C RR F						
Genotype	**n**	**% SR**	**% WR**	**% AR**	**TAU + SEM**	**RRP + SEM**
Uas-TrpA1/+; GMR78G02-gal4/+ 23°C DD M	13	84.62	15.38	0.00	23.92±0.10	2.100812887
Uas-TrpA1/+; GMR78G02-gal4/+ 23°C DD F	11	36.36	54.55	9.09	24.35±025	1.41±0.10
yw::GMR78G02-gal4/+ RR M	34	35.29	41.18	23.53	24.72±0.23	1.64±0.10
yw::GMR78G02-gal4/+ RR F	21	0.00	33.33	66.67	23.60±1.26	1.10±0.04
yw::GMR78G02-gal4/+ DD M	29	68.97	13.79	17.24	24.00±0.11	2.01±0.08
yw::GMR78G02-gal4/+ DD F	28	57.14	25.00	17.86	23.92±0.17	1.90±0.12
Uas-TeTxLC(NEG)/+; GMR78G02-gal4/+ RR M	11	81.82	9.09	9.09	24.50±0.07	2.32±0.15
Uas-TeTxLC(NEG)/+; GMR78G02-gal4/+ RR F	18	11.11	55.56	33.33	24.67±0.23	1.25±0.06
Uas-TeTxLC(NEG)/+; GMR78G02-gal4/+ DD M	11	100.00	0.00	0.00	23.5	2.23±0.09
Uas-TeTxLC(NEG)/+; GMR78G02-gal4/+ DD F	20	95.00	5.00	0.00	23.60±0.05	2.14±0.09
yw::GMR54D11-gal4/+ RR M	29	17.24	72.41	10.34	24.50±0.20	1.24±0.05
yw::GMR54D11-gal4/+ RR F	32	0.00	37.50	62.50	25.33±0.67	1.08±0.03
yw::GMR54D11-gal4/+ DD M	13	53.85	30.77	15.38	23.36±0.07	1.70±0.12
yw::GMR54D11-gal4/+ DD F	16	100.00	0.00	0.00	23.50±0.05	2.10±0.09
Uas-NaChBac/+; GMR54D11-gal4/+ RR M	13	84.62	15.38	0.00	27.77±0.37	1.81±0.12
Uas-NaChBac/+; GMR54D11-gal4/+ RR F	14	28.57	28.57	35.71	26.56±0.18	1.52±0.11
Uas-NaChBac/+; GMR54D11-gal4/+) DD M	16	62.50	31.25	6.25	27.10±0.09	1.63±0.09

Genotype	n	% SR	% WR	% AR	TAU + SEM	RRP + SEM
Uas-NaChBac/+; GMR54D11-gal4/+) DD F	16	18.75	62.50	18.75	26.04±0.13	1.38±0.14
Uas-TeTxLC/+; GMR54D11-gal4/+ RR M	15	0.00	53.33	46.67	23.69±0.30	1.17±0.05
Uas-TeTxLC/+; GMR54D11-gal4/+ RR F	13	0.00	23.08	76.92	22.50±2.02	1.08±0.03
Uas-TeTxLC/+; GMR54D11-gal4/+ DD M	14	35.71	64.29	0.00	23.96±0.12	1.43±0.07
Uas-TeTxLC/+; GMR54D11-gal4/+ DD F	15	26.67	40.00	33.33	24.30±0.20	1.45±0.12
Uas-TrpA1/+; GMR54D11-gal4/+ RR M 23°C	7	85.71	14.29	0.00	24.07±0.28	1.86±0.12
Uas-TrpA1/+; GMR54D11-gal4/+ RR F 23°C	8	25.00	12.50	62.50	23.83±0.33	1.35±0.19
Uas-TrpA1/+; GMR54D11-gal4/+ DD M 23°C	9	55.56	33.33	11.11	24.19±0.21	1.64±0.13
Uas-TrpA1/+; GMR54D11-gal4/+ DD F 23°C	5	40.00	20.00	40.00	23.67±0.17	1.45±0.14
Uas-TrpA1/+; GMR54D11-gal4/+ RR M 29°C	13	61.54	30.77	7.69	22.92±0.16	1.75±0.13
Uas-TrpA1/+; GMR54D11-gal4/+ RR F 29°C	16	6.25	50.00	43.75	22.33±0.20	1.28±0.08
Uas-TrpA1/+; GMR54D11-gal4/+ DD M 29°C	6	66.67	33.33	0.00	23.17±0.17	2.11±0.35
Uas-TrpA1/+; GMR54D11-gal4/+ DD F 29°C	12	58.33	33.33	8.33	23.32±0.08	1.70±0.09
Uas-TeTxLC(NEG)/+; GMR54D11-gal4/+ RR M	14	71.43	28.57	0.00	25.04±0.12	1.71±0.07
Uas-TeTxLC(NEG)/+; GMR54D11-gal4/+ RR F	12	8.33	58.33	33.33	24.19±0.19	1.27±0.07
Uas-TeTxLC(NEG)/+; GMR54D11-gal4/+ DD M	7	85.71	14.29	0.00	23.71±0.10	1.97±0.18
Uas-TeTxLC(NEG)/+; GMR54D11-gal4/+ DD F	3	66.67	33.33	0.00	23.67±0.17	1.78±0.35
Uas-TrpA1/+; Clk4.1M-	15	13.33	33.33	53.33	24.60±1.27	1.17±0.11

gal4/+ RR M 29°C						
Genotype	**n**	**% SR**	**% WR**	**% AR**	**TAU + SEM**	**RRP + SEM**
Uas-TrpA1/+; Clk4.1M-gal4/+ RR F 29°C	7	14.29	0	85.71	22	1.80
Uas-TrpA1/+; Clk4.1M-gal4/+ DD M 29°C	6	33.33	50	16.67	23.70±0.34	1.47±0.28
Uas-TrpA1/+; Clk4.1M-gal4/+ DD F 29°C	11	0	36.36	63.64	23.88±0.38	1.08±0.02
Uas-TrpA1/+; Clk4.1M-gal4/+ RR M 23°C	9	100.00	0.00	0.00	23.83±0.20	2.32±0.14
Uas-TrpA1/+; Clk4.1M-gal4/+ RR F 23°C	12	33.33	50.00	16.67	23.80±0.54	1.36±0.06
Uas-TrpA1/+; Clk4.1M-gal4/+ DD M 23°C	10	80.00	20.00	0.00	23.95±0.16	1.85±0.10
Uas-TrpA1/+; Clk4.1M-gal4/+ DD F 23°C	9	66.67	22.22	11.11	23.69±028	1.72±0.14
pdfgal80/+; crygal4/+ RR M	15	33.33	46.67	20.00	25.63±0.47	1.40±0.08
pdfgal80/+; crygal4/+ RR F	16	0.00	31.25	68.75	23.90±0.29	1.18±0.09
pdfgal80/+; crygal4/+ DD M	15	20.00	66.67	13.33	24.54±0.27	1.30±0.08
pdfgal80/+; crygal4/+ DD F	12	50.00	41.67	8.33	23.95±0.26	1.55±0.11
pdfgal80/NaChBac; crygal4/+ RR M	10	20.00	40.00	40.00	24.08±0.24	1.45±0.19
pdfgal80/NaChBac; crygal4/+ RR F	16	0.00	12.50	87.50	25.00±0.50	1.14±0.08
pdfgal80/NaChBac; crygal4/+ DD M	12	75.00	25.00	0.00	24.96±0.27	1.66±0.08
pdfgal80/NaChBac; crygal4/+ DD F	19	10.53	63.16	26.32	26.82±0.34	1.31±0.09
pdfgal80/TrpA1; crygal4/+ 29°C RR M	14	64.29	28.57	7.14	22.79±0.29	1.83±0.19
pdfgal80/TrpA1; crygal4/+ 29°C RR F	8	0	0	100	N/A	N/A
pdfgal80/TrpA1; crygal4/+ 29°C DD M	8	62.50	37.50	0.00	23.17±0.02	2.03±0.30
pdfgal80/TrpA1; crygal4/+ 29°C DD F	10	10.00	40.00	50.00	23.88±0.02	1.16±0.13

Genotype	n	% SR	% WR	% AR	TAU + SEM	RRP + SEM
pdfgal80/TeTxLC; crygal4/+ RR M	22	50.00	36.36	13.64	24.00±0.20	1.57±0.09
pdfgal80/TeTxLC; crygal4/+ RR F	26	0.00	30.77	69.23	23.79±1.78	1.20±0.10
pdfgal80/TeTxLC; crygal4/+ DD M	8	12.50	75.00	12.50	24.64±1.43	1.47±0.06
pdfgal80/TeTxLC; crygal4/+ DD F	5	60.00	20.00	20.00	24.50±1.47	1.52±0.12
pdfgal80/TeTxLC(NEG); crygal4/+ RR M	20	85.00	15.00	0.00	25.30±0.89	1.77±0.06
pdfgal80/TeTxLC(NEG); crygal4/+ RR F	6	0.00	16.67	83.33	23	1.11
pdfgal80/TeTxLC(NEG); crygal4/+ DD M	14	35.71	50.00	14.29	24.13±0.19	1.52±0.12
pdfgal80/TeTxLC(NEG); crygal4/+ DD F	15	6.67	46.67	46.67	24.19±0.25	1.23±0.06
pdfgal80/Kir2.1; crygal4/+ RR M	17	0.00	29.41	70.59	22.30±0.54	1.10±0.03
pdfgal80/Kir2.1; crygal4/+ RR F	14	0.00	42.86	57.14	29.75±1.06	1.25±0.05
pdfgal80/Kir2.1; crygal4/+ DD M	14	7.14	21.43	71.43	24.38±0.31	1.31±0.15
pdfgal80/Kir2.1; crygal4/+ DD F	19	0.00	15.79	84.21	24.50±0.29	1.19±0.08
TUG/Uas-NaChBac RR M	14	0	0	100	N/A	N/A
TUG/Uas-NaChBac RR F	15	0	33.33	66.67	28.10±2.14	1.06±0.02
TUG/Uas-NaChBac DD M	16	0	12.5	87.5	22.25±3.25	1.06±0.00
TUG/Uas-NaChBac DD F	16	0	6.25	93.75	27	1
TUG/uas-NaChBac; Crygal80/+ RR M	15	33.33	26.67	40	25.50±1.10	1.58±0.12
TUG/uas-NaChBac; Crygal80/+ RR F	15	33.33	33.33	33.33	25.90±0.19	1.56±0.11
TUG/uas-NaChBac; Crygal80/+ DD M	14	0	14.29	85.71	24.50±1.00	1.25±0.15
TUG/uas-NaChBac;	13	0	7.69	92.31	26	1.36

Crygal80/+ DD F						
Genotype	**n**	**% SR**	**% WR**	**% AR**	**TAU + SEM**	**RRP + SEM**
TUG/+; Crygal80/+ RR M	13	53.85	30.77	15.38	22.64±0.54	1.81±0.16
TUG/+; Crygal80/+ RR F	15	40	53.33	6.67	23.89±0.15	1.50±0.10
TUG/+; Crygal80/+ DD M	15	73.33	13.33	13.33	23.92±0.11	2.01±0.12
TUG/+; Crygal80/+ DD F	13	23.08	53.85	23.08	24.80±1.03	1.35±0.11

Appendix Table 25, Behavioural rhythmicities for various genotypes altering clock circuit connectivity or cell function in RR or DD. Data in red contributed in part by other lab members.

RR vs DD	**Distribution of rhythms**	**RRP**
Pdfr^{5304} M	0.029	0.041 *
Pdfr^{5304} F	0.527	0.043 *
Dh31$^{\#51}$ M	0.724	0.854
Dh31$^{\#51}$ F	0.532	0.529
PDF>LarKD M	>0.001***	>0.001 ***
PDF>LarKD F	0.999	0.759
Pdf; hid/+ M	0.657	0.719
Pdf; hid/+ F	1	0.434
Pdf/+;+;+ M	0.999	0.736
Pdf/+;+;+ F	0.002 **	0.003**
Pdf; NaChBac/+ M	0.999	0.584
Pdf; NaChBac/+ F	0.999	0.215
Pdf>TrpA1 29°C M	0.846	0.611
Pdf>TrpA1 29°C F	0.764	0.365
Pdf>TrpA1 23°C M	0.322	0.090
Pdf>TrpA1 23°C F	1	0.217
Pdf; Kir2.1 M	0.394	0.538
Pdf; Kir2.1 F	0.555	0.41
ds lar/ + M	1	0.346
ds lar/ + F	0.008 **	>0.001 ***
Uas-TeTxLC/+; GMR78G02-gal4/+ M	0.138	0.052
Uas-TeTxLC/+; GMR78G02-gal4/+ F	0.008 **	0.003**

RR vs DD	Distribution of rhythms	RRP
Uas-NaChBac/+; GMR78G02-gal4/+ M	0.007 **	>0.001 ***
Uas-NaChBac/+; GMR78G02-gal4/+ F	>0.001***	>0.001 ***
Uas-TrpA1/+; GMR78G02-gal4/+ 29°C M	0.002**	0.001 **
Uas-TrpA1/+; GMR78G02-gal4/+ 29°C F	0.001 **	0.002 **
Uas-TrpA1/+; GMR78G02-gal4/+ 23°C M	0.335	0.032*
Uas-TrpA1/+; GMR78G02-gal4/+ 23°C F	0.001 **	>0.001 ***
yw::GMR78G02-gal4/+ M	0.017 *	0.032 *
yw::GMR78G02-gal4/+ F	>0.001 ***	>0.001 ***
Uas-TeTxLC(NEG)/+; GMR78G02-gal4/+ M	0.476	0.884
Uas-TeTxLC(NEG)/+; GMR78G02-gal4/+ F	>0.001***	>0.001 ***
yw::GMR54D11-gal4/+ M	0.514	>0.001 ***
yw::GMR54D11-gal4/+ F	>0.001***	>0.001 ***
Uas-NaChBac/+; GMR54D11-gal4/+ M	0.514	0.289
Uas-NaChBac/+; GMR54D11-gal4/+ F	0.206	0.938
Uas-TeTxLC/+; GMR54D11-gal4/+ M	>0.001 ***	>0.001 ***
Uas-TeTxLC/+; GMR54D11-gal4/+ F	0.042 *	0.012*
Uas-TrpA1/+; GMR54D11-gal4/+ 23°C M	0.782	0.236
Uas-TrpA1/+; GMR54D11-gal4/+ 23°C F	0.584	0.532
Uas-TrpA1/+; GMR54D11-gal4/+ 29°C M	0.999	0.185
Uas-TrpA1/+; GMR54D11-gal4/+ 29°C F	0.009 **	>0.001 ***
Uas-TeTxLC(NEG)/+; GMR54D11-gal4/+ M	0.999	0.108
Uas-TeTxLC(NEG)/+; GMR54D11-gal4/+ F	0.13	0.009**
Uas-TrpA1/+; Clk4.1M-gal4/+ 29°C M	0.266	0.066
Uas-TrpA1/+; Clk4.1M-gal4/+ 29°C F	0.155	0.645
Uas-TrpA1/+; Clk4.1M-gal4/+ 23°C M	0.473	0.012*
Uas-TrpA1/+; Clk4.1M-gal4/+ 23°C F	0.359	0.033*
pdfgal80/+; crygal4/+ M	0.605	0.518
pdfgal80/+; crygal4/+ F	>0.001 ***	>0.001 ***
pdfgal80/NaChBac; crygal4/+ M	0.009 **	0.018*

RR vs DD	**Distribution of rhythms**	**RRP**
pdfgal80/NaChBac; crygal4/+ F	>0.001 ***	0.013*
pdfgal80/TeTxLC; crygal4/+ M	0.147	0;951
pdfgal80/TeTxLC; crygal4/+ F	0.003 **	>0.001 ***
pdfgal80/TeTxLC(NEG); crygal4/+ M	0.006 **	0.009**
pdfgal80/TeTxLC(NEG); crygal4/+ F	0.517	0.250
pdfgal80/Kir2.1; crygal4/+ M	0.68	0.654
pdfgal80/Kir2.1; crygal4/+ F	0.122	0.017*
TUG,NaChBac RR M	0.485	0.369
TUG,NaChBac RR F	0.083	0.041*
TUG/uas-NaChBac; Crygal80 RR M	0.026 *	0.006 **
TUG/uas-NaChBac; Crygal80 RR F	0.005 **	0.005 **
TUG/+; Crygal80 RR M	0.639	0.259
TUG/+; Crygal80 RR F	0.442	0.152
Other stats	**Distribution of rhythms**	**RRP**
$Dh31^{\#51}$ vs $Dh31^{\#51}$ /+ RR M	0.131	0.409
$Dh31^{\#51}$ vs $Dh31^{\#51}$ /+ RR F	0.32	0.086
$Dh31^{\#51}$ vs $Dh31^{\#51}$ /+ DD M	0.52	0.553
$Dh31^{\#51}$ vs $Dh31^{\#51}$ /+ DD F	0.067	0.011*
yw::GMR78G02-gal4/+ vs Uas-TeTxLC/+; GMR78G02-gal4/+ RR M	0.016	0.007* *
yw::GMR78G02-gal4/+ vs Uas-TeTxLC/+; GMR78G02-gal4/+ RR F	0.999	0.516
yw::GMR78G02-gal4/+ vs Uas-TeTxLC/+; GMR78G02-gal4/+ DD M	0.011 *	>0.001 ***
yw::GMR78G02-gal4/+ vs Uas-TeTxLC/+; GMR78G02-gal4/+ DD F	0.061	0.002 **
yw::GMR78G02-gal4/+ vs Uas-NaChBac/+; GMR78G02-gal4/+ RR M	0.377	0.623
yw::GMR78G02-gal4/+ vs Uas-NaChBac/+; GMR78G02-gal4/+ RR F	0.722	0.616
yw::GMR78G02-gal4/+ vs Uas-NaChBac/+; GMR78G02-gal4/+ DD M	0.503	0.133
yw::GMR78G02-gal4/+ vs Uas-NaChBac/+; GMR78G02-gal4/+ DD F	0.003 **	>0.001 ***

RR vs DD	Distribution of rhythms	RRP
Uas-TeTxLC/+; GMR78G02-gal4/+vs Uas-TeTxLC(NEG)/+; GMR78G02-gal4/+ RR M	>0.001 ***	0.006 **
Uas-TeTxLC/+; GMR78G02-gal4/+vs Uas-TeTxLC(NEG)/+; GMR78G02-gal4/+RR F	0.12	0.047*
Uas-TeTxLC/+; GMR78G02-gal4/+vs Uas-TeTxLC(NEG)/+; GMR78G02-gal4/+DD M	>0.001 ***	>0.001 ***
Uas-TeTxLC/+; GMR78G02-gal4/+vs Uas-TeTxLC(NEG)/+; GMR78G02-gal4/+ DD F	>0.001 ***	>0.001 ***
Uas-TrpA1/+; GMR78G02-gal4/+ 29°C vs 23°C RR M	0.017 *	0.001* *
Uas-TrpA1/+; GMR78G02-gal4/+ 29°C vs 23°C RR F	0.266	0.148
Uas-TrpA1/+; GMR78G02-gal4/+ 29°C vs 23°C DD M	0.181	0.021*
Uas-TrpA1/+; GMR78G02-gal4/+ 29°C vs 23°C DD F	0.788	0.691
R54D11/+ vs R54D11>TeTxLC RR M	0.017 *	0.933
R54D11/+ vs R54D11>TeTxLC RR F	0.491	0.602
R54D11/+ vs R54D11>TeTxLC DD M	0.002 **	0.244
R54D11/+ vs R54D11>TeTxLC DD F	>0.001 ***	>0.001 ***
R54D11/+ vs R54D11>NaChBac RR M	>0.001***	>0.001 ***
R54D11/+ vs R54D11>NaChBac RR F	0.011 *	>0.001 ***
R54D11/+ vs R54D11>NaChBac DD M	0.864	0.965
R54D11/+ vs R54D11>NaChBac DD F	>0.001 ***	>0.001 ***
R54D11> TeTxLC vs R54D11>TeTxLC (NEG) RR M	>0.001 ***	>0.001 ***
R54D11> TeTxLC vs R54D11>TeTxLC (NEG) RR F	0.065	0.009*
R54D11> TeTxLC vs R54D11>TeTxLC (NEG) DD M	0.063	0.003**
R54D11> TeTxLC vs R54D11>TeTxLC (NEG) DD F	0.588	0.079

RR vs DD	Distribution of rhythms	RRP
Uas-TrpA1/+; GMR54D11-gal4/+ 29°C vs 23°C RR M	0.741	0.408
Uas-TrpA1/+; GMR54D11-gal4/+ 29°C vs 23°C RR F	0.093	0.811
Uas-TrpA1/+; GMR54D11-gal4/+ 29°C vs 23°C DD M	0.999	0.098
Uas-TrpA1/+; GMR54D11-gal4/+ 29°C vs 23°C DD F	0.384	>0.001 ***
Uas-TrpA1/+; Clk4.1M-gal4/+ 29°C vs 23°C RR M	>0.001***	>0.001 ***
Uas-TrpA1/+; Clk4.1M-gal4/+ 29°C vs 23°C RR F	0.008 **	0.141
Uas-TrpA1/+; Clk4.1M-gal4/+ 29°C vs 23°C DD M	0.149	0.078
Uas-TrpA1/+; Clk4.1M-gal4/+ 29°C vs 23°C DD F	0.004 **	>0.001 ***
pdfgal80/+; crygal4/+ vs pdfgal80/NaChBac; crygal4/+ RR M	0.669	0.746
pdfgal80/+; crygal4/+ vs pdfgal80/NaChBac; crygal4/+ RR F	0.394	0.285
pdfgal80/+; crygal4/+ vs pdfgal80/NaChBac; crygal4/+ DD M	0.010 *	0.002**
pdfgal80/+; crygal4/+ vs pdfgal80/NaChBac; crygal4/+ DD F	0.067	0.036*
pdfgal80/+; crygal4/+ vs pdfgal80/Kir2.1; crygal4/+ RR M	0.003 **	0.003**
pdfgal80/+; crygal4/+ vs pdfgal80/Kir2.1; crygal4/+ RR F	0.707	0.173
pdfgal80/+; crygal4/+ vs pdfgal80/Kir2.1; crygal4/+ DD M	0.004 **	0.034*
pdfgal80/+; crygal4/+ vs pdfgal80/Kir2.1; crygal4/+ DD F	>0.001 ***	>0.001 ***
pdfgal80/TeTxLC; crygal4/+ vs pdfgal80/TeTxLC(NEG); crygal4/+ RR M	0.035 *	0.001**

RR vs DD	Distribution of rhythms	RRP
pdfgal80/TeTxLC; crygal4/+ vs pdfgal80/TeTxLC(NEG); crygal4/+ RR F	0.648	0.488
pdfgal80/TeTxLC; crygal4/+ vs pdfgal80/TeTxLC(NEG); crygal4/+ DD M	0.584	0.788
pdfgal80/TeTxLC; crygal4/+ vs pdfgal80/TeTxLC(NEG); crygal4/+ DD F	0.039 *	0.199
TUG-Cry80>NaChBac vs TUG-Cry80>+ RR M	>0.001 ***	0.002 **
TUG-Cry80>NaChBac vs TUG-Cry80>+ RR F	0.032 *	0.002 **
TUG-Cry80>NaChBac vs TUG-Cry80>+ DD M	0.999	0.360
TUG-Cry80>NaChBac vs TUG-Cry80>+ DD F	1	0.558
TUG-Cry80>NaChBac vs TUG>NaChBac RR M	0.400	0.134
TUG-Cry80>NaChBac vs TUG>NaChBac RR F	0.308	0.498
TUG-Cry80>NaChBac vs TUG>NaChBac DD M	>0.001 ***	>0.001 ***
TUG-Cry80>NaChBac vs TUG>NaChBac DD F	0.001 **	0.020 *
Pdf vs Pdf>NaChBac RR M	0.1	0.062
Pdf vs Pdf>NaChBac RR F	0.001 **	0.06 **
Pdf vs Pdf>NaChBac DD M	0.034 *	0.005**
Pdf vs Pdf>NaChBac DD F	>0.001 ***	0.004 **
Pdf vs Pdf>TrpA1 23 RR M	0.376	0.503
Pdf vs Pdf>TrpA1 23 RR F	0.125	0.035*
Pdf vs Pdf>TrpA1 23 DD M	0.31	0.069
Pdf vs Pdf>TrpA1 23 DD F	0.118	0.062
Pdf>TrpA1 29 vs Pdf>TrpA1 23 RR M	0.080	0.684
Pdf>TrpA1 29 vs Pdf>TrpA1 23 RR F	0.569	0.192
Pdf>TrpA1 29 vs Pdf>TrpA1 23 DD M	0.452	0.273
Pdf>TrpA1 29 vs Pdf>TrpA1 23 DD F	0.999	0.549

RR vs DD	Distribution of rhythms	RRP
Pdf vs Pdf>hid RR M	0.001 **	>0.001 ***
Pdf vs Pdf>hid RR F	0.102	0.008 **
Pdf vs Pdf>hid DD M	0.010 *	0.003 **
Pdf vs Pdf>hid DD F	>0.001 ***	0.001 **
Pdf vs Pdf>Kir2.1RR M	>0.001 ***	>0.001 ***
Pdf vs Pdf>Kir2.1RR F	0.004 **	0.001 **
Pdf vs Pdf>Kir2.1DD M	>0.001 ***	>0.001 ***
Pdf vs Pdf>Kir2.1DD F	>0.001 ***	>0.001 ***
Pdf>dslar vs +>dslar RR M	0.999	0.991
Pdf>dslar vs +>dslar RR F	0.019 *	>0.001 ***
Pdf>dslar vs +>dslar DD M	>0.001 ***	>0.001 ***
Pdf>dslar vs +>dslar DD F	>0.001 ***	>0.001 ***

Appendix Table 26, statistics comparing RR and DD rhythms for various genotypes in Appendix Table 25.

RR vs DD	Distribution of rhythms	RRP
TUG>*NaChBac* M	0.485	0.369
TUG>*NaChBac* F	0.083	0.041*
TUG-cry80>*NaChBac* M	0.026 *	0.006 **
TUG-cry80>*NaChBac* F	0.005 **	0.005 **
TUG-cry80>+ M	0.639	0.259
TUG-cry80>+ F	0.442	0.152
TUG-cry80>*NaChBac* vs TUG>*NaChBac* RR M	>0.001 ***	0.002 **
TUG-cry80>*NaChBac* vs TUG>*NaChBac* RR F	0.032 *	0.002 **
TUG-cry80>*NaChBac* vs TUG>*NaChBac* DD M	0.999	0.360
TUG-cry80>*NaChBac* vs TUG>*NaChBac* DD F	1	0.558
TUG-cry80>*NaChBac* vs TUG-cry80>+ RR M	0.400	0.134
TUG-cry80>*NaChBac* vs TUG-cry80>+ RR F	0.308	0.498
TUG-cry80>*NaChBac* vs TUG-cry80>+ DD M	>0.001 ***	>0.001

		***
TUG-cry80>*NaChBac* vs TUG-cry80>+ DD F	0.001 **	0.020 *

Appendix Table 27, P-values of significant differences between genotype and light condition for Excitation of TIM+ve CRY-ve cells. Distribution of rhythms is determined by 2x3 Fisher's exact test, and comparison of RRP by one-way ANOVA

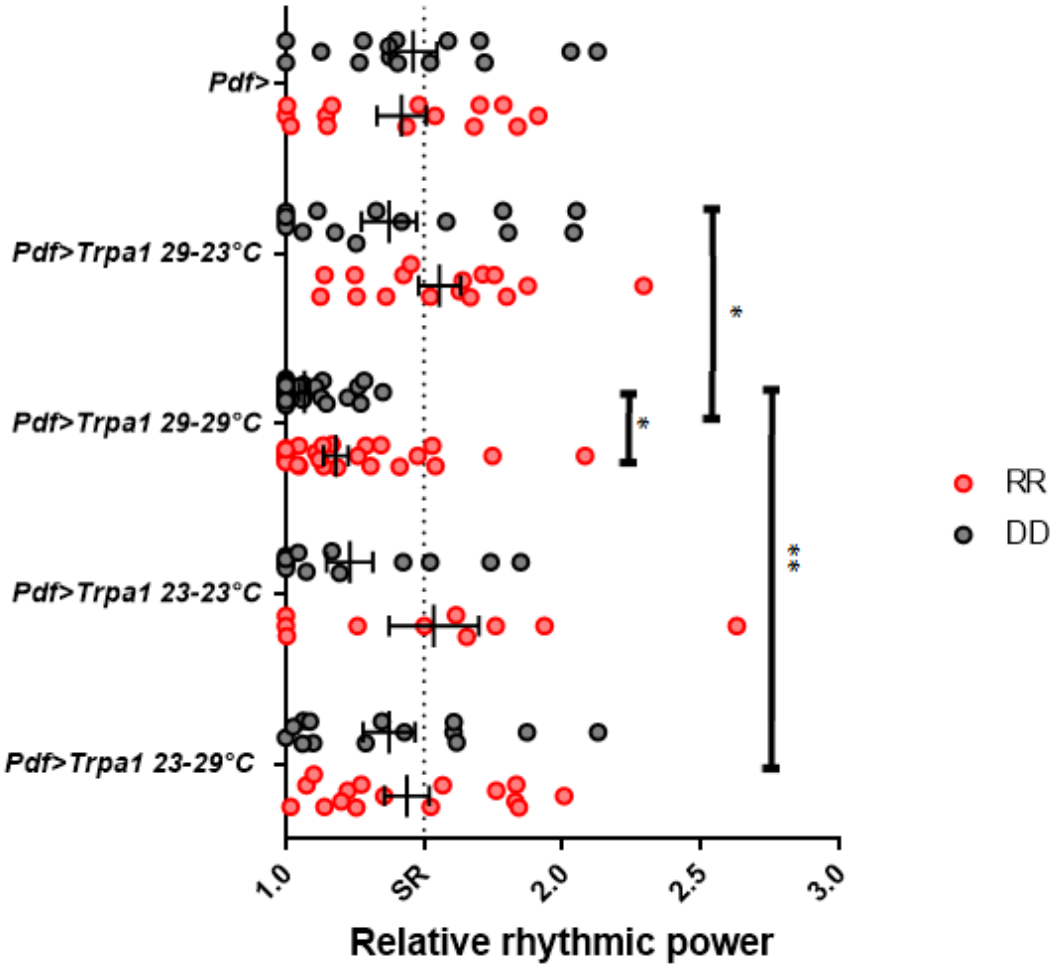

Appendix Figure 20, rhythmic strength of Pdf>TrpA1 flies with 29°C activation encompassing development, adulthood or both. Rhtyhmic data and statistics are presented in Appendix Tables 20 and 21, Wherein 29→29 °C males appear less rhythmic to other conditions. Females were excludied from the figure.

Genotype	**n**	**% SR**	**% WR**	**% AR**	**TAU + SEM**	**RRP + SEM**
***Pdf*; uas-*TrpA1*/+ 29→29 °C M RR**	8	25.00	50.00	25.00	21.33±0.11	1.37±0.07
***Pdf*; uas-*TrpA1*/+ 29→29 °C**	15	6.67	40.00	53.33	22.36±0.47	1.29±0.11

F RR						
Genotype	**n**	**% SR**	**% WR**	**% AR**	**TAU + SEM**	**RRP + SEM**
***Pdf*; uas-*TrpA1*/+ 29→29 °C M DD**	15	0.00	46.67	53.33	21.79±0.63	1.17±0.05
***Pdf*; uas-*TrpA1*/+ 29→29 °C F DD**	16	0.00	31.25	68.75	23.80±0.20	1.08±0.04
***Pdf*; uas-*TrpA1*/+ 29→23°C M RR**	16	56.25	43.75	0.00	25.47±0.12	1.56±0.08
***Pdf*; uas-*TrpA1*/+ 29→23°C F RR**	14	28.57	50.00	21.43	25.77±0.18	1.43±0.10
***Pdf*; uas-*TrpA1*/+ 29→23°C M DD**	15	33.33	46.67	20.00	25.18±0.10	1.51±0.11
***Pdf*; uas-*TrpA1*/+ 29→23°C DD**	15	26.67	66.67	6.67	25.21±0.13	1.48±0.08

Appendix Table 28, behavioural data for PDF cell hyperexcitation with TrpA1, raised at 29°C developmentally

RR vs DD	Distribution of rhythms	RRP
29→29 °C M	0.134	0.010 *
29→29 °C F	0.574	0.089
29→23°C M	0.198	0.154
29→23°C F	0.591	0.357
29→29 °C vs 29→23°C RR M	0.104	0.031 *
29→29 °C vs 29→23°C RR F	0.154	0.084
29→29 °C vs 29→23°C DD M	0.040 *	0.029 *
29→29 °C vs 29→23°C DD F	>0.001***	>0.001***
29→29 °C vs 23→29 °C RR M	0.003**	0.222
29→29 °C vs 23→29 °C RR F	0.004**	0.056
29→29 °C vs 23→29 °C DD M	>0.001***	0.005 **
29→29 °C vs 23→29 °C DD F	0.006**	>0.001***
23→23°C vs 29→23°C RR M	0.164	0.899
23→23°C vs 29→23°C RR F	0.592	0.170
23→23°C vs 29→23°C DD M	0.891	0.293
23→23°C vs 29→23°C DD F	0.294	0.472

Appendix Table 29, P-values derived from comparisons between behavioural data of

Pdf>TrpA1 raised and run at combinations of 23°C and 29°C. Comparisons between Distribution of rhythmicities was calculated using 2x3 Fisher's exact test, and RRP using one-way ANOVA

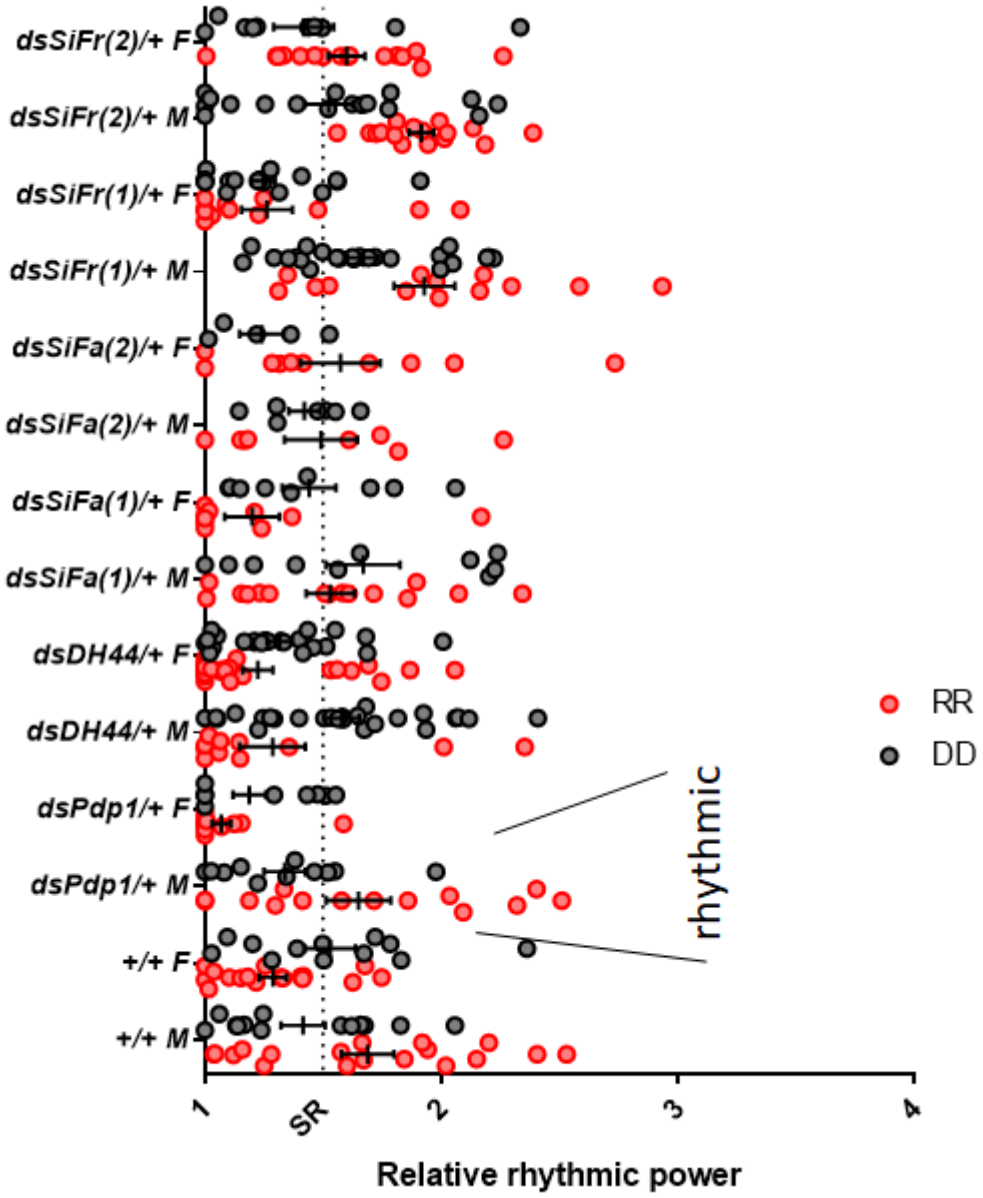

Appendix Figure 21, Displaying behavioural rhythmicities of genotype dcr; elav/+; N/N, expressing various RNAi lines on the 3rd chromosome in RR or DD. No noteworthy differences were apparent, including the positive control, dspdp1, which has previously shown demonstrated arrhythmicity when expressed with tim-UAS-gal4, and we are thus loathe to form conclusions from this data.

Genotype	n	% SR	% WR	% AR	TAU + SEM	RRP + SEM
***tubpgal80^{ts}*; TUG; Uasper 23→17°C M RR**	14	50.00	50.00	0.00	25.11±0.42	1.48±0.09
***tubpgal80^{ts}*; TUG; Uasper 23→17°C F RR**	15	6.67	60.00	33.33	23.55±1.86	1.12±0.07
***tubpgal80^{ts}*; TUG; Uasper 23→17°C M DD**	21	66.67	28.57	4.76	23.61±0.30	1.18±0.10
***tubpgal80^{ts}*; TUG; Uasper 23→17°C F DD**	14	57.14	21.43	21.43	23.10±0.21	1.11±0.09
***tubpgal80^{ts}*; TUG; Uasper 29→17°C M RR**	29	0.00	41.38	58.62	24.46±1.53	1.10±0.03
***tubpgal80^{ts}*; TUG; Uasper 29→17°C F RR**	29	0.00	10.34	89.66	22.17±3.39	1.10±0.03
***tubpgal80^{ts}*; TUG; Uasper 29→17°C M DD**	13	0.00	23.08	76.92	24.5±1.77	1.08
***tubpgal80^{ts}*; TUG; Uasper 29→17°C F DD**	13	0.00	15.38	84.62	22.5	1.13±0.03
***Elav-gal4*; Uasmyccyc#7/+; *tubpgal80^{ts}*cyc^{01}/cyc^{01} 17→29 °C M RR**	11	0.00	18.18	81.82	23.75±0.75	1.08±0.02
***Elav-gal4*; Uasmyccyc#7/+; *tubpgal80^{ts}*cyc^{01}/cyc^{01} 17→29 °C F RR**	12	0.00	25.00	75.00	22.17±0.6	1.17±0.08
***Elav-gal4*; Uasmyccyc#7/+; *tubpgal80^{ts}*cyc^{01}/cyc^{01} 17→29 °C M DD**	35	0.00	17.14	82.86	24.17±0.69	1.09±0.20
***Elav-gal4*; Uasmyccyc#7/+; *tubpgal80^{ts}*cyc^{01}/cyc^{01} 17→29 °C F DD**	43	0.00	11.63	88.37	22.70±0.12	1.14±0.19
***Elav-gal4*; Uasmyccyc#7/+; *tubpgal80^{ts}*cyc^{01}/cyc^{01} 29→29 °C M RR**	16	62.50	18.75	18.75	22.62±0.29	2.03±0.02
***Elav-gal4*; Uasmyccyc#7/+; *tubpgal80^{ts}*cyc^{01}/cyc^{01} 29→29 °C F RR**	13	69.23	30.77	0.00	22.73±0.12	2.06±0.04
***Elav-gal4*; Uasmyccyc#7/+;**	35	11.43	40	48.57	23.72±0.84	1.42±0.08

***tubpgal80^{ts}*cyc^{01}/cyc^{01} 29→29 °C M DD**						
Genotype	**n**	**% SR**	**% WR**	**% AR**	**TAU + SEM**	**RRP + SEM**
***Elav-gal4*; Uasmyccyc#7/+; *tubpgal80^{ts}*cyc^{01}/cyc^{01} 29→29 °C F DD**	31	83.87	12.90	3.23	23.50±0.37	2.48±0.12
***Elav-gal4*; Uasmyccyc#7/pdf*gal80*; *tubpgal80^{ts}*cyc^{01}/cyc^{01} 17→29 °C M RR**	11	0.00	0.00	100.00	N/A	N/A
***Elav-gal4*; Uasmyccyc#7/pdf*gal80*; *tubpgal80^{ts}*cyc^{01}/cyc^{01} 17→29 °C F RR**	9	0.00	0.00	100.00	N/A	N/A
***Elav-gal4*; Uasmyccyc#7/pdf*gal80*; *tubpgal80^{ts}*cyc^{01}/cyc^{01} 17→29 °C M DD**	8	0.00	0.00	100.00	N/A	N/A
***Elav-gal4*; Uasmyccyc#7/pdf*gal80*; *tubpgal80^{ts}*cyc^{01}/cyc^{01} 17→29 °C F DD**	12	0.00	0.00	100.00	N/A	N/A
***Elav-gal4*; Uasmyccyc#7/pdf*gal80*; *tubpgal80^{ts}*cyc^{01}/cyc^{01} 29→29 °C M RR**	33	6.06	63.64	30.30	22.70±0.30	1.29±0.06
***Elav-gal4*; Uasmyccyc#7/pdf*gal80*; *tubpgal80^{ts}*cyc^{01}/cyc^{01} 29→29 °C F RR**	35	14.29	40.00	45.71	23.32±0.30	1.48±0.08
***Elav-gal4*; Uasmyccyc#7/pdf*gal80*; *tubpgal80^{ts}*cyc^{01}/cyc^{01} 29→29 °C M DD**	12	0.00	16.67	83.33	23.75±0.25	1.12±0.00
***Elav-gal4*; Uasmyccyc#7/pdf*gal80*;**	19	0.00	5.26	94.74	24.50	1.23

***tubpgal80^{ts}*cyc^{01}/cyc^{01} 29→29 °C F DD**						
Genotype	**n**	**% SR**	**% WR**	**% AR**	**TAU + SEM**	**RRP + SEM**
TUG/uascyc; *tubpgal80^{ts}*cyc^{01}/cyc^{01} 29→29 °C DD	18	22.22	11.11	66.67	22.75±0.17	1.92±0.30
TUG/CyO; *tubpgal80^{ts}*cyc^{01}/cyc^{01} 29→29 °C DD	13	0.00	0.00	100.00	N/A	N/A
TUG/uascyc; *tubpgal80^{ts}*cyc^{01}/ser 29→29 °C DD	5	80.00	0.00	20.00	22.75±0.14	2.52±0.17
TUG/uascyc; *tubpgal80^{ts}*cyc^{01}/cyc^{01} 29→29 °C RR	5	40.00	40.00	20.00	24.25±0.78	1.51±0.22
TUG/CyO; *tubpgal80^{ts}*cyc^{01}/cyc^{01} 29→29 °C RR	5	0.00	0.00	100.00	N/A	N/A
pdf-*gal4*; uasmyccyc#7/+; *tubpgal80^{ts}*cyc^{01}/cyc^{01} 29→29 °C DD M	34	0.00	14.71	85.29	21.75±1.80	1.08±0.04
pdf-*gal4*; CyO/+; *tubpgal80^{ts}*cyc^{01}/cyc^{01} 29→29 °C DD M	18	0.00	16.67	83.33	23.75±2.25	1.05±0.02
pdf-*gal4*; uasmyccyc#7/+; *tubpgal80^{ts}*cyc^{01}/ser 29→29 °C DD M	21	52.38	38.10	9.52	23.45±0.10	1.60±0.13
pdf-*gal4*; uasmyccyc#7/+; *tubpgal80^{ts}*cyc^{01}/cyc^{01} 29→29 °C RR M	8	0.00	12.50	87.50	24.50	1.14
pdf-*gal4*; CyO/+; *tubpgal80^{ts}*cyc^{01}/cyc^{01} 29→29 °C RR M	3	0.00	0.00	100.00	N/A	N/A
***elav*; uascyc/*VGlut*80; *tubpgal80^{ts}*cyc^{01}/cyc^{01} 29→29 °C DD M**	19	26.32	42.11	31.58	23.88±0.63	1.26±0.08

Genotype	n	% SR	% WR	% AR	TAU + SEM	RRP + SEM
***elav*; uascyc/*VGlut*80; *tubpgal80^{ts}*cyc^{01}/cyc^{01} 29→29 °C DD f**	21	9.52	38.10	52.38	23.00±0.46	1.42±0.08
***elav*; uascyc/*VGlut*80; *tubpgal80^{ts}*cyc^{01}/cyc^{01} 29→29 °C RR M**	13	30.77	61.54	7.69	23.08±0.14	1.41±0.13
***elav*; uascyc/*VGlut*80; *tubpgal80^{ts}*cyc^{01}/cyc^{01} 29→29 °C RR f**	17	17.65	35.29	47.06	23.11±0.33	1.09±0.03
***elav*; uascyc/*VGlut*80; *tubpgal80^{ts}*cyc^{01}/TM3-sb^{1} 29→29 °C DD M**	6	0.00	50.00	50.00	23.67±0.18	1.48±0.16
***elav*; uascyc/*VGlut*80; *tubpgal80^{ts}*cyc^{01}/TM3-sb^{1} 29→29 °C DD f**	11	27.27	36.36	36.36	23.86±0.43	1.36±0.12
***elav*; uascyc/*VGlut*80; *tubpgal80^{ts}*cyc^{01}/TM3-sb^{1} 29→29 °C RR M**	4	25.00	75.00	0.00	22.88±0.75	1.26±0.21
***elav*; uascyc/*VGlut*80; *tubpgal80^{ts}*cyc^{01}/TM3-sb^{1} 29→29 °C RR f**	5	0.00	40.00	60.00	23.25±0.75	1.26±0.21
+/y; uas-cyc/+; *tubpgal80^{ts}*cyc^{01}/cyc^{01} 29→29 °C DD M	42	0.00	0.00	100.00	N/A	N/A
+/y; CyO/+; *tubpgal80^{ts}*cyc^{01}/cyc^{01} 29→29 °C DD M	18	0.00	0.00	100.00	N/A	N/A
+/y; uas-cyc/+; *tubpgal80^{ts}*cyc^{01}/cyc^{01} 29→29 °C RR M	8	0.00	0.00	100.00	N/A	N/A
+/y; CyO/+; *tubpgal80^{ts}*cyc^{01}/cyc^{01} 29→29 °C RR M	5	0.00	0.00	100.00	N/A	N/A
uas-cyc/+; *tubpgal80^{ts}*cyc^{01}/*R78G02*cyc^{01}	8	0.00	0.00	100.00	N/A	N/A

29→29 °C RR M						
Genotype	**n**	**% SR**	**% WR**	**% AR**	**TAU + SEM**	**RRP + SEM**
CyO/+; *tubpgal80^{ts}*cyc^{01}/*R78G02*cyc^{01} 29→29 °C RR M	13	0.00	0.00	100.00	N/A	N/A
uas-cyc/+; *tubpgal80^{ts}*cyc^{01}/*R78G02*cyc^{01} 29→29 °C DD M	5	0.00	0.00	100.00	N/A	N/A
CyO/+; *tubpgal80^{ts}*cyc^{01}/*R78G02*cyc^{01} 29→29 °C DD M	1	0.00	0.00	100.00	N/A	N/A
uas-cyc/+; *tubpgal80^{ts}*cyc^{01}/*Clk4.1M*cyc^{01} 29→29 °C DD M	25	12.00	8.00	80.00	22.40±0.73	1.48±0.12
CyO/+; *tubpgal80^{ts}*cyc^{01}/*Clk4.1M*cyc^{01} 29→29 °C DD M	5	0.00	0.00	100.00	N/A	N/A
uas-cyc/+; *tubpgal80^{ts}*cyc^{01}/ser 29→29 °C DD M	7	85.71	0.00	14.29	23.33±0.11	2.31±0.12
uas-cyc/pdf-*gal80*; *tubpgal80^{ts}*cyc^{01}/cry*gal4*13cyc^{01} 29→29 °C DD M	11	9.09	9.09	81.82	23.25±0.25	1.43±0.17
uas-cyc/pdf-*gal80*; *tubpgal80^{ts}*cyc^{01}/ser 29→29 °C DD M	1	100.00	0.00	0.00	23.50	1.52
uas-cyc/pdf-*gal80*; *tubpgal80^{ts}*cyc^{01}/cry*gal4*13cyc^{01} 29→29 °C RR M	7	14.29	0.00	85.71	21.00	1.61
uas-cyc/pdf-*gal80*; *tubpgal80^{ts}*cyc01/ser 29→29 °C RR M	3	100.00	0.00	0.00	23.83±0.29	1.87±0.05

Appendix Table 30: Behavioural datasets for various conditional CYC or PER manipulations of genotype cyc^{01} [pdf.cyc]^{ts} and [timP.per]^{ts} in RR and DD.

	Distribution of rhythms	RRP
cyc^{01} [pdf.cyc]^{ts} **RR vs DD**	1	0.641
cyc^{01} [pdf.cyc]^{ts} **vs** ***cyc^{01} [pdf.+]^{ts} CyO*** **RR**	1	0.568
cyc^{01} [pdf.cyc]^{ts} **vs** ***cyc^{01} [pdf.+]^{ts} CyO*** **DD**	0.999	0.818
cyc^{01} [elav-VGlut.cyc]^{ts} **M RR vs DD**	0.321	0.294
cyc^{01} [elav-VGlut.cyc]^{ts} **F RR vs DD**	0.813	0.558
cyc^{01} [elav.cyc]^{ts} **vs** ***cyc^{01} [elav-VGlut.cyc]^{ts}*** **RR M**	0.098	0.059
cyc^{01} [elav.cyc]^{ts} **vs** ***cyc^{01} [elav-VGlut.cyc]^{ts}*** **RR F**	0.002 **	>0.001 ***
cyc^{01} [elav.cyc]^{ts} **vs** ***cyc^{01} [elav-VGlut.cyc]^{ts}*** **DD M**	0.586	
cyc^{01} [elav.cyc]^{ts} **vs** ***cyc^{01} [elav-VGlut.cyc]^{ts}*** **DD F**	>0.001 ***	>0.001 ***
cyc^{01} [elav.cyc]^{ts} **vs** ***cyc^{01} [elav-Pdf80.cyc]^{ts}*** **RR M**	>0.001 ***	>0.001 ***
cyc^{01} [elav.cyc]^{ts} **vs** ***cyc^{01} [elav-Pdf80.cyc]^{ts}*** **RR F**	>0.001 ***	>0.001 ***
cyc^{01} [elav.cyc]^{ts} **vs** ***cyc^{01} [elav-Pdf80.cyc]^{ts}*** **DD M**	0.042 *	0.036 *
cyc^{01} [elav.cyc]^{ts} **vs** ***cyc^{01} [elav-Pdf80.cyc]^{ts}*** **DD F**	>0.001 ***	>0.001 ***
cyc^{01} [+.cyc]^{ts} **vs** ***cyc^{01} [pdf.cyc]^{ts}*** **RR**	0.499	0.334
cyc^{01} [+.cyc]^{ts} **vs** ***cyc^{01} [pdf.cyc]^{ts}*** **DD**	0.015 *	0.185
cyc^{01} [+.cyc]^{ts} **vs** ***cyc^{01} [R78G02.cyc]^{ts}*** **RR**	1	1
cyc^{01} [+.cyc]^{ts} **vs** ***cyc^{01} [R78G02.cyc]^{ts}*** **DD**	1	1
cyc^{01} [+.cyc]^{ts} **vs** ***cyc^{01} [cry-pdf.cyc]^{ts}*** **RR**	0.466	0.302
cyc^{01} [+.cyc]^{ts} **vs** ***cyc^{01} [cry-pdf.cyc]^{ts}*** **DD**	0.039 *	0.071
cyc^{01} [+.cyc]^{ts} **vs** ***cyc^{01} [TUG‐cyc]^{ts}*** **RR**	0.006 **	0.021*
cyc^{01} [+.cyc]^{ts} **vs** ***cyc^{01} [TUG‐cyc]^{ts}*** **DD**	>0.001 ***	0.031*
cyc^{01} [+.cyc]^{ts} **vs** ***cyc^{01} [elav.cyc]^{ts}*** **RR**	>0.001***	0.006 **
cyc^{01} [+.cyc]^{ts} **vs** ***cyc^{01} [elav.cyc]^{ts}*** **DD**	>0.001 ***	0.004 **
cyc^{01} [+.cyc]^{ts} **vs** ***cyc^{01} [elav-pdf.cyc]^{ts}*** **RR**	>0.001 ***	0.070
cyc^{01} [+.cyc]^{ts} **vs** ***cyc^{01} [elav-pdf.cyc]^{ts}*** **DD**	0.046 *	0.070
cyc^{01} [+.cyc]^{ts} **vs** ***cyc^{01} [elav-VGlut.cyc]^{ts}*** **RR**	>0.001 ***	0.002**
cyc^{01} [+.cyc]^{ts} **vs** ***cyc^{01} [elav-VGlut.cyc]^{ts}*** **DD**	>0.001 ***	0.001**
cyc^{01} [+.cyc]^{ts} **vs** ***cyc^{01} [Clk4.1M.cyc]^{ts}*** **DD**	0.005 **	0.147
cyc^{01} [pdf+Clk4.1M.cyc]^{ts} **vs** ***cyc^{01} [pdf.cyc]^{ts}*** **DD**	0.688	0.505
cyc^{01} [pdf+Clk4.1M.cyc]^{ts} **vs** ***cyc^{01} [elav.cyc]^{ts}*** **DD**	>0.001***	0.002**

Appendix Table 31, P values derived from comparisons of conditional CYC rescue in DD or RR, with various driver lines, pursuant to results in Appendix Table 30. Statistics comparing between conditions for genotypes tubpgal80^{ts}; TUG; Uasper ([timP.per]^{ts}), elav-gal4; Uasmyccyc#7/+; tubpgal80^{ts}cyc^{01}/cyc^{01} (cyc^{01} [elav.cyc]^{ts}) and elav-gal4; Uasmyccyc#7/pdfgal80; tubpgal80^{ts}cyc^{01}/cyc^{01} (cyc^{01} [elav-Pdf80.cyc]^{ts}) are included in the main body of the text, Tables 5.6, 5.7 and 5.8 respectively.

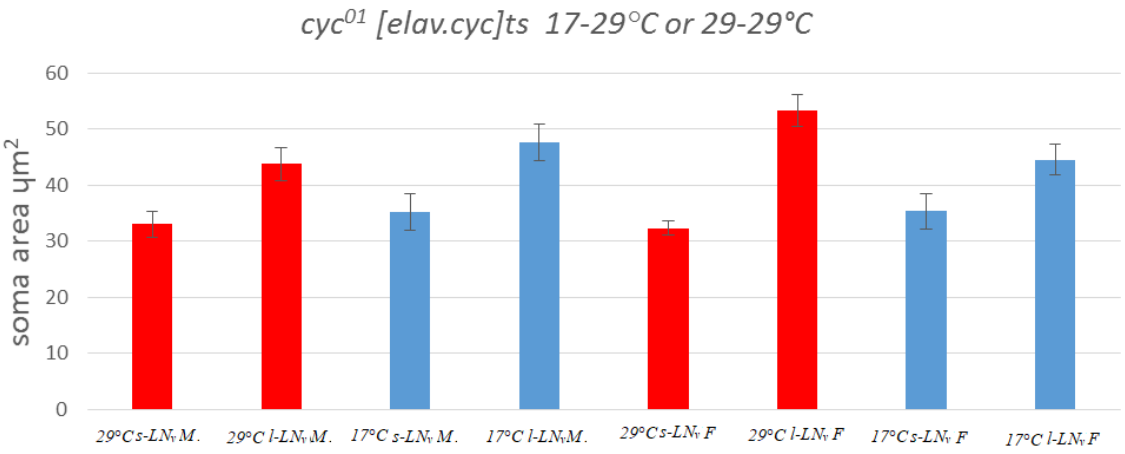

Appendix Figure 22: PDF+ve soma size in restrictively or permissively raised cyc^{01} [elav.cyc]^{ts}. s-LN$_v$ soma are predictably smaller than l-LN$_v$ soma, but no further trend is identifiable across the data.

	D/N ratio P value
cyc^{01} [elav.cyc]^{ts} M vs cyc^{01} [elav-Pdf80.cyc]^{ts} M	*0.008 ** *
cyc^{01} [elav.cyc]^{ts} M vs cyc^{01} M	*0.001*** *
cyc^{01} [elav-Pdf80.cyc]^{ts} M vs cyc^{01} M	*0.939*
cyc^{01} [elav.cyc]^{ts} F vs cyc^{01} [elav-Pdf80.cyc]^{ts} F	*0.267*
cyc^{01} [elav.cyc]^{ts} F vs cyc^{01} F	*0.001 *** *
cyc^{01} [elav-Pdf80.cyc]^{ts} F vs cyc^{01} F	*0.098*

Appendix Table 32, relevant to Figure 3.10, statistics comparing significance of difference between D/N ratios for cyc^{01} and conditional CYC rescue pan-neuronally or pan-neuronally excluding PDF cells, raised and run at 29→29°C in all cases.

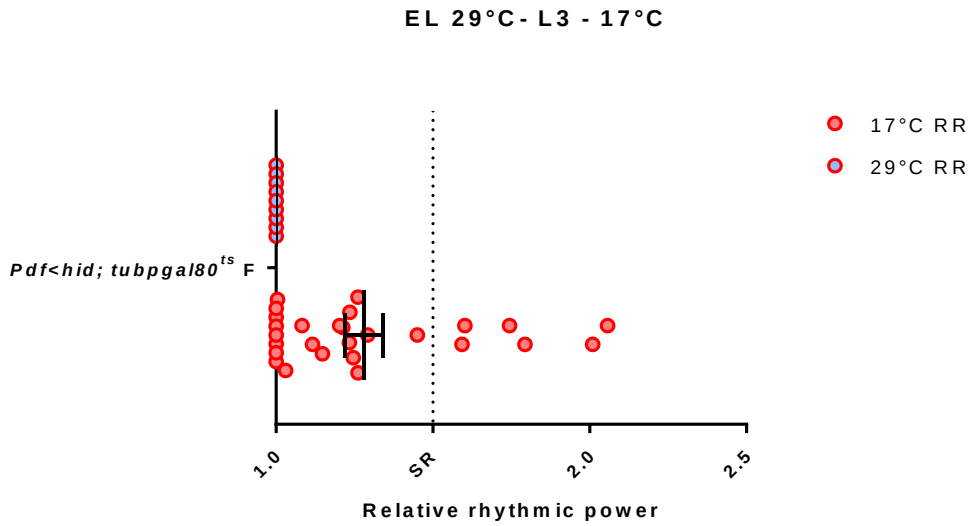

Appendix Figure 34, behavioural rhythmicities for Pdf-gal4(x)/Y; UAS-hid/+; tubpgal80^{ts}/+raised at 29°C from egg-laying and transferred to 17°C as third-instar larvae. Flies were run at 17°C RR followed by 29°C RR. At 17°C, flies should have l-LN$_v$s, but not s-LN$_v$s, which should be ablated upon transferral to 29°C midway through the behavioural assay. There were significant differences in rhythmicity between conditions (P=0.013), indicative of successful PDF cell ablation at 29°C. In support of conditional PDF ablation experiements in Figure 5.5, we can conclude therefore that a rhythmic population can be rendered arrhythmic through adult-specific PDF-cell ablation. There were no surviving males by the completion of the behavioural experiment.*

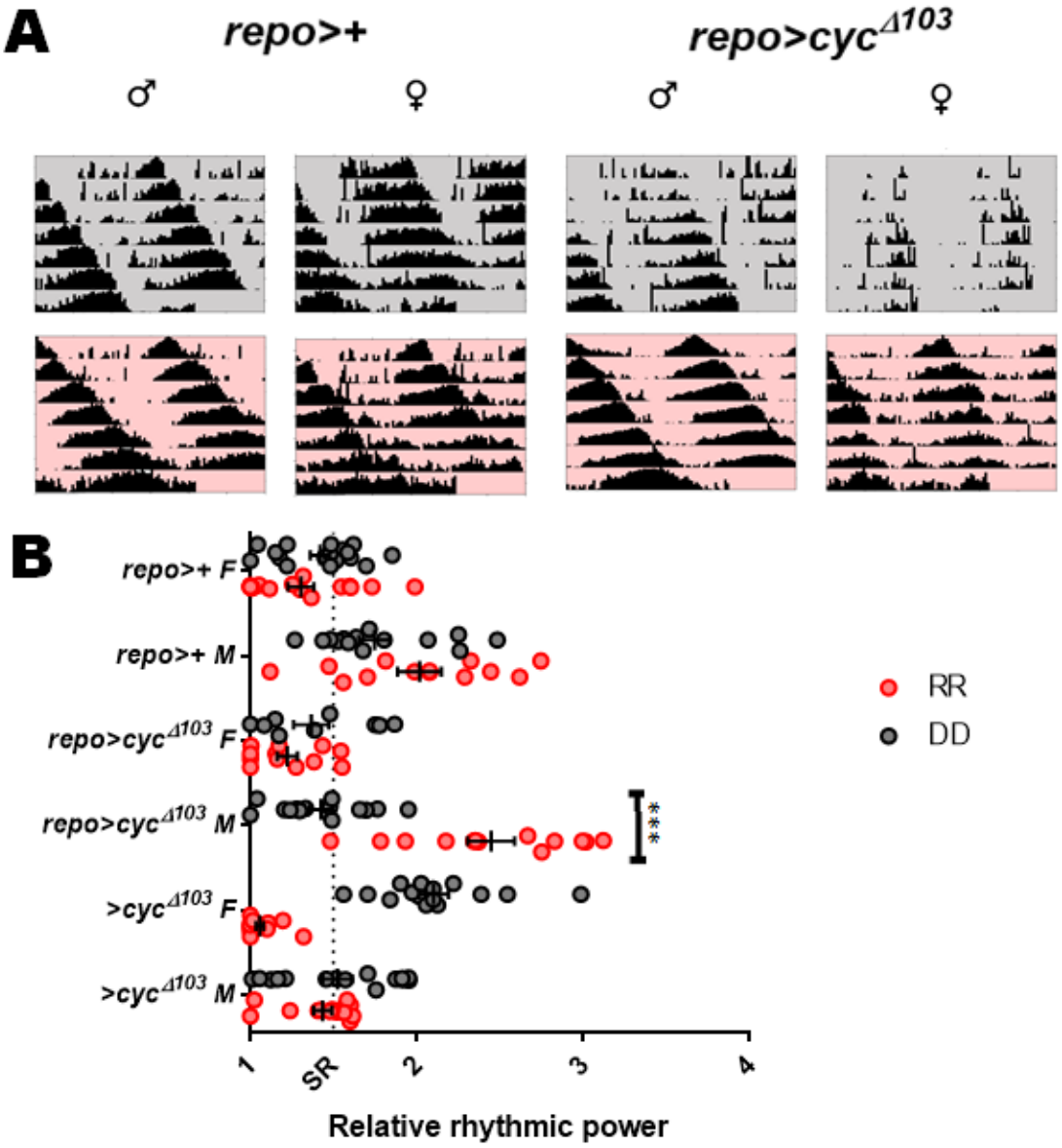

*Appendix Figure 23, Panel A shows actograms for repo> cyc$^{\Delta 103}$, removing oscillator function from the glia, and responderless controls, run in 23°C RR or DD. This demonstrates period lengthening is a result of genetic background rather than a glia-specific function, and overall rhythmicity does not appear decreased. Panel B shows RRP for the two conditions, with differences in rhythmicity for males (P<0.001***).*

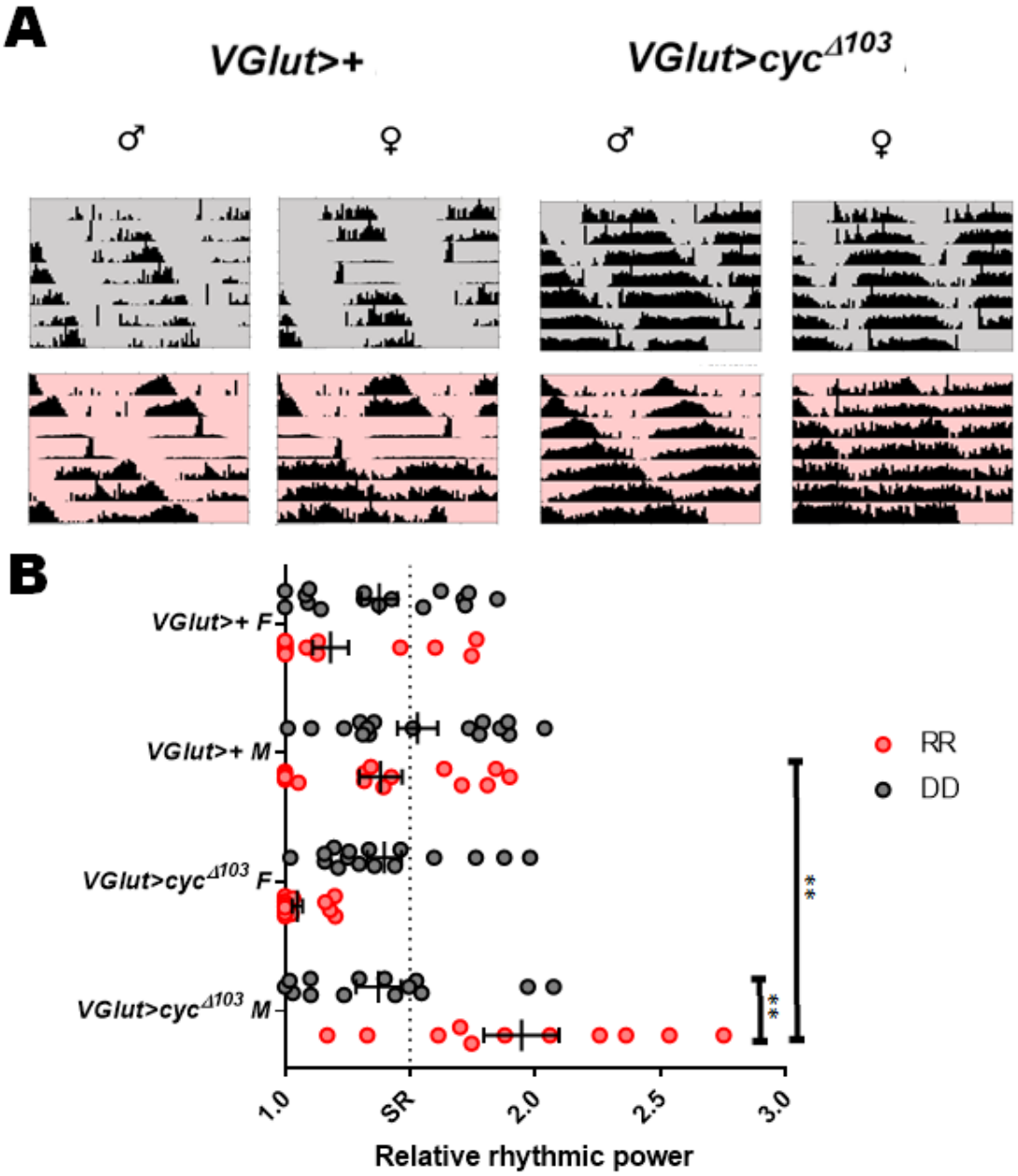

Appendix Figure 24, Panel A shows actograms and Panel B shows behavioural rhythmicity data for VGlut> cyc$^{\Delta 103}$ and responderless controls run in 23°C RR or DD, demonstrating a lack of notable phenotype when oscillator of select DN1 cells is halted. Similarly, a long period manifests in undriven controls.

RR vs DD		**Distribution of rhythms**	**RRP**
VGlut> *cyc$^{\Delta 103}$*	**M**	0.015 *	0.002**
VGlut> *cyc$^{\Delta 103}$*	**F**	>0.001 ***	>0.001 ***
VGlut>**+**	**M**	0.106	0.219

	Distribution of rhythms	RRP
***VGlut*>+ F**	0.156	0.091
driven vs undriven		
***VGlut* RR M**	0.046*	0.002**
***VGlut* RR F**	0.325	0.085
***VGlut* DD M**	0.142	0.944
***VGlut* DD F**	0.24	0.843

Appendix Table 33, P-values denoting significance of comparisons between behavioural rhythmicity of flies following expression of dominant-negative CYC to disrupt molecular oscillations in glutamatergic cells, in RR and DD.

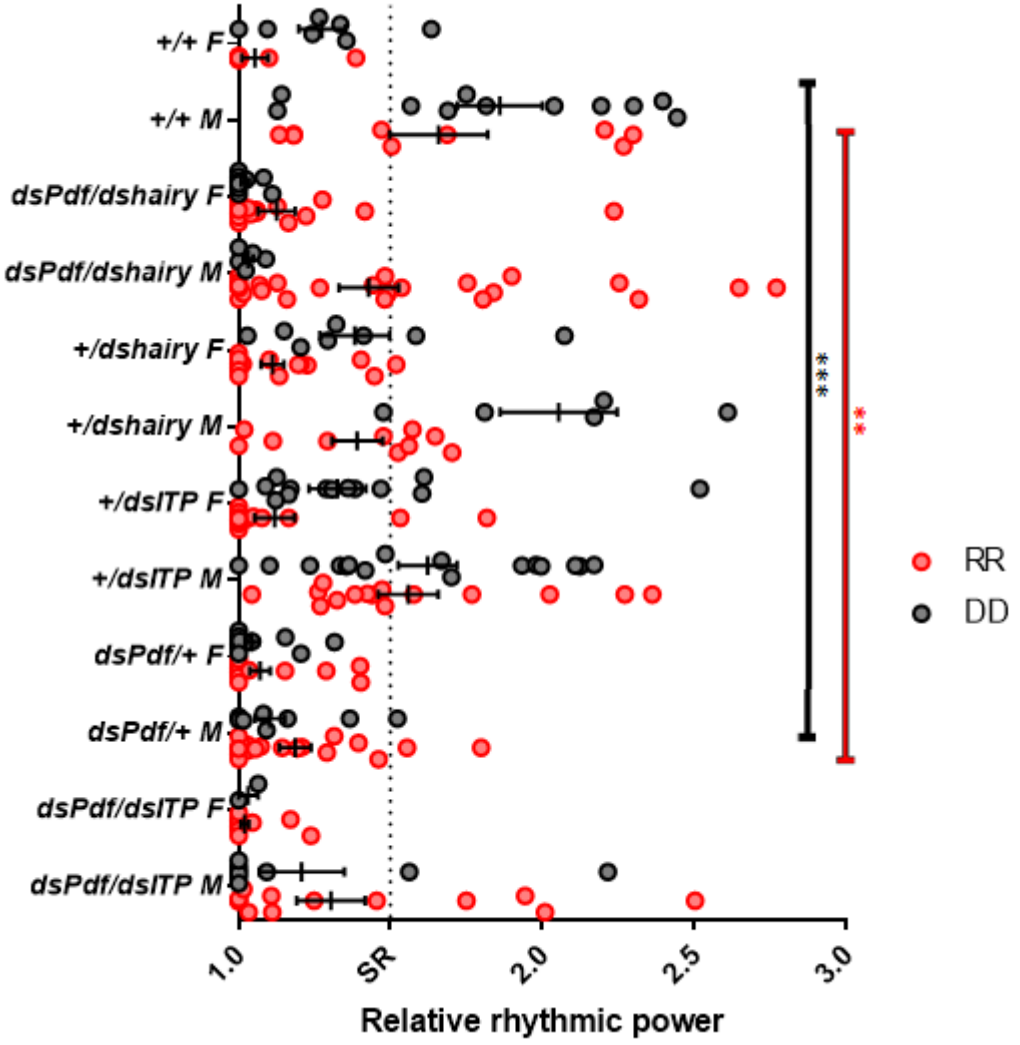

Appendix Figure 25: Relative rhythmic power of various lines of genotype dcr; TUG/+; /+, encompassing RNAi lines on the 3rd chromosome, run in 23°C RR or DD. ITP knockdown and hairy knockdown do not significantly differ whether knocked down alone or in conjunction with PDF and, both appear to amerliorate effect of heterozygous dspdf

knockdown on rhythms

Genotype	n	% SR	% WR	% AR	TAU + SEM	RRP + SEM
dcr; TUG; +/+ RR M	15	53.33	46.67	0.00	24.37±0.18	1.61±0.11
dcr; TUG; +/+ RR F	12	8.33	25.00	66.67	25.25±1.12	1.35±0.17
dcr; TUG; +/+ DD M	11	81.82	18.18	0.00	24.00±0.18	1.86±0.14
dcr; TUG; +/+ DD F	7	14.29	71.43	14.29	24.50±0.18	1.32±0.07
dcr; TUG; dspdf/+ RR M	17	17.65	58.82	23.53	23.54±0.41	1.37±0.11
dcr; TUG; dspdf/+ RR F	17	0.00	29.41	70.59	23.50±0.63	1.26±0.07
dcr; TUG; dspdf/+ DD M	25	4.00	36.00	60.00	24.65±0.49	1.16±0.052
dcr; TUG; dspdf/+ DD F	19	0.00	31.58	68.42	23.58±2.01	1.12±0.05
dcr; TUG; dspdf/dsITP RR M	20	40.00	25.00	35.00	24.04±0.17	1.76±0.16
dcr; TUG; dspdf/dsITP RR F	27	0.00	25.93	74.07	24.50±0.20	1.07±0.03
dcr; TUG; dspdf/dsITP DD M	21	9.52	28.57	61.90	25.19±0.99	1.29±0.14
dcr; TUG; dspdf/dsITP DD F	8	0.00	25.00	75.00	21.25±5.75	1.08±0.01
dcr; TUG; dspdf/dshairy RR M	29	31.03	34.48	34.48	23.53±0.19	1.72±0.13
dcr; TUG; dspdf/dshairy RR F	21	4.76	47.62	47.62	24.50±0.69	1.29±0.13
dcr; TUG; dspdf/dshairy DD M	5	0.00	60.00	40.00	21.50±2.75	1.05±0.02
dcr; TUG; dspdf/dshairy DD F	10	0.00	40.00	60.00	22.88±2.56	1.06±0.03
dcr; TUG; +/dsITP RR M	23	34.78	60.87	4.35	22.88±0.21	1.46±0.10
dcr; TUG; +/dsITP RR F	28	7.14	39.29	53.57	23.17±1.25	1.28±0.13
dcr; TUG; +/dsITP DD M	16	50.00	43.75	6.25	24.17±0.11	1.66±0.09
dcr; TUG; +/dsITP DD F	16	18.75	62.50	18.75	25.23±0.30	1.40±0.11
dcr; TUG; +/dshairy RR M	10	50.00	40.00	10.00	24.50±0.50	1.63±0.11

Genotype	n	% SR	% WR	% AR	TAU + SEM	RRP + SEM
dcr; TUG; +/dshairy RR F	22	4.55	45.45	50.00	24.00±0.69	1.27±0.06
dcr; TUG; +/dshairy DD M	5	80.00	20.00	0.00	23.60±0.10	2.05±0.19
dcr; TUG; +/dshairy DD F	8	25.00	75.00	0.00	23.63±0.16	1.38±0.11

Appendix Table 34, behavioural rhythmicities for dcr;TUG lines driving RNAi for pdf, ITP and hairy in RR and DD

RR vs DD	Distribution of rhythms	RRP
dcr; TUG; +/+ M	0.216	0.356
dcr; TUG; +/+ F	0.079	0.019*
dcr; TUG; dspdf/+ M	0.083	0.285
dcr; TUG; dspdf/+ F	0.999	0.508
dcr; TUG; dspdf/dsITP M	0.077	0.607
dcr; TUG; dspdf/dsITP F	1	0.795
dcr; TUG; dspdf/dshairy M	0.117	0.108
dcr; TUG; dspdf/dshairy F	0.802	0.256
dcr; TUG; +/dsITP M	0.58	0.647
dcr; TUG; +/dsITP F	0.053	0.090
dcr; TUG; +/dshairy M	0.72	0.002**
dcr; TUG; +/dshairy F	0.024 *	0.007**
Other stats		
+/+ vs dspdf/+ RR M	0.029 *	0.002**
+/+ vs dspdf/+ RR F	0.648	0.765
+/+ vs dspdf/+ DD M	>0.001***	>0.001***
+/+ vs dspdf/+ DD F	0.031 *	0.001**
+/+ vs dsITP/+ RR M	0.492	0.580
+/+ vs dsITP/+ RR F	0.759	0.476
+/+ vs dsITP/+ DD M	0.29	0.161
+/+ vs dsITP/+ DD F	1	0.743
+/+ vs dshairy/+ RR M	0.644	0.146
+/+ vs dshairy/+ RR F	0.439	0.366
+/+ vs dshairy/+ DD M	0.999	0.442
+/+ vs dshairy/+ DD F	0.999	0.463

	Distribution of rhythms	RRP
dspdf/+ vs dspdf/dshairy RR M	0.435	0.068
dspdf/+ vs dspdf/dshairy RR F	0.252	0.458
dspdf/+ vs dspdf/dshairy DD M	0.685	0.380
dspdf/+ vs dspdf/dshairy DD F	0.698	0.487
dspdf/+ vs dspdf/dsITP RR M	0.191	0.335
dspdf/+ vs dspdf/dsITP RR F	1	0.139
dspdf/+ vs dspdf/dsITP DD M	0.29	0.442
dspdf/+ vs dspdf/dsITP DD F	0.999	0.838
dspdf/dshairy vs dspdf/dsITP RR M	0.717	0.426
dspdf/dshairy vs dspdf/dsITP RR F	0.092	0.092
dspdf/dshairy vs dspdf/dsITP DD M	0.564	0.378
dspdf/dshairy vs dspdf/dsITP DD F	0.638	0.808

Appendix Table 35, P-values for comparisons between various knockdowns with genotype dcr; TUG; RNAi/RNAi in RR and DD in support of Appendix Table 34. Comparisons between distribution of rhythmicities was calculated using 2x3 Fisher's exact test, and RRP using one-way ANOVA.

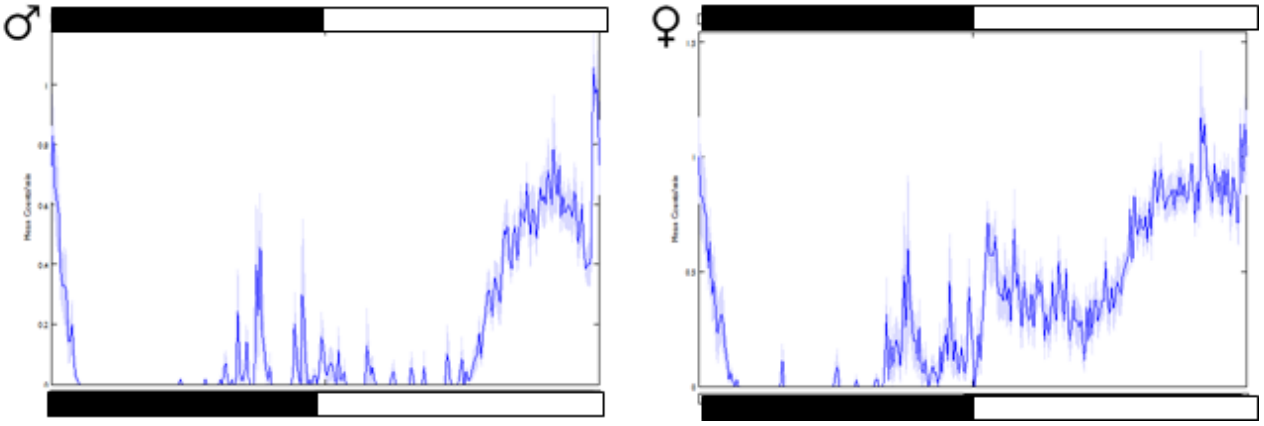

Appendix Figure 26, LD profiles for hdc^{jk910};Pdf^{01} males and females, ♂ n=14, ♀ n=11. Demonstrated is a clearly advanced E peak, analogous to regular Pdf^{01} mutants. This reassures us that flies are genuine Pdf^{01} mutants, despite relatively strong rhythmicity detailed in Appendix table 37.

Genotype	n	% SR	% WR	% AR	TAU + SEM	RRP + SEM
Pdf>hid;tubpgal80^{ts} 29->17 RR	15	0.00	20.00	80.00	24.00±1.15	1.05±0.01
Pdf>CyO;tubpgal80^{ts} 29->17 RR	15	20.00	73.33	6.67	24.36±0.24	1.35±0.07
Pdf>hid;+ 29->17 RR	5	0.00	60.00	40.00		
Pdf>hid;tubpgal80^{ts} 29->17 DD	15	0.00	26.67	73.33	23.67±3.18	1.06±0.05
Pdf>CyO;tubpgal80^{ts} 29->17 DD	15	20.00	26.67	53.33	24.14±0.51	1.53±0.11
Pdf>hid;+ 29->17 DD	5	0.00	0.00	100.00		
Pdf>hid;tubpgal80^{ts} 29->17 RR	18	0.00	5.56	94.44		
Pdf>CyO;tubpgal80^{ts} 29->17 RR	25	24.00	60.00	16.00	27.14±0.23	1.38±0.08
Pdf>hid;+ 29->17 RR	16	0.00	18.75	81.25		
Pdf>hid;tubpgal80^{ts} 29->17 DD	18	0.00	16.67	83.33	23.00	1.17±0.12
Pdf>CyO;tubpgal80^{ts} 29->17 DD	25	24.00	36.00	40.00	24.77±0.52	1.39±0.08
Pdf>hid;+ 29->17 DD	16	0.00	12.50	87.50		
Pdf>hid;tubpgal80^{ts} 17->17 RR	12	25.00	41.67	33.33	26.10±0.94	1.27±0.09
Pdf>CyO;tubpgal80^{ts} 17->17 RR	15	53.33	40.00	6.67	24.46±0.30	1.84±0.17
Pdf>hid;tubpgal80^{ts} 17->17 DD	15	0.00	26.67	73.33	20.88±1.55	1.13±0.01
Pdf>CyO;tubpgal80^{ts} 17->17 DD	15	60.00	40.00	0.00	24.20±0.32	1.70±0.12
Pdf>hid;tubpgal80^{ts} 17->17 RR	31	29.03	48.39	22.58	26.13±0.52	1.61±0.11
Pdf>CyO;tubpgal80^{ts} 17->17 RR	27	62.96	29.63	7.41	26.18±0.37	1.88±0.11
Pdf>hid;tubpgal80^{ts} 17->17 DD	25	0.00	32.00	68.00	26.00±1.64	1.19±0.05
Pdf>CyO;tubpgal80^{ts} 17->17	21	76.19	19.05	4.76	26.40±0.35	1.97±0.11

DD

Appendix Table 36, Behavioural data for Pdf; hid/+; tubpgal80^{ts}/+ and controls across various developmental temperature conditions and adult light conditions

Genotype	n	% SR	% WR	% AR	TAU + SEM	RRP + SEM
hdc^{jk910};Pdf^{01} RR M	17	5.88	47.06	47.06	24.00±1.56	1.25±0.12
hdc^{jk910};Pdf^{01} RR F	12	0.00	41.67	58.33	23.60±0.43	1.33±0.08
hdc^{jk910};Pdf^{01} DD M	19	15.79	36.84	47.37	24.00±0.27	1.35±0.12
hdc^{jk910};Pdf^{01} DD F	17	5.88	17.65	76.47	23.67±0.15	1.28±0.15
hdc^{jk910};Pdf^{01}/+ RR M	16	93.75	6.25	0	24.56±0.11	2.02+0.16
hdc^{jk910};Pdf^{01}/+ RR F	15	53.33	40	6.67	24.57±0.09	1.70+0.12
hdc^{jk910};Pdf^{01}/+ DD M	16	100	0	0	24.19±0.08	2.41+0.12
hdc^{jk910};Pdf^{01}/+ DD F	16	18.75	75	6.25	24.70±0.19	1.41+0.05
norpA;Pdf^{01} RR M	8	0.00	25.00	75.00	23.00±1.00	1.14±0.12
norpA;Pdf^{01} RR F	5	0.00	0.00	100.00	~	~
norpA;Pdf^{01} DD M	10	20.00	20.00	60.00	22.25±0.83	1.44±0.19
norpA;Pdf^{01} DD F	12	0.00	8.33	91.67	25.00	1.15
norpA:: Pdf^{01}/+ M DD	15	53.33	33.33	13.33	24.54±0.30	1.62±0.13
norpA:: Pdf^{01}/+ F DD	14	64.29	35.71	0.00	24.71±0.17	1.71±0.13
norpA:: Pdf^{01}/+ M RR	14	57.14	35.71	7.14	23.35±0.15	1.95±0.12
norpA:: Pdf^{01}/+ F RR	14	50.00	21.43	28.57	23.55±0.14	1.86±0.13
eya2;Pdf^{01} RR M	4	0.00	25.00	75.00	22.50	1.07
eya2;Pdf^{01} RR F	8	0.00	0.00	100.00		
eya2;Pdf^{01} DD M	10	0.00	30.00	70.00	27.17±3.94	1.16±0.06
eya2;Pdf^{01} DD F	6	0.00	0.00	100.00	~	~
eya2;Pdf^{01}/+ RR M	16	68.75	25.00	6.25	24.23±0.17	1.90±0.16
eya2;Pdf^{01}/+ RR F	13	38.46	46.15	15.38	23.82±0.17	1.54±0.14
eya2;Pdf^{01}/+ DD M	11	90.91	9.09	0.00	23.32±0.14	1.71±0.11
eya2;Pdf^{01}/+ DD F	16	62.50	31.25	6.25	23.63±0.14	1.82±0.14
disco^{1} RR M	24	0.00	33.33	66.67	16.69±1.13	1.16±0.04
disco^{1} RR F	6	0.00	50.00	50.00	25.83±6.36	1.11±0.07
disco^{1} DD M	17	0.00	0.00	100	~	~
disco^{1} DD F	7	0.00	0.00	100	~	~
Pdf^{01} RR M	29	10.00	13.00	6.00	22.56±0.11	1.51±0.08
Pdf^{01} RR F	8	1	1	6	22.25±0.25	1.54±0.34

Genotype	n	% SR	% WR	% AR	TAU + SEM	RRP + SEM
Pdf^{01} DD M	9	0	2	7	24.29±0.73	1.25±0.04
Pdf^{01} DD F	8	0	1	7	23	1.09
dcr; TUG; dspdf/dshiscl1 RR M	22	18.18	27.27	54.55	22.50±0.60	1.49±0.15
dcr; TUG; dspdf/dshiscl1 RR F	26	3.85	15.38	80.77	26.60±1.46	1.26±0.10
dcr; TUG; dspdf/dshiscl1 DD M	30	3.33	43.33	53.33	24.50±0.96	1.16±0.05
dcr; TUG; dspdf/dshiscl1 DD F	31	0.00	9.68	90.32	20.50±2.25	1.06±0.03
dcr; tug; +/dshiscl RR M	16	93.75	0.00	6.25	24.00±0.29	2.22±0.12
dcr; tug; +/dshiscl RR F	20	5	55	40	24.41±0.41	1.23±0.06
dcr; tug; +/dshiscl DD M	23	65.22	21.74	13.04	23.90±0.19	1.96±0.12
dcr; tug; +/dshiscl DD F	23	86.96	13.04	0.00	23.98±0.38	1.92±0.08

Appendix Table 37: Behavioural data encompassing rhythmic strength and period length for various lines challenging visual system or histamine signalling function in RR and DD. Data contributed entirely or in part from other lab members highlighted in Red.

	Distribution of rhythms	RRP
norpA;Pdf^{01} RR M vs Pdf^{01}	0.014 *	>0.001 ***
norpA;Pdf^{01} RR F vs Pdf^{01}	0.999	0.911
norpA;Pdf^{01} DD M vs Pdf^{01}	0.165	0.999
norpA;Pdf^{01} DD F vs Pdf^{01}	1	1
eya2;Pdf^{01} RR M vs Pdf^{01}	0.108	>0.001 ***
eya2;Pdf^{01} RR F vs Pdf^{01}	0.466	0.959
eya2;Pdf^{01} DD M vs Pdf^{01}	0.421	0.763
eya2;Pdf^{01} DD F vs Pdf^{01}	1	0.96
hdc^{jk910};Pdf^{01} RR M vs Pdf^{01}	0.05	0.021 *
hdc^{jk910};Pdf^{01} RR F vs Pdf^{01}	0.239	1
hdc^{jk910};Pdf^{01} DD M vs Pdf^{01}	0.404	0.523
hdc^{jk910};Pdf^{01} DD F vs Pdf^{01}	0.999	0.934
norpA;Pdf^{01} RR M vs "" Pdf^{01}/+	0.001 **	0.005 **
norpA;Pdf^{01} RR F vs "" Pdf^{01}/+	0.041 *	0.067

	Distribution of rhythms	**RRP**
norpA;Pdf^{01} DD M vs "" Pdf^{01}/+	0.07	0.774
norpA;Pdf^{01} DD F vs "" Pdf^{01}/+	>0.001 ***	0.012 *
eya2;Pdf^{01} RR M vs "" Pdf^{01}/+	0.005 **	0.017 *
eya2;Pdf^{01} RR F vs "" Pdf^{01}/+	>0.001 ***	0.201
eya2;Pdf^{01} DD M vs "" Pdf^{01}/+	>0.001 ***	0.008 **
eya2;Pdf^{01} DD F vs "" Pdf^{01}/+	>0.001 ***	0.006 **
hdc^{jk910};Pdf^{01} RR M vs "" Pdf^{01}/+	>0.001 ***	>0.001 ***
hdc^{jk910};Pdf^{01} RR F vs "" Pdf^{01}/+	0.001 **	0.071
hdc^{jk910};Pdf^{01} DD M vs "" Pdf^{01}/+	>0.001 ***	>0.001 ***
hdc^{jk910};Pdf^{01} DD F vs "" Pdf^{01}/+	>0.001 ***	0.002 **
Dcr; TUG; dspdf/+ vs dcr; TUG; dspdf/dshiscl1 RR M	0.196	0.255
Dcr; TUG; dspdf/+ vs dcr; TUG; dspdf/dshiscl1 RR F	0.55	0.986
Dcr; TUG; dspdf/+ vs dcr; TUG; dspdf/dshiscl1 DD M	0.888	1
Dcr; TUG; dspdf/+ vs dcr; TUG; dspdf/dshiscl1 DD F	0.146	0.624
RR vs DD		
norpA;Pdf^{01} M	0.614	0.044*
norpA;Pdf^{01} F	1	0.559
norpA;Pdf^{01}/+ M	0.999	0.242
norpA;Pdf^{01}/+ F	0.149	0.647
eya2;Pdf^{01} M	1	0.033*
eya2;Pdf^{01} F	1	0.304
eya2;Pdf^{01}/+ M	0.462	0.916
eya2;Pdf^{01}/+ F	0.476	0.022*
hdc^{jk910};Pdf^{01} M	0.718	0.671
hdc^{jk910};Pdf^{01} F	0.218	0.260
hdc^{jk910};Pdf^{01}/+ M	0.499	0.026*
hdc^{jk910};Pdf^{01}/+ F	0.096	0.897
disco^{1} M	0.012 *	0.054
disco^{1} F	0.076	0.575
dcr; TUG; dspdf/dshiscl1 RR M	0.525	0.367
dcr; TUG; dspdf/dshiscl1 RR F	0.824	0.392

dcr; tug; +/dshiscl RR M	0.082	0.803
dcr; tug; +/dshiscl RR F	>0.001 ***	>0.001 ***

Appendix Table 30: Stats for behavioural data in table N. P-values for distribution of rhtyhmicities were generated using 2x3 Fisher's exact test, whilst RRP P-values were generated using one-way ANOVA. Data in red contributed in part by other lab members.

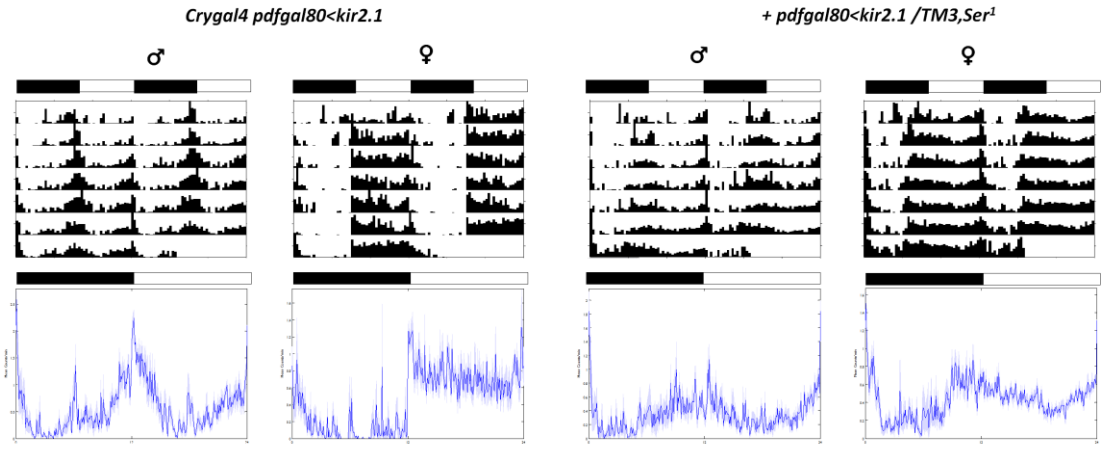

Appendix figure 27: Average actograms for Crygal4-pdfgal80>Kir2.1 in 12:12 LD. Visible in males is an abundant evening anticipation increase in spite of behavioural arrhythmicity in both RR and DD. n number from left to right = 6, 4, 4, 8.

Genotype	**n**	**% SR**	**% WR**	**% AR**	**TAU + SEM**	**RRP + SEM**
DH44>TrpA1 29C RR M	28	17.86	67.86	14.29	21.69±0.28	1.29±0.05
DH44>TrpA1 29C RR F	29	24.14	48.28	27.59	21.86±0.14	1.33±0.07
DH44>TrpA1 29C DD M	15	26.67	73.33	0.00	23.37±0.09	1.41±0.10
DH44>TrpA1 29C DD F	15	20.00	60.00	20.00	23.42±0.14	1.37±0.13
DH44>TrpA1 23C RR M	10	60	40	0	24.40±0.74	1.69±0.16
DH44>TrpA1 23C RR F	13	0	53.85	46.15	25.36±0.95	1.10±0.03

Genotype	n	% SR	% WR	% AR	TAU + SEM	RRP + SEM
DH44>TrpA1 23C DD M	14	78.57	21.43	0	23.89±0.13	1.89±0.11
DH44>TrpA1 23C DD F	16	37.5	50	12.5	24.21±0.20	1.50±0.12
DH44>+ 29C RR M	24	79.17	12.50	8.33	23.11±0.05	2.44±0.13
DH44>+ 29C RR F	17	11.76	76.47	11.76	23.30±0.18	1.35±0.06
DH44>+ 29C DD M	23	100.00	0.00	0.00	22.70±0.19	2.24±0.08
DH44>+ 29C DD F	26	84.62	15.38	0.00	22.88±0.16	1.93±0.08
DH44>+ 23C RR M	16	87.50	12.50	0.00	24.41±0.21	2.02±0.12
DH44>+ 23C RR F	14	42.86	35.71	21.43	24.45±0.11	1.61±0.11
DH44>+ 23C DD M	32	90.63	9.38	0.00	23.75±0.06	1.98±0.07
DH44>+ 23C DD F	21	80.95	19.05	0.00	23.90±0.11	2.11±0.13
SIFa>hid RR M	10	60	40.00	0.00	24.40±0.74	1.69±0.16
SIFa>hid RR F	13	0	53.85	46.15	25.36±0.95	1.10±0.03
SIFa>hid DD M	18	50	38.89	11.11	23.22±0.30	1.60±0.11
SIFa>hid DD F	22	22.73	31.82	45.45	24.83±0.89	1.38±0.12
lk^{c275} M RR	32	65.63	34.38	0.00	23.50±0.17	1.64±0.07
lk^{c275} F RR	15	6.67	13.33	80.00	23.17±1.09	1.32±0.15
lkr^{c003} M RR	28	32.14	60.71	7.14	24.73±0.27	1.45±0.06
lkr^{c003} F RR	11	9.09	27.27	63.64	25.63±2.28	1.26±0.12
lk^{c275} M DD	13	0.00	46.15	53.85	23.42±1.06	1.23±0.07
lk^{c275} F DD	8	0.00	75.00	25.00	23.42±2.16	1.11±0.04
lkr^{c003} M DD	11	9.09	36.36	54.55	24.20±0.12	1.35±0.18
lkr^{c003} F DD	9	0.00	33.33	66.67	23.67±4.28	1.12±0.06
lk^{c275}/+ M RR	21	47.62	47.62	4.76	23.98±0.14	1.66±0.08
lk^{c275}/+ F RR	17	0	29.41	70.59	24.60±0.29	1.21±0.13
lkr^{c003}/+ M RR	16	100	0	0	25.16±0.09	2.07±0.06
lkr^{c003}/+ F RR	13	7.69	61.54	30.77	23.89±0.74	1.16±0.07
lk^{c275}/+ M DD	46	32.61	56.52	10.87	23.84±0.09	1.47±0.04
lk^{c275}/+ F DD	16	81.25	18.75	0	23.59±0.05	1.89±0.10
lkr^{c003}/+ M DD	29	10.34	65.52	24.14	23.52±0.13	1.23±0.05
lkr^{c003}/+ F DD	21	90.48	9.52	0	23.57±0.04	1.84±0.05
SIFa-gal4/CyO RR M	7	100	0	0	23.71±0.15	2.37±0.07

Genotype	n	% SR	% WR	% AR	TAU + SEM	RRP + SEM
SIFa-gal4/CyO RR F	7	57.14	42.86	0	24.43±0.23	1.52±0.10
SIFa-gal4/CyO DD M	7	100	0	0	23.43±0.07	1.89±0.06
SIFa-gal4/CyO DD F	7	42.86	42.86	14.29	25.92±1.89	1.47±0.07

Appendix Table 39; Behavioural data for rhythmic strength and period length of various lines challenging clock output pathways

	Distribution of rhythms	RRP
RR vs DD		
DH44>TrpA1 23 M	0.392	0.100
DH44>TrpA1 23 F	0.022	0.803
DH44>TrpA1 29 M	0.352	0.106
DH44>TrpA1 29 F	0.768	0.904
DH44>+ 23 M	0.999	0.779
DH44>+ 23 F	0.031 *	>0.001 ***
DH44>+ 29 M	0.049 *	0.140
DH44>+ 29 F	>0.001 ***	>0.001 ***
***SIFa*> hid M**	0.849	0.424
***SIFa*> hid F**	0.196	0.304
***SIFa*>+ M**	1	>0.001***
***SIFa*>+ F**	0.999	0.418
LK^{c275} M	>0.001***	>0.001 ***
LK^{c275} F	0.011 *	0.912
LKR^{c003} M	0.001 **	0.024 *
LKR^{c003} F	0.402	0.107
LK^{c275} /+ M	0.490	0.051
LK^{c275}/+ F	>0.001 ***	>0.001 ***
LKR^{c003}/+ M	>0.001***	>0.001***
LKR^{c003}/+ F	>0.001 ***	>0.001 ***

driven vs undriven	**Distribution of rhythms**	**RRP**
DH44 23 M RR	0.163	0.334
DH44 23 F RR	0.029*	0.580
DH44 29 M RR	>0.001 ***	>0.001 ***
DH44 29 F RR	0.213	0.744
DH44 23 M DD	0.35	0.529
DH44 23 F DD	0.012 *	0.003 **
DH44 29 M DD	>0.001 ***	>0.001 ***
DH44 29 F DD	>0.001 ***	0.012 *
***SIFa* RR M**	0.103	0.004 **
***SIFa* RR F**	0.003**	>0.001***
***SIFa* DD M**	0.067	0.061
***SIFa* DD F**	0.304	0.310
23°C vs 29°C		
DH44>TrpA1 M RR	0.046 *	>0.001 ***
DH44>TrpA1 F RR	0.111	0.206
DH44>TrpA1 M DD	0.009 **	0.004**
DH44>TrpA1 F DD	0.006 **	0.350
DH44>+ M RR	0.818	0.038*
DH44>+ F RR	0.071	0.162
DH44>+ M DD	0.226	0.484
DH44>+ F DD	1	0.128
Het vs Hom		
LK^{c275} RR M	0.251	0.975
LK^{c275} RR F	0.411	0.384
LKR^{c003} RR M	>0.001 ***	>0.001 ***
LKR^{c003} RR F	0.291	0.859
LK^{c275} DD M	>0.001 ***	0.001 **
LK^{c275} DD F	>0.001 ***	>0.001 ***
LKR^{c003} DD M	0.063	0.606
LKR^{c003} DD F	>0.001 ***	>0.001 ***

Appendix Table 40: Stats for behavioural data in Appendix Table 39, relevant to TrpA1

expression within DH44+ve cells. P-values for distribution of rhythmicities were generated using 2x3 Fisher's exact test, whilst RRP P-values were generated using one-way ANOVA with Games-howell post-hoc test.

P-value vs	***cyc*^{01} M**	***cyc*^{01} F**	***cyc*^{01}/+ M**	***cyc*^{01}/+ F**	**17→29 *cyc*^{01} *[elav.sytgfp+cyc]*^{ts}**	**Pdf>CD8::GFP;*cyc*^{01}**
***cyc*^{01} M**		0.493	0.990	0.996	0.993	0.000
***cyc*^{01} F**	0.493		0.827	0.163	0.240	0.010
***cyc*^{01}/+ M**	0.990	0.827		0.812	0.854	0.000
***cyc*^{01}/+ F**	0.996	0.163	0.812		1.000	0.000
17→29 *cyc*^{01} *[elav.sytgfp+cyc]*^{ts}	0.993	0.240	0.854	1.000		0.000
Pdf>CD8::GFP;*cyc*^{01}	0.000	0.010	0.000	0.000	0.000	

Appendix Table 41: Statistics comparing number of PDF cell soma between various genotypes with manipulated CYC values

17°C vs 29°C	**Distribution of rhythms**	**RRP**
M RR	>0.001 ***	0.002**
F RR	>0.001 ***	>0.001 ***
RR vs DD		
29°C M	0.001 **	>0.001 ***
29°C F	0.349	0.111
17°C M	1	0.975
17°C F	0.345	0.191

Appendix Table 42, P-values comparing behavioural rhythmicity of permissively or restrictively raised cyc^{01} *[elav.cyc]*^{ts} *in RR and DD. Distribution of rhythmicity was calculated with 2x3 Fisher's exact test, and RRP by one-way ANOVA*

P	**Distribution of rhythms**	**RRP**
RR vs DD		
29→29 *°C* M	0.007**	0.062

29→29 °C F	0.001 **	0.027 *
17→29 °C M	1	1
17→29 °C F	1	1
17°C vs 29°C		
RR M	>0.001 ***	0.013 *
RR F	0.014 *	0.014 *
DD M	0.529	0.807
DD F	0.999	0.969

Appendix Table 43, P values for significance between behavioural rhythmicity of cyc^{01} [elav-Pdf80.cyc]^{ts} raised at 17°C or 29°C and run in 29°C RR or DD, demonstrating that permissively raised flies in RR differ to their restrictively-raised counterparts, whilst this is not the case in DD. Distribution of rhythmicity was calculated using 2x3 Fisher's exact test, and RRP by one-way ANOVA.

Comparison	**Distribution of rhythmicity**	**RRP**
[timP.per]^{ts} 23°C ♂ RR vs DD	0.374	0.056
[timP.per]^{ts} 23°C ♀RR vs DD	0.010 **	0.005**
[timP.per]^{ts} 29°C ♂ RR vs DD	0.314	0.274
[timP.per]^{ts} 29°C ♀RR vs DD	0.637	0.835
[timP.per]^{ts} ♂ RR 29°C vs 23°C	>0.001***	>0.001***
[timP.per]^{ts} ♀ RR 29°C vs 23°C	>0.001***	>0.001***

Appendix Table 44, P-values for comparisons in distribution of rhythmicity and RRP between [timP.per]^{ts} in RR and DD.

	n	**% SR**	**% WR**	**% AR**	**TAU ± SEM**	**RRP ± SEM**
cyc^{01} **17→17°C**	13	0	15.38	84.62	23.5±7.5	1.18±0.10
cyc^{01} **17→17°C**	16	0	6.25	93.75	33	1.05
cyc^{01} **17→29 °C**	3	0	0	100		
cyc^{01} **17→29 °C**	6	0	0	100		

	n	% SR	% WR	% AR	TAU ± SEM	RRP ± SEM
***cyc*^{01} 29→17°C**	19	0	0	100		
***cyc*^{01} 29→17°C**	22	0	0	100		
***cyc*^{01} 29→29 °C**	20	0	0	100		
***cyc*^{01} 29→29 °C**	24	0	12.5	87.5	26.67±2	1.21±0.11

Appendix Table 45, dataset of cyc^{01} behavioural rhythms in freerunning conditions.

Appendix Figures: Reproduced from other places

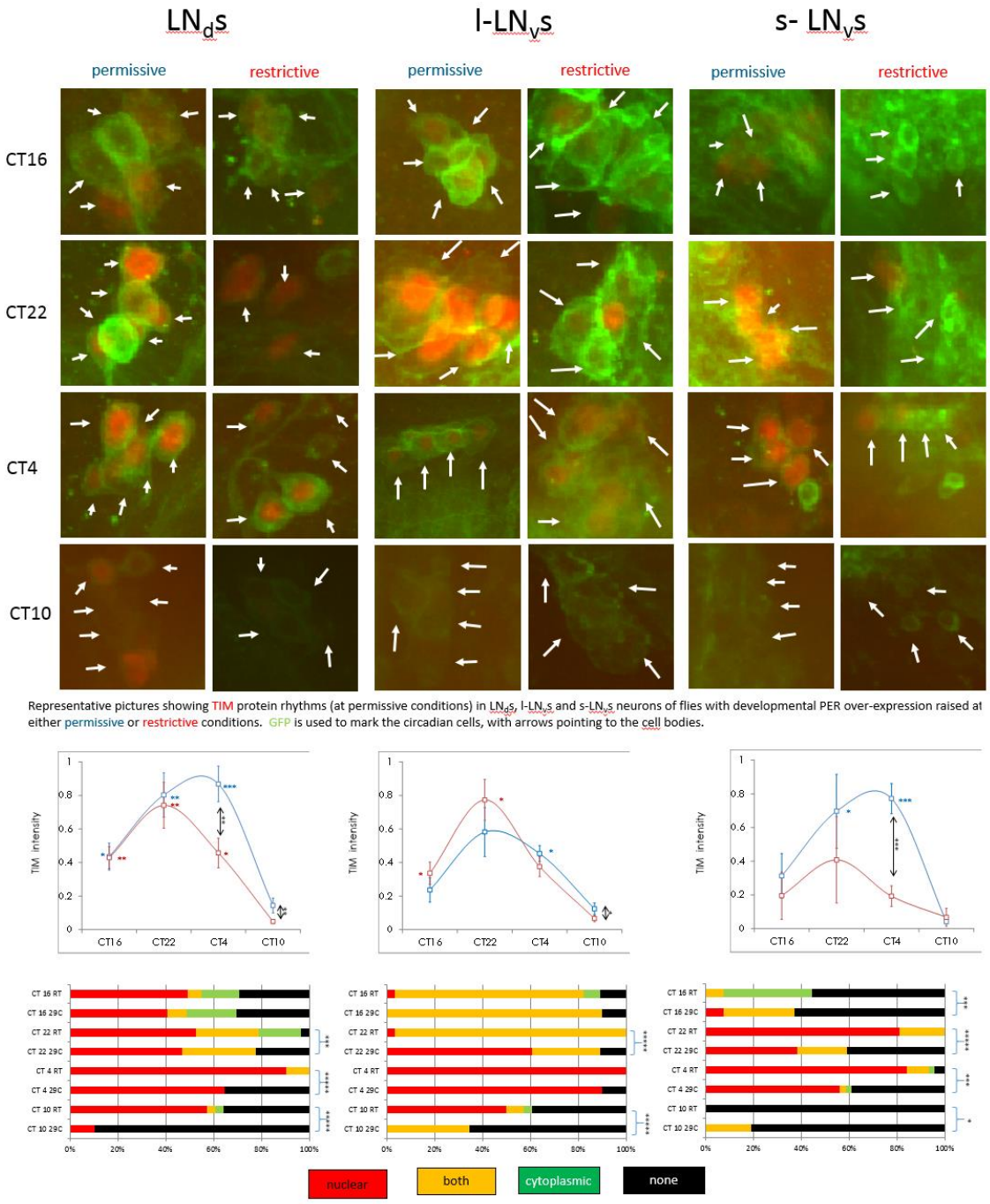

Representative pictures showing TIM protein rhythms (at permissive conditions) in LNds, l-LNvs and s-LNvs neurons of flies with developmental PER over-expression raised at either permissive or restrictive conditions. GFP is used to mark the circadian cells, with arrows pointing to the cell bodies.

Appendix Figure 28, taken from Karolina Mirowska thesis (2015). Demonstrated are the molecular rhythms of permissively and restrictively raised [timP.per]^{ts}

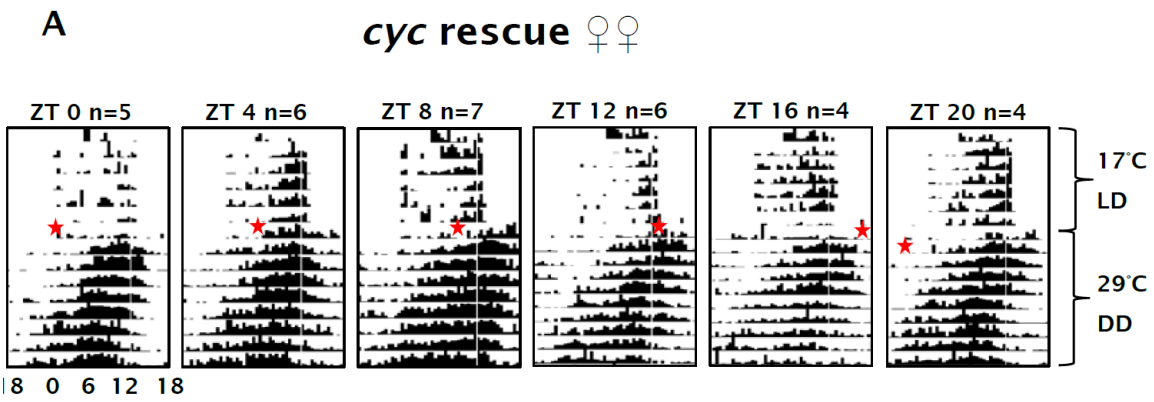

Appendix Figure 29, taken from Karolina Mirowska thesis, 23°C-raised cyc^{01} [elav.cyc]^{ts} run at 17°C LD and 29°C DD, moved into DD as varying phases. This demonstrates permissive freerunning phase is determined by restrictive entrainment phase rather than resumption of permissive temperature, suggesting the oscillator is not static in 17°C, but responsive to external cues and capable of altering phase information.

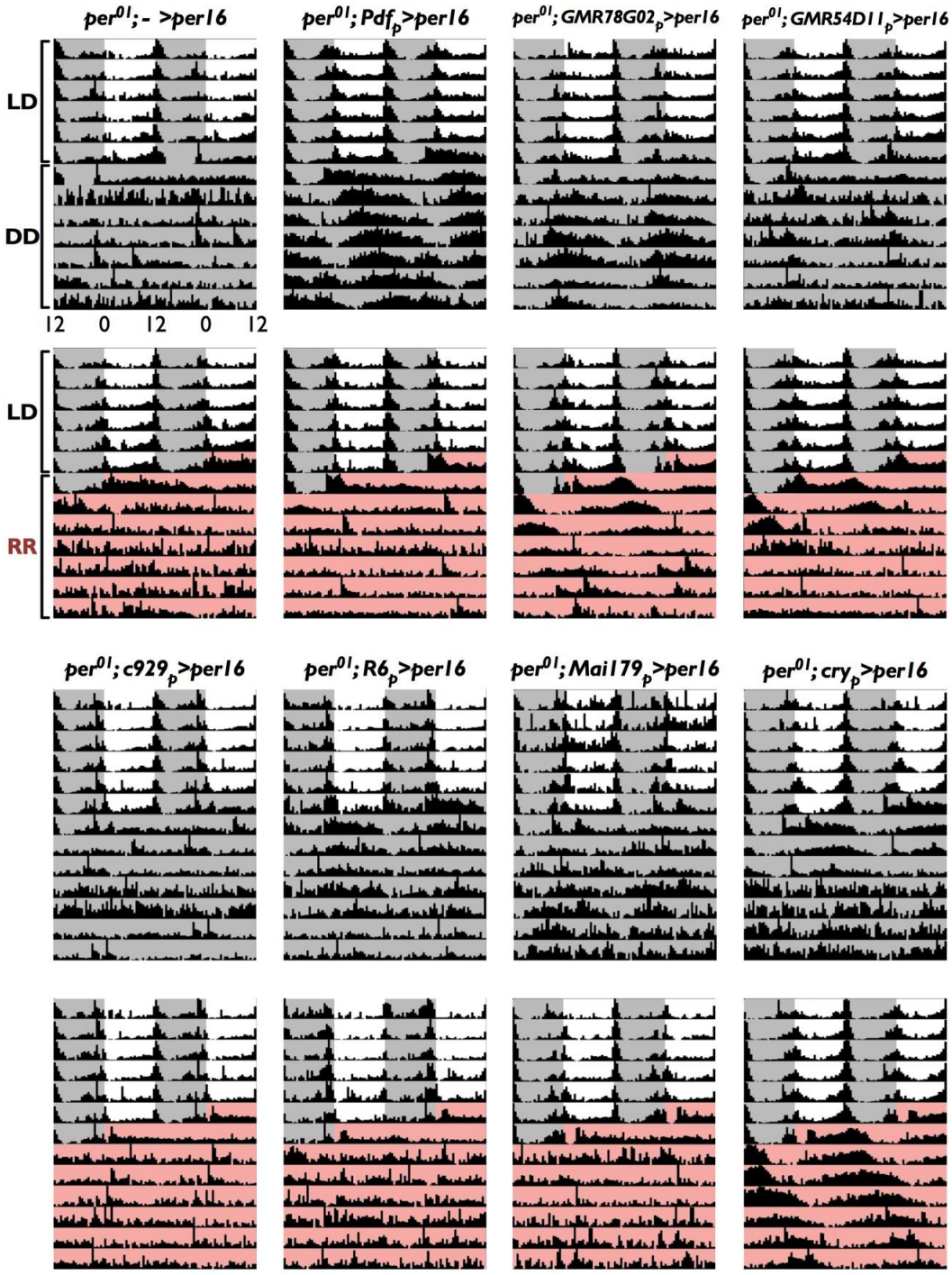

Appendix Figure 30, produced in entirety by Miguel Ramirez-Moreno, showing LD, DD and RR behavioural profiles for spatial re-introduction of PER on per^{01} background. Inclusion in the appendix is required to provide context for my contributions to this dataset, and to compare differences between required and sufficient oscillators.

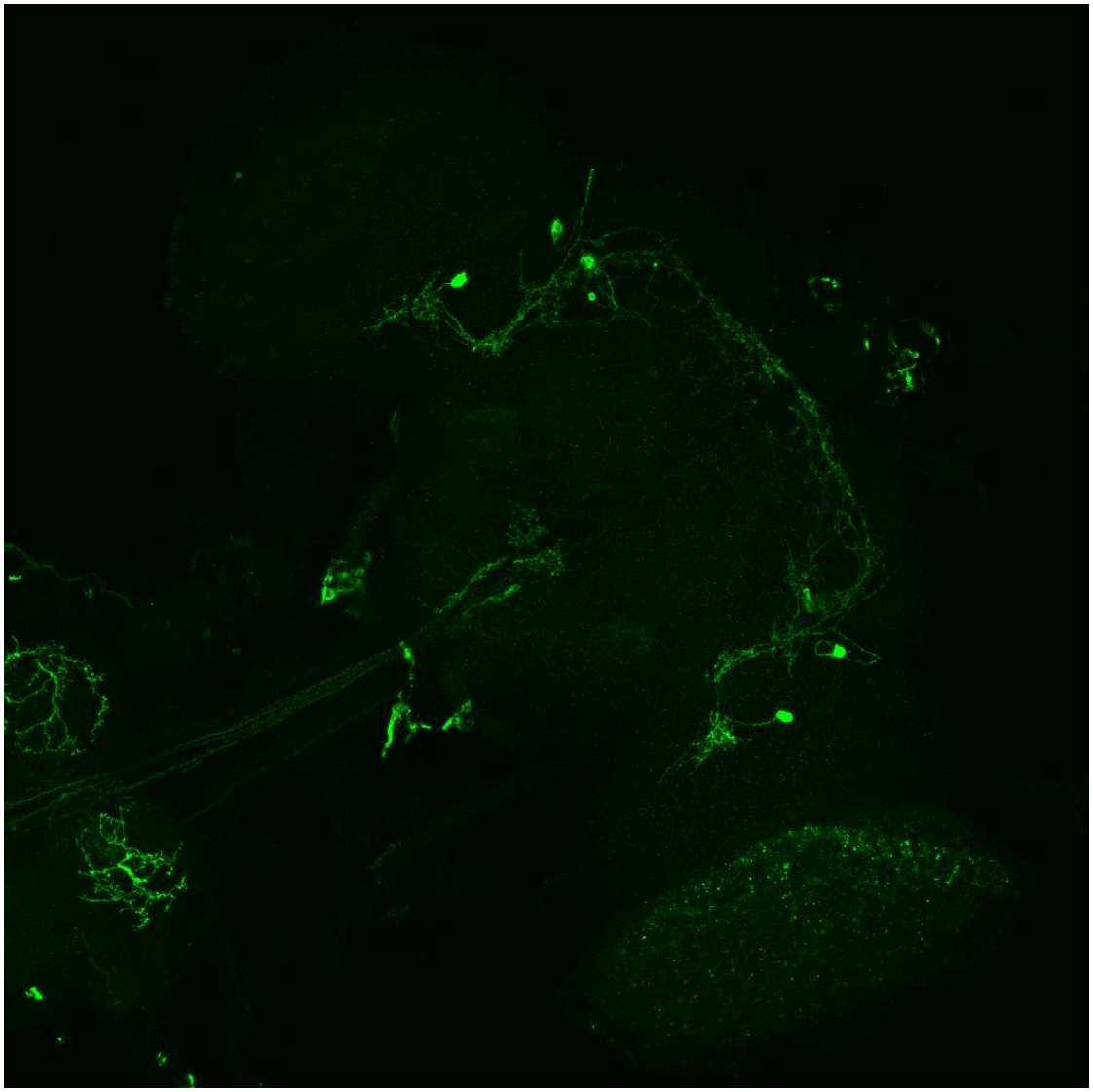

Appendix Figure 31, taken from the flylight website, staining pattern of R54D11-gal4, demonstrating expression in very few neurons, and arguably only 1-2 cells beyond the ITP+ve clock cells are encapsulated by this driver within the protocerebrum.

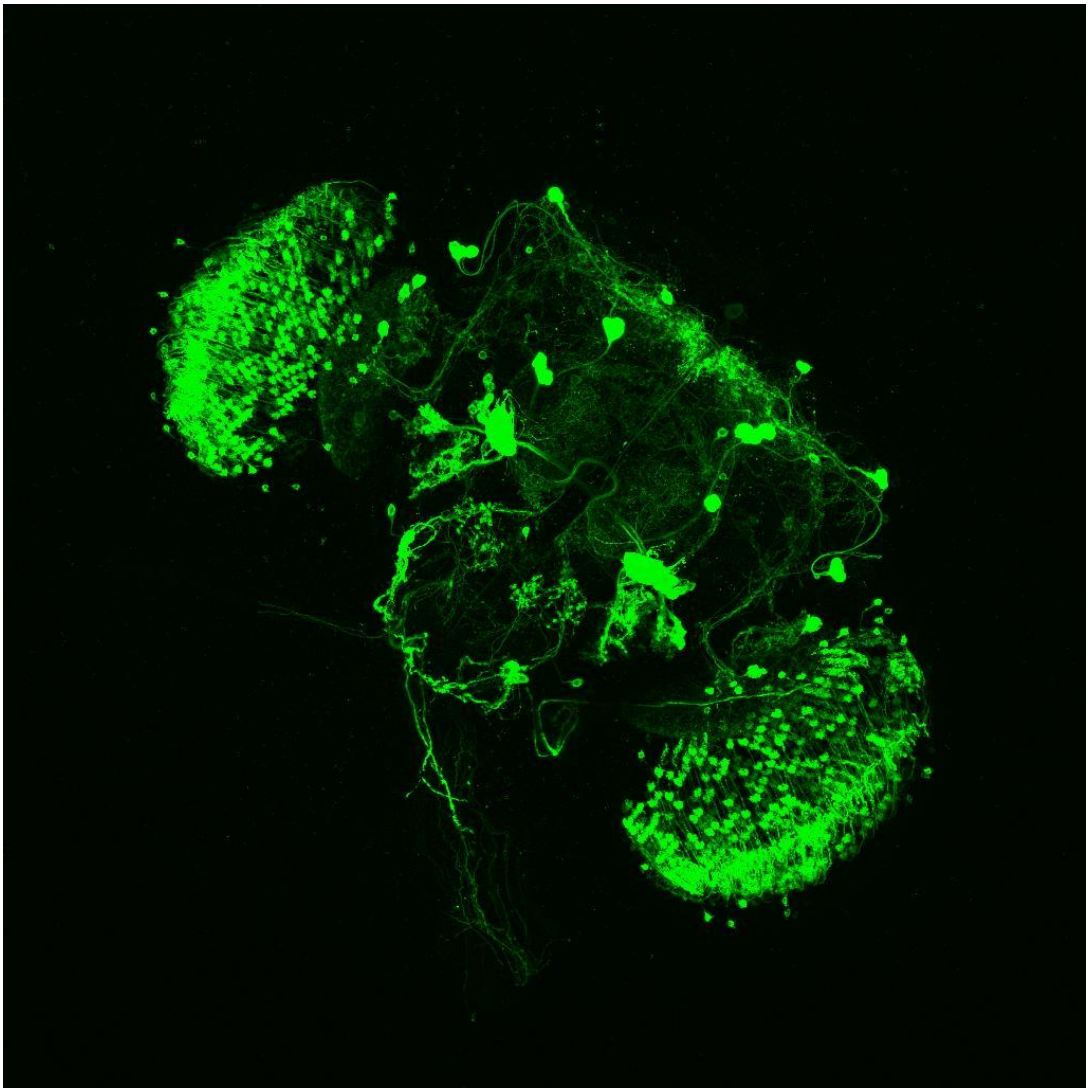

Appendix Figure 32, taken from the flylight website, staining pattern of R78G02-gal4, showing expression in numerous neurons. (Yoshii et al., 2015) has previously validated these express in the 3 LN_ds and 5^{th}-sLN_v, which are all clearly visible in this image. Other targeted cells include the non-clock ITP cells and cells located within the optic lobe and ellipsoid body

Chapter 8: References

ABRUZZI, K., CHEN, X., NAGOSHI, E., ZADINA, A., ROSBASH, M. 2015. RNA-seq Profiling of Small Numbers of *Drosophila* Neurons. *Methods in Enzymology*. 551, 369–386.

AGRAWAL, P. & HARDIN, P. E. 2016. The *Drosophila* Receptor Protein Tyrosine Phosphatase LAR Is Required for Development of Circadian Pacemaker Neuron Processes That Support Rhythmic Activity in Constant Darkness But Not during Light/Dark Cycles. *Journal of Neuroscience,* 36**,** 3860-3870.

AKERSTEDT, T., FREDLUND, P., GILLBERG, M. & JANSSON, B. 2002. A prospective study of fatal occupational accidents - relationship to sleeping difficulties and occupational factors. *Journal of Sleep Research,* 11**,** 69-71.

ALLADA, R., WHITE, N. E., SO, W. V., HALL, J. C. & ROSBASH, M. 1998. A mutant *Drosophila* homolog of mammalian Clock disrupts circadian rhythms and transcription of period and timeless. *Cell,* 93**,** 791-804.

ANDRETIC, R., VAN SWINDEREN, B. & GREENSPAN, R. J. 2005. Dopaminergic modulation of arousal in *Drosophila*. *Current Biology,* 15**,** 1165-1175.

BAE, K., LEE, C., HARDIN, P. E. & EDERY, I. 2000. dCLOCK is present in limiting amounts and likely mediates daily interactions between the dCLOCK-CYC transcription factor and the PER-TIM complex. *Journal of Neuroscience,* 20**,** 1746→1753.

BACH-Y-RITA, P. 1993. Non-synaptic diffusion neurotransmission (NDN) in the brain. *Neurochemistry International,* 23, 297-318.

BAHN, J. H., LEE, G. & PARK, J. H. 2009. Comparative Analysis of Pdf-Mediated Circadian Behaviors Between *Drosophila* melanogaster and D. virilis. *Genetics,* 181**,** 965-975.

BAINBRIDGE, S. P., AND BOWNES, M. 1981. Staging the metamorphosis of *Drosophila* melanogaster. Journal of Embryology and Experimental Morphology. 66, 57-80.

BATEMAN, J. R., LEE, A. M. & WU, C. T. 2006. Site-specific transformation of *Drosophila* via phi C31 integrase-mediated cassette exchange. *Genetics,* 173**,** 769-777.

BECKWITH, E. J., GOROSTIZA, E. A., BERNI, J., REZAVAL, C., PEREZ-SANTANGELO, A., NADRA, A. D. & CERIANI, M. F. 2013. Circadian Period Integrates Network Information Through Activation of the BMP Signaling Pathway. *Plos Biology,* 11.

BENITO, J., ZHENG, H. & HARDIN, P. E. 2007. PDP1 epsilon functions downstream of the circadian oscillator to mediate behavioral rhythms. *Journal of Neuroscience,* 27**,** 2539-2547.

BERDNIK, D., CHIHARA, T., COUTO, A. & LUO, L. Q. 2006. Wiring stability of the adult *Drosophila* olfactory circuit after lesion. *Journal of Neuroscience,* 26**,** 3367-3376.

BERNDT, A., KOTTKE, T., BREITKREUZ, H., DVORSKY, R., HENNIG, S., ALEXANDER, M. & WOLF, E. 2007. A novel photoreaction mechanism for the circadian blue light photoreceptor *Drosophila* cryptochrome. *Journal of Biological Chemistry,* 282**,** 13011-13021.

BEUCHLE, D., JAUMOUILLE, E. & NAGOSHI, E. 2012. The Nuclear Receptor unfulfilled Is Required for Free-Running Clocks in *Drosophila* Pacemaker Neurons. *Current Biology,* 22**,** 1221-1227.

BLANCHARD, F. J., COLLINS, B., CYRAN, S. A., HANCOCK, D. H., TAYLOR, M. V. & BLAU, J. 2010. The Transcription Factor Mef2 Is Required for Normal

Circadian Behavior in *Drosophila*. *Journal of Neuroscience,* 30**,** 5855-5865.
BLANCHARDON, E., GRIMA, B., KLARSFELD, A., CHELOT, E., HARDIN, P. E., PREAT, T. & ROUYER, F. 2001. Defining the role of *Drosophila* lateral neurons in the control of circadian rhythms in motor activity and eclosion by targeted genetic ablation and PERIOD protein overexpression. *European Journal of Neuroscience,* 13**,** 871-888.
BLAU, J. & YOUNG, M. W. 1999. Cycling vrille expression is required for a functional *Drosophila* clock. *Cell,* 99**,** 661-671.
BONINI, N. M., LEISERSON, W. M. & BENZER, S. 1993. The Eyes Absent Gene - Genetic-Control of Cell-Survival and Differentiation in the Developing *Drosophila* Eye. *Cell,* 72**,** 379-395.
BORBELY, A. A. & ACHERMANN, P. 1999. Sleep homeostasis and models of sleep regulation. *Journal of Biological Rhythms,* 14**,** 557-568.
BORNSTEIN, B., ZAHAVI, E.E., GELLEY, S., ZOOSMAN, M., YANIV, S.P., FUCHS, O., PORAT, Z., PERLSON, E. & SCHULDINER, O. 2015. Developmental axon pruning requires destabilization of cell adhesion by JNK signaling. *Neuron*. 88, 926–940.
BRAND, A. H. & PERRIMON, N. 1993. Targeted Gene-Expression as a Means of Altering Cell Fates and Generating Dominant Phenotypes. *Development,* 118**,** 401-415.
BROWN, S. A., KOWALSKA, E. & DALMANN, R. 2012. (Re)inventing the Circadian Feedback Loop. *Developmental Cell,* 22**,** 477-487.
BUHL, E., BRADLAUGH, A., OGUETA, M., CHEN, K. F., STANEWSKY, R. & HODGE, J. J. L. 2016. Quasimodo mediates daily and acute light effects on *Drosophila* clock neuron excitability. *Proceedings of the National Academy of Sciences of the United States of America,* 113**,** 13486-13491.
BUTLER, B,, PIRROTTA, V., IRMINGER-FINGER, I., AND NÖTHIGER, R. 1986. The sex-determining gene tra of Drosophila: molecular cloning and transformation studies. *EMBO Journal*. 5(13): 3607–3613.
BURG, M. G., SARTHY, P. V., KOLIANTZ, G. & PAK, W. L. 1993. Genetic and Molecular-Identification of a *Drosophila* Histidine-Decarboxylase Gene Required in Photoreceptor Transmitter Synthesis. *Embo Journal,* 12**,** 911-919.
BUSZA, A., EMERY-LE, M., ROSBASH, M. & EMERY, P. 2004. Roles of the two *Drosophila* CRYPTOCHROME structural domains in circadian photoreception. *Science,* 304**,** 1503-1506.
CANNELL, E., DORNAN, A. J., HALBERG, K. A., TERHZAZ, S., DOW, J. A. T. & DAVIES, S. A. 2016. The corticotropin-releasing factor-like diuretic hormone 44 (DH44) and kinin neuropeptides modulate desiccation and starvation tolerance in *Drosophila* melanogaster. *Peptides,* 80**,** 96-107.
CAVANAUGH, D. J., GERATOWSKI, J. D., WOOLTORTON, J. R. A., SPAETHLING, J. M., HECTOR, C. E., ZHENG, X. Z., JOHNSON, E. C., EBERWINE, J. H. & SEHGAL, A. 2014. Identification of a Circadian Output Circuit for Rest: Activity Rhythms in *Drosophila*. *Cell,* 157**,** 689-701.
CAVEY, M., COLLINS, B., BERTET, C. & BLAU, J. 2016. Circadian rhythms in neuronal activity propagate through output circuits. *Nature Neuroscience,* 19**,** 587-+.
CERIANI, M. F., DARLINGTON, T. K., STAKNIS, D., MAS, P., PETTI, A. A., WEITZ, C. J. & KAY, S. A. 1999. Light-dependent sequestration of TIMELESS by CRYPTOCHROME. *Science,* 285**,** 553-556.
CERIANI, M. F., HOGENESCH, J. B., YANOVSKY, M., PANDA, S., STRAUME, M. & KAY, S. A. 2002. Genome-wide expression analysis in *Drosophila* reveals genes controlling circadian behavior. *Journal of Neuroscience,* 22**,** 9305-9319.

CHATURVEDI, R., LUAN, Z., GUO, P. Y. & LI, H. S. 2016. *Drosophila* Vision Depends on Carcinine Uptake by an Organic Cation Transporter. *Cell Reports,* 14**,** 2076-2083.
CHOI, C., FORTIN, J. P., MCCARTHY, E. V., OKSMAN, L., KOPIN, A. S. & NITABACH, M. N. 2009. Cellular Dissection of Circadian Peptide Signals with Genetically Encoded Membrane-Tethered Ligands. *Current Biology,* 19**,** 1167-1175.
CLANDININ, T. R., LEE, C. H., HERMAN, T., LEE, R. C., YANG, A. Y., OVASAPYAN, S. & ZIPURSKY, S. L. 2001. *Drosophila* LAR regulates R1-R6 and R7 target specificity in the visual system. *Neuron,* 32**,** 237-248.
CLARIDGE-CHANG, A., WIJNEN, H., NAEF, F., BOOTHROYD, C., RAJEWSKY, N. & YOUNG, M. W. 2001. Circadian regulation of gene expression systems in the *Drosophila* head. *Neuron,* 32**,** 657-671.
COLLINS, B., KANE, E. A., REEVES, D. C., AKABAS, M. H. & BLAU, J. 2012. Balance of Activity between LN(v)s and Glutamatergic Dorsal Clock Neurons Promotes Robust Circadian Rhythms in *Drosophila*. *Neuron,* 74**,** 706-718.
CUSUMANO, P., KLARSFELD, A., CHELOT, E., PICOT, M., RICHIER, B. & ROUYER, F. 2009. PDF-modulated visual inputs and cryptochrome define diurnal behavior in *Drosophila*. *Nature Neuroscience,* 12**,** 1431-1437.
CYRAN, S. A., BUCHSBAUM, A. M., REDDY, K. L., LIN, M. C., GLOSSOP, N. R. J., HARDIN, P. E., YOUNG, M. W., STORTI, R. V. & BLAU, J. 2003. vrille, Pdp1, and dClock form a second feedback loop in the *Drosophila* circadian clock. *Cell,* 112**,** 329-341.
CYRAN, S. A., YIANNOULOS, G., BUCHSBAUM, A. M., SAEZ, L., YOUNG, M. W. & BLAU, J. 2005. The double-time protein kinase regulates the subcellular localization of the *Drosophila* clock protein period. *Journal of Neuroscience,* 25**,** 5430-5437.
CZARNA, A., BERNDT, A., SINGH, H. R., GRUDZIECKI, A., LADURNER, A. G., TIMINSZKY, G., KRAMER, A. & WOLF, E. 2013. Structures of *Drosophila* Cryptochrome and Mouse Cryptochrome1 Provide Insight into Circadian Function. *Cell,* 153**,** 1394-1405.
DE, J., VARMA, V., SAHA, S., SHEEBA, V. & SHARMA, V. K. 2013. Significance of activity peaks in fruit flies, *Drosophila* melanogaster, under seminatural conditions. *Proceedings of the National Academy of Sciences of the United States of America,* 110**,** 8984-8989.
DEPETRIS-CHAUVIN, A., BERNI, J., ARANOVICH, E. J., MURARO, N. I., BECKWITH, E. J. & CERIANI, M. F. 2011. Adult-Specific Electrical Silencing of Pacemaker Neurons Uncouples Molecular Clock from Circadian Outputs. *Current Biology,* 21**,** 1783→1793.
DIANGELO, J. R., ERION, R., CROCKER, A. & SEHGAL, A. 2011. The Central Clock Neurons Regulate Lipid Storage in *Drosophila*. *Plos One,* 6.
DIB, P. B., GNAGI, B., DALY, F., SABADO, V., TAS, D., GLAUSER, D. A., MEISTER, P. & NAGOSHI, E. 2014. A Conserved Role for p48 Homologs in Protecting Dopaminergic Neurons from Oxidative Stress. *Plos Genetics,* 10.
DIONNE, H., HIBBARD, K.L., CAVALLARO, A., KAO, J.C., AND RUBIN, G.M. 2018. Genetic Reagents for Making Split-*GAL4* Lines in *Drosophila*. *Genetics* 209, 31-35.
DISSEL, S., HANSEN, C. N., OZKAYA, O., HEMSLEY, M., KYRIACOU, C. P. & ROSATO, E. 2014. The Logic of Circadian Organization in *Drosophila*. *Current Biology,* 24**,** 2257-2266.
DOLEZELOVA, E., DOLEZEL, D. & HALL, J. C. 2007. Rhythm defects caused by newly engineered null mutations in *Drosophila*'s cryptochrome gene. *Genetics,*

177**,** 329-345.
DUFFY, J. B. 2002. *GAL4* system in *Drosophila*: A fly geneticist's Swiss army knife. *Genesis,* 34**,** 1-15.
DUNLAP, J. C. 1999. Molecular bases for circadian clocks. *Cell,* 96**,** 271→290.
ECK, S., HELFRICH-FÖRSTER, C. & RIEGER, D. 2016. The Timed Depolarization of Morning and evening Oscillators Phase Shifts the Circadian Clock of *Drosophila*. *Journal of Biological Rhythms,* 31**,** 428-442.
EMERY, P., SO, W. V., KANEKO, M., HALL, J. C. & ROSBASH, M. 1998. CRY, a *Drosophila* clock and light-regulated cryptochrome, is a major contributor to circadian rhythm resetting and photosensitivity. *Cell,* 95**,** 669-679.
EMERY, P., STANEWSKY, R., HELFRICH-FÖRSTER, C., EMERY-LE, M., HALL, J. C. & ROSBASH, M. 2000. *Drosophila* CRY is a deep brain circadian photoreceptor. *Neuron,* 26**,** 493-504.
EWER, J., HAMBLEN-COYLE, M.,. ROSBASH., M & HALL, J. 1990. Requirement for *period* gene expression in the adult and not during development for locomotor activity rhythms of imaginal *Drosophila melanogaster. Journal of Neurogenetics.,* 7, 31-73
FEINBERG, E. H., VANHOVEN, M. K., BENDESKY, A., WANG, G., FETTER, R. D., SHEN, K. & BARGMANNL, C. I. 2008. GFP reconstitution across synaptic partners (GRASP) defines cell contacts and Synapses in living nervous systems. *Neuron,* 57**,** 353-363.
FERNANDEZ, M. P., BERNI, J. & CERIANI, M. F. 2008. Circadian remodeling of neuronal circuits involved in rhythmic behavior. *Plos Biology,* 6**,** 518-524.
FISCHER, R., HELFRICH-FÖRSTER, C., & PESCHEL, N. 2016. GSK-3 β does not stabilize cryptochrome in the circadian clock of *Drosophila*. *PLoS ONE*. 11
FLOURAKIS, M., KULA-EVERSOLE, E., HUTCHISON, A. L., HAN, T. H., ARANDA, K., MOOSE, D. L., WHITE, K. P., DINNER, A. R., LEAR, B. C., REN, D. J., DIEKMAN, C. O., RAMAN, I. M. & ALLADA, R. 2015. A Conserved Bicycle Model for Circadian Clock Control of Membrane Excitability. *Cell,* 162**,** 836-848.
FOGLE, K. J., BAIK, L. S., HOUL, J. H., TRAN, T. T., ROBERTS, L., DAHM, N. A., CAO, Y., ZHOU, M. & HOLMES, T. C. 2015. CRYPTOCHROME-mediated phototransduction by modulation of the potassium ion channel beta-subunit redox sensor. *Proceedings of the National Academy of Sciences of the United States of America,* 112**,** 2245-2250.
FOGLE, K. J., PARSON, K. G., DAHM, N. A. & HOLMES, T. C. 2011. CRYPTOCHROME Is a Blue-Light Sensor That Regulates Neuronal Firing Rate. *Science,* 331**,** 1409-1413.
FRENKEL, L., MURARO, N.I., BELTRÁN GONZÁLEZ, A.N., MARCORA, M.S., BERNABÓ, G., HERMANN-LUIBL, C., ROMERO, J.I., HELFRICH-FÖRSTER, C., CASTAÑO, E.M., MARINO-BUSJLE, C., CALVO, D.J., CERIANI, M.F. 2017.
Organization of Circadian behavior relies on glycinergic transmission. *Cell reports.* 19, 72–85.
FRIGGI-GRELIN, F., ICHE, M. & BIRMAN, S. 2003. Tissue-specific developmental requirements of *Drosophila* tyrosine hydroxylase isoforms. *Genesis,* 35**,** 175-184.
GATTO, C. L. & BROADIE, K. 2009. Temporal requirements of the fragile X mental retardation protein in modulating circadian clock circuit synaptic architecture. *Frontiers in Neural Circuits,* 3.
GENGS, C. X., LEUNG, H. T., SKINGSLEY, D. R., IOVCHEV, M. I., YIN, Z., SEMENOV, E. P., BURG, M. G., HARDIE, R. C. & PAK, W. L. 2002. The target of *Drosophila* photoreceptor synaptic transmission is a histamine-gated chloride

channel encoded by ort (hclA). *Journal of Biological Chemistry,* 277**,** 42113-42120.
GIEBULTOWICZ, J. M. 2001. Peripheral clocks and their role in circadian timing: insights from insects. *Philosophical Transactions of the Royal Society of London Series B-Biological Sciences,* 356**,** 1791→1799.
GLICKMAN, M. H. & CIECHANOVER, A. 2002. The ubiquitin-proteasome proteolytic pathway: Destruction for the sake of construction. *Physiological Reviews,* 82**,** 373-428.
GLOSSOP, N. R. J., HOUL, J. H., ZHENG, H., NG, F. S., DUDEK, S. M. & HARDIN, P. E. 2003. VRILLE feeds back to control circadian transcription of Clock in the *Drosophila* circadian oscillator. *Neuron,* 37**,** 249-261.
GODA, T., MIROWSKA, K., CURRIE, J., KIM, M. H., RAO, N. V., BONILLA, G. & WIJNEN, H. 2011. Adult Circadian Behavior in *Drosophila* Requires Developmental Expression of cycle, But Not period. *Plos Genetics,* 7.
GODA, T., TANG, X., UMEZAKI, Y., CHU, M. L. & HAMADA, F. N. 2016. *Drosophila* DH31 Neuropeptide and PDF Receptor Regulate Night-Onset Temperature Preference. *Journal of Neuroscience,* 36**,** 11739-11754.
GOROSTIZA, E. A. & CERIANI, M. F. 2013. Retrograde Bone Morphogenetic Protein Signaling Shapes a Key Circadian Pacemaker Circuit. *Journal of Neuroscience,* 33**,** 687-696.
GOROSTIZA, E. A., DEPETRIS-CHAUVIN, A., FRENKEL, L., PIREZ, N. & CERIANI, M. F. 2014. Circadian Pacemaker Neurons Change Synaptic Contacts across the Day. *Current Biology,* 24**,** 2161-2167.
GREEN, E. W., O'CALLAGHAN, E. K., HANSEN, C. N., BASTIANELLO, S., BHUTANI, S., VANIN, S., ARMSTRONG, J. D., COSTA, R. & KYRIACOU, C. P. 2015. *Drosophila* circadian rhythms in seminatural environments: Summer afternoon component is not an artifact and requires *TrpA1* channels. *Proceedings of the National Academy of Sciences of the United States of America,* 112**,** 8702-8707.
GRIMA, B., CHELOT, E., XIA, R. H. & ROUYER, F. 2004. Morning and evening peaks of activity rely on different clock neurons of the *Drosophila* brain. *Nature,* 431**,** 869-873.
GROTH, A. C., FISH, M., NUSSE, R. & CALOS, M. P. 2004. Construction of transgenic *Drosophila* by using the site-specific integrase from phage phi C31. *Genetics,* 166**,** 1775→1782.
GUNAWARDHANA, K. L. & HARDIN, P. E. 2017. VRILLE Controls PDF Neuropeptide Accumulation and Arborization Rhythms in Small Ventrolateral Neurons to Drive Rhythmic Behavior in *Drosophila*. *Current Biology,* 27**,** 3442-+.
GUNTHORPE, D., BEATTY, K. E. & TAYLOR, M. V. 1999. Different levels, but not different isoforms, of the *Drosophila* transcription factor DMEF2 affect distinct aspects of muscle differentiation. *Developmental Biology,* 215**,** 130-145.
GUO, F., CERULLO, I., CHEN, X. & ROSBASH, M. 2014. PDF Neuron Firing Phase-shifts Key Circadian Activity Neurons in *Drosophila*. *Elife,* 3, 02780.
GUO, F., YU, J. W., JUNG, H. J., ABRUZZI, K. C., LUO, W. F., GRIFFITH, L. C. & ROSBASH, M. 2016. Circadian neuron feedback controls the *Drosophila* sleep-activity profile. *Nature,* 536**,** 292-297.
HARRIS, W.A.& STARK, W.S. 1977. Heriditary retinal degeneration in *Drosophila melanogaster*. *Journal of General Physiology*, 69,.261→291
HAMADA, F. N., ROSENZWEIG, M., KANG, K., PULVER, S. R., GHEZZI, A., JEGLA, T. J. & GARRITY, P. A. 2008. An internal thermal sensor controlling temperature preference in *Drosophila*. *Nature,* 454**,** 217-U55.

HAMASAKA, Y., RIEGER, D., PARMENTIER, M. L., GRAU, Y., HELFRICH-FÖRSTER, C. & NASSEL, D. R. 2007. Glutamate and its metabotropic receptor in *Drosophila* clock neuron circuits. *Journal of Comparative Neurology,* 505**,** 32-45.

HAMBY, K. A., KWOK, R. S., ZALOM, F. G. & CHIU, J. C. 2013. Integrating Circadian Activity and Gene Expression Profiles to Predict Chronotoxicity of *Drosophila* suzukii Response to Insecticides. *Plos One,* 8.

HANAI, S., HAMASAKA, Y. & ISHIDA, N. 2008. Circadian entrainment to red light in *Drosophila*: requirement of Rhodopsin I and Rhodopsin 6. *Neuroreport,* 19**,** 1441-1444.

HAO, H. P., ALLEN, D. L. & HARDIN, P. E. 1997. A circadian enhancer mediates PER-dependent mRNA cycling in *Drosophila* melanogaster. *Molecular and Cellular Biology,* 17**,** 3687-3693.

HARDIE, R. C. 1989. A Histamine-Activated Chloride Channel Involved in Neurotransmission at a Photoreceptor Synapse. *Nature,* 339**,** 704-706.

HARRINGTON, J. M. 2001. Health effects of shift work and extended hours of work. *Occupational and Environmental Medicine,* 58**,** 68-72.

HARRISINGH, M.C., WU, Y., LNENICKA, G.A., NITABACH, M.N. 2007. Intracellular Ca2+ regulates free-running circadian clock oscillation in vivo. *Journal of Neuroscience.* 27:12489–99

HEAD, L. M., TANG, X., HAYLEY, S. E., GODA, T., UMEZAKI, Y., CHANG, E. C., LESLIE, J. R., FUJIWARA, M., GARRITY, P. A. & HAMADA, F. N. 2015. The Influence of Light on Temperature Preference in *Drosophila*. *Current Biology,* 25**,** 1063-1068.

HEISENBERG, M., BUCHNER, E. 1977. The role of retinula cell types in visual behavior of *Drosophila* melanogaster. *Journal of Comparative Physiology,* 117**,** 127-162.

HELFRICH-FÖRSTER, C. 2003. The neuroarchitecture of the circadian clock in the brain of *Drosophila* melanogaster. *Microscopy Research and Technique,* 62**,** 94-102.

HELFRICH-FÖRSTER, C. 2004. The circadian clock in the brain: a structural and functional comparison between mammals and insects. *Journal of Comparative Physiology a-Neuroethology Sensory Neural and Behavioral Physiology,* 190**,** 601-613.

HELFRICH-FÖRSTER, C., SHAFER, O. T., WULBECK, C., GRIESHABER, E., RIEGER, D. & TAGHERT, P. 2007. Development and morphology of the clock-gene-expressing lateral neurons of *Drosophila* melanogaster. *Journal of Comparative Neurology,* 500**,** 47-70.

HELFRICH-FÖRSTER, C., TAUBER, M., PARK, J. H., MUHLIG-VERSEN, M., SCHNEUWLY, S. & HOFBAUER, A. 2000. Ectopic expression of the neuropeptide pigment-dispersing factor alters behavioral rhythms in *Drosophila* melanogaster. *Journal of Neuroscience,* 20**,** 3339-3353.

HELFRICH, C. & ENGELMANN, W. 1983. Circadian-Rhythm of the Locomotor-Activity in *Drosophila*-Melanogaster and Its Mutants Sine Oculis and Small Optic Lobes. *Physiological Entomology,* 8**,** 257-272.

HELFRICH-FÖRSTER, C. 1997. Development of pigment-dispersing hormone-immunoreactive neurons in the nervous system of *Drosophila* melanogaster. *Journal of Comparative Neurology,* 380**,** 335-354.

HERMANN-LUIBL, C., YOSHII, T., SENTHILAN, P. R., DIRCKSEN, H. & HELFRICH-FÖRSTER, C. 2014. The Ion Transport Peptide Is a New Functional Clock Neuropeptide in the Fruit Fly *Drosophila* melanogaster. *Journal of Neuroscience,* 34**,** 9522-9536.

HERRERO, A., DUHART, J. M. & CERIANI, M. F. 2017. Neuronal and Glial Clocks Underlying Structural Remodeling of Pacemaker Neurons in *Drosophila*. *Frontiers in Physiology,* 8.
HEWES, R. S., SCHAEFER, A. M. & TAGHERT, P. H. 2000. The cryptocephal gene (ATF4) encodes multiple basic-leucine zipper proteins controlling molting and metamorphosis in *Drosophila*. *Genetics,* 155**,** 1711→1723.
HONG, S. T., BANG, S., PAIK, D., KANG, J. K., HWANG, S., JEON, K., CHUN, B., HYUN, S., LEE, Y. & KIM, J. 2006. Histamine and its receptors modulate temperature-preference behaviors in *Drosophila*. *Journal of Neuroscience,* 26**,** 7245-7256.
HOUL, J. H., NG, F., TAYLOR, P. & HARDIN, P. E. 2008. CLOCK expression identifies developing circadian oscillator neurons in the brains of *Drosophila* embryos. *Bmc Neuroscience,* 9.
HOUL, J. H., YU, W. J., DUDEK, S. M. & HARDIN, P. E. 2006. *Drosophila* CLOCK is constitutively expressed in circadian oscillator and non-oscillator cells. *Journal of Biological Rhythms,* 21**,** 93-103.
HOYLE, N. P., SEINKMANE, E., PUTKER, M., FEENEY, K. A., KROGAGER, T. P., CHESHAM, J. E., BRAY, L. K., THOMAS, J. M., DUNN, K., BLAIKLEY, J. & O'NEILL, J. S. 2017. Circadian actin dynamics drive rhythmic fibroblast mobilization during wound healing. *Science Translational Medicine,* 9.
HUANG, T. C., TU, J., CHOW, T. J. & CHEN, T. H. 1990. Circadian-Rhythm of the Prokaryote Synechococcus Sp Rf-1. *Plant Physiology,* 92**,** 531-533.
HUANG, Y. M., AINSLEY, J. A., REIJMERS, L. G. & JACKSON, F. R. 2013. Translational Profiling of Clock Cells Reveals Circadianly Synchronized Protein Synthesis. *Plos Biology,* 11.
HUANG, Y. M., HOWLETT, E., STERN, M. & JACKSON, F. R. 2009. Altered LARK expression perturbs development and physiology of the *Drosophila* PDF clock neurons. *Molecular and Cellular Neuroscience,* 41**,** 196-205.
HUGHES, M. E., GRANT, G. R., PAQUIN, C., QIAN, J. & NITABACH, M. N. 2012. Deep sequencing the circadian and diurnal transcriptome of *Drosophila* brain. *Genome Research,* 22**,** 1266-1281.
IM, S. H., LI, W. H. & TAGHERT, P. H. 2011. PDFR and CRY Signaling Converge in a Subset of Clock Neurons to Modulate the Amplitude and Phase of Circadian Behavior in *Drosophila*. *Plos One,* 6.
IM, S. H. & TAGHERT, P. H. 2010. PDF Receptor Expression Reveals Direct Interactions Between Circadian Oscillators in *Drosophila*. *Journal of Comparative Neurology,* 518**,** 1925-1945.
ISAAC, R. E., LI, C. X., LEEDALE, A. E. & SHIRRAS, A. D. 2010. *Drosophila* male sex peptide inhibits siesta sleep and promotes locomotor activity in the post-mated female. *Proceedings of the Royal Society B-Biological Sciences,* 277**,** 65-70.
ITO, C., GOTO, S. G., SHIGA, S., TOMIOKA, K. & NUMATA, H. 2008. Peripheral circadian clock for the cuticle deposition rhythm in *Drosophila* melanogaster. *Proceedings of the National Academy of Sciences of the United States of America,* 105**,** 8446-8451.
JACKSON, F. R. 2011. Glial Cell Modulation of Circadian Rhythms. *Glia,* 59**,** 1341-1350.
JAUMOUILLE, E., ALMEIDA, P. M., STAHLI, P., KOCH, R. & NAGOSHI, E. 2015. Transcriptional Regulation via Nuclear Receptor Crosstalk Required for the *Drosophila* Circadian Clock. *Current Biology,* 25**,** 1502-1508.
JOHARD, H. A. D., YOISHII, T., DIRCKSEN, H., CUSUMANO, P., ROUYER, F., HELFRICH-FÖRSTER, C. & NASSEL, D. R. 2009. Peptidergic Clock Neurons

in *Drosophila*: Ion Transport Peptide and Short Neuropeptide F in Subsets of Dorsal and Ventral Lateral Neurons. *Journal of Comparative Neurology,* 516**,** 59-73.
JOUFFE, C., CRETENET, G., SYMUL, L., MARTIN, E., ATGER, F., NAEF, F. & GACHON, F. 2013. The Circadian Clock Coordinates Ribosome Biogenesis. *Plos Biology,* 11.
KADENER, S., MENET, J. S., SCHOER, R. & ROSBASH, M. 2008. Circadian transcription contributes to core period determination in *Drosophila*. *Plos Biology,* 6**,** 965-977.
KANEKO, M. & HALL, J. C. 2000. Neuroanatomy of cells expressing clock genes in *Drosophila*: Transgenic manipulation of the period and timeless genes to mark the perikarya of circadian pacemaker neurons and their projections. *Journal of Comparative Neurology,* 422**,** 66-94.
KANEKO, M., HELFRICH-FÖRSTER, C.H., HALL, J.C. 1997. Spatial and temporal expression of the period and timeless genes in the developing nervous system of *Drosophila*: newly identified pacemaker candidates and novel features of clock gene product cycling. *Journal of Neuroscience,* 17**,** 15.
KANEKO, M., PARK, J. H., CHENG, Y. Z., HARDIN, P. E. & HALL, J. C. 2000. Disruption of synaptic transmission or clock-gene-product oscillations in circadian pacemaker cells of *Drosophila* cause abnormal behavioral rhythms. *Journal of Neurobiology,* 43**,** 207→233.
KAYSER, M. S., YUE, Z. F. & SEHGAL, A. 2014. A Critical Period of Sleep for Development of Courtship Circuitry and Behavior in *Drosophila*. *Science,* 344**,** 269-274.
KEEGAN, K. P., PRADHAN, S., WANG, J. P. & ALLADA, R. 2007. Meta-analysis of *Drosophila* circadian microarray studies identifies a novel set of rhythmically expressed genes. *Plos Computational Biology,* 3**,** 2087-2110.
KEENE, A. C., MAZZONI, E. O., ZHEN, J., YOUNGER, M. A., YAMAGUCHI, S., BLAU, J., DESPLAN, C. & SPRECHER, S. G. 2011. Distinct Visual Pathways Mediate *Drosophila* Larval Light Avoidance and Circadian Clock Entrainment. *Journal of Neuroscience,* 31**,** 6527-6534.
KELLOGG, D. R., MITCHISON, T. J. & ALBERTS, B. M. 1988. Behavior of Microtubules and Actin-Filaments in Living *Drosophila* Embryos. *Development,* 103**,** 675-686.
KIDD, P. B., YOUNG, M. W. & SIGGIA, E. D. 2015. Temperature compensation and temperature sensation in the circadian clock. *Proceedings of the National Academy of Sciences of the United States of America,* 112**,** E6284-E6292.
KILMAN, V. L. & ALLADA, R. 2009. Genetic Analysis of Ectopic Circadian Clock Induction in *Drosophila*. *Journal of Biological Rhythms,* 24**,** 368-378.
KIM, E. Y. & EDERY, I. 2006. Balance between DBT/CKI epsilon kinase and protein phosphatase activities regulate phosphorylation and stability of *Drosophila* CLOCK protein. *Proceedings of the National Academy of Sciences of the United States of America,* 103**,** 6178-6183.
KING, A. N., BARBER, A. F., SMITH, A. E., DREYER, A. P., SITARAMAN, D., NITABACH, M. N., CAVANAUGH, D. J. & SEHGAL, A. 2017. A Peptidergic Circuit Links the Circadian Clock to Locomotor Activity. *Current Biology,* 27**,** 1915-+.
KLARSFELD, A., MALPEL, S., MICHARD-VANHEE, C., PICOT, M., CHELOT, E. & ROUYER, F. 2004. Novel features of cryptochrome-mediated photoreception in the brain circadian clock of *Drosophila*. *Journal of Neuroscience,* 24**,** 1468-1477.
KLARSFELD, A., PICOT, M., VIAS, C., CHELOT, E. & ROUYER, F. 2011. Identifying Specific Light Inputs for Each Subgroup of Brain Clock Neurons in

Drosophila Larvae. *Journal of Neuroscience,* 31**,** 17406→17415.
KO, H. W., JIANG, J. & EDERY, I. 2002. Role for Slimb in the degradation of *Drosophila* Period protein phosphorylated by Doubletime. *Nature,* 420**,** 673-678.
KOH, K., ZHENG, X. Z. & SEHGAL, A. 2006. JETLAG resets the *Drosophila* circadian clock by promoting light-induced degradation of TIMELESS. *Science,* 312**,** 1809-1812.
KOJIMA, S., SHER-CHEN, E. L. & GREEN, C. B. 2012. Circadian control of mRNA polyadenylation dynamics regulates rhythmic protein expression. *Genes & Development,* 26**,** 2724-2736.
KONOPKA, R. J. & BENZER, S. 1971. Clock Mutants of *Drosophila*-Melanogaster. *Proceedings of the National Academy of Sciences of the United States of America,* 68**,** 2112-&.
KULA-EVERSOLE, E., NAGOSHI, E., SHANG, Y. H., RODRIGUEZ, J., ALLADA, R. & ROSBASH, M. 2010. Surprising gene expression patterns within and between PDF-containing circadian neurons in *Drosophila*. *Proceedings of the National Academy of Sciences of the United States of America,* 107**,** 13497-13502.
KULA, E., LEVITAN, E. S., PYZA, E. & ROSBASH, M. 2006. PDF cycling in the dorsal protocerebrum of the *Drosophila* brain is not necessary for circadian clock function. *Journal of Biological Rhythms,* 21**,** 104-117.
KUMAR, S., CHEN, D. & SEHGAL, A. 2012. Dopamine acts through Cryptochrome to promote acute arousal in *Drosophila*. *Genes & Development,* 26**,** 1224-1234.
KUMAR, S., CHEN, D. C., JANG, C., NALL, A., ZHENG, X. Z. & SEHGAL, A. 2014. An ecdysone-responsive nuclear receptor regulates circadian rhythms in *Drosophila*. *Nature Communications,* 5.
KUNST, M., HUGHES, M. E., RACCUGLIA, D., FELIX, M., LI, M., BARNETT, G., DUAH, J. & NITABACH, M. N. 2014. Calcitonin Gene-Related Peptide Neurons Mediate Sleep-Specific Circadian Output in *Drosophila*. *Current Biology,* 24**,** 2652-2664.
KUO, C. T., JAN, L. Y. & JAN, Y. N. 2005. Dendrite-specific remodeling of *Drosophila* sensory neurons requires matrix metalloproteases, ubiquitin-proteasome, and ecdysone signaling. *Proceedings of the National Academy of Sciences of the United States of America,* 102**,** 15230-15235.
KYRIACOU, C. P., OLDROYD, M., WOOD, J., SHARP, M. & HILL, M. 1990. Clock Mutations Alter Developmental Timing in *Drosophila*. *Heredity,* 64**,** 395-401.
LEAR, B. C., LIN, J. M., KEATH, J. R., MCGILL, J. J., RAMAN, I. M. & ALLADA, R. 2005. The ion channel narrow abdomen is critical for neural output of the *Drosophila* circadian pacemaker. *Neuron,* 48**,** 965-976.
LEAR, B. C., ZHANG, L. Y. & ALLADA, R. 2009. The Neuropeptide PDF Acts Directly on Evening Pacemaker Neurons to Regulate Multiple Features of Circadian Behavior. *Plos Biology,* 7.
LEE, C., BAE, K. & EDERY, I. 1999. PER and TIM inhibit the DNA binding activity of a *Drosophila* CLOCK-CYC/dBMAL1 heterodimer without disrupting formation of the heterodimer: a basis for circadian transcription. *Molecular and Cellular Biology,* 19**,** 5316-5325.
LEE, G., KIKUNO, K., BAHN, J. H., KIM, K. M. & PARK, J. H. 2013. Dopamine D2 Receptor as a Cellular Component Controlling Nocturnal Hyperactivities in *Drosophila* melanogaster. *Chronobiology International,* 30**,** 443-459.
LEE, G. H., BAHN, J. H. & PARK, J. H. 2006. Sex- and clock-controlled expression of the neuropeptide F gene in *Drosophila*. *Proceedings of the National Academy of Sciences of the United States of America,* 103**,** 12580-12585.
LEE, T. & LUO, L. Q. 1999. Mosaic analysis with a repressible cell marker for studies of gene function in neuronal morphogenesis. *Neuron,* 22**,** 451-461.

LERNER, I., BARTOK, O., WOLFSON, V., MENET, J. S., WEISSBEIN, U., AFIK, S., HAIMOVICH, D., GAFNI, C., FRIEDMAN, N., ROSBASH, M. & KADENER, S. 2015. Clk post-transcriptional control denoises circadian transcription both temporally and spatially. *Nature Communications,* 6.
LEVINE, J. D., FUNES, P., DOWSE, H. B. & HALL, J. C. 2002. Resetting the circadian clock by social experience in *Drosophila* melanogaster. *Science,* 298**,** 2010-2012.
LIANG, X. T., HOLY, T. E. & TAGHERT, P. H. 2017. A Series of Suppressive Signals within the *Drosophila* Circadian Neural Circuit Generates Sequential Daily Outputs. *Neuron,* 94**,** 1173-1181.
LIANG, X. T., HOLY, T. E. & TAGHERT, P. H. 2016. Synchronous *Drosophila* circadian pacemakers display nonsynchronous $Ca2^{+}$ rhythms in vivo. *Science*. 351, 976–981
LIM, C., LEE, J., KOO, E. & CHOE, J. 2007. Targeted inhibition of Pdp1 epsilon abolishes the circadian behavior of *Drosophila* melanogaster. *Biochemical and Biophysical Research Communications,* 364**,** 294-300.
LIN, S. C., LIN, M. H., HORVATH, P., REDDY, K. L. & STORTI, R. V. 1997. PDP1, a novel *Drosophila* PAR domain bZIP transcription factor expressed in developing mesoderm, endoderm and ectoderm, is a transcriptional regulator of somatic muscle genes. *Development,* 124**,** 4685-4696.
LIN, S. C. & STORTI, R. V. 1997. Developmental regulation of the *Drosophila* Tropomyosin I (TmI) gene is controlled by a muscle activator enhancer region that contains multiple cis-elements and binding sites for multiple proteins. *Developmental Genetics,* 20**,** 297-306.
LIN, Y., HAN, M., SHIMADA, B., WANG, L., GIBLER, T. M., AMARAKONE, A., AWAD, T. A., STORMO, G. D., VAN GELDER, R. N. & TAGHERT, P. H. 2002. Influence of the period-dependent circadian clock on diurnal, circadian, and aperiodic gene expression in *Drosophila* melanogaster. *Proceedings of the National Academy of Sciences of the United States of America,* 99**,** 9562-9567.
LIN, Y., STORMO, G. D. & TAGHERT, P. H. 2004. The neuropeptide pigment-dispersing factor coordinates pacemaker interactions in the *Drosophila* circadian system. *Journal of Neuroscience,* 24**,** 7951-7957.
LIU, Q. L., LIU, S., KODAMA, L., DRISCOLL, M. R. & WU, M. N. 2012. Two Dopaminergic Neurons Signal to the Dorsal Fan-Shaped Body to Promote Wakefulness in *Drosophila*. *Current Biology,* 22**,** 2114-2123.
LIU, S., LAMAZE, A., LIU, Q. L., TABUCHI, M., YANG, Y., FOWLER, M., BHARADWAJ, R., ZHANG, J., BEDONT, J., BLACKSHAW, S., LLOYD, T. E., MONTELL, C., SEHGAL, A., KOH, K. & WU, M. N. 2014. WIDE AWAKE Mediates the Circadian Timing of Sleep Onset. *Neuron,* 82**,** 151-166.
LIU, T. X., MAHESH, G., HOUL, J. H. & HARDIN, P. E. 2015. Circadian Activators Are Expressed Days before They Initiate Clock Function in Late Pacemaker Neurons from *Drosophila*. *Journal of Neuroscience,* 35**,** 8662-8671.
LIU, T. X., MAHESH, G., YU, W. J. & HARDIN, P. E. 2017. CLOCK stabilizes CYCLE to initiate clock function in *Drosophila*. *Proceedings of the National Academy of Sciences of the United States of America,* 114**,** 10972-10977.
LIU, X., ZWIEBEL, L. J., HINTON, D., BENZER, S., HALL, J. C. & ROSBASH, M. 1992. The Period Gene Encodes a Predominantly Nuclear-Protein in Adult *Drosophila*. *Journal of Neuroscience,* 12**,** 2735-2744.
MAJERCAK, J., SIDOTE, D., HARDIN, P. E. & EDERY, I. 1999. How a circadian clock adapts to seasonal decreases in temperature and day length. *Neuron,* 24**,** 219→230.
MALPEL, S., KLARSFELD, A. & ROUYER, F. 2002. Larval optic nerve and adult extra-retinal photoreceptors sequentially associate with clock neurons during

Drosophila brain development. *Development,* 129**,** 1443-1453.
MARRUS, S. B., ZENG, H. K. & ROSBASH, M. 1996. Effect of constant light and circadian entrainment of per(S) flies: Evidence for light-mediated delay of the negative feedback loop in *Drosophila*. *Embo Journal,* 15**,** 6877-6886.
MARTELLI, C., PECH, U., KOBBENBRING, S., PAULS, D., BAHL, B., SOMMER, M. V., POORYASIN, A., BARTH, J., ARIAS, C. W. P., VASSILIOU, C., LUNA, A. J. F., POPPINGA, H., RICHTER, F. G., WEGENER, C., FIALA, A. & RIEMENSPERGER, T. 2017. *SIFa*mide Translates Hunger Signals into Appetitive and Feeding Behavior in *Drosophila*. *Cell Reports,* 20**,** 464-478.
MARTINEK, S., INONOG, S., MANOUKIAN, A. S. & YOUNG, M. W. 2001. A role for the segment polarity gene shaggy/GSK-3 in the *Drosophila* circadian clock. *Cell,* 105**,** 769-779.
MATSUMOTO, K., TOH-E, A., OSHIMA, Y. 1978. Genetic control of galactokinase synthesis in Saccharomyces cerevisiae: evidence for constitutive expression of the positive regulatory gene *gal4*. *Journal of Bacteriology,* 134**,** 11.
MAZZONI, E. O., DESPLAN, C. & BLAU, J. 2005. Circadian pacemaker neurons transmit and modulate visual information to control a rapid behavioral response. *Neuron,* 45**,** 293-300.
MCCABE, B. D., MARQUES, G., HAGHIGHI, A. P., FETTER, R. D., CROTTY, M. L., HAERRY, T. E., GOODMAN, C. S. & O'CONNOR, M. B. 2003. The BMP homolog Gbb provides a retrograde signal that regulates synaptic growth at the *Drosophila* neuromuscular junction. *Neuron,* 39**,** 241-254.
MCDONALD, M. J. & ROSBACH, M. 2001. Microarray analysis and organization of circadian gene expression *Drosophila*. *Cell,* 107**,** 567-578.
MEZAN, S., FEUZ, J. D., DEPLANCKE, B. & KADENER, S. 2016. PDF Signaling Is an Integral Part of the *Drosophila* Circadian Molecular Oscillator. *Cell Reports,* 17**,** 708-719.
MROSOVSKY, N. 1999. Masking: History, definitions, and measurement. *Chronobiology International,* 16**,** 415-429.
MURAD, A., EMERY-LE, M. & EMERY, P. 2007. A subset of dorsal neurons modulates circadian behavior and light responses in *Drosophila*. *Neuron,* 53**,** 689-701.
MURARO, N. I. & CERIANI, M. F. 2015. Acetylcholine from Visual Circuits Modulates the Activity of Arousal Neurons in *Drosophila*. *Journal of Neuroscience,* 35**,** 16315-16327.
MUSIEK, E. S. & HOLTZMAN, D. M. 2016. Mechanisms linking circadian clocks, sleep, and neurodegeneration. *Science,* 354**,** 1004-1008.
MYERS, E. M., YU, J. J. & SEHGAL, A. 2003. Circadian control of eclosion: Interaction between a central and peripheral clock in *Drosophila* melanogaster. *Current Biology,* 13**,** 526-533.
NAGOSHI, E., SUGINO, K., KULA, E., OKAZAKI, E., TACHIBANA, T., NELSON, S. & ROSBASH, M. 2010. Dissecting differential gene expression within the circadian neuronal circuit of *Drosophila*. *Nature Neuroscience,* 13**,** 60-U220.
NASH, H. A., SCOTT, R. L., LEAR, B. C. & ALLADA, R. 2002. An unusual cation channel mediates photic control of locomotion in *Drosophila*. *Current Biology,* 12**,** 2152-2158.
NG, F. S., TANGREDI, M. M. & JACKSON, F. R. 2011. Glial Cells Physiologically Modulate Clock Neurons and Circadian Behavior in a Calcium-Dependent Manner. *Current Biology,* 21**,** 625-634.
NITABACH, M. N., BLAU, J. & HOLMES, T. C. 2002. Electrical silencing of *Drosophila* pacemaker neurons stops the free-running circadian clock. *Cell,* 109**,** 485-495.
NITABACH, M. N., WU, Y., SHEEBA, V., LEMON, W. C., STRUMBOS, J.,

ZELENSKY, P. K., WHITE, B. H. & HOLMES, T. C. 2006. Electrical hyperexcitation of lateral ventral pacemaker neurons desynchronizes downstream circadian oscillators in the fly circadian circuit and induces multiple behavioral periods. *Journal of Neuroscience,* 26**,** 479-489.

O'BRIEN, M. A. & TAGHERT, P. H. 1998. A peritracheal neuropeptide system in insects: Release of myomodulin-like peptides at ecdysis. *Journal of Experimental Biology,* 201**,** 193-209.

OH, Y., JANG, D., SONN, J. Y. & CHOE, J. 2013. Histamine-HisCl1 Receptor Axis Regulates Wake-Promoting Signals in *Drosophila* melanogaster. *Plos One,* 8.

OSTERWALDER, T., YOON, K.S., WHITE, B.H., KESHISHIAN, H. 2001. A conditional tissue-specific transgene expression system using inducible *GAL4*. *Proceedings of the National Academy of Sciences of the United States of America*, 98

PARANJPE, D. A., ANITHA, D., CHANDRASHEKARAN, M., JOSHI, A. & SHARMA, V. K. 2005. Possible role of eclosion rhythm in mediating the effects of light-dark environments on pre-adult development in *Drosophila* melanogaster. *Bmc Developmental Biology,* 5.

PARISKY, K. M., AGOSTO, J., PULVER, S. R., SHANG, Y. H., KUKLIN, E., HODGE, J. J. L., KANG, K., LIU, X., GARRITY, P. A., ROSBASH, M. & GRIFFITH, L. C. 2008. PDF Cells Are a GABA-Responsive Wake-Promoting Component of the *Drosophila* Sleep Circuit. *Neuron,* 60**,** 672-682.

PARK, J. H. & HALL, J. C. 1998. Isolation and chronobiological analysis of a neuropeptide pigment-dispersing factor gene in *Drosophila* melanogaster. *Journal of Biological Rhythms,* 13**,** 219-228.

PARK, J. H., HELFRICH-FÖRSTER, C., LEE, G., LIU, L., ROSBASH, M. & HALL, J. C. 2000. Differential regulation of circadian pacemaker output by separate clock genes in *Drosophila*. *Proceedings of the National Academy of Sciences of the United States of America,* 97**,** 3608-3613.

PENG, Y., STOLERU, D., LEVINE, J. D., HALL, J. C. & ROSBASH, M. 2003. *Drosophila* free-running rhythms require intercellular communication. *Plos Biology,* 1**,** 32-40.

PESCHEL, N., CHEN, K. F., SZABO, G. & STANEWSKY, R. 2009. Light-Dependent Interactions between the *Drosophila* Circadian Clock Factors Cryptochrome, Jetlag, and Timeless. *Current Biology,* 19**,** 241-247.

PICOT, M., CUSUMANO, P., KLARSFELD, A., UEDA, R. & ROUYER, F. 2007. Light activates output from evening neurons and inhibits output from morning neurons in the *Drosophila* circadian clock. *Plos Biology,* 5**,** 2513-2521.

PITTENDRIGH, C. S. 1954. On temperature independence in the clock-system controlling emergence time in *Drosophila*. *Proceedings of the National Academy of Sciences,* 40**,** 1018-1029.

PLAUTZ, J. D., KANEKO, M., HALL, J. C. & KAY, S. A. 1997. Independent photoreceptive circadian clocks throughout *Drosophila*. *Science,* 278**,** 1632-1635.

PRICE, J. L. 2014. Translational Regulation of the *Drosophila* Post-Translational Circadian Mechanism. *Plos Genetics,* 10.

PRICE, J. L., BLAU, J., ROTHENFLUH, A., ABODEELY, M., KLOSS, B. & YOUNG, M. W. 1998. Double-time is a novel *Drosophila* clock gene that regulates PERIOD protein accumulation. *Cell,* 94**,** 83-95.

REDDY, K. L., WOHLWILL, A., DZITOEVA, S., LIN, M. H., HOLBROOK, S. & STORTI, R. V. 2000. The *Drosophila* PAR domain protein 1 (Pdp1) gene encodes multiple differentially expressed mRNAs and proteins through the use of multiple enhancers and promoters. *Developmental Biology,* 224**,** 401-414.

RENN, S. C. P., PARK, J. H., ROSBASH, M., HALL, J. C. & TAGHERT, P. H. 1999. A

pdf neuropeptide gene mutation and ablation of PDF neurons each cause severe abnormalities of behavioral circadian rhythms in *Drosophila*. *Cell,* 99**,** 791-802.
RIEGER, D., SHAFER, O. T., TOMIOKA, K. & HELFRICH-FÖRSTER, C. 2006. Functional analysis of circadian pacemaker neurons in *Drosophila* melanogaster. *Journal of Neuroscience,* 26**,** 2531-2543.
ROMAN, G., ENDO, K., ZONG, L. & DAVIS, R. L. 2001. P{Switch}, a system for spatial and temporal control of gene expression in *Drosophila* melanogaster. *Proceedings of the National Academy of Sciences of the United States of America,* 98**,** 12602-12607.
RORTH, P. 1996. A modular misexpression screen in *Drosophila* detecting tissue-specific phenotypes. *Proceedings of the National Academy of Sciences of the United States of America,* 93**,** 12418-12422.
ROTHENFLUH, A., YOUNG, M. W. & SAEZ, L. 2000. A TIMELESS-independent function for PERIOD proteins in the *Drosophila* clock. *Neuron,* 26**,** 505-514.
RUBIN, G. M. & SPRADLING, A. C. 1982. Genetic-Transformation of *Drosophila* with Transposable Element Vectors. *Science,* 218**,** 348-353.
RUTILA, J. E., SURI, V., LE, M., SO, W. V., ROSBASH, M. & HALL, J. C. 1998. CYCLE is a second bHLH-PAS clock protein essential for circadian rhythmicity and transcription of *Drosophila* period and timeless. *Cell,* 93**,** 805-814.
SABADO, V., VIENNE, L., NUNES, J. M., ROSBASH, M., AND NAGOSHI, E. 2017. Fluorescence circadian imaging reveals a PDF-dependent transcriptional regulation of the *Drosophila* molecular clock. *Scientific Reports.* 7. 41560
SAEZ, L. & YOUNG, M. W. 1996. Regulation of nuclear entry of the *Drosophila* clock proteins period and timeless. *Neuron,* 17**,** 911-920.
SCHLICHTING, M., MENEGAZZI, P., LELITO, K. R., YAO, Z. P., BUHL, E., DALLA BENETTA, E., BAHLE, A., DENIKE, J., HODGE, J. J., HELFRICH-FÖRSTER, C. & SHAFER, O. T. 2016. A Neural Network Underlying Circadian Entrainment and Photoperiodic Adjustment of Sleep and Activity in *Drosophila*. *Journal of Neuroscience,* 36**,** 9084-9096.
SCHRADER, H., BOVIM, G. & SAND, T. 1993. The Prevalence of Delayed and Advanced Sleep Phase Syndromes. *Journal of Sleep Research,* 2**,** 51-55.
SCHUBERT, F. K., HAGEDORN, N., YOSHII, T., HELFRICH-FÖRSTER, C., AND RIEGER, D. 2018. Neuroanatomical details of the lateral neurons of *Drosophila melanogaster* support their functional role in the circadian system. *Jouranl of Comparative Neurology.* 526, 1209–1231
SEHGAL, A., PRICE, J. & YOUNG, M. W. 1992. Ontogeny of a Biological Clock in *Drosophila*-Melanogaster. *Proceedings of the National Academy of Sciences of the United States of America,* 89**,** 1423-1427.
SEHGAL, A., PRICE, J. L., MAN, B. & YOUNG, M. W. 1994. Loss of Circadian Behavioral Rhythms and Per Rna Oscillations in the *Drosophila* Mutant Timeless. *Science,* 263**,** 1603-1606.
SELLAMI, A. & VEENSTRA, J. A. 2015. *SIFa*mide acts on fruitless neurons to modulate sexual behavior in *Drosophila* melanogaster. *Peptides,* 74**,** 50-56.
SEPP, K. J., SCHULTE, J. & AULD, V. J. 2001. Peripheral glia direct axon guidance across the CNS/PNS transition zone. *Developmental Biology,* 238**,** 47-63.
SHAFER, O. T., HELFRICH-FÖRSTER, C., RENN, S. C. P. & TAGHERT, P. H. 2006. Reevaluation of *Drosophila* melanogaster's neuronal circadian pacemakers reveals new neuronal classes. *Journal of Comparative Neurology,* 498**,** 180-193.
SHAFER, O. T., KIM, D. J., DUNBAR-YAFFE, R., NIKOLAEV, V. O., LOHSE, M. J. & TAGHERT, P. H. 2008. Widespread receptivity to neuropeptide PDF throughout the neuronal circadian clock network of *Drosophila* revealed by real-time cyclic AMP imaging. *Neuron,* 58**,** 223→237.

SHAFER, O. T., ROSBASH, M. & TRUMAN, J. W. 2002. Sequential nuclear accumulation of the clock proteins period and timeless in the pacemaker neurons of *Drosophila* melanogaster. *Journal of Neuroscience,* 22**,** 5946-5954.
SHAFER, O. T. & TAGHERT, P. H. 2009. RNA-Interference Knockdown of *Drosophila* Pigment Dispersing Factor in Neuronal Subsets: The Anatomical Basis of a Neuropeptide's Circadian Functions. *Plos One,* 4.
SHANG, Y. H., GRIFFITH, L. C. & ROSBASH, M. 2008. Light-arousal and circadian photoreception circuits intersect at the large PDF cells of the *Drosophila* brain. *Proceedings of the National Academy of Sciences of the United States of America,* 105**,** 19587-19594.
SHANG, Y. H., HAYNES, P., PIREZ, N., HARRINGTON, K. I., GUO, F., POLLACK, J., HONG, P. Y., GRIFFITH, L. C. & ROSBASH, M. 2011. Imaging analysis of clock neurons reveals light buffers the wake-promoting effect of dopamine. *Nature Neuroscience,* 14**,** 889-U110.
SHAW, P. J., TONONI, G., GREENSPAN, R. J. & ROBINSON, D. F. 2002. Stress response genes protect against lethal effects of sleep deprivation in *Drosophila*. *Nature,* 417**,** 287→291.
SHEEBA, V., FOGLE, K. J. & HOLMES, T. C. 2010. Persistence of Morning Anticipation Behavior and High Amplitude Morning Startle Response Following Functional Loss of Small Ventral Lateral Neurons in *Drosophila*. *Plos One,* 5.
SHEEBA, V., FOGLE, K. J., KANEKO, M., RASHID, S., CHOU, Y. T., SHARMA, V. K. & HOLMES, T. C. 2008a. Large Ventral Lateral Neurons Modulate Arousal and Sleep in *Drosophila*. *Current Biology,* 18**,** 1537-1545.
SHEEBA, V., SHARMA, V. K., GU, H., CHOU, Y. T., O'DOWD, D. K. & HOLMES, T. C. 2008b. Pigment dispersing factor-dependent and -independent circadian locomotor behavioral rhythms. *Journal of Neuroscience,* 28**,** 217-227.
SIEGMUND, T. & KORGE, G. 2001. Innervation of the ring gland of *Drosophila* melanogaster. *Journal of Comparative Neurology,* 431**,** 481-491.
SIVACHENKO, A., LI, Y., ABRUZZI, K. C. & ROSBASH, M. 2013. The Transcription Factor Mef2 Links the *Drosophila* Core Clock to Fas2, Neuronal Morphology, and Circadian Behavior. *Neuron,* 79**,** 281→292.
SMOLENSKY, M. H., HAUS, E. 2001. Circadian Rhythms and Clinical Medicine With Applications to Hypertension. *American Journal of Hypertension,* 14**,** 10.
STANEWSKY, R., KANEKO, M., EMERY, P., BERETTA, B., WAGER-SMITH, K., KAY, S. A., ROSBASH, M. & HALL, J. C. 1998. The cry(b) mutation identifies cryptochrome as a circadian photoreceptor in *Drosophila*. *Cell,* 95**,** 681-692.
STELLER, H., FISCHBACH, K. F. & RUBIN, G. M. 1987. Disconnected - a Locus Required for Neuronal Pathway Formation in the Visual-System of *Drosophila*. *Cell,* 50**,** 1139-1153.
STOLERU, D., NAWATHEAN, P., FERNANDEZ, M. D. L. P., MENET, J. S., CERIANI, M. F. & ROSBASH, M. 2007. The *Drosophila* circadian network is a seasonal timer. *Cell,* 129**,** 207-219.
STOLERU, D., PENG, Y., AGOSTO, J. & ROSBASH, M. 2004. Coupled oscillators control morning and evening locomotor behaviour of *Drosophila*. *Nature,* 431**,** 862-868.
STOLERU, D., PENG, Y., NAWATHEAN, P. & ROSBASH, M. 2005. A resetting signal between *Drosophila* pacemakers synchronizes morning and evening activity. *Nature,* 438**,** 238-242.
SUNDRAM, V., NG, F. S., ROBERTS, M. A., MILLAN, C., EWER, J. & JACKSON, F. R. 2012. Cellular Requirements for LARK in the *Drosophila* Circadian System. *Journal of Biological Rhythms,* 27**,** 183-195.
SWEENEY, S. T., BROADIE, K., KEANE, J., NIEMANN, H. & OKANE, C. J. 1995.

Targeted Expression of Tetanus Toxin Light-Chain in *Drosophila* Specifically Eliminates Synaptic Transmission and Causes Behavioral Defects. *Neuron,* 14**,** 341-351.

SZUPERAK,M., CHURGIN, M.A., BORJA, A.J., RAIZEN, D.M., FANG-YEN., C & KAYSER., M.S. 2018. A sleep state in *Drosophila* larvae required for neural stem cell proliferation. *elife*. 7.e33220.

TANOUE, S., KRISHNAN, P., KRISHNAN, B., DRYER, S. E. & HARDIN, P. E. 2004. Circadian clocks in antennal neurons are necessary and sufficient for olfaction rhythms in *Drosophila*. *Current Biology,* 14**,** 638-649.

TECHNAU, G. & HEISENBERG, M. 1982. Neural Reorganization during Metamorphosis of the Corpora Pedunculata in *Drosophila*-Melanogaster. *Nature,* 295**,** 405-407.

TERHZAZ, S., ROSAY, P., GOODWIN, S. F. & VEENSTRA, J. A. 2007. The neuropeptide *SIFa*mide modulates sexual behavior in *Drosophila*. *Biochemical and Biophysical Research Communications,* 352**,** 305-310.

TESSIER, C. M., BROADIE, K. 2009. Activity-Dependent Modulation of Neural Circuit Synaptic Connectivity. *Frontiers in Molecular Neuroscience,* 2.

TRUMAN, J. W. 1990. Metamorphosis of the Central-Nervous-System of *Drosophila*. *Journal of Neurobiology,* 21**,** 1072-1084.

UEDA, H. R., MATSUMOTO, A., KAWAMURA, M., IINO, M., TANIMURA, T. & HASHIMOTO, S. 2002. Genome-wide transcriptional orchestration of circadian rhythms in *Drosophila*. *Journal of Biological Chemistry,* 277**,** 14048-14052.

VACCARO, A., ISSA, A. R., SEUGNET, L., BIRMAN, S. & KIARSFEID, A. 2017. *Drosophila* Clock Is Required in Brain Pacemaker Neurons to Prevent Premature Locomotor Aging Independently of Its Circadian Function. *Plos Genetics,* 13.

VANIN, S., BHUTANI, S., MONTELLI, S., MENEGAZZI, P., GREEN, E. W., PEGORARO, M., SANDRELLI, F., COSTA, R. & KYRIACOU, C. P. 2012. Unexpected features of *Drosophila* circadian behavioural rhythms under natural conditions. *Nature,* 484**,** 371-U108.

VELERI, S., RIEGER, D., HELFRICH-FÖRSTER, C. & STANEWSKY, R. 2007. Hofbauer-Buchner eyelet affects circadian photosensitivity and coordinates TIM and PER expression in *Drosophila* clock neurons. *Journal of Biological Rhythms,* 22**,** 29-42.

VISWANATH, V., STORY, G.M., PEIER, A.M., PETRUS, M.J., LEE, V.M., HWANG, S.W., PATAPOUTIAN, A., JEGLA, T. 2003. Opposite thermosensor in fruitfly and mouse. *Nature,* 423(6942): 822--823.

VOSSHALL, L. B., PRICE, J. L., SEHGAL, A., SAEZ, L. & YOUNG, M. W. 1994. Block in Nuclear-Localization of Period Protein by a 2nd Clock Mutation, Timeless. *Science,* 263**,** 1606-1609.

VRAILAS-MORTIMER, A. D., RYAN, S. M., AVEY, M. J., MORTIMER, N. T., DOWSE, H. & SANYAL, S. 2014. p38 MAP Kinase Regulates Circadian Rhythms in *Drosophila*. *Journal of Biological Rhythms,* 29**,** 411-426.

WANG, W., BARNABY, J. Y., TADA, Y., LI, H., TOR, M., CALDELARI, D., LEE, D. U., FU, X. D. & DONG, X. N. 2011. Timing of plant immune responses by a central circadian regulator. *Nature,* 470**,** 110-U126.

WATTS, R. J., HOOPFER, E. D. & LUO, L. Q. 2003. Axon pruning during Drosphila metamorphosis: Evidence for local degeneration and requirement of the ubiquitin-proteasome system. *Neuron,* 38**,** 871-885.

WEISS, R., BARTOK, O., MEZAN, S., MALKA, Y. & KADENER, S. 2014. Synergistic Interactions between the Molecular and Neuronal Circadian Networks Drive Robust Behavioral Circadian Rhythms in *Drosophila* melanogaster. *Plos Genetics,* 10.

WIJNEN, H. & YOUNG, M. W. 2006. Interplay of circadian clocks and metabolic rhythms. *Annual Review of Genetics,* 40**,** 409-448.
WU, J. S. & LUO, L. 2006. A protocol for dissecting *Drosophila* melanogaster brains for live imaging or immunostaining. *Nat Protoc,* 1**,** 2110-5.
WULBECK, C., GRIESHABER, E. & HELFRICH-FÖRSTER, C. 2008. Pigment-dispersing factor (PDF) has different effects on *Drosophila*'s circadian clocks in the accessory medulla and in the dorsal brain. *Journal of Biological Rhythms,* 23**,** 409-424.
YADAV, P., THANDAPANI, M. & SHARMA, V. K. 2014. Interaction of light regimes and circadian clocks modulate timing of pre-adult developmental events in *Drosophila*. *Bmc Developmental Biology,* 14.
YAMAGUCHI, S., DESPLAN, C. & HEISENBERG, M. 2010. Contribution of photoreceptor subtypes to spectral wavelength preference in *Drosophila*. *Proceedings of the National Academy of Sciences of the United States of America,* 107**,** 5634-5639.
YAMANAKA, N., ROMERO, N. M., MARTIN, F. A., REWITZ, K. F., SUN, M., O'CONNOR, M. B. & LEOPOLD, P. 2013. Neuroendocrine Control of *Drosophila* Larval Light Preference. *Science,* 341**,** 1113-1116.
YANG, Z. H. & SEHGAL, A. 2001. Role of molecular oscillations in generating behavioral rhythms in *Drosophila*. *Neuron,* 29**,** 453-467.
YANIV, S. P., ISSMAN-ZECHARYA, N., OREN-SUISSA, M., PODBILEWICZ, B. & SCHULDINER, O. 2012. Axon Regrowth during Development and Regeneration Following Injury Share Molecular Mechanisms. *Current Biology,* 22**,** 1774→1782.
YAO, Z. 2016. *Connectivity, Organization, and Network Coordination of the Drosophila Central Circadian Clock.* PhD, University of Michigan.
YAO, Z. & SHAFER, O. T. 2014. The *Drosophila* Circadian Clock Is a Variably Coupled Network of Multiple Peptidergic Units. *Science,* 343**,** 1516-1520.
YAPICI, N., COHN, R., SCHUSTERREITER, C., RUTA, V. & VOSSHALL, L. B. 2016. A Taste Circuit that Regulates Ingestion by Integrating Food and Hunger Signals. *Cell,* 165**,** 715-729.
YASUYAMA, K. & MEINERTZHAGEN, I. A. 2010. Synaptic Connections of PDF-Immunoreactive Lateral Neurons Projecting to the Dorsal Protocerebrum of *Drosophila* melanogaster. *Journal of Comparative Neurology,* 518**,** 292-304.
YOSHII, T., FUNADA, Y., IBUKI-ISHIBASHI, T., MATSUMOTO, A., TANIMURA, T. & TOMIOKA, K. 2004. *Drosophila* cry(b) mutation reveals two circadian clocks that drive locomotor rhythm and have different responsiveness to light. *Journal of Insect Physiology,* 50**,** 479-488.
YOSHII, T., HERMANN-LUIBL, C., KISTENPFENNIG, C., SCHMID, B., TOMIOKA, K. & HELFRICH-FÖRSTER, C. 2015. Cryptochrome-Dependent and -Independent Circadian Entrainment Circuits in *Drosophila*. *Journal of Neuroscience,* 35**,** 6131-6141.
YOSHII, T., TODO, T., WULBECK, C., STANEWSKY, R. & HELFRICH-FÖRSTER, C. 2008. Cryptochrome is present in the compound eyes and a subset of *Drosophila*'s clock neurons. *Journal of Comparative Neurology,* 508**,** 952-966.
YOSHII, T., WULBECK, C., SEHADOVA, H., VELERI, S., BICHLER, D., STANEWSKY, R. & HELFRICH-FÖRSTER, C. 2009. The Neuropeptide Pigment-Dispersing Factor Adjusts Period and Phase of *Drosophila*'s Clock. *Journal of Neuroscience,* 29**,** 2597-2610.
YOUNG, M. W. & KAY, S. A. 2001. Time zones: A comparative genetics of circadian clocks. *Nature Reviews Genetics,* 2**,** 702-715.
YU, W. J., ZHENG, H., PRICE, J. L. & HARDIN, P. E. 2009. DOUBLETIME Plays a

Noncatalytic Role To Mediate CLOCK Phosphorylation and Repress CLOCK-Dependent Transcription within the *Drosophila* Circadian Clock. *Molecular and Cellular Biology,* 29**,** 1452-1458.

ZHANG, L. Y., CHUNG, B. Y., LEAR, B. C., KILMAN, V. L., LIU, Y. X., MAHESH, G., MEISSNER, R. A., HARDIN, P. E. & ALLADA, R. 2010a. DN1(p) Circadian Neurons Coordinate Acute Light and PDF Inputs to Produce Robust Daily Behavior in *Drosophila*. *Current Biology,* 20**,** 591-599.

ZHANG, L. Y., LEAR, B. C., SELUZICKI, A. & ALLADA, R. 2009. The CRYPTOCHROME Photoreceptor Gates PDF Neuropeptide Signaling to Set Circadian Network Hierarchy in *Drosophila*. *Current Biology,* 19**,** 2050-2055.

ZHANG, Y., LIU, Y. X., BILODEAU-WENTWORTH, D., HARDIN, P. E. & EMERY, P. 2010b. Light and Temperature Control the Contribution of Specific DN1 Neurons to *Drosophila* Circadian Behavior. *Current Biology,* 20**,** 600-605.

ZHANG, Y. Q., RODESCH, C. K. & BROADIE, K. 2002. Living synaptic vesicle marker: Synaptotagmin-GFP. *Genesis,* 34**,** 142-145.

ZHAO, J., KILMAN, V. L., KEEGAN, K. P., PENG, Y., EMERY, P., ROSBASH, M. & ALLADA, R. 2003. *Drosophila* clock can generate ectopic circadian clocks. *Cell,* 113**,** 755-766.

ZHENG, X. Z., KOH, K., SOWCIK, M., SMITH, C. J., CHEN, D. C., WU, M. N. & SEHGAL, A. 2009. An Isoform-Specific Mutant Reveals a Role of PDP1 epsilon in the Circadian Oscillator. *Journal of Neuroscience,* 29**,** 10920-10927.

ZHENG, Y. C., HIRSCHBERG, B., YUAN, J., WANG, A. P., HUNT, D. C., LUDMERER, S. W., SCHMATZ, D. M. & CULLY, D. F. 2002. Identification of two novel *Drosophila* melanogaster histamine-gated chloride channel subunits expressed in the eye. *Journal of Biological Chemistry,* 277**,** 2000-2005.